FACULTEIT LANDBOUWKUNDIGE EN
TOEGEPASTE BIOLOGISCHE
WETENSCHAPPEN

Academiejaar 2003-2004

SYSTEMATIC CALIBRATION OF ACTIVATED SLUDGE MODELS

SYSTEMATISCHE CALIBRATIE VAN ACTIEF SLIB MODELLEN

door

M.Sc. ir. Gürkan Sin

Thesis submitted in fulfillment of the requirements for the degree of Doctor (Ph.D) in Applied Biological Sciences: Environmental Technology

Proefschrift voorgedragen tot het bekomen van de graad van Doctor in de Toegepaste Biologische Wetenschappen: Milieutechnologie

op gezag van

Rector: **Prof. Dr. A. De Leenheer**

Decaan:
Prof. Dr. ir. H. VAN LANGENHOVE

Promotor:
Prof. Dr. ir. P. VANROLLEGHEM

ISBN 90-5989-024-8

Gent, February 2004

De promotor:

Prof. Dr. ir. Peter Vanrolleghem

De auteur:

Gürkan Sin, M.Sc. ir.

Dedicated to my beloved *sino* family
& to the life with its all-surrounding uncertainities & unknowns…

Acknowledgement

Finally, here I am facing the acknowledgement page of my PhD thesis. To come that far in this PhD adventure is certainly a great pleasure and relief. I think the words from the Russian writer Dostoyevski summarize quite well this particularly precious adventure of my life: it has been a “blood, sweat and tears” experience. But it was simply worth it not only with respect to the great perspectives and the expertise it added to my professional background, but also equally important was the great experiences and maturity it brought along with to my personal and inner development.

The story of my PhD started about 4 years ago back in March 2000 when I was fully busy writing my M.Sc. thesis in a gloomy teaching assistant office located at the basement of the Environmental Engineering Department of Middle East Technical University (METU) in Ankara. At a time when I was fed up with my M.Sc. thesis (I hardly remember the detail now but probably it was something to do with my English☺), I somehow decided to send around a dozen of application letters for doing a PhD study abroad and got (to my surprise) a quick reply from Prof. Dr. ir. Peter A. Vanrolleghem with lots of questions in it -probably to test my level of knowledge or whether or not I will be able to figure out my way in this wild PhD adventure. After a long period of exchanging emails with Prof. Dr. ir. Peter A. Vanrolleghem, to my great happiness, Prof. Dr. ir. Peter A. Vanrolleghem, my supervisor to be, offered me the opportunity to carry out a PhD research in BIOMATH. In this way, I arrived in Belgium in the late August of 2000.

Having said the brief story of how I ended up doing a PhD in Belgium, I want to express my gratitude and thanks to many people who supported me both scientifically and personally during this PhD study. First of all my sincere thanks go to Peter –my supervisor, for his amazing, full-time positive and energetic personality, unlimited source of knowledge, excellent guiding ability, for providing the financial support to carry out a PhD study in one of the leading-edge research departments and for helping me sorting out the meticulous details of bureaucracy, e.g. postponing my military service, extending the residence permit etc. Peter, it was great honor to work with you and learn from you. I look forward to continuing working with you in this field.

It was a great pleasure to be part of BIOMATH’s multilingual and multi-continental atmosphere. I want to mention some of my colleagues with whom I had the pleasure to work

and interact: Jurgen Meirlaen (thank you Jurgen, you are a big mentor of wild wild WEST), Henk Vanhooren, Tolessa Deksissa, Bob De Clercq, Frederik Verdonck, Ingmar Nopens, Dirk De Pauw, Klaas Malisse, Kathrin Kotte, Ruxandra Govoreanu, Güçlü Insel, Dae Sung Lee, Chang Kyoo Yoo, Jiang Tao, Usama Zaher, Eveline Volcke, Stijn Van Hulle and Griet Schelstraete. I want to thank you all for your positive and generous cooperation and interaction we had in various research activities/duties. I want to also thank Dr. Krist Gernaey (an ex-BIOMATHer) and Albert Guisasola a visiting colleague from Barcelona: I had a wonderful cooperation and teamwork experience with you.

I also want to mention my sysadmin teammates who keeps BIOMATH server running successfully (at least so far☺) against the hostile attacks from bad people, hackers looking for fun. Dirk, Ingmar, Stefaan, Frederik, Gaspard the linuxman, Sammy, Petra, it was a great fun (at the same time lots of workload) and experience to work with you.

Of course, life in BIOMATH is not all about research but also some fun (luckily☺). Thank you all for arranging and or joining many colorful and cheerful activities: BIOMATH weekends, BIOMATcH mini-football team (don't worry, we can only get better☺), BIOMATH out of control parties, spring walks, movie nights and so many other things.

I am also very thankful and grateful for the friendship of Annick and also to my roommate and colleague Güçlü. Special thanks go to my friend and colleague Ruxandra for her kind support and help during the though period of writing this thesis. And to Mahir, whom I had the pleasure to befriend only the last year of my PhD but still it was great pleasure to have your fellowship (…of the ring…) in this sometimes very lonely town of Ghent.

Last but not least, thanks from the bottom of my heart to my beloved family (the *betsino*) your unconditional love and beautiful support – Gülcan, Gülhan, Hakan, Nekiye and Nasreddin, thank you so much. *"Anne, baba ve sevgili kardeslerim, kocaman sevgi ve desteklerinizi icin sizlere sonsuz tesekkur etmek istiyorum. Sizlerin destegi ve sevgisi bu doktora surecinde bana inanilmaz yardimci oldu, bunu kesinlikle bilmenizi isterim."*

I guess that is it guys, thank you all again.

May 2004, Ghent
Gürkan Sin

Contents

Chapter 1

Introduction and problem statement

1. INTRODUCTION

The research carried out in this thesis is situated in the wastewater treatment branch of environmental engineering/technology. The particular objective of this thesis is explicitly specified in the next section. However in this section, history of wastewater treatment shall be briefly reviewed. The major sources of water pollution, i.e. the process in which *clean* water is converted into *wastewater,* are mainly anthropogenic i.e. due to man-made activities. Sources of water pollution are numerous, but they are related to the following main anthropogenic activities: water demand/consumption by a community, logarithmic increase in population, industrialization, agriculture and technological development (Metcalf and Eddy, 1991; Gijzen and Mulder, 2001).

In the early stages of wastewater treatment development, the need for treating the polluted water was triggered in the latter half of 1800s in Europe by serious concerns for sanitation soon after bacteriologists (Koch and Pasteur) had discovered the link between water pollution and disease. This concern of sanitation led to the development of the activated sludge process for wastewater treatment by Ardern and Locket in 1914 in England. It was operated as a fill and draw batch reactor (the first type of sequencing batch reactors used widely today). Therefore, the early history of wastewater treatment was mainly concerned with sanitation issues, i.e. removal of pathogenic microorganisms from polluted water.

Parallel to remarkable advances made in the civilization, particularly brought up by the heavy industrialization period until the end of the 1960s, the major concerns of wastewater treatment were extended to prevent/control deterioration/degradation of drinking water quality which started to become heavily polluted. For instance, the Environmental Protection Agency (EPA) in the United States was established in 1970 in response to the growing concerns for degradation of environmental resources: water, air and soil. This was an inevitable result since industrial development at that time completely ignored the impact of the discharge of polluted water to receiving bodies. On top of that, anthropogenic production of fertilizers (particularly after the development of the Haber-Bosch process that made production of fertilizers

technologically/economically feasible) for use in agriculture was increasing exponentially. This was required particularly to meet the food/protein demand of the exponentially increasing population (Gijzen and Mulder, 2001). This massive production of an anthropogenic source of nitrogen eventually accumulated in the biosphere and contributed significantly to the nitrogen pollution load in previously clean water bodies (e.g. rivers, groundwater, lakes). This triggered the well-known eutrophication problem in surface water bodies (Gijzen and Mulder, 2001). This has imposed serious threats to available drinking water resources and has also led to deterioration in biodiversity (Gijzen and Mulder, 2001). Becoming aware of these serious threats directed at essential components of nature - air, water and soil, upon which life depends, effluent discharge legislation became more stringent to safeguard the natural environment, see e.g. the recent European Union Water Framework Directive and EPA regulations.

At this point it is important to note that although more than 2/3rd of earth is made up of water, only a tiny fraction of this water ca 0.05% is expected to bear water quality standards suitable for drinking (UNESCO, 2003). Although water is a renewable resource, the available resources are becoming rapidly polluted. In response to this, there has been growing concerns for water-deficit areas, e.g. those countries located in the Middle East, that water may trigger conflicts over trans-boundary sharing/issues which may even lead to war (Water 21, 2003). This increases the significance of the proper management of the available water resources, which is based on more and more integrated approaches i.e. coupled to sewer, wastewater treatment and receiving water bodies (Meirlaen, 2002).

According to the United Nations, 1.1 billion people do not have access to safe water while 2.4 billion people still lack access to improved sanitation (UNESCO, 2003). These statistics indicate that the wastewater treatment community has two agenda points to focus on simultaneously: the first one is to meet the basic needs of mankind, i.e. access to safe water and improved sanitation in under-developed/poor countries (the total number of people affected is huge, equal to almost half of the total population of man on earth). A second agenda point is to control the heavily polluted water resources (particularly in terms of nitrogen and phosphorous) thereby safeguarding natural ecosystems in developed countries. In short, this means there is a lot of work waiting ahead and to be carried out by wastewater engineers. Note that the research of this PhD is performed in Belgium -a developed nation, and as such it focuses on the second agenda point: wastewater treatment technology oriented at control of nutrient pollution.

The dominant technology employed for wastewater treatment is the activated sludge process. It has been applied in numerous configurations e.g. extended aeration, suspended continuous systems, plug-flow systems, batch systems etc. (Metcalf and Eddy, 1991). Since it was first

discovered, the activated sludge process has been subjected to continuous growth/development in view of process design and operation. The accumulated experience/information/know-how about activated sludge processes was summarised/transformed into a mathematical model called Activated Sludge Model No.1 (ASM1) by the IWA (formerly IAWQ) Task Group on Mathematical Modelling for Design and Operation of Biological Wastewater Treatment Processes (Henze *et al*., 1987). The particular aim of this work was to provide a unified/common platform for wastewater engineers to exchange ideas and use modelling for design and optimisation of complex activated sludge processes (Henze *et al*., 2000).

2. STATEMENT OF PROBLEM AND OBJECTIVE

The introduction of ASM1 has significantly stimulated the application of dynamic modelling to wastewater treatment plants (WWTPs). Its use mainly aimed at optimisation of the design and operation of WWTPs for cost reduction and improvement in effluent quality (Coen *et al*., 1997; Carucci *et al*., 1999a; van Veldhuizen *et al*., 1999; among many others). Dynamic modelling of wastewater treatment plants has also challenged the state-of-the-art design of WWTPs, which is typically based on rules of thumb, empirical and steady-state equations (see e.g. Metcalf and Eddy, 1991). Another important stimulus of ASM1 was the common terminology introduced for modelling activated sludge processes, which indeed proved to be useful for facilitating the transfer of knowledge between researchers, for instance, by using a compact matrix formulation for the mathematical models. The full-scale application of ASM1 for the dynamic modelling of WWTPs removing COD and N, has also resulted in the rapid development of ASM2 (and ASM2d) for modelling biological phosphorous removal (Henze *et al*., 1995a). Parallel to the continuous accumulation of experience with full-scale applications of ASM1, ASM3 was developed to deal with the observed storage phenomena in activated sludge processes (Gujer *et al*., 1999).

As mentioned above, activated sludge models (ASMs) are indeed a compact and elegant summary of the state-of-the-art understanding of activated sludge processes. Calibration of ASMs, an inherent part of any type of model application, is strictly required prior to the application of dynamic models for a WWTP. It consists of several steps, including lab-scale experiments for the characterisation of the influent wastewater and the determination of the kinetics / stoichiometry of the biological processes ongoing in the WWTP. To this aim, numerous experimental methodologies have been developed and applied to full-scale systems (Ekama *et al*., 1986; Henze *et al*., 1987; Sollfrank and Gujer, 1991; Kappeler and Gujer, 1992; Spanjers *et al*., 1998; Vanrolleghem *et al*., 1999; among many others). These experimental designs are usually (if not mostly) based on respirometric techniques and were developed particularly for calibration of ASM1. For a thorough review on this issue the reader is referred to Petersen *et al*. (2003a). In addition to these lab-scale experiments, dedicated

measurement campaigns consisting of intensive sampling and measurements of influent and effluent variables every 2 or 4 hours over a period of a few days to a week, are required to adequately catch the dynamics in a WWTP (see e.g. Petersen, 2000).

The next step in the calibration is to transfer the results collected from the lab-experiments into the ASM model parameters. In this step, the influent COD fractions i.e. the ratios of S_S/COD_{tot}, S_I/COD_{tot}, X_S/COD_{tot}, X_I/COD_{tot} and influent Nitrogen fractions S_{ND}/TKN, X_{ND}/TKN determined from influent wastewater characterisation experiments are used to construct a dynamic input file for the treatment plant model. This is typically performed as follows:

1. The influent COD & Nitrogen fractionation results are assumed constant for the particular wastewater under study
2. These influent COD fractions are then multiplied with the dynamic COD and TKN measurements obtained e.g. every 2-4 hrs from the intensive measurement campaign data. In this way, the dynamic influent S_S, S_I, X_S, X_I, X_{ND} and S_{ND} profiles are estimated which are prerequisite for dynamic modelling of WWTP using e.g. ASM1.

After the dynamic input data is constructed, it is used as an input to calibrate the kinetic/stoichiometric parameters of the model so as to obtain a good fit to the measured dynamics in the WWTP, e.g. to measured MLSS, measured NO_3-N in the aeration tank, in the effluent, in the return cycle etc. At this stage, the calibration is mostly performed manually. This means the modeller tries to manually change one parameter at a time until a good model fit to the measurements is obtained (visual observation) following a step-wise procedure in which one after the other parameter of the model is manually changed. The information obtained about the kinetic/stoichiometric parameters of the biological processes from the lab-scale experiments is also used in this step. This way of calibration is simply based on expert-knowledge and driven by ad-hoc approaches. In fact, calibration of a model without expert-knowledge was reported to be a very dangerous task, bound to lead to nonsense results (Andrews, 1991).

Another common observation that can be made about the numerous calibration studies published in literature is that each calibration study has its own procedure in choosing the type of lab-experiments for the influent characterisation and the kinetic/stoichiometric parameter estimation, parameter subsets to be calibrated, hydraulic characterisation and settling characterisation. This makes it too difficult to compare and for quality check among different calibration studies since there is no common basis. To address these concerns, recently systematic calibration protocols have been proposed after recognizing this wide range of degree of freedoms used during calibration studies (Petersen, 2000; Hulsbeek *et al*., 2002, Petersen *et al*., 2002b; Langergraber *et al*., 2003a; WERF, 2003). Although the objective of

these calibration protocols is to aid modellers in calibration studies, the main message is that a standard procedure for calibration of ASMs (particularly ASM1) should be used for quality check and comparison reasons.

An obvious alternative method for calibration consists of using well-known optimisation algorithms, e.g. Simplex (Dochain and Vanrolleghem, 2001) to change the parameters until the optimal fit is obtained. However, this is not that straightforward. The major issue that makes the calibration of ASM1 (and this is also true for other ASM family models) too difficult is that the model structure is too complex compared to the available measurements (in terms of quality and quantity of the available measurements) (Ayesa *et al.*, 1995; Weijers and Vanrolleghem, 1997; Brun *et al*., 2002; Petersen *et al*., 2003b). This results in poor identifiability of the model, which means it is not possible to assign unique values to the parameters of the model. This makes the application of automatic calibration procedures practically impossible. However, this doesn't mean development of automatic calibration procedures is not possible/feasible. Researches aiming to lay down the basis for automatic calibration have already been started. Weijers and Vanrolleghem (1997) developed a methodology based on the Fisher Information Matrix (FIM) for selecting the best identifiable parameter sets to be used in calibration of ASM1 under a given measurement data set. Moreover, quite recently Brun *et al*. (2002) proposed and applied a methodology for selecting best identifiable parameter sub-sets for calibration of ASM2d mainly using output sensitivity functions of model parameters. Petersen *et al.* (2003b), on the other hand, intensively studied to improve identifiability of model parameters using combined respirometric and titrimetric measurement from lab experiments based on Optimal Experimental Design (OED) principles (Dochain and Vanrolleghem, 2001).

In this thesis the attention was mainly focused at the continuous development and application of systematic calibration protocols for activated sludge models for nitrogen removal. In the long-term, it was aimed to contribute to the development of automatic calibration protocols by developing robust sensors and experimental set-ups that will increase the quality of the available measurements to be used in calibration, in particular for the processes occurring under anoxic (denitrifying) conditions. Therefore, the research is carried out focusing in parallel on the following aspects of systematic calibration of ASMs:

1. **Development of lab-scale experimental methodologies particularly for the anoxic environment:** It was shown that the experimental designs developed for calibration of ASM1 are mainly based on respirometric measurements, which is valid only under aerobic conditions (Petersen *et al*., 2003a). In contrast to respirometry, which provides oxygen uptake rate measurements of biomass (Spanjers *et al*., 1998), there is a lack of a robust/simple device to quantify the stoichiometric and kinetics parameters of

activated sludge activity under anoxic conditions. Titrimetric measurements have been shown to allow unique parameter estimation from aerobic lab-experiments (Gernaey *et al*., 2002b). Since titrimetry also has a potential under anoxic conditions, a titrimetric set-up was studied and a reliable methodology to measure the nitrate uptake rate (NUR) of biomass, i.e. an anoxic respirometer, was developed.

2. **Development of model-based methods for interpretation of lab-scale experiments:**

   The experimental data resulting from the measurement of both aerobic and anoxic activities of activated sludge is interpreted using a model-based approach. This is needed to obtain mechanistically meaningful, unique parameter estimates allowing their transfer to the overall activated sludge model. In this regard the following issues are studied and discussed in detail:

   a. *Extensions to the titrimetric model of Gernaey et al. (2002a)*: The titrimetric model developed recently by Gernaey *et al*. (2002a) was shown to improve the identifiability of the ASM1 model. However, the applicability of the titrimetric model was limited to experimental data collected under strict conditions. To circumvent this problem, the Gernaey model is studied in detail and extended to describe titrimetric data collected under a wide range of experimental conditions.

   b. *Simultaneous storage and growth activities of activated sludge*: Estimation of yield coefficients from respirometric batch experiments leads to parameter values that are often higher than the default values. This is not surprising since it was recently shown by numerous studies both at lab-scale and full-scale experiments (van Loosdrecht *et al*., 1997; Beun *et al*., 2000a&b, Beccari *et al*., 2002; Dircks *et al*., 2001; Carucci *et al*., 2001; among many others) that the storage process has a significant role in overall substrate conversion processes occurring in WWTP. To this aim, experimental data collected under both aerobic and anoxic conditions are studied in detail using both ASM1 and ASM3e (an extended version of ASM3 see Chapter 4.2.2 and Chapter 4.3) models. A parameter estimation procedure for each model is developed in view of full-scale model applications.

   c. *The fast transient phenomenon observed in oxygen uptake rate (OUR) data*: OUR measurements resulting from respirometric batch experiments often display a fast transient in minute scale (see e.g. Gernaey *et al*., 2002b), which is usually ignored (Vanrolleghem *et al*., 1995). This transient in OUR is not predicted by ASM1 (which is the industry standard model). This fast transient is studied in detail within the frame of high quality and efficient calibration of activated sludge models and a hypothesis to explain the underlying mechanism

is proposed.

3. **Application of a systematic calibration protocol:**
   The systematic calibration protocol of Petersen *et al.* (2002b) is studied in detail and extended to generalize the protocol for various applications. This so-called BIOMATH calibration protocol is evaluated both at a full-scale continuous (carrousel type) activated sludge system and at a pilot-scale (80L) sequencing batch reactor (SBR) system. The latter was chosen to test the ability of the calibration protocol to work adequately under a completely different process configuration than in the continuous systems it was originally developed for. Particular emphasis is given to the life-cycle of a calibrated model in full-scale activated sludge system. It is ultimately aimed to gain insight into the following question: "How long and to what extent does a calibrated model remain valid in view of adequately representing dynamic behaviour of a WWTP?" This is a quite significant aspect of the modelling work in view of ensuring reliability/confidence in full-scale applications of calibrated models.

4. **Development and application of systematic optimisation protocol:**
   Much efforts have been invested to calibrate models. It is therefore of utmost importance that the calibrated models can be used efficiently to gain as much benefit as possible from the modelling. In this respect, a systematic protocol for model-based optimisation of process operation is developed and evaluated at a pilot-scale SBR. The objectives of an optimisation study can be numerous depending on the objective of the study itself, e.g. reduction of operational cost, improvement of effluent quality, improving the stability of operation etc. However, the main issue is that the optimisation study itself should also be systematized to ensure optimal application of the calibrated model, since in many studies one observes that is limited to the mere comparison of only a few scenarios.

3. OUTLINE

The research results presented in this thesis can be structured into four main parts corresponding with the objective of the thesis. In the first part, the development of sensors (particularly anoxic sensors) for high-quality data collection is presented. In the second part, the collected data is interpreted using model-based approaches. In the third part, the results obtained from the application of the BIOMATH calibration protocol to a pilot-scale SBR and a full-scale carrousel type WWTP are presented. In the fourth part, the application of a systematic protocol to the optimisation of SBR operation is presented.

Chapter 2 presents the BIOMATH protocol for calibration of activated sludge models. This protocol is based on the previous calibration protocol proposed by Petersen *et al.*

(2002b) and aims at giving thorough guidelines for performing a calibration study. Special attention is given to making the guidelines general rather than specific to a system since it is known that most WWTP have very different characteristics. *A main part of this chapter was presented as keynote lecture in WEFTEC 2003 conference, Los Angeles, California, USA, 11-15 October, 2003 (Vanrolleghem et al., 2003).*

PART 1: Development of lab-scale sensors/experimental methodologies

Chapter 3.1 introduces the integrated sensor developed for the overall monitoring of aerobic and anoxic activated sludge activities occurring in biological nutrient removal plants (BNR). The anoxic sensor in this study was based on an ion-selective nitrate electrode. *This chapter was published in Water Science and Technology (Sin et al., 2003).*

In Chapter 3.2 the methodology for the monitoring of anoxic activated sludge activity is improved by using a nitrate biosensor. This methodology was compared with the methodology based on an ion-selective nitrate electrode as presented in Chapter 3.1. Advantages and disadvantages of both methods are discussed. It is important to note that the anoxic methodology developed in this chapter is the first candidate anoxic respirometer ever developed to provide reliable, on-line, high-frequency (every 3 seconds) nitrate uptake measurements (NUR) of biomass with performance that is at least as good as a typical aerobic respirometer. *This chapter was presented as oral presentation in AutMoNet 2004 conference, Vienna, Austria, 19-20 April 2004 (Sin and Vanrolleghem, 2004).*

PART 2: Development of model-based methods for interpretation of lab-scale experiments

Chapter 4.1 describes the extension of the titrimetric model of Gernaey *et al.* (2002a) with a dynamic CO_2 model to interpret the titrimetric data resulting from aerobic batch experiments with pulse addition of carbon source. Particular emphasis is given to develop a method to calibrate the dynamic CO_2 module of the extended Gernaey model using titrimetric measurements alone. *This chapter is in preparation for publication.*

Chapter 4.2.1 compares the ASM1 and the ASM3 models using oxygen uptake rate (OUR) data obtained from full-scale WWTPs from Belgium and Spain. The major objective of this chapter is to reveal the limitations of both models in view of an accurate description of the OUR data obtained from typical calibration experiments. To this aim, the mechanistic meaning of parameter estimates and the practical identifiability of ASM3 are discussed and compared to ASM1. This chapter was accepted as platform/oral presentation in the *IWA 4th World Water Congress,19-24 September 2004, Marrakech, Morocco.*

Chapter 4.2.2 describes the development of a simultaneous storage and growth model by extending ASM3 to adequately describe OUR data obtained from batch experiments designed specifically for calibration of ASM1. A calibration methodology using OUR measurements alone is developed and applied for calibration of the extended ASM3 model. The model is validated using independent PHB measurements too. *This chapter is in preparation for publication to Biotechnology and Bioengineering.*

Chapter 4.3 compares ASM1 with the simultaneous storage and growth model developed in Chapter 4.2.2 and adopted to anoxic conditions in view of adequately and mechanistically describing the NUR obtained using the anoxic respirometer developed in Chapter 3.2. A calibration methodology using only NUR for both ASM1 and ASM3e models is developed in view of full-scale application. Moreover, titrimetric data are used to evaluate their impact on the identifiability of parameters. Finally, the significance of the initial substrate to biomass ratio, S_0/X_0, in anoxic batch experiments is discussed in view of its effect on the variability of parameter estimates. *This chapter is in preparation for publication in Biotechnology and Bioengineering.*

Chapter 4.4 describes and explains the fast transient observed in OUR data obtained from batch experiments designed for calibration purposes. Several hypotheses are considered for explanation of this observed transient in OUR. An empirical model is shown to predict and therefore account for the observed transient in the OUR data during parameter estimation. The effect of ignoring this transient on parameter estimates is also discussed. *This chapter was published in Biotechnology and Bioengineering (Vanrolleghem et al., 2004).*

PART 3: Application of systematic calibration protocol

Chapter 5.1 describes the application of the systematic BIOMATH protocol for calibration of an ASM2d type model for predicting nutrient removal in a pilot-scale SBR. A step-wise procedure is developed and applied to manually fine-tune the model parameters until a good fit to the measurements is obtained. *This chapter was accepted for poster presentation in the 3rd IWA conference on SBRs (SBR3), 22-26 February 2004, Noosa, Australia (Insel et al., 2004).*

Chapter 5.2 presents another application of the BIOMATH calibration protocol, this time to a full-scale carrousel type WWTP. The main objective of this chapter is to gain insight into the life-cycle of a calibrated model. In other words, it is attempted to answer “to what extent and how long a calibrated model remains valid in terms of adequately representing the dynamics of a WWTP?” In this chapter, the BIOMATH protocol is extended with a detailed procedure for model validation. *This chapter is in preparation for publication.*

PART 4: Development and application of systematic optimisation protocol

Chapter 6 describes the development and application of a systematic optimisation protocol to improve the effluent quality of a nutrient removing pilot-scale SBR. The model calibrated in Chapter 5.1 is used in this chapter. The systematic optimisation protocol is based on running a grid of scenarios using a previously determined set of operational parameters of the system. For the selection of the best operating scenario, a robustness index is also incorporated in the overall performance evaluation to address the desired stability of an operating model. *A main part of this chapter was presented in the 3rd IWA conference on SBRs (SBR3), 22-26 February 2004, Noosa, Australia and accepted for publication in a special issue of Water Science and Technology (Sin et al., 2004).*

Finally, Chapter 7 presents general discussions and also underlines/draws main conclusions of the research carried out in this thesis.

Chapter 2

BIOMATH Activated Sludge Model Calibration Protocol

ABSTRACT

Since the introduction of ASM1 in 1987 (Henze *et al*., 1987), numerous studies have been reported dealing with calibration of activated sludge models (particularly ASM1). A recent thorough review on calibration of activated sludge models (particularly ASM1) by Petersen *et al*. (2003a) has documented that there are a large number of experimental methodologies proposed and applied for the calibration. The choice of calibration approach and experimental procedures followed by practitioners during calibration depends heavily on the case under study i.e. *ad hoc* approaches are typically followed. This clearly indicates there is no unified approach towards calibration of activated sludge models worldwide. Moreover, there is a lack of systematic protocols to aid practitioners during a calibration study. In this section, a systematic methodology for calibration of the activated sludge plant models is proposed on the basis of consolidated engineering and scientific experience. It is called the BIOMATH protocol. The proposed protocol for the modelling of the treatment plant is refined on the basis of a previous protocol developed by Petersen *et al*. (2002b). In the BIOMATH protocol, the definition of the target(s) of the model usage plays a crucial role in the selection of the steps to be followed during calibration. For the activated sludge modellers this protocol tries to combine and link state of the art methodologies for calibration of different processes in a wastewater treatment plant (hydraulics, biological reactions, sedimentation processes, etc.), and it can thus be used as a complete guideline for extensive model calibration tasks.

Part of this chapter was published as:

Vanrolleghem P.A., Insel G., Petersen B., Sin G., De Pauw D., Nopens I., Weijers S. and Gernaey K. (2003) A comprehensive model calibration procedure for activated sludge models. In Proceedings: *76th Annual Technical Exhibition & Conference. WEFTEC 2003*. October 11 - 15, 2003, Los Angeles, California U.S.A. (on CD-ROM).

1. INTRODUCTION

Robust model-based optimisation of wastewater treatment plants necessitates successful calibration of complex wastewater treatment plant models. The word ‘successful’ relates to the prediction capability of activated sludge models under variable process conditions, where the model should describe the plant behaviour within realistic margins taking into account the uncertainties on the inputs and reactions taking place in the system.

In recent years, the complexity of the models has increased considerably with the discovery of new processes (Henze *et al.*, 2000; Barker and Dold, 1997), and as a result the modelling task became more time consuming with *ad hoc* calibration of the model parameters. In this context, a compromise should be found between the difficulties in parameter estimation with large models and the characterization of important processes taking place in the reactors. The model selection task is based on the target of the model use. Cost reduction and the search for operating conditions that allow achievement of appropriate effluent quality criteria (Nitrogen, Phosphate) are the most common targets to be achieved with the model studies. After the model selection task, the most important issue is using this model to characterize the overall activated sludge plant behaviour including the biological and physico-chemical phenomena (e.g. settling), the so-called model ‘calibration’. After a successful validation of the model, it can serve for its purpose.

In this study, a comprehensive model calibration procedure for the activated sludge model is proposed which accounts for the physical and biological processes occurring in a typical municipal wastewater treatment plant (WWTP). The methodology works for different activated sludge models, depending on the targets and the available engineering knowledge.

2. THE BIOMATH CALIBRATION PROTOCOL

The BIOMATH protocol for the calibration of activated sludge models is composed of four main stages and 12 modules (see Figure 1). The first stage is the definition of the target(s) of the modelling exercise followed by decision making on the necessary information to be obtained from the activated sludge (AS) plant such that the target of the modelling study can be reached. Some of the modules (1-11) can be skipped depending on the general evaluation whether the targets are reached. The second stage is the collection of detailed information on the activated sludge plant. The mass transfer (hydraulic and oxygen transfer), biological, settling and the influent characterizations are included in this step. In addition, the experimental or lab-scale work is incorporated with usage of the Optimal Experimental Design (OED) methodology to minimize the necessary experimental efforts and maximise the data quality. By averaging the influent and operational characteristics, steady state modelling is performed for the mass transfer, settler and the biological model (e.g. ASMs). The third step includes the complete calibration of the activated sludge model using the dynamic

influent data, and incorporating the parameter values obtained from lab scale experiments or full-scale data. During the last stage, decisions are made upon eventual re-iteration of a number of the modules.

The proposed protocol for the modelling of the treatment plant is refined on the basis of a previous protocol developed by Petersen *et al*. (2002b). The details of the modules underlying each step are shown in Figure 1, and are discussed below.

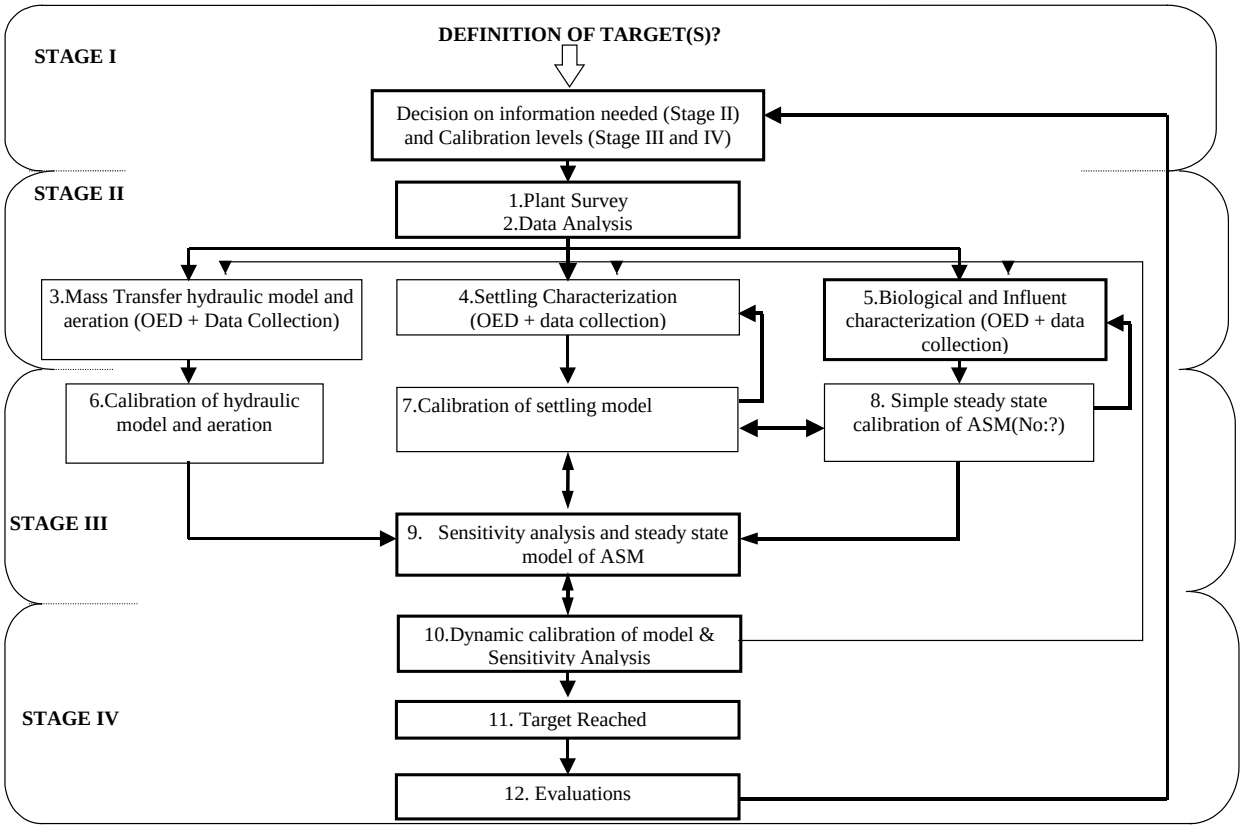

Figure 1. BIOMATH model calibration protocol

STAGE I. Definition of Target(s)

In the first step, the main objectives have to be defined for the modelling of continuous systems, sequencing batch reactors (SBR), alternating activated sludge plants etc. The decision is usually based on the time and/or budget necessary/available for the modelling task. Some of the stages can be omitted depending upon the objectives (see Figure 1). The main objectives for a modelling case can be:

- Optimisation and upgrading of an existing activated sludge plant
- Meeting the effluent criteria
- Cost reduction in plant operation
- Reuse of effluent wastewater

- Development of control strategies
- Design of the treatment plant.

Objective oriented BIOMATH protocol

This first step of the protocol is very important since the BIOMATH protocol is a general protocol and contains different options/choices to be made at different levels of the calibration (see below, e.g. simple or complex hydraulic models, settler models, detailed biological characterisation etc.). Depending on the objective of the study, the modeller may choose accordingly an appropriate option (simple or complex) and as such dynamically determine the calibration procedure that fits best the objective of the case under study. Similarly, the modeller may also skip some steps of the BIOMATH protocol, which may not be relevant for the objective of the calibration. E.g., if the aim is to obtain a calibrated model from only historical data, then there is no need to go through detailed biological characterisation steps etc.

STAGE II. Plant Survey/Data Analysis and process characterisation

1 & 2. Plant Survey and Data Analysis

A general description of the treatment plant to be used in the model calibration can be compiled from the operation database/log files of the activated sludge treatment plant itself, the design documents and/or personal communication with the plant operators.

The ***design data*** consist of the general plant layout and configuration, compartments/process units, volumes/areas/depths, water and sludge lines, installed capacities, pumps, aerators, P&I diagrams, hydraulic layout. On the other hand, the ***operational data*** concern the flow rates for influent, sludge recycles, sludge wastage and internal recirculation; sludge/wastewater distributions over parallel lines, step feed *etc.*; location, type and implementation of control strategies. The most important issue is the (available) ***measured data*** comprising the conventional characterization of influent & effluent (e.g. COD, TKN, PO_4, TP, NO_3, NH_4, TSS, pH, T (^{0}C)); on-line measurements from the treatment plant (dissolved oxygen, NO_3, SVI, ML(V)SS, PO_4, NH_4 , pH, T (^{0}C)); sludge blanket height in the clarifier, TSS concentration in the return sludge and effluent, P and N content of sludge, sludge age and daily sludge production, VSS/SS ratio of the sludge.

The information collected in this step is of great importance for the understanding of the capacity and the behaviour of the system. Therefore, the design, the operational data and the measured data should be evaluated and processed for understanding of the entire process. For data quality assessment, outlier detection is applied and interpolation of data can be done whenever it is appropriate and possible. Mass balances regarding the flow rate and the sludge

(considering the N and P content) are crucial for model calibration, particularly for the accurate estimation of the system sludge age (Barker and Dold, 1995; Nowak *et al.*, 1999). From a modelling point of view, it should be noted that the sludge age is the most influential parameter with respect to all model outputs.

For data quality assessment, outlier detection can be performed using several mass balances (particularly using inert components of the system). For instance, the mass balances for the flow rates and the solids are of great importance for the calibration. In case mass balances are not closed within an acceptable error, e.g. 5%, the corresponding data need to be re-checked or measured more precisely again. Detailed procedures for data quality analysis and data reconciliation techniques are already presented elsewhere e.g. among others in Meijer et al., 2002, WERF (2003).

Necessary information and relevant calculations for the assessment of the data quality are listed below:

- Sludge age calculation
- Mass balances (e.g. SS, P, COD, N, flow)
- Influent – Effluent concentrations
- Other perturbations (e.g. from other industrial discharges)
- Addition of chemicals (e.g. for settling improvement, carbon dosage, effluent quality amendment)
- Weather changes (e.g. Storm events)
- Energy Consumption or generation
- Daily/Monthly operational and maintenance costs.

In addition, some other factors that exert a critical influence on the system performance such as pH, temperature changes, industrial discharges, addition of auxiliary chemicals, energy consumption and generation of daily and monthly operational and maintenance costs etc., should be evaluated in this step.

3. Mass transfer characterization

In the mass transfer characterization, two main aspects have to be considered. The first one is the determination of the oxygen mass transfer coefficient (K_La) in all reactors (eg. surface aerators, brush-type or compressed air). The second aspect is the hydraulic characterization of the treatment plant. First, the influences of operational and biological factors on the oxygen transfer have to be considered. The volumetric mass transfer coefficient, K_La, should be estimated. Several methods are available in the literature for the determination of K_La and most practical methods are explained in sub-section 3.1. The K_La value for wastewater can be calculated from the formula given below if the K_La is given for clean water (see Eq. 1).

Typical values of α for diffused air and mechanical aeration equipment are in the range of 0.4 to 0.8 and 0.6 to 1.2, respectively (Metcalf and Eddy, 1991).

$$\alpha = \frac{K_L a_{wastewater}}{K_L a_{tapwater}} \quad (1)$$

In addition, the aeration efficiency is important for the appropriate selection of the aerators. Typical ranges for oxygen transfer efficiencies for various types of mechanical aerators are listed in Table 1. For fine-bubble aeration the K_La values are in the range of approx. 2 to 8 h^{-1} for an air flow rate per m^3 of basin ranging between 0.5 and 2.5 $m^3/h/m^3$ (Gillot, 2002).

Table 1. Typical ranges of oxygen transfer efficiencies for various types of mechanical aerators (Metcalf and Eddy, 1991).

Aerator type	*Oxygen transfer efficiency* KgO_2/kwh	
	Clean Water	*Field*
Surface low speed	1.21-3.04	0.72-1.46
Surface high speed	1.21-2.79	0.72-1.21
Surface downdraft turbine	1.21-2.42	0.61-1.21
Submerged impeller	1.21-2.42	0.72-1.09
Surface brush and blade	0.91-2.79	0.49-1.09

3.1 K_La determination

In a well-mixed region of a biological reactor the mass balance for oxygen under continuous operation can be written as:

$$V\frac{dS_O}{dt} = Q(S_{O,in} - S_O) + K_L a(S_{O,sat} - S_O).V + r_O V \quad (2)$$

The first term on the right hand side can be neglected, because it is comparably smaller than the other terms. Then, the equation is simplified into:

$$\left.\frac{dS_O}{dt}\right|_{ON} = K_L a(S_{O,sat} - S_O) + r_O \quad (3)$$

If the aeration is turned off, the equation (3) yields:

$$\left.\frac{dS_O}{dt}\right|_{OFF} = r_O \quad (4)$$

The K_La value can be calculated by using the equations 3 and 4 with the assumption that the oxygen utilization rate, r_O is constant during the experiments.

$$K_L a = \frac{\left.\frac{dS_O}{dt}\right|_{ON} - \left.\frac{dS_O}{dt}\right|_{OFF}}{S_{O2,sat} - S_{O2}} \quad (5)$$

In literature, several methods have been suggested for the determination of K_La under process conditions (Boyle and Campbell, 1984; Capela *et al.*, 1999; Gillot *et al.*, 1997; Mueller and Boyle, 1988). For details, the reader should consult the references indicated above. In case there is no dedicated experiment performed for the determination of K_La, then regular on-line oxygen measurements, which are available for the compartments of the activated sludge plant, can be used. In this way, the K_La values can be calibrated to fit those data during full-scale model calibration.

3.2 Hydraulic Characterization

Characterisation of the hydraulics of a treatment plant is essential for a reliable calibration. The reactor configuration and the modelling objectives will have an influence on the degree of accuracy imposed on the hydraulic characterization. Moreover, complex hydraulics may affect the sample location for a representative measurement (the measurable model component which has to be measured for the calibration). If it is difficult to understand the approximate hydraulics of the plant from the plant layout, a detailed hydraulic characterization is essential.

A “tracer test” can be performed in order to obtain rudimentary information about the hydraulic behaviour. Typically it allows determining the number of tanks-in-series. Dispersion models (or terms) can also be incorporated in the models in case it is necessary (Makinia and Wells, 2000; Stamou, 1997). The experiment may also provide more information about the dead volumes, short-circuiting and/or internal recycles in the reactors. If a detailed hydraulic characterisation is not required, possible assumptions can be made on the number of tanks-in-series based on the configuration of the compartments and the reactor dimensions (refer to Figure 2).

The amount of tracer (e.g. LiCl), the feeding pattern of the tracer (such as a square feed) and sampling period and frequency should be considered regarding the treatment plant configuration(s), recycles and the volumes of the tanks. In addition, the injection points together with the sampling points have to be decided if there is an unbalanced flow through the parallel lanes or in the flow distribution boxes. Moreover, the transient hydraulic

behaviour of the treatment system due to flow changes, on/off controls of pumps and flow smoothing of tanks are important factors with respect to the hydraulics (De Clercq *et al.*, 1999).

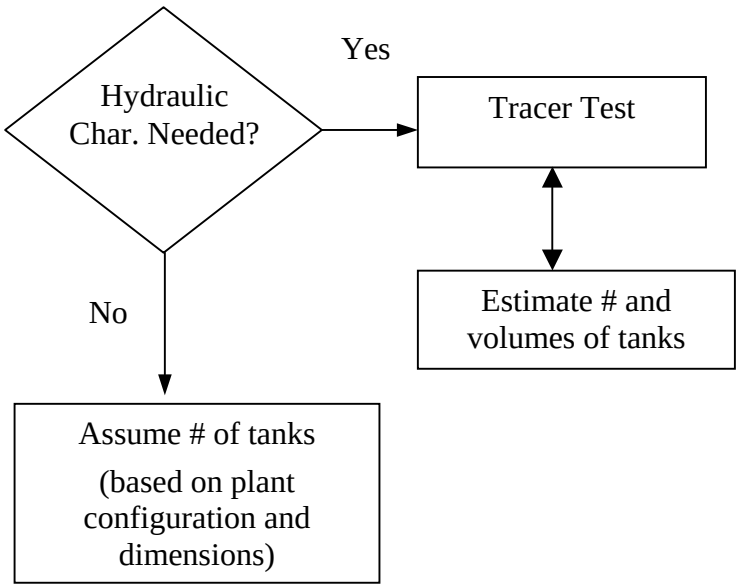

Figure 2. Hydraulic Characterization

In the hydraulic characterization of a treatment plant, the number of (perfectly mixed) tanks in series that correspond to the actual reactors (activated sludge unit, biofilter etc.) is determined. The tracer test is performed using an inert compound e.g. LiCl. A known amount of LiCl is injected into the inlet structure of the reactor. The concentration of LiCl (C(t)) as function of time is then measured at the outlet of the system under study. For the analysis, the volume (V) of the reactor and the volumetric flow-rate (Q) through the reactor has to be known. From these values the ideal hydraulic retention time (τ) can be calculated:

$$\tau = V/Q \tag{6}$$

Then one can calculate the dimensionless time t':

$$t' = t / \tau \tag{7}$$

From the measured concentration C(t) the hydraulic residence time distribution (E(t)) can be calculated:

$$E(t) = \frac{C(t)}{\int_0^\infty C(t)dt} \tag{8}$$

The dimensionless hydraulic residence time distribution (E(t')) is then equal to:

$$E(t') = \tau * E(t) \quad (9)$$

This dimensionless hydraulic residence time distribution is also equal to:

$$E(t') = \frac{n^n}{(n-1)!} t'^{n-1} e^{-nt'} \quad (10)$$

From the equation (10), the number of tanks-in-series, n, can be determined. In practice, one compares the calculated E(t')-curve calculated from the tracer test data with pre-calculated E curves as given in Figure 2. The best fit of the curve gives the number of tanks-in-series.

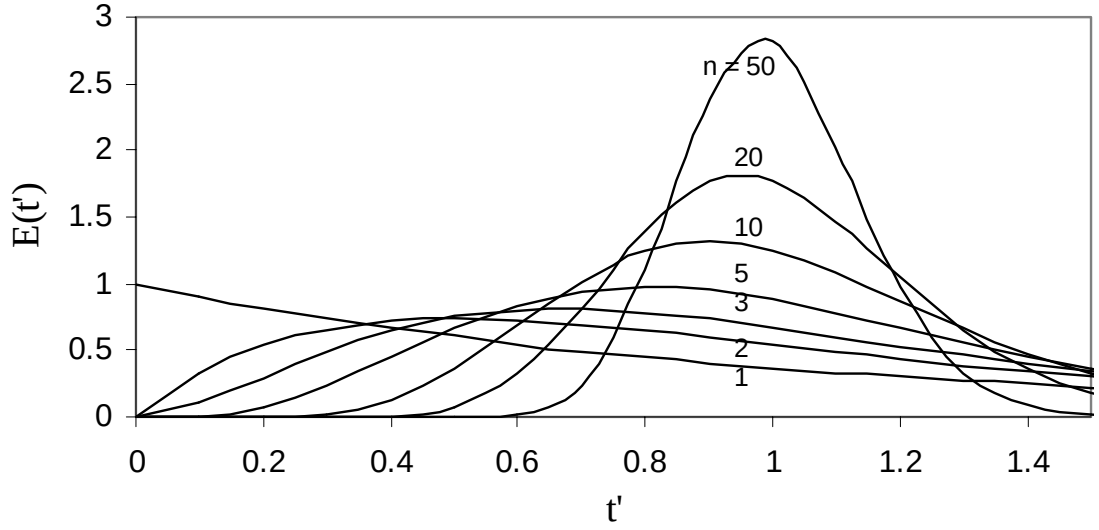

Figure 3. Pre-calculated E curves for n tanks in series

For rectangular tanks, the number of reactors, n, can also be calculated using the empirical formula given below (Chambers, 1992):

$$n = 7.4\ (B.H)^{-1}.L.Q\ (1+R) \quad (11)$$

where; n = number of reactors (-)
B = reactor width (m)
H = reactor depth (m)
R = Recirculation rate (-)
L = Reactor Length (m)
Q = average inflow-rate (m^3/sec)

This empirical formula is valid depending on the range of the variables given in the formula:
28 m< L <500 m
2 m < B <20 m
2.4 m < H <6 m
0.7 < R< 1.5
1.3 h < τ < 3 h

Here, the hydraulic retention time, τ time can be calculated by:
τ(h) = reactor volume* (3600.Q.(1+R)) (12)

4. Settling Characterization

A detailed settling characterization is necessary if the settling performance and the reactions during the settling influence the overall system behaviour (e.g. effluent COD, N). In addition, the target(s) might be the optimisation of settling or may be to solve effluent suspended solids problems. From a modelling point of view, the investigation could be focused on either settling in the primary or final clarifier, depending upon the objectives. If a detailed settling characterization is necessary, settling experiments and/or other relevant measurements such as SVI have to be carried out before selecting the settling model. In addition, reactions in the settler like denitrification and phosphorus release in have to be considered. This can be checked by calculating the mass balance of nitrate/phosphate around the settling tank or site observation such as nitrogen gas bubbles entrapped in the flocs. If the solid separation in the settler is working well, no detailed settling characterization is necessary. So, a point settler model can suffice to describe the separation of the suspended solids from the main stream. If much sludge is maintained in the (real) settler, a virtual reactor can be included in the model. The residence time in the settler can then be modelled by placing a tank with a volume equal to the volume of the settler in series with the settler.

As mentioned above, if a specific analysis of the plant is required and the settler affects plant performance, a more detailed model for the settler should be used. This can be done via one-, two- or three-dimensional settling models. Of course, the complexity of the model should meet the requirements. For operation and control of a WWTP a one-dimensional model is advised. The most commonly used one-dimensional model is the settling model of Takács *et al.* (1991), but alternatives (both simpler and more complex) exist (Ekama *et al*., 1997).

Selection of the appropriate model is based on the measurement of concentration profiles or sludge-blanket-height time profiles. The model which best fits the measured concentration profiles or the sludge blanket heights, should be selected. Reaction submodels should be included in the settler model if they affect the effluent quality. The smoothing effect of the secondary clarifier on the effluent quality with respect to COD, total nitrogen and phosphorus

etc. should also be accounted for. This can be done in the calibration step by introducing the smoothing effect of the secondary clarifier into the simulator. The flow diagram for the settling characterization is given in Figure 4.

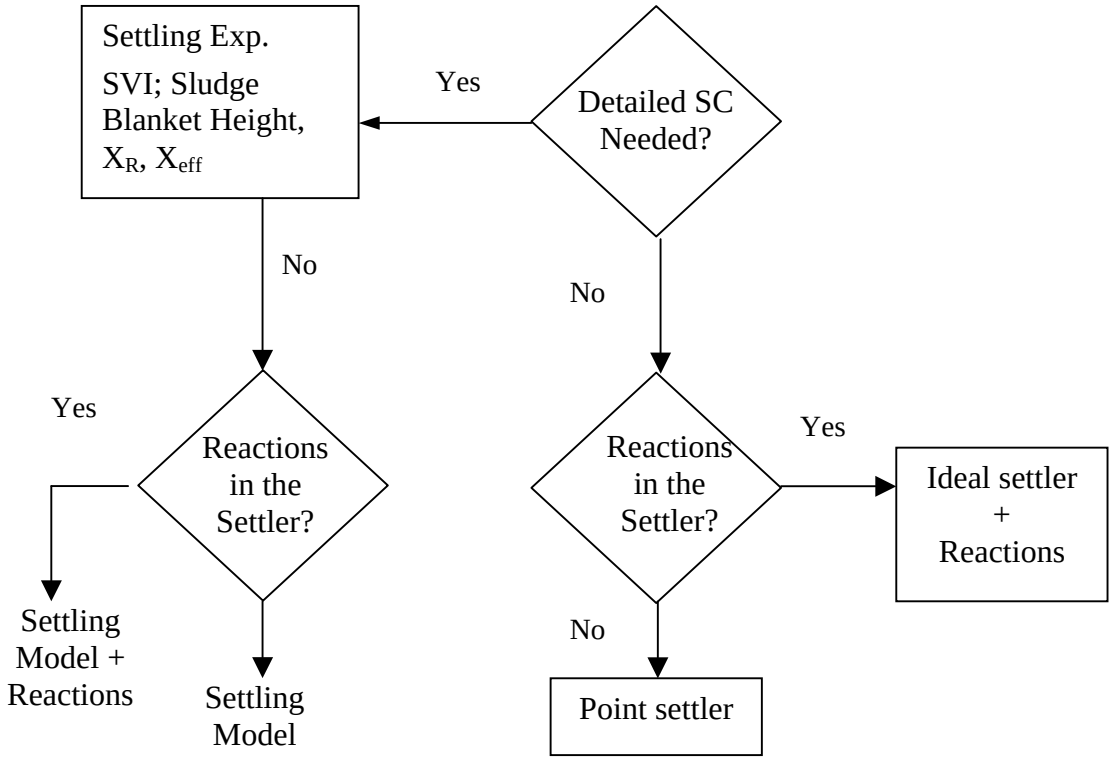

Figure 4. Settling Characterization

The primary clarifiers located upstream of the biological reactors also have a vital role since there might be activation and/or interactions between physico-chemical and biological reactions. For instance, in addition to biological reactions, the COD removal is also occurring via physico-chemical reactions such as flocculation and hydrolysis of particulate COD fractions into soluble ones. A large amount of COD is removed by plain settling. In primary settlers, the settleable COD fraction is removed at higher settling velocities than the velocities obtained in final clarifiers. The unsettled wastewater contains biomass, which leads to biological processes such as fermentation, acidification and ammonification due to heterotrophic activity (Gernaey *et al.*, 2001b; Orhon *et al.*, 2002). The settling and biological reactions should be incorporated in the model if the effect of the primary clarifier on the overall process performance is evident. The effect of a primary clarifier can be evaluated by performing some relevant experimental analysis including filtered/unfiltered COD, NH_4-N and VFA analysis etc. in the influent and the effluent streams of a primary clarifier.

5. Model-Based Characterization of the Biological Processes

Activated Sludge Models (ASM1, ASM2-ASM2d, ASM3) proposed by the IWA (formerly

IAWPRC, then IAWQ) task group on Mathematical Modelling for Design and Operation of Biological Wastewater Treatment (Henze *et al*., 2000) are the most commonly applied mathematical models for the modeling of the biological compartments of wastewater treatment plants. The ASM family of models has been applied successfully to full-scale treatment plants and has been shown to be a good compromise between the complexity of the activated sludge processes and the quality of prediction of the plant behaviour under dynamic conditions. Therefore, in the proposed Biomath protocol the calibration methodology is focused on the ASM models.

5.1 Model Selection

The selection of models describing the biological activity is dependent on: (a) the biological processes/activity (e.g. COD removal, N removal or P removal) occurring in the treatment plant and (b) the purpose of the model application. Model selection should be based on the targets of the modeling in order to optimise the calibration efforts. The following models, which have been applied successfully for municipal wastewater treatment plant modeling, are suggested:

- Choose ASM1 for COD and N removing biological wastewater treatment plants:
- Choose ASM2 for COD, N and P removing biological wastewater treatment plants
- Choose ASM2d if in addition to item 2, denitrifying phosphorous activity is observed in the biological wastewater treatment plant.
- Choose ASM3 if in addition to item 1, considerable storage phenomena are observed in the pant.

Based on the purpose of the model, modifications or extensions of the proposed models should be considered. For example, if build-up of nitrite (e.g. in denitrification) is observed in the treatment plant and if the target is set to diagnose the problem and therefore prevent nitrite build-up then the ASM models should be modified to include 2- step nitrification and 2-step denitrification processes. For an example of this type of extension of the ASM1 model, the reader can refer to Sin *et al*. (2001). With such model, the rather complex intermediate steps of the nitrification and denitrification processes can be studied in detail to understand the cause of the problem and suggest a solution. Although in the proposed BIOMATH protocol focus is given to the calibration of the ASMs, with appropriate modifications the proposed protocol can aid the calibration of other ASM type mathematical models.

5.1.1 Selection of parameters for calibration

The determination of all model parameters is an expensive and time-consuming process. Therefore, whenever possible it is suggested that the default values reported in previous applications should be assigned to the model parameters (Henze *et al.*, 2000). In this context, a sensitivity analysis allows, based on the target of the modelling exercise, to discriminate

between the relatively less sensitive and the most sensitive parameters (De Pauw *et al.*, 2003; Weijers and Vanrolleghem, 1997; Brun *et al.*, 2002). The sensitivity of a parameter can be determined by increasing and/or decreasing its value and by observing the resulting changes in the simulation output. Another approach for the selection of the parameter subset for the calibration is to apply the collinearity index (Brun *et al.*, 2002; Reichert and Vanrolleghem, 2001). The information of the sensitivity analysis should be used in the calibration protocol and is expected to minimize the calibration efforts and therefore optimise the overall calibration procedure towards the objectives of the modelling. For instance, the most important (sensitive) parameters for the prediction of MLSS in the system are mainly the particulate inert materials concentration (or COD) in the influent (X_I), the heterotrophic biomass yield coefficient (Y_H), the heterotrophic biomass decay coefficient, (b_H) and the sludge retention time (Nowak *et al.*, 1999).

5.1.2 Optimal Experimental Design (OED)

Calibration of a mathematical model asks for at least the determination of a couple of parameters that can be selected among all model parameters by analysing the sensitivity functions. In the context of calibration of the Activated Sludge Models, several lab-scale experiments and full-scale measurement campaigns are usually needed (Henze *et al.*, 1987; Carucci *et al.*, 1999; Coen *et al.*, 1997; Petersen *et al.*, 2002b, 2003a) which are expensive and time consuming.

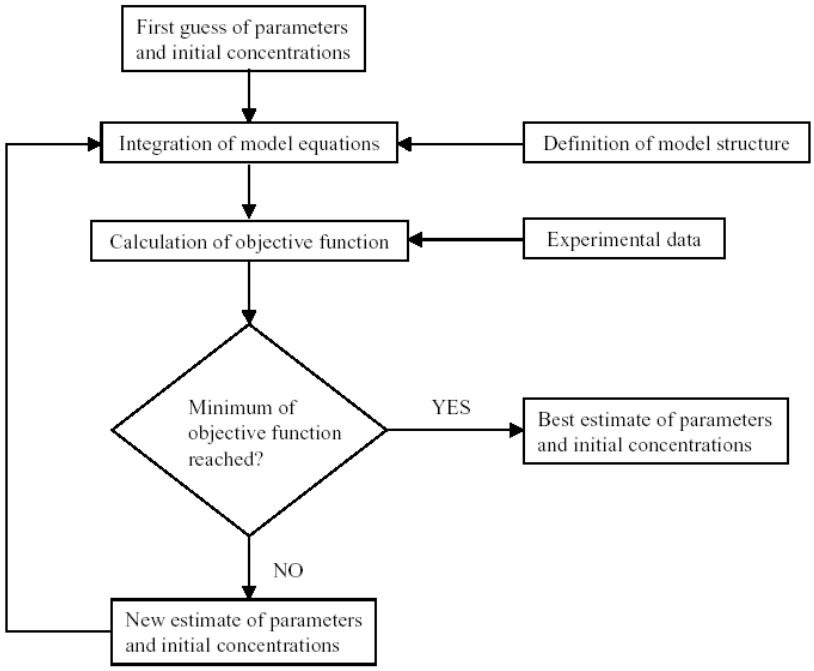

Figure 5. Parameter estimation procedure (Wanner *et al.*, 1992)

The optimal experimental design (OED) concept should be incorporated into the calibration protocol to maximize the information content of each of the experiments (Dochain and Vanrolleghem, 2001). This approach therefore, is expected to minimize time and cost aspects of the laboratory work. Optimal experimental design methodology can be applied for lab-scale experimental set-ups or even for full-scale measurement campaigns. However, OED applications to full-scale systems need a high level of *a priori* information and expert knowledge.

5.1.3 Parameter estimation

Parameter estimation consists of determining the 'optimal' values of the parameters of a selected model with the aid of measured data (Petersen *et al.*, 2003b). Here the 'optimal' value means the parameter value which gives the best fit to the measured data. Initially, the model structure of which the parameter(s) need to be estimated, the initial concentrations of the components and experimental data are necessary (Petersen *et al*., 2003b). According to Figure 5, initial estimates of the parameters and initial conditions have to be specified. Then, the actual parameter estimation is performed and is terminated when the objective function reaches a minimum with a certain accuracy. Different numerical techniques for parameter estimation can be found in Dochain and Vanrolleghem (2001).

5.2 Calibration of Activated Sludge Model No.1 (ASM1)

ASM1 introduced by Henze *et al.* (1987) essentially models a single-stage activated sludge system performing simultaneous COD oxidation, nitrification and denitrification. The matrix format representation of the ASM1 is presented in Table 2. Such matrix must be read as follows: the first column contains the processes included in ASM1, while the last column contains the process rates (kinetics) of these processes. The model components are given in the first row of Table 2. The stoichiometric coefficient of each component for each process is given in the cell corresponding to the intersection of the row of the process and the column of the component (see Table 2). A detailed description and explanation of the model processes and components can be found in the technical report of the IWA task group (Henze *et al.*, 1987).

Application of the ASM1 to a specific treatment plant, i.e. simulation of an activated sludge system based on ASM1, requires the calibration of the ASM1 model to the system under study. This means that the parameters and components presented in Table 2 should all be known for the case under study. That requires the estimation of the parameters (stoichiometric and kinetic) and characterization of wastewater and biomass of the system in accordance with the ASM1 model. This overall process is called calibration of the ASM1 model.

In this section, a calibration protocol for ASM1 will be presented mainly based on dedicated lab-scale experimental methods for wastewater characterization and estimation of the kinetic and stoichiometric parameters. However, it is important to stress that not all experiments presented in this section should be performed. Only the experiments aiming at providing data to identify the relevant parameters shown to be influential in the sensitivity analysis should be carried out. In other words, the experiments that have to be performed will be dependent on the system under study as well as on the target of the modelling study. In this context, the proposed model calibration procedure is not fixed but it should be considered as dynamic depending on each specific study. In the following, the methods for the influent wastewater characterization and estimation of kinetic/stoichiometric parameters for ASM1 mainly using respirometeric methods are presented. The extension of the influent wastewater characterisation for the ASM2d model is presented in section 5.3.

Table 2. The matrix representation of the ASM1 model (Henze *et al*., 1987)

Component (i) → ↓ Process (j)	1 S_I	2 S_S	3 X_I	4 X_S	5 X_{BH}	6 X_{BA}	7 X_P	8 S_O	9 S_{NO}	10 S_{NH}	11 S_{ND}	12 X_{ND}	13 S_{ALK}	Process rate (ρ_j)
1 Aerobic growth of heterotrophic biomass		$-\frac{1}{Y_H}$			1			$-\frac{1-Y_H}{Y_H}$		$-i_{XB}$			$-\frac{i_{XB}}{14}$	$\mu_{max\,H}\frac{S_S}{K_S+S_S}\frac{S_O}{K_{OH}+S_O}X_{BH}$
2 Anoxic growth of heterotrophic biomass		$-\frac{1}{Y_H}$			1					$-i_{XB}$			$\frac{1-Y_H}{14\cdot 2.86Y_H}$ $-\frac{i_{XB}}{14}$	$\eta_g\mu_{max\,H}\frac{S_S}{K_S+S_S}\frac{K_{OH}}{K_{OH}+S_O}$ $\frac{S_{NO}}{K_{NO}+S_{NO}}X_{BH}$
3 Aerobic growth of autotrophic biomass						1		$-\frac{4.57-Y_A}{Y_A}$	$-\frac{1}{Y_A}$	$-i_{XB}-\frac{1}{Y_A}$			$-\frac{2}{14Y_A}-\frac{i_{XB}}{14}$	$\mu_{max\,A}\frac{S_{NH}}{K_{NH}+S_{NH}}\frac{S_O}{K_{OA}+S_O}X_{BA}$
4 Decay of heterotrophic biomass				$1-f_p$	-1		f_p					$i_{XB}-f_p i_{XB}$		$b_H X_{BH}$
5 Decay of autotrophic biomass				$1-f_p$		-1	f_p					$i_{XB}-f_p i_{XB}$		$b_A X_{BA}$
6 Ammonification of soluble organic nitrogen										1	-1		$\frac{1}{14}$	$k_a S_{ND} X_{BH}$
7 Hydrolysis of slowly biodegradable substrate		1		-1										$k_h\frac{X_S/X_{BH}}{K_X+X_S/X_{BH}}X_{BH}$ $\left[\frac{S_O}{K_{OH}+S_O}+\eta_h\frac{K_{OH}}{K_{OH}+S_O}\frac{S_{NO}}{K_{NO}+S_{NO}}\right]$
8 Hydrolysis of organic nitrogen											1	-1		$\rho_7(X_{ND}/X_S)$

5.2.1. Influent Wastewater Characterization

In most of the cases, the daily monitoring of an ordinary wastewater treatment plant consists of measuring influent and effluent COD, TKN, NH_4 and PO_4-P. On the other hand, the wastewater components included in the ASM1 are different than those being measured in the treatment plant.

Influent COD components

The influent COD is subdivided into several components (see Figure 6).

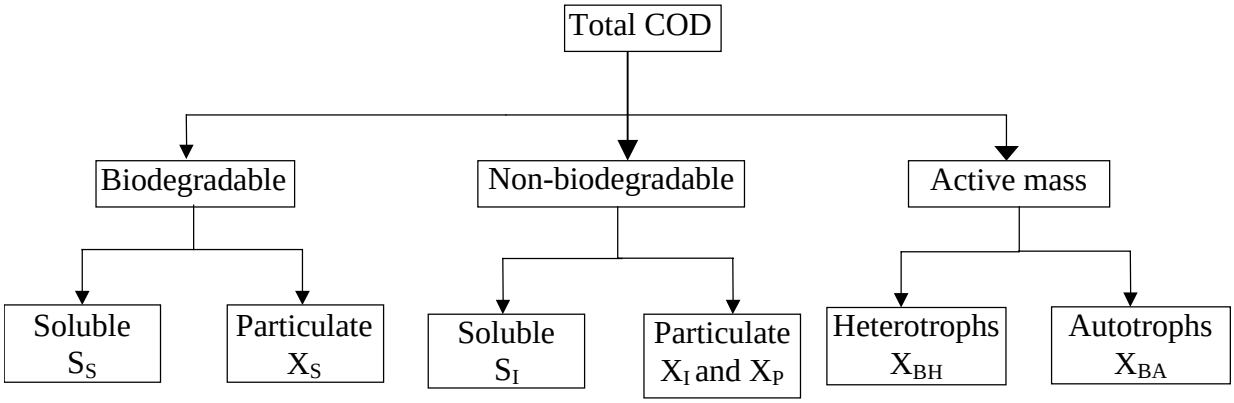

Figure 6. COD components in ASM1 (adopted from Petersen *et al.*, 2003a)

The biomass fractions in the influent COD are assumed to be negligible. The remaining fractions for the influent total COD are then given by:

$$CODtot = S_I + S_S + X_I + X_S \tag{13}$$

In the following an experimental methodology for determining the remaining fractions of the influent COD are presented. This methodology is a combination of biological (respirometric) and physical-chemical methods and was applied by Petersen *et al.* (2002b).

Determination of influent soluble inert COD, S_I:

The effluent soluble inert COD is assumed to be equal to the influent inert soluble COD of the treatment plant if it is operated at an SRT at least higher than 3 days (Mamais *et al.*, 1993). The effluent inert soluble COD can be estimated by subtracting the effluent readily biodegradable COD from the effluent total soluble COD. This is formulated and given in equation (14):

$$S_{I,\text{influent}} = S_{I,effluent} - 0.1 \times COD^{removed} = (CODsol_{effluent} - S_{S,effluent}) - 0.1 \times COD^{removed} \tag{14}$$

Where $COD^{removed}$ refers to the COD removed in the aeration tank. The 10% term is included to correct for the soluble microbial product formation by the biological activity (Henze *et al.*, 1992). Furthermore, the effluent readily biodegradable COD can be approximated from the effluent BOD samples as follows:

$$S_{S,effluent} = \frac{F_{BOD/COD,eff} * COD_{tot,effluent}}{(1 - Y)} \quad (15)$$

Where Y is the BOD yield coefficient assumed as 0.2 (or can be calculated based on lab-scale experiments) and $F_{BOD/COD,eff}$ is the ratio of effluent BOD_5 to effluent COD_{tot}:

$$F_{BOD/COD,eff} = Average\left(\frac{BOD_{5,effluent}}{COD_{tot,effluent}}\right) \quad (16)$$

It is suggested that weekly BOD_5 effluent data of the treatment plant with corresponding $COD_{tot,effluent}$ data should be used for the calculation of effluent and thus influent S_I. Once the $S_{S,effluent}$ is known, the effluent inert soluble COD can be determined easily from equation 14 and thus the influent inert soluble COD too.

Determination of influent readily biodegradable COD, S_S:
The influent readily biodegradable COD can be estimated from a respirometric batch test. The respirometric batch test should be carried out with an unfiltered influent sample and nitrification inhibitor (ATU) should be added to prevent oxygen uptake interference from nitrification. It is important to note that this approach is based on respirometry while there is an alternative approach requiring the use of long-term BOD data (e.g. 14 days or 28 days) of influent wastewater. This BOD-based characterisation of readily biodegradable substrate is employed in the STOWA protocol (Hulsbeek *et al*., 2002). An extensive application of this approach for characterisation of readily biodegradable COD is already presented both in Roeleveld and van Loosdrecht (2002) and Weijers (1999).

In this respirometric method, the readily biodegradable COD content of the influent can be determined as follows:

$$COD_{st} = \frac{BODst}{(1 - Y_H)} \quad (17)$$

Where BOD_{st} is the area under the exogenous oxygen uptake rate profile in the respirogram (the plot of oxygen uptake rate versus time as illustrated in Figure 7) and represents the short term BOD of the sample. Y_H is assumed to be 0.67 in this batch test. It is assumed that the model S_S is equal to the experimentally determined COD_{st} and, therefore, the S_S in the influent wastewater can be calculated by taking into account the following volume correction:

$$S_S = \frac{CODst}{V_{SAMPLE}} \cdot V_{REACTOR} \tag{18}$$

where, V_{SAMPLE} refers to the volume of sample of wastewater added to the batch reactor while $V_{REACTOR}$ represents the total volume of the batch reactor used in the experiment.

It is significant to note that this method is quite sensitive to two parameters on which the method's accuracy critically depends: (1) the assumed Y_H value and (2) the determination of endogenous and exogenous OUR profiles. One approach would be to discern the two levels of OUR manually by eye-visualisation of the respirogram obtained. However, a more accurate / reliable approach consists of a model-based interpretation of the respirograms (see e.g. Gernaey *et al*., 2001a).

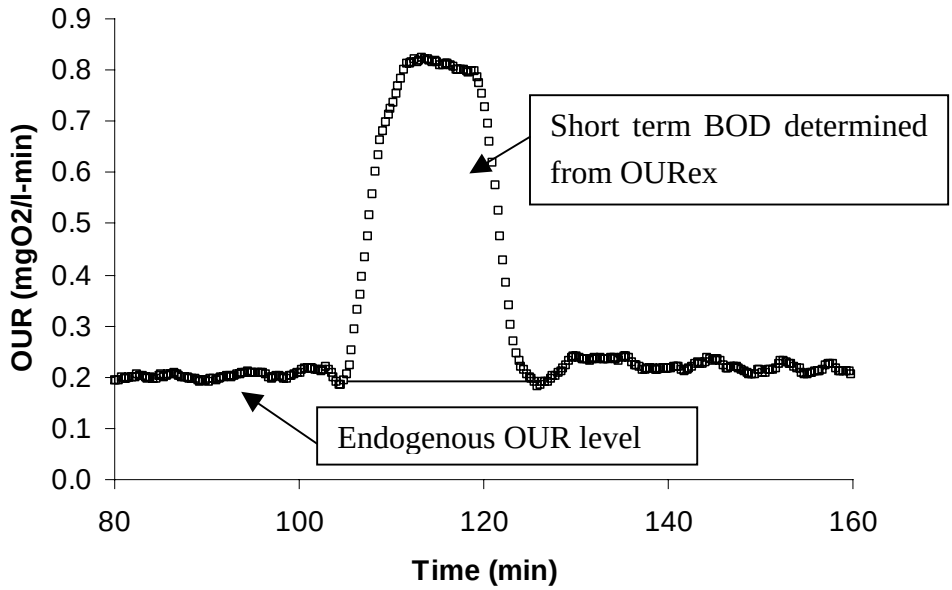

Figure 7. An OUR profile obtained after addition of 300 mg Acetate to a 2.57 l activated sludge at time 104 min. The BOD_{st} is given by the area under the OUR_{ex} ($r_{O2,ex}$) profile which is the total OUR minus the endogenous OUR ($r_{O2,end}$).

The reproducibility of the first approach was shown to be poor (Carucci *et al.*, 1999), since it is subjective. In some experimental results, it would be quite difficult to discriminate X_S from

the S_S part. The interpretation and estimation of the influent S_S becomes more complicated when a storage phenomenon is observed. In this case, it would be quite impossible to discriminate between an X_S tail and the oxygen consumption related to the degradation of the internal storage products (van Loosdrecht *et al*., 1997) by the first approach. In this case, it is suggested to keep Y_H value higher than the default ones to compensate for the storage phenomenon (e.g. 0.75). However, the best approach is the model-based data interpretation and this should be certainly preferred whenever possible.

Note that for cases where the BOD_{st} value resulted from an experiment in which no ATU is added, the COD_{st} concentration can be determined according to:

$$BOD_{st} = BOD_{st,total} - BOD_{st,TKN} \quad (19)$$

The BOD_{st} requirement for the oxidation of TKN ($BOD_{st,TKN}$) is determined using the TKN concentrations obtained from the chemical analyses of the wastewater (Eq. 20). The value of Y_A is set to 0.24 (Henze *et al*., 1987).

$$BOD_{st,TKN} = (4.57 - Y_A) \cdot TKN \quad (20)$$

However, ATU addition is advised in order to prevent possible errors that may result from the experimental errors (determination of TKN, OUR etc). Another significant remark about the proposed method is that storage phenomena may interfere with the determination of S_S. Under certain circumstances the biomass may store COD_{st} as internal storage products which may lead to underestimation of the COD_{st} from the OUR data (Vanrolleghem *et al*., 1997). In order to get a realistic value for S_S, a higher yield coefficient Y_H can be adopted (e.g. up to 0.75; see chapter 4.2.2), but the reliability of the method would be tightly linked with the assumed value of Y_H. For systems where the storage phenomenon is not dominant, the interference is not expected to be a problem.

As a final step it is advised to check the soluble COD balance:

$$COD_{sol,influent} = S_S + S_I + S_{rest} \quad (21)$$

In case $COD_{sol,influent}$ in Eq.21 is higher than $S_S + S_I$, S_{rest} can be added to the slowly biodegradable substrate, X_S (Orhon *et al.*, 1998). On the contrary, if $COD_{sol,influent}$ is lower than $S_S + S_I$, part of the measured BOD_{st} may be considered to be originating from X_S.

Determination of influent total particulate COD, X_I and X_S:

Once the soluble fractions of the influent COD are determined, the particulate fraction of the influent COD can be determined from the mass balance equation (13). The unique values for X_S and X_I will be assigned during the steady-state model calibration:

$$COD_{tot} - COD_{sol} = X_S + X_I \quad (22)$$

The X_S concentration contains the S_{rest} from the mass balance in equation (21) and is partly determined from steady state model evaluations.

The X_I is suggested to be estimated by comparing the measured and predicted sludge concentration and sludge production. The X_I influent concentration is typically used as a "tuning component" in the model calibration of the sludge balance and the X_S concentration is adjusted accordingly via mass balance E.q.22 (assuming that X_{BH} and X_{BA} are negligible, see above).

Finally, the influent COD characterization methodology is summarised in Figure 8.

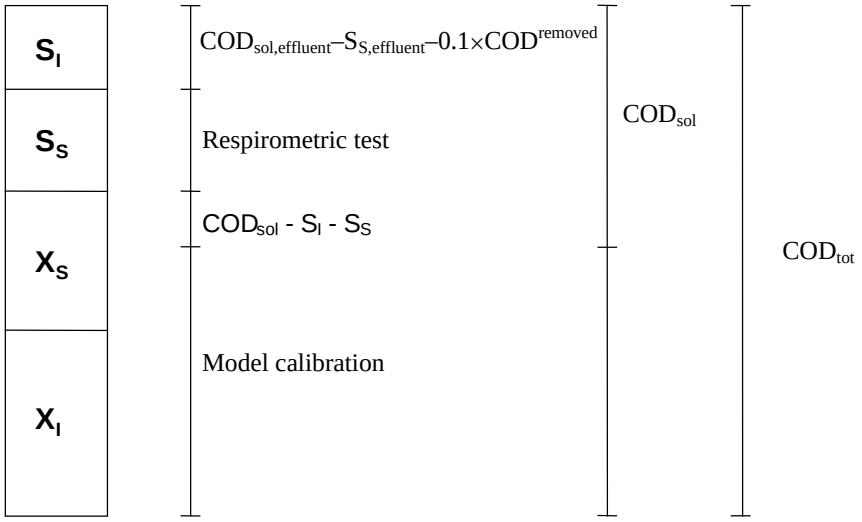

Figure 8. Summary of the influent characterisation methodology for considering the ASM1 model.

Influent nitrogen components

In Figure 9 the ASM1 model nitrogen components are presented. For the nitrogen fractions a similar approach to the COD fractionation is proposed both for influent and effluent nitrogen characterisation. It is assumed that the influent contains negligible concentrations of nitrate (S_{NO}) unless influent nitrate measurements are available. Assuming there is no or negligible biomass in the influent wastewater, the total Kjeldhal nitrogen can be fractionated according to Eq. 23 (Henze *et al*., 1987).

$$TKN = X_{NI} + X_{ND} + S_{NI} + S_{ND} + S_{NH} \quad (23)$$

Ammonia nitrogen (S_{NH})

The analytically measured NH_4-N concentration following the Standard Methods (APHA, 1995) is considered to be equal to S_{NH}. This component is expected to be available in the monitoring programme of most wastewater treatment plants.

Soluble biodegradable organic nitrogen (S_{ND})

It is assumed that the ratio of soluble to total TKN is proportional with the ratio of COD_{sol} to COD_{tot}. Thus, the soluble Kjeldhal nitrogen (SKN) can be approximated via Eq.24, and by assuming that the nitrogen content of inert soluble organic matter (i_{NSI}) equals 1.5% (Henze *et al*., 1995) the concentration of S_{ND} can be determined via Eq.25.

$$SKN = \frac{CODsol}{CODtot} \cdot TKN = S_{NI} + S_{ND} + S_{NH} \quad (24)$$

$$S_{ND} = SKN - i_{NSI} \cdot S_I - S_{NH} \quad (25)$$

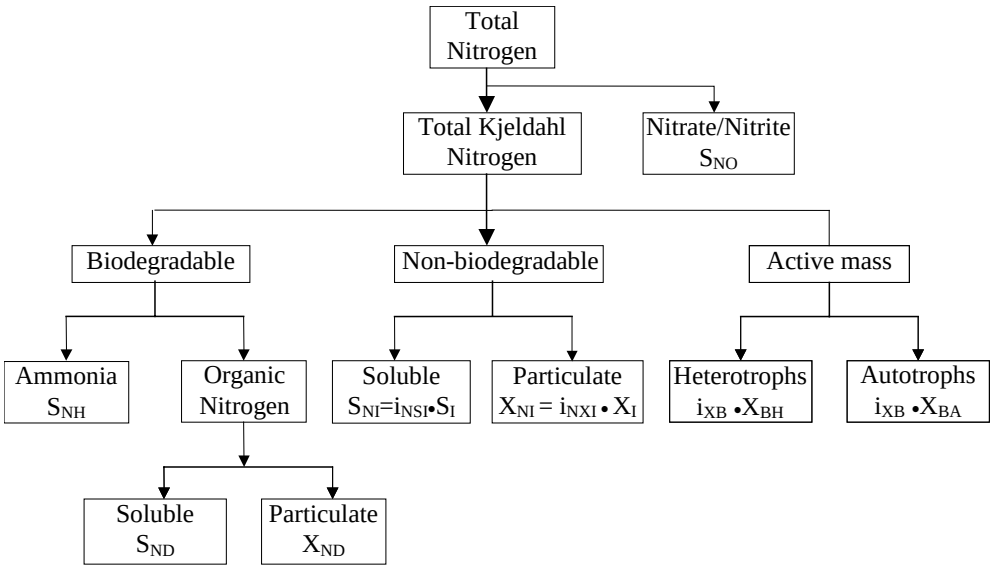

Figure 9. Nitrogen components in ASM1 (adopted from Petersen *et al*., 2003a)

Slowly biodegradable organic nitrogen (X_{ND})

The nitrogen content of inert suspended organic matter (i_{NXI}) is initially assumed to be 1% (Henze *et al*., 1995) resulting in Eq. 26 for the determination of X_{ND}.

$$X_{ND} = TKN - i_{NXI} \cdot X_I - SKN \quad (26)$$

The overall procedure for influent characterisation is summarised in Table 3.

Table 3. Summary of COD and nitrogen components determination

COD fractionation	
Inert soluble COD, S_I	$S_{I,\text{inf luent}} = (COD_{sol,effluent} - S_{S,effluent}) - 0.1 \times COD^{removed}$
Readily biodegradable COD, S_S	$S_S = \frac{COD_{st}}{V_{SAMPLE}} \cdot V_{REACTOR}$ Where $COD_{st} = \frac{BOD_{st}}{(1-Y_H)}$
Inert particulate COD, X_I	Model calibration where $COD_{tot} - COD_{sol} = X_S + X_I$
Slowly biodegradable COD, X_S	$X_S = (COD_{tot} - COD_{sol}) + S_{rest} - X_I$
Nitrogen fractionation	
Ammonia nitrogen, S_{NH}	Analytical measurement of NH_4-N
Soluble biodegradable organic-N, S_{ND}	$S_{ND} = SKN - i_{NSI} \cdot S_I - S_{NH}$ Where
	$SKN = \frac{CODsol}{CODtot} \cdot TKN = S_{NI} + S_{ND} + S_{NH}$
Slowly biodegradable organic-N, X_{ND}	$X_{ND} = TKN - i_{NXI} \cdot X_I - SKN$

5.2.2 Kinetic Parameter Determination

The methodology described below is advised for the determination of key kinetic parameters of the activated sludge processes included in ASM1, i.e. those related to heterotrophic and autotrophic activity.

Maximum specific growth rates

Regarding the determination of the maximum specific growth rates for heterotrophs and nitrifiers a respirometric batch test is proposed. The identifiable parameter combinations for heterotrophic growth using OUR data obtained from batch experiments are given in Table 4. These parameter combinations are advised to be used during parameter estimation using batch respirograms (see e.g. Figure 11). Separate/unique parameter estimation is possible if the initial amount of substrate, $S_S(0)$, in the batch experiment is known. In this case, there is a unique/single solution for the 3 identifiable parameter combinations listed in the Table 4.

Table 4 Identifiable parameter combinations for growth and hydrolysis kinetics.

Growth (Dochain *et al.*, 1995).		**Hydrolysis (Insel *et al.*, 2003a)**	
No biomass growth	Biomass growth	No biomass growth	Biomass growth
$\frac{1-Y_H}{Y_H}\mu_H X_H(0)$	$\frac{1-Y_H}{Y_H} X_H(0)$	$(1\text{-}Y_H)\ k_h\ X_H(0)$	$(1\text{-}Y_H)\ K_x\ X_H(0)$
$(1\text{-}Y_H)\ S_S(0)$	$(1\text{-}Y_H)\ S_S(0)$	$(1\text{-}Y_H)\ K_x\ X_H(0)$	$(1\text{-}Y_H)\ X_S(0)$
$(1\text{-}Y_H)\ K_S$	$(1\text{-}Y_H)\ K_S$	$(1\text{-}Y_H)\ X_S(0)$	$(1\text{-}Y_H)\ X_H(0)$
	μ_H		k_h

Index "(0)" indicates the initial value

These respirometric experiments are good examples of experiments where the Optimal Experimental Design (OED) methodology can be applied. Indeed, in one batch experiment proper addition of wastewater and ammonium (S_0/X_0) as determined by OED allows to determine the nitrification kinetics together with the COD degradation kinetics. This was successfully applied by Petersen (2000) (see Figure 10). The design of these experiments is described in more detail elsewhere (Petersen, 2000), but consisted of simultaneous addition of wastewater and ammonium, thus allowing to estimate the nitrification kinetics and the degradation of COD in a single experiment. The exogenous oxygen uptake rate, $r_{O,ex}$, resulting from the addition of wastewater and ammonium respectively is given in Figure 10 and can be described by the following equation (Eq. 27):

$$r_{O,ex} = (1 - Y_H) \cdot \frac{\mu_{max\,H} X}{Y_H} \cdot \frac{S_S}{K_S + S_S} + (4.57 - Y_A) \cdot \frac{\mu_{max\,A} X}{Y_A} \cdot \frac{S_{NH}}{K_{NH} + S_{NH}} \quad (27)$$

Using model-based parameter estimation and assuming the yield coefficients are a priori known e.g. by taking Y_H and Y_A as 0.67 and 0.24 respectively (since initial amount of S_S is not a priori known), the maximum heterotrophic and nitrifying biomass growth rates and the Monod affinity constants K_S and K_{NH} can be determined. If the aim is only to determine the maximum growth rates for the heterotrophic and nitrifying growth rates then the Monod affinity constants could simply be fixed to their ASM1 default values together with the yield coefficients. The reader is advised to consult the IWA task group report on ASM1 for default values (Henze *et al.*, 1987).

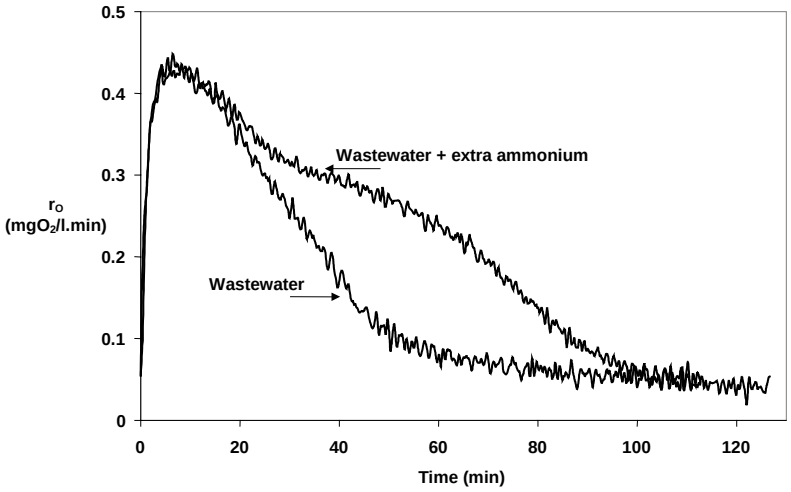

Figure 10. Example of respirograms obtained from respirometric tests with wastewater and wastewater mixed with ammonium (Petersen *et al.*, 2002b).

The parameter estimation can also be performed in two steps for heterotrophic and nitrifying biomass. In the first step, the heterotrophic parameters can be identified from an experiment with ATU addition (thereby inhibiting nitrification). The resulting respirogram will provide

the information necessary to determine the parameters for COD degradation. In the second step, an experiment without ATU addition can be performed and the resulting OUR data can be used to determine the nitrification kinetics by fixing the heterotrophic parameters determined in the first experiment. Either approach can be expected to yield the same results for heterotrophs and nitrifiers.

It is quite important to note that if a storage phenomenon is observed, the ASM1 model presented in Eq. 27 will fail to model the OUR data obtained from the experiment. This means that the method proposed will fail to determine the kinetic parameters. In order to model the system, a more suitable mathematical model (see e.g. Chapter 4.2.2; ASM3) should be applied.

Hydrolysis

The hydrolysis process incorporated in the ASM models is expressed with the surface saturation type equation (see Table 2). Generally speaking, this equation is governed by the maximum hydrolysis rate, k_h and the half saturation constant for hydrolysis, K_X (Henze *et al.*, 1999; Henze *et al.*, 1987; Orhon *et al.*, 1999; Orhon *et al.*, 1998; Mino *et al.*, 1995). In the literature, some researchers suggest that the hydrolysis kinetics can also be expressed by a first order equation (Sperandio and Paul, 2000; Spanjers and Vanrolleghem, 1995; Sollfrank and Gujer, 1991; Kappeler and Gujer 1992).

In this report, the experimental procedures suggested by Ekama *et al.* (1986) and Insel *et al.* (2003a) are proposed for surface saturation type hydrolysis. According to the method proposed by Ekama *et al.* (1986), the determination of the parameters for hydrolysis is carried out by a "cyclic square wave feed" experiment. To determine the hydrolysis parameters the data obtained after the drop in respiration rate are important. For details the reader is referred to Ekama *et al.* (1986).

The identifiable parameter combinations of the hydrolysis process based on OUR measurements were recently studied by Insel *et al*. (2003a) and they are given in Table 4. These parameter combinations can be used to estimate the parameters of the hydrolysis process from batch OUR experiments.

Decay rates

The endogenous respiration rate, $r_{O,end}$, can be measured simply as function of time in a long term (e.g. 5-7 days) aerated batch test without substrate supply. The endogenous decay rate, b_H', can be determined as the slope of the curve consisting of $\ln(r_{O,end}(0))/\ln(r_{O,end}(t))$ data points plotted as function of time (Ekama *et al*., 1986). This decay rate should be transformed into the model decay rate based on the death regeneration concept via Eq. 28 (Henze *et al*.,

1987), where Y_H is assumed to be a priori known, e.g. 0.67 (ASM1 default), and f_p to 0.08 according to the ASM1 default parameters.

$$b_H = \frac{b'_H}{1 - Y_H(1 - f_p)} \tag{28}$$

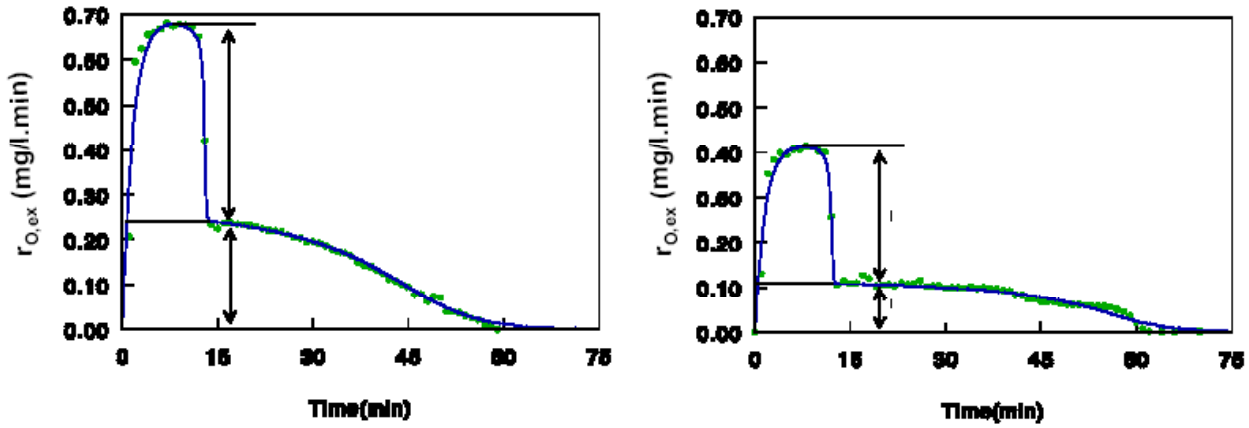

Figure 11. Determination of the OUR_{max} of a sludge sample after an incubation time of 1 day (left) and 7 days (right) (Spanjers and Vanrolleghem, 1995).

Another method for the determination of b_H was proposed by Spanjers and Vanrolleghem (1995). The model for carbon oxidation and nitrification is applied to the respiration data from acetate/ammonium addition. According to this method, the heterotrophic and autotrophic endogenous decay rate can be found by curve fitting. In this method, the sludge is sampled from the main reactor without any continuous feed during the experiment. Then a known amount of a readily biodegradable substrate (e.g. an acetic acid and ammonium mixture) is spiked into the sludge at different times. The resulting respirograms are plotted versus time scale (Figure 11). The decrease in the maximum OUR levels corresponds to the decrease in the active biomass due to decay. By fitting the model to the OUR data and assuming that biological kinetics remain unchanged (e.g. yield coefficients and maximum growth rates), the decrease in the biomass concentration can be calculated and used to determine the decay rate coefficient of biomass (Spanjers and Vanrolleghem, 1995).

Temperature correction

As there might be differences between the temperatures under the lab experimental conditions and the treatment plant under study, the temperature effect can be modelled using the modified Arrhenius equation:

$$r(T) = r(20\ ^0C) \cdot \theta^{.(T-20)} \tag{29}$$

where the temperature correction coefficient, θ, can be found from the literature or determined experimentally for each process under consideration. For example, it is reported to range between 1.01 and 1.08 for the maximum growth rate of heterotrophs in Metcalf and Eddy (1991).

5.2.3 Biomass Characterization

The particulate COD balance in the aeration reactor will result in the following equation:

$$X = X_I + (X_P) + X_{BH} + X_{BA} \quad (30)$$

The concentration of X_S may be assumed negligible or estimated from steady-state simulations with the model. The concentrations of the remaining particulate, slowly varying components must be assessed: X_{BH}, X_{BA} and X_I ($+X_P$). Only two concentrations must be assessed since the sum of the concentrations is equal to the particulate COD (X) of the sludge that can be measured by using traditional COD analysis. Eq. 30 then allows to estimate the missing fraction.

The following fast and direct methods for assessing sludge components are proposed for the protocol. Notice that the particulate nitrogen components, X_{ND}, are also considered negligible here (see Eq. 30). However, similar to the X_S as mentioned above, the X_{ND} can also be approximated using steady-state simulations with the model.

Heterotrophic biomass X_{BH}

The concentration of heterotrophs in a continuous system under steady state conditions is equal to:

$$X_{BH} = Y_H \cdot \frac{\theta_X}{\theta_H} \cdot \frac{COD^{Degraded}}{1 + b'_H \theta_X} \quad (31)$$

where θ_X is the sludge age, θ_H is the hydraulic retention time, $COD^{Degraded}$ the total amount of COD removed (taken over a sufficiently long period, e.g. one sludge age), b'_H the decay rate coefficient and Y_H the yield coefficient. The parameters b'_H and Y_H can be either determined from the respirometric methods or can be assigned to their default values reported in Henze *et al.* (1987). The $COD^{Degraded}$ can be determined from the respirometric measurements of biodegradable COD fractions (S_S, X_S) that are already discussed in the influent COD characterization section of the protocol.

Autotrophic organisms X_{BA}

In much the same way, the concentration of nitrifying organisms in the activated sludge can be evaluated by means of a mass balance for the autotrophs (over a sufficiently long time) (Dupont and Sinkjær, 1994):

$$X_{BA} = Y_A \cdot \frac{\theta_X}{\theta_H} \cdot \frac{f^{Aerobic} \cdot N^{Nitr}}{1 + b_A . \theta_X} \tag{32}$$

where $f^{Aerobic}$ is the aerobic fraction of the reactor, N^{Nitr} the amount of nitrified nitrogen, b_A the autotrophic decay rate coefficient and Y_A the autotrophic yield coefficient. The methods to determine the parameters b_A and Y_A were already discussed in the kinetic parameters estimation section of the protocol. N^{Nitr} can be quantified using the respirometry-based nitrifiable nitrogen evaluation methods as described below.

A respirometric batch test can be performed similar to the batch measurements for S_S and X_S estimation. The test should be performed with nitrifying activated sludge and the oxygen consumption for nitrification should be separated from the other oxygen consuming processes. N^{Nitr} can be estimated using the area under the OUR profile:

$$N^{Nitr} = \frac{\int OUR\, dt}{4.57 - Y_A} \tag{33}$$

The term (4.57 - Y_A) is needed to convert the oxygen consumed by nitrification to a nitrogen concentration. In this term, 4.57 indicates the mass of oxygen needed to oxidise one mass of ammonium nitrogen to nitrate. The value of the autotrophic yield coefficient,Y_A, is typically 0.24 g COD (biomass)/g N (Henze *et al*., 2000).

Produced inert suspended organic matter X_P

To determine the produced inert matters, X_P, an evaluation of the mass balance of X_P in steady state can be made. Assuming that the autotrophic biomass can be neglected, Eq. 34 is obtained:

$$X_P = f'_p \cdot b'_H \cdot X_{BH} \cdot \theta_X \tag{34}$$

where f'_p is the inert particulate fraction of biomass produced due to decay (0.2 gCOD-X_P/gCOD-X_{BH}) and b'_H is the traditional endogenous decay coefficient. The total concentration of inert matters, including the often-significant contribution of suspended inert material from the influent, is given in Eq. 35.

$$X_P = \frac{\theta_X}{\theta_H} X_I + f'_P \cdot b'_H \cdot X_H \cdot \theta_X \quad (35)$$

The only unknown particulate COD component, X_I in this case can be determined as suggested above by a model fitting procedure during the calibration, in other words by tuning the simulated X with the measured or observed X (Eq. 30).

5.2.4 Alternative Methods for Biological Characterization of ASM1

The introduction of the ASM1 (Henze *et al.*, 1987) to the scientific and wastewater treatment community has unleashed an immediate need for development of experimental methods for the calibration of the ASM1. In fact, that development of calibration methodologies was the bottleneck step for ASM1 to gain acceptance for full-scale application in the wastewater treatment community. The IWA Task Group on Mathematical Modelling suggested a calibration methodology, which required tedious and time-consuming lab-work for the ASM1 with the provision that a better methodology is possible to be developed. In view of this, many researchers have focused their attention on developing experimental methods to facilitate the application of ASM1 for full-scale systems. As a result of these considerable efforts, many experimental methods have been developed and proposed for the calibration of the ASM1 (see Petersen *et al*., 2003a). However, there is no common and standard ASM1 calibration methodology available yet in the literature. It seems a rather challenging task to develop a standard calibration procedure due to the very uniqueness of each treatment plant installed and operated around the world.

In addition to the BIOMATH calibration protocol, which was initially developed in Petersen (2000) and Petersen *et al*. (2002b) and refined in this study, several other calibration approaches have recently been proposed. These are the STOWA protocol (Hulsbeek *et al*., 2002), the HSG guidelines (Langergraber *et al*., 2003a) and the WERF calibration methodology (WERF, 2003). The main common objective of these calibration protocols is to standardise the calibration of activated sludge models for full-scale WWTPs (e.g. ASM1, ASM2d, etc.). This is essentially needed to enable an internal quality check for the calibration study and to be able to compare different calibration studies. A second common aspect of these protocols is that they are developed on the basis of regional experiences with the calibration of ASMs. For example, the STOWA protocol was developed and applied to more than 100 WWTPs operated in The Netherlands (Hulsbeek *et al*., 2002). The HSG guidelines were developed based on the experiences of University researchers from Austria, Germany and Switzerland (Langergraber *et al*., 2003a). Last, the WERF calibration methodology was developed focusing on the North American practice for the calibration of models of full-scale

WWTPs (WERF, 2003). A critical and detailed comparison of these systematic protocols are provided below using a SWOT analysis.

Moreover, as aforementioned, the experimental methods available in the literature for ASM1 calibration have been extensively reviewed in Petersen *et al.* (2003a). A summary table adopted from Petersen *et al.* (2003a) is provided that contains references for full-scale ASM1 applications employing different calibration strategies. More information about various experimental methods designed and applied for ASM1 wastewater characterization and parameter estimation can be found in the same reference (Petersen *et al.*, 2003a).

Table 5. Reference table for ASM1 calibration cases (Alternatives) adapted from Petersen *et al*. (2003a).

Reference	**Purpose**	**Calibration strategy**	**Characterisation**						
			Wastewater				***Sludge***	***Kinetic and stoichiometric***	
			Full-scale data	Model components			Lab-scale analyses	Model calibration	Lab-scale experiments
				Mass balances	Lab-scale	Model calibration			
ST92	Description: Nitrification, COD removal	Steady state Dynamic	3,7,8,9	S_I	X_I			Y_H, μ_H, K_S, k_h, K_X, b_H, μ_A, K_{NH}	
L92	Optimisation: N-removal	Steady state	3,4,8,9	S_S, X_S, X_{BH}	S_I, X_I		1,2,3,7	K_X, k_h	μ_A, b_A
PS92	Description: N-removal	Steady state Dynamic	3,4,5,7,8,9	S_S, S_I, X_I				μ_A, K_S, η_g	
DS94	Optimisation: N-removal	Steady state Dynamic	3,4,5,7,8,9					K_S, η_g	μ_A, b_A, K_{NH}, K_{OA}
S93	Description: Nitrification, COD removal	Steady state Dynamic	1,3,5,6,8				1,2,3	μ_H, K_S, μ_A	
dS94	Optimisation: All processes	Steady state Dynamic	3,5,7,8,9,10			All	1,2,3,7	μ_A, b_A, μ_H, K_S, k_h, K_X, K_{NO}, η_g, η_h,	
XH96	Description: COD removal, N removal	Steady state Dynamic	3,4,6,8,9	S_I, S_S	S_S, X_{BH}, X_S	X_I	1	μ_A, K_{OH}, K_{NH}, η_g	
K98	Description: COD & N removal	Steady state Dynamic	1,2,3,4,7,8,9		S_S		1,2	k_h, K_X, b_H, η_g, K_{OH}	b_H, μ_H, μ_A, K_{OA}
C99	Optimisation: COD & N removal	Steady-state	3,7	X_S	S_S,S_I	X_I	Not available		μ_H, μ_A & η_g

1. SS : Suspended Solids
2. VSS : Volatile Suspended Solids
3. CODtot : total COD & CODsol : soluble COD
4. BOD_5 : Biological Oxygen Demand (5days)
5. TN : Total Nitrogen & TKN : Kjeldahl Nitrogen
6. NH_4-N : Ammonium Nitrogen
7. NO_x-N : Nitrate + Nitrite Nitrogen
8. (10) PO_4-P : Ortho-phosphate

dS94 de la Sota *et al*., (1994)
DS94 Dupont and Sinkjær (1994)
K98 Kristensen *et al*., (1998)
L92 Lesouef *et al*., (1992)
PS92 Pedersen and Sinkjær (1992)
ST92 Siegrist and Tshui (1992)
S93 Stokes *et al*. (1993)
XH96 Xu and Hultman (1996) & C99 Carucci *et al*., (1999)

5.2.5 SWOT analysis of the systematic calibration protocols

The systematic calibration protocols have a lot in common. First of all, all of them start with a clear definition of the objective of the model calibration and emphasize the importance of data quality checking and verification (and ultimately correcting). Further, they demand a similar validation step after the calibration. However, there are also significant points where each protocol has a different approach. For example, the experimental methods for determining influent wastewater characterisation, kinetic/parameter estimation are all different in BIOMATH, STOWA and WERF protocols, how to design a dynamic measurement campaign, how to perform the calibration of model parameters etc.

In order to make the picture clearer and thoroughly compare these protocols, a Strengths, Weaknesses, Opportunities and Threats (SWOT) analysis was performed and it is summarised in Table 5bis. In what follows the SWOT analysis of the protocols is presented in detail.

The BIOMATH calibration protocol

The BIOMATH protocol has a detailed procedure for the characterisation of settling, hydraulic and biological sub-models of the WWTP. For characterization of each sub-model, several (at least two) methods are proposed, each associated with different underlying assumptions and calibration accuracies.

But the influent wastewater characterisation and the kinetic/stoichiometric parameter estimation of the biological processes are heavily relying on respirometric measurements. These respirometry-based methods have both positive and negative aspects. First of all, it is a more mechanistic approach in which the biomass response to different fractions of wastewater is analysed in contrast to the physical–chemical methods which only evaluates physical properties of the wastewater. However, it is not always straightforward to interpret OUR profiles and quantitatively determine readily biodegradable COD, S_S, and slowly biodegradable COD, Xs without the use of a model. Moreover, storage phenomena are increasingly shown to occur in activated sludge treatment plants. In this case, it becomes too difficult to separate the degradation of the X_S wastewater fraction from the utilisation of internal storage polymers, X_{STO}. This will add some uncertainty to the correct determination of the S_S and the X_S fractions in the influent wastewater.

The estimation of kinetic and stoichiometric parameters of the biological model from OUR measurements has been shown to be possible with a high accuracy. However, it requires a model-based approach and demands dedicated software and trained users.

Sensitivity analysis is proposed as a tool to point out the parameters that influence the process behaviour most. Based on this sensitivity analysis the choice can be made which parameters

should/can be calibrated. Moreover, Optimal Experimental Design (OED) is proposed as a tool for design and comparison of (dynamic) measurement campaigns and batch experiments. As such it contributes to increasing the parameter accuracy in both full-scale and lab-scale data collection steps. The downside of this OED is that not all modelling and simulation software have an OED module and so far a high degree of specialisation is required for the use of such a tool. However, the increased automation and efforts in improving user support should alleviate this.

Further, the BIOMATH protocol does not emphasize in sufficient detail the methods for data reconciliation like the STOWA and WERF protocols do. Further, from the structure of the BIOMATH protocol, it is not clear/easy to determine how the objective of the calibration study determines the final specific calibration procedure to follow for a particular case study. This should be improved and clarified by mentioning from the start the different calibration levels and associated procedures similar to the *tiered approach* used in the WERF protocol.

Overall, the BIOMATH protocol is oriented at employing scientifically more exact methods rather than using practically more applicable methods. This makes the BIOMATH protocol the most sophisticated of all four protocols but it may not be the most user friendly for new modelers entering the field. Still, once the OED methodology and sensitivity analysis can be incorporated into the calibration procedure, it may provide a good opportunity/perspective to move further into developing *a fully automatic* calibration procedure.

The STOWA calibration protocol

In the STOWA calibration protocol, the influent wastewater characterisation is based on combined BOD measurement and physical-chemical methods. Although physical-chemical methods give reproducible/consistent results, the BOD method has a major uncertainty with the determination/assumption of the inert particulate fraction, f_P, (Roeleveld and Van Loosdrecht, 2002). The results of the BOD method are very important since they determine the biodegradable fraction of the wastewater or alternatively the inert fraction of wastewater, which is a key/critical ratio determining the remaining other fractions of the influent COD. Weijers (1999) has investigated the use of model-based interpretation of the BOD profiles/curves using a simplified ASM1 model, showing promising results that can be used to extend the STOWA protocol. Further investigation to improve the reproducibility of the BOD method could significantly improve this part of the STOWA protocol.

The steady-state calibration of the protocol is not acknowledged specifically in the main structure of the model calibration. However, steady-state calibration results could be used to double-check the results of the mass balances (particularly the solids balance used to check the SRT of the system) similar to the other protocols, i.e. BIOMATH, HSG and WERF.

Biomass characterisation, i.e. the determination of the initial autotrophic and heterotrophic biomass concentrations in the WWTP, are not specified/provided in the protocol. Moreover, detailed guidelines or remarks concerning the design of dynamic measurement campaigns are not discussed/provided in detail even though this is the most expensive aspect of a model calibration study.

The STOWA protocol is the only protocol where a time estimate for the different steps involved in calibration is mentioned/included. However, it may not generally be applicable for different systems as the protocol is based on the range of studied WWTPs. Settling and biological characterization are addressed in detail, but relatively little details are provided on hydraulic characterization of the aeration tanks.

Further, the protocol puts little or negligible emphasise on mathematical and/or statistical methods such as OED that can be used for design and comparison of measurement campaigns and lab-scale batch tests. Moreover, although the proposed manual calibration procedure is a great help for beginners, it may be dangerous to generalize it for full-scale applications. By definition, it is too difficult if not impossible to expect that the fixed parameter subsets proposed by the STOWA protocol (and the order of calibration of these parameter subsets) remain valid for various/different WWTPs, even operated *only* in the Netherlands. The possibility to calibrate these parameter subsets given in the STOWA protocol depends strictly on the available information content of the plant data (quality, quantity, etc.) and plant operation/configuration. It would therefore be useful to check whether these proposed parameter subsets remain indeed sensitive in each calibration study.

Overall, the STOWA protocol among others is the most straightforward, practical, easy to follow/read and easy to implement protocol. In that context, this protocol (in addition to the WERF protocol, see below) is most suited for practical applications and as such it is expected to become popular among consultants. A very important function of the STOWA protocol could also be to guide the inexperienced/ new modellers to understand the significant steps underlying a calibration study and perform a good quality calibration study.

The HSG guidelines

This protocol presents general guidelines to be followed and documented during a calibration study and is therefore generally applicable. It is aimed towards the performance evaluation of existing plants with the highest requirements regarding model calibration and validation. The ultimate goal is to systematize the documentation of the overall calibration study. However, no feed back loops are incorporated in the scheme implying all calibration steps are straightforward and no internal-check of each step is necessary.

On the other hand, the HSG guidelines do not prefer to propose any particular experimental methodologies for influent characterization and kinetic parameter determination nor do they provide specific details on how to calibrate a selected ASM model. This certainly gives extra freedom of choice for the modelers to decide which experimental methodologies to employ. However in this way it may be questionable to what extent the calibration procedure is systematized. In other words, not imposing a certain experimental methods may conflict with the ultimate aim of the protocol, which is to bring a standard for the overall calibration study. Also new practitioners are not guided by the protocol to find elsewhere the correct experimental methods for parameter determination and influent characterization.

Similarly, the choice of the parameters to be calibrated is also left to the practitioners. Important though a sensitivity analysis is proposed to identify the most sensitive parameters, which may help improving the choice of parameters subsets for calibration. However, quantitative criteria are needed to rank/choose the most sensitive parameters among each other e.g. as it is employed in Brun et al., (2002). This comment is true for all protocols where sensitivity analysis is proposed.

An important point in HSG guidelines is the proposal to use CFD as a tool in characterizing the hydraulic (mixing behavior) of the aeration tanks. This indeed could provide a better alternative to the tracer experiments proposed by all other protocols. However, a detailed procedure of using such a CFD tool is needed to facilitate the use of such a sophisticated tool. Further, it should be mentioned that the use of CFD would further complicate and extend the model calibration exercise.

At present, the HSG guidelines do not have a case study where the implementation of the protocol is illustrated on a full-scale WWTP. This would have improved the transfer of the protocol among practitioners. Overall the HSG guidelines are the only protocol which proposes a certain format for reporting the overall calibration study thoroughly, and this may indeed remarkably improve the ability to read and compare different calibration studies.

The WERF protocol

The WERF protocol lacks a structured approach to the different levels of the calibration procedure, which makes it not user-friendly to read and to follow. Further, the WERF protocol presents detailed experimental methods for influent wastewater characterization and fractionation of active biomass, yet it provides relatively few explanations and methods for hydraulic and settling characterisation of the treatment plant. It is particularly important to note that the WERF protocol misses to adequately mention/discuss the significance of biological reactions (particularly denitrification) ongoing in clarifiers and the need to consider them in the model-formulation step.

The experimental methodologies were particularly oriented at determination of nitrification parameters (particularly growth rate and decay rate of autotrophs). On one hand, this is a good point since determination of, for instance, decay rate of autotrophs was lacking in the current literature. However, the significance of the nitrification kinetics should not underestimate the significance of adequately describing the kinetics of other biological processes, e.g. denitrification, EBPR etc. Moreover, the experimental methodologies proposed to determine growth rate of autotrophs are rather laborious as opposed to, for instance, simple respirometric experiments (Vanrolleghem and Spanjers, 1998). The respirometric experiments are also more rapid and more cost-effective compared to the SBR-based procedure of the WERF protocol. In that respect, the protocol lacks to justify the selection of laborious SBR-based procedure over simpler experimental methods.

General guidelines to design a dynamic measurement campaign are proposed, however it is still plant-specific and certainly cannot readily be extrapolated to other WWTPs. In that sense, the design of a measurement campaign is left yet again to the practitioners. Moreover, the proposed length of the dynamic measurement campaign is rather short i.e. 1-2 days. This short-term is certainly not expected to adequately reflect the long-term dynamics of the plant. In that respect, the WERF protocol may imply that the model calibration results aim to catch daily dynamics of the plant rather than slower dynamics.

Overall the WERF protocol summarises a huge number of full-scale model calibration experiences. It manages also to present a so called *tiered approach* for model calibration which makes it possible for the new modellers to choose a calibration procedure depending on the objective of the goal of the calibration. A very important point in this respect, is the calibration level 2 which is based on the historical data of the plant. Such data are available for most of the WWTPs and can be used by the new modellers as a learning step before performing dynamic measurements campaign data, which is the most expensive step of the overall calibration study. In that respect, this protocol in addition to the STOWA protocol, is expected to be attractive /useful for new modellers and consultants.

Table 5bis. Strengths, Weaknesses, Opportunities and Threats (SWOT) of the different calibration protocols

	Strengths	Weaknesses	Opportunities	Threats
BIOMATH	Detailed settling, hydraulic & biological characterisation Detailed influent characterisation Biomass characterisation Sensitivity analysis/parameter selection, OED for MC design Structured overview of protocol Feed back loops	Respirometric influent characterisation requires model-based interpretation OED has not been applied yet in practice but research is ongoing OED software and specialist required No detailed methodology for data quality check No practical procedure for parameter calibration	Generally applicable Works efficiently once implemented in a simulator Dynamic measurement campaigns can be designed and compared based on OED	Not all modelling and simulation software have OED High degree of specialisation is required for the application
STOWA	Detailed settling and biological characterisation Process control Time estimate for different calibration steps Detailed data quality check Step-wise calibration of biological process parameters Structured overview of protocol Feed back loops	Not detailed hydraulic characterisation BOD test gives problems (*f*p) No biomass characterisation No guidance for MC design No detailed info on sensitivity analysis Fixed parameter subsets for calibration of biological processes	Easy to use Practical experimental methods No specialist required Good for consultants and new modellers	No mathematical/statistical approach for parameter selection for calibration May not be applicable for different systems since parameter subset for calibration may change for different WWTPs
HSG	CFD for hydraulic characterisation Biological characterisation Design of measurement campaign A standard format for documentation Data quality check Structured overview of protocol	No feed back loops Provides only general guidelines Not detailed settling characterisation No particular methods for influent characterisation or parameter estimation No detailed sensitivity analysis/parameter selection	Generally applicable A standard format for thorough documentation/reporting of calibration studies	Not detailed/practical enough for new practitioners The free choice of experimental methodologies for influent/kinetic characterisation may jeopardise standardization of calibration studies
WERF	Detailed influent characterisation Detailed μ_A and b_A determination Biomass characterisation Sensitivity analysis/parameter selection Detailed data quality check A *tiered approach* for calibration Several examples of case studies	Settling process less emphasized Almost no emphasize on other kinetic parameters of the model No structured overview of protocol	Based on practical experience A tiered approach for calibration provides different calibration levels for different goals and accuracy of calibration	Focus on μ_A determination and influent characterisation Ignoring the significance of the other compartments of the full-scale model

5.3 Calibration of ASM2/2d Model

The ASM2d model includes the enhanced biological phosphate removal processes on top of the carbon and nitrogen removal (21 processes and 19 parameters). According to the model Phosphorous Accumulating Organisms (PAOs) responsible for phosphorus removal, can store volatile fatty acids (S_A) in the form of Polyhydroxy-alkanoate (PHA) and release phosphate into the bulk-liquid in anaerobic conditions. In the presence of electron acceptors (in the presence of oxygen or nitrate), they are able to take up phosphate and consume the storage materials for their growth and phosphate sequestration. The matrix representation of ASM2d model is given in the Table 7 (Henze *et al.*, 1999).

5.3.1. Influent Wastewater Characterization

The components of the influent wastewater according to the ASM2d model are given in Table 6. The new components (and the state variables) for ASM2d are given as follows: acetic acid, S_A, fermentable substrate, S_F, for dissolved components; phosphorus accumulating organisms, X_{PAO}, stored polyphosphate in PAOs, X_{PP}, and organic storage products, X_{PHA}, for particulate components. Chemical precipitation and dissolution reactions together with the state variables ferric hydroxide ($Fe(OH)_3$), X_{MeP}, and ferric phosphate ($FePO_4$), X_{FeP}, are not included here.

Table 6. Components of the ASM2d model

Dissolved Components		Particulate Components	
S_{O2}	Dissolved oxygen	X_I	Inert non-biodegradable organics
S_F	Fermentable substrate	X_S	Slowly biodegradable substrate
S_A	Fermentation product	X_H	Heterotrophic biomass
S_{NH4}	Ammonium	X_{PAO}	Phosphorus accumulating organisms
S_{NO3}	Nitrate (plus nitrite)	X_{PP}	Stored poly-phosphate of PAO
S_{PO4}	Phosphate	X_{PHA}	Organic storage products of PAO
S_I	Inert non-biodegradable organics	X_{AUT}	Autotrophic biomass
S_{ALK}	Bicarbonate alkalinity	X_{TSS}	Particulate material as a model component
S_{N2}	Nitrogen gas (N_2), 0.78 atm at 20^0C		

In this section, the state variables and kinetic parameters regarding the PAOs will be discussed. In addition, some relevant measurements and lab-scale tests, which are necessary for the characterization, will be provided in this section. Since the ASM2d model is an extended version of ASM1 model, the characterization studies only focused on the phosphorus removal processes. The user should refer to the previous section if information is needed for other components and kinetics, which are the same as in the ASM1 model.

Influent COD fractionation

The influent COD fractionation for ASM2d is the same as the one presented for ASM1 with one exception, i.e. where the readily biodegradable COD, S_S, is sub-divided into two

fractions: volatile fatty acids (S_A) and fermentable COD (S_F). The determination of these tow sub-fractions of S_S is presented below.

Fermentation product (acetic acid), S_A

The acetic acid component can be determined directly by Gas Chromatography (GC) and/or the titration procedure (Van Vooren, 2000). Chemical Oxygen Demand (COD) measurements are not recommended due to the volatilisation characteristics of acetate.

Table 7. Matrix Representation ASM 2d model (depicted from Henze *et al.*, 1999)

Component (i) → ↓ Process (j)	1 S_{O2}	2 S_F	3 S_A	4 S_{NH4}	5 S_{NO3}	6 S_{PO4}	7 S_I	8 S_{ALK}	9 S_{N2}	10 X_I	11 X_S	12 X_H	13 X_{PAO}	14 X_{PP}	15 X_{PHA}	16 X_{AUT}	17 X_{TSS}
1 Aerobic Hydolysis		1-fsi		$\nu_{i,NH4}$		$\nu_{i,PO4}$	f_{si}				-1						$\nu_{i,TSS}$
2 Anoxic Hydrolysis		1-fsi		$\nu_{i,NH4}$		$\nu_{i,PO4}$	f_{si}				-1						$\nu_{2,TSS}$
3 Anaerobic Hydrolysis		1-fsi		$\nu_{i,NH4}$		$\nu_{i,PO4}$	f_{si}				-1						$\nu_{3,TSS}$
4 Aerobic Growth on S_F	$1-(1/Y_H)$	$-1/Y_H$										1					
5 Aerobic growth on S_A	$1-(1/Y_H)$		$-1/Y_H$									1					
6 Anoxic Growth on S_F	$1-(1/Y_H)$	$-1/Y_H$			$-(1-Y_H)$ $/2.86\ Y_H$				$(1-Y_H)$ $/2.86\ Y_H$			1					
7 Anoxic Growth on S_A			$-1/Y_H$		$-(1-Y_H)$ $/2.86\ Y_H$				$(1-Y_H)$ $/2.86\ Y_H$			1					
8 Fermentation		-1	1														
9 Lysis										f_{Xi}	$1- f_{Xi}$	-1					
10 Storage of X_{PHA}			-1			Y_{PO4}								$-Y_{PO4}$	1		
11 Aerobic storage of X_{PP}	$-Y_{PHA}$					-1								1	$-Y_{PHA}$		
12 Anoxic storage of X_{PP}					$\nu_{i2,NO3}$	-1			$-\nu_{i2,NO3}$					1	$-Y_{PHA}$		
13 Aerobic growth of X_{PAO}	$\nu_{i3,O2}$					$-i_{PBM}$							1		$-1/Y_H$		
14 Anoxic growth of X_{PAO}					$\nu_{i4,NO3}$	$-i_{PBM}$			$-\nu_{i4,NO3}$				1		$-1/Y_H$		
15 Lysis of X_{PAO}						$-\nu_{i5,NO3}$				f_{Xi}	$1- f_{Xi}$		-1				
16 Lysis of X_{PP}						1								-1			
17 Lysis of X_{PHA}			1												-1		
18 Aerobic growth of X_{AUT}	$(4.57-Y_A)$ $/ Y_A$			$\nu_{i8,NH4}$	$1/Y_A$	$-i_{PBM}$										1	
19 Lysis of Autotrophs				$\nu_{i9,NH4}$		$\nu_{i9,PO4}$				f_{Xi}	$1- f_{Xi}$					-1	
20 Precipitation						-1		$\nu_{20,ALK}$									1.42
21 Redissolution						1		$\nu_{21,ALK}$									-1.42

Fermentable substrate (acetic acid), S_F

The definition of readily biodegradable substrate, according to the ASM1 and ASM2d model is the sum of acetic acid, S_A and the fermentable substrate, S_F fractions. The expression

regarding their concentrations can be written as:

$$S_S = S_F + S_A \quad (36)$$

Then, the fermentable COD fraction can be calculated with equation Eq. 37 if S_A is previously determined:

$$S_F = S_S - S_A \quad (37)$$

Particulate COD components

The particulate components in the influent wastewater are the phosphorus accumulating organisms, X_{PAO}s, the polyphosphate stored in PAOs, X_{PP} and the organic storage products $X_{PHA.}$ The COD values of these components in the influent can be regarded as negligible compared to total influent COD. As a result, there is at present no available method for the determination of each component in the raw wastewater.

Phosphorus components

In the ASM2d model, the phosphorus component is sub-divided into two parts. The first one is the ortho-phosphate fraction available in the bulk liquid, not only playing a role as a nutrient for the ordinary heterotrophs and autotrophs but also for PAOs. The second one is the organic phosphate fraction, which is incorporated in the influent components (S_F, X_I, X_S, X_H). As a result, the total phosphorus content of the wastewater is the sum of ortho-phosphate and organically bound phosphate. The phosphorus components can be determined according to the APHA, Standard Methods (1998)

5.3.2 Stoichiometry and kinetics characterization of PAOs

In the literature, there are numerous calibration studies carried out for full-scale EBPR using the ASM2/2d model (e.g. UCT, Modified Bardenpho). The calibration of the plants is primarily based on tuning some relevant parameters related to hydrolysis and PAO kinetics which have a big influence on the effluent phosphate and COD concentration (Makinia *et al*. 2001; Dudlry *et al*., 2000; Larrea *et al*., 2001; Carette *et al*., 2001; Satoh *et al*. 2000; Cinar *et al*., 1998; Daigger and Nolasco, 1995; Kim *et al*., 2001).

Anaerobic batch release test (maximum phosphorus release test)

The magnitude of P uptake is strongly linked to the phosphorus release under anaerobic conditions (Wentzel *et al*., 1985). The phosphorus content of biomass (Bio-P sludge) can be calculated according to the method proposed by Wentzel *et al.* (1985). The anaerobic batch test should be performed with the addition of acetate (or sewage) to the mixed liquor sampled from the EBPR plant. However, the nitrate already present in the mixed liquor should be

taken into consideration (Comeau *et al.*, 1990) since ordinary heterotrophs consume part of the acetate for denitrification if nitrate is present. Therefore, an excess amount of acetate has to be injected or the sludge should be washed. In addition, the pH value of the mixed liquor should be kept constant during the experiment since the P release is influenced by the external pH (Smolders *et al.*, 1994). A typical phosphorous profile measured during an anaerobic phosphorous release test with an excess amount of acetate is given in Figure 12. The maximum phosphorus concentration can be calculated with:

$$P(t) = P_{max}\left(1 - \frac{P_{max} - P_{t=0}}{P_{max}} e^{-kt}\right) \quad (38)$$

where P(t) = phosphorus concentration at time t, mgP/l
P_{max} = the maximum potential phosphorus concentration, mgP/l
and $P_{t=0}$ = initial phosphorus concentration, mgP/l
k= first order rate constant

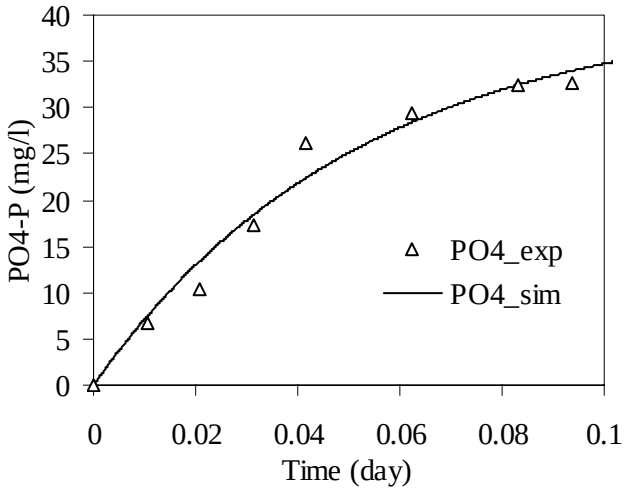

Figure 12. Phosphorus release test result

Aerobic batch uptake test (maximum phosphorus uptake test)
Aerobic (or anoxic) batch tests with oxygen (or nitrate) and orthophosphate measurements allow to estimate the kinetics of the phosphorous uptake rate of PAOs as described in ASM2d. Basically, the proposed method is based on a batch experiment conducted with the sludge sampled from a bio-P treatment plant. The sludge is first subjected to anaerobic conditions with the addition of an excess amount of acetate as described above. In the following stage the sludge is washed and aerated with the addition of certain amount of phosphate. During the aeration phase, respirometric data (nitrate in anoxic experiments) together with the filtered orthophosphate measurements are collected. The initial phosphate concentration at the start of the experiments can be adjusted using OED techniques to achieve

optimal parameter accuracy. The other parameters have to be taken as default or should be calibrated using full-scale treatment plant data.

STAGE III: Steady state calibration of the selected model

In this phase, the data from the full-scale wastewater treatment plant are averaged using a flux-based approach to obtain a good approximation to the steady state of the plant, and the model is calibrated to fit to the average effluent concentration and sludge waste data (calculated based on flux analysis). In this step, only those parameters which influence the long-term behaviour of a wastewater treatment plant (WWTP) should be modified during calibration, e.g. Y_H, b_H, f_p, X_I. Steady-state calibration is composed of two consecutive steps: (i) simple steady-state calibration (see Figure 1- Stage II/Module 8) and (ii) steady-state calibration (see Figure 1 – Stage III/Module 9). The main motivation of dividing the steady-state calibration into two complementary steps is to speed up the simulation and therefore reduce the calibration time. Indeed, the simulation of *a simple steady-state* configuration of a plant is much faster than the simulation of the *steady-state* configuration of the plant that also includes hydraulic and controller configurations (compare the plant layouts in Figure 13 and Figure 14).

In the *simple steady-state calibration* the different reactors in the treatment plant are represented by an ideal perfectly mixed tank to approximate a simple treatment plant configuration. This is illustrated in Figure 13 for a carrousel type WWTP that is studied in detail in Chapter 5.2. The calibration of the activated sludge model and the settler are linked to each other in order to describe the final effluent quality. At this stage, the interaction between the steady state calibration and the settler model calibration is taken into consideration.

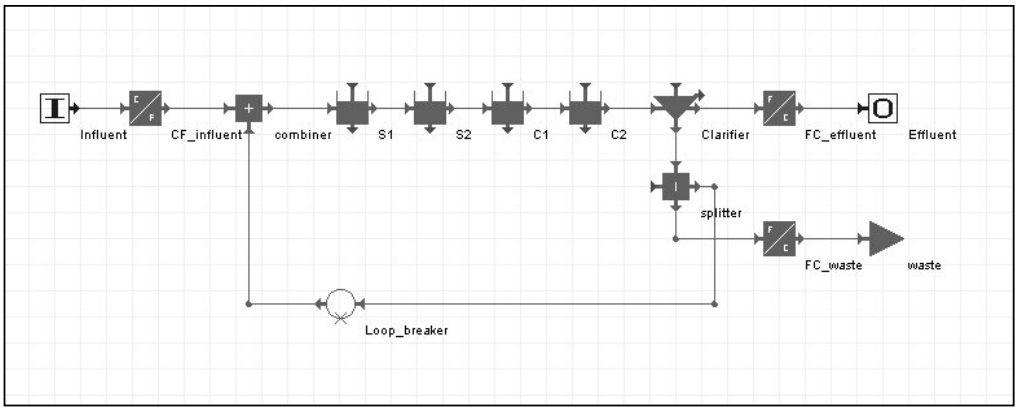

Figure 13. Plant layout for simple steady state calibration (WEST)

In the *steady state calibration,* the controllers (aeration, return and internal recycle rates etc.) and detailed hydraulic characterisation of the plant are incorporated in the model (see Figure 14 as illustrated for the same carrousel WWTP studied in Chapter 5.2). The main idea is to

estimate the appropriate biomass composition in the reactors or settler. It should be noted here that the biomass composition obtained from the steady state calibration is used in the dynamic model calibration as the initial biomass composition.

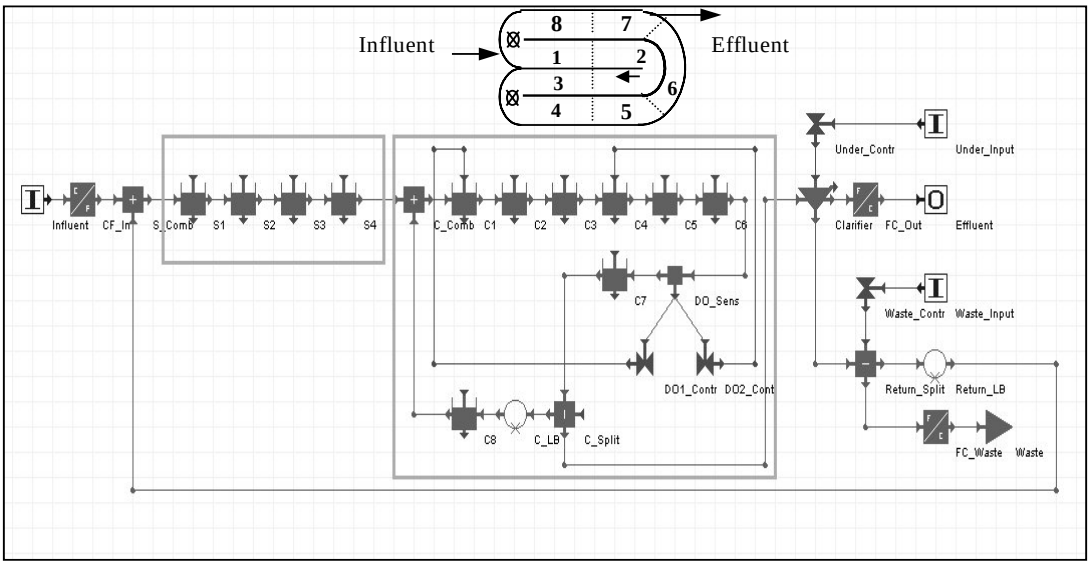

Figure 14. Plant layout implemented in WEST software

The steady state calibration is then done for each of the sub-models, i.e. the calibration of the mass transfer model (K_La), the settling model (e.g. point-settler) and the biological model (X_I, Y_H, b_H, f_p). Depending on the objectives and/or conditions of the treatment plant, these sub-models can be omitted or considered as a sub-model in the general steady state calibration task. The steady-state calibration results can be compared on the basis of averaged (flux-based) effluent COD, N and P concentrations, oxygen consumption and sludge production as mentioned above. If the simulated steady state performance is in good agreement with the data collected in Stage II or with the long-term data, the dynamic calibration of the general model can be performed. What is most important in the steady-state calibration is the accurate modelling of the sludge production. This should be in good agreement with the reality before proceeding into the dynamic calibration of the model.

STAGE IV: Dynamic calibration and evaluation of the results

In Stage IV, the dynamic calibration of the activated sludge model is performed. For the initial conditions, the biomass composition resulting from the steady state calibration in Stage III is used. The dynamic calibration of the model necessitates the availability of dynamic influent concentration profiles. A large amount of data and optimised sampling both provide sufficient information on the understanding of the system behaviour and allow a precise estimation of parameters. This should be a key point of attention in Stage II.

Now, the decision has to be made on the parameters to be estimated (i.e. kinetic or stoichiometric constants for the biological model). Further, a sensitivity analysis is necessary. It uses the dynamic influent data and the parameters obtained in Stage III. The output variables again, have to be selected upon the objectives of the modelling study or the availability and the quality of the data. For instance, if the effluent nitrate concentration is measured or the objective is the optimisation of the effluent nitrate concentration, the sensitivity functions of the parameters should be carried out with respect to effluent nitrate. In this way, one may conclude which parameters are more influential to the available effluent nitrate data. Then, the calibration of the model can be done by fine-tuning the parameters on the basis of fitting the model to dynamic data obtained from the measurement campaign. If the standard deviations for the most sensitive parameters are still quite high after the dynamic calibration, additional lab experiments could be performed. In this respect, one should refer to Stage II and Stage III for the experimental study.

The calibration can be performed manually or by using an optimiser (or parameter estimation) module available in the various wwtp simulators. The first approach is expert-knowledge driven and requires a sound insight into the system. The latter approach requires a priori information about model structure and quality of the available information obtained from the measurement campaign. In other words, it usually requires an analysis of the parameter identifiability (structural and/or practical) (Weijers and Vanrolleghem, 1997; Reichert and Vanrolleghem, 2001; Brun *et al.*, 2002; De Pauw *et al*., 2003) where the parameter sub-sets that can be reliably estimated under the available measurement campaign data are determined. From a practical application point of view, this approach is usually not preferred since it is found cost-prohibitive, tedious, time consuming and requiring special expertise for the identifiability study (De Pauw *et al*., 2003). It is therefore not surprising to see that in almost all of the calibration studies dealing with ASMs the parameters are calibrated manually.

Following the calibration of the activated sludge model, a final evaluation should be performed within the context of the objectives i.e. whether or not the objective is reached. The success of the calibrated model should be judged. If it is found that the calibrated activated sludge model does not mimic the dynamic behaviour of the system, solutions have to be investigated by re-evaluation of the plant data, the sub-models or even the targets defined in the first step. Additionally, it can be proposed that the existing model needs to be modified or that an alternative activated sludge model is used in the calibration. However, in this situation, the protocol must be followed again for the new activated sludge model.

3. DISCUSSION

The proposed methodology for activated sludge model calibration consists of modules for hydraulic characterization, settling characterization and biological characterization of the

treatment plant under study. The crucial points in this procedure are the definition of the target of the modelling study, and the selection of further necessary steps within the proposed model calibration framework. As discussed in the presentation of the procedure, the selection of the modules is dependent on the assumptions made. In addition, depending on the targets of the modelling study or the problems experienced during the data collection, the relative importance of the modules may change. Although each module is regarded as an individual section they are interrelated to each other. Thus, these interactions have to be considered to get to a model of the general behaviour of the system. For instance, if there is a problem with the hydraulic characterization, this problem will consequently influence the calibration of the biological processes/compartment. Hence, the hydraulic characterisation of the system should be improved, e.g. by considering dispersion models or using tracer studies for accurate determination of the number of CSTR tanks-in-series.

The application of the methodology is dynamic in such a way that it can be used for designing the measurement campaign or modelling the wastewater plant on the basis of the available short or long term data provided. Lab-scale, pilot-scale or on-site experiments dedicated to the assessment of certain parameters decrease the uncertainty on the parameter estimates, especially when OED techniques are used. From a modelling point of view, the steady state calibration of the model has to mimic the activated sludge performance on the long run by disregarding sudden process disturbances. Thus, long-term data are important in terms of understanding the plant performance. On the other hand, a short-term intensive measuring campaign reflects the responses under dynamic variations (e.g. diurnal load variations). As an example, it should be noted here that some disturbances such as temperature changes have to be considered during long-term simulations since they might directly affect the oxygen transfer and the biological reactions etc. There might also be short-term disturbances, e.g. inhibition, aeration controller failure, etc. These factors should also be taken into consideration. Important to realise is also that the lack of knowledge on the operational changes (mostly manually controlled activated sludge treatment plants) often introduces large uncertainties in understanding the system behaviour, which is then difficult to interpret and to consider in the final plant model.

The most important factors in modelling are the accurate influent wastewater characterization and the solids retention time (SRT) in the system. On the other hand, characterisation of the particulate fraction of the influent wastewater and the SRT of a system have been shown to be correlated. For instance, by manipulating the inert fraction of the influent one can compensate for an uncertainty in the SRT of a system. In the case of calibrating an activated sludge plant using full scale data, the uncertainty will be mostly on the influent particulate COD components (particularly X_I), if the operating SRT of a treatment plant system is not accurately known. To circumvent this problem, it is important to accurately calculate the SRT

of the system and to determine the influent inert particulate fraction of wastewater in each modelling study. The SRT can be calculated using daily sludge wastage data, which can be also checked using a mass balance of phosphate around the system. And, the influent inert particulate COD, X_I, can be determined accurately based on biological characterization, i.e. respirometric batch tests.

A sensitivity analysis can be performed in the steady state and the dynamic calibration stage to determine which subsets of parameters can be selected for the calibration of the model (Weijers and Vanrolleghem, 1997; Petersen *et al*., 2002b; Brun *et al*., 2002). The results of the sensitivity analysis vary depending on the plant configuration (e.g. Volume, recycle rates, recirculation, HRT, SRT) and controller strategy/strategies. It is important to note that the sensitivity of the parameters of a controller (e.g. on-off aeration) is often higher than the sensitivity of activated sludge model parameters.

The main issue in the validation step is to test the model by using an independent data set, which was not used in the calibration. Ideally, a separate measurement campaign data performed under different operating conditions (e.g. different season, temperature, period etc) should be used for validation of the model. However this is usually a cost-prohibitive. In case the calibrated model fails to predict the new dynamic data “reasonably” good, it is advised to iterate the calibration modules (see Figure 1). In the second iteration, the following options can be considered:

- Modification of the model structure. For example, addition of specific components and or processes to the model (two-step nitrification/denitrification, etc.)
- Apply an in-depth calibration for a particular module in the calibration protocol
    - Perform tracer studies for accurate hydraulic characterization,
    - Implement a more complex settler model (e.g. Takacs) for a better prediction of the settler performance
- Perform dedicated lab-scale experiments (preferably designed by OED principles) for accurate quantification of the biomass activity under anoxic, aerobic and anaerobic conditions.

Upon “successful” calibration and validation of the model, the calibrated model can finally be used to achieve the modelling objectives, e.g. decreasing the aeration demand, improve effluent nitrogen and phosphorous concentrations of the plant.

The BIOMATH calibration protocol and the thorough review of experimental methodologies applied for calibration of ASMs (particularly ASM1) as performed by Petersen *et al*. (2003a) indicate that:

(1) In contrast to the respirometric techniques which are well-established and most frequently used for the calibration of aerobic compartments of ASMs, there is a lack of a robust/simple sensor for quantifying the stoichiometric and kinetics parameters of sludge activity under anoxic conditions. In other words, there is no sensor available for on-line, high frequency and high quality measurement of nitrate similar to oxygen measurements by DO electrodes.
(2) The storage phenomenon may interfere with the respirometric characterization of influent S_S as well as stoichiometric and kinetic parameter estimation for activated sludge. Therefore, a model-based interpretation of respirometric profiles taking into account the storage phenomenon may be needed to evaluate the extent of storage for the activated sludge under study.
(3) The calibration of ASMs is mostly ad-hoc which makes it difficult to check its quality and to compare different calibration studies. There is a need for standardizing the calibration of ASMs, which is possible by following a systematic calibration protocol such as the BIOMATH calibration protocol proposed here.

This thesis focuses on ultimately systemizing the current calibration practices applied for simulations of full-scale WWTPs. To this aim, part of the thesis is devoted to developing an anoxic sensor that can be used to collect high frequency and quality data (similar to aerobic respirometers) under anoxic conditions (Part 1). In the following part of the thesis (Part 2), model-based methodologies also explicitly considering storage phenomenon are developed to interpret the experimental data and to transfer the parameter estimates to the full-scale model. In the remainder of the thesis, the systematic BIOMATH calibration protocol is evaluated both at full-scale and lab-scale activated sludge treatment plants. In addition to the systematic calibration protocol, a systematic optimisation protocol for application of calibrated models to optimise the operation of activated sludge treatment plants is also proposed and evaluated on a lab-scale SBR.

It is ultimately expected that the application of systematic approaches to model wastewater treatment plants will contribute to an improved reliability and objectivity of the calibration studies, thereby improving the credibility and validity of modelling and its various applications e.g. upgrade, design, reduction of operation costs, improving effluent quality etc.

4. CONCLUSIONS

For modelling wastewater treatment plants, a calibration protocol based on consolidated scientific and engineering experience is presented. The protocol is composed of a set of interactive and independent modules for the calibration of hydraulic, settling and biological characterization of the treatment plant.

The protocol is designed to provide guidelines for the new modellers in this field. The major features of the protocol are highlighted as follows:

- Objective-oriented flexible calibration protocol: The targets of modelling and the availability of the data for calibration determine the overall procedure/steps to be executed during the calibration.
- Data collection and quality is of crucial importance for a reliable calibration, hence data quality should be checked e.g. via mass balances.
- The influent wastewater characterization and the solids mass balance of the system (SRT) are essential for a successful calibration.
- The influent wastewater characterization is based on respirometric methods in contrast to physico-chemical methods.
- The OED principle is incorporated in the design of experiments (lab-scale as well as full-scale). In this way, uncertainty of the estimates of the model parameters is reduced as well as the required experimental work.
- The calibration is based on an iterative approach until reaching a “reasonably” good agreement between model results and measurements.

Further, the calibration protocol has a dynamic structure can be updated straightforwardly parallel to the new developments (new experimental methodologies etc.) in the field of activated sludge modelling.

Two major problems were also identified. First, there is a lack of robust/simple sensor to quantify the stoichiometric and kinetics parameters of anoxic sludge activity. This is mainly a technical limitation i.e. there has been no sensor available for on-line, high frequency and high quality measurement of nitrate similar to oxygen measurements by DO electrodes. Second, the storage phenomenon may interfere with the respirometric characterization of influent S_S as well as with the estimation of stoichiometric and kinetic parameters. As such the extent of the storage phenomenon should be evaluated for accurate interpretation of respirometric profiles obtained from batch experiments.

PART 1
-
DEVELOPMENT OF LAB-SCALE SENSORS/EXPERIMENTAL METHODOLOGIES

Chapter 3.1

An integrated sensor for the monitoring of aerobic and anoxic activated sludge activities in biological nitrogen removal plants

ABSTRACT

An integrated sensor is developed as a tool for monitoring the activated sludge activity on which the performance of the treatment plant depends. The sensor provides information-rich data of high frequency obtained from respirometric-titrimetric and nitrate measurements in one single set-up. The sensor is shown to successfully monitor and provide in depth insight into nitrification, denitrification and carbon source degradation processes occurring in BNR plants. Based on the experimental results it is hypothesized that the ratio of NUR to OUR rather reflects the rate of carbon source uptake (storage) under anoxic and aerobic conditions than growth process.

This chapter was published as:

Sin G., Malisse K. and Vanrolleghem P.A. (2003) An integrated sensor for the monitoring of aerobic and anoxic activated sludge activities in biological nitrogen removal plants. *Wat. Sci. Tech.*, 47(2), 141-148.

1. INTRODUCTION

Nitrogen removal is mostly accomplished through biological processes. The most commonly designed process configuration is the combination of nitrification and denitrification processes in aerobic and anoxic environments. For biological treatment, although way cheaper than its counterpart the chemical treatment, the process stability is still a major concern. Coupled with the recent demand by ever more stringent effluent criteria set by EU guidelines, process stability and performance of the biological treatment plants has been challenged seriously. Modelling and control of the biological processes seems promising to meet these challenges for biological nitrogen removal (BNR) plants. The availability of sensors able to provide online and reliable information is central to the development and further application of process control.

In this context, a number of methods and (bio)-sensors have been and still being developed. Respirometry has been shown to be a valuable technique in probing information from the activated sludge processes: e.g., monitoring activated sludge activity (Gernaey *et al.*, 2001a), determination of inhibition kinetics (Kong *et al.*, 1996), characterization of influent wastewater and estimation of biokinetic parameters of the activated sludge process (Kappeler and Gujer, 1992; Vanrolleghem and Spanjers, 1998; Vanrolleghem *et al.*, 1999; Petersen *et al.*, 2003a). Regarding the anoxic biomass activity, nitrate measurements replace the respirometric methods (McClintock *et al.*, 1988; Kristensen *et al.*, 1992; Naidoo *et al.*, 1998) where nitrate is generally measured offline using traditional colorimetric methods or autoanalyser at a low measurement frequency (around 5 – 10 min). In addition, titrimetry –an indirect measurement of pH effect of the biomass on the medium, has been well applied for monitoring and quantifying both anoxic and aerobic activated sludge activities (Ramadori *et al.*, 1980; Massone *et al.*, 1996; Bogaert *et al.*, 1997; Gernaey *et al.*, 2002a,b).

Table 1. The information matrix delivered by the integrated sensor.

Processes	Aerobic Heterotrophs	Anoxic Heterotrophs	Aerobic Autotrophs
Aerobic COD - Oxidation	OUR and HP		
Denitrification		NU and HP	
Nitrification			OUR, NP and HP

In this study, a method based on integrated aerobic and anoxic sensors is developed to monitor the entire activated sludge activity occurring in biological nitrogen removal (BNR) plants. The integrated sensor works by sequentially monitoring the aerobic and anoxic activity of the biomass. The aerobic part of the sensor is based on respirometric–titrimetric measurements (Gernaey *et al.*, 2001a) while the anoxic part of the sensor is based on nitrate–titrimetric measurements (Foxon *et al.*, 2002; Petersen *et al.*, 2002a). For nitrate measurements, an ion-selective nitrate electrode is employed to provide online, fast and

continuous data. The well-known electrode drift phenomenon of the nitrate probe (Pedersen *et al.,* 1990) is overcome by implementing the following automatic in situ calibration procedure: the initial nitrate concentration that should be added to start an anoxic experiment is dosed to the reactor in two steps: in the first step 2/3rd of the nitrate is added and this is followed by the addition of the remaining (1/3rd) nitrate. In this way, two points of nitrate versus electrode potential are available for the in situ calibration.

By merging the aerobic and anoxic sensors in one single set-up, the integrated sensor provides the information-rich matrix of data presented in Table 1. The sensor is tested for three distinctive activated sludge activities: carbon degradation, nitrification and denitrification processes. The quality of the experimental data is analysed and the titrimetric data is interpreted based on the conceptual proton production model of Gernaey *et al.* (2002a) and Petersen *et al.* (2002a).

2. MATERIALS AND METHODS

The set-up of the integrated sensor shown in Fig. 1 consists of an aeration (2.5 l) and a respiration 1 l) vessel which is made strictly airtight (Gernaey *et al.,* 2001a). A cooling system (Lauda Ecoline E303) is used to control the temperature of the reactors. Data acquisition, pH control and data processing are implemented by Labview software (National Instruments, NIDAQ 6.9 with AT-MIO-16XE-50 DAQ card and Labview 6.i). The dissolved oxygen is measured by Inpro 6100/120/T/N (Mettler Toledo) type oxygen electrodes, which are connected to Knick Process 73 and Knick Stratos 2401 oxygen transmitters respectively.

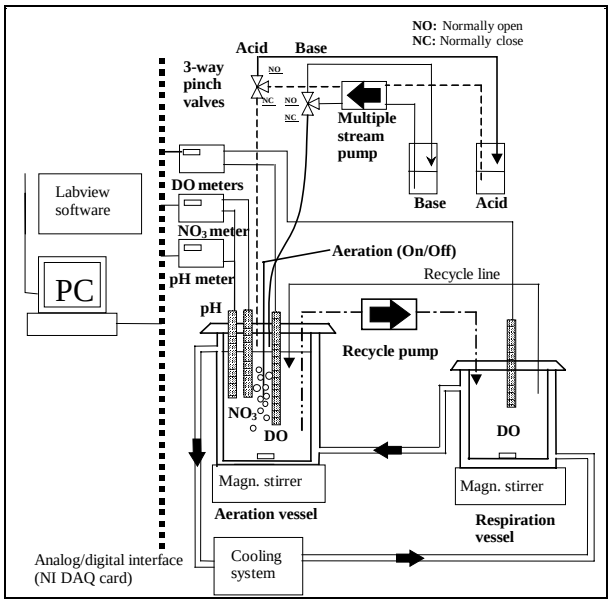

Figure 1. Illustration of the integrated sensor set-up.

The pH is measured in the aeration vessel with a HA405-DXK-S8/120 type pH electrode

(Mettler Toledo), which is connected to a Knick Stratos 2401 pH transmitter, and nitrate is measured with a type S7/120 ion-selective electrode (Mettler Toledo) in combination with a reference electrode, which are both connected to a Knick Process 73 pH transmitter.

The data acquisition frequency of the sensor is set to 3 seconds. High frequency noise known to be present in the weak analog signals of the electrodes of the set-up are filtered using a low pass Savitzky-Golay least square polynomial filter (Press *et al.*, 1992), through a Labview Matlab script node (Matlab R12, The MathWorks Inc.). The pH is controlled within a narrow pH set-band ± 0.03 as described in detail in Gernaey *et al.* (2001a).

Activated sludge monitoring methodology

For the experimental work activated sludge was sampled from a lab scale 80 l SBR reactor (Govoreanu *et al.*, 2003; Chapter 5.1). During the experiments small substrate pulses (e.g. 15-20 ml) of acetate or dextrose (10 g COD/l), ammonium (1 g N/l) and nitrate (10 g N/l) stock solutions were dosed to the activated sludge. All experiments were performed at 15.3 ±0.1 ^{0}C. The following experimental procedure is applied for on-line data collection:

1. Initialisation phase: A sludge sample (3 L) taken from the second aeration phase of the SBR is pumped into the reactor. The sample is brought into the endogenous state,
2. Aerobic experimental phase: The aerobic cycle is started by addition of a substrate sample (COD, NH_4-N). The pH is fixed to a desired level similar to the operational conditions of the plant. The duration of the cycle is 2-4 hrs depending on the S_0/X_0 ratio,
3. Anoxic experimental phase: After the aerobic cycle reaches a steady-state level (relatively constant DO), aeration is switched off. The initial nitrate concentration is measured with the nitrate probe. Nitrate is added step-wisely for in situ calibration. This is followed by addition of a COD source (e.g. acetate, dextrose) according to the desired C/N ratio (advised to be sufficiently high, e.g. 8). The duration of the experiment is 2-3 hrs depending on the C/N ratio, and
4. Discharge of the sample.

3. RESULTS AND DISCUSSION

The potential use of the integrated sensor for monitoring carbon source degradation, nitrification and denitrification processes was evaluated following the experimental procedure outlined above.

3.1 Monitoring carbon source degradation processes under aerobic and anoxic conditions

During the aerobic phase, the sensor essentially works according to the methodology of respirometric-titrimetric measurements developed and tested for activated sludge by Gernaey

et al. (2001a, 2002a). In fig. 2A and fig.2B, a typical response of activated sludge to a pulse addition of acetate and dextrose is presented respectively. As expected, the addition of the readily degradable substrate acetate induces a rapid depletion of oxygen in the reactor, which is accompanied by an increased rate of acid addition to keep the pH constant. As explained in detail in the titrimetric model of Gernaey *et al.* (2002a), 4 processes basically influence the proton concentration during the course of aerobic acetate degradation: the uptake of carbon source (for weak acids) leads to proton consumption, uptake of ammonia for growth will release protons, CO_2 production as a result of carbon source oxidation will release protons and finally the CO_2 stripping from the reactor due to aeration will consume protons from the medium. From the proton production model, it is apparent that two processes dominate the proton consumption from the medium (which is compensated by acid addition to keep the pH constant): uptake of acetate and CO_2 stripping from the medium.

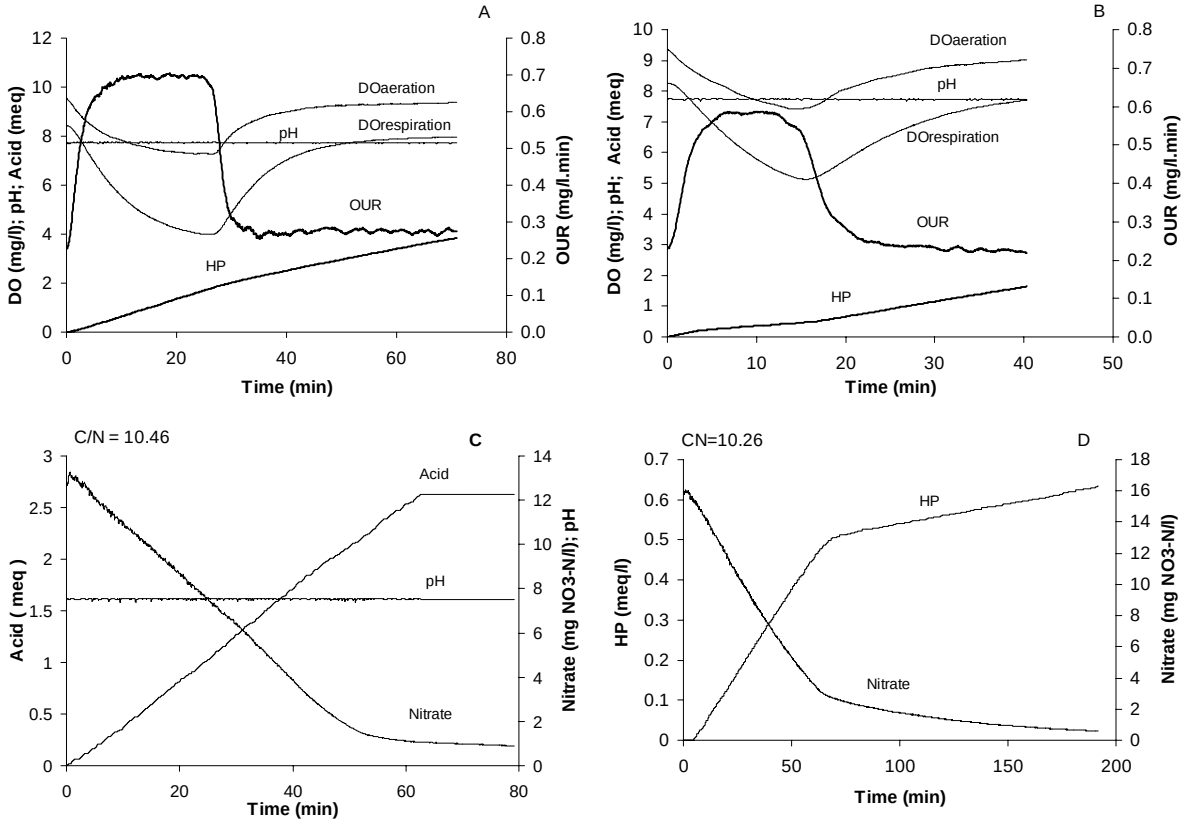

Figure 2. Typical experimental results from the integrated sensor. The aerobic phase of the sensor: 15 ml acetate addition with pH set point 7.7 (A), 15 ml dextrose addition with pH set point 7.5 (B). The anoxic phase of the sensor: acetate addition with C/N 10.46 and pH set point 7.7 (C), dextrose addition with C/N 10.26 and pH set point 7.5 (D).

In fig.2A, two acid addition rates can be discerned: one is corresponding to rapid uptake of acetate by biomass plus CO_2 stripping and the second one is the acid addition rate due to the CO_2 stripping effect. In other words, the increased rate of cumulative acid addition indicates an increased rate of acetate uptake, which ceases once all the acetate is consumed. After that

point on, the acid addition is required mainly to compensate for the proton consumption by CO_2 stripping process, which is assumed to be constant for short-term experiments (Gernaey *et al.*, 2002a). It is known, however, that the acid addition rate due to CO_2 stripping will decrease exponentially in the long term as the bicarbonate system in the medium tends to attain its equilibrium (Iversen *et al.*, 1994).

The oxygen uptake rate of the biomass attains its maximum in a very short time after the addition of the acetate. The observed transient delay (2 to 5 minutes in fig.2A) in reaching the maximum activity is typical for batch experiments and is conceived to be the start-up phenomena of the biomass (Vanrolleghem *et al.*, 1998; Chapter 4.4).

The activated sludge response to dextrose addition presented in fig.2B demonstrates the effect of the carbon source on the titrimetric profile. Contrary to the acetate addition, the uptake of dextrose (present in bulk liquid in undissociated form) induces no effect on the proton concentration in the medium. In this case, the ammonia uptake for growth and CO_2 production processes release protons to the medium, which is accompanied by a decreased rate of acid addition during the dextrose uptake phase. After all dextrose is consumed from the medium, the acid addition increases immediately to compensate for the proton consumption due to CO_2 stripping (Gernaey *et al.*, 2002a).

The response of activated sludge to pulse additions of acetate and dextrose under anoxic conditions is presented in fig.2C and fig.2D respectively. Under anoxic conditions, the denitrifying fraction of the biomass starts immediately to take up acetate (shown by acid addition in fig.2C) and use nitrate. Since CO_2 stripping is quite small (Bogaert *et al.*, 1997) during anoxic experiments but still cannot be assumed zero due to surface mass transfer, the dominant effect on the proton consumption is induced by acetate uptake. In addition to acetate uptake, uptake of nitrate and nitrite as electron acceptor will induce proton consumption from the medium too as explained in detail in Petersen *et al.* (2002a). The acid addition ceases when all the acetate is taken up from the medium (fig.2C), while nitrate reduction continues, albeit at a drastically lowered rate.

The anoxic response of activated sludge to dextrose addition is a base addition (fig.2D), in contrast to the acetate, which agrees with the proton production model of Petersen *et al.* (2002a). Apparently, in this case, the proton production processes, which are ammonia uptake and CO_2 production, dominate the proton concentration in the medium. The exogenous nitrate reduction (i.e. the nitrate reduction by exogenous carbon source) is fast and follows zero order kinetics (indicating the Monod terms for substrate and other growth limiting nutrients are close to unity). After the external carbon source (dextrose) is completely removed from the mixed liquor, as indicated by the breakpoint in the base addition profile and the nitrate

reduction curve, the base addition as well as the nitrate reduction rates continue at a lower rate for quite a long time (over 100 min). The explanation for these phenomena could be either endogenous nitrate reduction or nitrate reduction due to endogenous processes and degradation of internally stored products (Daigger and Grady, 1982). The latter seems to be plausible when considering the history of the sludge. The SBR is operated batch-wise, where the biomass is exposed to feast and famine periods. It is well observed fact that the response of activated sludge to this environment is to form storage products (Daigger and Grady, 1982; Dircks *et al.*, 2001; Dionisi *et al.*, 2001).

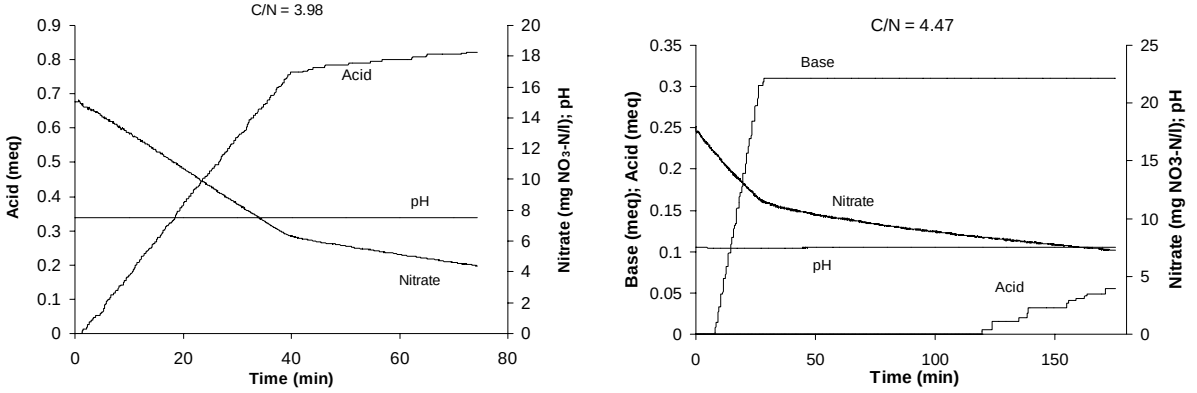

Figure 3. Anoxic activated sludge response to low COD/N conditions: acetate addition with C/N 3.98 and pH set point 7.5 (left), dextrose addition with C/N 4.47 and pH set point 7.5 (right).

The experimental results obtained at lower C/N ratios (presented in fig.3) support this hypothesis. As shown in fig.3 (right), base addition accompanies the nitrate reduction by dextrose, which ceases once the external dextrose is removed from the medium. The base addition after a pause period (a number of minutes depending on the bandwidth of the pH controller) swaps to acid addition indicating a change in the dominance of the pH affecting processes. Preliminary simulations with the conceptual proton production model of Petersen *et al.* (2002a) indicate that the endogenous process causes slight proton consumption from the medium (increase in alkalinity). Based on these arguments, it can be concluded that the activated sludge seems to reduce nitrate (and other denitrification intermediates) by the internally stored products at a quite lower rate than the exogenous nitrate reduction rate. The anoxic phase of the integrated sensor is thus able to successfully monitor the response of the activated sludge under anoxic conditions for various substrate sources including storage phenomena.

3.2 Anoxic reduction factor of heterotrophic growth

The anoxic growth reduction factor (Henze *et al.*, 1987), becomes identifiable straightforwardly with the online information obtained from the integrated sensor by comparing the aerobic (OUR) and anoxic heterotrophic activities (NUR) as follows: $\eta_g = 2.86$

x NUR/OUR. Where NUR is the nitrate uptake rate of the biomass, determined from the derivative (slope) of the nitrate uptake curve. The η_g for acetate and dextrose is found to be 0.953 and 1.06 respectively. The results suggest that the biomass is very well able to denitrify under anoxic conditions.

Table 2. Anoxic activated sludge monitoring results for exogenous and endogenous processes

	Exogenous		Endogenous	
	NUR (mg NO_3-N/l-min)	HPR (meq H^+/min)	NUR (mg NO_3-N/l-min)	HPR (meq H^+/min)
Acetate (high C/N)	0.2347	-0.0439	-	-
Acetate (low C/N)	0.22578	-0.01978	0.05356	-0.0016
Dextrose (high C/N)	0.21935	0.02537	0.02939	0.0034
Dextrose (low C/N)	0.2275	0.01229	0.0261	0

The nitrate uptake rate of biomass (NUR) given in Table 2 is observed not to change under high and low C/N ratios, which seems reasonable as the major fraction of the biomass is expected to favour carbon source uptake under aerobic and anoxic conditions rather than growth (Daigger and Grady, 1982; van Loosdrecht and Heijnen, 2002). In fact, considering the anoxic reduction factor (the ratio of NUR to OUR) is approximately 1 implies that the growth is not affected under anoxic conditions. However, model based interpretation of aerobic and anoxic data (results not shown) showed that the yield coefficient under aerobic and anoxic conditions is considerably higher than the accepted default value of 0.67 for heterotrophs (Henze *et al.*, 1987). Under these conditions, the comparison of NUR and OUR will not truly reflect the anoxic growth reduction. Rather, it is expected to determine the ratio of NUR to OUR dominated by the storage rate under anoxic (Dionisi *et al.,* 2001) and aerobic conditions (Dircks *et al.,* 2001). Therefore, it may seem reasonable to conclude that the uptake rate of carbon source remains equal in aerobic and anoxic conditions. It is also observed that the NUR after the external carbon source is removed from the medium is different for experiments with acetate and dextrose. This suggests that the utilisation rate of stored products with dextrose is slower than that of acetate. This is in accordance with the findings of Dircks *et al.* (2001). It is clear that these arguments need to be confirmed with dedicated experiments.

However, it is not clear as to why the proton production rate determined from the slope of the cumulative acid (acid addition means proton consumption) or base addition (proton production) curves (HPR) is halved for low C/N ratios. This point is currently investigated with a mathematical model developed to simulate the experimental results.

3.3 Monitoring simultaneously nitrification and carbon source degradation kinetics

Combining the nitrate electrode with the respirometric-titrimetric measurements offers the opportunity to monitor the nitrification and carbon degradation processes in a single

experiment as presented in fig.4, in this way excluding the need to perform at least two independent experiments (one with nitrification inhibitor (e.g. ATU) addition and the other without inhibiting the nitrifiers (Kong *et al.,* 1996)). Cross-analysing the OUR, titrimetric data and nitrate shows that the acetate uptake and the nitrification start immediately and reach their maximum conversion rate after a start-up phenomenon. The additional availability of nitrate measurements provides an independent observer that can be used to at least qualitatively check the results of simultaneous carbon source degradation and nitrification kinetics.

The titrimetric profile obtained from this experiment confirms the proton production model of Gernaey *et al.* (2001a, 2002a). During the first phase, increased acid addition occurs due to rapid acetate uptake (see fig.4). In the second stage, no acid and base addition is necessary due to the equilibrium between two competing pH-affecting processes: ammonium oxidation (first step nitrification) releases protons that are compensated by the proton consumption due to CO_2 stripping. Soon after the endpoint of the 1st step nitrification (see fig.4), the acid addition is resumed due to the CO_2 stripping effect.

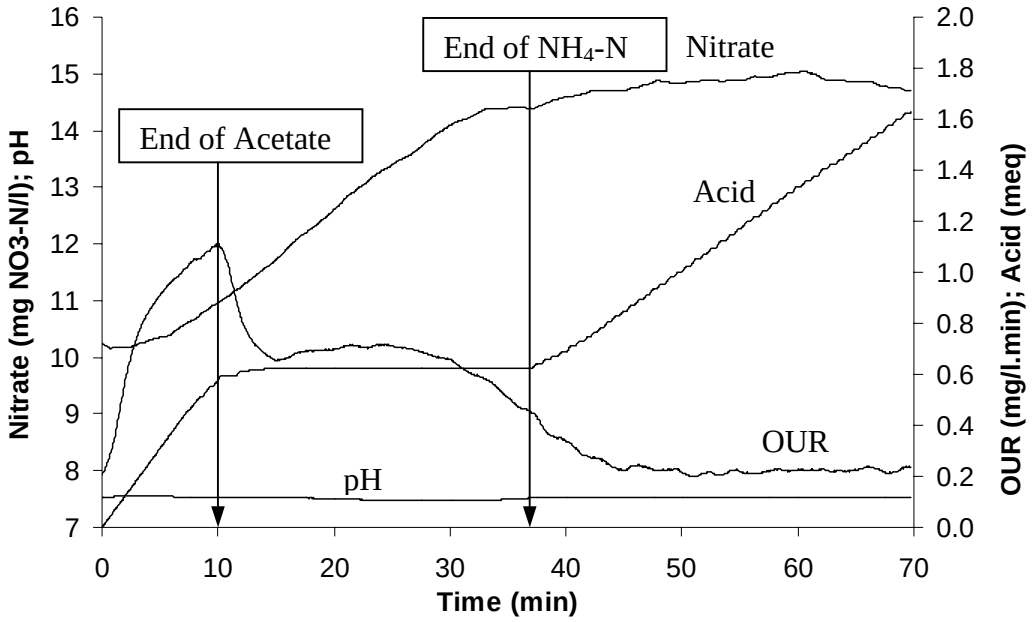

Figure 4. Monitoring carbon source degradation and nitrification processes in single batch reactor: pulse addition of 8.5 ml acetate and 15 ml ammonium nitrogen with pH-set point 7.5.

4. CONCLUSIONS AND PERSPECTIVES

The integrated sensor developed here essentially is a tool for monitoring activated sludge activities occurring in BNR plants in a single set-up. The integrated sensor is shown to successfully monitor nitrification, denitrification and aerobic carbon source degradation processes. The information rich matrix of data (OUR, HP and NU or NP) provided by the integrated sensor can be used to quantify and estimate activated sludge activities.

Furthermore, each independent measured variable can be used as an internal check for the quality of the experimental results. The information provided by the sensor (titrimetry mainly monitors the carbon source uptake while OUR and NU monitor the energy generation of the biomass) is shown to be equally powerful in studying the quite significant storage response of the activated sludge in batch experiments for anoxic and aerobic conditions. The conceptual proton production model proposed elsewhere was shown to explain the titrimetric results well. Based on the experimental results it is hypothesized that the ratio of NUR to OUR rather reflects the rate of carbon source uptake (storage) under anoxic and aerobic conditions than the energy generation process. This reduction factor was close to 1 for the activated sludge under study, which means that carbon source uptake was similar in both conditions.

5. ACKNOWLEDGEMENT

The research was financially supported by the European Community EESD EVK1-CT-2000-00054.

Chapter 3.2

A nitrate biosensor based methodology for monitoring anoxic activated sludge activity

ABSTRACT

An improved methodology based on a nitrate biosensor is developed and applied successfully for in-depth monitoring and study of anoxic activated sludge activities. The major advantages of the methodology are its simplicity, reliability and high data quality. The resulting data allowed for the first time to monitor anoxic respiration rate of activated sludge (nitrate uptake rate (NUR)) at a high time resolution making it clearly comparable with high frequency oxygen uptake rate (OUR) measurements obtained under aerobic conditions. Further, the anoxic respiration data resulting from a pulse addition of carbon source to endogenously respiring anoxic activated sludge shows a clear start-up phenomenon and storage tail that is usually also observed in high-frequency OUR measurements. Finally, the improved methodology can be expected to serve as an anoxic respirometer for activated sludge treatment plants where denitrification process occurs in single-step. Further, it can be used for a variety of purposes e.g. for anoxic activity monitoring, process control and parameter estimation of the activated sludge process, similar to the aerobic respirometers.

The main part of this chapter was presented as oral presentation in AutMoNet2004:
Sin G. and Vanrolleghem P.A. (2004) A nitrate biosensor-based methodology for monitoring anoxic activated sludge activity. In proceedings: *2nd IWA* conference on Automation in Water Quality Monitoring (AutMoNet2004), April 19-20, Vienna, Austria, pp 61-68.

1. INTRODUCTION

Techniques and methods currently available to study the anoxic respiration rate of the biomass defined as nitrate uptake rate (NUR), are rather limited and under-developed compared to the tools available for studying the aerobic processes. One example is respirometry, the measurement of the oxygen uptake rate (OUR) of the biomass (Spanjers *et al*., 1998). It has been shown to be a powerful tool to study in-depth the aerobic processes for various purposes: monitoring toxicity (Kong *et al*., 1996), characterisation of wastewater, estimation of kinetics and stoichiometric parameters (Vanrolleghem *et al*., 1999) and control (Spanjers *et al*., 1998).

The major limitation to obtain an equally popular tool for monitoring anoxic respiration has been mainly technical (Lynggaard-Jensen, 1999). In other words, a reliable, simple and on-line sensor for the measurement of nitrate at least as powerful as oxygen electrodes used in respirometry was not available. The anoxic respiration rate has been usually measured using automatic analysers based on colorimetric methods (Kristensen *et al*., 1992; Naidoo *et al*., 1998) or ion chromatography (McClintock *et al*., 1988) with 10–35 minutes of measurement interval. However this is not sufficient to adequately monitor process dynamics that is often occurring at the minute scale (Chapter 4.4). Recently, several other methods were developed for on-line and reliable in situ measurement of nitrate based on various principles (Lnyggaard-Jensen, 1999): potentiometric, e.g. ion selective electrode (ISE) (Rieger *et al*., 2002), photometric, e.g. UV-based sensors (Langergraber *et al*., 2003b) and biosensors (Larsen *et al*., 2000).

Each technique has limitations as well as advantages. The bottleneck of UV-based nitrate measurements is the likely interference of organic compounds present in the complex matrix of wastewater to the nitrate absorbance at 205 nm (Lynggaard-Jensen, 1999). In order to overcome this interference, tedious and sophisticated calibration techniques (Roig *et al*., 2003; Langergraber *et al*., 2003b) are usually required in which interfering organic compounds are compensated for by performing UV measurements at different wavelength of the absorbance spectrum (Lynggaard-Jensen, 1999).

The principle of the potentiometric sensor is to measure the difference between the potential of a reference electrode and an ion-selective electrode that is usually log-linear to the concentration of the target ion, in this case nitrate (Rieger *et al*., 2002). A previously developed anoxic activated sludge monitoring methodology was based on an ion-selective nitrate electrode (Chapter 3.1). Long-term experience/working with this type of ion-selective electrode showed that the slope of the electrode drifts usually in a rather random and unpredictable way and even during the course of a relatively short (less than 1 hour) batch

experiment (Petersen *et al*., 2002a; Malisse, 2002). Moreover, it was rather sensitive towards ionic strength of the medium particularly to the nitrite concentration (Malisse, 2002). Further, the sensor signals were not log-linear to nitrate concentrations in the lower range, particularly below 2 mgN/l (Malisse, 2002). The frequent drift problem of the slope of the ISE electrodes was previously reported too (Pedersen *et al*., 1992; Petersen *et al*., 2002a). Based on this long-term experience, it appeared that this type of nitrate sensor was not sufficiently advanced to live up to the high requirements for a robust nitrate sensor.

The main motivation of this study is to develop a more robust, simple and reliable anoxic methodology for the monitoring of activated sludge based on the previously developed anoxic methodology (Chapter 3.1). Particularly, the aim is that the methodology can be used as a reliable anoxic respirometer that provides high frequency (on-line) and high quality data to be used for a variety of purposes (mentioned above). To this aim, the ion-selective nitrate electrode of the previous methodology (Chapter 3.1) is replaced with a novel nitrate measurement technique, a nitrate biosensor, demonstrated to provide reliable, online and fast measurements (Larsen *et al*., 2000). The paper is structured as follows: first, the step-response of the biosensor, which is a significant property of a sensor in view of high-frequency measurements, is analysed. This is followed by a rigorous analysis of the slope of the biosensor in relation to its robustness/stability. Further, the improved methodology will be applied to different activated sludge samples for the monitoring of anoxic activity. Finally, the results of the anoxic respirometer will be compared to the result of an aerobic respirometer for the same activated sludge.

2. MATERIALS AND METHODS

The anoxic respirometer developed in this study is shown in Fig. 1. The set-up consists of a 1 L reactor with thermal jackets for temperature control by a cooling system (Lauda Ecoline E303). Data acquisition, pH control and data processing are implemented by Labview software (National Instruments, NIDAQ 6.9 with AT-MIO-16XE-50 DAQ card and Labview 6.i). The nitrate is measured by a biosensor shown in Fig. 1 (right) (Unisense, Denmark) and connected to a picoammeter (Unisense, Denmark) where the raw signals (nA) of the nitrate biosensor are amplified (mV) and sent to the DAQ card.

The principle of the biosensor is simply that nitrate in the medium diffuses through the nitrate ion selective membrane into the biochamber. The nitrate is then reduced to nitrogen dioxide (N_2O) by specialised bacteria, which is then measured by a Clark-type N_2O transducer (Larsen *et al*., 2000). The pH is measured in the aeration vessel with a HA405-DXK-S8/120 type pH electrode (Mettler Toledo), which is connected to a Knick Stratos 2401 pH transmitter. The data acquisition frequency of the sensor is set to 3 seconds. High frequency

noise known to ride on top of the weak analog signals of electrodes were filtered using a low pass Savitzky-Golay filter (Chapter 3.1) with central moving window size 11 and polynomial order 1. The pH is controlled within a pH set-band ± 0.03 as described in detail in Gernaey *et al.* (2001a).

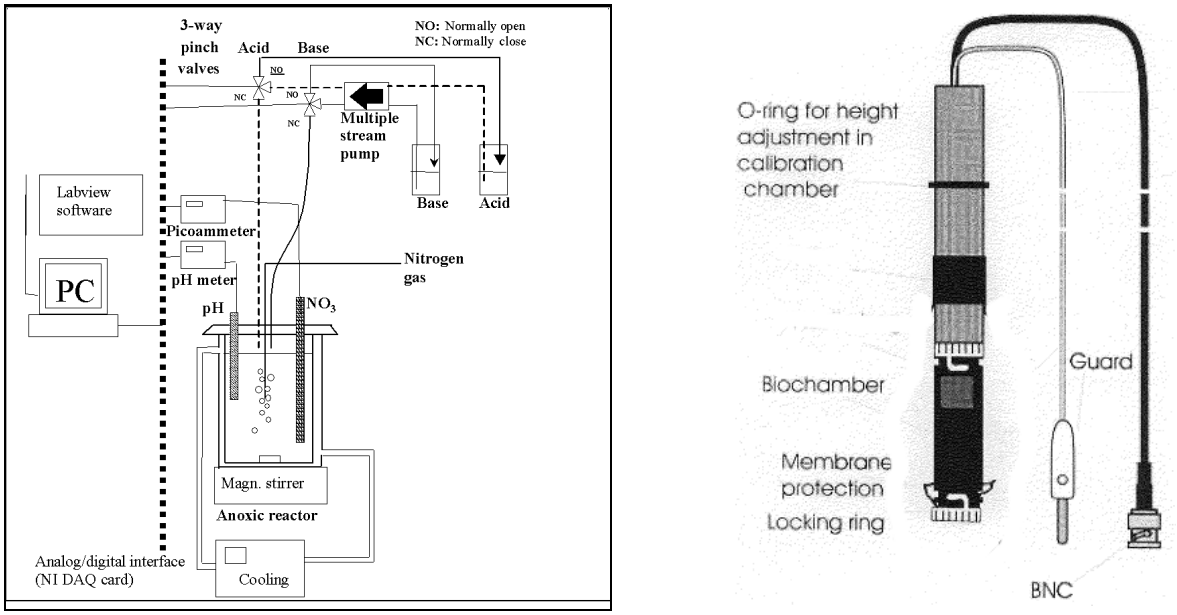

Figure 1. Illustration of the anoxic respirometer (left) Nitrate biosensor (right)

Activated sludge monitoring methodology

For the experimental work activated sludge was sampled from either a pilot scale 80-l SBR reactor (Chapter 5.1) or Gent-Ossemeersen WWTP receiving mainly domestic wastewater (Aquafin, Belgium). During the experiments small substrate pulses of acetate (10 g COD/l), nitrate (1 g NO_3-N/l) and ammonium (1 gNH_4-N/l) stock solutions were dosed to the activated sludge. All experiments were performed at 20 ±0.1 ^{0}C. The following procedure was applied during the anoxic experiments:

(1) Transfer 900 ml fresh sludge sample into the anoxic reactor.
(2) Aerate the sludge sample over-night.
(3) Stop aeration and provide N_2 gas to ensure anoxic conditions.
(4) Wait for 20-30 min to determine the anoxic endogenous baseline.
(5) Add 5 mg NH_4-N to ensure no ammonia limitation for growth.
(6) Add nitrate (NO_3-N) step wisely for in-line calibration.
(7) Add acetate as carbon source according to certain C/N ratios.
(8) Take regular samples for off-line nitrate/nitrite measurements.

3. RESULTS AND DISCUSSION

3.1 Step response of the nitrate biosensor and reconstruction of true nitrate concentration

Every sensor has a transient dynamic response to a step change in the physical quantity under measurement, e.g. nitrate (see e.g. for DO sensors in Lee and Tsao (1979)). It is, therefore, important to identify and account for the dynamic response of the biosensor to prevent measurement errors. This is especially significant in studies dealing with the determination of the kinetics of the biological processes (Chapter 4.4). To this aim, the step-response of the nitrate biosensor was analysed and shown in Fig. 2(left) for two different nitrate pulse additions (3.45 and 6.9 $mgNO_3$-N/l). Similar to the oxygen electrodes (Lee and Tsao, 1979), the response of the biosensor can be modelled by a first order model (see Eq.1 and Fig.2 (right)):

$$E_{real}(t) = E(t) + \tau \bullet \frac{dE(t)}{dt} \qquad \text{Eq. 1}$$

$$E(t) = A \bullet \left(1 - e^{-t/\tau}\right) \qquad \text{Eq. 2}$$

Where $E_{real}(t)$ is the ideal output of the nitrate biosensor ($mgNO_3$-N/l), $E(t)$ is the output of the nitrate biosensor ($mgNO_3$-N/l), τ is the first order time constant of the nitrate biosensor (min) and t is time (min). The time constant of the biosensor, τ, can be estimated using Eq. 2 which is valid for a step-increase in nitrate concentration. In Eq.2, A is a constant referring to the ideal output of the biosensor after nitrate pulse addition ($mgNO_3$-N/l). With Eq.2 the model fit to the biosensor output is shown for the first nitrate pulse in Fig.2(right). Using non-linear regression, the time constant was determined to be 0.31 ±0.01 (min) (where A was also simultaneously estimated and found to be 3.39±0.04 $mgNO_3$-N/l). The time constant of the nitrate biosensor is in the same order of magnitude as that of oxygen electrodes (Lee and Tsao, 1979; Chapter 4.4).

The reconstruction of the true nitrate measurements using Eq.1 is also shown in Fig.2 (right). From a practical application point of view, the results are acceptable and show that it is possible to approximate the actual nitrate concentrations in the medium.

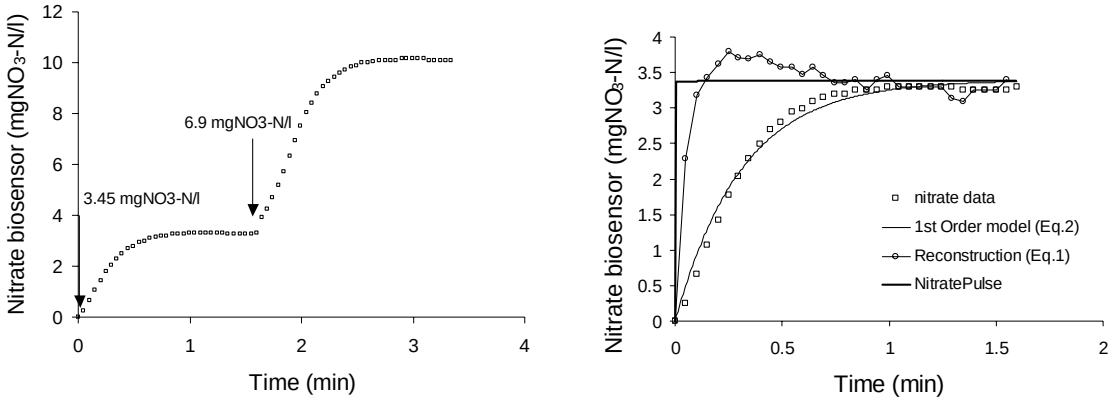

Figure 2. Step-response of the nitrate biosensor to 2 consecutive additions of known nitrate pulses (left), first order model prediction (Eq.2) fitted to the first step response and reconstruction of the real nitrate concentration in the medium (using Eq.1) (right).

3.2 Slope of the nitrate biosensor: In-line calibration

In contrast to ion-selective that show log-linear behaviour, the biosensor provides mV signals linearly proportional to the nitrate concentration in the medium (Larsen *et al*., 2000) and has no intercept i.e. absence of nitrate gives a 0 mV signal. Nitrate is therefore obtained simply by multiplying the biosensor signals with its slope. The accurate estimation of the slope is therefore essential to obtain accurate nitrate measurements. Equally significant is the stability/drift of the slope for short-term (during an experiment) and long-term applications. With this in mind, the drift/stability of the biosensor's slope were studied in two different activated sludge samples: a pilot-scale SBR and the Ossemeersen WWTP.

The slope of the biosensor in the activated sludge from pilot-scale SBR was found to be higher than the slope in the sample from the Ossemeersen WWTP (almost twice, see Table 1). The reason of this change in the characteristics of the biosensor in different samples could be due to the differences in composition of the samples e.g. salinity (Manual, Unisense). However it is beyond the scope of this study to go into detail on the causes. In short, the biosensor should be calibrated in the medium in which it is being used.

Table 1. The slope of the biosensor in experiments with different activated sludge samples

Activated Sludge Source	Slope mV/(mgN/l)	Drift (%/day)
Pilot-scale SBR	0.022	-32% over 12 days (-2.68%/day)
Ossemeersen WWTP	0.013	-14% over 3 days (-4.65%day)

The slope of the biosensor was observed to drift in time albeit at a different rate depending on the activated sludge (see Fig.3 for activated sludge from SBR). In comparison, the slope and the offset of the ion-selective nitrate electrode used in the previous methodology (Chapter 3.1) was also monitored for long-term in the same pilot-scale SBR (Malisse, 2002).

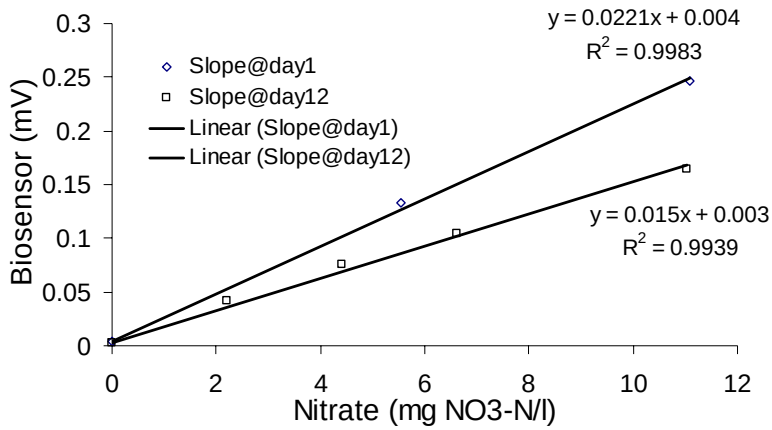

Figure 3. Drift of the biosensor slope in SBR sludge.

It was clearly observed that the drift in the slope of the ion-selective electrode is rather random and chaotic with no specific pattern and ranging between 45 and 75 mV/log(NO_3-N/l) on consecutive days (results not shown). Moreover, the offset of the ion-selective electrode was rather high and changing randomly between 230 – 280 mV (results not shown). In contrast, the drift in the slope of the biosensor is rather stable/predictable in the sense that it is decreasing linearly in time. Moreover, the offset of the biosensor was observed to be rather stable and almost zero (between 0.003 – 0.004 mV) in different activated sludge samples. A regular calibration therefore seems appropriate to deal with the drift for the biosensor.

It is important to note that in combined nitrate-titrimetric experiments, the ionic strength of the medium may change slightly due to, for instance, continuous addition of acid (see Fig.4). This was also observed to affect the slope of the biosensor (results not shown) but could also be compensated for appropriately with the in-line calibration that is available in each pulse addition of nitrate.

3.3 Application of the improved methodology

The improved anoxic methodology was applied to the pilot-scale SBR to study the anoxic response of activated sludge to pulse additions of carbon source (see Fig.4). From now on, the presented nitrate measurements are all corrected for the response time of the biosensor and for the slope drift. The nitrate uptake rate (NUR) indicating the denitrification activity of the biomass is calculated as follows (similar to the calculation of OUR in LSS type respirometers (Spanjers *et al*., 1998)):

$$NUR = -\frac{dNO_3}{dt} \qquad \text{(Eq.3)}$$

where the right hand side is the derivative of the nitrate concentration which is calculated by taking the slope of the nitrate profile using a central moving window approach with 3 data points.

The response of the endogenously respiring biomass to the first pulse addition of substrate (see Fig.4) shows that the maximum nitrate uptake rate (NUR_{max}) is reached following a fast transient response taking 2-3 minutes to complete. This transient phenomenon is often observed in OUR from similar batch experiments (Chapter 4.4). Further, after the external carbon source is removed completely from the medium (this is indicated by a strong bending point in the nitrate and acid addition profiles see Fig.4 (left)), NUR decreases drastically to a level clearly higher than the previous endogenous level (see Fig.4 (left)). This elevated endogenous level implies that the nitrate reduction continues at a rate higher than the endogenous rate probably using intracellular storage polymers produced during the feast phase (Beun *et al*., 2000b; Van Loosdrecht and Heijnen, 2002). The sharp decrease (around 80%) in the denitrification rate of the biomass when the external carbon source is depleted is noteworthy. It clearly indicates the bottleneck of denitrification i.e. the availability of a readily biodegradable carbon source. Further on, the endogenous level drops to zero when all nitrate is removed from the reactor (around t=250 min., Fig.4 (left)). Moreover, it is worth to mention that the anoxic response of biomass to the pulse addition of acetate is repeated in a similar way in the following two pulse additions, with one exception: In the third pulse addition NUR reaches a maximum plateau implying that the previous two acetate pulse additions induced a wake-up effect on the biomass as discussed in Vanrolleghem *et al*. (1998) for OUR. This issue is addressed further below.

Similar results were obtained and discussed with the previous version of the anoxic methodology (Chapter 3.1). However, the significance of the modification presented in this paper is its high-quality nitrate measurements, which enable much higher-quality NUR calculation thereby improving the quality of the anoxic activated sludge monitoring. In addition, the nitrate biosensor provides linear signals and can also measure at the low concentration range as opposed to the log-linear signals of the ion-selective electrode in the previous methodology that were practically limited to concentrations above 2 $mgNO_3$-N/l. As a result, the biosensor enables to study/estimate nitrate affinity constants of biomass, which was not possible with the ion-selective electrode used in the previous methodology. Moreover, it is easy to calibrate the biosensor and convert its signals into the nitrate data. Finally, although the drift in the slope of the biosensor exists, it is predictable (see above) which allows it to be compensated for appropriately by in-line calibration in contrast to the chaotic drift in the ion-selective electrode.

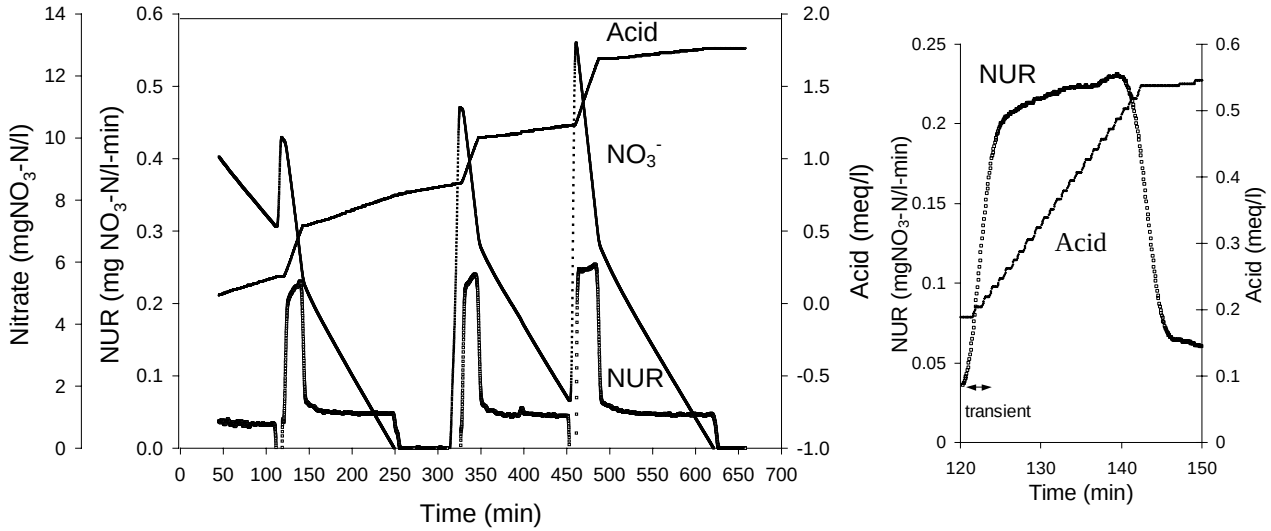

Figure 4. Anoxic monitoring of pilot-scale SBR sludge with 3 consecutive pulse additions: (10 $mgNO_3$-N + 30 mgCOD), (11 mg NO_3-N+ 30 mgCOD) and (12.5 mgN + 40 mgCOD). NO_3, NUR and titrimetric data (left) Transient response in NUR zoomed from the first pulse addition (right).

For the interpretation of the titrimetric data, the conceptual model developed and described in detail elsewhere (Petersen *et al*., 2002a; Chapter 3.1) is used. The conceptual model in general takes into account various pH effects of biological and physico-chemical processes occurring during anoxic batch experiments. In the endogenous period before the first pulse addition, a linear acid addition rate (i.e. proton consumption rate) is observed (see Fig.4) mainly to compensate for the protons removed due to CO_2 stripping by the nitrogen gas. Upon pulse addition of acetate, the acid addition rate is immediately increased (see Fig.4 (left)). This is mainly required to compensate for the immediate uptake of the acetate, which is accompanied by removal of protons from the medium (by stoichiometry, each mmol of acetate removed consumes approximately 1 mmol of proton from the medium, see Petersen *et al*. (2002a) and Chapter 3.1. During the feast period, i.e. in the presence of the external carbon source, the acid addition rate is maximum and linear in time; however, the acid addition rate decreases drastically to a lower rate similar to the previous level i.e. during the famine period. The titrimetric data is also observed to produce reproducible results in 3 consecutive pulse additions of acetate. For the famine period, however, the titrimetric data show a slow-down in the rate due to the reduction in the CO_2 stripping process (rate).

The nitrate and titrimetric data are observed to display different dynamics about the denitrification process. The acid addition is immediately started after pulse addition of substrate but a transient is clearly shown in the NUR data (see Fig.4 (right)). The same phenomenon was also observed in combined OUR-titrimetric measurements (Gernaey *et al*., 2002a; Chapter 4.4). The difference in the observed dynamics is hypothesised to be resulting from the substrate metabolism of the cell where substrate uptake is an earlier process in the

metabolism than the nitrate uptake. The experimental results obtained here further support the aforementioned hypothesis developed in Chapter 4.4 as it is obtained here under anoxic conditions.

3.4 Comparison of NUR and OUR under high resolution

In Fig.5, the anoxic respiration rate (NUR) is compared with the aerobic respiration rate (OUR) of the sludge from the Ossemeersen WWTP. The aim is to compare the performance of the anoxic respirometer developed in this study with a well-established aerobic respirometer (Chapter 3.1). The NUR was obtained using the methodology described above with C/N equal to 1 while the OUR was obtained with a pulse addition of 46.88 mgCOD /l acetate following the methodology and the respirometer described in Chapter 3.1. Biomass concentrations in both experiments were significantly different, 6800 versus 2700 mgVSS/l for aerobic and anoxic tests respectively. The data frequency and quality of NUR is the same as the OUR. These results firmly suggest that the anoxic respirometer developed in this study is an equally powerful tool as the aerobic respirometer.

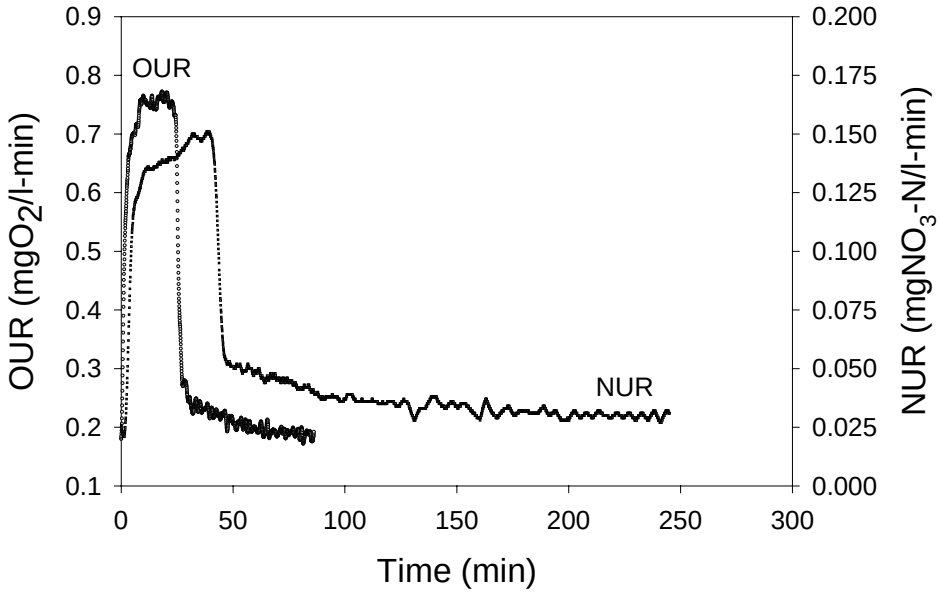

Figure 5. Comparison of OUR (46.88 mgCOD/l) and NUR (38.89 mgCOD/l) for the Ossemeersen sludge

Further, the anoxic set-up is ready to meet the high requirements for reliable, robust and accurate determination of respiration rate under anoxic conditions. It is observed that the pattern of acetate degradation is similar under aerobic and anoxic conditions under feast and famine periods albeit, as expected, that the rate and the stoichiometry of the processes are different. However, no rate and stoichiometric comparison is made between OUR and NUR here, as it is part of Chapter 4.

3.5 Comparison of the dynamic response of biomass under aerobic and anoxic conditions

The high-frequency and quality NUR measurements enable to study and compare the dynamics of anoxic activity of activated sludge with the dynamics of aerobic activity observed in OUR obtained from batch experiments conducted under similar conditions (see Figure 6). The NUR measurements were obtained as explained above whereas the OUR measurements were obtained from pulse addition of acetate to endogenously respiring activated sludge (not fed during 12 hours) (Vanrolleghem *et al.*, 1998).

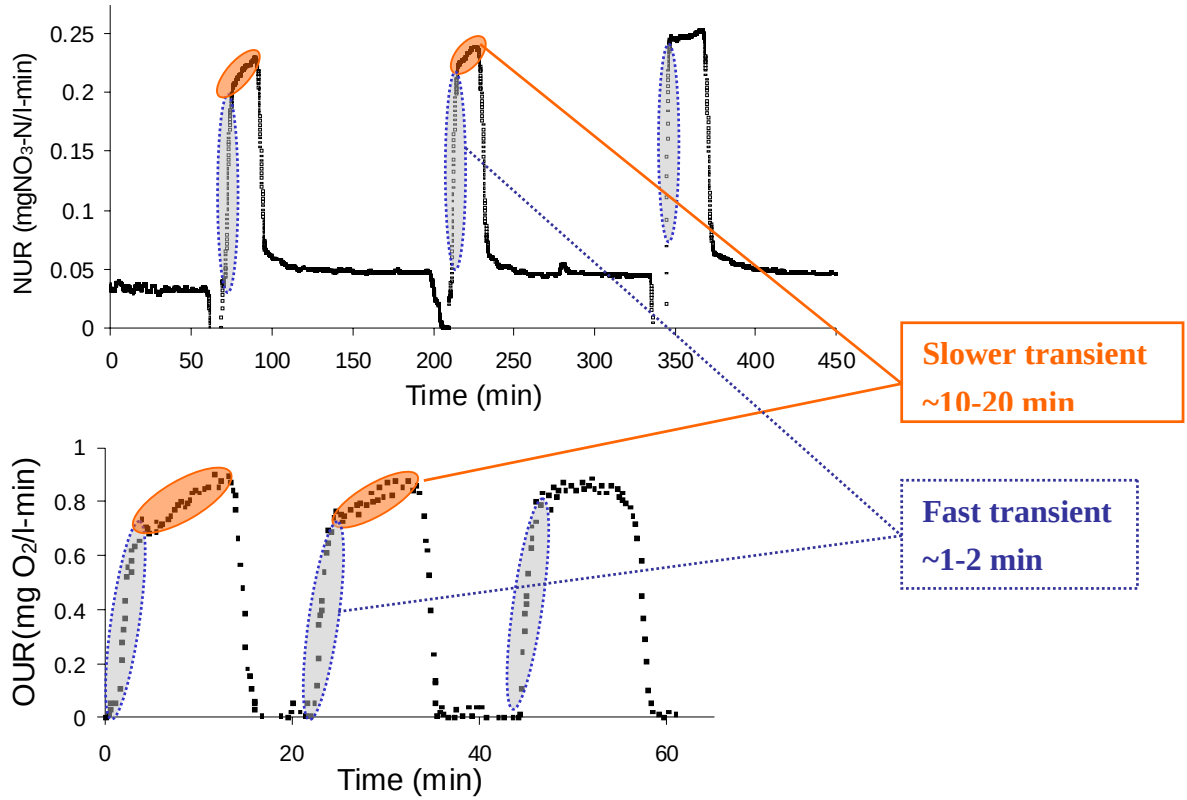

Figure 6. Dynamic response of activated sludge under anoxic conditions (top) and aerobic conditions data taken from Vanrolleghem *et al.*, 1998 (down). See the text for explanation.

Two transient phenomena, with fast and slower dynamics respectively were observed both in NUR and OUR measurements (see Figure 6). The fast transient occurs every time right after the pulse addition of acetate, and takes around 2-5 minutes. It is encircled with the dashed ellipsoid in Figure 6. This fast transient is observed in many OURs obtained from batch experiments (Chapter 4.4). Referring to studies dealing with dynamic metabolic network modelling of pure cultures, in Chapter 4.4 it was hypothesized that the way substrate is metabolised at the cellular level may lead to this observed transient.

The slower transient, on the other hand, is observed to take place right after the fast transient and it may continue until all the acetate is taken up by biomass (indicated with bold circles in Figure 6). However, this slower transient is observed to disappear after, in these two examples, two consecutive pulse additions of acetate (see Figure 6). This indicates that the order of magnitude of this slower transient is around 10-20 minutes. The observed time constant in the order of 10 minutes can be explained by RNA regulation at the cellular level as discussed in detail in Vanrolleghem *et al*. (1998) referring to Roels (1983).

In short, the observed dynamic responses of activated sludge activity to pulse addition of acetate under anoxic (NUR) and aerobic (OUR) conditions are similar. This is in accordance with the findings of Beun *et al.* (2000a,b) based on studies dealing with metabolism of acetate and degradation of storage products under aerobic and anoxic conditions.

3.6 Limitation of the improved methodology

The application of the improved anoxic methodology has one significant limitation due to a drawback of the biosensor. It is the fact that the biosensor measures both nitrate and nitrite. In fact, the ion-selective electrode used in the previous methodology (Chapter 3.1) was also sensitive to nitrite concentrations. Therefore, it is of utmost importance, particularly for parameter estimation, that nitrite is quantified and corrected for. Different and conflicting results have been reported in literature concerning nitrite build-up during denitrification (Betlach and Tiedje, 1982; Thomsen *et al*., 1994; Almeida *et al*., 1995; von Schultess and Gujer, 1996; Oh and Silverstein, 1999; Beun *et al*., 2000b). In this study, the nitrite build-up was monitored regularly using off-line nitrite measurements and was observed to be always below/around 0.22 mgNO_2-N/l. This indicates that nitrite build-up was negligible in this study and that denitrification processes occurred in single step.

Further, since the biosensor is also sensitive to possible N_2O build-up during denitrification (Larsen *et al.*, 2000; McMurray *et al.*, 2004), the anoxic respirometer based on the biosensor becomes *essentially* more suitable to study the single-step denitrification process with negligible intermediate accumulation. On the other hand, the anoxic methodology developed in this chapter can easily be extended to study denitrification intermediates as new sensors/tools become available to measure nitrite and N_2O separately (see e.g. McMurray *et al.*, 2004).

4. CONCLUSIONS

An improved methodology has been developed and successfully applied for the monitoring of anoxic activated sludge activity. The major improvement of the methodology is its simplicity, robustness and high quality data resulting from the use of a novel nitrate biosensor. The

output of the biosensor is quite fast with a first order time constant equal to 0.31 min. Moreover, the drift of the biosensor slope was observed to be stable in the sense that it decreases linearly in time (-2.65%/day), which can easily be corrected for by in-line calibration i.e. using the known nitrate additions that are regularly performed in the operation of the sensor. The resulting high frequency data allowed for the first time to monitor anoxic respiration rate of activated sludge, NUR, at a higher resolution, i.e. every 3 seconds, and down to lower nitrate concentrations than ever before allowing to even estimate nitrate affinity constants. Similar to the OUR, the NUR resulting from a pulse addition of carbon source to endogenously respiring anoxic activated sludge exhibits a clear storage tail. Moreover, activated sludge is observed to display a similar dynamic response (characterised with fast and slower transients) to pulse addition of acetate under anoxic (NUR) and aerobic (OUR) conditions. Finally, the methodology developed in this study is expected to serve as an anoxic respirometer to study the anoxic behaviour of activated sludge, particularly single-step denitrification process. Ultimately, the anoxic respirometer can be used for various purposes, e.g. process control, monitoring and characterisation of the denitrification process in view of calibration of activated sludge models.

PART 2
-
DEVELOPMENT OF MODEL-BASED METHODS FOR INTERPRETATION OF LAB-SCALE EXPERIMENTS

Chapter 4.1

Extensions to the modelling of aerobic carbon source degradation using titrimetric data

ABSTRACT

Recently Gernaey *et al*. (2002a) developed a model to interpret respirometric (OUR) –titrimetric (Hp) data obtained from aerobic oxidation of different carbon sources in view of the calibration of Activated Sludge Model No.1 (ASM1). The carbon dioxide transfer rate (CTR) was observed relevant for the description of the titrimetric data but was assumed to be constant during these experiments. However, this assumption of constant CTR is only valid under certain experimental conditions. To improve its range of applicability, the Gernaey model is extended in this study with a dynamic model to describe the dynamic CTR process based on the CO_2 gas-liquid interaction (stripping) and the aqueous CO_2 equilibrium system. A calibration methodology for the dynamic CO_2 model with only titrimetric data collected under endogenous conditions was developed after intensively studying the CO_2 model in relation to its practical (local) identifiability. Accordingly, it is proposed to calibrate the dynamic CO_2 model by first estimating the equilibrium constant of the aqueous CO_2 system, pK_1, and the initial aqueous CO_2 concentration, C_{Tinit}, using titrimetric data. The CO_2 mass transfer coefficient, K_La_{CO2}, can be calculated using the K_La_{O2} determined from oxygen measurements. The extended Gernaey model was successfully applied to interpret typical data obtained from respirometric-titrimetric experiments characterised by a non-linear CO_2 stripping process. The parameter estimation results using the titrimetric data alone were rather close to the estimation results using the respirometric data (OUR) or using the combined OUR and Hp data, thereby supporting the validity of the dynamic CO_2 model and its calibration approach. The increased range of applicability and accurate utilization of the titrimetric data is expected to contribute particularly to the improvement of the identification of the over-parameterised ASM models.

This chapter is in preparation for publication.

1. INTRODUCTION

Modelling activated sludge processes e.g. by the Activated Sludge Model (ASM) suite of Henze *et al.* (2000) has gained significant popularity in the last decade. The crucial step in the application of the models is the calibration step. Calibration of the models consists of estimating the biokinetic and stoichiometric parameters of the sludge/wastewater interaction and requires additional information about the kinetics and stoichiometry of the processes under study.

Respirometry which is the measurement of the respiration rate of biomass (OUR) (Spanjers *et al*., 1998) has been a well-established methodology for the calibration of the activated sludge models (Kappeler and Gujer, 1992; Vanrolleghem *et al.*, 1999; Petersen *et al.*, 2003a; etc.). However, the increased complexity of the activated sludge models (ASM) weakened the identifiability of the models. In other words, it becomes increasingly difficult to find unique and reliable values for the model parameters. Additional measurements besides OUR are quite essential for improving the identifiability of the models (Weijers and Vanrolleghem, 1999; Weijers, 2000; Brun *et al.*, 2002).

Titrimetry, which is the indirect measurement of the pH effects resulting from the biomass metabolic activity, has recently reached a level of precision which makes it useful for quantifying the kinetics of the activated sludge processes (Ramadori *et al*., 1982; Gernaey *et al.*, 2002a,b; Petersen *et al*., 2002a; Foxon *et al*., 2002; Pratt *et al*., 2003; Sin *et al*., 2003). Titrimetry is a rather simple method where the resulting data is the cumulative acid or base addition needed to keep the pH of the medium constant during a batch experiment.

Unlike respirometric data which are a direct result of the carbon oxidation process, the titrimetric data are the result of the pH effect of several processes occurring during aerobic carbon degradation experiment: substrate uptake, ammonium uptake for growth, CO_2 production due to carbon oxidation and the CO_2 stripping processes. It is therefore very crucial to accurately decouple the contribution of the physical-chemical processes to the titrimetric data from that of the biological processes. A mathematical model that accounts for the pH effect of each process mentioned above is needed to link the titrimetric data to the biological activity. Gernaey *et al.* (2002a) developed a mathematical model that accounts for the pH effects of the aforementioned processes (biomass metabolic activity and the gas-liquid CO_2 equilibrium) to describe the titrimetric data resulting from aerobic carbon source degradation processes.

2. PROBLEM STATEMENT

In the Gernaey model (2002a), the pH effect of the CO_2 stripping process, in other words the CO_2 transfer rate (CTR), is described as part of the background proton production rate (b_C).

The b_C was observed to be constant before and after the experiments reported in Gernaey *et al*. (2002a) and therefore it was assumed constant in the model. The assumption that the pH effect of CTR is constant (or changing negligibly) is however only valid for experiments with the following conditions: (1) Addition of a small amount of carbon source, (2) Low K_La – oxygen mass transfer coefficient and therefore low mass transfer coefficient of CO_2. The mass transfer coefficient of CO_2 is linked to the K_La of oxygen with a constant value determined by the diffusion coefficients for O_2 and CO_2 (Spérandio and Paul, 1997), (3) High pH set point (e.g. 8) and (4) Short-term experiments, e.g. 15-20 min for aerobic oxidation of the carbon source.

Figure 1 illustrates what happens if this assumption is not valid, e.g. when K_La_{O2} (and therefore K_La_{CO2}) is set high (0.37 min^{-1}). The background proton production rate (b_C) mainly induced by CTR is not constant beyond the point where the acetate is completely oxidized. It is clear that the Gernaey model cannot be applied for this type of experimental results.

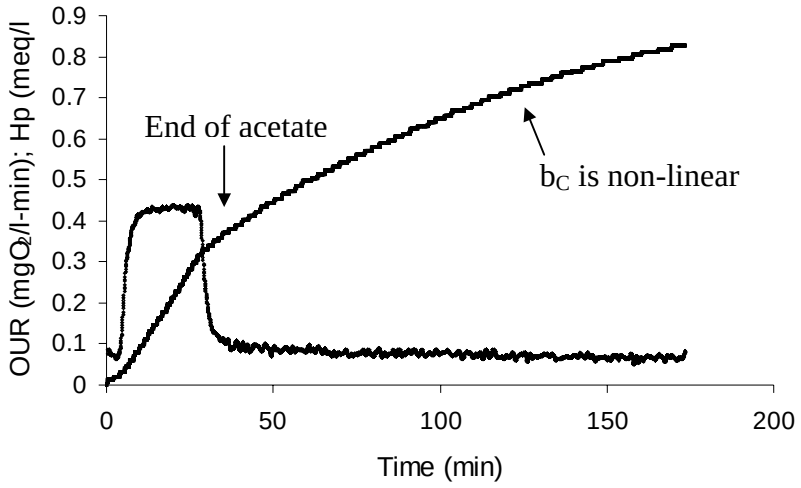

Figure 1. An experimental result from a pulse addition of 50 mgCOD/l acetate to an endogenously respiring activated sludge in a combined respirometric-titrimetric setup.

A proper and more general method for the description of the CO_2 stripping phenomenon is to consider the dynamics of the stripping and the gas-liquid equilibrium of CO_2 (Spérandio and Paul, 1997; Noorman *et al*., 1992; etc.). Pratt *et al.* (2003) applied such a model to describe the pH effect of the CTR in their methodology proposed to describe the titrimetric data resulting from various biological processes. The method provided by Pratt *et al.* (2003) however requires a sophisticated and expensive set-up for off-gas CO_2 measurements, which is unable to adequately deal with dynamic conditions.

The objective of this research

The main motivation of this study is to model the dynamic CO_2 stripping process during aerobic carbon source degradation experiments without the need to measure off-gas CO_2. In this study, the methodology developed by Gernaey *et al.* (2002a) is extended to describe experiments with nonlinear background proton production rates (see Figure 1). To this aim, in the first part of this study, a dynamic model based on kinetic considerations of gas and liquid phase CO_2 dissociation equilibria is developed. Then the Gernaey model is extended with this dynamic CO_2 model. A calibration methodology only based on titrimetric data is presented for the calibration of the dynamic CO_2 model using experiments under endogenous conditions. In the second part of this study, the extended titrimetric methodology is applied for the modelling of aerobic carbon source degradation process. The parameter estimation and model-fits using titrimetric data versus respirometric-titrimetric data are compared to check the credibility/reliability of the extended titrimetric model.

3. MATERIAL AND METHODS

The experiments were performed using the integrated sensor described in detail in Chapter 3.1 and shown in Figure 2. The integrated sensor basically consists of an aeration reactor (2.5 l) and a respiration 1 l) vessel which is made strictly airtight (Gernaey *et al.*, 2001a).

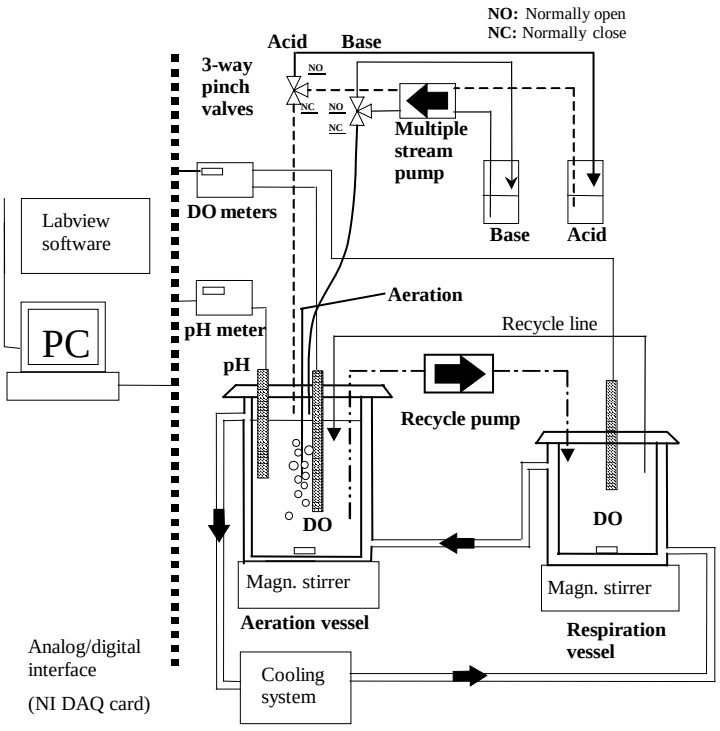

Figure 2. Schematic illustration of the integrated sensor

A cooling system (Lauda Ecoline E303) is used to control the temperature of the reactors. Data acquisition, pH control and data processing are implemented by Labview software

(National Instruments, NIDAQ 6.9 with AT-MIO-16XE-50 DAQ card and Labview 6.i). High frequency noise known to be present in the weak analog signals of the electrodes of the set-up are filtered using a low pass Savitzky-Golay least square polynomial filter through a Labview Matlab script node (Matlab R12, The MathWorks Inc.) (see Chapter 3.1).

For the experimental work, activated sludge was sampled from the Maria Middelares WWTP (Gent, Belgium), which performs nitrification and COD removal. During the experiments, ATU was added (ca 20 mg/l) to inhibit nitrification and small substrate pulses (e.g. 15-20 ml) of acetate from a 10 gCOD/l stock solution were dosed to the activated sludge. All experiments were performed at 15.3 ±0.1 ^{0}C. The pH is controlled within a narrow pH set-band ± 0.03 as described in detail in Gernaey *et al.* (2001a).

All model simulations and parameter estimation were performed using WEST® (Hemmis NV, Kortrijk, Belgium), a dedicated software for the modelling of wastewater treatment plants (Vanhooren *et al.*, 2003).

4. MODEL DEVELOPMENT

4.1 Carbon dioxide (CO_2) gas-liquid equilibrium

It is assumed that the CO_2 produced by the biological activity in the various steps of the carbon metabolism is transferred passively through the cellular membrane to the medium, mainly in the form of CO_2 (Noorman *et al.*, 1992).

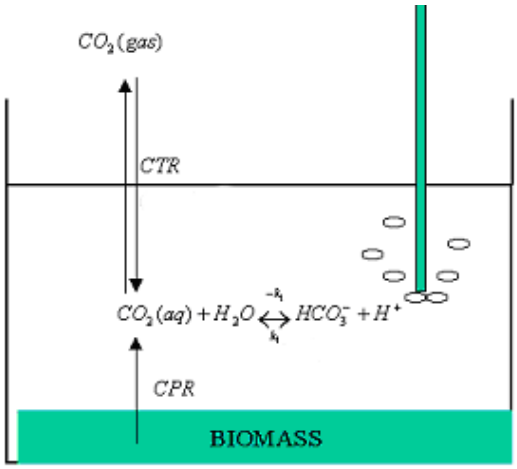

Figure 3. The simplified description of complex CO_2 system in a typical batch reactor containing activated sludge sample.

Once the CO_2 is excreted, it will be involved in several reversible chemical reactions (see below). The major processes involving CO_2 in a typical batch experiment can be schematically represented in Figure 3. Three major processes can be identified for proper

description of CO_2 in the system: CO_2 production from biological activity, CO_2 buffer system and CO_2 stripping process.

4.2 Dissolved carbon dioxide equilibria

The equilibria of the dissolved carbon dioxide system can be written as follows (Stumm and Morgan, 1996):

$$CO_2 + H_2O \longleftrightarrow H_2CO_3 \longleftrightarrow HCO_3^- + H^+ \longleftrightarrow CO_3^{2-} + 2H^+ \quad (1)$$

The hydration reaction of CO_2 to form H_2CO_3 is a slower process compared to the dehydration of H_2CO_3 to form CO_2 (Stumm and Morgan, 1996). This intermediate step is therefore usually neglected from the carbonate system. Activated sludge systems operate near neutral pH conditions and at this pH, the fraction of carbonate (CO_3^{2-}) at neutral pH is quite negligible (E.g. 0.001 at pH 7.5). The simplified dissolved CO_2 equilibria in the activated sludge mixed liquor system therefore reduces to the following relation:

$$CO_2 + H_2O \underset{k_{-1}}{\overset{k_1}{\rightleftharpoons}} HCO_3^- + H^+ \quad (2)$$

Note that another possible reaction involving CO_2 is shown in Eq. 3. However, the impact of this reaction on total inorganic carbon equilibrium at neutral pH conditions is negligible as well (Spérandio and Paul, 1997). However, Eq.3 is included in the model to quantitatively demonstrate the impact on the equilibrium concentrations of aqueous carbonate system.

$$CO_2 + OH^- \underset{k_{-2}}{\overset{k_2}{\rightleftharpoons}} HCO_3^- \quad (3)$$

The equilibrium constant of the reactions are given by:

$$K_1 = \frac{[H^+]\cdot[HCO_3^-]}{[CO_2]} \text{ and } K_2 = \frac{[HCO_3^-]}{[OH^-]\cdot[CO_2]} \text{ where } K_2 = \frac{K_1}{K_W} \quad (4)$$

In this study, the kinetics of aqueous CO_2 equilibria is considered explicitly in order to obtain an accurate description of the dynamics of the CO_2 in the system. An alternative approach could be to assume that the equilibrium is attained instantaneously (Iversen *et al.*, 1994; Gernaey *et al.*, 2002a; Pratt *et al.*, 2003). The reactions involving CO_2 and HCO_3 can be described as follows:

$$r_1 = k_1[CO_2] - k_{-1}[HCO_3^-][H^+] = k_1[CO_2] - \frac{k_1}{10^{-pK_1}}10^{-pH}[HCO_3^-] \quad (5)$$

$$r_2 = k_2[CO_2][OH^-] - k_{-2}[HCO_3^-] = k_2 10^{pH-pKw}[CO_2] - \frac{k_2}{10^{-pK_2}}[HCO_3^-] \quad (6)$$

where $k_{-1} = k_1/K_1$ and $k_{-2} = k_2/K_2$.

4.3 Carbon dioxide transfer rate (CTR)

Aqueous CO_2 is transferred to the gas phase through the stripping process at a rate called carbon dioxide transfer rate (CTR). This transfer rate is known to be limited by the liquid side resistance (Ho *et al*., 1987; Spérandio and Paul, 1997; Noorman *et al*., 1992; see time constant analysis below). Therefore the CTR will be limited by the mass transfer coefficient of CO_2 and the liquid-gas phase equilibrium concentration of CO_2:

$$CTR = K_L a_{CO2} * (CO_2^* - CO_{2[aq]}) \quad (7)$$

Where CO_2^* represents the dissolved CO_2 concentration which is in equilibrium with the partial pressure of CO_2 in the atmosphere (gas phase) and $K_L a_{CO2}$ represents the mass transfer coefficient of CO_2. The $K_L a_{CO2}$ can be determined from the oxygen transfer coefficient ($K_L a$) using the ratio of their corresponding diffusivity coefficients (Noorman *et al*., 1992; Sperandio and Paul, 1997):

$$\frac{K_L a_{CO_2}}{K_L a_{O_2}} = \sqrt{\frac{D_{CO_2}}{D_{O_2}}} = 0.91 \quad (8)$$

The equilibrium concentration of CO_2 is governed by the Henry law and described as follows:

$$CO_2^* = P_{CO2} * K_H \quad (9)$$

where K_H is the Henry coefficient for CO_2 ($atm^{-1}.mol.L^{-1}$) and P_{CO2} is the partial pressure of CO_2 (atm). The parameter K_H depends on the temperature and ionic strength of the medium (Noorman *et al*., 1992; Stumm and Morgan, 1996). However, since there is no value available for activated sludge conditions, the value reported in Stumm and Morgan (1996) for water at 15 ^{0}C is considered in this study.

The partial pressure of CO_2 in the air (P_{CO2}) is typically around 0.038% of the atmospheric pressure (e.g. 1 atm) (Royce, 1992). Hence, the saturation concentration of carbon dioxide in the water can be predicted once the ambient air pressure is known.

4.4 Carbon dioxide production rate (CPR)

Both exogenous and endogenous activities of biomass are accompanied by CO_2 production. The CO_2 produced by biomass enters into mixed liquor and reacts with the complex aqueous-gas phase CO_2 system. In short, biological, chemical and physical processes influence the CO_2 equilibrium in a batch reactor, as schematically shown in Figure 3. The CO_2 production rate (CPR) is stoichiometrically linked to the oxygen uptake rate of the biomass (OUR) via the respiration quotient (RQ) (Royce, 1992; Bonarius *et al.*, 1995; etc.).

CPR due to aerobic oxidation of carbon source

The respiration quotient (RQ) can be calculated from the given stoichiometry of the aerobic carbon oxidation using the convention described in Heijnen (1999):

$$\frac{1}{Y_H}(mgCOD)\ CH_yO_z + \left(1-\frac{1}{Y_H}\right)(mgCOD)\ O_2 + \frac{14c}{8\gamma_x}(mgN)NH_3 \rightarrow 1mgCOD\ CH_aO_bN_c + \frac{1}{8}\left(\frac{1}{\gamma_s Y_H}-\frac{1}{\gamma_x}\right)(mmol)\ CO_2 + (\ldots)\ H_2O \qquad (10)$$

The stoichiometric coefficients shown in Eq. 10 are determined using elemental conservation equations and a balance of degrees of reduction of the considered component (Heijnen, 1999). In eq.10 biomass and substrate are represented by $CH_aO_bN_c$ and CH_yO_z respectively based on their C-mol content for straightforward calculation of the degree of reduction. The corresponding degree of reduction of the biomass (γ_x) and the substrate (γ_s) are calculated as follows: (i) $\gamma_x = 4+a-2b-3c$ and (ii) $\gamma_s = 4+y-2z$. By definition the nitrogen content of biomass, $i_{NBM,}$ is equal to $\frac{14c}{8\gamma_x}$ whereas the stoichiometric coefficient of water can be calculated using the mass conservation for oxygen in Eq.10.

The oxygen uptake rate and CO_2 production rate of aerobic heterotrophic growth can be calculated as follows:

$$OUR = \left(\frac{1-Y_H}{Y_H}\right) * r_x\ (mgO_2/l\text{-}min) \text{ and } CPR = \frac{1}{8\gamma_s}\left(\frac{1}{Y_H}-\frac{\gamma_s}{\gamma_x}\right) * r_x\ (mmol\ CO_2/l\text{-}min)$$

Where r_x stands for the biomass growth rate (see Table 3). Finally, RQ can be calculated straightforwardly from the stoichiometric ratio of CO_2 to O_2 on molar basis:

$$\text{RQ} = \frac{CPR}{OUR/32} = 4\frac{\gamma_x - \gamma_s Y_H}{\gamma_s \gamma_x (1 - Y_H)} \text{ (mmol } CO_2\text{/ mmol } O_2\text{)}$$

The RQ is a function of the yield coefficient of biomass as well as of the degree of reduction of substrate and biomass. In the following table, the respiration quotient for different substrate sources are calculated using yield coefficients reported in literature as typical values for aerobic heterotrophic growth (Heijnen and van Dijken, 1992). Table 1 indicates that using methanol and ethanol as substrate source for aerobic heterotrophic growth results in much lower amounts of CO_2 production compared to glucose and propionate as substrate source.

Table 1. Calculation of CO_2 production and respiration quotient for different carbon sources considering biomass composition as $CH_{1.8}O_{0.5}N_{0.2}$ with γ_x= 4.2.

Substrate	γ_s	Y_{SX}*	Y_H	O_2	CO_2	RQ**
		mmol/mmol	mgCOD/mgCOD	mgCOD	mmol	
Glucose (CH_2O)	4	0.61	0.64	0.5613	0.0190	1.0848
Methanol (CH_4O)	6	0.54	0.37	1.6954	0.0264	0.4981
Ethanol ($CH_3O_{0.5}$)	6	0.53	0.38	1.6455	0.0254	0.4930
Propionate ($CH_2O_{2/3}$)	4.7	0.48	0.43	1.3148	0.0322	0.7847

*Taken from Heijnen and Van Dijken (1992)

** in mmolCO_2/mmolO_2

CPR due to endogenous process

Similar to the exogenous activity, the CO_2 production resulting from the endogenous process is linked to the endogenous consumption of oxygen. The calculation of the respiration quotient for the endogenous process can be performed straightforwardly from the stoichiometric relation of the endogenous process, which is given in Eq.11. The endogenous respiration of biomass can be described as follows (on C-mol basis):

$$CH_aO_bN_c + \frac{4 + a - 2b - 3c}{4} O_2 \rightarrow CO_2 + \frac{a - 3c}{2} H_2O + cNH_3 \qquad (11)$$

Recalling the definition of γ_x, which is mentioned above, Eq. 11 can be rearranged as follows:

$$CH_aO_bN_c + \frac{\gamma_x}{4} O_2 \rightarrow CO_2 + \frac{a - 3c}{2} H_2O + cNH_3 \qquad (12)$$

In this case, the respiration quotient can be determined as follows (on mol basis):

$$RQ_{end} = CPR_{end}/OUR_{end} = \frac{4}{\gamma_x} \quad (13)$$

The degree of reduction of the biomass plays a significant role in determining the extent of the CO_2 production during the endogenous process. For biomass with degrees of reduction of 4 and 4.2, the endogenous respiration quotient is equal to 1 and 0.952 respectively. In this study, it is assumed that the endogenous CPR is equal to the endogenous OUR on a molar basis in view of the average biomass composition generally accepted in literature (Metcalf and Eddy, 1991; Henze *et al*., 1987). Several researchers have also assumed CPR_{end} equal to the OUR_{end} (Gernaey *et al*., 2002b; Petersen *et al*., 2002a; Pratt *et al*., 2003).

4.5 Extending the Gernaey model with the dynamic CO_2 system

The Gernaey model is essentially based on the ASM1 model with the exception of the Hp column. The Hp column indicates the amount of proton production from the processes included in the model (meq or mmol). Two additional components are required in order to implement the dynamic CO_2 system into the Gernaey model: namely CO_2 and HCO_3. The extended mathematical model is shown in Table 3 and the default values of the model parameters (particularly for the CO_2 system) are given in Table 2. The Hp column in Table 3 includes the pH effects of the three processes: (1) Heterotrophic growth, (2) Endogenous respiration and (3) aqueous CO_2 equilibrium.

The two sub-processes associated with the heterotrophic growth, substrate (column 2 Table 3.) and ammonia uptake (see column 3 Table 3) are particularly influencing the Hp column. The Gernaey model assumes that the substrate is taken up by the biomass in undissociated form. That means if a substrate is present in undissociated form, it will have no effect on the proton concentration, e.g. dextrose. However, the uptake of a substrate which is present in ionized form (e.g. weak acids) will be accompanied by the uptake of a proton from the medium. The extent of the proton taken up from the medium is determined by the fraction m (see Gernaey *et al.* (2002a) for more details). The fraction m is the ratio of the ionized weak acids to the total amount of weak acid present in the medium, given by Eq. 14:

$$m = \frac{[A^-]}{[HA]+[A^-]} = \frac{10^{-pKa}}{10^{-pH}+10^{-pKa}} = \frac{1}{1+10^{pKa-pH}} \quad (14)$$

where $[A^-]$ ionized form of the weak acid (e.g. acetic acid)

[HA] unionized form of the weak acid (acetate)

pK_a negative logarithm of the acidity constant

By the same token, the uptake of ammonia from the medium will release protons to the medium. The extent of protons produced will again depend on the pH of the medium and is determined by the fraction of ammonium present in the medium, p, described by Eq.15:

$$NH_3 + H^+ \leftrightarrow NH_4^+ \qquad p = \frac{10^{-pH}}{10^{-pH} + 10^{-pKNH4}} = \frac{1}{1 + 10^{pH - pKNH4}} \tag{15}$$

The release of ammonia during the endogenous process will also affect the proton concentration in the medium. The stoichiometric coefficient of this influence needs to be corrected for the nitrogen content of the inert fraction of the COD released during the decay process as shown in Table 3 (column 6 & row 2).

The net effect of the CO_2 system on the Hp column is a result of the difference between the CO_2 production rate and the CO_2 transfer rate. This difference is in fact equivalent to the amount of HCO_3 accumulation in the system. From the stoichiometry of Eq.2 (see also Table 3), it is obvious that for each mmol of HCO_3^- produced 1 mmol of protons (H^+) will be produced. The rate of accumulation of HCO_3^- (i.e. the protons) on the other hand depends on the kinetics of each process involved in the CO_2 system: the CPR, the CTR and the aqueous CO_2 equilibrium.

It is clear that the CO_2 system has a major impact on the Hp component. However, the main motivation of this study is to investigate the biological activity. That means that the CPR signal should be accurately calculated back from the Hp component in order to link the titrimetric data to the biological activity. This in turn requires that the CTR and kinetics of the aqueous CO_2 equilibrium should be accurately described and identified.

An important question in relation to the reliability of the CTR and aqueous CO_2 equilibrium model is: " What is the uncertainty introduced by assuming the CO_2 model parameters (e.g. k_1, pK_1, K_H etc) default values as they are reported in the literature for water systems?" This point is unfortunately often neglected (Yegneswaran and Gray, 1990; Royce, 1992; Bonarious *et al*., 1995; etc.). It is known for instance that equilibrium constants (in particular for the CO_2 system) depend very much on the ionic strength of the medium (Noorman *et al.*, 1992; Stumm and Morgan, 1996). This implies that all model parameters need to be determined for different ionic strengths for an accurate description of the CO_2 system. In the following section, this uncertainty issue is going to be discussed using model-based simulations and sensitivity analysis of the CO_2 model parameters.

Table 2. Default values of the model parameters used in this study (The kinetic values are reported for 15 ^{0}C)

Parameter	Description	Default	Reference
P_{CO2}	Partial pressure of CO_2 in air, atm	0.00038	Royce (1992)
K_H	Henry coefficient for CO_2, mole.atm^{-1}.l^{-1}	0.045	Stumm and Morgan, (1996)
S_{CO2}^*	CO_2 saturation coefficient at 1 atm, mol/l	0.017 10^{-3}	Stumm and Morgan, (1996)
S_O^*	Oxygen saturation concentration, mg/l	10	Estimated
K_1	Forward reaction rate for aqueous CO_2 equilibrium, min^{-1}	2.4	Stumm and Morgan (1996)
k_{-1}	Backward reaction rate for aqueous CO_2 equilibrium, L.mole^{-1}.min^{-1}	4.74 10^6	Stumm and Morgan (1996)
pK_1	Negative logarithm of the first acidity constant in the CO_2 equilibrium (K_1)	6.42	Stumm and Morgan (1996)
pK_2	Negative logarithm of the equilibrium constant (K_2) of Eq.3	-7.92	Sperandio and Paul (1997)
K_2	Forward reaction rate of Eq.3, L.mole^{-1}.min^{-1}	72	Sperandio and Paul (1997)
k_{-2}	Backward reaction rate of Eq.3, min^{-1}	8.6	Sperandio and Paul (1997)
pK_W	Equilibrium constant for water	14.34	Stumm and Morgan, (1996)
pK_A	Equilibrium constant for acetate dissociation	4.75	Stumm and Morgan, (1996)
pK_{NH}	Equilibrium constant for NH_4^+ dissociation	9.25	Stumm and Morgan, (1996)
C	Molecular weight of 1 mol of acetate, gCOD/mol	64	Calculated
f_{XI}	Inert fraction of biomass, gCOD/gCOD	0.2	Henze *et al*. (2000)
i_{NXI}	Nitrogen content of the inert fraction of biomass, gN/gCOD	0.02	Henze *et al*. (2000)
i_{NBM}	Nitrogen content of biomass, gN/gCOD	0.07	Henze *et al*. (2000)
Y_H	Yield coefficient of biomass, gCOD/gCOD	0.67	Henze *et al*. (2000)
γ_S	Degree of reduction of S_S (for acetate $C_2H_4O_2$)	4	Calculated
γ_X	Degree of reduction of X_H (e.g. $CH_{1.8}O_{0.5}N_{0.2}$)	4.2	Assumed
μ_{maxH}	Maximum growth rate of biomass, d^{-1}	2	Estimated
b_H	Endogenous decay coefficient of biomass, d^{-1}	0.24	Estimated
K_S	Substrate affinity constant of biomass, mgCOD/l	0.5	Estimated
K_O	Oxygen affinity constant of biomass, mgCOD/l	0.2	Henze *et al*. (2000)
K_La_{O2}	Oxygen mass transfer coefficient, min^{-1}	0.37	Estimated
K_La_{CO2}	Carbon dioxide mass transfer coefficient, min^{-1}	0.34	Estimated

Table 3. Matrix representation of the mathematical model of Gernaey *et al.*(2002a) extended with the dynamic CO_2 system

Component (i)→ **Process (j) ↓**	1. S_O	2. S_S	3. S_{NH}	4. S_{HCO3}	5. S_{CO2}	6. S_{Hp}	7. X_H	8. X_I	**Kinetics**
1.Growth of Heterotrophs	$-\frac{1-Y_H}{Y_H}$	$-\frac{1}{Y_H}$	- i_{NBM}		$\frac{1}{8\gamma_s}\left(\frac{1}{Y_H}-\frac{\gamma_s}{\gamma_x}\right)$	$\frac{p\cdot i_{NBM}}{14}+\frac{m}{Y_H\cdot C}$	+1		$\mu_{\max H} M_S M_O M_{NH} X_H$
2.Endegenous respiration	$-(1-f_{XI})$		i_{NBM} - f_{XI}*i_{NXI}		$\left(\frac{1-f_{XI}}{8\cdot\gamma_X}\right)$	$-\frac{(i_{NBM}-f_{XI}\cdot i_{NXI})\cdot p}{14}$	-1	f_{XI}	$b_H M_O X_H$
3.Aqueous CO_2 equilibrium				1	-1	1			$\left(k_1+k_2 10^{pH-pKw}\right)\cdot S_{CO2} - \left(k_1\cdot 10^{pK_1-pH}+k_{-2}\right)\cdot S_{HCO3}$
4. CO_2 stripping					-1				$K_L a_{CO2}\cdot\left(S^*_{CO2}-S_{CO2}\right)$
5. Aeration	1								$K_L a\cdot\left(S^*_O-S_O\right)$

Where **M** stands for the Monod function. E.g. $M_S=\frac{S_S}{S_S+K_S}$; and the constants m and p are pH dependent functions (see the text).

5. RESULTS

The results are presented in two main parts. In the first part, the extended titrimetric model is studied in detail in order gain a better insight and confidence into the model structure and therefore come up with a reliable calibration methodology. In the second part of the results, the extended model is applied using the calibration methodology to interpret a typical respirometric-titrimetric data set in view of calibration of ASM1 type models.

5.1 Evaluation of the extended titrimetric model under endogenous respiration

In this part, the extended titrimetric model, particularly the dynamic CO_2 module, is studied in detail in order to gain a deeper insight into the model structure. This is required in order to develop a simple calibration methodology for the model using titrimetric data alone. Moreover, it is also essential in order to gain confidence into the extended model in view of a reliable description of the titrimetric data resulting from typical batch experiments designed for calibration of ASMs.

To this aim, titrimetric data were collected under endogenous conditions where the main biological influence on the titrimetric data is endogenous CO_2 production and release of nitrogen due to decay, which was determined experimentally. Moreover, using the mass transfer coefficient of oxygen, the K_La_{CO2} was calculated to quantify the CO_2 stripping kinetics. After that the remainder of the mass transfer model is calibrated using the titrimetric data. In order to understand the slow dynamics observed in the titrimetric data a time constant analysis of the dynamic CO_2 model is performed. Further, to understand the practical identifiability of the model based on the titrimetric data, output sensitivity functions of the dynamic CO_2 model parameters were investigated. The effect of uncertainty in the default CO_2 model parameters (model assumptions) on the calibrated parameters is also investigated to determine to what extent the assumptions are valid. Based on these investigations a calibration methodology is proposed. Finally, the Fisher Information Matrix (FIM) is used to investigate the optimal (i.e. minimum) duration required for a titrimetric experiment under endogenous conditions to provide a reliable calibration of the dynamic CO_2 model. The results are presented in the following structure:

- *Determination of the endogenous decay rate, b_H, and the nitrogen content of biomass, i_{NBM}*
- *Determination of the mass transfer coefficient of carbon dioxide*
- *Parameter estimation results for the complete CTR model using titrimetric data*
- *Time constant analysis of the slow dynamics of the titrimetric data*
- *Sensitivity analysis of the parameters of the dynamic CO_2 model*
- *Effect of parameter uncertainty on the estimation results*
- *A simple calibration methodology for the dynamic CO_2 model using titrimetric data*

- *Optimal duration of titrimetric experiment for reliable calibration of the dynamic CO_2 model*

5.1.1 Determination of the endogenous decay rate, b_H, and the nitrogen content of biomass, i_{NBM}

The endogenous decay rate b_H and the coefficient of the ammonia release i_{NBM} were determined experimentally to evaluate the effect of the endogenous process on the titrimetric data. In this way, the effect of a biological process (i.e. endogenous respiration) on the Hp is quantified and the Hp data could be used to calibrate the parameters of the chemical and physical processes affecting the Hp data, as done below (see Figure 3).

A 3 L activated sludge sample was brought into the integrated sensor and ATU (18.6 mg/L) was added to inhibit nitrification (if any) during the experiment. The oxygen concentration was maintained high enough (around 9.0 mgO_2/l) during aeration to ensure oxygen unlimited conditions. After aerating the biomass more than one day at endogenous state, OUR of the biomass was monitored for three days (endogenous OUR was measured for 30 minutes once per day). During this period the ammonium nitrogen was also measured using commercial kits (Dr. Lange).

Table 4. Monitoring the OUR and NH_4 release during the endogenous respiration

Day	Time	NH_4-N (mg N/l)	OUR (mg O_2/l*min)
12.10.02	12:25	2.81	0.0957
14.10.02	14:40	7.59	0.0565
15.10.02	11:38	-	0.0464

The endogenous OUR of the biomass decreases exponentially as described in Eq. 16 and Eq.17. The slope of the natural logarithm of OUR versus time is equal to the decay rate constant of the biomass shown in Eq.18. In this case, the decay rate constant of the biomass was determined to be 0.24 d^{-1}. This value is in the typical range of values reported for activated sludge systems (Henze *et al*., 2000).

$$OUR_{end} = (1 - f_{XI}) \cdot b_H \cdot X_H(t) \tag{16}$$

with

$$X_H(t) = X_{H0} \cdot e^{-b_H \cdot t} \tag{17}$$

$$\ln(OUR_{end}) = \ln\left((1 - f_{XI}) \cdot b_H \cdot X_{H0}\right) - b_H \cdot t \tag{18}$$

The release rate of ammonium nitrogen during the endogenous process is described by Eq. 19. The nitrogen content of the biomass can be determined using Eq.20, which is simply comparing the amount of nitrogen released by amount of the biomass lost during the endogenous respiration:

$$\frac{dS_{NH}}{dt} = (i_{NBM} - f_{XI} \cdot i_{NXI}) \cdot b_H \cdot X_H \quad (19)$$

$$i_{NBM} = \frac{S_{NH}(t_2) - S_{NH}(t_1)}{X_H(t_1) - X_H(t_2)} + f_{XI} \cdot i_{NXI} \quad (20)$$

The amount of biomass $X_H(t)$ can be estimated from Eq. 16, which is rewritten as:

$$X_H(t) = \frac{OUR_{end}(t)}{(1 - f_{XI}) \cdot b_H} \quad (21)$$

The i_{NBM} can then be calculated by assuming the nitrogen content of the inert fraction of the biomass known (f_{XI}=0.2 and i_{NXI} = 0.02), measurements of released ammonia and two measurements of OUR_{end}:

$$i_{NBM} = \frac{4.78}{703.68 - 415.44} + 0.2 \cdot 0.02 = 0.021\ mgNH_4^+ - N / mgCOD_{biomass}$$

The i_{NBM} value "0.021" is rather low compared to the typical value "0.07" reported in Henze *et al*. (2000). However, it is important to notice that the i_{NBM} is determined on the basis of NH_4-N measurements. It means that it does not include the particulate nitrogen which was probably also released from the biomass decay leading to the estimation of a low i_{NBM} value. For a realistic determination of the nitrogen content of the biomass, it is more appropriate to directly measure total nitrogen, TKN. However, from the pH effect point of view, i_{NBM} based on NH_4-N should be used in the titrimetric models since only the ammonium nitrogen that is released has an effect on the Hp data.

5.1.2 Determination of the mass transfer coefficient of carbon dioxide, K_La_{CO2}

The CO_2 mass transfer coefficient, K_La_{CO2}, can be determined from the oxygen mass transfer coefficient, K_La_{O2}, using Eq.22.

$$\frac{K_L a_{CO_2}}{K_L a_{O_2}} = \sqrt{\frac{D_{CO_2}}{D_{O_2}}} = 0.91 \quad (22)$$

The ratio of 0.91 is a default value corresponding to the diffusivity coefficients of oxygen and CO_2. However, it was shown that this ratio may be changing depending on the experimental conditions (Noorman *et al*., 1992; Spérandio and Paul, 1997). This point is evaluated further in the following endogenous experiment where the titrimetric data is used to directly estimate the K_La_{CO2}.

The K_La_{O2} was determined from an aeration experiment in which the sludge was in the endogenous state. Only the aeration reactor of the integrated sensor was used in this experiment and was filled with 2 L of biomass. The aeration in the experimental set-up was essentially a fine-bubble aeration in which compressed air was continously passed through a tube with fine-holes located at the bottom of the reactor. The airflow rate and the positon of the aeration tube were fixed throughout the experiments performed with this set-up.

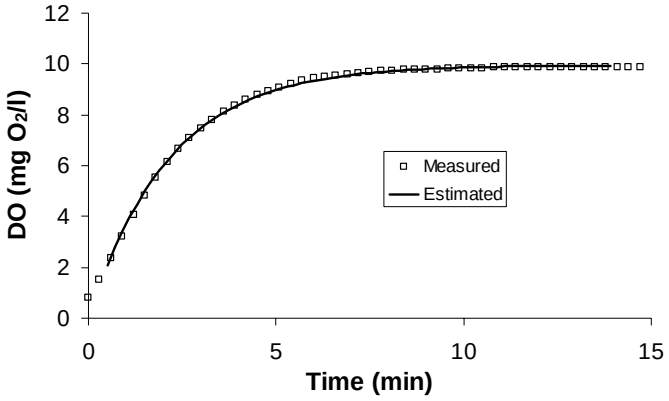

Figure 4. Measured and model predicted oxygen concentration during the aeration experiment

In the reaeration experiments, the aeration was first switched off and then the aeration reactor was flushed with nitrogen gas.After dissolved oxygen concentration was decreased in the reactor to a low level, the aeration was resumed in the reactor. As a result, the dissolved oxygen concentration increased in a first order manner during the aeration period and reached the saturation concentration in 10 min (see Figure 4). For parameter estimation, the oxygen data was truncated according to the ASCE guidelines **(**1992**)** (data which is below 20% of S_O^* and above 95% of S_O^*).

The results of the parameter estimation are given in Table 5. During parameter estimation, the endogenous process was modelled by using the b_H determined in the previous section ($0.24d^{-1}$ = $0.00017\ min^{-1}$). It was observed that the influence of the endogenous respiration on the K_La estimation was quite negligible (see Table 5 for b_H equal to zero). This is probably because the duration of the experiment was rather short. The endogenous respiration has a slight impact on the estimation of the S_O^* parameter as this parameter can correct for endogenous respiration. The K_La was estimated to be $0.46\ min^{-1}$.

Table 5. Parameter estimation results for K_La_{O2} and S_O^* during the aeration experiments.

	S_O^* (mg O_2/l)	K_La_{O2} (min^{-1})	b_H (min^{-1})	X_H (mg COD/l	SSE
b_H estimated	10.24 ±0.011	0.463 ± 0.003	0.00017	1000	1.24
b_H assumed	9.96 ±0.01	0.463 ± 0.003	0	1000	1.23

5.1.3 Parameter estimation results using titrimetric data

The CTR model given in Eq.7 contains three parameters that need to be identified: K_La_{CO2}, CO_2^* and initial $CO_{2,aq}$. The equilibrium concentration of carbon dioxide is fixed which is estimated using Eq. 9. The initial concentration of aqueous CO_2 however needs to be estimated in addition to the K_La_{CO2}. The fraction of total inorganic carbon present as CO_2 , $C_{T,init}$, is a function of medium pH and equilibrium constant pK_1. In order to determine the initial distribution of the CO_2 species during an experiment the following functions – determined assuming equilibrium at that time instant, are used:

$$CO_{2,init} = C_{T,init} \frac{1}{1+10^{pK1-pH}} \tag{23}$$

$$HCO_{3,init} = C_{T,init} \frac{1}{1+10^{pH-pK1}} \tag{24}$$

Calibration of the CTR model now requires the estimation of the K_La_{CO2} and the initial concentration of the total inorganic CO_2 in the reactor.

A typical titrimetric profile resulting from an endogenous experiment is shown in Figure 5. The proton consumption from the medium is indicated by a negative proton production i.e. Hp in Figure 5-top. In order to compensate for the proton consumption, acid is added to the medium by the titrimetric setup.

In the beginning, the proton consumption occurs at a high rate due to the large driving force (see Eq.7) i.e. the difference between the equilibrium CO_2^* concentration and the aqueous CO_2 concentration is large. The driving force decreases exponentially in time until the aqueous CO_2 reaches an equilibrium point determined by the partial pressure of CO_2 in the atmosphere (air) (see Figure5-down). Consequently, the proton consumption rate decreases exponentially as a result of the exponential removal rate of HCO_3 from the medium (see Figure 5). However, the liquid-gas equilibrium point for CO_2 may not be reached for an even longer time due to the continuous and varying CPR from endogenous respiration (in fact CPR will decrease exponentially due to endogenous respiration too).

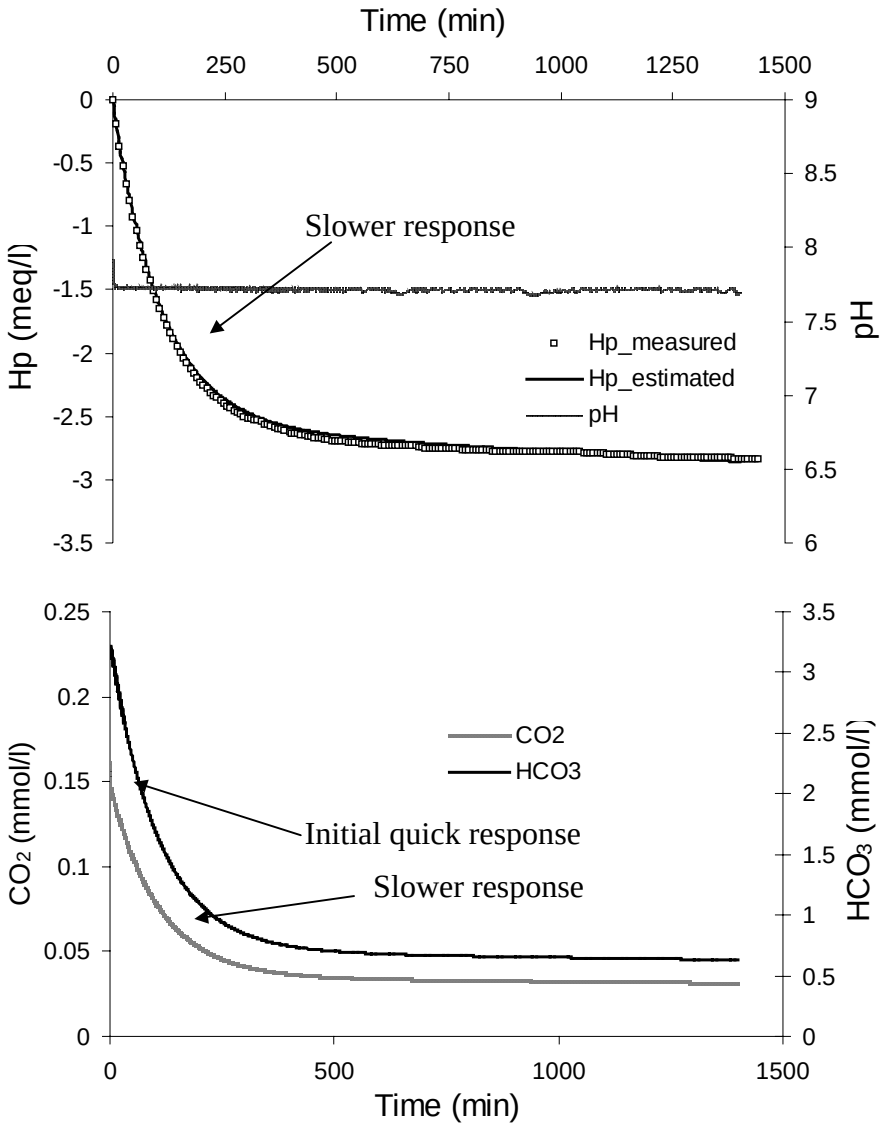

Figure 5. The model fit to titrimetric data (Hp) (continuous line) (top) and simulation results for the CO_2 and HCO_3 during the experiment (down). See the text for explanation. (1 out of 150 data points are plotted in order not to overload the graph).

The parameter estimation results for three different experiments including the one shown in Figure 5 are given in Table 6. During parameter estimation, the endogenous process parameters (b_H, i_{NBM}) were fixed using the experimentally derived values using the method presented in the previous section. The initial biomass concentration which is a crucial parameter regarding the endogenous process is estimated using Eq.21 from the endogenous OUR values monitored during each experiment. The K_La_{CO2} is estimated to be 0.36 min^{-1} as an average of the three experiments. In this case, the experimentally determined ratio of the mass transfer coefficients for CO_2 and O_2 is 0.86, which is quite close to the default value 0.91 (see Eq. 22). The deviation from the default ratio is not surprising since it is known that the experimental conditions influence the estimation of K_La_{CO2}.

Table 6. Parameter estimation results with the dynamic CO_2 model. All experiments performed at pH 7.72 under endogenous conditions (see text for details)

Experiments	K_La_{CO2} (min^{-1})	C_{Tinit} (mmol/l)	X_H (mgCOD/l)	SSE
12.10.2002	0.32 ± 0.00007	3.31 ± 0.0008	700	0.07
07.10.2002	0.40 ± 0.0007	2.06 ± 0.0007	660	0.65
16.10.2002	0.38 ± 0.001	1.45 ± 0.0006	350	0.68

5.1.4 Time constant analysis of the slow dynamics of the titrimetric data

It is observed that the time constant of the dynamic CO_2 stripping process monitored by the Hp data (see Figure 5-top) is quite slow. This phenomenon however cannot be explained straightforward by analyzing only the rate constants of the processes involved in the CO_2 system i.e. K_La_{CO2} and k_1 are in the order of 0.36 min^{-1} and 2.4 min^{-1} respectively. In order to understand the underlying reason for this phenomenon the time constant analysis of the dynamic CO_2 system is performed below.

During an endogenous experiment, the gas-liquid dynamic CO_2 equilibrium presented above (see Table 3) is described by the following state equations:

F_1: $dS_{CO2}/dt = K_La_{CO2} * (S_{CO2} - S_{CO2}^{*}) - k_1*S_{CO2} + k_1*10^{(pK1-pH)}*S_{HCO3} + CPR_{end}$
F_2: $dS_{HCO3}/dt = k_1*S_{CO2} - k_1*10^{(pK1-pH)}*S_{HCO3}$

Where $CPR_{end} = RQ_{end} * (1-f_{XI})*b_H*X_H$

Note that the alternative reaction of CO_2 with the hydroxyl ion (Eq.3) is not included since it was shown that its contribution to the dynamic CO_2 system is negligible. The jacobian matrix of the dynamic CO_2 system is then given by:

$$J = \begin{bmatrix} \frac{\partial F_1}{\partial CO_2} & \frac{\partial F_1}{\partial HCO_3} \\ \frac{\partial F_2}{\partial CO_2} & \frac{\partial F_2}{\partial HCO_3} \end{bmatrix}$$

The four differential equations are differentiated resulting in the following system matrix:

$$J = \begin{bmatrix} -k_1 - K_L a_{CO2} & k_1 10^{(pK_1 - pH)} \\ k_1 & -k_1 10^{(pK_1 - pH)} \end{bmatrix}$$

The eigenvalues of the jacobian matrix are calculated and found out to be complex functions of model parameters and operating variables (e.g. pH, K_La_{CO2} etc.):

$$\lambda_{1,2} = -\frac{1}{2}\left(k_1 + K_L a_{CO2} + k_1 10^{(pK_1 - pH)} \pm \beta\right)$$

where, $\beta = \sqrt{\left(k_1^2 + 2k_1 K_L a_{CO2} + 2k_1^2 10^{(pK_1 - pH)} + {K_L a_{CO2}}^2 - 2K_L a_{CO2} k_1 10^{(pK_1 - pH)} + k_1^2 10^{2(pK_1 - pH)}\right)}$

The time constants of the CO_2 system can be determined by taking the inverse of the eigenvalues (Noorman *et al*., 1992). These time constants are calculated for different model parameters and operating variables and are given in Table 8 for illustrative purposes. Two different time constants are observed. τ_1 indicates a process/processes with fast dynamics while τ_2 shows a process/processes with slower dynamics. It can be roughly stated that τ_1 corresponds to equilibrium processes at the gas-liquid interface, which is rather quick (in the order of minutes) while τ_2 corresponds to slower aqueous CO_2 equilibrium processes i.e. inter-conversion between CO_2 and HCO_3^- species (Ho *et al*., 1987; Noorman *et al*., 1992).

Table 8. Time constant analysis of the CO_2 system

k_1 min^{-1}	pK_1	K_La_{CO2} min^{-1}	pH_{set}	$\tau_1=-1/\lambda_1$ min	$\tau_2=-1/\lambda_2$ min
2.4	6.42	0.37	8.5	0.36	384
2.4	6.42	0.37	8.0	0.35	123
2.4	6.42	0.22	7.72	0.37	103
2.4	6.42	0.22	7.52	0.36	67
2.4	6.42	0.37	7.72	0.35	65
2.4	6.42	0.37	7.52	0.34	42

These results (particularly the time constant τ_2) explain the underlying mechanism for the slow dynamics observed in the titrimetric data (see Figure 5-top), which is in the order of 100 min depending on the operating variables and model parameters (see Table 8). One important remark concerning time constant 2 is the fact that it depends on the system pH (i.e. the pH set-point) and K_La_{CO2} during an experiment. The lower the pH the faster the response of the CO_2 system becomes (see Table 8). In contrast, the slower the K_La_{CO2}, the slower the response of the dynamic CO_2 system is (see Table 8). This is not surprising since decreasing pH increases the fraction of $CO_{2,aq}$ in the system.

On the other hand, the fast time constant, τ_1, explains the initial quick equilibrium observed in the CO_2 simulations (see Figure 5-down). These observations are in close agreement with the findings of Noorman *et al*. (1992) reported for the dynamic CO_2 model including an off-gas CO_2 balance for alkalophilic processes.

5.1.5 Sensitivity analysis of the parameters of the dynamic CO_2 model

The dynamic CO_2 model successfully predicts the dynamic behavior of the experimental data presented in Figure 5. In this section, a sensitivity analysis of the parameters contained in the CO_2 model is performed in order to assess the practical identifiability of the CO_2 model using titrimetric data alone. For the evaluation of the sensitivity function, the experimental conditions simulated for Figure 5A are used. It is important to note that the sensitivity function is dependent on the initial conditions and the assumptions (default values) made for the model parameters.

The output sensitivity functions are calculated for k_1, k_2, pK_1, K_La_{CO2} and C_{Tinit} parameters and plotted against the sensitivity function of the K_La_{CO2} (see Figure 6). In general, it is observed that the highest sensitivity of the parameters is exhibited around 100 min during the experiment. Among the parameters considered, the k_2 -the rate constant of the CO_2 reaction with hydroxyl ion to form HCO_3^- has the lowest sensitivity (in the order of 10^{-9}, see Figure 6C). This certainly confirms that the contribution of the alternative reaction of CO_2 with hydroxyl ion is negligibly small at neutral pH conditions. The CO_2 model can therefore be further simplified by excluding this reaction i.e. Eq.3 from the extended model presented in Table 3.

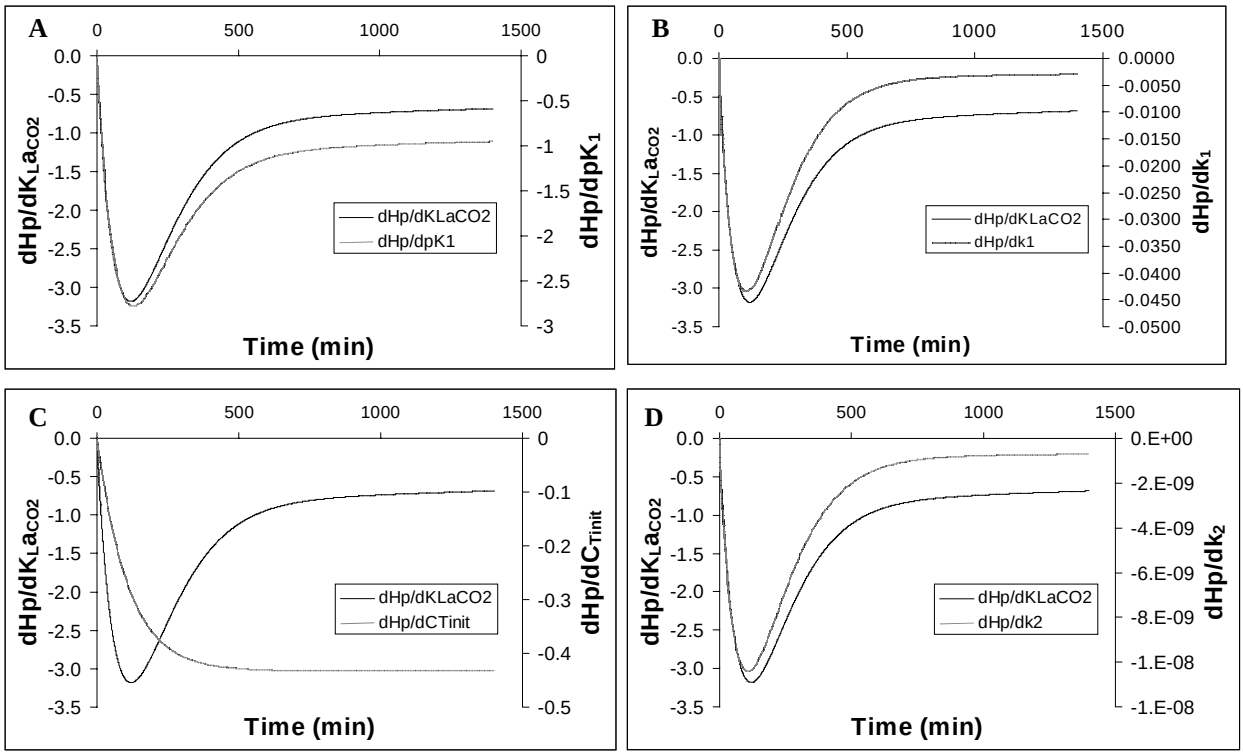

Figure 6. Output sensitivity functions calculated for the main CO_2 model parameters.

The sensitivity functions of pK_1 and k_1 are almost perfectly correlated with the sensitivity of the K_La_{CO2} until the peak level is reached in the corresponding sensitivity function. Beyond

the peak level, some degree of correlation between these parameters still exists yet it decreases in time (see Figure 6A&B). That decrease, on the other hand, is observed in all sensitivity functions. This is not surprising since in the long term, the CO_2 system is driven more and more to an equilibrium point where the impact of the CO_2 stripping on the Hp data becomes less important.

The sensitivity functions of K_La_{CO2} and C_{Tinit} are observed to be correlated in the beginning of the experiment, yet the correlation is broken after the peak is reached in the sensitivity function of the K_La_{CO2} (see Figure 6C). This suggests that both parameters are identifiable from the Hp data, which is already confirmed by the parameter estimation results (see Table 6). However, in the long term the sensitivity of both parameters decreases considerably which means that long-term experiments are not needed for the identification of these two parameters from the Hp data. In this context, a useful way to determine the optimal duration of an experiment in relation to parameter estimation is the study of the Fisher Information Matrix (FIM) (see below).

5.1.6 Effect of parameter uncertainty on estimation results

It was demonstrated in the previous section that a correlation exists between the parameters k_1, pK_1 and K_La_{CO2}. It is known that the medium composition, e.g. the ionic strength, may influence especially equilibrium constants, i.e. pK_1, which is usually set to a default value reported for water systems with a low ionic strength (Stumm and Morgan, 1996). It is therefore clear that uncertainty may exist in the value for pK_1. In this section, the influence of a change in pK_1 value on the parameter estimation for K_La_{CO2} and C_{Tinit} is investigated. For this purpose, K_La_{CO2} and C_{Tinit} are re-estimated considering 1% and 5% deviation in pK_1 using the first 300 min of the experimental data presented in Figure5A. Moreover, the influence of a change in k_1 is also investigated although it is reported that rate constants are not influenced much by the ionic strength of the medium (Ho *et al*., 1987; Stumm and Morgan, 1996).

The parameter estimation results for different values of pK_1 and k_1 are shown in Table 7. These results reveal the following main conclusions:

1. A change in pK_1 or k_1 values is compensated by a change in the K_La_{CO2} and C_{Tinit} estimates. The estimate of the K_La_{CO2} is influenced to a larger extent than the estimate of the initial total aqueous CO_2 concentration.
2. Even a very small (1%) change in pK_1 induces a considerable impact on the K_La_{CO2} estimate (16.35%). A larger change (5%) in pK_1 induces an unreasonable estimate for K_La_{CO2} with 135.85% deviation from the default conditions. This estimate mechanistically has no meaning e.g. K_La_{CO2} is almost two times bigger than K_La_{O2}. This indicates a clear parameter identifiability problem.

3. A relatively larger change (e.g. 10%) in k_1 induces almost negligible impact on the K_La_{CO2} (0.63% change) and C_{Tinit} (-0.14% change) estimates. Therefore, the k_1 can be assumed reliably from the range reported for water media (Stumm and Morgan, 1996).

However, a very important remark is that each parameter combination given in Table 7 predicted the entire experimental data set (data up to 1400 min) presented in Figure 5A equally perfect. This is an important outcome in relation to the applicability of the model. Indeed, the main objective of this study is not to uniquely identify parameters of the dynamic CO_2 model. Rather, the main goal is to describe and accurately predict the pH effect of the dynamic CO_2 system (CO_2 equilibrium and CTR processes) and this is achieved quite successfully using any parameter combination given in Table 7.

Table 7. Influence of possible parameter uncertainties in pK_1 and k_1 on the estimation of the K_La_{CO2} and C_{Tinit}.

	Fixed		**Estimated**				
Parameter uncertainty	k_1	pK_1	K_La_{CO2}	Error (%)*	C_{Tinit}	Error(%)*	SSE
(default)	2.4	6.42	0.318	-	3.36	-	0.07
1% change in pK_1	2.4	6.36	0.37	16.35	3.39	0.95	0.07
5% change in pK_1	2.4	6.10	0.75	135.85	3.64	8.25	0.07
10% change in k_1	2.16	6.42	0.32	0.63	3.35	-0.14	0.07
25% change in k_1	1.8	6.42	0.33	3.77	3.35	-0.41	0.08

*The deviation of a parameter from its default value calculated as the relative percent error.

5.1.7 Conclusion: A simple calibration methodology for the dynamic CO_2 model using titrimetric data

Considering the sensitivity analysis and correlations existing between the model parameters (see above), it is suggested to calculate K_La_{CO2} from the mass transfer coefficient of oxygen (K_La_{O2}) using Eq. 22 and setting k_1 to its typical value reported for water media (Stumm and Morgan, 1996). In this way, the dynamic CO_2 model can be calibrated successfully only by estimating pK_1 and C_{Tinit} using the titrimetric data under endogenous conditions. In this calibration approach, the need to experimentally determine pK_1 and C_{Tinit} for experiments with different ionic strentgths is eliminated thereby facilitating the application of the titrimetric methodology.

5.1.8 Optimal duration of titrimetric experiment for reliable calibration of the dynamic CO_2 model

In this section, the FIM is used to monitor the information content of the experiment described above as a function of time and thereby to find optimal duration of the titrimetric data in view of reliable parameter estimation. The reason is simply that batch experiments for calibration of ASMs are typically designed to be short (30 – 80 minutes). Since calibration of the dynamic CO_2 model needs additional measurements prior to substrate addition (see

below), it is desired to keep the length of the experiment under endogenous conditions prior to substrate addition short while maintaining a reliable parameter estimation using the resulting titrimetric data.

The FIM is a measure of quality and quantity of the experimental information and is calculated using the output sensitivity functions as shown in Eq. 25.

$$\mathbf{FIM} = \sum_{i=1}^{N} \mathbf{Y_P}\left(\mathbf{t_i}, \underline{\mathbf{p}}\right)^{\mathbf{T}} \underline{\mathbf{Q_i}}\, \mathbf{Y_P}\left(\mathbf{t_i}, \underline{\mathbf{p}}\right) \tag{25}$$

where Y_P are the output sensitivity functions with respect to the parameters at the measurement time instant and Q_i is a weighting matrix and is usually chosen to be the inverse of the measurement error covariance matrix. The FIM serves as the main basis for the optimal experimental design (OED), which has been applied successfully for improving identifiability of Monod-type models (Baltes *et al.*, 1994; Vanrolleghem *et al*., 1995; Petersen, 2000; Dochain and Vanrolleghem, 2000; Insel *et al*., 2003; etc…).

The parameters pK_1 and C_{Tinit} selected for estimation using the proton production data (Hp) (see above) are used to construct the FIM. As a result, the FIM can be formulated as follows (note that since there is only one measurement and its error is assumed constant in time, the weighting matrix Q_i is assumed 1):

$$FIM = \sum_{i}^{N} \begin{bmatrix} \dfrac{\partial Hp}{\partial pK_1} \\ \dfrac{\partial Hp}{\partial C_{Tinit}} \end{bmatrix} \cdot \begin{bmatrix} \dfrac{\partial Hp}{\partial pK_1} & \dfrac{\partial Hp}{\partial C_{Tinit}} \end{bmatrix} = \begin{bmatrix} \sum_{i}^{N} \dfrac{\partial Hp}{\partial pK_1}\dfrac{\partial Hp}{\partial pK_1} & \sum_{i}^{N} \dfrac{\partial Hp}{\partial pK_1}\dfrac{\partial Hp}{\partial C_{Tinit}} \\ \sum_{i}^{N} \dfrac{\partial Hp}{\partial pK_1}\dfrac{\partial Hp}{\partial C_{Tinit}} & \sum_{i}^{N} \dfrac{\partial Hp}{\partial C_{Tinit}}\dfrac{\partial Hp}{\partial C_{Tinit}} \end{bmatrix} \tag{26}$$

The FIM is calculated using the output sensitivity functions of the parameters pK_1 and C_{Tinit} as a function of time i.e. the number of considered measurements N in the FIM calculation (E.q. 26) is increasing with increasing time. The FIM has several properties, so called A, B, D, E and Mod-E criteria, that can be used to evaluate the information content of an experiment (see Dochain and Vanrolleghem, 2001). They are plotted in Figure 7.

Among the FIM properties, the D and Mod-E criteria are most relevant since they provide an idea about the parameter estimation accuracy and parameter correlation under a given set of measurements (Dochain and Vanrolleghem, 2001). The D-criterion is based on the determinant of the FIM. Increase in the D-criterion, indicating an increase in the information content of the experiment, is observed (see Figure 7) and continues during the experiment time. This means that the longer the experiment is, the better the accuracy of parameter

estimation becomes (Dochain and Vanrolleghem, 2001). On the other hand, the Mod-E, which is based on the ratio of the maximum eigenvalue of the FIM to its minimum eigenvalue, increases in the beginning of the experiment up to a peak and then decreases drastically (see Figure 7). This means that the parameter correlation is very high in the beginning of the experiment (in this case up to 5-6 minutes) and then decreases in time.

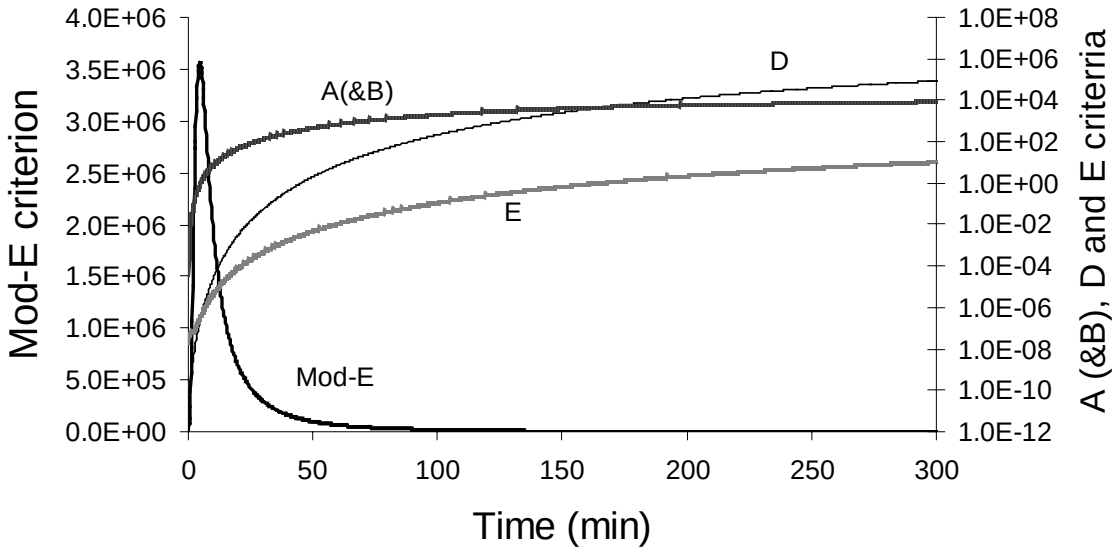

Figure 7. Different properties of the FIM (see the text for explanation) as a function of time during the experiment presented in Figure 5 (the second Y-axis is based on a logarithmic scale to compare small and large values of different criteria).

Since particularly parameter correlation was found significant (as shown above) during calibration of the dynamic CO_2 model, the Mod-E criterion can be used for the determination of optimal duration of the titrimetric experiment. Therefore, based on the Mod-E, it can be said that the duration of the titrimetric experiment should be higher than 50 min while certainly less than 100 minutes, as this provides sufficient information with improved identifiability of the dynamic CO_2 model.

5.2 Application of the extended titrimetric methodology under exogenous respiration

Figure 8 shows a typical set of respirometric-titrimetric data resulting from 2 consecutive additions of acetate (30 mgCOD/l) to endogenously respiring activated sludge. Upon pulse addition of acetate, the oxygen uptake rate (OUR) of the biomass displays a fast transient, which takes 2-5 minutes before reaching the maximum OUR level possible under the given conditions (Chapter 4.4).

The proton consumption (i.e. negative Hp), however, increases immediately to a maximum rate (with no or negligible transient) upon pulse addition of acetate (see Figure 8). These

dynamics in the OUR and Hp data have been observed and discussed in detail in Chapter 4.4. After acetate has been removed from the medium (indicated by the sharp decrease in OUR and a sharp bending point in the Hp profile), the proton consumption continues due to stripping of CO_2 from the reactor.

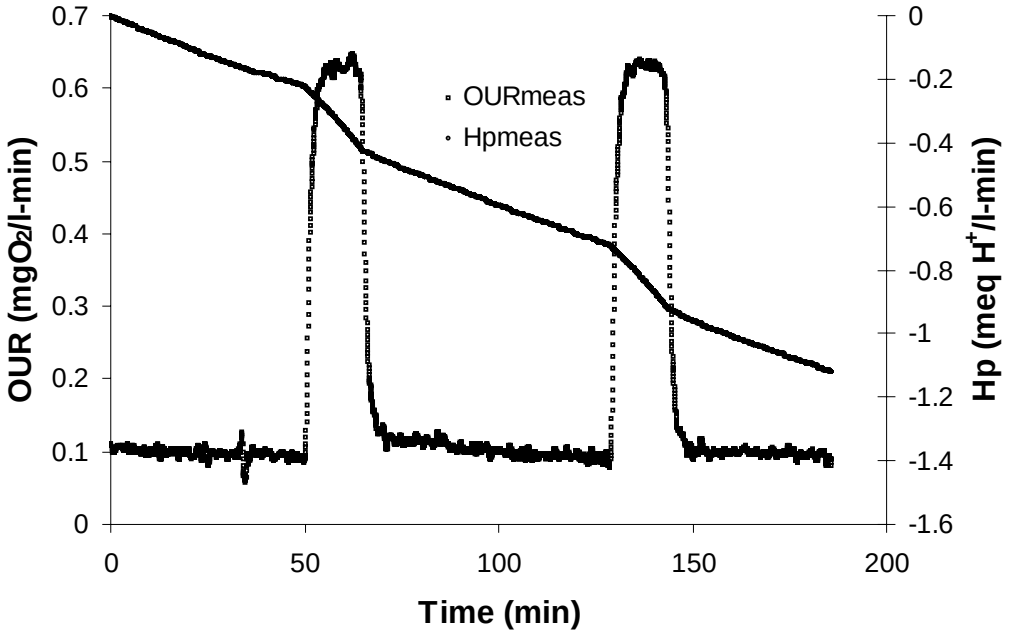

Figure 8. Typical respirometric-titrimetric measurements from batch experiments with pulse additions of ca 30-mgCOD/l acetate to endogenously respiring activated sludge.

5.2.1 Parameter estimation results

The entire data set presented in Figure 8 was used to obtain the parameter estimates shown in Table 8. The reason of this choice is twofold: first for the calibration of the extended titrimetric model the endogenous phase before and after the pulse addition of substrate needed. Second, the objective is to improve reliability and accuracy of the parameter estimates by considering two pulses of OUR (rather than using the two OUR pulses separately and then take the average of the parameter estimates).

In the parameter estimation, the endogenous decay coefficient was fixed to the experimentally determined value i.e., 0.24 d^{-1} (or 0.000167 min^{-1}, see first results section). The initial active fraction of biomass, $X_H(0)$, was determined using the endogenous part of the OUR prior to substrate addition (using Eq. 21). Finally, the structurally identifiable parameter combinations corresponding to each measured variable (see Gernaey *et al*., 2002b) were estimated using the measured variables separately or combined (see Table 9). For the parameter estimation using titrimetric data, however, the yield coefficient was fixed to its estimate based on OUR since it was shown that either i_{NBM} or yield is structurally identifiable (Gernaey *et al*., 2002b).

Table 9. Parameter estimation results using respirometric-titrimetric measurements. *Italics* indicates the parameters fixed during parameter estimation.

	OUR and Hp		**OUR**		**Hp**	
Parameters	Value	Error*	Value	Error*	Value	Error*
Y_H (mgCOD/mgCOD)	0.756	2.5E-4	0.755	3.3E-4	*0.755*	
K_S (mgCOD/l)	0.69	1.8E-3	0.69	2.9E-3	0.42	2.3E-4
μ_H (min^{-1})	0.00236	1.2E-6	0.00236	3.1E-6	0.00204	1.9E-6
$X_H(0)$ (mg COD/l)	*773*		*773*		*773*	
b_H (min^{-1})	*0.000167*		*0.000167*		*0.000167*	
τ_{OUR} (min)	1.63	4.6E-3	1.627	1.5E-2	-	
τ_{Hp} (min)	0.043	2.4E-4	-		0.067	6.2E-5
i_{NBM} (mgN/mgCOD)	0.057	3.0E-4	-		0.055	6.2E-5
C_{Tinit} (mmol/l)	2.24	4.3E-3	-		2.26	2.1E-3
pK1	6.366	7.6E-4	-		6.367	3.9E-4
k_1 (min^{-1})	*100*		-		*100*	
K_La_{CO2} (min^{-1})	*0.313*		-		*0.313*	
K_La_{O2} (min^{-1})	*0.344*		*0.344*		*0.344*	
SSE	1.02		0.92		0.12	

* Parameter estimation errors calculated for 95% confidence intervals

Parameter estimation results using OUR, Hp and simultaneous OUR and Hp data are summarized in Table 9. Model fits to the measurements in each case are found to be acceptable (see Figure 9). The parameter estimation errors, however, are too optimistic (see Table 9). This is because the algorithm used to calculate the parameter estimation errors is known to give optimistic results particularly when the total number of measurements is high and when autocorrelation exists in the experimental data (Dochain and Vanrolleghem, 2001; Petersen, 2000). In general the parameters estimated using the titrimetric data (Hp) are confirmed by the parameter estimates using the well-established oxygen measurements (OUR) (see Table 8).

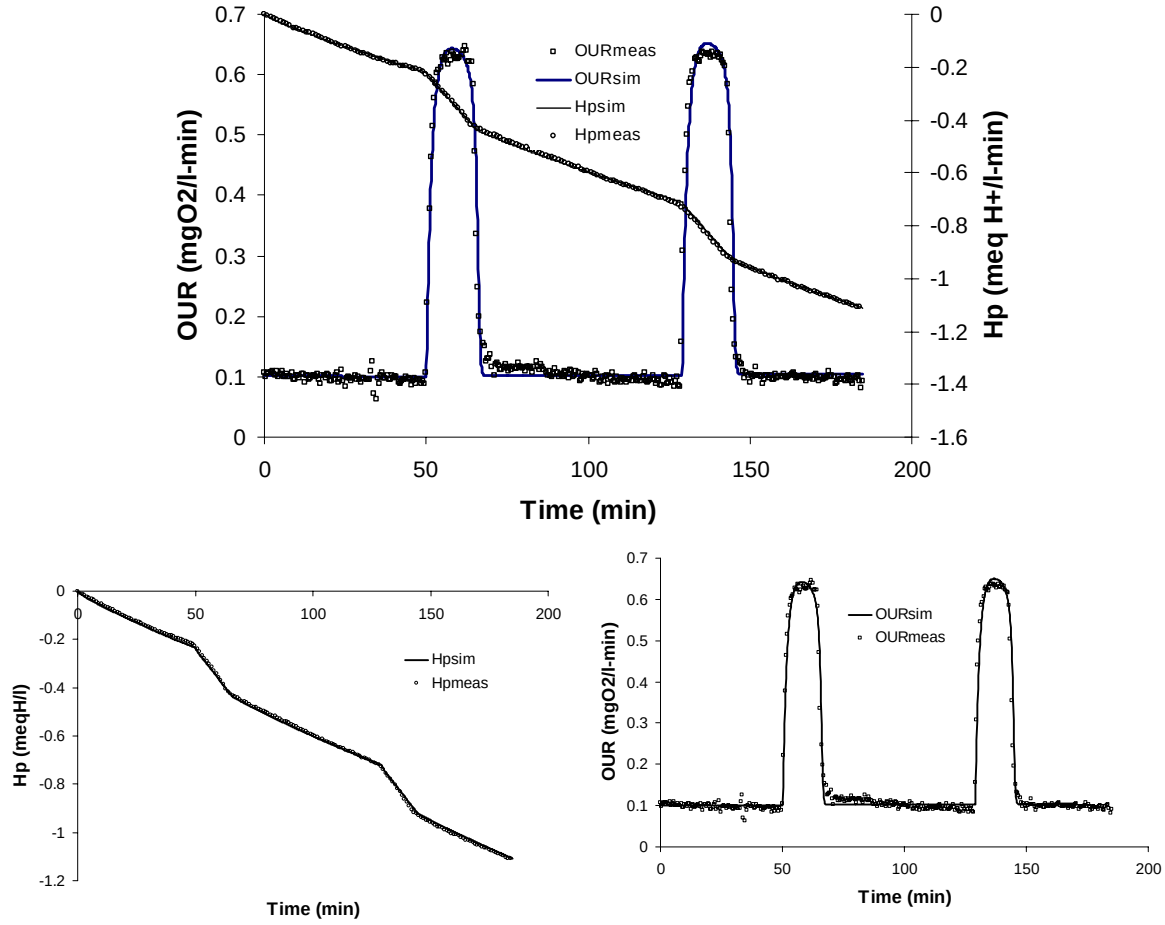

Figure 9. The model fit to the experimental data after parameter estimation using OUR & Hp (top), Hp (down-left) and OUR (down-right).

6. DISCUSSION

In the first part of this study, the Gernaey model was extended by the dynamic CO_2 model and used successfully to interpret titrimetric data collected from endogenous experiments. A calibration methodology for the dynamic CO_2 model using titrimetric data alone has been applied successfully (see above) after analyzing in detail the model structure and the identifiability of the dynamic CO_2 model. Accordingly, it is suggested that K_La_{CO2} is calculated from the K_La_{O2} determined from the oxygen measurements, similar to previous works (Noorman *et al.*, 1992; Sperandio and Paul, 1997). Since the k_2 parameter has negligible effect on the titrimetric data, it was eliminated from the model. In fact this was expected since at neutral pH, the reaction of CO_2 with the hydoxyl ion to form HCO_3^- is usually negligible (Stumm and Morgan, 1996; Sperandio and Paul, 1997). Moreover, uncertainty analysis of parameter k_1 showed that this parameter could be fixed to its default value reported for water systems. This assumption causes negligible change in the parameter estimation results. Therefore, the remaining parameters pK_1 and C_{Tinit} (the initial molar concentration of total inorganic carbon in the medium) can be reliably estimated from the titrimetric data collected from the endogenous part. The parameters of the endogenous

process, i.e. b_H and i_{NBM}, have an influence on the titrimetric data during endogenous part. Therefore, it is suggested to fix these parameters by determining them from a separate long-term decay experiment.

The time constant analysis of the dynamic CO_2 model has shown that the slow response dynamics observed in the titrimetric data with a time constant of ca 100 min (see Table 8) is due to the inter-conversions between aqueous CO_2 and HCO_3^- ions in the liquid. This is confirmed by the findings of Noorman *et al*. (1992) and reported in Ho *et al*. (1987). Moreover, the dynamics of the titrimetric data were observed to depend on the system pH and the mass transfer coefficient of CO_2.

In the second part of this study, the extended titrimetric model was applied successfully to interpret the titrimetric data resulting from an aerobic carbon source degradation experiment in view of model calibration. The estimated parameters are comparable within the range reported in the literature (Gernaey *et al*., 2002b). Moreover, the parameters estimated using Hp are quite close to the values estimated using OUR or combined OUR and Hp data (see Table 8). These results support the validity of the dynamic CO_2 model and its calibration procedure.

The yield coefficient (0.75) is estimated to be higher than the default value of ASM1 (0.67) indicating the possible existence of the storage phenomenon (Van Loosdrecht and Heijnen, 2002). However, the typical storage tail in the OUR was not observed (see Figure 8). On the contrary, the OUR profiles could be modeled straightforwardly using the ASM1 model (see Table 3).

The extended titrimetric model is more complicated than its predecessor i.e. Gernaey model since it models the non-linear effect of the dynamic CO_2 system on the resulting titrimetric data. However, the application of the model remains possible with titrimetric data alone. However, in this way, the range of applicability of titrimetric methods is increased. Because, titrimetric data resulting from experiments with pronounced and non-linear CO_2 stripping can now be interpreted and modeled reliably, e.g. for parameter estimation for aerobic carbon source degradation in view of model calibration (Gernaey *et al*., 2002b; Gernaey *et al*., 2001), monitoring and parameter estimation of nitrification kinetics (Ramadori *et al*., 1982; Gernaey *et al*., 1998; Gerneay *et al*., 2001; Yuan and Bogaert, 2001).

Moreover, the increased range of applicability and accurate utilization of the titrimetric data is expected to contribute particularly to the improvement of the identification of the over-parameterized ASM models (e.g. ASM1, ASM2, ASM3). For instance, it has been shown that titrimetric data in addition to respirometric data, make the yield coefficient identifiable during

carbon source degradation processes (Gernaey *et al*., 2002b).

On the other hand, one important drawback associated with the titrimetric methodology is that the elemental composition of the biomass and carbon source should be a priori known (i.e. the degrees of reduction of biomass and substrate). This is not the case for wastewater, which has a complex composition. However, the extended model is still valuable for many applications. For example, it is particularly significant when studying and identifying the two-step nitrification kinetics. Moreover, it is a useful, simple and cheap tool to study the degradation of known carbon sources by activated sludge.

7. CONCLUSIONS

In this study, the Gernaey model was successfully extended with a dynamic CO_2 model to describe titrimetric data resulting from titrimetric experiments with time-varying CO_2 stripping rates. The dynamic CO_2 model was based on the CO_2 gas-liquid equilibrium and the aqueous CO_2 system. The dynamic CO_2 model in the extended Gernaey model required more parameters to be estimated than the Gernaey model.

Therefore, a simple calibration procedure was developed which makes it possible to calibrate the dynamic CO_2 model using titrimetric data alone, e.g. about 50 minutes collected under endogenous conditions. Accordingly, the CO_2 mass transfer coefficient, $K_La_{CO2,}$ can be calculated using the K_La_{O2} obtained from oxygen measurements, while the k_1 forward reaction rate constant of the first equilibrium reaction of CO_2 can be assumed from literature. The remaining parameters pK_1 and C_{Tinit} were shown to be estimated reliably from short-term titrimetric data (e.g. 50 minutes).

The time constant analysis of the dynamic CO_2 model has shown that the slow response dynamics observed in the titrimetric data (with a time constant of ca 100 min) is due to the transfer resistance of CO_2 at the liquid side. Further, the time constant observed in the titrimetric data depends on several degrees of freedom in the experimental conditions, e.g. pK_1, pH and K_La_{CO2}.

Using the calibration procedure developed above, the extended Gernaey model was used successfully to interpret typical data colelcted during combined respirometric-titrimetric experiments. The parameter estimation results using titrimetric data alone were confirmed remarkably well by the parameter estimates based on respirometeric measurements. This supports the validity of the Gernaey model extended with the dynamic CO_2 model.

The extended Gernaey model is expected to contribute to the improvement of the identifiability of increasingly complex activated sludge models (Henze *et al*. 2000). Although

the titrimetric methodology requires the substrate composition to be a priori known, it is a valuable and cheap tool for many applications: identifying two-step nitrification kinetics and studying degradation kinetics of known carbon sources by activated sludge.

Chapter 4.2.1

Limitations of ASM1 and ASM3: A comparison based on batch OUR profiles from different full-scale WWTP

ABSTRACT

The two most popular models for the description of the biological COD removal are ASM1 and ASM3. However, some numerical inconsistencies arise when using these models to interpret the data obtained in short-term respirometric batch experiments. In this study, both models are fitted to four different respirometric batch profiles obtained with biomass from different WWTP. The parameter estimation results and the practical (local) identifiability are analysed, and the limitations of both models are discussed. Based on this discussion, possible improvements to the modelling of the biological COD removal, such as the inclusion of simultaneous growth and storage on external substrate, are proposed.

This chapter is accepted as platform presentation in 4th IWA World Water Congress:

Guisasola A., Sin G., Baeza J.A., Carrera J. And Vanrolleghem P (Accepted) Limitations of ASM1 and ASM3: a comparison based on batch OUR profiles from different full-scale WWTPs. *IWA 4th World Water Congress*, 19-24 September 2004, Marrakech, Morocco.

1. INTRODUCTION

In 1987, the International Water Association (IWA) introduced the Activated Sludge Model nº1 (ASM1) for the description of the biological COD and nitrogen removal (Henze *et al.,* 2000). In this model, biomass was considered to grow solely on the external substrate present and the oxygen consumption after the external substrate depletion was explained with the decay of biomass. In the conventional activated sludge processes, the feed regime is highly variable and biomass is subjected to alternating conditions of external substrate availability (feast phase) and absence of external substrate (famine phase). Under these dynamic conditions, internal storage polymers play an important role in the substrate consumption (van Loosdrecht *et al.,* 1997). Recently, a new model for the COD removal (ASM3) has been developed mainly to take this storage phenomenon into account (Henze *et al.,* 2000). The main innovation of this model is the assumption that all the readily biodegradable organic substrates taken up under feast conditions are directly converted into stored material. These stored compounds become the carbon and energy source for growth purposes in the subsequent famine period. In ASM3, the decay processes are replaced with the endogenous processes. The conceptual basis of ASM3 has been largely criticized and alternatives models taking into account simultaneous storage and growth processes were proposed (e.g. van Aalst-van Leeuwen *et al.,* 1997, Krishna and Van Loosdrecht, 1999; Beccari *et al.,* 2002, van Loosdrecht and Heijnen 2002, Karahan-Gül *et al.,* 2003).

In this study, parameter estimation and identifiability issues of ASM3 in view of model calibration are addressed and compared with the well-studied ASM1 model. To this aim, oxygen uptake rate measurements (OUR) of biomass sampled from 3 different full-scale wastewater treatment plants (WWTPs) were used. The parameter estimation results of both models are interpreted and discussed in view of their possible (mechanistic) biological meaning. Further, the practical (local) identifiability of both models is compared in view of unique parameter estimations. Based on the mechanistic meaning and the identifiability of the parameter estimates, possible improvements to modelling substrate conversion processes are discussed.

2. MATERIALS AND METHODS

2.1 Experimental set-up

The experimental work was performed in two different set-ups. On the one hand, experiments A and B were performed in an LFS type respirometer, which was developed in a previous work (Guisasola *et al.* in press). On the other hand, experiments C and D were performed using the hybrid-respirometric set-up described in a previous study (Chapter 3.1). The pH is fixed during these experiments to 7.80±0.03 using a pH controller.

In both set-ups, the biomass was first aerated overnight to reach the endogenous-state. Then, a first pulse of acetate was added to induce a "wake-up" effect on the biomass activity (Vanrolleghem *et al.*, 1998) At the same time, ammonia in excess and ATU (30 mg/l) was added to avoid growth-limitation and nitrification, respectively. Activated sludge sampled from three different WWTP was used during experimental work: experiment D used biomass from the Maria Middlelares WWTP (Gent, Belgium), which performs COD removal and nitrification. Experiment C used biomass from Ossemeersen WWTP (Gent, Belgium), which performs COD removal, nitrification and denitrification the same way as Granollers WWTP (Catalonia, Spain) whose biomass was used for experiments A and B. These biomass samples were analysed for TSS and VSS according standard methods (APHA, 1995).

2.2 Parameter estimation and confidence intervals

Modelling, simulation and parameter estimation were performed using MATLAB 6.5 (The MathWorks, Natick, MA). The differential equations were solved using an explicit Runge-Kutta (4,5) formula. Parameter estimation was carried out by using the Nelder-Mead Simplex search method, where the weighed sum J (Eq. 1) of squared errors between model outputs $y(t_k,\theta)$ and the measured outputs $y_M(k)$, with Q_k as weighting matrix (equal to the inverse of the measurement error covariance matrix), is minimised:

$$J = \sum_{k=1}^{N} \left[y(t_k,\theta) - y_M(k) \right]^T Q_k \left[y(t_k,\theta) - y_M(k) \right] \quad (1)$$

where N is the number of measurements. Each of the output signals can be linearised in the neighbourhood of the optimal vector of parameters θ_O (Dochain and Vanrolleghem, 2001):

$$y(t,\theta_O + \delta\theta) = y(t,\theta_O) + \left[\frac{\delta y(t,\theta_O)}{\delta \theta^T} \right]_{\theta_O} \cdot \delta\theta = y(t,\theta_O) + Y_\theta^T(t)\delta\theta \quad (2)$$

where $Y_\theta(t)$ is the so called output sensitivity function. If Q_k is the covariance matrix of the measurement noise, the FIM is defined as:

$$FIM = \sum_{k=1}^{N} Y_\theta^T(t_k) Q_k Y_\theta(t_k) \quad (3)$$

The FIM matrix summarises the quantity and quality of information obtained in each experiment because it considers the output sensitivity functions and the measurement errors of an experimental data (i.e. accuracy of an experiment). Assuming white measurement noise and no model mismatch, the inverse of the FIM provides the lower bound of the parameter

estimation error covariance matrix that can be used to assess the estimation uncertainty of θ_O:

$$COV(\theta_O) \geq FIM^{-1} \quad (4)$$

Moreover, since output sensitivities of parameters with respect to measurement(s) are calculated using a model, the FIM also depends on the structure of the model. This property of FIM can be used to study the practical identifiability (local) of the model under the available experimental data (Dochain and Vanrolleghem, 2001).

3. RESULTS AND DISCUSSION

In this study, four different OUR profiles (Figures 1a-d) obtained from three different full-scale WWTPs were used to investigate the model-fit performance and identifiability for ASM1 and ASM3. These OUR profiles show different behaviours despite a pulse of the same substrate (acetate) was added (see Fig. 1), because the biomass used in each experiment came from a different WWTP. The differences appreciated among the OUR profiles are probably linked to the operational conditions of the plant i.e. alternating feed and famine conditions.

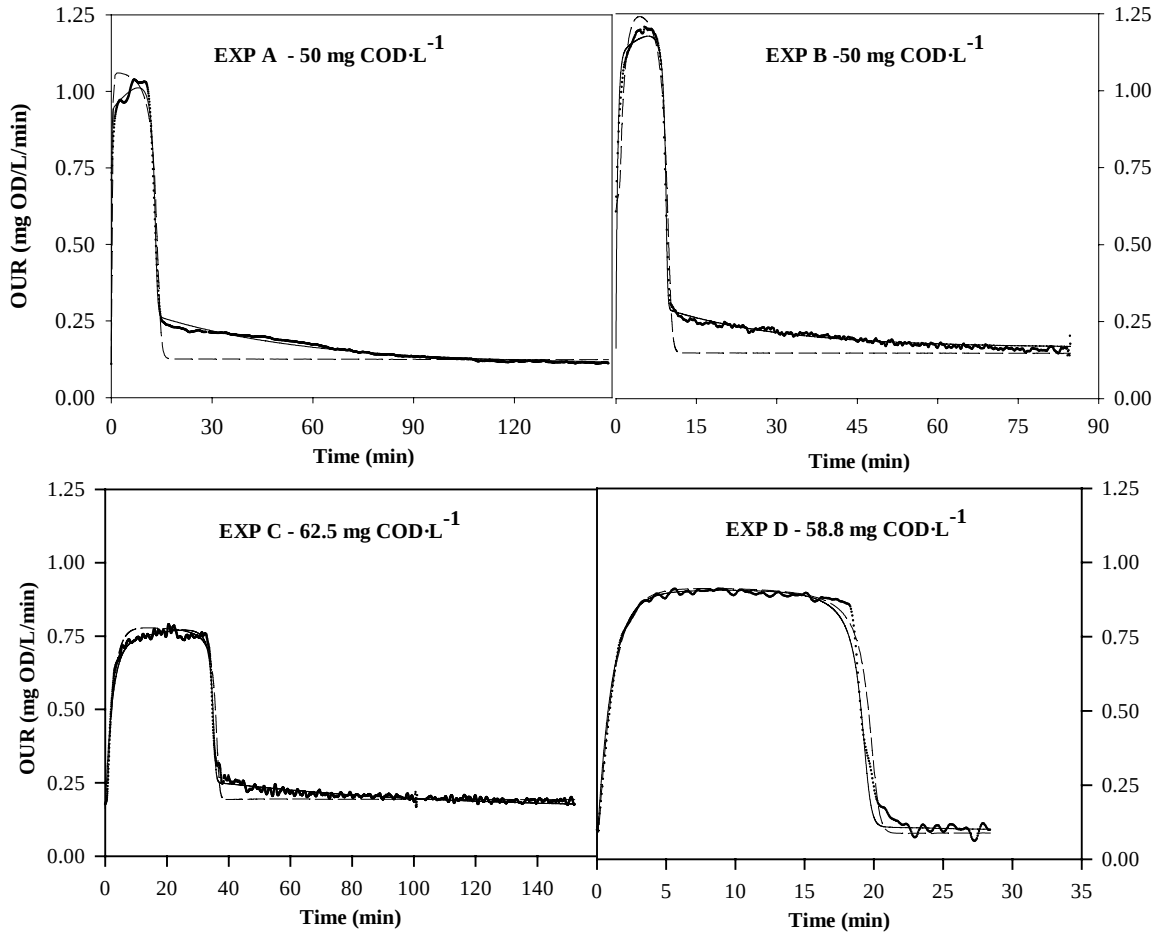

Figures 1 (A-D)- Experimental data (dotted line) and modelled OUR profiles. The ASM1 and ASM3 fittings are depicted with short-dashed and solid lines respectively.

For instance, in experiments A, B and C two different phases can be easily distinguished. The first phase is related to the external substrate consumption, while the second phase corresponds to the consumption of the previously stored internal polymer (van Loosdrecht *et al.*, 1997). In Granollers and Ossemeersen WWTPs, both nitrification and denitrification take place and the biomass is subjected to alternating anoxic and aerobic conditions under the dynamic influent substrate/wastewater pattern. Under these conditions of alternating external substrate availability, bacteria capable of storing substrate have a competitive advantage because they are able to balance their growth rate under continuously changing conditions. Under the periods of excess substrate, non-storage bacteria have to invest extra energy to grow faster in the presence of substrate and will deteriorate in the periods without substrate (van Loosdrecht *et al.*, 1997). On the other hand, in experiment D only one phase can be distinguished which is a typical ASM1 type OUR profile. The biomass used in this experiment came from the Maria Middlelares WWTP, which is continuously aerated, and is probably subjected to rather stable influent dynamics. In other words, the feast and famine phases are probably less pronounced in this WWTP.

3.1 Parameter estimation procedure

The mathematical models used (see Table 1) to interpret the experimental data are simplified versions of ASM1 and ASM3 respectively: aerobic degradation of COD as substrate. The processes included in Table 1 are described in detail in Henze *et al.* (2000).

Table 1. The simplified ASM1 and ASM3 models used in this work (M stands for the Monod kinetics of the corresponding parameter: e.g. $M_O = S_O/(S_O + K_O)$

ASM1 Processes	X_H	X_{STO}	X_S	S_S	S_O	Kinetics
1. Growth on S_S	**1**			$-\frac{1}{Y_{H,S}}$	$-\frac{1-Y_{H,S}}{Y_{H,S}}$	$\mu_H M_S \cdot M_O X_H \cdot (1-e^{-\frac{t}{\tau}})$
2. Biomass decay	**-1**		**(1-fp)**			$b_H X_H$
3. Hydrolysis			**-1**	**1**		$k_H M_{X_S/X_H} \cdot M_O \cdot X_H$
ASM3 Processes	X_H	X_{STO}	X_S	S_S	S_O	Kinetics
4. S_S Storage		**1**		$-\frac{1}{Y_{STO}}$	$-\frac{1-Y_{STO}}{Y_{STO}}$	$k_{STO} \cdot M_S \cdot M_O \cdot X_H \cdot (1-e^{-\frac{t}{\tau}})$
5. Growth on X_{STO}	**1**	$-\frac{1}{Y_{H,STO}}$			$-\frac{1-Y_{H,STO}}{Y_{H,STO}}$	$\mu_H \cdot M_{X_{STO}/X_H} \cdot M_O \cdot X_H$
6. Endogenous respiration	**-1**				**-1**	$b_H \cdot M_O \cdot X_H$
7. X_{STO} respiration		**-1**			**-1**	$b_{STO} \cdot M_O \cdot X_H$

An empirical factor was added in the kinetics of two processes (processes nº 1 and 4) to describe the fast transient period (1-3 minutes) in reaching the maximum OUR observed after

the substrate addition. This phenomenon, known as "start-up", can be mathematically described by a first order model (Chapter 4.4; Guisasola *et al.,* 2004).

For the parameter estimation, the initial concentration of biomass, $X_H(0)$ is estimated using the baseline endogenous OUR level prior to substrate addition, while fixing the decay rate coefficient b_H to its default value assigned in the corresponding model. This approach was adopted since it is not possible to obtain unique values of both b_H and $X_H(0)$ using OUR measurements alone. Hence, only one of the two parameters can be estimated and the other one should be fixed. In this study, b_H was fixed to its default value since it does not vary significantly among different WWTPs. The fittings of the models (ASM1 and ASM3) are given in Figure 1(a-d) and the results of the parameter estimation are given in Table 2. The parameter estimation errors obtained are quite good (see Table 2). This is because the method used to estimate these estimation errors is known to give too optimistic results due to autocorrelation in the OUR data (Dochain and Vanrolleghem, 2001).

3.2 Evaluation of the quality of the fit of ASM1 and ASM3

A first glance at Figure 1 shows that ASM1 is not able to describe the tail observed in experiments A and B, where the storage effect is emphasized. Many respirograms can be found in the literature with this tail, and the main criticism that ASM1 may receive is that these tails are not predicted when the feed solely contains readily biodegradable substrate. In contrast, when using typical raw wastewater the effect of storage would be lumped in the hydrolysis process and, hence, ASM1 could describe correctly the experimental OUR profile.

Table 2 – Parameter estimation results and confidence intervals (COD_X – COD biomass, COD_S – COD external substrate, COD_P – COD PHA)

ASM1 fittings	**EXP A**	**EXP B**	**EXP C**	**EXP D**
μ_H (d^{-1})	3.876±0.003	4.112±0.009	1.020±0.001	2.951±0.001
$Y_{H,S}$ (g $COD_X \cdot g^{-1}$ COD_S)	0.757±0.001	0.792±0.001	0.666±0.001	0.726±0.001
K_S (mg $COD \cdot L^{-1}$)	1.789±0.005	1.63±0.02	0.558±0.008	0.718±0.005
τ (min)	0.240±0.007	0.95±0.05	2.072±0.006	1.065±0.007
$X_H(0)$ (mg $COD_X \cdot L^{-1}$)	1250	1800	2300	1250
SSE	2.386	2.192	1.673	0.966
ASM3 fittings	**EXP A**	**EXP B**	**EXP C**	**EXP D**
k_{STO} (d^{-1})	4.88±0.009	4.679±0.009	1.056±0.002	3.027±0.007
Y_{STO} (g $COD_P \cdot g^{-1}$ COD_S)	0.796±0.006	0.831±0.006	0.715±0.005	0.75±0.01
K_S (mg $COD \cdot L^{-1}$)	0.80±0.02	0.91±0.02	0.69±0.02	0.79±0.02
μ_H (d^{-1})	28.1±0.5	64±2	19.8±0.4	51± 32
$Y_{H,STO}$ (g $COD_X \cdot g^{-1}$ COD_P)	0.804±0.002	0.921±0.002	0.838±0.002	0.96±0.01
τ (min)	0.123±0.005	0.34±0.01	2.21±0.03	1.02±0.03
$X_H(0)$ (mg $COD_X \cdot L^{-1}$)	1000	1500	2000	1000
SSE	0.560	0.744	0.999	0.755

As shown in Table 2, ASM3 better describes all the experimental profiles when comparing the sum of squared errors (SSE). The clearer the storage effect is, the higher the improvement

of using ASM3 instead of ASM1. This improvement is observed even in the experiment D, where no storage can be appreciated. When comparing the fittings of ASM1 and ASM3, it has to be taken into account that 7 parameters are estimated in ASM3, while only five are estimated in ASM1. The more parameters to be estimated, the more chances to obtain better fittings. However, once a good fitting is obtained, an analysis on the mechanistic meaning of the parameter estimation results is required. In the following, the analysis of the parameter estimation results of both models is developed.

3.3 Evaluation of the parameter estimation results of the models

In the experiments with apparent storage (A and B) two different shoulders can be easily distinguished. According to ASM1, the direct growth on external substrate is the cause of the first shoulder, whereas the ASM3 model links this first consumption to the storage of substrate into internal polymer. These processes have different default yield values: 0.67 for the growth yield in ASM1 and 0.85 for the storage yield in ASM3, because less energy is required to store external substrate than to produce new cells. When fitting experimental data to ASM1, the growth yields obtained (0.76 and 0.79) are higher than 0.67. This finding indicates the storage presence because less oxygen consumption is observed while the majority of the substrate flux is incorporated into biomass (e.g. as new cells in ASM1 or internal storage products + new cells in ASM3).

On the other hand, the storage yields obtained by fitting ASM3 (0.79 and 0.83) are a bit lower than the default one of ASM3 (0.85), probably reflecting that not all the acetate consumed is stored. Yield values for storage with acetate in this range are also experimentally observed in other similar works (van Aalst-van Leeuwen *et al.*, 1997 (0.75), Krishna and van Loosdrecht 1999 (0.73), Koch *et al.*, 2000 (0.72), Karahan-Gül *et al.*, 2003 (0.78)). These observations i.e. higher growth yield in ASM1 and lower storage yields in ASM3, support the concept that both growth and storage processes occur simultaneously and part of acetate is used for growth and the rest is stored.

Although the tail is accurately fitted by ASM3, the mechanistic meaning of the parameters related to this tail is highly questionable. First of all, the parameter estimation error of μ_H is the highest of all the parameters (especially in experiment where no/negligible storage effect is observed). Moreover, both the maximum growth rate (μ_H) and the growth yield ($Y_{H,STO}$) estimated by ASM3 (see Table 2) are noticeably higher than the default ones, 2 d^{-1} and 0.63 respectively. The reason for these high values could be that the real production of X_{STO} (e.g. PHA) during the experiment is less than the one predicted by the model. This is not surprising since ASM3 considers that all the acetate is stored. Hence, the experimentally observed tail (see Fig. 1-a) is much smaller than the one predicted by the ASM3 with its default values. From a model-fit point of view, the μ_H must be increased so that the endpoint of the PHA

consumption can be predicted correctly. From a parameter identifiability point of view, however, $Y_{H,STO}$ is correlated with μ_H (See below). Therefore an increase in μ_H is compensated by an increase in the estimate of $Y_{H,STO}$ so that the total oxygen consumed is correctly predicted. High values of the growth yield, $Y_{H,STO}$, are also observed in the literature when fitting ASM3 to experimental data (Koch *et al.*, 2000; Karahan-Gül *et al.*, 2003; Beccari *et al.*, 2002). This is however contradicting the conceptual basis of ASM3 since the predicted growth yield does not have any longer mechanistic meaning. On the other hand ASM1 is not able to predict the tail often observed in OUR obtained from batch experiments. However, for a profile with low storage effect (as experiment C) an increase in the b_H value could result in better model-fit.

Experiment D seems to be the only OUR profile which is in agreement with ASM1 because the typical storage tail is not observed. However, the estimated growth yield (0.73) (see Table 2) is still higher than the default value in ASM1 (0.67). This observation strongly suggests the presence of storage phenomenon and as such, it again supports the aforementioned simultaneous storage and growth phenomenon. Concerning the fit of ASM3 to experiment D, non-reliable/non-mechanistic parameter estimates were obtained (see Table 2), especially the values referring to the growth on storage product (e.g. μ_H) is around 50 d^{-1} for the same reason explained below, i.e. the actually experimental produced X_{STO} is lower than what the ASM3 predicts.

3.4 Simultaneous growth and storage on external substrate

In general, more reliable parameter values would be obtained if the model could describe that part of the acetate was used directly for growth. In this case, the model would predict less PHA production and the predicted tail would be lower and, then, closer to the experimental data. Moreover, a decrease on the values of μ_H and $Y_{H,STO}$ would be necessary to describe the tail. The reduction of the tail as a function of a percentage of the acetate used directly for growth is depicted in Figure 2. In this figure, four simulations with a model coming from a combination of ASM1 and ASM3 are performed (see chapter 4.2.2).

The simultaneous storage and growth models have been recently developed using a metabolic approach in van Aalst-van Leeuwen *et al.*, 1997, in the works of van Loosdrecht and Heijnen (2002) and Karahan-Gül *et al.* (2003). Apart from a more reliable description of the reality, these models can overcome another described failure of ASM3. ASM3 fails in predicting the maximum growth rate profile on these short-term respirometric batch experiments. Krishna and van Loosdrecht (1999) pointed out the presence of a discontinuity on this profile. In other words, the growth rate observed in the feast phase is higher than the one observed in the famine phase. ASM1 correctly describes this observation, because the oxygen consumption is solely related to the growth process, so both the OUR and the growth rate profiles have the

same trend. In contrast, according to ASM3, the growth rate must be constant and continuous along the experiment corresponding to the maximum growth rate on storage product. Two different growth rates are predicted with the introduction of simultaneous growth and storage on external substrate.

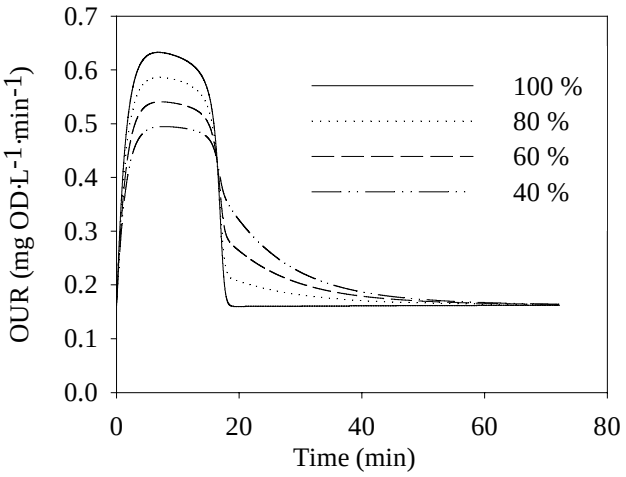

Figure 2 – Simulation of the effect of a percentage of the acetate being used directly for growth

3.5 Practical (local) identifiability ASM3 using OUR

An important issue that should be considered in modeling, particularly in view of calibration, is the identifiability of the models. The identifiability of the ASM1 model based on short-term respirometric profiles is already discussed in detail in Dochain and Vanrolleghem (2001). ASM3 introduces the storage process in addition to the growth process for the description of the tail. The growth process on X_{STO} of ASM3, is a totally different model structure, which contains three parameters: μ_H, K_{STO} and $Y_{H,STO}$ (see Table 1). As shown in Figure 3-upleft, the output sensitivity functions of μ_H and K_{STO} (calculated for exp C) are correlated with each other. This implies that both parameters cannot be identified uniquely. The correlation between these two parameters becomes clear when the shape of the objective function, J, (Eq.1) is calculated around an optimum as a function of μ_H and $K_{STO.}$ The shape of objective function (see Fig 3-upright) shows a flat valley with a certain direction in the plane (μ_H and K_{STO}). This has often been observed in Monod-type models (e.g. Dochain and Vanrolleghem, 2001). This means that several different combinations of μ_H and K_{STO} can fit the experimental data equally well. This observation was also confirmed when both parameters were considered for parameter estimation. In that case, the parameter estimation error (uncertainty in parameter estimation) of μ_H and K_{STO} increased considerably, up to 300% of relative errors, indicating no reliable estimates for both parameters are possible.

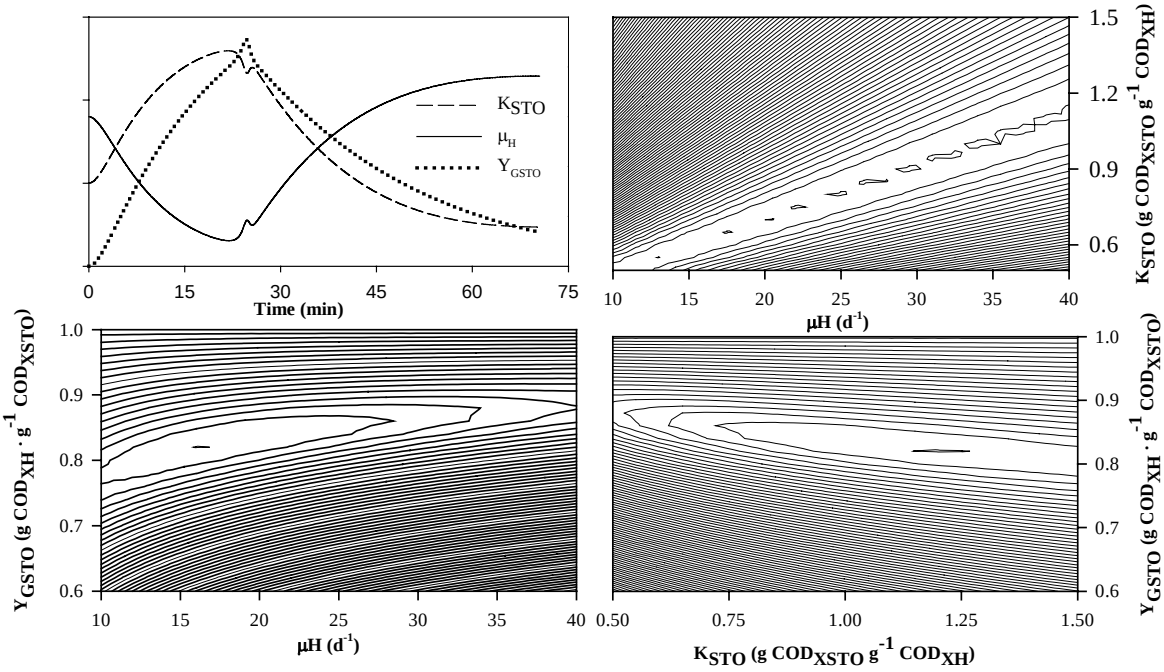

Figure 3 – Sensitivity functions of μ_H (solid line), K_{STO} (short-dashed line) and $Y_{H,STO}$ (dotted line) (upleft) and correlation of μ_H and K_{STO} (upright), μ_H and $Y_{H,STO}$ (downleft) and K_{STO} and $Y_{H,STO}$ (downright).

On the other hand, the shape of the objective function as a function of μ_H and $Y_{H,STO}$ depicted in Figure 3-downleft does not show linearity in the plane (μ_H and $Y_{H,STO}$). However, the contour plots of the objective function are rather large which indicates that still a high correlation exists between these two parameters (Dochain and Vanrolleghem, 2001). The same conclusion can be obtained from the plot of the objective function as a function of K_{STO} and $Y_{H,STO}$ (Figure 3 – downright). This implies the existence of a severe correlation between K_{STO} and $Y_{H,STO.}$ In this study, K_{STO} was not estimated together with μ_H and $Y_{H,STO}$ and it was fixed to its default value in ASM3 i.e. 1 g $COD_{XSTO} \cdot g^{-1}COD_{XH}$.

4. CONCLUSIONS

In this study, ASM1 and ASM3 models were compared in view of mechanistically predicting Oxygen Uptake Rate (OUR) measurements of activated sludge. It was observed that the ASM3 model better describes all the experimental profiles when comparing the sum of squared errors. However, it has to be taken into account that seven parameters are estimated in this model in contrast with ASM1, where only five parameters are estimated. Moreover, in experiments with considerable storage, ASM1 is not able to predict the tail observed due to the internal polymer consumption. In contrast, ASM3 can describe this second tail accurately, but non-mechanistic parameters are obtained.

The growth yield (Y_H) obtained by fitting ASM1 to the short-term respirometric batch profiles was observed to be higher than the default one (0.67) and the storage yield (Y_{STO}) obtained by fitting ASM3 is lower than the default one (0.85). These values may support the simultaneous storage and growth models already proposed in other works (e.g. van Loosdrecht and Heijnen, 2002). The introduction of simultaneous storage and growth models would also help to improve the mechanistic meaning of the estimated parameters.

From a practical identifiability point of view, this study shows the difficulty to obtain reliable values of the parameters related to the ASM3-growth process because μ_H and K_{STO} are not identifiable, and high correlation exists between $Y_{H,STO}$ and μ_H, and $Y_{H,STO}$ and K_{STO}. Future model developments should take into account the identifiability issues. Non-identifiable model structures should be avoided to improve the mechanistic meaning of model parameters thereby facilitating model validation tasks.

5. ACKNOWLEDGEMENTS

Albert Guisasola is grateful for the grant received from the Spanish government (Ministerio de Educacion y Ciencia). His work is supported by CICYT (project REN2000-0670/TECNO).

Chapter 4.2.2

A new approach for modelling simultaneous storage and growth processes for activated sludge systems under aerobic conditions

ABSTRACT

Based on critically evaluating previous models available in literature, a new mechanistic model is developed to describe simultaneous storage and growth processes occurring in activated sludge systems under aerobic conditions Two important aspects of the proposed model are (1) the branch-pipe analogy introduced for the modelling of the distribution of substrate flux between storage and growth under feast conditions and (2) the second order model developed for the description of the degradation of the storage products under famine conditions. With this new approach, it is now possible to *explicitly* separate substrate uptake kinetics from growth kinetics. The model is successfully calibrated using *only* the OUR data obtained from batch experiments with biomass from full-scale WWTPs in Belgium and Spain. Moreover, the predictions of the calibrated model were successfully confirmed using offline PHB measurements, supporting the validity of the proposed model. An iterative experimental design procedure was successfully applied and found to remarkably improve the parameter estimation accuracy for the growth on storage parameters K_1 and K_2, which used to have large confidence intervals. The parameter estimation results showed that the storage ratio, f_{STO}, ranged from 0.3 to 0.65 mgCOD/mgCOD for the biomass examined in this study. Moreover, the estimated biomass growth yield on substrate (0.58 mgCOD/mgCOD) is quite close to the theoretically expected range for heterotrophic growth. This became possible thanks to the storage process that is properly accounted for. The maximum substrate uptake rate was observed to be 5 times higher than the maximum growth rate of the biomass. Moreover, the maximum growth rate was predicted in the range 0.7 –1.3 d^{-1}. This range, albeit quite lower than the values reported for the growth-based ASM models, is believed to be more realistic. Finally, the new model is expected to better and mechanistically describe simultaneous storage and growth activities of activated sludge systems and as such to contribute to improved design, operation and control of those systems.

This chapter is *in preparation* for publication in Biotech. Progress.

1. INTRODUCTION

The modelling of activated sludge processes, particularly the biological substrate conversions, has evolved fundamentally in the last two decades from simple growth-based kinetics (ASM1, Henze *et al*., 2000) to more complicated models involving the description of storage phenomena (ASM3, Henze *et al*., 2000). The major driving force behind this modelling trend was the increased understanding of storage polymers to be an essential intermediate in the overall substrate removal in (full-scale) activated sludge systems, particularly subjected to feast and famine conditions (van Loosdrecht *et al*., 1997; Krishna and van Loosdrecht, 1999; Beun *et al*., 2000a; Henze *et al*., 2000; Dircks *et al*., 2001; Carucci et al., 2001; Beccari *et al*., 2002).

The storage phenomenon in activated sludge is conceived to be due to microbial selection in relation to limited and alternating availability of substrate in activated sludge systems. The selective forces are thought to be the dynamic/fluctuating nature of the substrate input to WWTPs and the inherent characteristics of certain designs of WWTPs, i.e. SBRs, plug-flow type reactors, selectors for bulking control, anaerobic compartments with short residence time for phosphorous removal, etc. (van Loosdrecht *et al*., 2001; Dircks *et al*., 2001). These result in an uneven/irregular spatial and temporal distribution of substrate in WWTP systems creating alternating feast and famine conditions. In this type of systems, it is hypothesised that microorganisms tend to maximise their substrate uptake (requiring less energy than growth, van Loosdrecht and Heijnen, 2002) to form storage polymers in the presence of external substrate (feast phase) and then to grow using the previously stored polymers in absence of substrate (famine phase) (van Loosdrecht *et al*., 1997). In this way, microorganisms that can maximise substrate uptake gain selective advantage against those that maximise growth rate or are directly growing on substrate during the feast phase, i.e. ASM1 type biomass (van Loosdrecht *et al*., 1997).

ASM3 is one of the first models to address the storage phenomenon. To keep the modeling exercise simple (Gujer *et al*., 1999), it assumed that all readily biodegradable substrate (S_S) is first stored as internal storage products (X_{STO}) before it is used for growth during the famine phase. Being the first attempt to evaluate ASM3 using experimental data, Krishna and van Loosdrecht (1999) has observed that ASM3 failed to model two significant experimental observations:

(i) The discontinuity in the growth rate of biomass observed experimentally in feast and famine phases

(ii) It required prediction of higher levels of internal storage polymers than measured to fit the oxygen consumption during feast and famine phases.

The major reason of this failure was the experimentally observed fact that storage and growth occur simultaneously during the feast phase as opposed to the assumption of ASM3 that only

storage occurs during feast phase (van Aalst-van Leeuwen *et al*., 1997; Krishna and van Loosdrecht, 1999; Beun *et al*., 2000a). This fact led to the formulation of the first simultaneous storage and growth model to better interpret the experimental data by Krishna and van Loosdrecht (1999). This exclusive storage/growth assumption of ASM3 has often been challenged/criticised by numerous results obtained with biomass both from lab-scale (Beun *et al*., 2000a,b; Karahan-Gul *et al*., 2003;etc) and full-scale experiments (Dircks *et al*., 2001; Carucci *et al*., 2001; Beccari *et al*., 2002). In Chapter 4.2.1, moreover, it was shown that this assumption of ASM3 also causes severe practical identifiability problems that results in unrealistic/not-mechanistic parameter estimates using batch OUR profiles, the traditional way of model calibration. From a mechanistic modelling point of view, it becomes clear that ASM3 should be extended to account for simultaneous storage and growth. In addition to Krishna and van Loosdrecht (1999), several models have been proposed to improve the mechanistic modelling of simultaneous storage and growth processes in activated sludge systems (see below), however there is no commonly agreed model yet.

This research aims to further improve the understanding and mechanistic modelling of simultaneous storage and growth processes occurring in activated sludge systems with slowly growing biomass under low F/M in view of application to the modelling of full-scale WWTPs. To this aim, a new model is developed by critically evaluating previously proposed models for feast and famine conditions. A particular emphasis is given to the kinetic description of the degradation of storage polymers under famine conditions for biomass with low PHB content, as typically found in full-scale WWTPs. A simple calibration methodology only based on batch oxygen uptake rate (OUR) data has been developed to facilitate full-scale application of the model. The model is applied to batch OURs obtained with biomass sampled from two WWTPs in Belgium and Spain respectively. Practical identifiability analysis of the model parameters is performed to gain better insight into the model structure in view of improving the parameter estimation procedure. Finally, optimal experimental design (OED) is used as a tool to improve parameter estimation accuracy using OUR measurements alone.

2. MATERIALS AND METHODS

2.1 Experimental set-up

The experimental work was performed in two different set-ups. Experiment A was performed using the hybrid-respirometric set-up described in Sin *et al*. (2003). During this experiment, the pH was fixed to 7.80±0.03 using a pH controller. On the other hand, experiments B were performed in a 10 L reactor operated as an LFS type respirometer (Spanjers *et al*., 1998), which was developed in previous work (Guisasola *et al.*, 2003).

PHB was measured according to the modified method of Comeau *et al.* (1988). Forty mg of lyophilised sludge samples were digested and methylated with 4 ml of acidulated methanol (3% H_2SO_4) and 4 ml of chloroform during 3.5 hours at 100 ºC. Benzoic acid was used as internal standard. The analyses were performed in a GC system (Hewlett Packard 5890). Triplicates of each sample were done.

In both set-ups, the biomass was first aerated overnight to reach an endogenous state. Then, a first pulse of acetate was added to induce a "wake-up" effect on the biomass activity (Vanrolleghem *et al.*, 1998). At the same time, ammonia in excess and ATU (30 mg/l) were added to avoid growth-limitation and nitrification, respectively. Activated sludge sampled from two different WWTPs was used during the experimental work: experiment A used biomass from the Ossemeersen WWTP (Gent, Belgium) whereas Experiment B used biomass from Granollers WWTP (Catalonia, Spain). Both WWTPs perform COD removal, nitrification and denitrification. These biomass samples were analysed for TSS and VSS according to Standard Methods (APHA, 1995).

2.2 Parameter estimation and confidence intervals

All modelling and simulation works including parameter estimation were performed using MATLAB 6.5 (The MathWorks, Natick, MA). The differential equations were solved using an explicit Runge-Kutta (4,5) formula. The procedure for parameter estimation and confidence intervals used here is described in Chapter 4.2.1.

3. MODEL DEVELOPMENT

3.1 Feast phase

Modelling simultaneous storage and growth consists of two distinct but complementary phases: feast and famine. Under feast conditions, two modelling approaches have been employed: traditional and metabolic approaches. In the first approach based on a traditional ASM-type model structure, three distinctive yield coefficients independent from each other are used for storage, direct growth on external substrate and growth on internal storage products processes respectively (Krishna and van Loosdrecht, 1999; Beccari *et al*., 2002; Karahan-Gul *et al*., 2003; Carucci *et al*., 2001).

The second approach is based on the metabolic model of van Aalst-van Leeuwen *et al.* (1997) for pure cultures (Beun *et al*., 2000a; Beun *et al*., 2002; Van Loosdrecht and Heijnen, 2002). In this metabolic model, it has been demonstrated that the yield coefficients of storage, direct growth on substrate and growth on internal storage products respectively are linked to each other through metabolism of the substrate. Further, the yield coefficients are observed to depend on the efficiency of the oxidative phosphorylation i.e. efficiency of energy (ATP)

generation in cells (van Aalst-van Leeuwen *et al*., 1997; Beun *et al*., 2000a). This approach makes it possible to restrict the calibration to the estimation of only one parameter (δ) instead of three yield coefficients.

$$Y_{H\,S} = \frac{4\cdot\delta - 2}{4.2\cdot\delta + 4.32}.\frac{4.2}{4};\; Y_{STO} = \frac{4\cdot\delta - 2}{4.5\cdot\delta}.\frac{4.5}{4} \text{ and } Y_{H\,STO} = \frac{4.5\cdot\delta - 0.5}{4.2\cdot\delta + 4.32}.\frac{4.2}{4.5}$$

where $Y_{H,S}$ is the growth yield on substrate (mgCOD-X/mgCOD-S), Y_{STO} is the storage yield on substrate (mgCOD-STO/mgCOD-S) and $Y_{H,STO}$ is the growth yield on storage products (mgCOD-X/mgCOD-STO). These relationships were derived by van Aalst-van Leeuwen *et al.* (1997) using a metabolic model describing simultaneous storage and growth on acetate in pure cultures. The numbers appearing in these yield-coefficients are basically related to the degree of reduction of biomass (4.2), acetate (4.0) and PHB (4.5), see van Aalst-van Leeuwen *et al.* (1997) for further details.

3.2 Kinetic modelling of substrate flux under feast phase

An extensive review on experimental observations with biomass displaying the storage phenomenon under aerobic conditions (Beun *et al*., 2002) has shown that the ratio of PHB produced to acetate taken up is constant and is found to be 0.67 gCOD/gCOD.

Studies of the storage phenomenon with pure cultures at low SRT's (i.e. high growth rate) showed that storage is dependent on the growth rate of the culture (van Aalst-van Leeuwen, *et al*., 1997). In other words, the accumulation rate of storage products was linearly correlated to the difference between the maximum substrate uptake rate and the substrate uptake rate required for growth. When the culture is operated at a growth rate close to its maximum substrate uptake rate, negligible storage is observed. This also means that if the culture is operated under zero growth conditions, the majority of the substrate flux will be diverted to the formation of storage products (van Aalst-van Leeuwen *et al*., 1997).

On the other hand, most WWTPs are typically operated at high SRT's to achieve complete biological nutrient removal resulting in biomass with a rather low average growth rate (~1/SRT). In these systems, it is hypothesized that the maximum substrate uptake rate (q_{MAX}) of the biomass is higher than the average growth rate. This is understandable since growth requires more energy (induction of enzymes, monomers, macromolecules (RNA, DNA, ribosome, etc) for the new cells) than substrate uptake (Roels, 1983; van Loosdrecht and Heijnen, 2002). Consequently, the maximum substrate flux into the cell exceeds the maximum growth of the biomass and the difference is diverted to formation of the storage polymers. In this range, the q_{MAX} is slightly changing with SRT (Van Loosdrecht and Heijnen, 2002). Since the storage becomes the dominant process under these conditions, the

ratio of PHB produced per acetate taken up can be considered constant as confirmed experimentally (Beun *et al*., 2000a; Beun *et al*., 2002; Dircks *et al*., 2001; etc). From a mathematical point of view, the biological control of substrate flux into the cell can be illustrated using branch-pipe analogy (see Figure 1).

In the branch-pipe analogy, the flow F1 stands for the substrate influx into the cell (substrate uptake rate), F3 for the substrate flux diverted to growth and F2 for the substrate flux diverted to storage. Experimental observations show that the ratio of storage products to substrate taken up (F2/F1) is constant around a certain value (e.g. 0.67 gCOD/gCOD; van Loosdrecht and Heijnen, 2002). The remaining substrate flux is diverted to growth (F3). This experimental observation can be modelled by considering a ratio controller on the flow F2 that is indicated by valve A. In this way, the flow of F2 can be controlled by fixing its value to a certain fraction of F1, f_{STO} (i.e. F2 = f_{STO} * F1) which means that the substrate flow to F3 is also controlled at (F1-F2= F3; F3 = (1-f_{STO}) * F1).

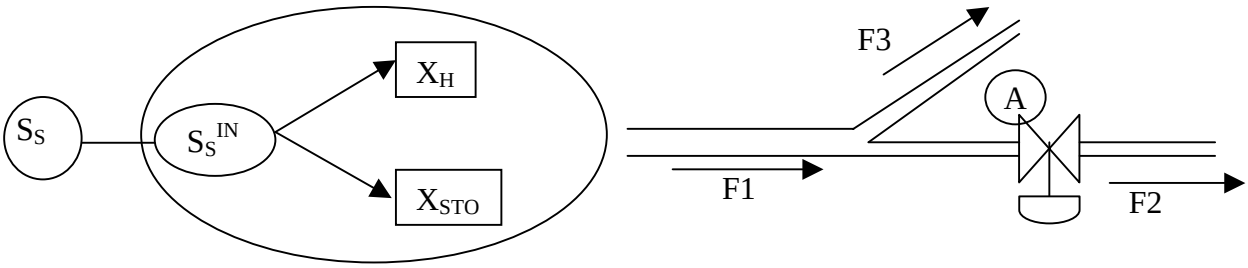

Figure 1. Illustration of substrate flux into the cell (left) and branch-pipe analogy for control of substrate flux under feast conditions (right) (see text for explanation).

From a mathematical point of view, it is not important where the control valve is employed. However, it will have absolutely two different meanings. If the control valve is on F2, this means that the biomass is trying to maximise its storage rate while the remaining substrate is used for growth. By the same token, if the control valve is considered on F3 then this means the biomass is trying to maximise its growth rate while the remaining substrate is used for storage. Most probably the reality consists of a mixture of biomass with the two strategies. However, the mathematical representation of the reality under both strategies remains the same. Consequently, the substrate flux under feast conditions can be modelled as follows:

$$r_S^{IN} = r_S - \frac{1}{Y_{HS}} r_{XH} - \frac{1}{Y_{STO}} r_{STO} \qquad \text{Eq.5}$$

The internal substrate concentration, S_S^{IN}, is assumed at steady state due to the metabolic control of the biomass (see Eq1 and Eq2 in Table 1). The steady state assumption of S_S^{IN} (i.e.

r_S^{IN} = 0) is mostly correct during the feast phase, except for the two short unsteady-state/transient phases occurring in a pulse experiment: (i) at the time of S_S pulse addition and (ii) just after depletion of S_S respectively. The description of the first unsteady-state part can be lumped into the description of the transient response usually observed in batch experiments (see Chapter 4.4), and the second unsteady-state phase is assumed to have a negligible effect on the substrate affinity constant (K_S). Therefore:

$$r_S = \frac{1}{Y_{H\,S}} r_{XH} + \frac{1}{Y_{STO}} r_{STO} \qquad \text{Eq.6}$$

Eq. 6 can be translated into the following equality (assuming no limitations in Eq.5 & Eq.6):

$$q_{MAX} = \frac{\mu_{MAX,S}}{Y_{H,S}} + \frac{k_{STO}}{Y_{STO}} \qquad \text{Eq.7}$$

Based on experimental observations of the constant ratio of substrate uptake/storage as discussed above in detail, the control is assumed on F2 which means that biomass is maximising storage rate (see above):

$$k_{STO} = f_{STO} \cdot q_{MAX} \cdot Y_{STO} \text{ and } \mu_{MAX,S} = (1 - f_{STO}) \cdot q_{MAX} \cdot Y_{H,S} \qquad \text{Eq. 8}$$

where f_{STO} is the fraction of the substrate flux diverted to the storage products (mgCOD-STO/mgCOD-S). In this way, modelling the rates of simultaneous storage and growth reduces to two parameters i.e. f_{STO} and q_{MAX}.

It is important to note that from a metabolic point of view Eq.7 also includes a fraction of substrate used for maintenance i.e. the Herbert-Pirt equation (Beun *et al*., 2000a; van Loosdrecht and Heijnen, 2002). However, in traditional ASM models (Henze *et al*., 2000) the maintenance concept of the biomass is already lumped into the endogenous decay coefficient describing many other processes e.g. death, predation, lysis etc. In this study, therefore, the maintenance of biomass is implicitly included in the endogenous decay coefficient (see Table 1) in order to keep the model at a reasonable complexity.

Although based on the same conceptual background, the major difference between the proposed model and the model of van Loosdrecht and Heijnen (2002) is the mathematical formulation (see Figure 2). The model of van Loosdrecht and Heijnen (2002) uses the X_{STO} component to divert the substrate flux to growth and to storage in order to keep the model simple (see Figure 2). However, in this way, the interpretation of the mathematical model

becomes dangerous since it implies that the biomass grows both in the feast phase and the famine phase using X_{STO} but then in two different ways, with two different yields and two different growth rates.

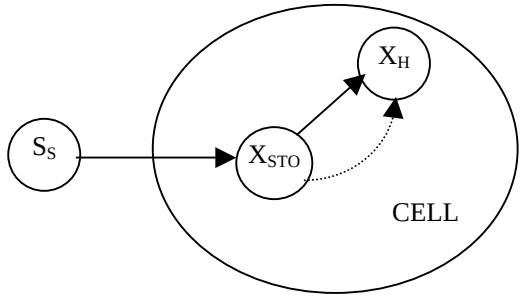

Figure 2. Mathematical formulation used in the model of van Loosdrecht and Heijnen (2002) (—— feast phase, ------- famine phase)

Kinetic modelling of storage products under famine phase

It is commonly observed that degradation of the storage polymers is the rate-limiting step and as such determines the growth rate under famine conditions. However, there is no commonly agreed mathematical model yet. Two approaches have been usually employed to describe the kinetics of degradation of X_{STO} under famine conditions: surface saturation-type kinetics (Henze *et al.*, 2000; Krishna and van Loosdrecht, 1999; Beccari *et al.*, 2002; Karahan-Gul *et al.*, 2003) and a first-order model (van aalst-van Leeuwen *et al.*, 1997; Beun *et al.*, 2000a; Beun *et al.*, 2002; Dircks *et al.*, 2001; van Loosdrecht and Heijnen, 2002).

The surface saturation type kinetics, e.g. as in ASM3, has been shown to cause severe practical identifiability problems due to its structure resulting in unrealistic parameter estimates (see Chapter 4.2.1). Moreover, so far the first-order type models were developed and applied for experimental conditions having biomass with a high content of internal storage products (Beun *et al.*, 2002; Dircks *et al.*, 2001). However, activated sludge from full-scale WWTPs has a relatively much lower fraction of storage products due to the limited availability of external substrate sources as opposed to the studies in well-controlled lab environments.

In this study several model structures including the above mentioned models have been applied to OUR data obtained from full-scale WWTPs with low PHB content (results not shown). The following kinetic expression was found to describe the degradation of storage products reasonably good:

$$f(X_{STO}/X_H) = \frac{X_{STO}/X_H}{K_{STO} + X_{STO}/X_H} \cdot \frac{X_{STO}/X_H}{f_{XSTO}^{REG}} \qquad \text{Eq.9}$$

In this mathematical expression the first part describes the surface-saturation type degradation kinetics of X_{STO} –similar to the concept employed in ASM3 (Henze *et al*., 2000). The second part assumes that the degradation of X_{STO} is regulated as function of the storage content of the cell, $f_{XSTO} = X_{STO}/X_H$ (see Dircks *et al*., 2001). This means that when f_{XSTO} is high, the degradation of X_{STO} is faster, depending on the regulation constant of the cell, f_{XSTO}^{REG}. However, when f_{XSTO} is decreasing and approaching a minimum level in the biomass, the biomass starts to limit the degradation rate of X_{STO}. The particular reasons behind the choice of this kinetic expression are the following:

i. Dircks *et al*. (2001) showed explicitly that the degradation rate of PHB strongly depends on the PHB content of the cell. The authors concluded that at least 4 kinetic expressions (zero order, 2/3rd order, first order and 2nd order) would be needed to accurately describe the PHB degradation rate considering the entire range of PHB contents in the cell.
ii. (ii) Referring to the experimental studies conducted under carbon-limited chemostat conditions, van Aalst-van Leeuwen *et al*. (1997) hypothesised that biomass always contains a minimum PHB content. This implies that biomass is likely to control the degradation rate of storage products such that a minimum level of storage products can be maintained.
iii. (iii) Experimental observations (particularly OUR from batch experiments) showed that there are at least two phenomena corresponding to a fast and a slow degradation rate of X_{STO} under famine conditions (see below).

Eq.9 can be rewritten as follows, resulting in a second order-type kinetic expression:

$$f\left(X_{STO}/X_H\right) = \frac{\left(X_{STO}/X_H\right)^2}{K_2 + K_1 . X_{STO}/X_H} \quad \text{where } K_2 = K_{STO} * f_{XSTO}^{REG} \text{ and } K_1 = f_{XSTO}^{REG}. \qquad \text{eq.10}$$

In this expression, K_2 becomes the affinity of the biomass as a function of X_{STO}/X_H (mg COD/mgCOD) and K_1 is nothing but the regulation constant of the biomass as function of X_{STO}/X_H (mg COD/mgCOD).

The model developed in this study is summarised in matrix format in Table 1. Similar to previous studies (e.g. van Loosdrecht and Heijnen, 2002), the growth rate of biomass on X_{STO} is assumed to occur under strictly famine conditions, i.e. a Monod inhibition function for external substrate is added to the kinetic description of r_{STO} (see Eq.3 in Table 1).

Table 1. Matrix representation of the extended ASM3 model (see text for explanation)

Processes	1. S_O	2. S_S	3. S_{NH}	4. X_H	5. X_I	6.X_{STO}	**Kinetics**
	g O_2	g COD	g N	G COD	g COD	g COD	
1. Formation of storage products, X_{STO}	$-\frac{1-Y_{STO}}{Y_{STO}}$	$\frac{-1}{Y_{STO}}$				1	$\left(1-e^{t/\tau}\right)k_{STO}\cdot M_O\cdot M_S\cdot X_H$
2. Aerobic growth on external substrate, S_S	$-\frac{1-Y_{H_S}}{Y_{H_S}}$	$-\frac{1}{Y_{H_S}}$	$-i_{NBM}$	+1			$\left(1-e^{t/\tau}\right)\mu_{MAX,S}\cdot M_S M_O M_{NH} X_H$
3. Aerobic growth on storage products, X_{STO}	$-\frac{1-Y_{H_{STO}}}{Y_{H_{STO}}}$		$-i_{NBM}$	1		$-\frac{1}{Y_{H_{STO}}}$	$\mu_{\max STO} M_O M_{NH} \frac{\left(X_{STO}/X_H\right)^2}{K_2+X_{STO}/X_H\cdot K_1}\cdot\frac{K_S}{S_S+K_S}X_H$
4.Endogenous respiration	$-\left(1-f_{XI}\right)$		$i_{NBM}-i_{NXI}f_{XI}$	-1	f_{XI}		$b_H M_O X_H$
5.Endogenous respiration of X_{STO}	-1					-1	$b_{STO} M_O X_{STO}$
6. Aeration	1						$K_L a\cdot\left(S_O^*-S_O\right)$

$k_{STO}=f_{STO}\cdot q_{MAX}\cdot Y_{STO}$; $\mu_{MAX,S}=\left(1-f_{STO}\right)\cdot q_{MAX}\cdot Y_{H,S}$; M stands for a Monod kinetic function (the substrate considered is indicated in the subscript) e.g. $M_S = S_S/(K_S+S_S)$.

The first-order empirical model ($1-e^{t/\tau}$) is used to model the transient response observed in OUR data obtained from batch experiments (Chapter 4.4; Guisasola *et al.*, 2004)

4. RESULTS

4.1 OUR for monitoring simultaneous storage and growth processes

Respirometry, defined as the measurement of the oxygen uptake rate of biomass (Spanjers *et al*., 1998), is used in this study to support model development and calibration. From now on, the biomass sampled from Ossemeersen (Belgium) and Granollers WWTP (Catalonia, Spain) will be referred to as biomass A (experiment A) and biomass B (experiment B). Respirometric measurements with biomass A obtained after pulse addition of a certain amount of acetate to endogenously respiring activated sludge are shown in Figure 3.

Upon pulse addition of substrate i.e. under the feast conditions, the oxygen uptake rate (OUR) of biomass A increases gradually to a maximum level following a fast transient (ca 3-4 minutes) (see Figure 3). This transient period is frequently observed in OUR obtained from batch experiments with pulse addition of substrate (see Chapter 4.4). The biomass i.e. OUR activity continues at this maximum level until all external substrate is taken up by biomass for storage and growth. After the external substrate is removed, i.e. in the famine phase, the OUR of biomass A drops from the maximum level to a level higher than the endogenous OUR level maintained prior to substrate addition (see Figure 3). Under famine conditions, biomass grows using X_{STO} internal storage products produced in the previous phase. A similar pattern of acetate oxidation is observed with biomass B (Figure 4-right).

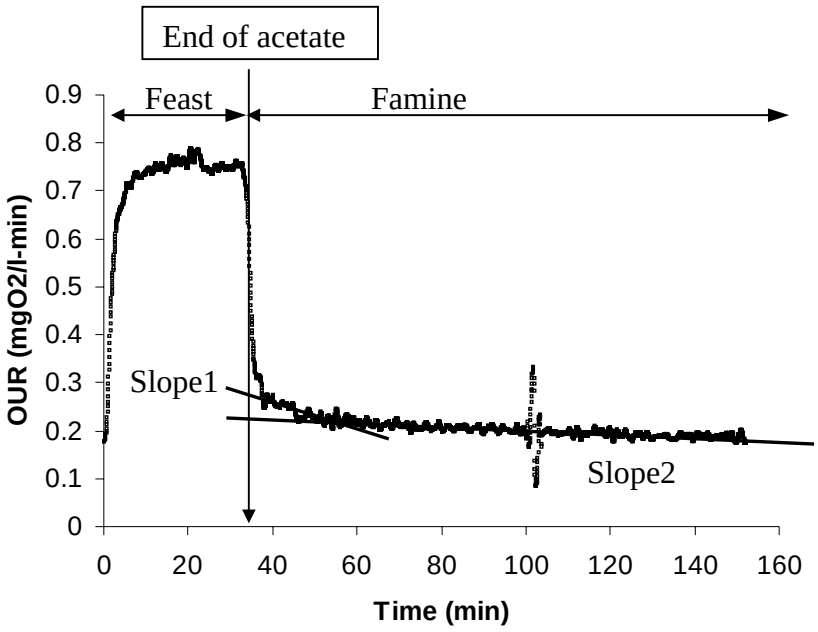

Figure 3. Oxygen uptake rate measurements after pulse addition of acetate to endogenously respiring biomass A (See text for explanation).

The oxygen uptake rate is observed to have two different slopes indicating two phenomena under famine conditions (see Figure 3). This observation was the particular reason for the choice of second order kinetics for the description of the degradation of storage products (see the model development section).

4.2 Calibration of the model: Parameter estimation procedure

For the calibration of the model, the initial concentration of active biomass, $X_H(0)$ is estimated using the baseline endogenous OUR level prior to substrate addition, while fixing the decay rate coefficient b_H to its default value advised in the ASM models (Henze *et al*., 2000) i.e. 0.2 d^{-1} (see Table 2). The endogenous OUR prior to substrate addition is equal to:

$$OUR_{end}(0) = (1 - f_{XI}) \cdot b_H \cdot X_H(0) \qquad \text{Eq.11}$$

In our approach, f_{XI} is also fixed in this equation to its default value advised in ASM3, 0.2 mgCOD/mgCOD. From a structural identifiability point of view, it is not possible to obtain unique values of both b_H and $X_H(0)$ using short-term (e.g. 10 – 15 minutes) endogenous OUR measurements. In other words, there are an infinite number of solutions (parameter combinations of b_H and $X_H(0)$) to Eq.11. This is because the decay of biomass is practically negligible within such short-period. Long-term (e.g. 10 days) monitoring of endogenous OUR is needed for unique estimation of b_H (Keesman *et al*., 1997; Henze *et al*., 2000). Moreover, the endogenous utilisation rate of X_{STO}, b_{STO}, is linked to the endogenous decay rate of biomass, b_H, similar to the approach adopted in ASM3 (Henze *et al*., 2000).

The initial concentration of storage products, $X_{STO}(0)$, is either measured (in experiment B and the OED experiment) or estimated (in experiment A). The estimation of the initial concentration of storage products, $X_{STO}(0)$ was observed to cause severe identification problems (results not shown), i.e. it has a too large confidence interval. To deal with this, this parameter was estimated using a step-wise procedure for experiment A. In the first step, $X_{STO}(0)$ was included in the parameters subset used in the parameter estimation. Then, in the second step, the $X_{STO}(0)$ was eliminated from the parameters subset (see Table 2) and the parameter estimation was run again, but this time the $X_{STO}(0)$ was fixed to the estimated value in the first step. The practical identifiability of this parameter is discussed in detail below (see the discussion section).

This issue is addressed in detail below in the discussion section. The maximum growth rate of biomass on X_{STO}, $\mu_{MAX,STO}$, is assumed to be in the same order of magnitude as the maximum growth rate of biomass on external substrate, $\mu_{MAX,S}$, in order to keep the model calibration exercise at a reasonable complexity. It is important to note that from a parameter estimation

point of view, any possible error involved in this assumption is most likely compensated by the estimate of K_2 or K_1 (see Eq. 3 in Table 1).

The yield coefficients for storage, Y_{STO}, direct growth on S_S, $Y_{H,S}$, and growth on X_{STO}, $Y_{H,STO}$ are calibrated by estimating the δ parameter using the relations given above. The maximum storage rate, k_{STO}, and the maximum growth rate of biomass, μ_{MAX}, are calculated from the estimates of the maximum substrate uptake rate, q_{MAX}, and the fraction of substrate used for storage f_{STO} using the substrate flux model described above. The remaining parameters (see Table 2) were estimated using the Nelder-Mead simplex minimisation algorithm (Nelder and Mead, 1964).

4.3 Parameter estimation results

Parameter estimation results obtained using OUR measurements with biomass A and biomass B are summarised in Table 2 while best fits of the model to the experimental data are shown in Figure 4. The model fits are quite acceptable/plausible (see Figure 4).

The ratio of substrate uptake to substrate used for storage, f_{STO}, was found low in experiment A (for biomass A) compared to the average value 0.67 mgCOD/mgCOD considered as a constant for WWTPs (Beun *et al*., 2002; van Loosdrecht and Heijnen, 2002). On the other hand, the storage fraction of biomass B is in good agreement with the typical value mentioned above.

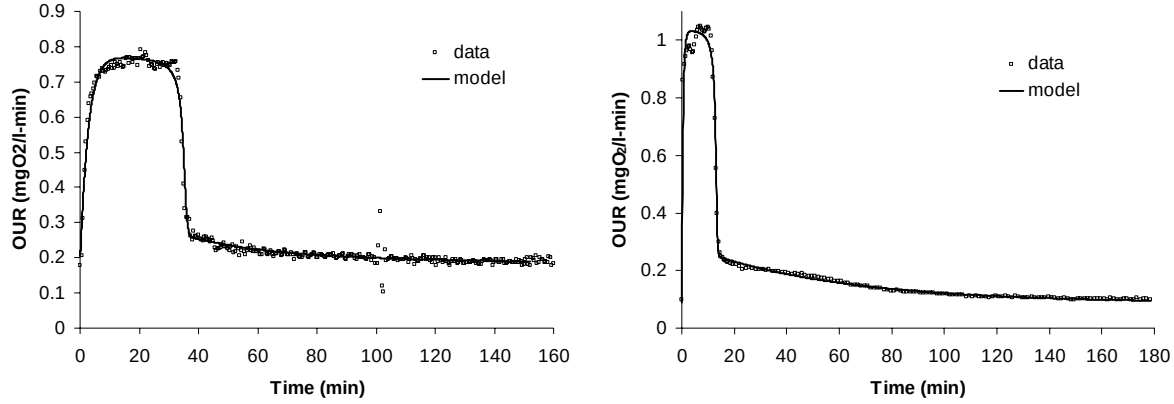

Figure 4. Model fits to the experiments A (left) and experiment B (right) (see Table 2 for the calibrated parameters). Only every 10th data point is shown to keep the figure clearer.

The substrate uptake rate of biomass A (i.e. $q_{MAX} * X_H(0)$) is observed to be ca half that of the substrate uptake rate of biomass B. As a result, the kinetic parameters estimated for biomass A were also slower than the kinetic parameters estimated for biomass B (see Table 2). Nonetheless, the μ_{MAX} estimates of both biomass samples are noticeably lower than the typical range of values reported in literature for the maximum heterotrophic growth rate for

municipal WWTPs (Henze *et al*., 2000; Gernaey *et al*., 2002b; Vanrolleghem *et al*., 2004; etc.). Moreover, the substrate affinity constants, K_S, of biomass A and biomass B (see Table 2) were also found to be in the same order of magnitude of the values obtained from other batch experiments (Gernaey *et al*., 2002b; Chapter 4.4).

Table 2. Parameter estimation results with the simultaneous storage and growth model.

Parameters	Experiment A	Confidence Interval**	Experiment B	Confidence Interval**
Parameters estimated				
q_{MAX} (d^{-1})	1.67±0.09*	5.39%	6.43±0.05*	0.78%
f_{STO} (mgCOD/mgCOD)	0.29±0.07	24.14%	0.65±0.09	13.85%
δ (mol/mol)	2.88±0.16	5.56%	2.57±0.22	8.56%
K_S (mgCOD/l)	0.6±0.4	66.67%	0.67±0.11	16.42%
K_1 (mgCOD/mgCOD)	0.015±0.029	193.33%	0.053±0.041	77.36%
K_2 (mgCOD/mgCOD)	$1.7\cdot10^{-4}\pm3\cdot10^{-4}$	182.35%	$9.8\cdot10^{-4}\pm1\cdot10^{-3}$	102.04%
τ (min)	2.73±0.12	4.40%	0.51±0.05	10%
Parameters estimated using the step-wise procedure (see text for explanation)				
$X_{STO}(0)$ (mgCOD/l)	0.99 (estimated)		6.8 (measured)	
Parameters assumed				
b_H (d^{-1})	0.2		0.2	
b_{STO} (d^{-1})	0.2		0.2	
f_{XI}(mgCOD/mgCOD)	0.2		0.2	
Parameters calculated				
$X_H(0)$ (mgCOD/l)	1650		800	
q_{MAX} * $X_H(0)$ (mgCOD/l-d)	2755		5144	
$\mu_{MAX,S}$ (d^{-1})	0.72		1.3	
k_{STO} (d^{-1})	0.4		3.31	
$\mu_{MAX,STO}$ (d^{-1})	0.72		1.3	
Y_{STO} (mgCOD/mgCOD)	0.83		0.81	
$Y_{H,S}$ (mgCOD/mgCOD)	0.61		0.58	
$Y_{H,STO}$ (mgCOD/mgCOD)	0.71		0.68	

* Parameter estimates are given together with 95% confidence interval

** Confidence intervals are presented in these columns as absolute relative percentage of the parameter estimates, i.e. (confidence interval/parameter)*100.

4.4 Practical parameter identifiability

Practical identifiability of a model structure is important as it tells which parameter combinations can be estimated under given measurement accuracy and quantity (Dochain and Vanrolleghem, 2001). Parameters which are not identifiable or only with large confidence intervals, can (and should) be eliminated from the parameters subset that is chosen for estimation. In this way, one can improve the reliability and accuracy of the parameter estimation (Dochain and Vanrolleghem, 2001). For such identifiability study, output sensitivity functions of parameters and contour plots of the objective functional will be evaluated.

Output sensitivities of model parameters calculated using best-fit parameters obtained in experiment B (see Table 2) are shown in Figure 5. The output sensitivity function of q_{MAX} is observed to be correlated with the output sensitivity function of f_{STO} and δ during the feast phase. However these correlations are broken to a large extent in the famine phase, thereby making it possible to estimate those parameters simultaneously using OUR measurements (see Table 2). The sensitivity function of K_S also has a different trajectory than that of the sensitivity of q_{MAX} unlike what happens in pure-growth models where it is often the case that μ_{MAX} is correlated with K_S (Dochain and Vanrolleghem, 2001). Moreover, the output sensitivity functions of f_{STO} and δ are also almost perfectly correlated under the feast phase but again this correlation is interrupted during the famine phase, making these parameters uniquely identifiable as well.

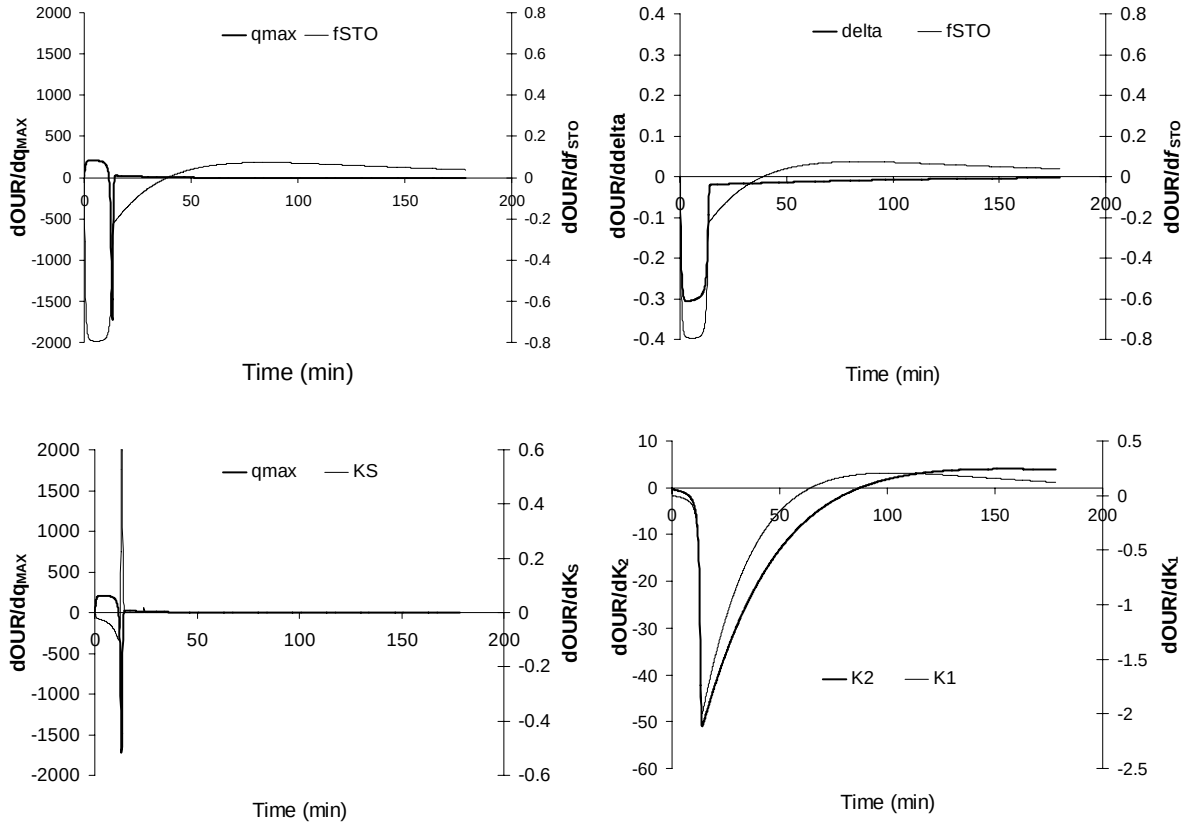

Figure 5. Output sensitivity functions of model parameters calculated around best-fit conditions for experiment B (see text for explanation). Note that 'delta' is 'δ'.

The output sensitivity functions for K_1 and K_2, i.e. the two parameters of the second order model used in this study to describe degradation of storage products under famine conditions, are observed to be correlated until a certain time instant beyond which the correlation is broken (see Figure 5). In this regard, the length of the famine phase becomes extremely important for reliable estimation of these parameters. The output sensitivities of K_1 and K_2

have no specific correlation with the sensitivity functions of q_{MAX}, f_{STO} and δ respectively. This ensures reliable estimation of parameters K_1 and K_2 from the part of data collected under famine conditions.

In short, the output sensitivity functions of the model parameters estimated in Table 2 suggests that they are practically identifiable using OUR measurements alone. These positive results of the parameter sensitivity analysis are confirmed with the analysis of the shape of the cost/objective functional performed below.

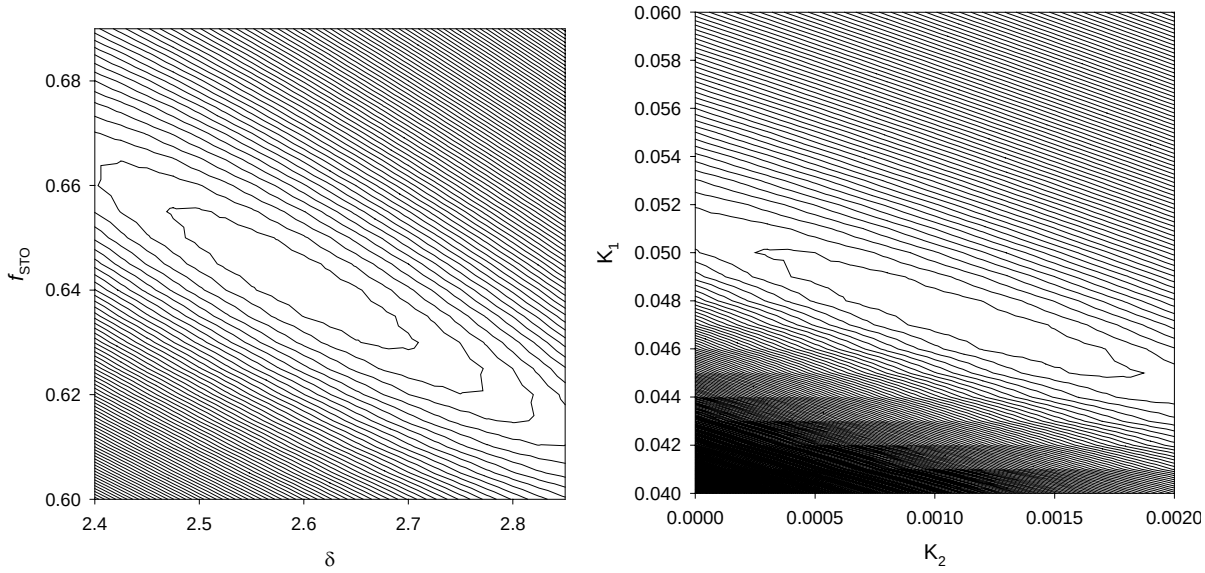

Figure 6 – Contour plots of the objective functional used for parameter estimation as function of two parameters; f_{STO} and δ (left) and K_1 and K_2 (right).

The contour plots of the objective function shown in Figure 6 were calculated around the optimum for different combinations of parameters: f_{STO} and δ (Figure 4-left) and K_1 and K_2 (Figure 6-right). The contours of the objective functions are large in both planes of the two-parameter subsets i.e. f_{STO} - δ plane and K_1 - K_2 planes respectively. Moreover, the objective function is observed to be valley-like in a certain direction particularly in the plane K_1 and K_2 (see Figure 6-right). This means that several combinations of parameters K_1 and K_2 will give almost equally good fits to the data leading to large confidence intervals in the parameter estimates (Baltes *et al.*, 1994; Dochain and Vanrolleghem, 2001). This is indeed observed in the parameter estimation results. The relative errors on parameter estimates K_1 and K_2 are calculated to be 77% and 102% respectively in experiment B (see Table 2). When confronted with such situation, optimal experimental design (OED) has been shown to be a good tool to improve parameter estimation accuracy (Dochain and Vanrolleghem, 2001; Petersen, 2000). This is investigated below.

4.5 Optimal experimental design (OED) for parameter estimation

The optimal experimental design procedure presented in Dochain and Vanrolleghem (2001) is used to improve the confidence interval for parameter estimation. The reference experiment was chosen to be experiment B. The parameter subset considered for parameter estimation consists of q_{MAX}, f_{STO}, K_1, K_2, τ, K_S and δ. The experimental degrees of freedom were chosen to be (1) single or two consecutive pulse additions of acetate (2) amounts of first (and second) pulse additions and (3) time instant of the second pulse addition. The duration of each experiment was fixed to 200 minutes. The substrate to biomass ratio, S/X, was constrained to 0.1 (mgCOD/mgCOD) in order to prevent any possible physiological change at the cellular level (Chudoba *et al*., 1992; Grady *et al*., 1999). Considering that the $X_H(0)$ was approximated as 800 mgCOD/l (see Table 2), the total added substrate was fixed to 80 mgCOD/l.

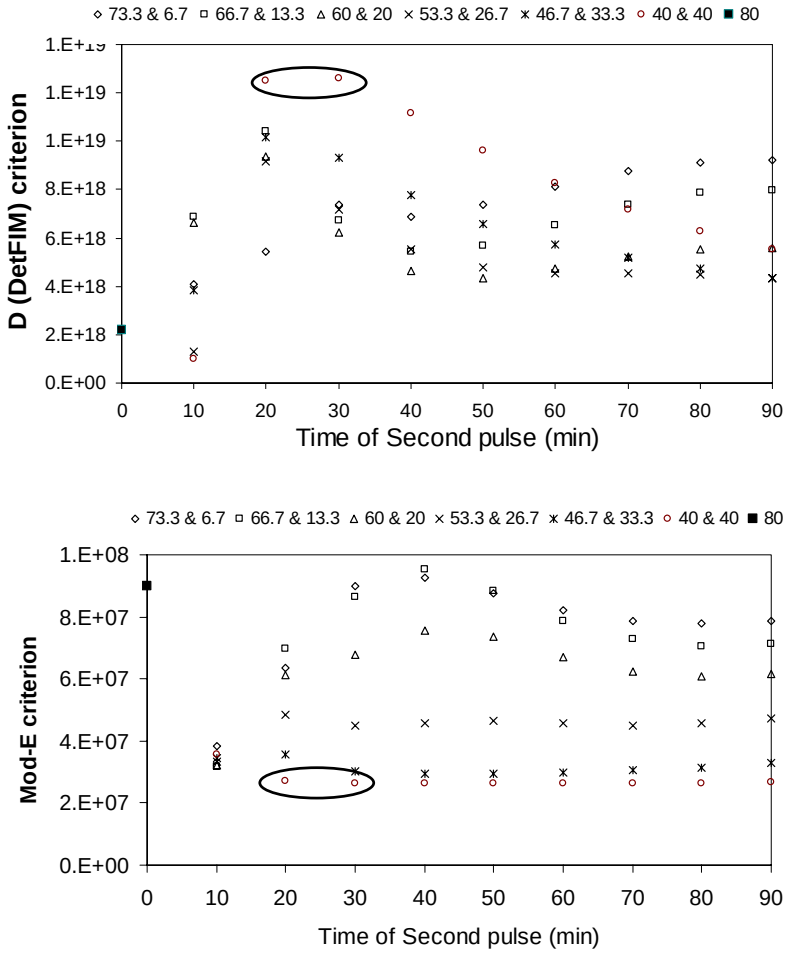

Figure 7. Properties of FIM as a function of the pulse time and the concentration of the pulses: D-criterion (top) and Mod-E criterion (down) (see text for explanation).

An iterative OED procedure was followed. The Fisher Information Matrix (FIM), which is the basis for OED, is calculated to summarise the information content of each hypothetical experiment under different combinations of the above-mentioned degrees of freedom

(Dochain and Vanrolleghem, 2001). The D and Mod-E criteria of FIM, the most frequently used properties of FIM for optimisation of the experiment, are used in this study. The D-criterion, i.e. the determinant of FIM, aims at increasing the overall information content of the experiment thereby improving as well the overall parameter estimation accuracy. The Mod-E criterion focuses on decreasing the parameter correlation by decreasing the condition number of the FIM, i.e. the ratio of the largest to the lowest eigenvalues of the FIM (Dochain and Vanrolleghem, 2001).

The results of OED under various combinations of degrees of freedom are shown in Figure 5. The objective is to find an experiment with the lowest Mod-E and the highest D criteria values. It can be seen from Figure 7 (see the circled regions) that the optimal experiment according to the OED analysis is a two pulse addition of (40 mg COD/l each) where the second pulse is added around 20 min, which corresponds to an addition just before the first pulse of substrate is completely taken up by the biomass. The optimal experiment results in two peaks in the OUR profile that contains more information under feast conditions and thereby improves the accuracy of parameter estimation, particularly for those parameters related to feast conditions i.e. q_{MAX}, τ, f_{STO}, δ and also K_S. After the second pulse of substrate is consumed by biomass, the OUR tail under famine conditions where the effect of storage products produced in the previous two pulses is observed, becomes obviously very important. In this way, the estimation of parameters related to degradation of storage products for biomass growth, i.e. K_1 and K_2, are improved.

Implementation of the OED experiment

The optimal experiment resulting from the OED study was applied to biomass B and the experimental results are shown in Figure 8 including off-line PHB measurements in triplicate. Upon the first pulse addition of acetate, the OUR immediately increases to a maximum level following a fast transient. Parallel to this increase in the OUR, the PHB content of the biomass also increases linearly in time confirming that part of the acetate is diverted to storage while the rest is used for growth at the same time (see Figure 8). This observation i.e. simultaneous storage and growth, has been frequently reported for activated sludge (Beun *et al*., 2000a; Beun *et al*., 2002; Dircks *et al*., 200; Carucci *et al*., 2001; Beccari *et al*., 2002).

After the first pulse of acetate is completely consumed by the biomass, the OUR drops immediately. The same phenomenon as in the first acetate pulse is repeated in the second pulse addition of acetate (see Figure 8). The formation of PHB is continued with a linear increase for as long as acetate is present in the medium. After the second pulse of acetate is completely consumed by biomass, PHB starts to decrease gradually following a non-linear pattern. Concomitantly, the OUR is also decreased and followed a non-linear uptake rate due to the oxygen uptake for biomass growth on PHB.

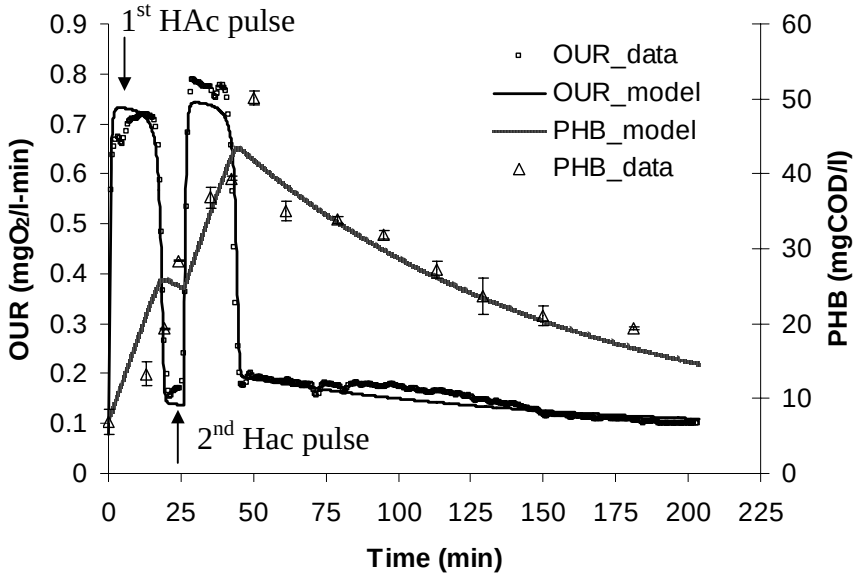

Figure 8. Implementation of the OED experiment with two pulse additions of equal amounts of acetate (40 mgCOD/l) where the second acetate pulse is added after ca 20 minutes.

The parameter estimation results for the OED experiment only using OUR measurements are shown in Table 3. The model predictions are compared both with OUR and PHB measurements in Figure 8. The model fit to the OUR measurements is acceptable. However, the model was unable to perfectly fit the second peak in the OUR profile. This is discussed in detail below (see discussion section).

It is important to stress that the PHB measurements were not used for the parameter estimation/model calibration, but instead they are compared with the predictions of the model calibrated using only OUR measurements. The model predictions for the PHB concentrations are in very good agreement with the measured PHB content during the two consecutive pulse additions of acetate (see Figure 8).

From a parameter estimation point of view, a remarkable improvement in parameter estimation accuracy was obtained from the OED experiment (compare Table 2 and Table 3). Particularly the huge confidence intervals of K_1 and K_2 (see Table 2) could be reduced from 77% and 102% to 12% and 25% respectively. In this regard, the application of the OED methodology for improving parameter estimation accuracy is clearly valuable.

Although the confidence intervals of the parameter estimates have been reduced in the OED experiment, the parameter estimates themselves did not vary significantly compared to the values obtained in the reference experiment (i.e. experiment B). For instance, the estimate of δ remained quite close to the value estimated in the reference experiment (see Table 2 and

Table 3). However, the estimate of q_{MAX} was found lower than the value estimated in the reference experiment (see Table 2 and Table 3) indicating that in the OED experiment biomass may have not yet reached its maximum substrate uptake rate. Since q_{MAX} was lower, the $\mu_{MAX,S}$, k_{STO} and $\mu_{MAX,STO}$ were also calculated to be lower compared to the reference experiment (compare Table and Table 3). A possible explanation for this observation could be physiological adaptation, which is discussed below.

Table 3. Parameter estimation results for the OED experiment using only OUR data.

Parameters	The OED experiment	Confidence interval**
Parameters estimated		
q_{MAX} (d^{-1})	4.27±0.03*	0.70%**
f_{STO} (mgCOD/mgCOD)	0.60±0.03	5.00%
δ (mol/mol ATP)	2.56±0.08	3.13%
K_S (mgCOD/l)	0.70±0.1	14.29%
K_1 (mgCOD/mgCOD)	0.102±0.012	11.76%
K_2 (mgCOD/mgCOD)	$1.2\cdot10^{-3}\pm3\cdot10^{-4}$	25%
τ (min)	0.51±0.07	13.73%
Parameters measured		
$X_{STO}(0)$ (mgCOD/l)	6.8	
Parameters assumed		
b_H (d^{-1})	0.20	
b_{STO} (d^{-1})	0.20	
f_{XI} (mgCOD/mgCOD)	0.20	
Parameters calculated		
$X_H(0)$ (mgCOD/l)	800.00	
$\mu_{MAX,S}$ (d^{-1})	0.97	
k_{STO} (d^{-1})	2.02	
$\mu_{MAX,STO}$ (d^{-1})	0.97	
Y_{STO} (mgCOD/mgCOD)	0.80	
$Y_{H,S}$ (mgCOD/mgCOD)	0.57	
$Y_{H,STO}$ (mgCOD/mgCOD)	0.68	

* & ** see the footer of Table 2 for the explanation

Finally, it was observed experimentally that the amount of PHB formed per amount of acetate consumed, f_{STO}, is equal to 0.54 mgCOD-PHB/mgCOD, which is quite close to the estimated value for f_{STO}, 0.60 mgCOD/mgCOD (see Table 3). Moreover, both measured and estimated values fall in the range reported by Beun *et al.* (2002) for aerobic, slowly growing activated sludge cultures. This result supports the validity of the model as well as the calibration procedure using OUR measurements alone.

5. DISCUSSION

5.1 The model performance: Parameter estimation results

From the parameter estimation results with both biomass A and biomass B (Table 2), it is observed that the maximum growth rate of biomass, μ_{MAX}, estimated in this study is

noticeably lower than the values reported for μ_{MAX} in the growth-based ASM models (Vanrolleghem *et al*., 1999; Gernaey *et al*., 2002b; Chapter 4.4). However, the parameter estimates obtained for K_S in this study (see Table 2) are clearly comparable with the parameter estimates obtained for K_S in the traditional growth-based ASM models (Vanrolleghem *et al*., 1999; Gernaey *et al*., 2002b; Chapter 4.4). On the other hand, the maximum growth rate, $\mu_{MAX,}$ of both biomass samples estimated in this study is expected to provide more realistic predictions of the true growth rate of activated sludge in municipal WWTPs. Moreover, the maximum substrate uptake rate of biomass, q_{MAX}, is estimated to be considerably higher (e.g. up to 5 times see Table 2) than the maximum growth rate of biomass. These results support the hypothesis that activated sludge growth is slower than the maximum substrate uptake rate (Beun *et al*., 2002; van Loosdrecht and Heijnen, 2002)

The efficiency of the oxidative phosphorylation, δ, was found in the theoretically expected range i.e. 1 – 3 mol/mol for both biomass samples (Beun *et al*., 2000a). Moreover, the yield coefficients calculated using the estimated δ for biomass A and biomass B were very similar even though biomass A and biomass B have different growth and storage kinetics. This result certainly supports the validity of the proposed model structure, which assumes that the macroscopic yield coefficients are independent of the growth rate, and can be estimated using a metabolic relation (see model development; Beun *et al*., 2000a; van Loosdrecht and Heijnen, 2002).

The second order model adopted in this study to describe the utilisation of storage products under famine conditions successfully fitted the OUR tail under famine conditions. The parameter K_2, defined as the affinity of biomass to storage products as function of the storage content of biomass i.e. X_{STO}/X_H, was found to be low for both biomass. Moreover, the traditional affinity constant of biomass to storage products, K_{STO}, which can be calculated as K_2/K_1 (see model development) was found to be around 0.01 mgCOD/mgCOD which is in good agreement with the default value proposed for PAOs in ASM2d, which is also 0.01 mgCOD/mgCOD (Henze *et al*., 2000). Moreover, Koch et al. (2000) estimated for K_{STO} a value as low as 0.1 mgCOD/mgCOD using the ASM3 model. Note that the K_{STO} value estimated in this study is significantly lower than the default value proposed for K_{STO} in ASM3 which is 1.0 mgCOD/mgCOD (Henze et al., 2000). We believe that the default value of ASM3 is too high which is most probably due to the severe parameter correlations with the maximum growth rate of biomass as studied in detail in Chapter 4.2.1. On the other hand, the parameter K_1 defined as the regulation constant of biomass controlling the degradation of the storage product, was observed to change from one experiment to another experiment, making it difficult to comment on. This variability is most probably due to the problems of practical identifiability encountered with the estimation of these two parameters K_2 and K_1 (see Figure 6). One way to improve the identifiability of this parameter is to apply an OED methodology,

as done in this study. Another way of improving the identifiability of these parameters is naturally to use PHB measurements for parameter estimation on top of the OUR data. It is clear that further research is needed in this direction.

Direct biomass growth on substrate (acetate) can be compared with the biomass production based on internally stored PHB using the following ratio:

$$\frac{Y_{STO} \times Y_{H,STO}}{Y_{H,S}}$$

This ratio is calculated to be 1.00 for biomass A and 0.95 for biomass B. This means there is no biomass reduction when PHB is used for growth in experiment A while there is around 5% reduction in biomass production in experiment B. These values indicate that biomass capable of storage has no or negligible disadvantage compared to biomass capable of only growth. This is in agreement with the findings of Beun *et al*. (2000a).

5.2 Practical identifiability of the model

The study of the model using output sensitivity functions (see Figure 5) and contour plots of the objective functional (see Figure 6) showed that it is possible to identify the feast-phase parameters q_{MAX}, δ, f_{STO} and K_S using OUR alone. Moreover, identification of the K_1 and K_2 parameters related to the famine phase is also possible using the OUR tail but this goes together with large uncertainties (see Figure 4-right).

To facilitate the full-scale applications of the model, the calibration procedure developed in this study is based on OUR measurements alone since PHB measurements are assumed hardly available due to the analytical skills and equipment required. However, an important issue in this context, is the evaluation of the initial concentration of storage products in biomass, $X_{STO}(0)$.

Estimation of this parameter was observed to cause severe parameter identification problem when OUR is used alone as aforementioned. To understand the reason of this difficulty, the objective functional was calculated as a function of $f_{XSTO}(0)$ (i.e. the storage fraction of biomass expressed as 100 * $X_{STO}(0)/X_H(0)$), δ and f_{STO}. The contour plots of the objective function in both planes i.e. $f_{XSTO}(0)$- δ and $f_{XSTO}(0)$-f_{STO} are large and have a valley-like shape with a very flat bottom (see Figure 7). This valley-like cost-functional shape with a flat bottom is known to cause severe problems to optimisation algorithms in finding the minimum (Dochain and Vanrolleghem, 2001). Moreover, large (and unclosed) contour plots of the objective functional indicate that there are many combinations of parameters that give an almost equally good fit to the measurements. This implies that the confidence intervals of the

parameter estimates would also be very large. In short, the analysis of the shape of the objective functional implies that the simultaneous estimation of parameters $f_{XSTO}(0)$ (and $X_{STO}(0)$), δ and f_{STO} is difficult.

In fact, these correlations are not surprising since the f_{STO} is practically/experimentally calculated from the difference between the initial X_{STO} and the final X_{STO} content of biomass under feast conditions (i.e. $f_{STO} = (f_{XSTO}(0) - f_{XSTO}(\text{final}))/S_S(0)$. In this way, estimation of f_{STO} is clearly dependent on the true value of $f_{XSTO}(0)$. Since $f_{XSTO}(0)$ is influencing the calculation of f_{STO}, the estimation of δ becomes also correlated with the estimate of $f_{XSTO}(0)$ to compensate for an error in the estimate of f_{STO}. These correlations are manifested in the contour plots of the objective functional as discussed above (see Figure 9).

To resolve this issue the $f_{XSTO}(0)$ should be fixed to either a measured value or by using step-wise parameter estimation (Dochain and Vanrolleghem, 2001). This step-wise parameter estimation procedure is already explained above (see calibration of the model).

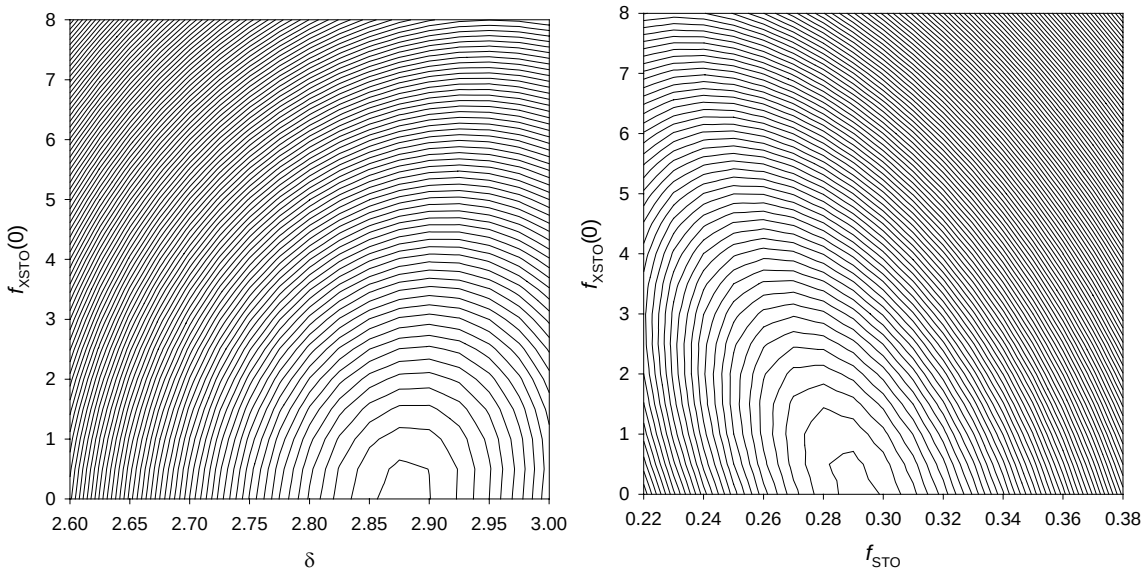

Figure 9. Contour plots of the objective functional as a function of 2 parameters $f_{XSTO} - \delta$ (left) and $f_{XSTO} - f_{STO}$ (right).

5.3 Implementation of OED for parameter estimation

The application of the OED methodology was observed to provide remarkable improvements to the parameter estimation accuracy (compare Table 2 and Table 3). For instance, it was possible to reduce the large confidence intervals of the parameters K_1 and K_2 from 77% and 102% to 12% and 25% respectively.

However, the model could not perfectly describe the second peak in the OUR profile corresponding to the second acetate pulse (see Figure 8). This discrepancy may be due to the

not modelled physiological adaptation of the biomass. In other words, after the first pulse of acetate, the biomass increases its RNA and protein content and activity to sustain a higher growth rate (Vanrolleghem *et al*., 1998; van Loosdrecht and Heijnen, 2002). In this respect, it is also important to note that parameter estimates with the OED experiment remained close to the ones of the reference experiment except q_{MAX}, which was found lower than the reference experiment. This supports the above-mentioned hypothesis that the biomass in the OED experiment undergoes a transient to increase its substrate uptake rate until it reaches the maximum substrate uptake, see e.g. the q_{MAX} obtained in the reference experiment. Similar phenomena were reported and discussed in detail in Vanrolleghem *et al*. (1998). Since the model developed in this study aims at modelling stable activated sludge cultures for WWTPs, the 10% increase in maximum OUR can be considered negligible in view of model calibration purposes. On the other hand, for a better experimental design for model-calibration purposes this adaptation phenomenon can be overcome e.g. by adding a wake-up pulse of substrate (Vanrolleghem *et al*., 1998).

5.4 Significance of the research

Ultimately this research aims to extend ASM3 by critically considering previous attempts to better describe the aerobic heterotrophic growth in full-scale WWTPs in a mechanistically sound way. The model developed in this study has been applied successfully to OUR data obtained from short-term batch experiments. It is now possible with the model to *explicitly* separate substrate uptake kinetics from growth kinetics thereby facilitating the application of the extended ASM3 model to better describe/model aerobic carbon oxidation processes in full-scale WWTPs. A particular emphasise was given to develop a practical and easy calibration methodology based only on OUR to facilitate the application this type of activated sludge models. It has been shown that the model has no or negligible impact on the prediction of sludge production for full-scale WWTPs, which is an important aspect of activated sludge modelling.

It is expected that improved mechanistic modelling of biological processes in WWTPs will deliver a better insight into the system, which can be used to improve design, operation and control of the biological processes. Since most of the WWTPs also operate under anoxic conditions it is important to extend the model developed here to describe simultaneous storage and anoxic growth for full-scale WWTPs. This extension is done in the next chapter.

6. CONCLUSION

In this study, the ASM3 model was successfully extended to describe simultaneous storage and growth activities of activated sludge under aerobic conditions. Two features distinguish the model from other previously presented models: (i) a branch-pipe analogy for modelling the distribution of substrate flux over growth and storage under feast conditions. This

approach makes it possible to *explicitly* separate substrate uptake from growth kinetics, (ii) a second order type kinetics expression to model the degradation of storage products under famine conditions.

A practical calibration procedure requiring only OUR data obtained from batch experiments was developed and applied successfully to calibrate the model. The predictions of the calibrated model were also confirmed by independent PHB measurements, supporting the validity of the model. The Optimal Experimental Design (OED) methodology was shown to be valuable in view of improving the parameter estimation accuracy, particularly for the identification of the second order model developed in this study.

The maximum growth rate of heterotrophs was estimated to be between 0.7 – 1.3 d^{-1}. These values are quite lower than the values reported in literature for the growth-based ASM models. Similarly, the yield coefficient for heterotrophic growth on acetate was estimated to be around 0.58, which is lower than the values reported in literature for growth-based models. It is believed that the proposed model gives a better prediction of the growth yield and the maximum growth rate of biomass in full-scale WWTPs since it accounts for the storage phenomenon. Moreover, the maximum substrate uptake rate of the biomass was estimated to be as much as 5 times higher than the maximum growth rate of the biomass. This supports the hypothesis that in full-scale WWTPs, substrate uptake rate is higher than the growth rate.

7. ACKNOWLEDGEMENT

One of the authors wishes to sincerely thank Prof. dr. ir. Mark van Loosdrecht for the valuable/generous discussions they had over the storage phenomenon during the course of his PhD research. These discussions were very much helpful and appreciated.

Chapter 4.3

Modelling simultaneous storage and growth activities of slowly growing activated sludge cultures under anoxic conditions

ABSTRACT

In this study, a previously developed mechanistic model (Chapter 4.2.2) was extended to describe the simultaneous storage and growth activities of denitrifiers under feast and famine conditions. This new extended model is called ASM3e. The ASM3e model was successfully applied to interpret the high frequency and high quality NUR data obtained from batch experiments with acetate as carbon source and compared with an alternative model, an extended version of the ASM1 model called ASM1e. Parameter estimation results showed that ASM3e was able to provide more realistic estimates for the yield of anoxic growth on substrate (0.49) than the ASM1e model (0.66). Moreover, the maximum growth rate of denitrifiers predicted by ASM3e was ca 5 times lower than the maximum growth rate predicted by the ASM1e model. The discrepancies between ASM3e and ASM1e are due to the storage phenomenon, which was predicted to consume as much as 60% of the acetate used in the studied batch experiments. As such, it is expected that ASM3e is closer to reality.

Affinity constants for substrate and nitrate predicted by both ASM1e and ASM3e were in very close agreement. However, the K_{NO3} value was estimated to be as low as 0.015 mgN/l, which is significantly lower than the default values reported for full-scale activated sludge systems. The second order model adopted to describe degradation of storage products was observed to adequately fit the NUR tail reflecting usage of stored substrate under famine conditions. The affinity constant for storage products, K_{STO}, was estimated to be ca 0.02 mgCOD/l, which is in agreement with the default value in ASM3.

Moreover, both ASM1e and ASM3e were further extended with a titrimetric model to interpret the titrimetric data resulting from anoxic batch experiments. Both models could describe the titrimetric data sufficiently well. However, further research is required to improve the identifiability of the titrimetric models under combined titrimetric and nitrate measurements.

The substrate to biomass (S_0/X_0) ratio in anoxic batch experiments was shown to remarkably influence the parameter estimation results. It is hypothesised that when subjected to higher S_0/X_0, biomass

simultaneously increases its maximum substrate uptake rate and maximum growth rate while keeping its maximum storage rate unchanged. This hypothesis is complementary to the hypothesis of Chudoba *et al*. (1992).

Finally, with the mechanistic models developed in Chapter 4.2.2 and in this study, it is now possible to use the overall, extended ASM3 model for better description of both aerobic and anoxic activities of heterotrophs in nitrogen removing plants. Full-scale applications of these models warrant a better insight into the dynamics found in biological nitrogen removal plants.

This chapter is *in preparation* for publication.

1. INTRODUCTION

Simultaneous storage and growth activities of activated sludge have been demonstrated to occur and quantified both at lab- and full-scale activated sludge systems. This was supported by recent researches on the underlying mechanisms of substrate removal in activated sludge systems under aerobic (van Loosdrecht *et al*., 1997; Krishna and van Loosdrecht, 1999; Beun *et al*., 2000a; Dircks *et al*., 2001; Beccari *et al*., 2002; Carucci *et al*., 2002) and anoxic conditions (Beun *et al*., 2000b; Dionisi *et al*., 2001). This result is not surprising as it was already theoretically expected in the unified model of Daigger and Grady (1982) for bacterial growth on soluble components. Moreover, from a microbial survival point of view it is clear that bacteria capable of storing substrate as internal storage polymers (e.g. PHB) when external substrate is available, will gain a selective advantage in famine conditions compared to bacteria with only growth strategy (van Loosdrecht and Heijnen, 2002). This alternating feast and famine conditions are not the exception but the rule in many full-scale wastewater treatment plants (WWTP) (van Loosdrecht *et al*., 1997).

Moreover, several other experimental observations, which imply the existence of storage phenomenon, were often reported. For instance, higher growth yields e.g. 0.75, were usually required to be able to adequately describe the oxygen uptake rate (OUR) of activated sludge obtained from batch experiments (Henze *et al*., 2000; Gernaey *et al*., 2002b; Chapter 4.1; Chapter 4.2.1). This means part of the substrate was channelled/used for other purposes than only formation of new bacterial cells i.e. growth. Moreover, in a typical batch-OUR experiment (see e.g. Gernaey *et al*., 2002b; see Chapter 4.2.1 and Chapter 4.4) it has also been observed that the endogenous OUR level of biomass prior to substrate addition and after external substrate is completely removed does not remain the same. On the contrary, the endogenous OUR level increases considerably after the substrate addition and it takes a very long time to return to the baseline endogenous OUR level prior to substrate addition. This elevated endogenous level may indeed, be due to additional OUR consumption required for degradation of internal storage polymers on top of the endogenous respiration of biomass which is due to lysis, maintenance, decay and predation by higher organisms, e.g. protozoa, rotifiers etc (van Loosdrecht and Henze, 1999).

In short, the existence of the storage phenomenon challenges the current understanding and therefore modelling of substrate removal in activated sludge systems, which is solely based on growth processes, e.g. Activated Sludge Model no.1 (ASM1) of Henze *et al*., (2000). As a result Activated Sludge Model no.3 was developed to take into account the storage phenomenon of activated sludge both under aerobic and anoxic conditions (Henze *et al*., 2000). To keep the modelling at an acceptable complexity, ASM3 assumed that substrate is first stored completely before it is used for growth. However, this assumption was demonstrated to be untenable: (1) it is unable to model the experimentally observed

discontinuity in the growth rate of biomass under feast and famine conditions (Krishna and van Loosdrecht, 1999) (2) it predicts formation of more storage products than experimentally observed when trying to fit a typical oxygen uptake rate profile of biomass under feast and famine phases (Krishna and van Loosdrecht, 1999) (3) growth is found to occur simultaneously with storage under feast conditions (Krishna and van Loosdrecht, 1999; Beun *et al*., 2000a; Beun *et al*., 2002;) and (4) severe practically identifiability problems are reported when trying to fit ASM3 to OUR data from typical batch experiments and leads to mechanistically not meaningful parameter values (Chapter 4.2.1).

Consequently, several mathematical models were proposed to improve the modelling of aerobic simultaneous storage and growth processes. These models were based on either the metabolic model of the Delft research group (van Aalst-van Leeuwen *et al*., 1997; Beun *et al*., 2000a; van Loosdrecht and Heijnen, 2002) or using traditional ASM approaches (Krishna and van Loosdrecht, 1999; Carucci *et al*., 2001; Beccari *et al*., 2002; Karahan-Gul *et al*., 2003). The above mentioned models for the aerobic storage phenomenon were usually developed or studied using OUR measurements obtained from respirometers. These are well-established tools for monitoring biomass activity under aerobic conditions (Spanjers *et al*., 1998).

The modelling of the storage phenomenon under anoxic conditions has remained less studied compared to its aerobic counterpart and it is typically based on extending the models developed under aerobic conditions to anoxic conditions, see e.g. Beun *et al*. (2000b) and van Loosdrecht and Heijnen (2002). This could be due to practical/technical limitations with the measurement of the anoxic activity of biomass, which is usually monitored with off-line nitrate measurements at low frequency (measurement interval typically 10-20 minutes). In this study, a recently developed anoxic respirometer (Chapter 3.2) able to provide high frequency data with a quality that is at least as good as a typical respirometer, will be used to evaluate the model proposed to describe anoxic storage activity of biomass (see below model development). In addition to NUR measurements, titrimetric measurements are also employed to increase the amount of information about the anoxic heterotrophic activity during batch experiments.

The main objectives of this study are to improve the understanding and mechanistic modelling of simultaneous storage and growth processes of activated sludge occurring under anoxic conditions. This research is a follow-up study of the simultaneous storage and growth of activated sludge under aerobic conditions presented in the previous chapter (see Chapter 4.2.2). The research is organized in three main parts: In the first part, the simultaneous storage and growth model developed in the previous chapter (Chapter 4.2.2) is adapted to anoxic conditions and used to interpret high frequency NUR data obtained from anoxic batch experiments. Then, the results from the anoxic model are compared with the industry standard ASM1 model (Henze *et al*., 2000) in view of the mechanistic meaning of parameter estimates.

In the second part of the study, additional titrimetric measurements are used to investigate a possible improvement on parameter estimation and model calibration in view of full-scale applications. Finally, in the third part, the influence of the initial substrate to biomass ratio in batch experiments designed for model calibration is demonstrated.

2. MATERIALS AND METHODS

The anoxic respirometer developed in a previous study (see Chapter 3.2) is used to measure the nitrate uptake rate (NUR) of biomass. The anoxic set-up consists of a 1 L reactor with thermal jacket for temperature control by a cooling system (Lauda Ecoline E303). Nitrate is measured by a biosensor (Larsen *et al.*, 2000; Unisense, Denmark). The pH is measured in the aeration vessel with a HA405-DXK-S8/120 type pH electrode (Mettler Toledo) and controlled within a pH set-band ± 0.03 as described in detail in Gernaey *et al.* (2001a). The data acquisition frequency in the anoxic experiments is set to 3 seconds. High frequency noise known to ride on top of the weak analog signals of electrodes were filtered using a low pass Savitzky-Golay filter (Chapter 3.1) with central moving window size 11 and polynomial order 1.

For the experimental work activated sludge was sampled from either a pilot scale 80-l SBR reactor (see Chapter 5.1) called experiment A or Ossemeersen WWTP receiving mainly domestic wastewater (Aquafin, Belgium) called experiment B. During the experiments small substrate pulses of acetate (10 g COD/l), nitrate (1 g NO_3-N/l) and ammonium (1 gNH_4-N/l) stock solutions were dosed to the activated sludge. All experiments were performed at 20 ±0.1 ^{0}C. N_2 gas was provided continuously onto the surface of the reactor during the experiments to ensure anoxic conditions. Regular samples were taken to check nitrite build-up during the experiments via commercial kits (Dr. Lange). MLSS and MLVSS concentration of activated sludge was measured following Standard Methods (APHA, 1995).

Model implementation, simulations, parameter estimation and confidence interval for parameter estimates were all performed using WEST software (Hemmis NV, Kortrijk, Belgium; Vanhooren *et al.*, 2003). The methodology proposed in Dochain and Vanrolleghem (2001) was used to calculate the confidence intervals for parameter estimates, which is described in detail in Chapter 4.2.2.

3. MODEL DEVELOPMENT

In this section, two models used in this study will be described. The aim of using these two models is to compare the well-established and widely used growth kinetics based ASM1 model with substrate uptake kinetics based models i.e. the simultaneous storage and growth developed in the previous study (Chapter 4.2.2), in view of a better and mechanistic description of anoxic activity of biomass in full-scale activated sludge systems.

3.1 ASM1e: ASM1 model extended with proton production under anoxic conditions

In activated sludge models (Henze *et al*., 2000), denitrification is often modelled assuming complete denitrification in one step (from NO_3^- to nitrogen gas) using Monod kinetics for growth and a reduced yield coefficient. On the other hand, numerous studies have demonstrated that denitrification occurs following a sequential reduction path for oxidised nitrogen species: $NO_3^- \rightarrow NO_2^- \rightarrow NO \rightarrow 0.5N_2O \rightarrow 0.5N_2$ (Betlach and Tiedje, 1982; Zumft, 1997; Thomsen *et al*., 1994; Almeida *et al*., 1995; Wild *et al*., 1996). Moreover, it is often shown that partial denitrification may or may not occur depending on several factors e.g. COD/N, type of substrate, type of biomass, pH and temperature etc. (Betlach and Tiedje, 1982; Thomsen *et al*., 1994; von Schulthess and Gujer, 1996; Oh and Silverstein, 1999). Since there is still no consensus – rather conflicting results, on the underlying mechanisms and occurrence of partial denitrification, e.g. nitrite build up or emission of N_2O during denitrification, it was decided to model denitrification in a single step following the conceptual approach of ASM1 (Henze *et al*., 2000) which has been applied successfully for numerous full-scale wastewater treatment plants (WWTP).

However, the ASM1 model is extended to describe the pH effect of denitrification process, since it was shown previously to provide additional insight into the denitrification process (Bogaert *et al*., 1997; Petersen *et al*., 2002a; Foxon *et al*., 2002; Sin *et al*., 2003). The conceptual anoxic titrimetric model proposed by Petersen *et al*. (2002a), which extended the aerobic titrimetric model of Gernaey *et al*. (2002a) to anoxic conditions, is adopted in this study to describe the pH effect of denitrification. However, for the calculation of the stoichiometric coefficients of the titrimetric model, the stoichiometry of the denitrification process is employed (see Annex 1). Each stoichiometric coefficient shown in the CO_2 and Hp columns of the ASM1e model (see Table 2) is derived using conservation balances for degree of reduction, carbon (COD) and nitrogen as detailed in Annex 1.

In short, the following processes included in ASM1 are considered to induce a pH effect during denitrification:

1. Substrate uptake for growth (for a weak acid type substrate)
2. Nitrate uptake as e-acceptor
3. Ammonium uptake for growth
4. CO_2 production from anoxic growth
5. CO_2 production from endogenous activity
6. CO_2 stripping (surface stripping during anoxic batch experiments)

It is assumed that the uptake of a weak acid type substrate (e.g. acetate which is in majority present in dissociated form in the liquid at pH equal to 7) consumes protons from the medium since biomass needs to preserve its charge balance at the cellular level (Gernaey *et al*.,

2002a). On the other hand, uptake of substrate present in undissociated form will not consume protons e.g. dextrose. The extent of proton consumption is determined by the fraction of acetate present in ionic form (dissociated) defined by *m*, which is determined by the acidity constant and the pH of the medium:

$$m = \frac{1}{1+10^{pKa-pH}} \quad (1)$$

where pK_a stands for the negative logarithm of the acidity constant. Similarly, the uptake of ammonia from the medium will release protons to the medium. The extent of proton produced will again depend on the pH of the medium and is determined by the fraction of ammonium present in the medium, *p*:

$$p = \frac{1}{1+10^{pH-pKNH}} \quad (2)$$

CO_2, produced both during growth and decay processes (see Annex 1), enters into the complex aqueous CO_2 equilibrium and forms a new equilibrium with bicarbonate ions, thereby directly influencing the proton concentration in the medium. The extent of this influence depends on the equilibrium constant of the CO_2 -HCO_3^- reaction and the pH of the medium. Moreover, since stripping transfers CO_2 from the liquid to the gas phase it is inherently part of the aqueous CO_2 system too. This complex gas-liquid CO_2 equilibrium system is studied in detail in Chapter 4.1 and adopted here to describe the pH effect of the CO_2 system during an anoxic batch experiment.

Default parameters used in the ASM1e model are summarised in Table 1. It is important to note that some of these parameters are unique for the experimental conditions studied in this research. Particularly the affinity constants for nitrate and substrate (i.e. acetate) are quite low compared to the default value proposed by Henze *et al.* (2000) for full-scale systems. This issue is further addressed below in the discussion section.

3.2 ASM3e: Simultaneous storage and growth model of Chapter 4.2.2 adopted to anoxic conditions

The model developed here only holds for single step denitrification process (see above) and is essentially based on the simultaneous storage and growth model developed for aerobic conditions in the previous study (see Chapter 4.2.2). In the previous study, the model was developed by critically evaluating several models available in the literature that describe storage phenomenon and has the following distinct features: (1) diversion of substrate flux for growth and storage is modelled using a pipe-branch analogy (2) yield coefficients are

calculated using a metabolic model developed in van Aalst-van Leeuwen *et al*. (1997) (3) a second order model is used to describe degradation of storage products under famine conditions.

In a recent review on storage by activated sludge (Beun *et al*., 2002) it was shown that the fraction of substrate used for storage is a constant ratio, 0.67 gCOD-PHB/gCOD-HAc and 0.5 gCOD-PHB/gCOD-HAc under aerobic and anoxic conditions respectively. This assumption of a constant ratio, amount of substrate used for storage per amount of substrate consumed, f_{STO}, makes the modelling of simultaneous storage and growth processes under anoxic conditions relatively easy/practical. It requires only two parameters to be identified for the description of substrate flux into the cell: a maximum substrate uptake rate, q_{MAX} and a fraction of substrate flux diverted for storage, f_{STO} (see Chapter 4.2.2).

In the famine phase, the degradation of storage products is modelled using a second order model developed in the previous study (see Chapter 4.2.2) and adapted here to anoxic conditions:

$$\frac{dX_{STO}}{dt} = -\frac{1}{Y_{H,STO}} r_{H,STO} \qquad \text{with} \tag{3}$$

$$r_{H,STO} = \mu_{MAX,STO} \frac{\left(X_{STO} / X_H \right)^2}{K_2 + K_1 . X_{STO} / X_H} \frac{K_S}{K_S + S_S} \frac{S_{NO3}}{S_{NO3} + K_{NO3}} \frac{S_{NH}}{S_{NH} + K_{NH}} X_H \tag{4}$$

where K_2 is the affinity of the biomass as a function of X_{STO}/X_H (mg COD/mgCOD) and K_1 is a regulation constant controlling the degradation rate of X_{STO} as function of f_{XSTO} (see Chapter 4.2.2). Similar to the previous study (Chapter 4.2.2), $\mu_{MAX,STO}$ is in this study assumed to be equal to $\mu_{MAX,S}$ as a compromise between model complexity and practical applicability of the model. The yield coefficients for the growth on substrate and storage, and the yield for the storage process under anoxic conditions are calculated using the following relationships derived using the metabolic model of van Aalst-van Leeuwen *et al*. (1997) and adapted to anoxic conditions by Beun *et al*. (2000b):

$$Y_{H,S} = \frac{4 \cdot \delta_n - 2}{4.2 \cdot \delta_n + 4.32} . \frac{4.2}{4} ; \; Y_{STO} = \frac{4 \cdot \delta_n - 2}{4.5 \cdot \delta_n} . \frac{4.5}{4} \text{ and } Y_{H,STO} = \frac{4.5 \cdot \delta_n - 0.5}{4.2 \cdot \delta_n + 4.32} . \frac{4.2}{4.5}$$

where δ_n is the efficiency of oxidative phosphorylation under anoxic conditions (mol/mol) assumed to be 60% of the corresponding efficiency of oxidative phosphorylation under aerobic conditions (Beun *et al*., 2000b).

As a result, the nitrate uptake rate of denitrifiers under anoxic conditions will be equal to the sum of 5 different processes consuming nitrate under feast and famine conditions:

$$NUR = \left(\frac{1-Y_{H,S}}{2.86Y_{H,S}} r_{X,S} + \frac{1-Y_{STO}}{2.86Y_{STO}} r_{STO} + \frac{1-Y_{H,STO}}{2.86Y_{H,STO}} r_{X,STO} + \frac{1-f_{XI}}{2.86} b_H \right) X_H + \frac{1}{2.86} b_{STO} X_{STO}$$

The description of the endogenous activity of biomass, i.e. the decay of biomass and storage products, were modelled using the approach proposed in ASM3 (Henze *et al*., 2000). The mathematical model presented above for the description of simultaneous storage and growth activities of denitrifiers called ASM3e is given in Table 4 and Table 5 for stoichiometric and kinetic matrices respectively. The stoichiometric matrix given in Table 4 was checked using continuity equations for COD, charge, and nitrogen.

Similar to ASM1e, ASM3e is also extended to describe the pH effect of all processes involved in the description of anoxic storage and growth of denitrifiers, i.e. storage, growth, degradation of storage and endogenous processes. Since it was shown that titrimetric measurements provide additional insight into the denitrification process and improve the practical identifiability of relatively complex models (see e.g. Gernaey *et al*., 2002b), CO_2, HCO_3 and Hp columns are added to the matrix representation of ASM3e (see Table 4). The stoichiometric coefficients of CO_2 and proton components are calculated using the process stoichiometry of each process included in ASM3e. In the titrimetric model, it is assumed that biomass uses only VFA type carbon sources for the formation of storage products (see Annex 2). The stoichiometry of each process and the detailed calculation procedure are given in Annex 2. Moreover, the gas-liquid CO_2 system was described using the dynamic CO_2 model developed in Chapter 4.1.

The default values of the ASM3e model are shown in Table 1. It is useful to note that the reduction factor for heterotrophic activity under anoxic conditions is included in the model but its default value is set to 1. The reason of this choice is twofold: (1) Identifiability of this parameter was not possible using NUR measurements alone, as the determination of the reduction obviously also requires the measurement of OUR of biomass under aerobic conditions. (2) The default value was set to one thereby enabling direct comparison of the parameter estimates of the denitrification process with those obtained under aerobic conditions elsewhere (see e.g. Chapter 4.2.2).

Table 1. Default values of the parameters used in ASM1e and ASM3e developed in this study (The kinetic values are reported for 20 ^{0}C)

Parameter	Description	ASM1e	ASM3e
b_H	Endogenous decay rate for heterotrophs, d^{-1}	0.17	0.17
b_{STO}	Endogenous decay rate for X_{STO}, d^{-1}	-	0.17
δ_n	Efficiency of oxidative phosphorylation with NO_3^-, mol/mol	-	1.5
f_{STO}	Fraction of substrate diverted to storage, gCOD/gCOD	-	0.4
f_{XI}	Inert fraction of biomass, gCOD/gCOD	0.2	0.2
γ_x	Degree of reduction of biomass (e.g. $CH_{1.8}O_{0.5}N_{0.2}$)	4.2	4.2
γ_s	Degree of reduction of substrate (for acetate)	4	4
γ_{STO}	Degree of reduction of storage products (for PHB)	4.5	4.5
i_{NXI}	Nitrogen content of the inert fraction of biomass, gN/gCOD	0.02	0.02
i_{NBM}	Nitrogen content of biomass, gN/gCOD	0.086	0.086
i_{CSS}	C-mol content of substrate (e.g. $C_2H_4O_2$)	2	2
K_{NO3}	Biomass affinity constant for NO_3, mgN/l	0.05	0.05
K_{NH}	Biomass affinity constant for NH_4, mgN/l	0.01	0.01
K_S	Biomass affinity constant for substrate, mgCOD/l	0.5	0.5
K_O	Biomass affinity constant for oxygen, mgCOD/l	0.2	0.2
K_1	Regulation constant for degradation of X_{STO}, gCOD/gCOD	-	0.05
K_2	Biomass affinity constant for X_{STO}/X_H, gCOD/gCOD	-	0.001
K_H	Henry coefficient for CO_2, mole/(atm.l)	0.045	0.045
k_1	Forward reaction rate for aqueous CO_2 equilibrium, d^{-1}	3456	3456
K_La_{CO2}	Mass-surface transfer coefficient for CO_2, d^{-1}	4	4
k_{STO}	Maximum storage rate of denitrifiers, d^{-1}	-	0.8
μ_{maxH}	Maximum growth rate of denitrifiers on S_S, d^{-1}	2	0.7
μ_{maxSTO}	Maximum growth rate of denitrifiers on X_{STO}, d^{-1}	-	0.7
η	Anoxic reduction factor for growth/storage	1	1
P_{CO2}	Partial pressure of CO_2 in air, atm	0.00038	0.00038
pK_1	The first acidity constant in the aqueous CO_2 system (K_1)	6.35	6.35
pH	Negative logarithm of proton concentration	7.5	7.5
pK_A	Acidity constant for the dissociation of acetate	4.75	4.75
pK_{NH}	The equilibrium constant for the dissociation of NH_4^+	9.57	9.57
τ_{NO}	First order time constant observed in NUR, d	0.0007	0.0007
τ_{HP}	First order time constant observed in HP, d	0.00007	0.00007
S_{CO2}^*	CO_2 saturation coefficient (at 1 atm ambient pressure), mmol/l	0.017	0.017
q_{max}	Maximum substrate uptake rate of denitrifiers, d^{-1}	-	3
$Y_{H,S}$	Anoxic yield coefficient for growth on S_S, gCOD/gCOD	0.60	0.40
Y_{STO}	Yield coefficient for storage on S_S, gCOD/gCOD	-	0.55
$Y_{H,STO}$	Yield coefficient for growth on X_{STO}, gCOD/gCOD	-	0.67

Table 2. Matrix representation of the ASM1 model extended with proton production (ASM1e). See Annex 1 for calculation of the stoichiometry of the model for CO_2 and Hp components.

	1. S_S	2. S_{NH}	3. S_{NO3}	4. S_{N2}	5.S_{HCO3}	6. S_{CO2}	7. S_{Hp}	8. X_H	9. X_I
Process (j)	g COD	g N	g N	gN	mol	mol	mol	g COD	g COD
1.Anoxic Growth of Heterotrophs	$-\frac{1}{Y_{H,S}}$	$-i_{NBM}$	$-\frac{1-Y_{H,S}}{2.86Y_{H,S}}$	$\frac{1-Y_{H,S}}{2.86Y_{H,S}}$		$\left(\frac{1}{8\gamma_s Y_{H,S}}-\frac{1}{8\gamma_x}\right)$	$\frac{p\cdot i_{NBM}}{14}-\frac{m}{Y_H\cdot 8\gamma_S i_{CSS}}-\frac{1-Y_{H,S}}{40\cdot Y_{H,S}}$	+1	
2.Anoxic endogenous respiration		$i_{NBM}-f_{XI}\cdot i_{NXI}$	$-\frac{(1-f_{XI})}{2.86}$	$\frac{(1-f_{XI})}{2.86}$		$(1-f_{XI})\frac{1}{8\gamma_x}$	$-\frac{(i_{NBM}-f_{XI}\cdot i_{NXI})\cdot p}{14}-\frac{(1-f_{XI})}{40}$	-1	f_{XI}
3.Aqueous CO_2 equilibrium					1	-1	1		
4. CO_2 stripping						-1			

Table 3. Kinetics of the processes included in ASM1e

PROCESS	KINETICS
1. Anoxic growth of heterotrophs	$\mu_{\max H}\cdot\eta\frac{S_S}{S_S+K_S}\frac{S_{NO3}}{S_{NO3}+K_{NO3}}\frac{K_O}{S_O+K_O}\frac{S_{NH}}{S_{NH}+K_{NH}}X_H$
2.Anoxic endogenous respiration	$b_H\cdot\eta\frac{S_{NO3}}{S_{NO3}+K_{NO3}}\frac{K_O}{S_O+K_O}X_H$
3.Aqueous CO_2 equilibrium	$k_1\cdot S_{CO2}-\left(k_1\cdot 10^{pK_1-pH}\right)\cdot S_{HCO3}$
4. CO_2 stripping	$K_L a_{CO2}\cdot\left(S^*_{CO2}-S_{CO2}\right)$

Table 4. Matrix representation of the extended ASM3 model (developed in Chapter 4.2.2) adapted to anoxic conditions and extended with the pH effect of denitrification (see Annex 2 for the calculation of the stoichiometry of the model): ASM3e

	1.S_S	2.S_{NH}	3.S_{NO3}	4.S_{N2}	5.S_{HCO3}	6.S_{CO2}	7.S_{Hp}	8.X_H	9.X_I	10.X_{STO}
	g COD	g N	g N	g N	mol	Mol	Mol	g COD	g COD	g COD
1. Anoxic formation of storage products	$\frac{1}{Y_{STO}}$		$-\frac{1-Y_{STO}}{2.86Y_{STO}}$	$\frac{1-Y_{STO}}{2.86Y_{STO}}$		$\frac{1}{8}\left(\frac{1}{Y_{STO}\cdot\gamma_S}-\frac{1}{\gamma_{STO}}\right)$	$-\frac{m}{8\cdot\gamma_S\cdot Y_{STO}\cdot i_{CSS}}$ $-\frac{1-Y_{STO}}{14\cdot 2.86Y_{STO}}$			1
2. Anoxic growth on S_S	$-\frac{1}{Y_{H,S}}$	$-i_{NBM}$	$-\frac{1-Y_{H,S}}{2.86Y_{H,S}}$	$\frac{1-Y_{H,S}}{2.86Y_{H,S}}$		$\frac{1}{8}\left(\frac{1}{Y_{H,S}\gamma_S}-\frac{1}{\gamma_X}\right)$	$\frac{p\cdot i_{NBM}}{14}-\frac{m}{8\cdot\gamma_S\cdot Y_{HS}\cdot i_{CSS}}$ $-\frac{1-Y_{H,S}}{14\cdot 2.86Y_{H,S}}$	1		
3. Anoxic growth on storage products, X_{STO}		$-i_{NBM}$	$-\frac{1-Y_{H,STO}}{2.86Y_{H,STO}}$	$\frac{1-Y_{H,STO}}{2.86Y_{H,STO}}$		$\frac{1}{8}\left(\frac{1}{Y_{H,STO}\gamma_{STO}}-\frac{1}{\gamma_X}\right)$	$\frac{p\cdot i_{NBM}}{14}-$ $-\frac{1-Y_{H,STO}}{14\cdot 2.86Y_{H,STO}}$	1		$-\frac{1}{Y_{H,STO}}$
4.Anoxic endogenous respiration		$i_{NBM}-f_{XI}i_{NXI}$	$-\frac{(1-f_{XI})}{2.86}$	$\frac{(1-f_{XI})}{2.86}$		$\left(\frac{1-f_{XI}}{8\cdot\gamma_X}\right)$	$-\frac{(i_{NBM}-f_{XI}\cdot i_{NXI})\cdot p}{14}$ $-\frac{(1-f_{XI})}{40}$	-1	f_{XI}	
5.Anoxic Respiration of X_{STO}			$-\frac{1}{2.86}$	$\frac{1}{2.86}$		$\frac{1}{8\cdot\gamma_{STO}}$	$-\frac{1}{40}$			-1
6.Aqueous CO_2 equilibrium					1	-1	1			
7. CO_2 stripping						-1				

Table 5. Kinetics of the processes included in ASM3e

PROCESS	KINETICS
1. Anoxic formation of storage products	$k_{STO}\eta \frac{S_S}{S_S+K_S}\frac{S_{NO3}}{S_{NO3}+K_{NO3}}\frac{K_O}{S_O+K_O}\frac{S_{NH}}{S_{NH}+K_{NH}}X_H$
2. Anoxic growth on S_S	$\mu_{\max H}\eta \frac{S_S}{S_S+K_S}\frac{S_{NO3}}{S_{NO3}+K_{NO3}}\frac{K_O}{S_O+K_O}\frac{S_{NH}}{S_{NH}+K_{NH}}X_H$
3. Anoxic growth on X_{STO}	$\mu_{\max STO}\eta \frac{S_{NO3}}{S_{NO3}+K_{NO3}}\frac{S_{NH}}{S_{NH}+K_{NH}}\frac{\left(X_{STO}/X_H\right)^2}{K_2+X_{STO}/X_H\cdot K_1}\frac{K_S}{K_S+S_S}\frac{K_O}{K_O+S_O}X_H$
4.Anoxic endogenous respiration	$b_H\cdot\eta \frac{S_{NO3}}{S_{NO3}+K_{NO3}}\frac{K_O}{S_O+K_O}X_H$
5.Anoxic Respiration of X_{STO}	$b_{STO}\cdot\eta \frac{S_{NO3}}{S_{NO3}+K_{NO3}}\frac{K_O}{S_O+K_O}X_{STO}$
6.Aqueous CO_2 equilibrium	$k_1\cdot S_{CO2}-\left(k_1\cdot 10^{pK_1-pH}\right)\cdot S_{HCO3}$
7. CO_2 stripping	$K_L a_{CO2}\cdot\left(S^*_{CO2}-S_{CO2}\right)$

Where $k_{STO}=f_{STO}\cdot q_{MAX}\cdot Y_{STO}$ and $\mu_{MAX,S}=\left(1-f_{STO}\right)\cdot q_{MAX}\cdot Y_{H,S}$

4. RESULTS

The results are presented in three main parts. In the first part, the experimental data consisting of combined nitrate and titrimetric measurements are presented. Next, ASM1e and ASM3e models are applied to interpret the NUR measurements obtained with biomass A and B respectively and to compare the models with each other. In the second part, combined titrimetric and nitrate measurements are used for parameter estimation with both models to investigate if there is an improvement on parameter estimation accuracy compared to that of using NUR data alone. In the third part, the effect of the initial substrate to biomass ratio (S_0/X_0) on parameter estimation during short-term batch experiments designed for calibration is presented.

4.1 Experimental data: monitoring denitrification processes with combined NUR and titrimetric measurements

Monitoring the denitrification process with high frequency nitrate measurements combined with titrimetric measurements obtained in the recently developed anoxic respirometer (Chapter 3.2) is shown in Figure 1. The typical nitrate and titrimetric measurements obtained with consecutive additions of substrate to endogenously respiring denitrifiers are given in Figure 1-top. The nitrate uptake rate (NUR) of denitrifiers calculated from the nitrate measurements –using a central moving window approach with 3 data points (see Chapter 3.2), are shown in Figure 1-down.

It is important to note that acid addition (see Figure 1-top) during the denitrification means that the anoxic biological activity is consuming protons from the medium, which is regularly observed elsewhere too (Petersen *et al*., 2002a; Foxon *et al*., 2002). In view of the titrimetric model that focuses on proton production, proton consumption must be converted to a negative proton production, as plotted in Figure 1-down.

Nitrite build-up was checked regularly during the experiment and found negligible with a maximum NO_2^- concentration ca 0.22 mgN/l. This is not surprising since Malisse (2002) also did not observe nitrite accumulation in denitrification with acetate using biomass sampled from the same SBR. Oh and Silverstein (1999) also observed no nitrite build-up during denitrification with acetate under COD/N ratio equal to 2. However, in several other studies nitrite build-up was clearly observed to occur during denitrification (Beun *et al*., 2000b; Almeida *et al*., 1995; Wild *et al*., 1996; etc)

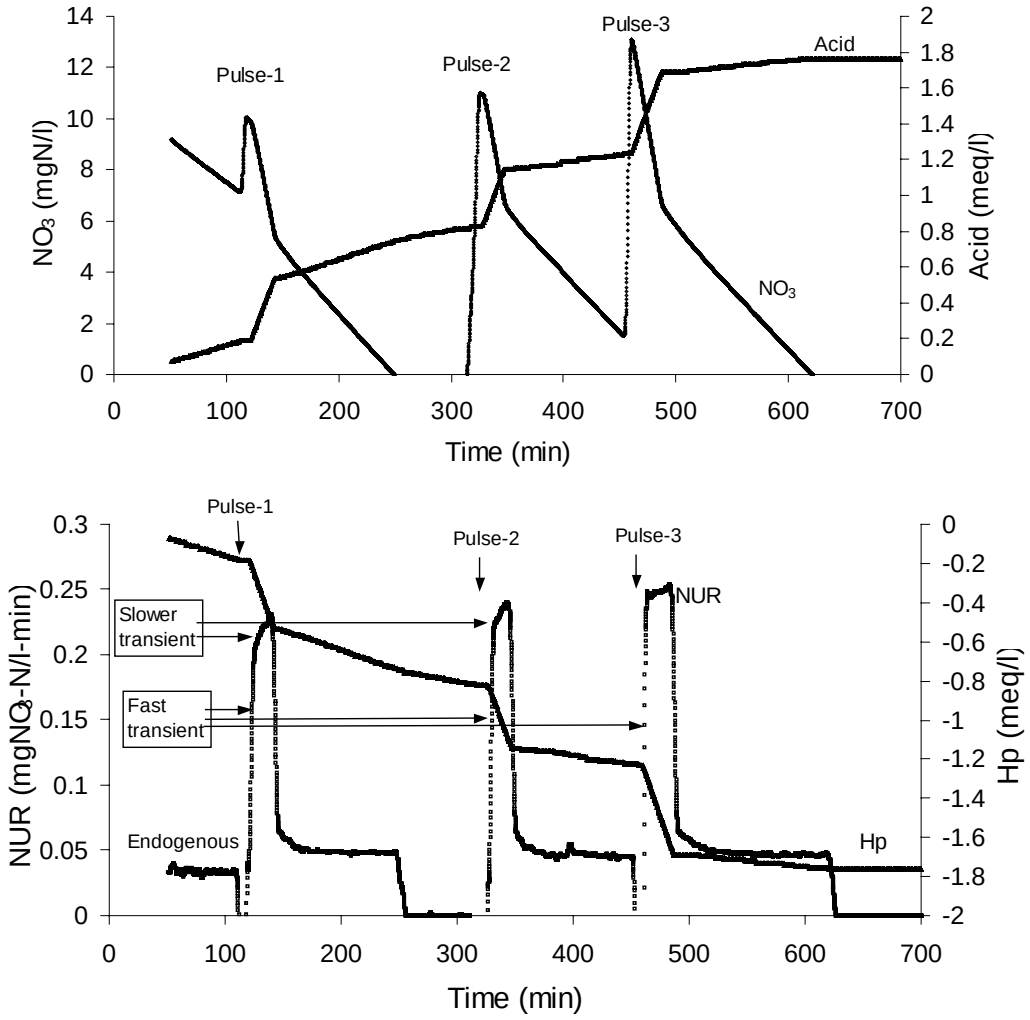

Figure 1. Typical nitrate and titrimetric measurements obtained using biomass A; pulse 1 with 33 mgCOD/l acetate and COD/N equal to 3.3, pulse 2 with 33 mgCOD/l acetate and COD/N equal to 3.0 and pulse 3 with 41 mgCOD/l acetate and COD/N equal to 3.3.

Upon pulse addition of acetate, NUR starts immediately to increase to a maximum rate following a first order transient, which takes ca 2-3 minutes (see Figure 1-down and pulse-1). This first order transient is often observed in OUR data obtained from batch experiments with activated sludge under aerobic conditions and is hypothesised to result from the cellular metabolism of substrate (see Chapter 4.4). Following this fast transient and after reaching a maximum level i.e. after about 3 minutes, the NUR is observed to keep increasing further albeit at a slower rate (see Figure-1 down and pulse-1). This second transient observed in NUR is relatively slow and takes around 10-20 minutes.

This slower transient towards the maximum NUR is also observed in OUR data obtained from pulse additions of substrate to endogenously respiring activated sludge (see Vanrolleghem *et al.*, 1998). Vanrolleghem and co-workers hypothesised that the underlying reason for this slower transient phenomenon could be physiological adaptation of biomass occurring at the RNA level and inducing more enzymes such that the maximum growth rate of biomass can be

increased (see also for a detailed discussion in Chapter 3.2). This phenomenon is often reported in studies with pure and mixed cultures too (Daigger and Grady, 1982; Grady *et al*., 1996; Chudoba *et al*., 1992). This slower transient phenomenon is repeated in the second pulse addition of acetate (see Figure 1-down) but it is no longer visible after the third acetate pulse addition (see Figure 1-down). This implies that the biomass has attained its maximum nitrate uptake rate possible under the new process conditions following a transient period, which took ca 40 minutes. This issue is further discussed in the discussion section below.

After acetate is completely consumed by biomass indicated by the sharp bending point in Hp, the NUR decreases to a baseline endogenous level clearly higher than the endogenous NUR level observed prior to addition of acetate (see Figure 1-down). This elevated level of NUR during an endogenous phase could be due to additional uptake of nitrate for oxidation of previously stored carbon polymers e.g. PHB. This point is further discussed below using model-based evaluation of the experimental data. Such elevated respiration rate after addition of acetate/substrate is also often observed in OUR with activated sludge under aerobic conditions (Chapter 4.2.1)

Titrimetric measurements display no or negligible transient upon pulse addition of acetate to a denitrifying culture (see Figure 1-down in pulse-1). Assuming that titrimetric data indirectly reflect the acetate consumption (Gernaey *et al*., 2002a; Petersen *et al*., 2002a; Chapter 4.4), this implies that the acetate uptake is very fast compared to the uptake of nitrate. The fast transients observed in NUR and Hp are analysed using the first order empirical model proposed in Chapter 4.4. After pulse addition of acetate, the proton consumption is linear in time suggesting that the uptake of acetate is also linear in time (see Figure 1-down in pulse 1). It is important to note that the Hp data do not display a second transient i.e. the slower transient that is observed in the NUR data. During the endogenous phase, consumption of protons continues at a non-linear rate due to stripping of CO_2 from the reactor (see Figure 1-down). According to the dynamic CO_2 model developed in Chapter 4.1, this is mainly dependent on the surface mass transfer coefficient of CO_2 and the aqueous concentration of CO_2.

The high frequency combined NUR and titrimetric data, with frequency and quality comparable to those of an aerobic respirometer (see e.g. Gernaey *et al*., 2001a) suggest that the response of activated sludge to pulse addition of acetate under anoxic conditions is quite similar to the aerobic oxidation of acetate by activated sludge (see Chapter 4.4). In the following section, however, the stoichiometry and the kinetics of the anoxic oxidation of acetate by activated sludge will be investigated in detail.

4.2 Parameter identifiability

4.2.1 ASM1e

An important aspect of parameter estimation for activated sludge models concerns the identifiability of the model structure under a given data set. Parameter estimation is usually complex in view of the limited availability of measurements (Dochain and Vanrolleghem, 2001; Brun *et al*., 2002; Petersen *et al*., 2003b). In other words, it is important to know beforehand which parameters or parameter combinations can be estimated using a certain measurement, e.g. NUR. The structural identifiability of growth based Monod-type models using combined respirometric and titrimetric measurements has recently been studied in detail (Dochain and Vanrolleghem, 2001; Gernaey *et al*., 2002b; Petersen *et al*., 2003b). Based on these studies, Petersen *et al*. (2003b) recently suggested a generalized method for determining the structurally identifiable parameters in ASM-like model structures. Using this generalized method, the identifiable parameter combinations of ASM1e using NUR and Hp measurements under negligible growth and un-limiting nitrate conditions are given in Table 6.

Table 6. Structurally identifiable parameter combinations of ASM1e (determined according to Petersen *et al*., 2003b) with different measurements assuming negligible growth and un-limiting nitrate conditions

Variables	Structurally identifiable parameter combinations
NUR	$\frac{1-Y_{HNO\,3}}{2.86\cdot Y_{HNO\,3}}\mu_{\max\,H}\eta X_{\,H}(0)\,;\frac{1-Y_{HNO\,3}}{2.86}\cdot K_S\,;\frac{1-Y_{HNO\,3}}{2.86}\cdot S_S(0)$
Hp	$\frac{\beta}{Y_{HNO3}}\cdot\mu_{\max H}\eta X_{\,H}(0);\beta\cdot K_S\,;\beta\cdot S_S(0)$ where $\beta=-\frac{m}{8\gamma_S i_{CSS}}+\frac{p}{14}i_{NBM}\cdot Y_{HNO3}-\frac{1}{14}\cdot\frac{1-Y_{HNO3}}{2.86}$
NUR & Hp	$\frac{1-Y_{HNO\,3}}{2.86\cdot Y_{HNO\,3}}\mu_{\max\,H}\eta X_{\,H}(0)\,;\frac{1-Y_{HNO\,3}}{2.86}\cdot K_S\,;\frac{1-Y_{HNO\,3}}{2.86}\cdot S_S(0)\ \frac{2.86}{1-Y_{HNO3}}\beta$

If the initial amount of substrate, $S_S(0)$, is known, the previously unidentifiable parameters Y_{HNO3}, K_S and μ_{maxH} can be identified uniquely, i.e. they can be calculated separately using the parameter combinations given for NUR in Table 6. In this study, the anoxic reduction factor η, is assumed 1 (see model development) which means that μ_{maxH} refers to the maximum growth rate of denitrifiers. Moreover the initial biomass concentration, $X_H(0)$, is estimated using endogenous NUR measurements prior to substrate addition where b_H was assumed a default value (Henze *et al*., 2000). Additional titrimetric measurements make also the i_{NBM} parameter identifiable (see Table 6) again assuming the yield is known.

The first order time constants for NUR and Hp measurements were shown to be uniquely identifiable too particularly using the data from the first 2-5 minutes of the experiment

(Gernaey *et al*., 2002b). It is important to stress that the parameter combinations given in Table 6 were determined assuming unlimiting nitrate conditions. It is expected that when nitrate is completely reduced to nitrogen gas in the medium, the affinity constant of nitrate should become identifiable too. This is discussed in detail below (see discussion section).

4.2.2 ASM3e

The generalized method of Petersen *et al*. (2003b) could not be applied to study the structural identifiability of the ASM3e model, because the model is rather complex and has a different structure compared to ASM1. Instead, the results obtained from the practical identifiability study of the ASM3e model under aerobic conditions performed before (see Chapter 4.2.2) is used here.

The endogenous decay coefficients of biomass and storage products, b_H and b_{STO} respectively, are fixed to their default values reported in literature (see e.g. ASM3 of Henze *et al*., 2000). The initial active biomass concentration, $X_H(0)$, is estimated using endogenous NUR measurements prior to substrate addition as mentioned above. The initial concentration of storage products, $X_{STO}(0)$, was shown to be poorly identifiable when only respirometric measurements are used (see Chapter 4.2.2). This consequently leads to large confidence intervals in the parameter estimates. To eliminate this problem, therefore, $X_{STO}(0)$ is estimated from NUR measurements using a two-step iterative estimation-method as proposed by Dochain and Vanrolleghem (2001). In the first iteration, $X_{STO}(0)$ is included in the parameter estimation, whereas in the second iteration, $X_{STO}(0)$ is fixed to its value estimated in the previous iteration (see Chapter 4.2.2).

The practical parameter identifiability of ASM3e performed in the previous study (Chapter 4.2.2) showed that δ, f_{STO}, q_{max}, K_S, K_1 and K_2 are identifiable with respirometric measurements. This parameter subset can, therefore, also be used in this study for parameter estimation using NUR measurements. However, when nitrate becomes limiting during the denitrification experiment, the affinity constant of nitrate should become identifiable too and therefore K_{NO3} is also estimated in experiment A, as discussed below (see discussion section).

4.3 Parameter estimation results with ASM1e and ASM3e models using NUR

Both models were calibrated using NUR measurements obtained from experiments A and B respectively. Parameter estimation and calculation of the corresponding confidence intervals of parameter estimates were performed in WEST (Hemmis NV, Kortrijk, Belgium; Vanhooren *et al*., 2003) using the simplex-search algorithm (Nelder and Mead, 1964). These parameter estimation results with their 95% confidence intervals are given in Table 7. The model fits to NO_3 and NUR measurements are plotted in Figure 2. In these plots, only each 15^{th} data point (i.e. data every 45 seconds) is shown to keep the figure from becoming too overloaded.

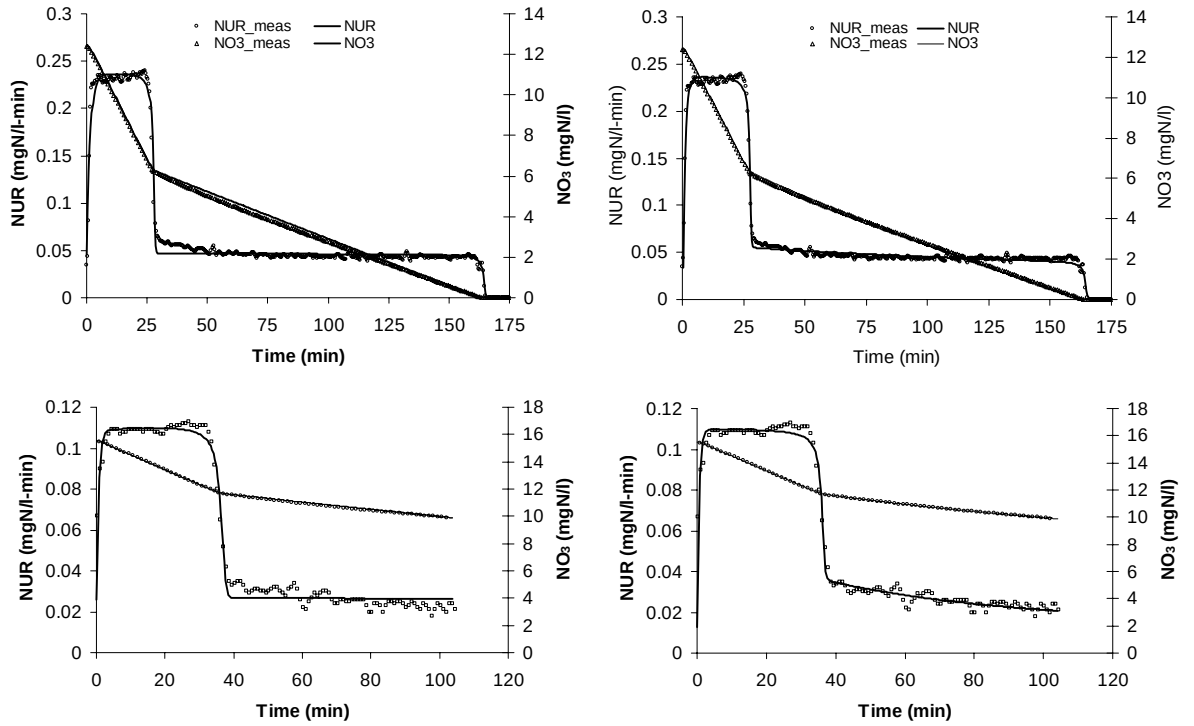

Figure 2. Model fits to experimental data using NUR. ASM1e (left) and ASM3e (right) with experiment A (top) and experiment B (down) respectively. Only every 15th data point is shown to keep the figure comprehensive (see the text for explanation).

The fits of both ASM1e and ASM3e models to NUR and NO_3 measurements from experiment A and B are good (see Figure 2). Still, the fit of ASM3e to NUR measurements is superior to the fit of ASM1e particularly during endogenous/famine phase (see e.g. Figure 2-top). The NUR obtained from both experiments showed a decreasing tail during the famine phase, which cannot be modelled by just using the endogenous process of ASM1e. On the contrary, ASM3e has one more process, i.e. degradation of storage products on top of the endogenous processes, and is therefore able to better fit the decreasing tail observed in NUR.

Although both models were calibrated using NUR, the model prediction of the nitrate data in both experiments A and B is almost equally good. Of course, this is theoretically expected and it is also worthwhile to note that the parameter estimation results with NO_3 and NUR are in very good agreement with each other (results not shown).

The parameter estimation results with ASM1e (see Table 7) showed that the anoxic yield coefficient for growth is in the range reported in ASM1 (Henze *et al*., 2000) but it was considerably higher than the yield recently reported by Muller *et al*. (2003), which is 0.58. Particularly, the yield in the experiment B is observed to be higher with a value of about 0.7 (see Table 7). An important parameter to be considered in view of yield estimation is the value of the endogenous decay coefficient of biomass. The endogenous decay rate of biomass

had to be increased by 40% and 100% in experiment A and B respectively to fit the endogenous NUR attained after substrate addition (see Figure 1-down and Table 7).

In ASM3e, on the other hand, the estimate for the anoxic yield for growth on substrate (0.49) in both experiments is closer to the usually observed value in activated sludge (0.58) (Muller *et al*., 2003). Moreover, the estimates of the storage yield, Y_{STO}, and growth yield on storage products, $Y_{H,STO}$, were quite the same in both experiments even though both experiments employed different biomass (see Table 7). Although the anoxic oxidative phosphorylation is found in the range 1 – 3 (Beun *et al*., 2000a), it is higher than the value reported by Beun *et al.* (2000b) for anoxic conditions (1.5).

Table 7. Parameter estimation results with NUR using ASM1e and ASM3e models. Parameters in **Bold** are estimated*, the rest are either *fixed* or calculated (see the text for explanation)

Parameter	Experiment A		Experiment B	
	ASM1e	ASM3e	ASM1e	ASM3e
$q_{MAX}(d^{-1})$	-	**2.31 (0.1%)**	-	**2.96 (0.12%)**
δ (mol/mol)	-	**1.96 (1.25%)**	-	**1.99 (5.82%)**
f_{STO}	-	**0.58 (0.99%)**	-	**0.64 (9.97%)**
K_1	-	**0.048 (8.84%)**	-	**0.026 (57.3%)**
K_2	-	**0.00089 (10.42%)**	-	**0.00077 (54.8%)**
K_{NO3} (mgN/l)	**0.016 (29.9%)**	**0.012 (7.31%)**	**0.012 (167.7%)**	*0.012*
K_S (mgCOD/l)	**0.37 (10.11%)**	**0.33 (2.59%)**	**0.42 (8.55%)**	**0.32 (10.1%)**
τ_{NO} (min)	**0.73 (1.77%)**	**0.71 (1.34%)**	**0.75 (9.04%)**	**0.63 (3.10%)**
b_H (d^{-1})	**0.24 (0.58%)**	*0.17*	**0.34 (1.24%)**	*0.17*
b_{STO} (d^{-1})	-	*0.17*	-	*0.17*
k_{STO} (d^{-1})	-	0.99	-	1.42
$\mu_{MAX,S}$ (d^{-1})	**1.52 (0.29%)**	0.48	**2.04 (0.54%)**	0.52
$\mu_{MAX,STO}$ (d^{-1})	-	0.48	-	0.52
$X_H(0)$ (mgCOD/l)	1000	1000	397	397
$X_{STO}(0)$ (mgCOD/l)	-	8.17	-	0.65
$Y_{H,S}$	**0.66 (0.22%)**	0.49	**0.699 (0.29%)**	0.49
$Y_{H,STO}$	-	0.62	-	0.62
Y_{STO}	-	0.74	-	0.75
SSE	0.049	0.032	0.020	0.011

*95% confidence intervals of parameter estimates are given in parenthesis as relative percentage of the corresponding parameter estimate.

Parameter estimation with ASM3e moreover showed that the fraction of substrate diverted for storage is remarkably high in both experiment A and B (see Table 7). These values are

slightly higher than the range reported for anoxic storage (0.5) but close to the range reported for aerobic storage (0.67) (Beun *et al.*, 2002). Moreover the growth rate of biomass estimated in ASM3e was considerably lower than the growth rate of biomass estimated for ASM1e (see Table 7).

Estimation of the affinity constant for nitrate, K_{NO3}, was possible for both models in experiment A as nitrate became limiting at the end of the experiment. The estimated value for K_{NO3} was significantly lower than the range reported for ASM models (Henze *et al.*, 2000; Wild *et al.*, 1996). However, it was not possible to reliably estimate K_{NO3} in experiment B since nitrate never became limiting throughout the experiment. This issue will be further investigated using sensitivity analysis in the discussion section.

The parameter estimation accuracy was found quite good/acceptable for both with ASM1e and ASM3e. However, the confidence intervals for K_1 and K_2 parameters, which are related to the degradation of X_{STO} during the famine phase in ASM3e, were found quite large in experiment B (see Table 7).

4.4 Additional titrimetric measurements for parameter estimation

In this section, titrimetric measurements obtained in experiment A (see Figure 1-down) are also used, along with NUR measurements, for parameter estimation. The fits of both ASM1e and ASM3e to the combined and NUR and titrimetric data are plausible with one exception (see Figure 3). Compared to the fit of the ASM1e model, the ASM3e model could not fit the titrimetric data very well during the endogenous phase (see Figure 3-down).

During the parameter estimation using combined NUR and Hp data, weighting factors were used for each variables. The weighting factors were determined using the inverse of the covariance of the measurement errors. To calculate the covariance of the measurement errors in NUR and Hp, a method proposed elsewhere was used (Petersen, 2000; Dochain and Vanrolleghem, 2001). The covariance of the measurement errors in NUR and Hp data were calculated as 4.7E-6 and 1.6E-5 respectively. These errors show that the Hp data contains more noise than the NUR data and as such it is weighted less during the parameter estimation with combined NUR and HP data.

The parameter estimation results with Hp and with combined NUR and Hp are given in Table 8. During parameter estimation based on only Hp data with ASM1e, Y_{HNO3} and endogenous decay parameters were fixed to the values determined using the NUR measurements (see Table 7). As far as the ASM1e model is concerned, combining titrimetric measurements with NUR data resulted in an improvement in parameter estimates related to the denitrification activity i.e. Y_{HNO3}, K_S, μ_{maxH} (see Table 8). Moreover the i_{NBM} parameter could also be

estimated with acceptable accuracy although its estimate is lower than the default value of ASM1. The first order time constant of titrimetric data, τ_{HP}, was observed to be low, 0.12 min on average (see Table 8). This implies there is almost no transient in the titrimetric data compared to the first order time constant, τ_{NO}, (ca 0.7 min) in the NUR measurements.

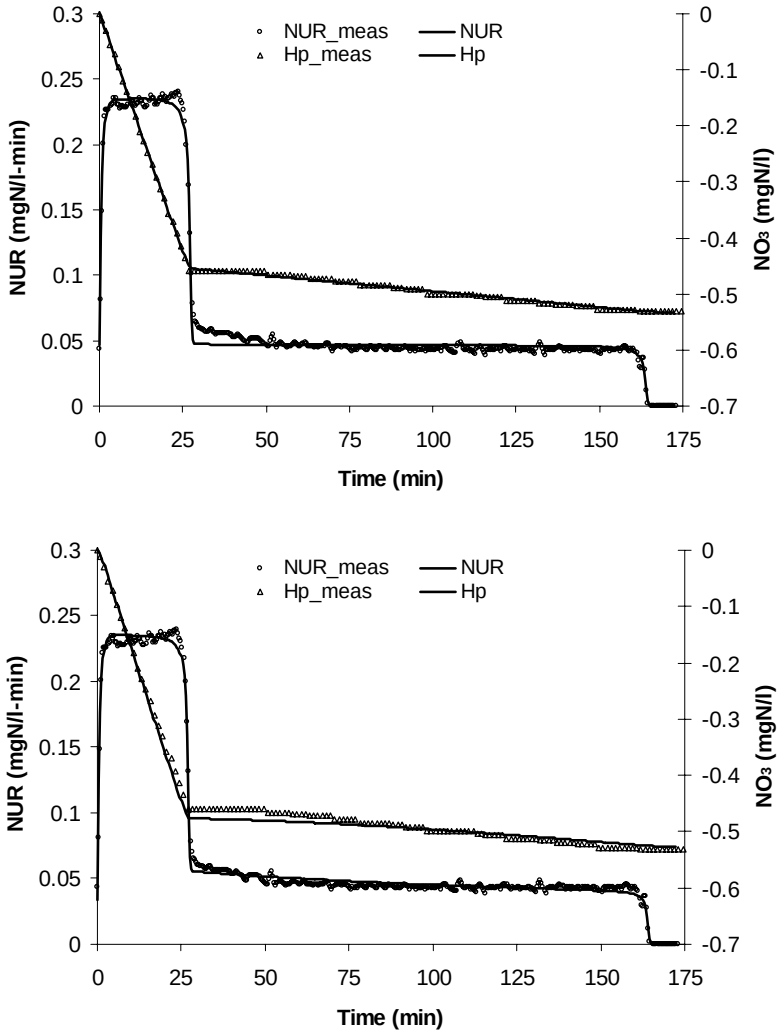

Figure 3. Model fits to combined NUR and titrimetric measurements in experiment A. ASM1e model (top) ASM3e model (down). Only every 15th data points is shown to keep the figure clear.

It is worthwhile to note that the confidence interval of the estimates of the dynamic CO_2 model parameters (K_La_{CO2}, C_{Tinit}) using only Hp data and using combined Hp and NUR data show significant differences (see Table 8). In other words, the confidence interval of the parameter estimates becomes remarkably larger when estimated on combined NUR and Hp data. This implies that they become practically unidentifiable. In contrast, the parameter estimates using only Hp data are quite good. This might be due to parameter correlations (particularly between the dynamic CO_2 model parameters and the denitrification parameters) that may exist during parameter estimation using combined NUR and Hp data. To better

understand and circumvent this problem, further research is required in the direction of the identifiability of both models under combined NUR and Hp data.

Table 8. Parameter estimation results with combined Hp and NUR measurements. Parameters in **Bold** are estimated* whereas the rest are either *fixed* or calculated (see text for explanation).

Parameter	ASM3e		ASM1e	
	Hp	Hp and NUR	Hp	Hp and NUR
$q_{MAX}(d^{-1})$	**2.40 (0.24%)**	**2.31 (0.06%)**	-	-
δ (mol/mol)	*1.96*	**1.94 (0.07%)**	-	-
f_{STO}	**0.30 (15.28%)**	**0.60 (0.16%)**	-	-
K_1	*0.048*	**0.047 (6.56%)**	-	-
K_2	*0.00089*	**0.00092 (3.31%)**	-	-
K_{NO3} (mgN/l)	*0.012*	**0.011 (3.60%)**	*0.016*	**0.016 (21.6%)**
K_S (mgCOD/l)	**0.99 (4.63%)**	**0.32 (2.06%)**	**0.12 (33.3%)**	**0.37 (2.24%)**
i_{NBM} (gN/gCOD)	**0.08 (1.4%)**	**0.11 (10.2%)**	**0.061 (0.42%)**	**0.06 (25.6%)**
K_La_{CO2} (d^{-1})	**1.20 (3.91%)**	**4.91 (24.9%)**	**3.8 (7.89%)**	**2.81 (145.6%)**
C_{Tinit} (mmol/l)	**0.93 (0.04%)**	**1.1 (78.1%)**	**1.1 (26.9%)**	**1.1 (212.3%)**
τ_{NO} (min)	*0.71*	**0.71 (36.9%)**	*0.73*	**0.74 (1.25%)**
τ_{HP} (min)	**0.03 (193.4%)**	**0.91 (256.7%)**	**0.063(33.7%)**	**0.18(16.8%)**
k_{STO} (d^{-1})	0.53	1.17	-	-
$\mu_{MAX,S}$ (d^{-1})	0.82	0.5	**1.50 (0.28%)**	**1.51 (0.22%)**
$\mu_{MAX,STO}$ (d^{-1})	0.82	0.5	-	-
b_H (d^{-1})	*0.17*	*0.17*	*0.239*	*0.239*
b_{STO} (d^{-1})	*0.17*	*0.17*	-	-
$X_H(0)$ (mgCOD/l)	1000	1000	1000	1000
$X_{STO}(0)$ (mgCOD/l)	8.17	8.17	-	-
$Y_{H,S}$	0.49	0.48	0.66	**0.66 (0.16%)**
$Y_{H,STO}$	0.62	0.61	-	-
Y_{STO}	0.74	0.74	-	-
SSE	**0.017**	**0.031**	**0.017**	**0.049**

*95 % confidence intervals of parameter estimates are given in the parenthesis as relative percentage of the corresponding parameter estimate.

During parameter estimation based on Hp data with ASM3e, the $X_{STO}(0)$, $X_H(0)$ and δ_n were fixed to the values determined using NUR measurements (see Table 7). It was observed, however, that the resulting parameter estimates for f_{STO} and growth rates based on only Hp data differed considerably from the parameter estimates obtained with combined NUR and Hp data (see Table 8). This could be due to parameter correlations as discussed below.

On the other hand, the parameter estimates related to denitrification activity (e.g. q_{MAX}, f_{STO}, δ_n K_S, K_{NO3}, K_1 and K_2) using combined NUR and Hp measurements were in close agreement with the parameter estimates obtained using NUR measurements (compare Table 7 and Table 8). However, the additional parameters determined using the information contained in the Hp data, particularly i_{NBM} and τ_{HP}, are observed to have physically not meaningful values and with a large confidence interval for τ_{HP} (which means it is practically not identifiable; see Table 8). The reason is suspected to be parameter correlations that may exist between the parameters of the titrimetric and biological models (see Table 4) as also observed above with the ASM1e model. It appears therefore that the titrimetric data under the famine phase are not sufficiently informative (e.g. compared to the information quality of NUR) to accurately estimate the titrimetric model parameters (see Figure 3). This is understandable from the observation that the titrimetric data during the famine phase did not show a typical non-linear CO_2 stripping trend as often observed in similar aerobic experiments (see Chapter 4.1). The underlying reason is quite obvious to be the surface mass transfer rate of CO_2, K_La_{CO2}. The value of K_La_{CO2} is low, e.g. in the order of 3 min (see Table 8) since no gas flow was sent through the mixed liquor.

Based on these observations, it is difficult to conclude that the additional titrimetric measurements are useful for the identifiability of ASM3e model, as it is partially the case for ASM1e (see above). Further research is clearly needed to improve the identifiability of the dynamic CO_2 model by designing experiments under different experimental conditions e.g. non-linear stripping of CO_2 with higher K_La_{CO2} (e.g. by N_2 sparging) similar to the conditions employed in aerobic experiments (see e.g. Chapter 4.1).

4.5 Adaptation of denitrifiers to pulse addition of substrate: effect of S_0/X_0

In this section, the NUR measurements obtained with consecutive substrate (acetate) additions to biomass B sampled from Ossemeersen WWTP are evaluated using the ASM3e model. Four acetate pulses were added consecutively to the activated sludge sample within a 12 hour period and the NUR obtained from the first pulse and the fourth acetate pulses are shown in Figure4-left and Figure4-right respectively.

The S_0/X_0 ratio was calculated using the initial biomass concentration estimated above using the endogenous NUR prior to substrate addition (see above-Table 7). In the fourth acetate pulse, S_0/X_0 was calculated by considering the previously added acetate to the reactor, i.e. S(0) in the fourth pulse was calculated as the total amount of acetate added (total amount of 4 additions) to the batch reactor.

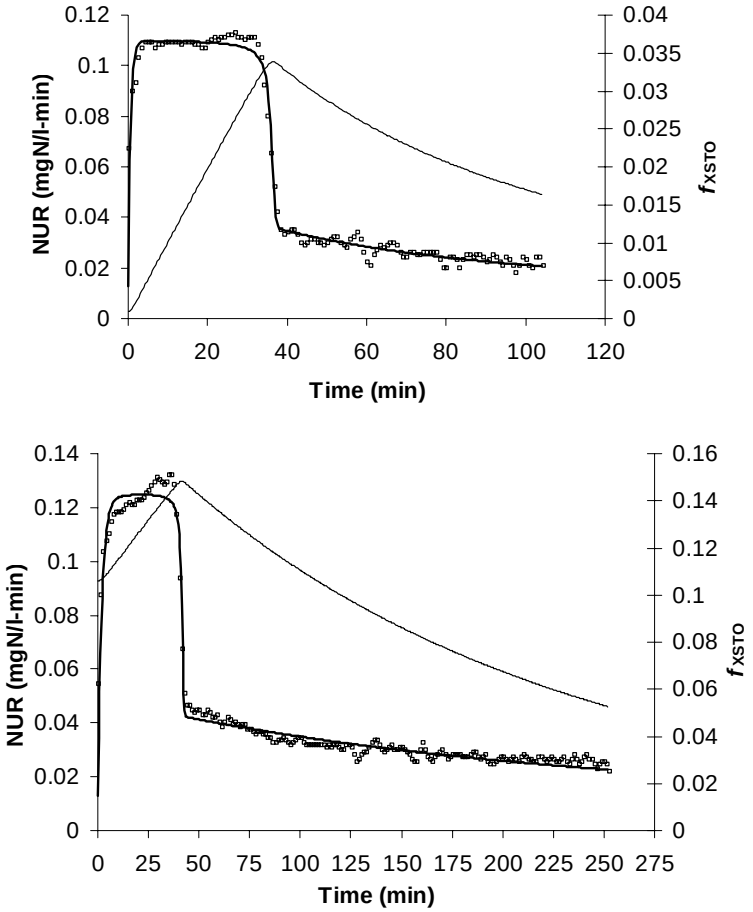

Figure 4. Model fit to experiment B (ASM3e) first pulse with 25 mgCOD/l where S/X = 0.06 (top) fourth pulse with 35 mgCOD/l where S/X =0.325 (down).

Model fits to the experimental data and the model prediction of the fraction of storage products of biomass are plotted in Figure 4. The model fits are observed to be good under both data sets. It is important to note that the initial fraction of storage products, $f_{XSTO}(0)$, predicted prior to the first acetate addition is around 0.16% i.e. 0.65 mgCOD/l as X_{STO} while it increased up to 37 mgCOD/l at the end of the three consecutive acetate pulses (in total 105 mgCOD/l added during a 7 hrs period). This increase in the storage content of biomass is expected since part of the substrate added (e.g. 60% average of Table 9) is diverted to the formation of storage products. Parameter estimation results with the NUR from the first and fourth acetate pulses are shown in Table 9.

The anoxic efficiency of oxidative phosphorylation, δ_n, is observed to remain the same in both pulses (see Table 9). This means also that the yield coefficients, Y_{STO}, $Y_{H,S}$ and $Y_{H,STO}$ remained the same since they are calculated using δ_n value (see Table 9). The fraction of substrate diverted to storage, f_{STO}, however, is observed to decrease from 0.64 to 0.56 whereas the maximum substrate uptake rate, q_{MAX}, increased by a factor 24% from 2.96 to 3.66 d^{-1}.

The maximum storage rate remained more or less unchanged (see Table 9) but the maximum growth rate of biomass increased by 50% (see Table 9). These results are discussed below.

Table 9. Parameter estimation results under low and high S_0/X_0 ratio. Parameters in **Bold** are estimated*, the rest are either *fixed* or calculated (see text for explanation).

	Nitrate Uptake Rate (NUR)	
Parameter	Pulse-1	Pulse-4
S/X (mgCOD/mgCOD)	0.06	0.35
$q_{MAX}(d^{-1})$	**2.96 (0.12%)**	**3.66 (0.41%)**
δ (mol/mol)	**1.99 (5.82%)**	**1.99 (2.61%)**
f_{STO}	**0.64 (9.97%)**	**0.56 (5.36%)**
K_1	**0.026 (57.3%)**	**0.018 (44.0%)**
K_2	**0.00077 (54.8%)**	**0.00040 (54.8%)**
K_{NO3} (mgN/l)	*0.012*	*0.012*
K_S (mgCOD/l)	**0.32 (10.1%)**	**0.29 (8.16%)**
k_{STO} (d^{-1})	1.42	1.53
$\mu_{MAX,S}$ (d^{-1})	0.52	0.80
$\mu_{MAX,STO}$ (d^{-1})	0.52	0.80
τ (d)	**0.63 (3.10%)**	**2.01 (3.37%)**
b_H (d^{-1})	*0.17*	*0.17*
b_{STO} (d^{-1})	*0.17*	*0.17*
$X_H(0)$ (mgCOD/l)	397	397
$X_{STO}(0)$ (mgCOD/l)	0.65	36.78
$Y_{H,S}$	0.49	0.49
$Y_{H,STO}$	0.62	0.62
Y_{STO}	0.75	0.75

*95 % confidence intervals of parameter estimates are given in the parenthesis as relative percentage of the corresponding parameter estimate.

5. DISCUSSION

5.1 Comparison of ASM1e with ASM3e: Biomass production and NUR

Prediction of biomass production is an important aspect in view of full-scale WWTP model applications. Biomass production of ASM1e and ASM3e models can be compared using the concept of yield coefficients as follows:

$$\frac{Y_{STO} \times Y_{H,STO}}{Y_{H,S}}$$

This ratio is calculated for experiment A and B to be 0.94 and 0.95 respectively. This means

ASM3e predicts a lower biomass production of about 5-6%. Simulations of biomass production during experiment A indeed show that ASM3e predicts a lower biomass production (see Figure 5). The difference is due to the fact that ASM3e diverts an important fraction of acetate -in this experiment it is 58%, to synthesis of PHB while the rest of the acetate is used for growth (see Figure 5). In ASM1e, the acetate is directly used for biomass production.

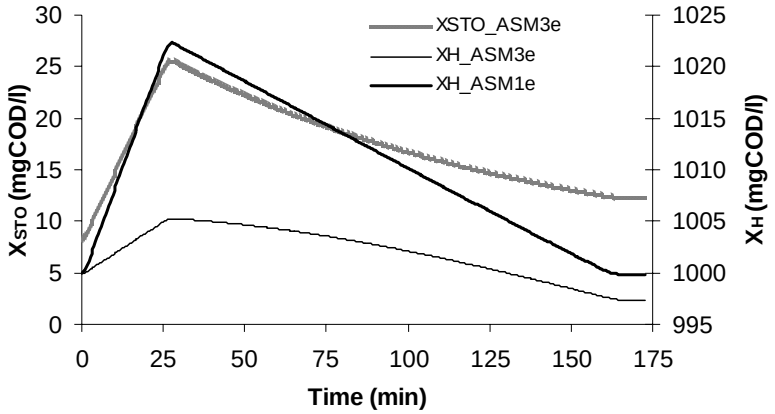

Figure 5. Model predictions of ASM1e and ASM3e for biomass production in experiment A

Another important difference between ASM1e and ASM3e can be observed in the modelling of the famine phase. In ASM1e biomass decays much faster compared to ASM3e to fit the increased NURend (see Figure 6-down). The difference between NURend predicted by ASM1e and the experimentally observed NURend (see dashed lines in Figure 6-down) is 40% for experiment A. This overestimation of the decay rate in ASM1e, therefore, partially explains the high value for the estimated anoxic growth yield in experiments A and B (see Table 7). Whereas in ASM3e direct growth on substrate is slower during the feast phase (see Figure 5), biomass continues to grow during the famine phase consuming additional nitrate (see Figure 6-top NUR_growth_sto). The net effect of secondary growth in ASM3e and decay of biomass during famine phase is a much slower decrease in biomass concentration compared to the biomass decay predicted by ASM1e (see Figure 5).

In ASM3e, consumption of nitrate during the feast phase is caused by growth and storage (see Figure 6-top). It is observed that the storage process consumes less nitrate (therefore energy) compared to the production of biomass (see Figure 6-top). This is, in fact, theoretically expected (Roels, 1983; van Loosdrecht and Heijnen, 2002). In the famine phase, nitrate is consumed by a secondary growth process on internal substrate, X_{STO}, and decay of biomass (see Figure 6-top). In this way, ASM3e is able to model the famine phase more mechanistically compared to ASM1e, which needs to overestimate the decay of biomass in order to fit the endogenous NUR. However, both the ASM1e and ASM3e models are able to successfully predict the overall NUR consumption by denitrifiers (see Figure 6-down). This is

a significant outcome supporting the validity of the ASM3e model for use in full-scale applications.

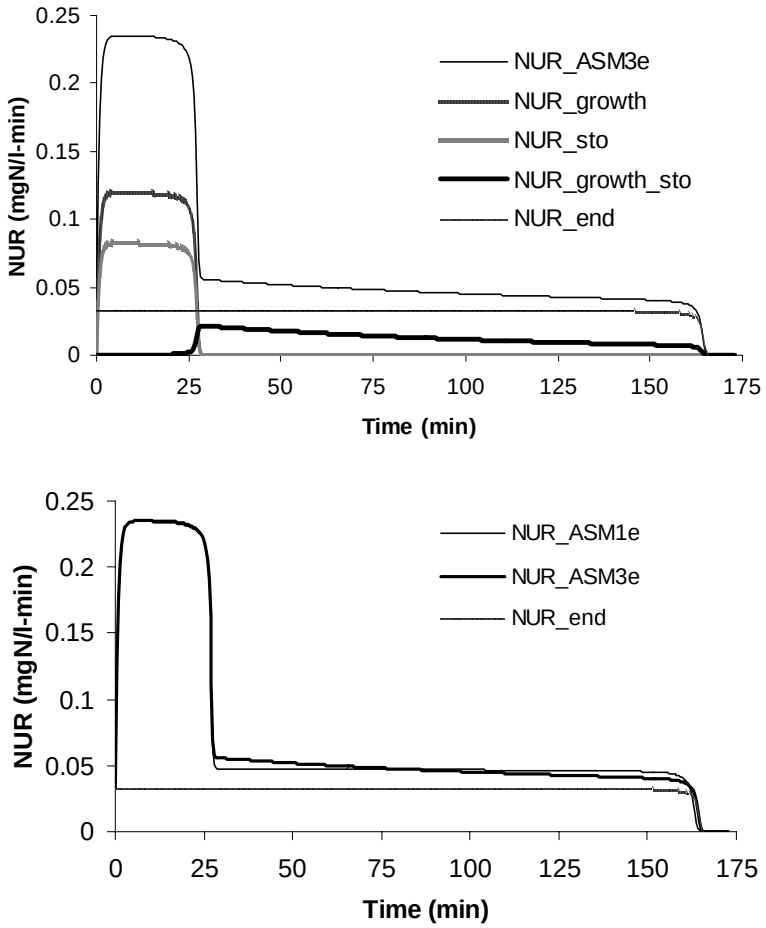

Figure 6. Prediction of contributions to the nitrate uptake rate (NUR) in ASM3e (top) and ASM1e (down) for experiment A.

5.2 Comparison of ASM1e and ASM3e: Parameter estimation results from NUR data

The ASM3e model successfully described the NUR data obtained from two different biomass samples (from pilot-scale SBR and full-scale WWTP, see Figure 2). The parameter estimation results for experiment A and B suggest that around 60% of the supplied acetate is used for the synthesis of storage PHB (see Table 7). Although this value is somewhat lower than the value reported in Beun *et al*. (2000b) which is 75%, the biomass studied here can be considered to exhibit a considerable storage capacity. The estimated anoxic yield coefficients were found to be close to the theoretically expected range (Heijnen and van Dijken, 1992). However, the anoxic efficiency of oxidative phosphorylation, δ_n, was found to be around 2 for both biomass samples. This is higher than the range reported in Beun *et al*. (2000b) which is 1.2±0.3. However, δ_n, is still in the range 1-3 mol/mol reported by Beun *et al*. (2000a&b) from Stouthamer (1988). Possible reason for this high estimate of δ_n could be the parameter correlations, which were shown to exist in a previous study (see Chapter 4.2.2). The existence

of parameter correlations means that several parameter combinations exist that give a good fit to the experimental observations despite the fact that one or more parameters may be assigned a mechanistically doubtful value.

The ASM3e model predicted ca 3 –4 times lower maximum growth rate for denitrifiers compared to the estimate of ASM1e (see Table 7). This is not surprising since both biomass samples used in this study was sampled from a system with an SRT equal to or longer than 10 days leading to biomass with low growth rates (van Loosdrecht and Heijnen, 2002). The reason for the difference between both models is simply that in ASM3e a fraction of substrate is channelled for storage in lieu of diverting all the substrate for growth. We expect that this lower value of the maximum growth rate for denitrifiers is closer to reality than the higher estimate of ASM1e.

Another important outcome of this study is the fact that the affinity constant of nitrate, K_{NO3}, could indeed be identified for both models (ASM1e and ASM3e) thanks to the high frequency and high quality NUR data obtained from a batch experiment where nitrate becomes the limiting substrate in the end of the experiment (see experiment A in Figure 2). The identifiability of the nitrate affinity constant on top of the affinity constant for acetate is also confirmed by the output sensitivity analysis of K_S and K_{NO3} (see Figure 7). The sensitivity function of K_S peaks around 25 minutes coinciding with the moment where acetate is completely taken up by the biomass. Although the sensitivity function of K_{NO3} displays a similar peak around 25 minutes, the most pronounced peak is observed around 160 min coinciding with the moment where nitrate is reduced completely by denitrifiers. At this peak, the sensitivity of K_S remains basically negligible.

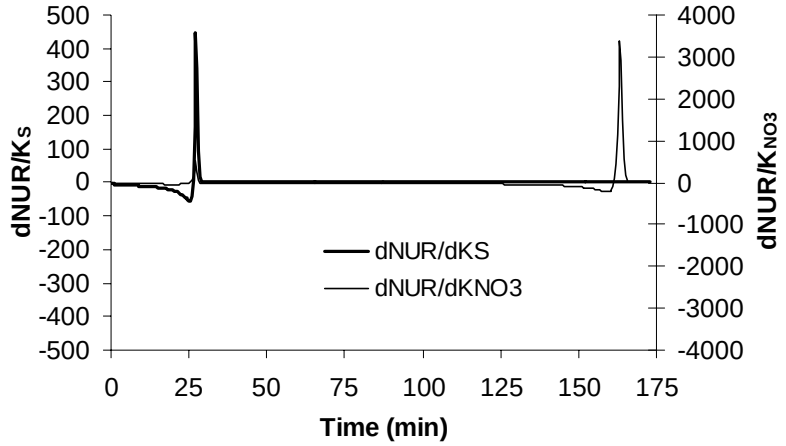

Figure 7. Output sensitivity function of K_S and K_{NO3} calculated for experiment A for the ASM1e model.

K_{NO3} is estimated to be around 0.015±0.005 mgN/l by both ASM1e and ASM3e models. This value is low compared to the default value proposed in the literature, which is in the order of

0.5 mgN/l (Henze *et al*., 2000; Wild *et al*., 1996). It is important to point to the frequency and accuracy of the nitrate measurements used here as they very much influence the quality of determination of the affinity constant in batch experiments. However, Betlach and Tiedje (1982) already reported that the estimate of K_{NO3} should at least be as low as 0.077±0.022 mgN/l. The low K_{NO3} values estimated in this study imply that the high values of K_{NO3} reported usually in full-scale model applications are probably required to compensate for diffusion limitations and or imperfect mixing conditions, which is very likely to occur in large tanks of full-scale WWTPs.

5.3 Modelling X_{STO} degradation during the famine phase

The degradation of X_{STO} during the famine phase is modelled using a second order model as already suggested by Dircks *et al*. (2001) for low storage content of biomass and employed successfully in the previous study (Chapter 4.2.2). The two parameters of this model are the affinity constant of biomass to f_{XSTO}, K_2, and K_1, a regulation constant controlling the degradation rate of X_{STO} (see chapter 4.2.2 for model development). These parameters were found to have large confidence intervals (see Table 7). Note that it was previously shown that K_1 and K_2 are both identifiable from respirometric measurements but with large correlations (Chapter 4.2.2). Similar observation was made in this study also.

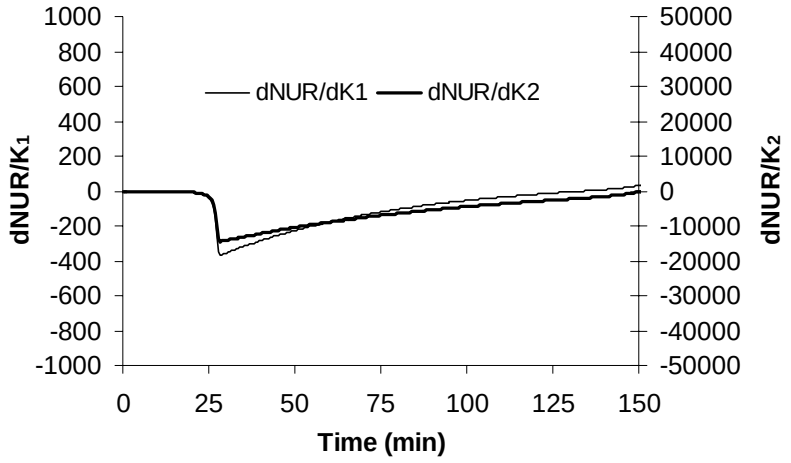

Figure 8. Output sensitivity functions of K_1 and K_2 (for experiment A)

The output sensitivity functions of K_1 and K_2 in Figure 8 show a close resemblance with each other, which explains the large correlation between these two parameters. Therefore, it is suggested to fix one of these parameters for future model applications. The affinity constant of biomass to X_{STO}, K_{STO}, is equal to K_2/K_1 (see model development Chapter 4.2.2). K_{STO} was found to range between 0.02 and 0.03 mgCOD/l in this study for biomass sampled from two different WWTPs. This range is quite close to the range found in Chapter 4.2.2 i.e. 0.01-0.02. Apparently, the affinity of biomass to X_{STO} (in this case PHB) is similar under aerobic and anoxic conditions but this is theoretically expected. Based on these results, it appears that the

parameter ratio, K_2/K_1, can be fixed to a certain value e.g. equal to the affinity of biomass to storage products. In this way, the endogenous tail of NUR can be fitted by fine-tuning *only* one of the two parameters, e.g. K_1 parameter. This approach will improve the confidence in parameter estimation.

5.4 Additional titrimetric measurements

Titrimetric models developed in this study (see Table 2&4 and Annex 1&2) were used to interpret the titrimetric data collected during denitrification experiments. Particularly the ASM1e model fitted the titrimetric data successfully. Moreover, the parameter estimation results showed that additional titrimetric measurements were indeed useful to improve the confidence intervals of the parameter estimates, particularly those related to the denitrification process (see Table 8). However, the parameters of the dynamic CO_2 model (K_La_{CO2} and C_{Tinit}) were observed to have large confidence intervals when estimated using combined NUR and Hp data (see Table 8). This might be due to the parameter correlation between titrimetric and biological model as aforementioned. This point requires further investigation, particularly the identifiability of the model under combined NUR and Hp data.

Nonetheless, the i_{NBM} parameter became identifiable when using combined nitrate and titrimetric measurements. Similar to Gernaey *et al*. (2002b), the i_{NBM} parameter was estimated to be 0.06, which is lower than the default value of ASM1, which is 0.086 mgN/mgCOD. The reason is explained above in Figure 5 where it was shown how ASM1e overestimates biomass production. Since in reality biomass production is probably less, the estimate of i_{NBM} will also be lower to compensate for this.

Although the first order time constant of Hp, τ_{HP}, was estimated with a large relative confidence interval, the estimated value is lower than the first order time constant observed in NUR, τ_{NO} (see Table 8 for ASM1e). These first order time constants were also observed to be different in combined OUR and titrimetric measurements (Gernaey *et al*., 2002b). The reason of this difference is hypothesised to be due to the metabolism of acetate at the cellular level (see Chapter 4.4). In other words, the substrate uptake is a process with faster dynamics (at the beginning of the substrate degradation pathway) compared to the nitrate uptake process (at the end of the substrate degradation pathway). These observations further support the hypothesis that the anoxic metabolism of substrate is quite similar to the aerobic metabolism (Beun *et al*., 2000a,b).

The ASM3e model could not be applied as successfully to the titrimetric data as ASM1e. For example f_{STO} was estimated to be 0.30. This is remarkably different than its estimate using NUR data (Table 7) and combined NUR and Hp data (see Table 8). Moreover, the i_{NBM} and τ_{HP} parameters were estimated to be 0.11 mgN/mgCOD and 0.9 min respectively (see Table

8), which makes it again difficult to claim any physical meaning for these parameters. An important issue related to these results is the identification of the dynamic CO_2 model included for the modelling of CO_2 stripping process as mentioned above. It becomes clear that particularly the Hp data during the famine phase do not contain sufficient information (dynamics) to accurately estimate the parameters of the titrimetric model (including the dynamic CO_2 model). A useful way to improve the identifiability of the model structure is to design better experimental conditions by using e.g. OED methodology, which is shown to be valuable in increasing the information content of the experimental data (see Chapter 4.2.2).

5.5 Effect of the S_0/X_0 ratio during anoxic batch experiments

The initial substrate to biomass ratio, S_0/X_0, is observed to impact the values of the kinetic parameters estimated from the NUR data obtained from batch experiments (see Table 9). It is important to mention that the S_0/X_0 was not observed to affect the estimate of the yield coefficients related to storage, Y_{STO}, direct growth, $Y_{H,S}$ and growth on storage, $Y_{H,STO}$ (see Table 9). The fraction of substrate diverted for storage, f_{STO}, however, is observed to decrease from 0.64 to 0.56 parallel to the increase in S_0/X_0 ratio. Further, the maximum substrate uptake rate, q_{MAX}, is increased by 24% from 2.96 to 3.66 d^{-1}. The maximum storage rate, k_{STO}, remained almost unchanged but the maximum growth rate of biomass increased by 50% parallel to the increase in S_0/X_0 ratio (see Table 9).

The finding that the maximum substrate uptake rate is increased while the maximum storage rate remained unchanged implies that the substrate flux, which becomes available for the synthesis of new biomass, is increased (see the simple steady-state substrate flux model in Chapter 4.2.2). Indeed, it is observed that the denitrifiers increased their maximum growth rate to make use of the increased availability of substrate in the medium (see Figure 9-left). In view of the physiological state of biomass (defined as the macromolecular composition of a cell at a given time (Grady *et al*., 1996)), it is possible that a culture undergoes adaptation to a new environment (physiological change induced by increased availability of acetate in this study) by regulating enzyme levels in the cell (Daigger and Grady, 1982; Roels, 1983; Chudoba *et al*., 1992; Grady *et al*., 1996; Vanrolleghem *et al*., 1998; van Loosdrecht and Heijnen, 2002). Although the ASM3e model does not contain expressions for changing enzymes levels in the biomass (see e.g. van Loosdrecht and Heijnen, 2002), it was nonetheless able to point out in which direction the adaptation on the physiological state of the biomass occurred. These findings are in accordance with the results obtained in studies dealing with the S_0/X_0 effect on parameter estimation using batch experiments (Chudoba *et al*., 1992; Grady *et al*., 1996; Sperandio and Paul, 2000). For instance, Chudoba *et al*. (1992) reported that at a low S_0/X_0 ratio in batch experiments, substrate is used mainly for the formation of internal polymers, while at high S_0/X_0 substrate is mainly used for the formation of new cells. This hypothesis was recently confirmed by Stasinakis *et al*. (2003).

The hypothesis of Chudoba *et al*. (1992) concerning the effect of S_0/X_0 on biomass during batch experiments is compared in Figure 9 with the hypothesis developed in this study. Chudoba and co-workers hypothesised that a mixed culture of microorganisms usually contains different bacterial species with different growth kinetics, which can be divided, for the sake of argument, into two main sub-groups: fast-growers versus slow-growers. The ratio of the concentration of these two groups in the biomass are determined by the operating parameters of the system they are sampled from, most important of all is the SRT. If the S_0/X_0 in a batch reactor is high, this will induce a substantial cell-multiplication which will lead to a change in the proportion of the slow growers over the fast growers in the batch reactor (see Figure 9-right). And the kinetic constants obtained under these circumstances will no longer represent the original system.

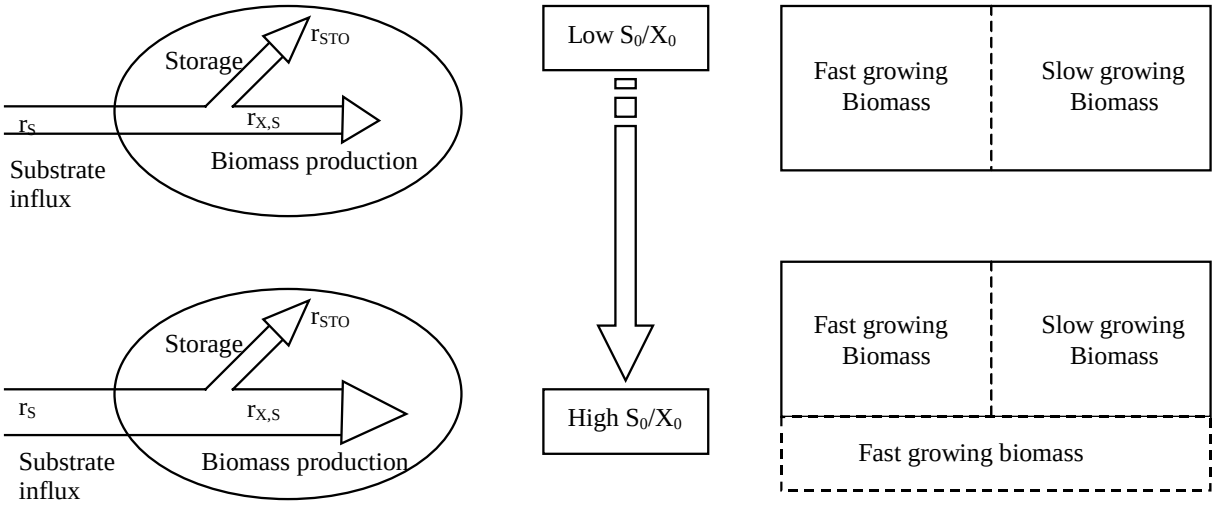

Figure 9. Effect of S_0/X_0 on biomass in batch experiments: comparison of the hypothesis developed in this study (left) with the hypothesis of Chudoba *et al*. (1992) (right).

The hypothesis developed in this study is complementary to the hypothesis of Chudoba *et al*. (1992), which deals with a time frame between 20 hrs and 120 hrs in batch reactors (substrate degradation ongoing). The hypothesis developed here deals with the observations in a batch reactor within a relatively shorter time, e.g. consecutive pulse addition of substrate within 7 hrs similar to the experiments performed in this study. At low S_0/X_0, a major fraction of the substrate will be channelled to storage (e.g. 60%) and the rest will be used for biomass production related activities. The fraction of the substrate flux used for storage is expected to be determined by the SRT (van Loosdrecht and Heijnen, 2002; Beun *et al*., 2002). As the level of S_0/X_0 increases in a batch reactor approaching to a critical level which can trigger/sustain substantial biomass production, biomass starts to increase its maximum substrate uptake rate and maximum growth rate while keeping the maximum storage rate unchanged (see Figure 9-left). In this way, the faster growing biomass will be favoured

instead of the slower biomass (the winner will be those that can consume most of the substrate). If this increase in S_0/X_0 is continued in a batch experiment (e.g. several consecutive pulse additions of substrate), it will eventually lead to a substantial change in the microbial populations as explained by the hypothesis of Chudoba *et al*. (1992) (Figure 9-right).

Furthermore, the results found in this section have two distinct consequences. First, from a calibration point of view, it is desirable to obtain parameter values representative for the system under study. This particular case shows that the S_0/X_0 ratio may influence the parameter estimation results remarkably leading to unrepresentative values of the system from which biomass was originally sampled. Based on this study, it is advised to keep the amount of substrate added in batch experiments as low as possible and maximum S_0/X_0 ratio should not exceed 0.1 throughout a batch experiment. Although there is an agreement in literature that this ratio should be kept low, there is no consensus on the magnitude of the value itself. For instance, Grady *et al*. (1996) advised a value around 0.025 to be low while a ratio of 20 is considered too high. Chudoba *et al*. (1992) advised a low S_0/X_0 ratio around 1 mgCOD-substrate/mg-biomass. Since this ratio is reported to depend on the history of the biomass culture, more research is needed before concluding for a common value.

Second, the results indicate that the biomass which was sampled from a full-scale WWTP indeed has a low growth rate. This means that the denitrification is indeed operated under sub-optimal conditions due to the limited availability of substrate, which was observed to quickly increase significantly upon pulse addition of substrate during a batch experiment (e.g. by 50% increase in growth rate see Table 9).

Finally, the ASM3 model was successfully extended to better describe the simultaneous storage and growth processes under anoxic conditions too. It is now possible to combine the model developed in Chapter 4.2.2 for aerobic conditions with the model developed here for anoxic conditions. The resulting model will describe both aerobic and anoxic activities of heterotrophs in nitrogen removing plants. It is expected that full-scale applications of these models warrant a better insight/understanding of the dynamics occurring in biological nitrogen removal plants. This can be used for optimisation of operation, upgrade and even design of new WWTPs.

6. CONCLUSION

A simultaneous storage and growth model (based on an extension of ASM3 which was developed in a previous study, see Chapter 4.2.2) was adapted to the denitrifying conditions and successfully applied to interpret NUR from batch experiments. The so-called ASM3e model was compared to the growth only based ASM1e model. The ASM3e model was found to lead to more realistic estimates for the yield coefficient for anoxic growth (0.49) than the

ASM1e model, which predicted a rather high value of about 0.66 for the anoxic growth yield. Moreover, the maximum growth rate of biomass predicted by ASM3e is 3-4 times lower than the growth rate estimated by ASM1e. This outcome was expected since ASM3e is based on the assumption of biomass that maximises substrate uptake in lieu of growth rate.

The ASM3e model was demonstrated to provide a better/detailed insight into the substrate removal mechanism under anoxic conditions. The model-based evaluation of the nitrate uptake rate showed that around 60% of the acetate was used for the synthesis of PHB while the rest is used for the production of new cells. The nitrate affinity constant, K_{NO3}, however, was estimated in the order of 0.015 mgN/l, which is low compared to the default values of ASM1 model. This discrepancy could be due to lumping of diffusion limitations occurring in full-scale WWTPs.

The S_0/X_0 in batch experiments was shown to remarkably influence the estimates of kinetic parameters whereas the estimate of yields was not affected. Based on the results of this study, it is hypothesised that at high S_0/X_0, biomass simultaneously increases its maximum substrate uptake and maximum growth rate while maintaining its maximum storage rate unchanged. This hypothesis is complementary to the hypothesis of Chudoba *et al*. (1992) that focuses on population changes. It is advised to keep the S_0/X_0 ratio below 0.1 mgCOD/mgCOD during anoxic batch experiments designed for calibration.

Finally, with the models developed in this study for anoxic conditions and in Chapter 4.2.2 for aerobic conditions, it is now possible to describe the entire activity of heterotrophs in BNR plants. Full-scale applications of this model warrants a better insight into the dynamics occurring in BNR plants which can be used for process design, optimisation and upgrade.

Annex 1. Determination of the stoichiometric coefficients of ASM1e that is extended with biological CO_2 and proton production

In this section, the extension of the ASM1 model to include biological CO_2 and proton production are presented. The CO_2 production and pH effect of each process included in ASM1e is evaluated in the following sub-sections. In order to make the model applicable for various cases, e.g. under different substrate type, storage product and biomass, the degree of reduction convention is used (Heijnen and van Dijken, 1992).

1. Anoxic growth of heterotrophs: Exogenous CO_2 production

CO_2 production resulting from the carbon metabolism of the heterotrophs under anoxic conditions using nitrate as e-acceptor can be obtained using the stoichiometry of the denitrification process.

$$\frac{1}{Y_{SX}}\mathrm{CH_yO_z}\ (mmol\text{-}C) + \frac{1}{5}\left(\gamma_x - \frac{\gamma_s}{Y_{SX}}\right)\ N\mathrm{O_3^-}\ (mmol\text{-}N) + c\mathrm{NH_3}\ (mmol\text{-}N) + \frac{1}{5}\left(\gamma_x - \frac{\gamma_s}{Y_{SX}}\right)\mathrm{H^+}$$

$$(mmol\ H^+) \rightarrow 1\mathrm{CH_aO_bN_c}\ (mmol\text{-}C) + \left(\frac{1}{Y_{SX}} - 1\right)\mathrm{CO_2}\ (mmol\text{-}C) + 0.5\frac{1}{5}\left(\gamma_x - \frac{\gamma_s}{Y_{SX}}\right)\mathrm{N_2}\ (mmol\text{-}N) + (\ldots)\ \mathrm{H_2O} \qquad (1)$$

The coefficient for CO_2 is worked out from the C-balance, while the coefficient for NO_3^- is obtained from the balance on degree of reduction known as the redox balance. The coefficient for H^+ is obtained from the charge balance, while the coefficient of water can be determined using e.g. the oxygen balance.

Converting units from mmol into mgCOD basis and then dividing both sides of Eq.1 with $8\gamma_x$ the stoichiometry of the denitrification process can be rearranged as follows:

$$\frac{\gamma_s}{\gamma_x Y_{SX}}\mathrm{CH_yO_z}\ \ (mgCOD)\ \ + \frac{14}{8*5}\left(1 - \frac{\gamma_s}{\gamma_x Y_{SX}}\right)\ \ N\mathrm{O_3^-}\ \ (mgN)\ \ +\ \ \frac{14c}{8\gamma_x}\mathrm{NH_3}\ \ (mgN)$$

$$+\frac{1}{8*5}\left(1 - \frac{\gamma_s}{\gamma_x Y_{SX}}\right)\mathrm{H^+}\ (mmol\text{-}H^+) \rightarrow 1\mathrm{CH_aO_bN_c}\ (mgCOD) + \left(\frac{1}{8\gamma_x Y_{SX}} - \frac{1}{8\gamma_x}\right)\mathrm{CO_2}\ (mmol\text{-}C)$$

$$+\ \frac{14}{8*5}\left(1 - \frac{\gamma_s}{\gamma_x Y_{SX}}\right)\mathrm{N_2}\ (mgN) + (\ldots)\ \mathrm{H_2O} \qquad (2)$$

The ASM models use a yield coefficient, $Y_{H,S}$, based on mgCOD/mgCOD basis, which is equal to:

$$\frac{1}{Y_{H,S}} = \frac{\gamma_s}{\gamma_x Y_{SX}}$$

Moreover, the nitrogen content of biomass, i_{NBM}, is by definition equal to $\frac{14c}{8\gamma_x}$. Using these definitions, Eq.2 can be rearranged as follows:

$$\frac{1}{Y_{H,S}} CH_yO_z\ (mgCOD) + \frac{1}{2.86}\left(1-\frac{1}{Y_{H,S}}\right) NO_3^-\ (mgN) + i_{NBM}\ NH_3\ (mgN) + \frac{1}{40}\left(1-\frac{1}{Y_{H,S}}\right) H^+$$

$$(mmol\text{-}H^+) \rightarrow 1X_H\ (mgCOD) + \left(\frac{1}{8\gamma_s Y_{H,S}} - \frac{1}{8\gamma_x}\right) CO_2\ (mmol\text{-}C) + \frac{1}{2.86}\left(1-\frac{1}{Y_{H,S}}\right) N_2\ (mgN) +$$

$$(\ldots)\ H_2O \qquad (3)$$

2. Endogenous decay of heterotrophs: endogenous CO_2 production:

In addition to the exogenous denitrification activity, anoxic endogenous respiration is the second significant source of CO_2 in the system. The endogenous respiration of biomass can be described as follows:

$$1\ CH_aO_bN_c\ (mmol\text{-}C) + \frac{\gamma_x}{5} NO_3^-\ (mmol\text{-}N) + \frac{\gamma_x}{5} H^+\ (mmol\text{-}H^+) \rightarrow CO_2\ (mmol\text{-}C) + (\ldots)\ H_2O$$

$$+ cNH_3\ (mmol\text{-}N) + 0.5\frac{\gamma_x}{5} N_2\ (mmol\text{-}N) \qquad (4)$$

Eq.5 can be rearranged by converting molar units into COD and dividing both sides of the equation by $8\gamma_x$:

$$1\ CH_aO_bN_c\ (mgCOD) + \frac{1}{2.86} NO_3^-\ (mgN) + \frac{1}{40} H^+\ (mmol\text{-}H^+) \rightarrow \frac{1}{8\gamma_x} CO_2\ (mmol\text{-}C) + (\ldots)$$

$$H_2O + i_{NBM}\ NH_3\ (mmol\text{-}N) + 2.86\ N_2\ (mgN) \qquad (5)$$

A relation between the endogenous nitrate uptake rate and the CO_2 production rate can be established using the stoichiometric coefficients of nitrate and CO_2:

$$CPR_{end} = \frac{5}{14\gamma_x} * NUR_{end} \qquad (6)$$

Annex 2. Determination of the stoichiometric coefficients of ASM3e

In this section, the pH effect of each process involved in ASM3e, i.e. storage of substrate, direct growth on substrate, growth on storage products, decay of storage products and decay of biomass is presented. Conservation balances of carbon, nitrogen, degree of reduction and charge are used to calculate the stoichiometric coefficients of the components following the convention of Heijnen and van Dijken (1992). In order to make the model applicable for various situations, substrate type, storage product and biomass types are described using degree of reduction convention (Heijnen and van Dijken, 1992).

1. Formation of storage products: External substrate (CHyOz) uptake for storage as CHpOq

Formation of storage products from a known a carbon source can be described as follows:

$$\frac{1}{Y_{STO,C}}\,CHyOz + x_1\,NO_3^- + z_1H^+ \rightarrow CHpOq + c_1\,CO_2 + d_1\,N_2 + (...)\,H_2O \quad \text{(mole basis)} \quad (7)$$

Performing carbon, nitrogen, degree of reduction and charge balances to determine the unknown coefficients leads to :

$$\frac{1}{Y_{STO,C}}\,CHyOz + \left(\gamma_{STO} - \frac{\gamma_S}{Y_{STO,C}}\right)\frac{1}{\gamma_{NO3}}\,NO_3^- + \left(\gamma_{STO} - \frac{\gamma_S}{Y_{STO,C}}\right)\frac{1}{\gamma_{NO3}}H^+ \rightarrow$$

$$CHpOq + \left(\frac{1}{Y_{STO,C}} - 1\right)CO_2 + \left(\gamma_{STO} - \frac{\gamma_S}{Y_{STO,C}}\right)\frac{1}{2\gamma_{NO3}}N_2 + (...)\,H_2O \quad (8)$$

Substrate, biomass and nitrogen are converted into COD basis:

$$\frac{8\gamma_S}{Y_{STO,C}}\,CHyOz + 14\left(\gamma_{STO} - \frac{\gamma_S}{Y_{STO,C}}\right)\frac{1}{\gamma_{NO3}}\,NO_3^- + \left(\gamma_{STO} - \frac{\gamma_S}{Y_{STO,C}}\right)\frac{1}{\gamma_{NO3}}H^+ \rightarrow$$

$$8\gamma_{STO}\,CHpOq + \left(\frac{1}{Y_{STO,C}} - 1\right)CO_2 + 28\left(\gamma_{STO} - \frac{\gamma_S}{Y_{STO,C}}\right)\frac{1}{2\gamma_{NO3}}N_2 + (...)\,H_2O \quad (9)$$

Both sides of Eq.9 are divided by $8\cdot\gamma_{STO}$ such that the stoichiometry can be written in reference to 1 g COD of storage product and the molar yield is replaced by a COD-based yield which is: $Y_{STO} = \frac{8\gamma_{STO}Y_{STO,C}}{8\gamma_S}$

and,

$$\frac{1}{Y_{STO}}\ \mathrm{CHyOz} + \frac{1-Y_{STO}}{2.86Y_{STO}}\ \mathrm{NO_3^-} + \left(\frac{1}{8\gamma_{NO3}} - \frac{1}{8\gamma_{NO3}Y_{STO}}\right)\mathrm{H^+} \rightarrow$$

$$\mathrm{CHpOq} + \left(\frac{1}{8\gamma_S Y_{STO}} - \frac{1}{8\gamma_{STO}}\right)\mathrm{CO_2} + \frac{1-Y_{STO}}{2.86Y_{STO}}\mathrm{N_2} + (...)\ \mathrm{H_2O} \qquad (10)$$

Example: The degree of reduction for acetate as substrate, γ_S, is 4, for nitrate, γ_{NO3}, is 5 and for PHB as storage product, γ_{STO}, 4.5. Moreover, assuming an anoxic storage yield of 0.75, the process stoichiometry becomes:

1.33 mgCOD $C_2H_4O_2$ + *0.12 mgN* NO_3^- *-0.0083 mmol* $H^+ \rightarrow$
1 mg COD $(CH_3O)_n$ + *0.014 mmol* CO_2 + *0.12 mgN* N_2 +(...) H_2O

According to the titrimetric model of Gernaey *et al*. (2002a), consumption of 1 mole acetate removes approximately 1 mole of protons at neutral pH (see model development). Then the pH effect of substrate uptake can be calculated to be: 1.33/64 = *0.021* mmol H^+/mgCOD-STO. where 64 is the g COD equivalent of 1 mole acetate.

Further, once the CO_2 produced inside the cell is excreted outside the cell, it will be readily dissociated into HCO_3^- and release approximately 1 mole of proton per mole of CO_2 at neutral pH (depending on pK1 and temperature, see Chapter 4.1). Then the pH effect of CO_2 production can be approximated as *0.014* mmol H^+/mgCOD-STO

The net pH effect of the production of 1 mgCOD PHB using acetate as carbon source can be calculated by summing all pH affecting processes:

proton balance = -0.021 – 0.0083 + 0.014 = *-0.015* mmol H^+/mgCOD PHB.

This means that formation of storage products (PHB in this case) from acetate has a proton consumption effect.

2. Anoxic growth of biomass (ChaObNc) on external substrate (CHzOy):
The anoxic growth of biomass can be described as follows:

$$\frac{1}{Y_{H,C}}\ \mathrm{CHyOz} + x_2\ \mathrm{NO_3^-} + y_2\ \mathrm{NH_3} + z_2\mathrm{H^+} \rightarrow \mathrm{CHaObNc} + c_2\ \mathrm{CO_2} + d_2\ \mathrm{N_2} + (...)\ \mathrm{H_2O}\ \ \text{(mole)} \qquad (11)$$

Performing carbon, nitrogen, degree of reduction and charge balances to determine the unknown coefficients (as above) and converting the mole unit into mass units (similar to above) leads to:

$$\frac{1}{Y_{H,S}}\ \mathrm{CHyOz} + \frac{1-Y_{H,S}}{2.86Y_{H,S}}\ \mathrm{NO_3^-} + i_{NBM}\mathrm{NH_3} + \left(\frac{1}{8\gamma_{NO3}} - \frac{1}{8\gamma_{NO3}Y_{H,S}}\right)\mathrm{H^+} \rightarrow$$

$$\mathrm{CHaObNc} + \left(\frac{1}{8\gamma_S Y_{H,S}} - \frac{1}{8\gamma_X}\right)\mathrm{CO_2} + \frac{1-Y_{H,S}}{2.86Y_{H,S}}\mathrm{N_2} + (...)\ \mathrm{H_2O} \qquad (12)$$

Example: The degree of reduction for acetate as substrate, γ_S, is 4, for nitrate, γ_{NO3}, is 5 and for biomass, γ_X, 4.2. Moreover, assuming an anoxic growth yield of 0.63, the process stoichiometry becomes:

1.587 mgCOD $C_2H_4O_2$ + *0.205 mgN* NO_3^- *+0.07 mgN* NH_3 *-0.015 mmol* $H^+ \rightarrow$
1 mg COD CHaObNc + *0.02 mmol* CO_2 + *0.205 mgN* N_2 +(...) H_2O

The pH effect of acetate uptake and CO_2 production can be calculated using the aforementioned assumptions:

pH effect of acetate uptake: 1.587/64 = *-0.025* mmol H^+/mgCOD-X
pH effect of CO_2 production: *0.02* mmol H^+/mgCOD-X

Assuming also that uptake of NH_3 for growth will release approximately 1 mole of H^+ per mole of NH_3 at neutral pH (see model development): 0.07/14 = +0.005 mmol H^+/mgCOD-X

The pH effect of the anoxic growth using acetate as carbon source can then be calculated by summing up all pH influencing sub-processes:

The net proton balance: – 0.025 – 0.015 + 0.005 + 0.02 = *-0.015* mmol H^+/mgCOD biomass

Similar to the anoxic storage process, the pH effect of the growth of denitrifiers is proton consumption.

3. Anoxic growth of biomass (CHaObNc) on storage product (CHpOq)
The indirect growth of biomass on storage products under anoxic conditions is described by:

$$\frac{1}{Y_{H,STO,C}}\,CHpOq + x_3NO_3^- + y_3NH_3 + z_3H^+ \rightarrow CHaObNc + c_3CO_2 + d_3N_2 + (...)H_2O \text{ (mole)} \quad (13)$$

Performing carbon, degree of reduction and charge balances to determine the unknown coefficients (as above) and converting the mole unit into mass units (similar to above) leads to:

$$\frac{1}{Y_{H,STO}}\,CHpOq + \frac{1-Y_{H,STO}}{2.86Y_{H,STO}}\,NO_3^- + i_{NBM}NH_3 + \left(\frac{1}{8\gamma_{NO3}} - \frac{1}{8\gamma_{NO3}Y_{H,STO}}\right)H^+ \rightarrow$$

$$CHaObNc + \left(\frac{1}{8\gamma_{STO}Y_{H,STO}} - \frac{1}{8\gamma_X}\right)CO_2 + \frac{1-Y_{H,STO}}{2.86Y_{H,STO}}\,N_2 + (...)\,H_2O \quad (14)$$

Example: The degree of reduction for PHB as substrate, γ_{STO}, is 4.5, for nitrate, γ_{NO3}, is 5 and for biomass, γ_X, 4.2. Moreover, assuming an anoxic growth yield on storage of 0.70, the process stoichiometry becomes:

1.43 mgCOD $(CH_3O)_n$ + *0.15 mgN* NO_3^- *+0.07 mgN* NH_3 *-0.0011 mmol* $H^+ \rightarrow$
1 mg COD CHaObNc + *0.0099 mmol* CO_2 + *0.15 mgN* N_2 +(...) H_2O

The pH effect of CO_2 production and NH_3 uptake for growth can be calculated using the aforementioned assumptions:

pH effect of CO_2 production: *0.0099* mmol H^+/mgCOD-X
pH effect of NH_3 uptake: 0.07/14 = *0.005* mmol H^+/mgCOD-X

The pH effect of the secondary growth of denitrifiers on storage products (PHB) can be calculated by summing up all sub-processes involved:

Then net proton balance: – 0.00107 + 0.005 + 0.0099 = *0.014* mmol H^+/mgCOD-X

This means that the anoxic growth on storage products has a proton production effect. This is contrary to the pH effect of storage and direct growth using acetate (see above).

4. Endogenous respiration of storage products, X_{STO}:
The endogenous respiration of X_{STO} can be described as follows:

$$CHpOq + x_4\,NO_3^- + z_4\,H^+ \rightarrow c_4\,CO_2 + d_4\,N_2 + (...)\,H_2O \quad (15)$$

Performing degree of reduction, nitrogen, carbon and charge balances on mole basis, gives the following:

$$CHpOq + \frac{\gamma_{STO}}{\gamma_{NO3}} NO_3^- + \frac{\gamma_{STO}}{\gamma_{NO3}} H^+ \rightarrow CO_2 + \frac{1}{2} \cdot \frac{\gamma_{STO}}{\gamma_{NO3}} N_2 + (...) H_2O \quad (16)$$

Converting from a molar basis to a mass basis (however the unit of CO_2 is kept at a molar basis), results in the following:

$$8 \cdot \gamma_{STO} \cdot CHpOq + 14 \cdot \frac{\gamma_{STO}}{\gamma_{NO3}} NO_3^- + \frac{\gamma_{STO}}{\gamma_{NO3}} H^+ \rightarrow CO_2 + 28 \cdot \frac{1}{2} \cdot \frac{\gamma_{STO}}{\gamma_{NO3}} N_2 + (...) H_2O \quad (17)$$

Dividing both sides of the equation by $8\gamma_{sto}$, leads to:

$$CHpOq\ (mgCOD) + \frac{14}{8\gamma_{NO3}}\ (mgN)\ NO_3^- + \frac{1}{8\gamma_{NO3}} H^+(mmol) \rightarrow \frac{1}{8\gamma_{STO}} CO_2\ (mmol) + \frac{14}{8\gamma_{NO3}} N_2 + (...) H_2O \quad (18)$$

Using the above-mentioned values for the degree of reduction, the stoichiometric coefficient for the decay of storage products can be calculated as follows:

$$CHpOq\ (mgCOD) + \frac{1}{2.86}\ (mgN)\ NO_3^- + \frac{1}{40} H^+(mmol) \rightarrow \frac{1}{36} CO_2\ (mmol) + \frac{1}{2.86} N_2 + (...) H_2 \quad (19)$$

This means that the endogenous decay of storage products has a very small effect on pH (*+0.0028* $meqH^+$/ $mgCOD\text{-}_{STO}$). Considering the fact that decay of the storage products is relatively slow, it can be concluded that this process has almost no effect on the pH of the medium.

5. Anoxic endogenous respiration of biomass:

The endogenous respiration of the biomass can be described as follows:

$$1\ CH_aO_bN_c\ \textit{(mmol-C)} + \frac{\gamma_X}{5} NO_3^-\ \textit{(mmolN)} + \frac{\gamma_X}{5} H^+\ (mmol\text{-}H^+) \rightarrow CO_2\ \textit{(mmol-C)} + (\ldots) H_2O + cNH_3\ \textit{(mmol-N)} + 0.5\frac{\gamma_X}{5} N_2\ \textit{(mmol-N)} \quad (20)$$

Eq.20 is rearranged by converting the molar units into COD units and dividing both sides of the equation by $8\gamma_x$, as follows:

$$1\ CH_aO_bN_c\ \textit{(mgCOD)} + \frac{1}{2.86} NO_3^-\ \textit{(mgN)} + \frac{1}{40} H^+\ (\text{mmol-}H^+) \rightarrow \frac{1}{8\gamma_x} CO_2\ \textit{(mmol-C)} + (\ldots)$$

$$H_2O + i_{NBM}\ NH_3\ \textit{(mgN)} + 2.86\ N_2\ \textit{(mgN)} \qquad (21)$$

The proton balance of the anoxic decay of biomass (considering CO_2 production, release of nitrogen and uptake of nitrate) is *-0.0014* $meqH^+/mgCOD\text{-}X_H$, assuming the degree of reduction of biomass is 4.2 and the i_{NBM} is 0.086 mgN/mgCOD. Since the decay of biomass is relatively slow, the anoxic decay of biomass is not expected to contribute significantly to the proton consumption in the medium.

Chapter 4.4

Transient response of aerobic and anoxic activated sludge activities to sudden substrate concentration changes

ABSTRACT

The state of the art understanding of activated sludge processes as summarized in the activated sludge models (ASM) of Henze *et al.* (2000) predicts an instantaneous increase in the biomass activity (which is measured e.g. by the corresponding respiration rate OUR, NUR, etc…) under sudden substrate concentration changes. Experimental data (e.g. short-term batch respiration experiments under aerobic or anoxic conditions) collected for the calibration of the dynamic models (ASM) often exhibit a transient phenomenon while attaining the maximum activity which can not be explained by the current understanding of the activated sludge process. That transient phenomenon exhibits itself immediately upon addition of a substrate source to an endogenously respiring activated sludge sample and it usually takes a few minutes until the activated sludge reaches its maximum possible rate under given environmental conditions. This discrepancy between the state of the art model and the experimental data is addressed in detail in this contribution. Among the hypotheses proposed, it appears that this transient response of the activated sludge is most likely resulting from the sequence of intracellular reactions involved in the substrate degradation by the activated sludge. Results from studies performed elsewhere with pure cultures (*S. cerevisae* and *E. coli*) support the hypothesis. The transient phenomenon can be described by a dynamic metabolic network model such as the one proposed by Chassagnole *et al.* (2002) or by a simple first order model as adopted in this study. The transient phenomenon occurring in short-term batch respiration experiments is shown to interfere severely with parameter estimation if not modelled properly (2.8 %, 11.5% and 16.8% relative errors (average of 3 experiments) on Y_H, μ_{maxH} and K_S respectively). Proper modelling of this transient phenomenon whose time constant is in the order of minutes (1 –3 min) is expected to contribute fundamentally to a better understanding and modelling of ORBAL, carrousel and SBR type treatment plants with fast-alternating process conditions, but such study is beyond the scope of the current contribution.

This chapter is published as:
Vanrolleghem P.A., Sin G. and Gernaey K. (2004) Transient response of aerobic and anoxic activated sludge activities to sudden concentration changes. *Biotechnol. Bioeng.*, 86: 277-290.

1. INTRODUCTION

Short-term batch substrate degradation experiments, usually initiated by pulse substrate additions to activated sludge that was previously sampled from a full-scale plant, are often used in the frame of full-scale wastewater treatment plant (WWTP) model calibrations. Such experiments produce data that are sufficiently informative for estimating kinetic and/or stoichiometric parameters of the activated sludge (Vanrolleghem *et al.*, 1995, 1999). Biomass oxygen uptake rates (OUR), ammonium uptake rates (AUR), nitrate uptake rates (NUR), or biomass proton production rates (HpR) are examples of data sets that most often result from the batch experiments. An overview of available methodologies for data collection can be found in Vanrolleghem *et al.* (1999) and Petersen *et al.* (2003a). The data, representing the response of the activated sludge sample to a pulse substrate addition, are often interpreted using a model, i.e. the model is fitted to the data by modifying the values of kinetic and/or stoichiometric model parameters. The resulting parameters are subsequently transferred to the full-scale plant model and combined with others (Petersen *et al.*, 2002b).

In this study, it will first be shown that the experimental observations during a short-term batch substrate degradation experiment following a pulse substrate addition do not correspond to the expectations based on the state of the art activated sludge models. A transient initial response is often observed in the experimental data that is not accounted for by the activated sludge models. The main objective of this paper is to investigate, understand and mathematically describe the underlying mechanisms for this experimentally observed transient response, because it bears a major limitation regarding the applicability of short-term batch experiments with activated sludge in dynamic model calibration procedures. After describing the nature of the observed phenomena, several hypotheses will be formulated to explain the experimental observations. In view of the experimental results, the importance of a correct understanding and modelling of the dynamic transient response phenomenon will be highlighted not only for the interpretation of the short term calibration experiments but also for the modelling of the full-scale WWTP.

2. PROBLEM STATEMENT

Note that from here on, the term “batch experiment” will be used to indicate short-term (e.g. between 15 – 60 min) batch substrate degradation experiments with activated sludge following a pulse substrate addition. In the following paragraphs the state of the art activated sludge models and typical experimental data obtained from batch experiments will be introduced. The problem statement will originate from the confrontation of these models with the data.

2.1 Expected activated sludge response to sudden concentration changes: The state of the art description

Simulation of full-scale WWTPs as well as interpretation of experimental results from batch experiments is based on the state of the art understanding of activated sludge behaviour, which is summarized in the Activated Sludge Models (ASM) (Henze *et al.*, 2000). For a batch experiment with a pulse substrate addition, the models (see Table 1) predict an instantaneous increase in the biomass activity (Figure 1). The activated sludge is in endogenous state at t = 0, and according to the model the biomass reacts to the pulse substrate addition with an immediate increase of the OUR to a maximum level of 0.83 mg O_2/l.min, indicating that the substrate is immediately metabolized at the maximum rate.

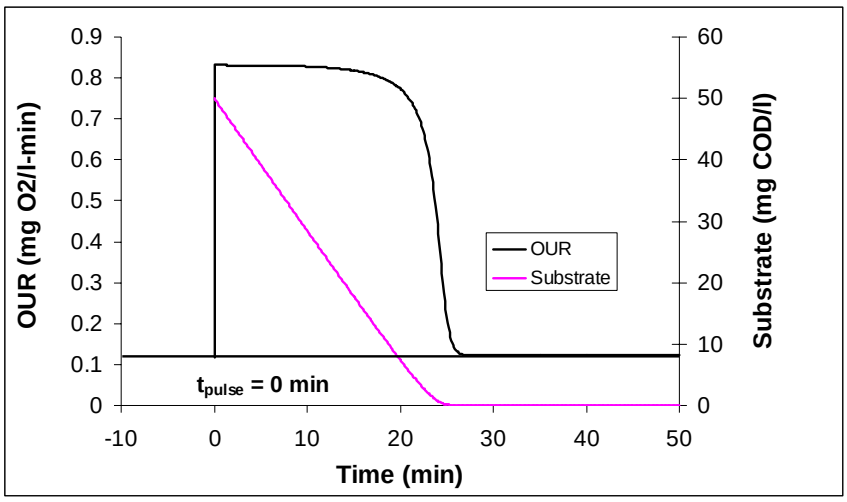

Figure 1. Simulation of activated sludge response to a pulse addition of readily biodegradable substrate in a batch reactor based on ASM1 (Henze *et al.*, 2000). The following parameters were used in the simulation: $S_S(0)$ = 50 mg COD/l; Y_H = 0.67 mg COD/mg COD, $\mu_{maxH}*X_H$ = 1.5 mg COD/l.min, K_S = 1 mg COD/l and b_H = 0.00015 1/min..

2.2 Experimental observation of activated sludge response to sudden concentration changes: Reality

A clear discrepancy between model predictions (Figure 1) and the experimental response obtained in a batch experiment can be observed during the first minutes of the experiment. Indeed, the OUR in Figure 2 shows a clear transient response following the pulse acetate addition. Note that the transient response to a pulse substrate addition can only be observed on condition that the data acquisition frequency is in the order of seconds. In the work of Orhon *et al.* (1995) for example, an OUR sampling interval of 10 minutes did not allow to observe the transient phenomenon in the OUR profiles, although a similar experimental design was used as for the experiment in Figure 2.

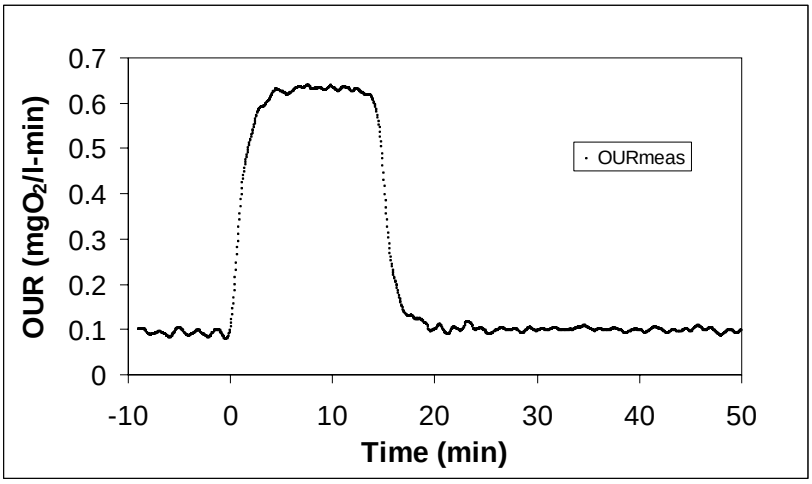

Figure 2. Typical activated sludge response to acetate addition (30.32 mg COD/l acetate) in batch experiments. The maximum OUR is reached after a transient period.

2.3 The discrepancy between model and data is a more general phenomenon

The observation of the transient response during batch experiments is not limited to the data presented in this paper. In many cases, published data show similar phenomena (Spanjers and Vanrolleghem, 1995; Kong *et al.*, 1996; Spérandio and Paul, 1997; Strotmann *et al.*, 1999; Ning *et al.*, 2000; Ficara *et al.*, 2000). In these papers, however, the transient phenomenon did not receive any attention and was neglected during the interpretation of the data. In some studies the author(s) apparently preferred to present only that particular part of the OUR data that can be explained with Monod kinetics (e.g. Vanrolleghem *et al.*, 1995), whereas the initial part of the data including the transient phenomenon is not shown.

Observations of the transient phenomenon are not limited to heterotrophic substrate degradation processes under aerobic conditions. The transient response was also observed for respirometric experiments with nitrifying biomass (Spanjers and Vanrolleghem, 1995; Ficara *et al.*, 2000; Gernaey *et al.*, 2001a). Furthermore the transient phenomenon was also observed in anoxic experiments with heterotrophic biomass (see Chapter 3.1; Chapter 3.2 and Chapter 4.3).

Observing the transient phenomenon is not limited to OUR data based on DO electrodes. OUR data can be extracted from off-gas oxygen measurements too. Pratt *et al.* (2002) argued that the transient phenomenon in their data might be due to the lag-time of the off-gas measurement system, but did not test this hypothesis in detail. A transient phenomenon was also present in the OUR profiles reported by Tusseau-Vuillemin *et al.* (2002), who measured the OUR using two different respirometric methods: titrimetric addition of H_2O_2 versus aeration in batch reactors. Again no assessment of the behavior was conducted.

The examples suggest that the transient phenomenon occurs in every experiment with pulse substrate additions to activated sludge. The measurement frequency during respirometric measurements is very important, since the transient phenomenon is fast with a time constant in the order of 1 – 3 minutes. Thus, although it is expected that the transient response occurs in most respirometric assays, it can only be detected in set-ups with a sufficiently high measurement frequency.

3. MATERIALS AND METHODS

Most of the data presented in this study were obtained using the RODTOX sensor (Vanrolleghem *et al.*, 1994). The RODTOX (Kelma bvba, Niel, Belgium) is a batch respirometer. The reactor vessel, filled with 10 litres of activated sludge, is constantly aerated, stirred and thermostated. In the cover of the bioreactor, dissolved oxygen (DO) and pH probes are installed. Two different types of Endress and Hauser DO electrodes were used during the investigation, i.e. the Conducta 905 and the Conducta 905 S.

Some data were obtained with the combined respirometric-titrimetric sensor (Gernaey *et al.*, 2001a), which allows measurement of combined OUR and HpR data. Data sets under anoxic conditions were collected using the integrated sensor developed in Chapter 3.1, which allows measurement of combined NUR and HpR data. An explanation of the operating principles of these sensors is not essential for the message of this paper. Basically, both sensors allow to obtain data that are similar to the data of the RODTOX sensor.

Simulations were performed using WEST® (Hemmis) a dedicated software for WWTP modelling (Vanhooren *et al*., 2003). The mathematical model is based on the ASM1 model structure (Henze *et al*., 2000), unless explicitly specified otherwise.

4. RESULTS

The experimental set-up, a physico-chemical phenomenon or insufficient description of the biological response with the model used for interpretation of the experimental data could all be reasons for the observed discrepancy between model predictions (Figure 1) and experimental observations obtained from batch experiments (Figure 2). Below, it will be attempted to answer the following question: “Is the observed discrepancy due to an error or misinterpretation of the experimental data, is it due to a physico-chemical phenomenon or is it a modelling error?”

4.1 Analysis of experimental set-up and data

The following properties of the experimental set-up may contribute significantly to the observed transient phenomenon (Figure 2):

a. Dynamics of the DO electrodes

b. Mixing characteristics of the experimental set-up

Each of these hypothetical explanations of the transient will be assessed in the frame of its potential contribution to the observed discrepancy between model predictions and experimental data.

4.1.1 Dynamics of the dissolved oxygen electrode

The dynamics of DO electrodes have been described most often as a first order process with time constants between 5 and 100 seconds (Lee & Tsao, 1979). Knowing the DO electrode model (Eq. 1) and its experimentally determined parameter τ, the actual DO concentration S_O can be retrieved from the electrode output E.

$$\frac{dE}{dt} = \frac{1}{\tau}(S_O - E) \qquad (1)$$

In Eq. 1, S_O is the true DO concentration in the liquid phase (mg O_2/l), E is the DO concentration measured by the DO electrode, and τ is the experimentally determined first order time constant of the DO electrode.

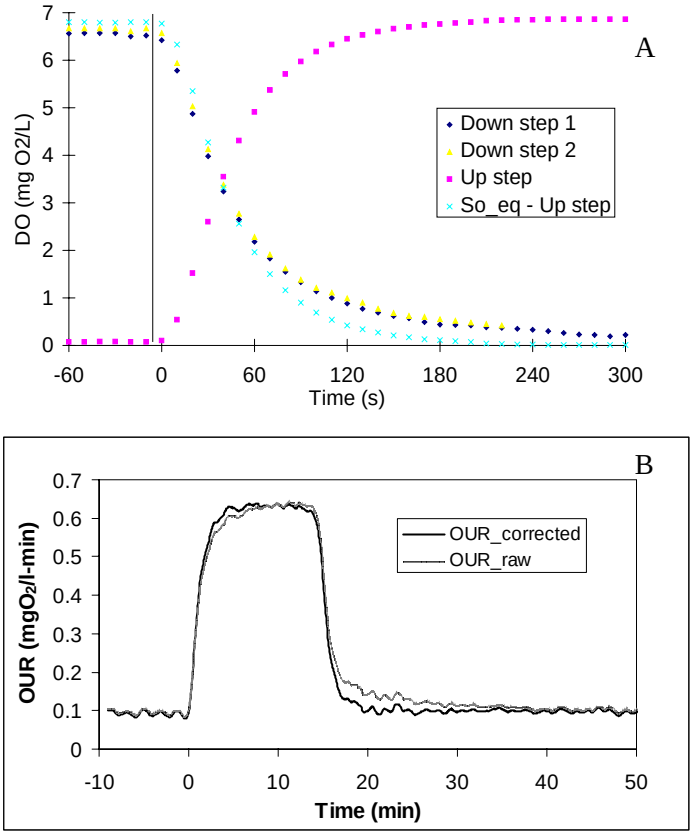

Figure 3. Typical up- and down step responses of DO-electrodes (Conducta 905, E+H) (A) Comparison of OUR corrected (solid line) and OUR_raw not corrected (dashed line) for the response time constant of the DO probe dynamics (B).

Up-step responses of the DO electrode have been recorded applying an experimental approach as described by Philichi & Stenstrom (1989). The down-step response of the DO electrodes was measured in the same set-up, but this time the electrode is removed from the reactor containing water saturated with oxygen and inserted into deoxygenated water. Figure 3A shows the response (both up-step and down-step) for the Conducta 905 electrode. Because both S_O and E are known in the experiment, the data allow determination of the first order time constant τ (see Eq. 1). For the Conducta 905 electrode the value of τ was 55 s, while for the Conducta 905S it was 12.5 s.

It is apparent that the time constant of DO electrodes has to be taken into account to appropriately model the dynamics of batch experiments. In addition, attention must be paid to noise elimination (Chapter 3.1), since taking derivatives during the OUR calculation enhances the effect of noise. Applying this probe model (Eq. 1), it was found that the electrode dynamics are only partially explaining the transient phenomenon (see Figure 3B). Yet, it is important to stress that the DO probe dynamics should be taken into account properly (e.g. by applying Eq.1) while calculating the OUR in any experimental set-up. In this study, the OUR values were always corrected for the response time of the DO probes.

4.1.2 Mixing characteristics in batch reactors (verification of the CSTR assumption)

The transient phenomenon in the data (Figure 2) could be the consequence of insufficient mixing. A colorimetric method was used to evaluate the mixing characteristics of the reactor vessel. Phenolphthalein was added to the RODTOX vessel filled with 10 liters of water. Addition of an excess base causes the colour of the phenolphthalein to immediately change from colourless to violet. Samples were taken automatically every 2 seconds in the reactor at a location close to the DO electrode. The colour intensity was analysed using spectrophotometry. Two series of mixing experiments were performed: one series with stirring and aeration on (aeration intensity 15 l/min.) and another series with stirring but no aeration (Figure 4). The degree of mixing, *m*, is used in this study to quantitatively describe the tracer experiments (Nielsen *et al.*, 2003):

$$m = \frac{s(t) - s(0)}{s_\infty - s(0)} \qquad (2)$$

Where *s(t)* is the concentration of the tracer at time *t* (in this case it is the phenolphthalein concentration measured indirectly as color intensity), *s(0)* is the initial concentration of the tracer and s_∞ is the concentration as time approaches to infinity where *m* becomes 1. The *mixing time*, t_m is defined as the time needed to reach a value of *m* equal to 95%. The mixing time is about 10 s in case of stirring only. With aeration the mixing is very fast, as the sample taken after 2 seconds already shows the final concentration. Hence, it can be concluded that

mixing of the substrate injected in the aerated batch reactor occurred significantly faster than the transient phenomenon observed in the experimental data. Thus, improper mixing does not contribute significantly to the transient phenomenon.

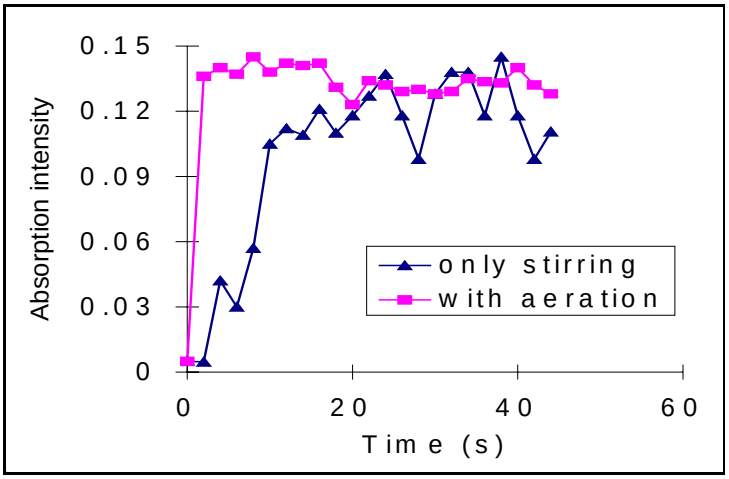

Figure 4. Absorption intensity measured at the position of the DO electrode for a mixing experiment with only stirring and an experiment with stirring and aeration.

Physico-chemical phenomena: Diffusion of the substrate into activated sludge flocs

Activated sludge grows in flocs. The flocs are nothing else than clumps of bacteria that stick together, for example because of the presence of significant amounts of exopolymers. Diffusion phenomena around the activated sludge flocs might be a determining factor to the transient phenomenon. This hypothesis can be qualitatively described as follows: Just before the pulse substrate addition, the sludge flocs can be assumed fully penetrated with oxygen and lacking substrate. When a substrate pulse is added to the bulk liquid, substrate diffuses into the activated sludge flocs where aerobic micro-organisms oxidize it, thereby consuming a significant amount of oxygen. This induces a difference in oxygen concentration between the flocs and the bulk liquid phase, and oxygen diffuses from the bulk liquid phase into the flocs. Finally, the decrease in oxygen concentration in the bulk is measured by the DO electrode. This would mean that the respirometric response to a pulse substrate addition may be influenced by diffusion limitations of either substrate or oxygen, or both.

In order to evaluate diffusion limitations, the following empirical approach was employed. An experiment was set up in which the respiration response of a single, non-flocculating *Pseudomonas* culture was compared to the response of an activated sludge sample. In the *Pseudomonas* culture no diffusion limitations for substrate or oxygen can exist as the cells do not flocculate. Addition of an acetate pulse to the *Pseudomonas* culture resulted in the respirogram of Figure 5. The time between substrate addition and measurement of the maximum OUR is still 3 to 4 minutes. It can be concluded that the hypothesis of diffusion limitation in the sludge flocs does not seem adequate to explain the transient behaviour

observed in microbial cultures following a pulse substrate addition. It appears to be a characteristic of the bacterial cell.

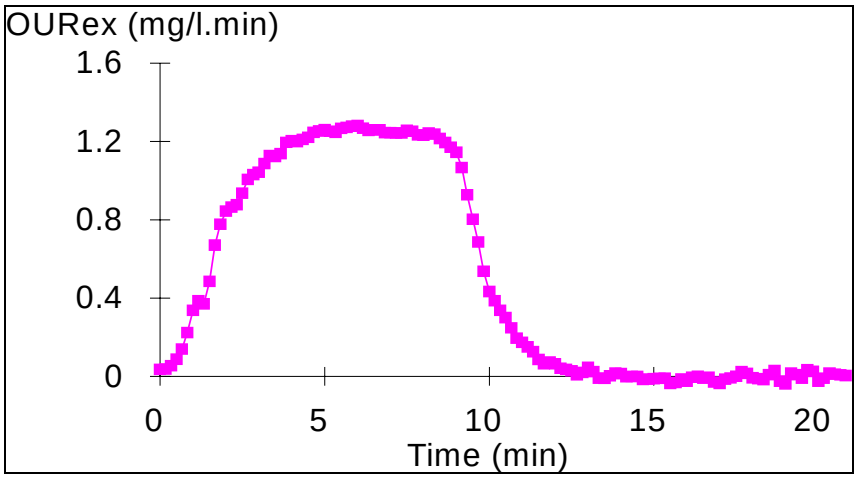

Figure 5. OUR profile (where endogenous OUR level was subtracted from the original OUR data) for a pulse addition of acetate to a *Pseudomonas aeruginosa* culture at t = 0.

The experiment with the *Pseudomonas* culture showed that the transient phenomenon couldn't be explained by transport limitations in the flocs. In support of this result, Li & Ganczarczyk (1992) stated that sludge flocs may be permeable, depending on their size and the plant operating conditions. They also suggested that advective transport through channels in the sludge flocs could be the main mass transfer mechanism, which could explain the absence of transport limitations in the flocs.

4.1.3 Summary: evaluation of the hypotheses

The 3 above hypotheses can only offer a partial explanation of the observed discrepancy between model predictions and the experimental data. Thus, the hypothesis that the experimental set-up or that physico-chemical phenomena cause the discrepancy has to be rejected in favour of the alternative hypothesis: "the discrepancy is caused to a large extent by a modelling error". A final argument to support the thesis that the transient phenomenon is not due to the experimental set-up used in our work is that the transient response phenomenon has also been observed in many different experimental set-ups, as indicated in the literature survey given above.

4.2 Empirical modelling of the transient response of activated sludge in batch experiments

4.2.1 First order model

The observed transient phenomenon can be modelled in a very simple but appropriate way by means of the following first order model of the observed growth rate:

$$\mu_{obs} = Trans \cdot \mu \quad (3)$$

$$Trans = (1 - e^{-t/\tau}) \quad (4)$$

where *Trans* is the transient term associated to the 1st order model (dimensionless), τ is the first order time constant (T), t is time (T), μ_{obs} is the observed growth rate of the activated sludge (T^{-1}) and μ is the maximum growth rate of the activated sludge (T^{-1}).

This first order approach was used by Vanrolleghem and co-workers as early as 1992 in De Schryver (1992). Since then, the first order model has been regularly mentioned and used by the same group in studies dealing with various applications of respirometric batch experiments (Vanrolleghem and Spanjers, 1998; Vanrolleghem *et al.*, 1998; Gernaey *et al.*, 2001a, 2002a, 2002b; Chapter 3.1; Chapter 4.1; Chapter 4.2.1). Quite recently, Guisasola *et al.* (2004) independently adopted the first order model, however still without providing a plausible explanation of the observed transient phenomenon.

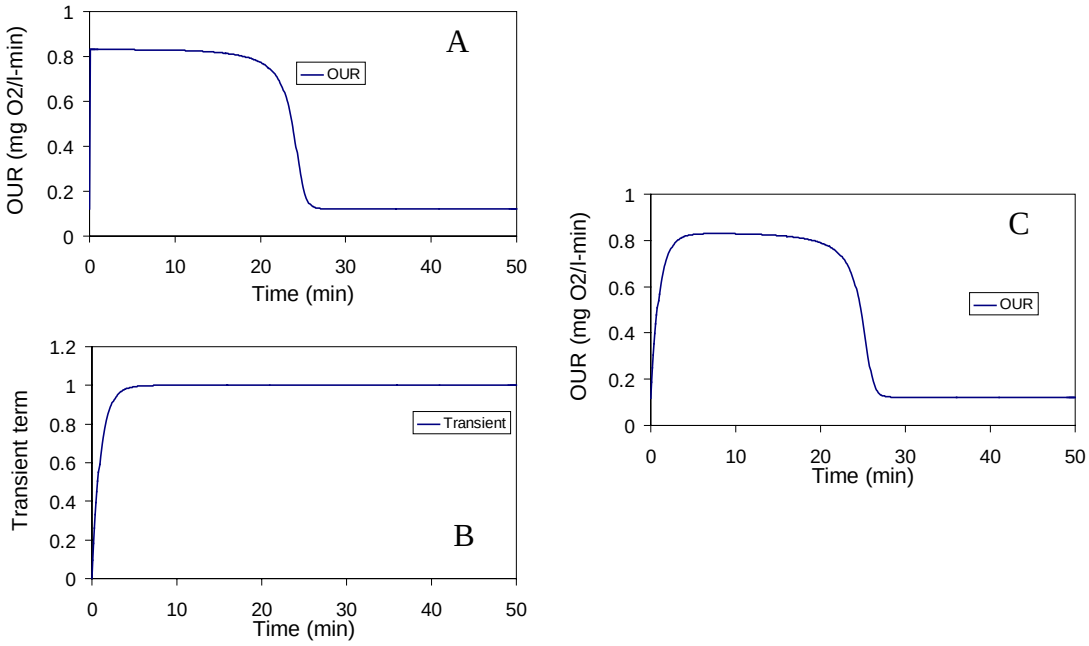

Figure 6. A typical simulated OUR profile in batch experiments using Monod kinetics (refer to Figure 1 for simulation conditions) (A). The simulated first order model transient for t = 1 min (B). Simulated OUR obtained by multiplying the OUR based on Monod kinetics with the first order model, resembling the experimental observations (see Figure 2)(C).

The concept of the empirical model is illustrated in Figure 6. The Monod based model prediction of the OUR is given in Figure 6A whereas the 1st order model of Eq. 3 was simulated for a time constant of 1 min (Figure 6B). The transient response observed in

experimental OUR data can be reproduced almost perfectly by multiplying the Monod model prediction with the first order model. It is obvious that employing this rather simple empirical approach is only one of the solutions to model the batch experiments. I

It should be noted that this approach implies that there is not only a transient in OUR but also in the substrate uptake. This is because, from a modelling point of view, the substrate and oxygen uptake are both directly linked to the growth process in ASM1-like models (Henze *et al.*, 2000). This issue will be addressed in the general discussion.

4.2.2 Application of the 1st order model to experimental data

The empirical first order model of Eq. 3 and 4 was applied to experimental data sets. The mathematical model that incorporates the first order response model is presented in a compact matrix format in Table I (see Henze *et al.*, 2000 for detailed information).

Table I. Matrix representation of the mathematical model used to interpret respirometric data

Component → Process ↓	1. S_S	2. S_O	3. S_{NH}	4. X_A	5. X_H	Process rate
1. Growth of Heterotrophs	$-\frac{1}{Y_H}$	$-\frac{1-Y_H}{Y_H}$	$-i_{XB}$		1	$\mu_{\max H}\left(1-e^{-t/\tau_H}\right)\frac{S_S}{S_S+K_S}X_H$
2. Growth of Nitrifiers		$-\frac{4.57-Y_A}{Y_A}$	$-i_{XB}-\frac{1}{Y_A}$	1		$\mu_{\max A}\left(1-e^{-t/\tau_A}\right)\frac{S_{NH}}{S_{NH}+K_{NH}}X_A$

Batch experiments with aerobic activated sludge (Heterotrophs)

A typical response of an activated sludge culture to a pulse addition of carbon source (here acetate) is shown in Figure 7. The biomass OUR reaches its maximum level after a transient phenomenon (see Figure 7).

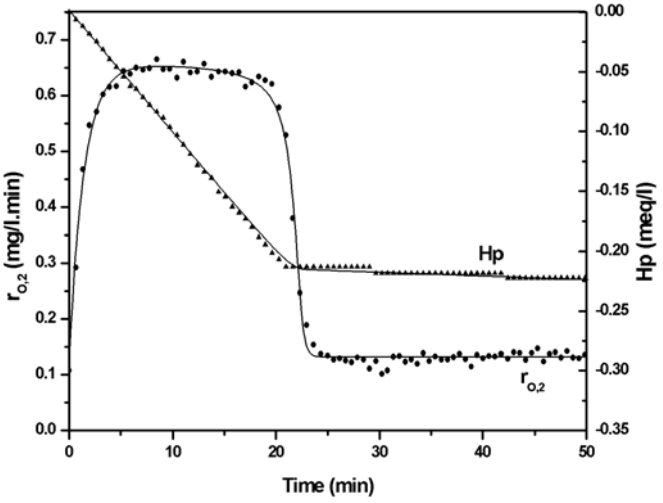

Figure 7. The response of aerobic heterotrophs to a pulse addition of (49.72 mg COD/l) acetate. Model fits to the OUR and Hp (titrimetric data) are also shown (Gernaey *et al.*, 2002b).

A discussion of the titrimetric data shown in this figure will follow below. As shown in Figure 7, the first order model describes the transient response occurring in the OUR profiles sufficiently well. In general, the first order time constants observed with aerobic heterotrophs seem to change with different activated sludge samples shown in Table II.

Table II. Estimates of 1st order time constants and substrate affinity constants for various activated sludge activities ($S_{NH}(0)$ and K_{NH} are relevant for experiments with nitrifiers; $S_S(0)$ and K_S are relevant for experiments with heterotrophs)

Exp. Id.	Initial substrate $S_{NH}(0)$ or $S_S(0)$	Substrate affinity K_{NH} or K_S	τ (min)	Reference
Experiments with nitrifiers: Ammonium as substrate-source				
1	5.02	0.43	2.907	Gernaey *et al*., 2001a
Day-1	3.3	0.25	0.91	Spanjers and Vanrolleghem, 1995
Day-2	3.3	0.15	3.0	Spanjers and Vanrolleghem, 1995
Experiments with aerobic heterotrophs: acetate as substrate-source				
1	25.22	0.72	1.88	Gernaey *et al*., 2002b
2	37.61	0.63	1.74	Gernaey *et al*., 2002b
3	49.72	0.62	1.42	Gernaey *et al*., 2002b
4	61.39	0.58	1.7	Gernaey *et al*., 2002b
5	45.9	0.66	1.25	This study
6	48.4	0.72	2.24	Kotte, 2002

Batch experiments with aerobic nitrifiers

The transient phenomenon is also observed in batch experiments with ammonium pulse additions for the kinetic characterization of nitrifying biomass (Figure 8). Similar to the heterotrophic bacteria, the OUR of the nitrifiers reaches a maximum OUR after a transient response.

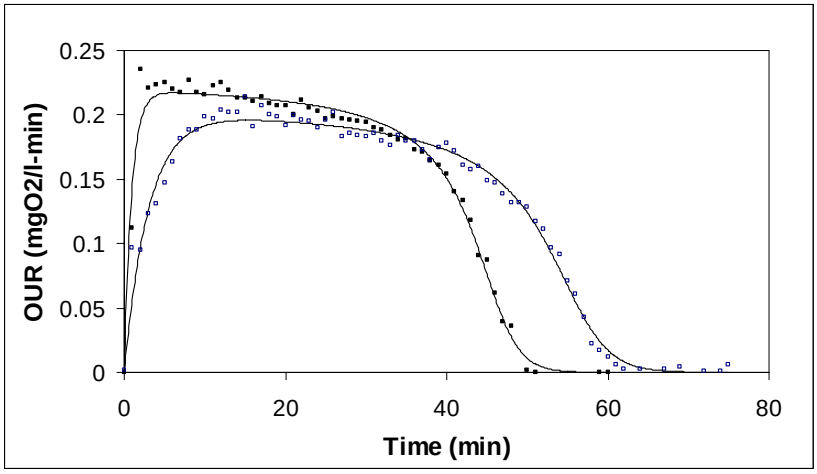

Figure 8. Transient response of nitrifying biomass to a pulse addition of 3.3 mg ammonium in 1.4 L batch reactor. Filled markers indicate day-1; open markers indicate experiment at day-2 and smooth lines indicate simulation results (Spanjers and Vanrolleghem, 1995).

A prolonged transient is observed with nitrifiers subjected to 1-day famine (aerobic endogenous respiration) conditions as demonstrated with the open square-marked OUR in the same figure. This change in the time constant might be resulting from physiological adjustments of the nitrifiers in response to changing environmental conditions (i.e. enzyme activity level, protein synthesis level, etc.). This hypothesis will be further discussed below.

4.2.3 Bias induced in biodegradation parameters by neglecting the transient phenomenon

The bias induced in parameters estimated from respirograms obtained by not properly accounting for the transient phenomenon is illustrated for the two experiments taken from Vanrolleghem *et al.* (1995) shown in Figure 9 and for one experiment performed specifically for this study (see Table III).

The original experimental data of Vanrolleghem *et al.* (1995) shown in Figure 9A & C clearly show the transient phenomenon. In order to be able to model it using Monod kinetics, the authors cut out the transient period from the original data and only used that part of the data that could be explained by the Monod model (Figure 9B & D). The original complete data sets were used to compare the parameter estimation results with or without considering the transient period.

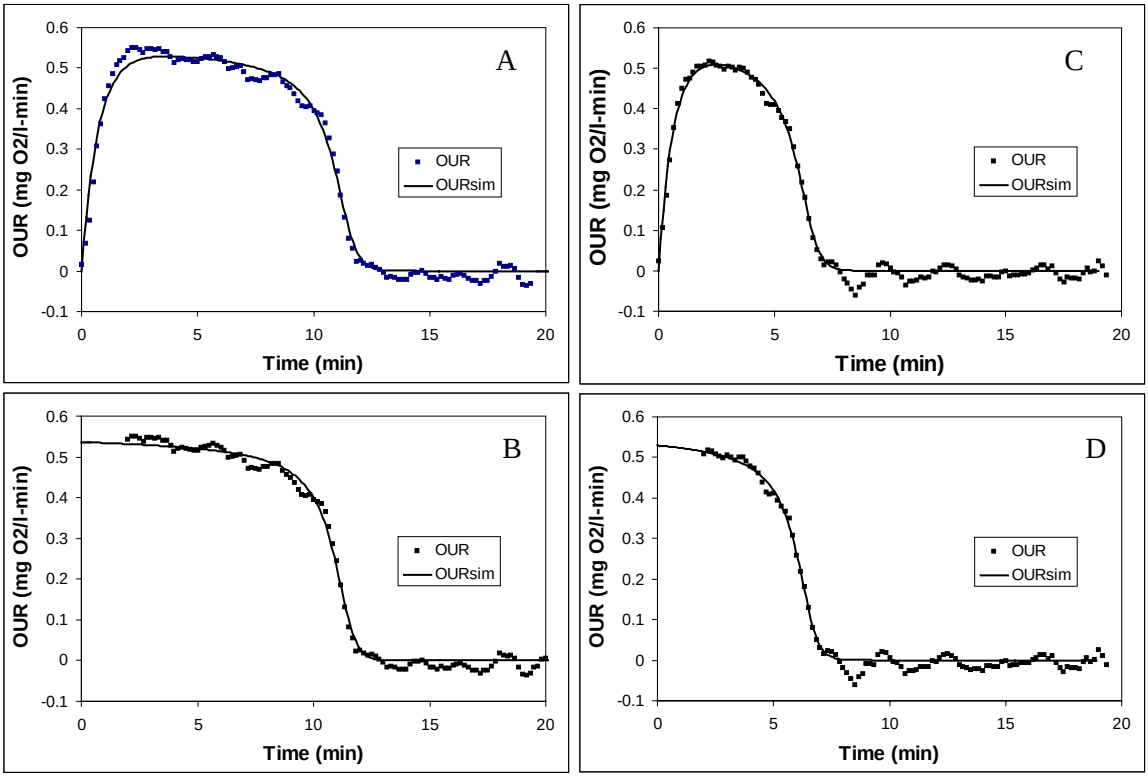

Figure 9. OUR profiles obtained from pulse addition of 20 mg COD/l acetate (A+B) and 10 mg COD/l (C+D) to an aerobic activated sludge sample. Model fits are based on ASM1 model. Deleting the transient responses from the OUR data (B & D) is compared with 1st order dynamic modelling of the transient phenomenon (A & C) (data from Vanrolleghem *et al.*, 1995).

Table III. Parameter estimation results with and without considering the transient response (see text for details about the estimation procedure. Units of the other parameters are as presented in the nomenclature).

PE approach	Duration**	$S_S(0)$	$\frac{1-Y_H}{Y_H}\mu_{\max H} X_H(0)$	$(1-Y_H)S_S(0)$	$(1-Y_H)K_S$	Y_H	μ_{maxH} (min^{-1})	K_S	τ (min)
Experiment A from Vanrolleghem *et al.* (1995)									
Model transient	12	20	0.57	5.2	0.18	0.74	0.00081	0.70	0.7
Ignore transient	12	20	0.57	5.6	0.17	0.72	0.00073	0.61	
ε_R* (%)						-2.78	-10.38	-14.75	
Experiment C from Vanrolleghem *et al.* (1995)									
Model transient	7	10	0.58	2.7	0.18	0.73	0.00078	0.67	0.61
Ignore transient	7	10	0.57	3.0	0.17	0.70	0.00066	0.55	
ε_R*(%)						-4.29	-18.18	-21.82	
Experiment from this study									
Model transient	30	45.9	0.40	10.2	0.15	0.78	0.00071	0.66	1.25
Ignore transient	30	45.9	0.40	10.6	0.13	0.77	0.00067	0.58	
ε_R*(%)						-1.30	-5.97	-13.79	

* Relative error in percentage.

** Time needed to oxidize the initial amount of carbon source i.e. the duration of the OUR due to external carbon source

When considered, the transient period is modelled using the 1st order model introduced above. For the parameter estimation (PE) procedure, it is assumed that no significant growth takes place during the short-term batch experiments and that the initial biomass concentration is fixed to 2000 mgCOD/l. Moreover, the initial amount of substrate added is a priori known. Under these assumptions, the identifiable parameter combinations shown in Table III can be estimated using OUR as a measured variable (Dochain and Vanrolleghem, 2001).

The results (see Table III and Figure 9) show that ignoring the transient period leads to a considerable underestimation of the yield coefficient, Y_H. This is because the identifiable parameter combination $(1-Y_H)S_S(0)$ changes when the transient period is considered or not (see Table III). Since the initial amount of substrate addition is a priori known, the error made in the estimate of $(1-Y_H)S_S(0)$ propagates directly into the estimate of Y_H. This result is not surprising since modelling the transient period provides a more accurate calculation of the area under the OUR profile (see Figure 9). This area is basically used to estimate the $Y_{H,}$ as it determines the oxygen consumed for the degradation of the substrate.

One could argue that Y_H could be estimated separately by calculating the area under the measured OUR curve (rather than by fitting a whole model to it). However, by working in this way a bias may be introduced in the other parameters (Dochain and Vanrolleghem, 2001). All parameters should be estimated simultaneously.

An error in the estimate of Y_H is quite critical since the estimate of Y_H is used to calculate μ_{maxH} and K_S from their respective parameter combinations (see Table III). The error in the estimate of Y_H is thus propagated into the estimate of μ_{maxH} and K_S. For instance, Y_H is underestimated by 2.78% in experiment A (see Table III). As a result, the estimates of μ_{maxH} and K_S are underestimated by 10.38% and 14.75% respectively. It is significant to stress that the absolute values of the estimate of the identifiable parameter combination, $\frac{1-Y_H}{Y_H}\mu_{\max H} X_H(0)$ does not change when ignoring the transient period (see Table III) since the error in Y_H is compensated by an error in μ_{maxH} as mentioned above. Clearly, it can be concluded that ignoring the transient period in the original OUR data induces a bias in the separate parameter estimation results.

The absolute errors in the parameter estimation results depend both on the initial amount of the substrate pulse and on the duration of the transient period (see Table III). Obviously one could minimize the bias in the parameter estimates by increasing the amount of substrate injected. However, the initial amount of substrate addition in short-term batch experiments should be limited, i.e. a low S_0/X_0 ratio should be applied, to prevent the biomass from significantly altering/adapting its physiological state during the experiment (Chudoba *et al.*, 1992; Novák *et*

al., 1994; Grady *et al.*, 1996). Consequently, performing short-term batch experiments with small substrate additions is the usual practice when aiming at experimental data that should provide representative, so-called 'extant', kinetic information to be used later for the calibration of full-scale WWTP models. Having recognized the impact of the transient period on the parameter estimates from short-term batch experiments, it can be inferred that the transient phenomenon may be one of the reasons contributing to the variability in the kinetic parameter estimates published in the literature (Grady *et al.*, 1996).

5. DISCUSSION

In this general discussion, the question "To what extent is the transient response observed in the batch OUR profiles related to a biological response, more particularly related to the substrate metabolism at the cellular level of the activated sludge culture?" will be addressed. Glycolysis will be used to illustrate the concept. The elucidation of the dynamics of cellular metabolism and its regulation is a challenging field of metabolic engineering (Stephanopoulos and Stafford, 2002) and results obtained in this field will be used here to support the substrate metabolism hypothesis.

5.1 Fundamental understanding

Carbon source degradation evaluated at the cellular level of heterotrophic bacteria is not a simple and straightforward process, but involves a complex system in which a myriad of enzymes, intermediate metabolites and metabolic pathways are coordinated and regulated (Kramer and Sprenger, 1991). An illustrative and detailed account of glucose metabolism is illustrated in Figure 10bis (left) for the yeast *Saccharomyces cerevisiae* which is reprinted from Theobald *et al.* (1997). The metabolites formed during the transformations are essential for the cell and are used to produce building blocks e.g. amino acids, nucleotides that are used later by the cell to synthesise proteins and to form macromolecules such as RNA, DNA and membrane polymers used in the production of new cells.

Activated sludge microorganisms, in particular those exposed to time-varying (dynamic) environmental conditions (e.g. temperature, supply of nutrients and substrates, pH etc.) need to be able to respond fast and properly (through regulation and coordination of the metabolism) to cope with a frequently changing environment and to survive (Kramer and Sprenger, 1991). Microorganisms can regulate their metabolism mainly on two levels (Kramer and Sprenger, 1991):

- **Regulation at the protein synthesis level**: This regulation takes place at the transcription (DNA→mRNA) and translation (mRNA→protein) level and is generally more cost-effective than the degradation of already synthesized proteins (leading to loss of building blocks and ATP). This eventually results in regulation of the enzyme levels in the cell.

- **Regulation at the enzyme activity level:** This regulation takes place at the crucial steps of the metabolic pathways. It results in a fast response by controlling the activities of the enzymes present in the cell using allosteric control mechanisms available to the cell.

Theobald *et al.* (1997) measured in vivo dynamics of the metabolites during glucose metabolism of *Saccharomyces cerevisiae* upon pulse addition of glucose to a steady state culture of *Saccharomyces cerevisiae* (Figure 10bis(right)).

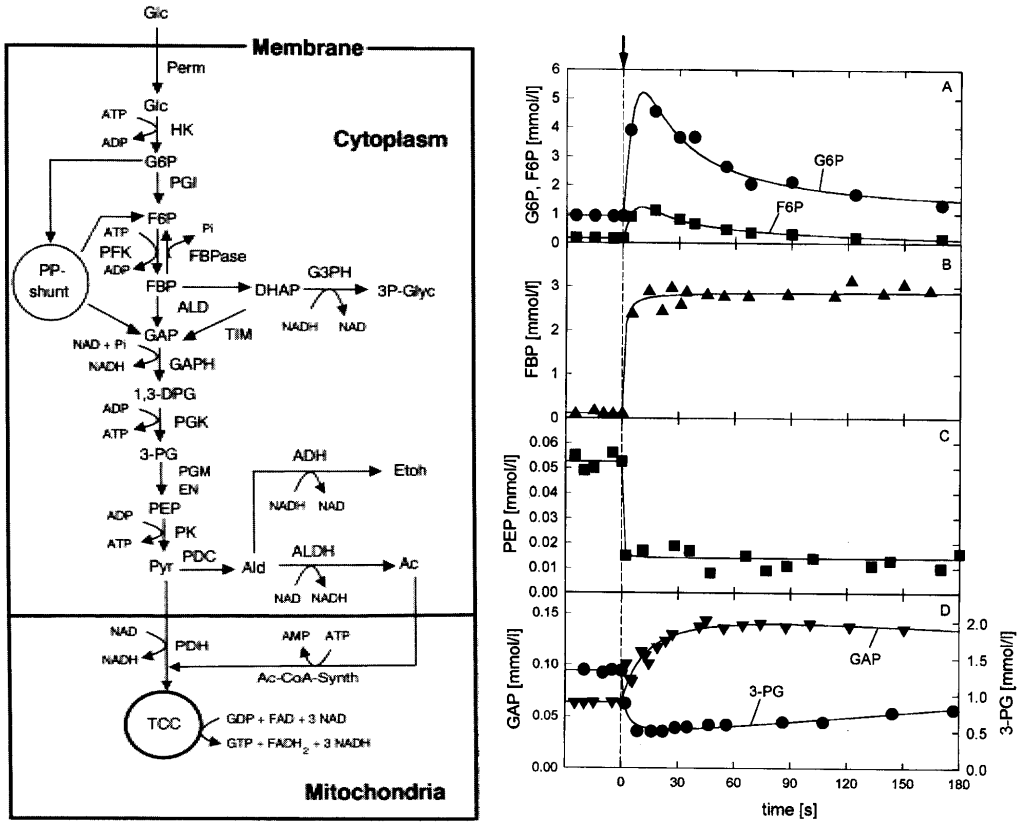

Figure 10bis The central carbon metabolism in *S. cerevisiae* (left) The dynamic change in the level of intermediates from their steady state levels after a glucose pulse (↓) (right). Reprinted from Theobald *et al.*, 1997. Copyright © 1997 John Wiley & Sons Inc. Reprinted by permission of Wiley-Liss Inc.

A very dynamic change in the intracellular metabolite concentrations can be observed upon pulse glucose addition. The time constant of the dynamic response in the intracellular metabolites to this pulse varies as the carbon (glucose) flux moves downward into the central metabolic pathway shown in Figure 10bis(left). For example the time constant of the dynamic response observed in the glucose-6-phosphate (G6P) concentration is around 5 s whereas the time constant of the dynamic response observed in the glyceraldehydes-3-phosphate (GAP) concentration which is situated in the middle of the glycolysis pathway is already around 30 s (see Figure 10bis). It is important to note here that the respiration rate measurements (OUR) take place at the end of the catabolic pathway. That means that the time constant of the respiration response would be expected to be even higher.

Quite recently, in a dynamic metabolic modelling study of *Escherichia coli* performed by the same group (Chassagnole *et al.*, 2002), it has been shown that the time constants of the numerous steps involved in the metabolic network of the central carbon metabolism of *E. coli* vary between 29 ms to 85 secs. It can be inferred from the time constants identified for central carbon metabolism that delays in the substrate metabolism might be the underlying mechanism of the transient phenomenon observed in the OUR measurements.

The substrate metabolism hypothesis is schematically described in Figure 10. Pulse addition of the substrate is the input to the system and the OUR measurements can be considered the measurements of the output i.e. the pulse response of the system. In this case, the resulting transient phenomenon observed in the OUR measurements is dependent on the characteristic time of the system which is the entire metabolic network of the cell. The left hand side of Figure 10 illustrates the substrate metabolism and its regulation to fine-tune the substrate flux through the different metabolic pathways, which is determined essentially by the physiological state of the cell. For example, if the cell is exposed to feast and famine conditions then most probably the cell will optimise the storage and growth processes in order to gain a selective advantage in the famine conditions (Daigger and Grady, 1982; Van Loosdrecht and Heijnen, 2002).

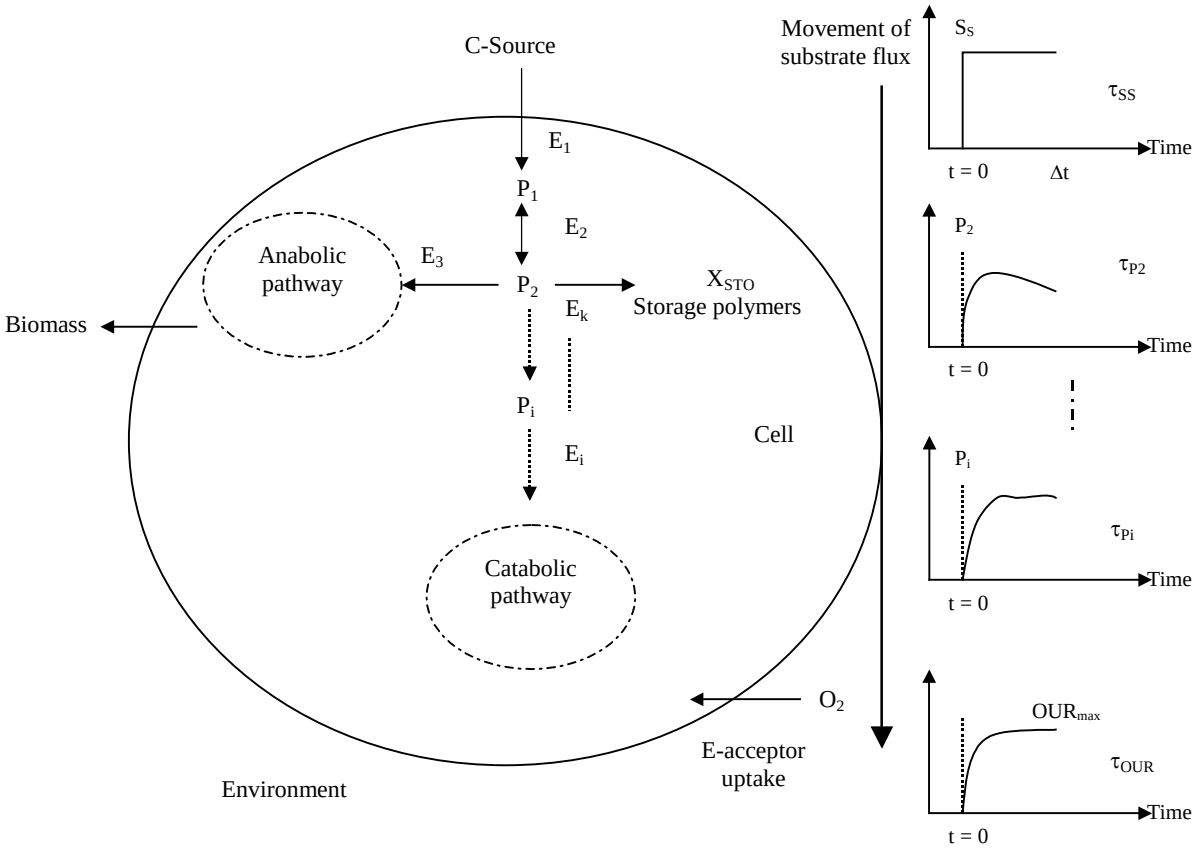

Figure 10. An illustrative description of the substrate metabolism hypothesis for the activated sludge mixed culture.

5.2. Input/Output behaviour: Substrate uptake rate / OUR measurements in batch experiments with aerobic carbon source degradation

In aerobic batch experiments with acetate, the substrate uptake rate can be monitored indirectly using the titrimetric methodology of Gernaey *et al.* (2002a). This titrimetric methodology for substrate uptake monitoring is based on the fact that at pH 7 to 8 the acetate is present in dissociated form. Consequently, since it is the undissociated form that is taken up, every mmol of acetate consumed removes approximately 1 mmol of protons from the medium. This proton consumption is compensated by the acid addition in the experimental set-up and this addition is recorded during the experiment. For a detailed explanation of this titrimetric methodology, the reader is referred to Gernaey *et al.* (2002a).

Table IV. Estimates of 1st order time constants and substrate affinity constants for aerobic activated sludge in various experiments with acetate addition as carbon source

Exp. No.	$S_S(0)$ (mg COD/l)	τ_{HP} (min)	τ_{OUR} (min)	K_{S_HP} (mg COD/l)	K_{S_OUR} (mg COD/l)	Reference
1	25.22	0.18	1.88	0.3	0.72	Gernaey *et al*., 2002b
2	37.61	0.1	1.74	0.1	0.63	Gernaey *et al*., 2002b
3	49.72	0.1	1.42	0.1	0.62	Gernaey *et al*., 2002b
4	61.39	0.1	1.7	0.6	0.58	Gernaey *et al*., 2002b
5	72.49	0.13	1.95	0.17	0.71	Gernaey *et al*., 2002b
6	45.9	-	1.25	-	0.66	This study
7	48.4	-	2.24	-	0.72	Kotte, 2002
Average		0.12	1.74	0.25	0.68	

Table IV summarizes the range of time constants for the transient phenomenon observed in OUR and Hp measurements, and the corresponding references to the publications with the experimental data. In general it is observed in aerobic experiments that the acetate uptake after a pulse addition is a very fast process with hardly any detectable transient phenomenon (see Figure 7), i.e. with a very small time constant (0.12 min average in Table IV). . The OUR data result from a slower process and therefore exhibit a clear initial transient phenomenon, characterized by a longer time constant (1.74 min average in Table IV).

A result of the difference between titrimetric and OUR data in experiments with acetate are the differences in estimated biomass Monod substrate affinity constants. The sharp bending point at the end of the substrate degradation process observed in the Hp data results in very low substrate affinity constants estimated from Hp data (Figure 7). The average K_S estimate was 0.25 mg COD/l. For comparison, the OUR data resulted in an average K_S estimate of 0.68 mg COD/l. These results mean that the substrate uptake process suddenly stops (according to high affinity –transport– enzyme kinetics) when the substrate is exhausted from the medium, while

the OUR only slows down at a lower pace after substrate is depleted due to the intracellularly accumulated intermediates that can still be oxidized.

5.3 Input/Output behavior: Batch experiments with anoxic acetate degradation

Anoxic respiration of activated sludge as measured by the titrimetric method proposed elsewhere (Petersen *et al.,* 2002a; Chapter 3.1) is shown in Figure 11. The titrimetric data in this experiment are assumed to be the combined effect of 4 processes influencing the proton concentration of the medium. These processes, explained in detail in Petersen *et al.* (2002a) and in Chapters 3.1 and 4.2 are: the substrate (carbon source) uptake (proton consumption effect), nitrate uptake as electron acceptor (proton consumption effect), CO_2 production due to biomass respiration (proton production effect) and ammonia uptake for growth (proton production effect). Anoxic oxidation of acetate typically results in acid addition for pH control during titrimetric experiments, indicating a consumption of protons from the medium. The analysis in Petersen *et al.* (2002a) shows that the proton consumption is basically due to rapid uptake of acetate as carbon source and nitrate uptake as electron acceptor. Once the acetate is removed from the medium, which took about 28 min in this experiment, the acid addition decreases drastically to a background rate determined by the pH effects of endogenous processes. For the first pulse addition of acetate (23.5 mg COD/l), acid addition starts soon to keep the pH of the medium constant, following a transient period with a time constant of 0.47 min^{-1} (see Figure 11). For the second pulse addition of acetate (46.7 mg COD/l), the transient response phenomenon is repeated with a time constant of 0.42 min^{-1}.

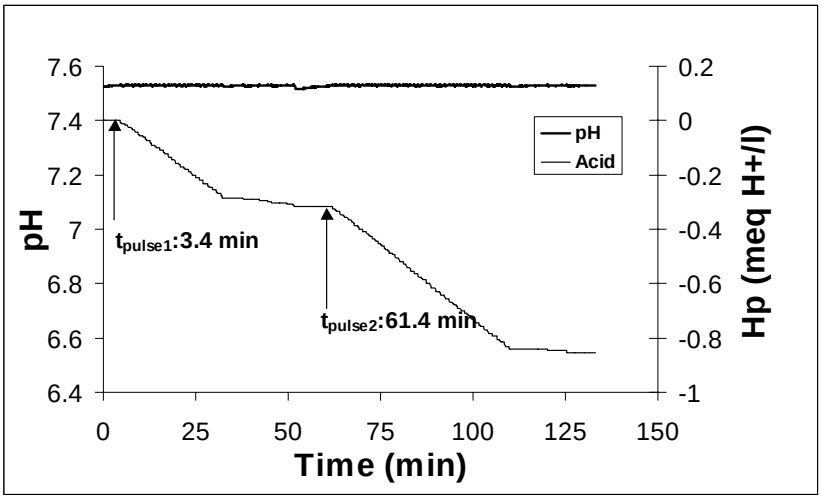

Figure 11. Consecutive addition of two acetate pulses to an anoxic batch reactor. The first acetate pulse (23.5 mg COD/l) was given to the reactor at 3.4 min, SNO3(0)=12.5 mg N/l. The second acetate pulse (46.7 mg COD/l) was injected to the anoxic reactor at 61.4 min, SNO3(0)=8.6 mg N/l.

The time constants observed on titrimetric data with anoxic acetate oxidation are 3 times (on average) higher than the values for aerobic acetate oxidation. This difference might be caused by the difference in the metabolism of acetate under aerobic and anoxic conditions. More

probably, the titrimetric data under anoxic conditions are influenced by nitrate uptake also, which is not the case for the aerobic conditions where oxygen uptake has no pH effect on the titrimetric data. As a result, the titrimetric data under anoxic conditions will reflect lumped dynamics of two processes: 1) Acetate uptake that is determined by the very fast substrate uptake kinetics and 2) Nitrate (e-acceptor) uptake that is driven mainly by the growth kinetics.

Summarizing, the experimental observations with (aerobic and anoxic) activated sludge activities provided additional support of the aforementioned substrate metabolism hypothesis. Regarding aerobic acetate oxidation, the time constant of the substrate uptake process, which is monitored by the titrimetric data, is in the order of 0.1 min with a very high substrate affinity (K_S = 0.25 mg COD/l), indicating that substrate uptake is a fast process with fast dynamics. On the other hand, the time constant obtained from the OUR data is in the order of 1.75 min with a relatively lower estimated substrate affinity (K_S = 0.68 mg COD/l), indicating that the OUR has comparatively slower dynamics. Van Loosdrecht and Heijnen (2002) observed in their experimental studies that the substrate uptake process is a very fast process compared with the growth process.

These experimental data fit very well with the hypothesis formulated in Figure 10. The substrate uptake as a starting point in the metabolic network of the cell has fast dynamics and does not depend on preceding reactions (Chassagnole *et al.*, 2002). Moving down the chain of metabolic reactions, some time passes until the electrons of the substrate finally reach the oxygen (or nitrate) reduction sites situated at the end of the metabolic network. As a result, a dynamic transient response occurs in the uptake of oxygen from the surrounding environment, which can be observed from OUR data. It can be expected that the dynamics determining the transient phenomenon will depend on the structure of the metabolic network, which is also determined by the physiological state of the culture. In this regard, this might explain the change in the time constant of the nitrifiers when having a different culture history (see Figure 8 and Table II).

It is obvious that modelling the transient phenomenon occurring in batch experiments should be possible with mechanistic dynamic metabolic network models, e.g. Chassagnole *et al.* (2002). However, such an approach is an extremely complex solution, which in the case of activated sludge mixed cultures is hardly applicable. However, the formulated hypothesis helps to understand the observed phenomenon from a mechanistic point of view.

The approach adopted here, i.e. a simple empirical first order process works fine to describe the batch experimental results and allows to obtain good biokinetic parameters despite the transient phenomenon. Moreover, it allowed us to study the differences in observed time constants (e.g. difference in the time constants of the substrate uptake versus oxygen uptake; effect of famine

state on the time constants for the nitrifiers), which led us to the metabolic hypothesis presented above.

If we want to adopt this first order approach to other situations than the ones encountered in a batch experiment, another mathematical formulation than the one in Eq. 3 and 4 will be required. A very natural approach would be to introduce an additional state variable, e.g. the intracellular substrate that is linked to the external substrate via a first order differential equation. This would also allow to decouple the substrate uptake from the growth process. However, when such approach is adopted, considerable problems surface when confronting substrate uptake data and oxygen uptake data for a complete batch experiments (results not shown). Further research is currently ongoing to find a simple mathematical description of the observations that would also work under fast alternating conditions different from batch experiments (e.g. the example given in Figure 12 where a substrate addition took place both at t = 0 min and t = 11.6 min).

5.4 Significance of modelling the transient phenomenon for activated sludge processes

One could wonder whether the observed discrepancy between model and experimental data has any practical importance? First of all, explicitly accounting for the transient phenomenon in the data interpretation is important to achieve correct interpretation of the experimental data, i.e. it will result in more realistic model parameter estimates, as illustrated in Table III. It was shown that if the transient period is not taken into account, erroneous biomass yield values would result from short-term batch experiments. Moreover, an error in the yield coefficient is amplified into the estimates of the maximum growth rate and the substrate affinity constant, with errors as much as 18% and 22% respectively (see Table III).

When approximating the observed transient phenomenon by a first order model, the time constant of the transient phenomenon typically is in the order of minutes. Thus, such transient phenomenon cannot be ignored for many types of full-scale WWTPs where the biomass is exposed to fast alterations in substrate and electron acceptor concentrations. In this respect, the similarities between batch substrate degradation experiments and full-scale plug-flow WWTP behaviour should be considered. In both systems, rapid biomass activity changes occur. In the batch experiment, the biomass activity will rapidly change following a batch substrate addition (see Figure 2). Once all substrate is consumed, the measured OUR rapidly decreases to zero, and the biomass resumes its endogenous state. In many full-scale plug-flow like activated sludge systems, such as oxidation ditches (Metcalf and Eddy, 1991) or Orbal WWTPs (Daigger and Littleton, 2000), the activated sludge is cycled around a circular reactor, thereby passing the influent feeding point every 5 to 15 minutes, depending on the configuration and the operating parameters. During each cycle, the biomass can experience aerobic, anoxic and anaerobic conditions. Thus, in these full-scale systems the activated sludge is subject to batch-

like conditions similar to pulse substrate additions every time it passes the influent feeding point.

Rapidly changing conditions similar to the ones induced by a pulse substrate addition also exist in fast alternating systems, for example:

a) In sequencing batch reactors (SBR) (Demuynck *et al.*, 1994) or standard activated sludge treatment plants (Wouters-Wasiak *et al.*, 1994) with high frequency intermittent aeration cycles or alternating aeration plants such as Biodenitro/Biodenipho systems (Bundgaard *et al.*, 1989)
b) In plug-flow type pre-denitrification systems (Wentzel *et al.*, 1992) with short anoxic residence times, in particular when considering the single-pass hydraulic retention time in the reactor, i.e. the ratio of the volume of the reactor over the total inflow to the reactor (influent plus recycle plus internal recirculation flows)
c) Plug-flow type selectors, usually situated in front of the main aeration tanks (plug-flow and/or carrousel) to enhance biological phosphorus removal and prevent sludge bulking have a short hydraulic retention time (e.g. in the order of 10 – 25 minutes as reported in Meijer *et al.*, 2002) which implies even shorter single-pass biomass residence times in the order of minutes (Vanrolleghem *et al.*, 2003).
d) In oxidation ditch systems with short phases e.g. ORBAL plants (Daigger and Littleton, 2000) and carrousel plants (Vanrolleghem *et al.*, 2003; Meijer *et al.*, 2002), where circulation times are also in the order of minutes.

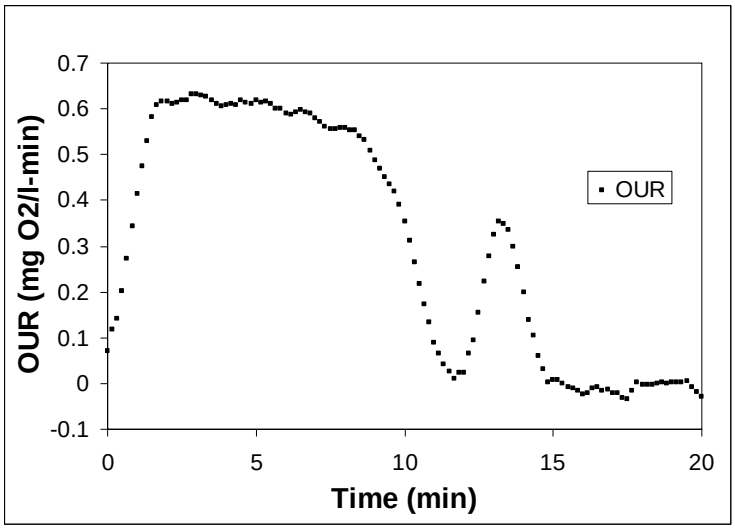

Figure 12. Repeatability of the transient phenomenon in response to pulse additions of acetate during a batch degradation experiment. The first pulse is 20 mg COD/l and the second pulse is 4 mg COD/l (Dochain and Vanrolleghem, 2001).

In many types of biological WWTPs the transient phenomenon can therefore be expected to occur and it will be an inherent characteristic of the biomass activity that will influence the

process every time the biomass is exposed to feast (feed) conditions. This is further illustrated in Figure 12 where a substrate addition took place both at t = 0 min and t = 11.6 min. In both cases the transient phenomenon is clearly observed. Therefore, proper understanding and modelling of the transient phenomenon can contribute to improved full-scale WWTP modelling. The inclusion of the transient behaviour in full-scale models requires the extension of the first order model (Eq. 3) which is only applicable to batch reactors to continuous systems. Preliminary investigations (not shown) have indicated that development of such a continuous model is not straightforward, and it is subject to ongoing research. Important to mention already is that it requires description of at least three processes, i.e. substrate uptake, metabolism in the metabolic network (as a first (or higher) order system) and growth, instead of the single process (i.e. growth) of ASM1 (Henze *et al.*, 2000).

6. CONCLUSION

The underlying mechanisms of the transient phenomenon that is often observed in the experimental data (e.g. OUR) obtained from short-term batch assays with activated sludge following a pulse substrate addition is investigated in detail in this study. Detailed analysis of the dynamics of the experimental set-up could partially explain the observed transient phenomenon, yet cannot describe it completely. Among the hypotheses proposed it appears that the transient response of the activated sludge following a pulse substrate addition is most likely resulting from the metabolism of the substrate by the mixed activated sludge culture.

It is shown that the transient phenomenon can be described by a first order model. It is demonstrated that an erroneous estimate of the biomass yield is obtained if the transient period is not taken into account during model-based parameter estimation. This error is propagated (and amplified) into the estimates of the maximum growth rate and the substrate affinity constant.

The first order time constant of the transient phenomenon observed in the experimental data shows that the substrate uptake process has a faster response (0.12 min on average) compared to the oxygen uptake dynamics (1.74 min on average), which is basically reflecting the dynamics of the overall substrate degradation process in the model. These results suggest that the substrate uptake processes should be decoupled from the growth processes in future activated sludge WWTP models.

Taking this transient phenomenon properly into account is expected to yield a better understanding and modelling of fast alternating biological systems such as ORBAL, carrousel type treatment or other fast-alternating plants, but the analysis of its impact is beyond the scope of the current contribution.

7. ACKNOWLEDGEMENT

The constructive comments by all three reviewers of this manuscript were very much appreciated. This study was supported by the EU by means of the ICON project, no. EVK1-CT2000-00054 and by the Belgian National Science Fund through grant G.0286.96.

PART 3
-
APPLICATION OF SYSTEMATIC CALIBRATION PROTOCOL

Chapter 5.1

A calibration methodology and model-based systems analysis for SBR's removing nutrients under limited aeration conditions

ABSTRACT

A methodology was proposed for the model calibration of nutrient removing lab-scale SBR's under limited aeration. Based on in-process measurements and influent wastewater characterization, the ASM2d model was modified by adding an organic nitrogen module linked to the hydrolysis mechanism. After calibration the simulation results showed that enhanced biological nutrient removal occurred during the fill-period and under reduced aeration that achieves so-called 'Simultaneous Nutrient Removal'. A model-based systems analysis was performed in terms of the contributions of the different processes to overall oxygen, nitrogen and phosphate utilization. In addition, simultaneously occurring biological reactions were compared during the different phases.

This chapter was presented in the 3rd IWA conference on SBR as:

Insel G., Sin G., Lee D.S. and Vanrolleghem P. A. (2004) A calibration methodology and model-based systems analysis for SBR's removing nutrients under limited aeration conditions. 3rd IWA International conference on SBR, Noosa, Queensland, Australia, 22-26 February 2004.

1. INTRODUCTION

Sequencing batch reactors (SBR) are mainly characterized by sequential process phases of fill, react, settle, decant and idle periods that allow considerable flexibility in the design and operation in view of different biological wastewater treatment alternatives (Irvine *et al.*, 1997; Ketchum, 1997). This flexibility is provided by the unique features of SBRs which are: (a) influent and effluent flows are uncoupled by time sequencing (b) the clarification occurs in the same reactor (c) biological processes take place in a cyclic or periodic manner (d) a portion of the treated water is replaced by untreated wastewater for each cycle distinguishing the SBR process from other continuous flow type activated sludge systems (Wilderer *et al.*, 2001; Artan *et al.*, 2001). The design of an SBR for nutrient (nitrogen) removal is mainly based upon the selection of some relevant parameters (e.g. sludge age, volume exchange ratio, cycle time, SVI) as described in, for instance, the ATV guidelines (Teichgräber *et al.*, 2001) in combination with stoichiometric mass balance calculations on the denitrification potential, N_{DP} and available nitrogen, N_A (Artan *et al.*, 2001). In reality, the resulting wastewater treatment plants are mostly over-designed to sustain efficient carbon and nutrient removal under varying environmental and operating conditions. However, attention should be paid to the operating conditions, which may positively or negatively affect the overall system performance, even if the system is designed with safety margins. On the other hand, the optimization of operating parameters (e.g. aeration control) can be an asset to take advantage of simultaneous nitrogen removal together with enhanced biological phosphorous removal known as 'simultaneous nutrient removal' (Daigger and Littleton, 2000).

An existing SBR plant may require a trustable optimisation in terms of nutrient removal, but that necessitates better understanding and quantification of the biological processes occurring in each phase. A calibrated activated sludge model is a practical tool to try numerous operation scenarios within a short evaluation time when an upgrade of the SBR is considered (see Chapter 6). In this way, the effect of changes in process configuration/control and environmental factors can be simulated and appropriate measures can be taken in due course. However, model calibration requires expert knowledge on the influent wastewater characterization, on-line/off-line measurements, operating conditions and the treatment system itself. The model-based interpretation of the system can be used to obtain a better understanding into the biological processes and also to select/identify the most appropriate operating variables to manipulate during model-based optimisation (see Chapter 6) such as cycle times, aeration capacity *etc.*

In this respect, this paper describes a 'calibration methodology' for a lab-scale SBR performing simultaneous nutrient removal under limited aeration conditions. In addition, a systems analysis is performed via the investigation of individual biological process contributions to phosphate utilization, oxygen consumption and nitrogen removal by using the calibrated model.

2. MATERIALS AND METHODS

A pilot-scale sequencing batch reactor (SBR) with a working volume of 80 L was seeded with sludge from the Ossemeersen wastewater treatment plant (Gent, Belgium) and operated for a 2 year period. The hydraulic retention time (HRT) and solids retention time (SRT) are maintained at 12 hrs and 10 days, respectively. Each cycle comprises an unaerated fill phase (60 min), aeration phase (150 min), anoxic phase (60 min), aerated phase (30 min), settling (45 min) and draw (15 min) phases. The total cycle time, C_T was set to 6 hours (4 cycles per day) with volumetric exchange ratio (V_0/V_{Total}) of 0.5.

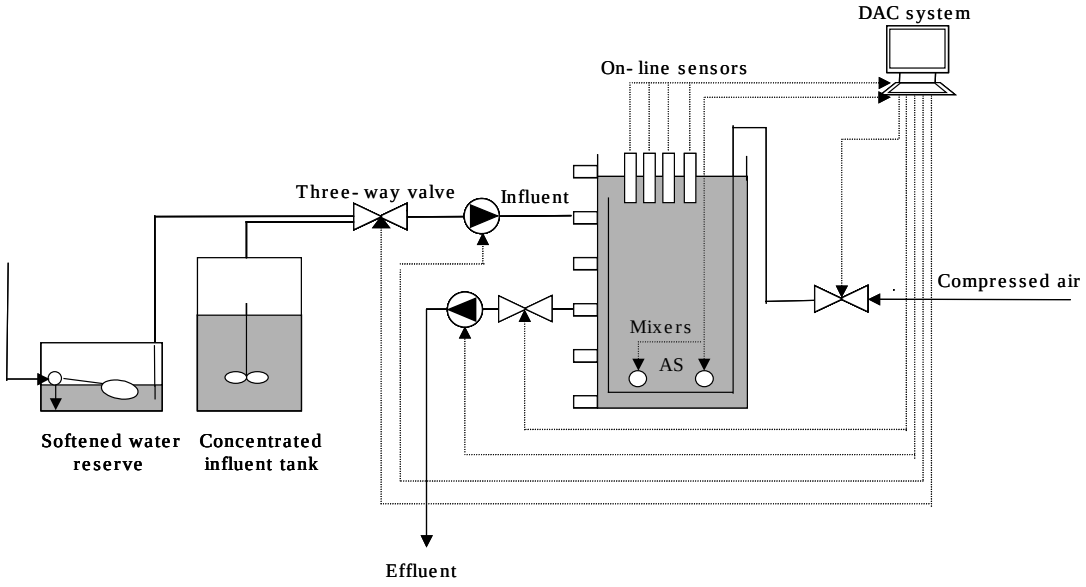

Figure 1. Schematic diagram of the SBR system

The excess sludge is wasted from the end of the aerobic phase for each cycle. A schematic diagram of the SBR system is given in Figure 1. The controls of the duration/sequence of phases and on/off status of peristaltic pumps, mixer and air supply are automatically achieved by a Labview data acquisition and control (DAC) system. The DAC system consists of computer, interface cards, meters, transmitters and solid-state relays. Electrodes for pH, ORP (oxidation-reduction potential), DO (dissolved oxygen), temperature, weight and conductivity are installed and connected to the individual meters. The status of the reactor is displayed on the computer and the time series of the electrode signals are stored in a data log-file. The aeration is controlled by turning on-off the aeration valve. The oxygen is kept around 2 mgO_2/L with an on-off controller with 0.5 mgO_2/L dead band.

Synthetic sewage, which mimicks real pre-settled domestic wastewater (Boeije *et al.*, 1999), is used as SBR influent. Based on the model, the influent wastewater characterization in terms of COD fractions, nitrogen and phosphorus components are summarized in Table 1 whihc is adopted from Boeije, 1999. The measured output variables of ortho-phosphate, dissolved

oxygen, ammonia and nitrate nitrogen were used in the calibration study. The volumetric oxygen mass transfer coefficient, K_La, was measured to be 255 d^{-1}. All measurements were carried out according to Standard Methods (APHA, 1998). In the modeling studies, a modification of ASM2d (Henze *et al.*, 1999) was used by the addition of ammonification and hydrolysis of organic nitrogen processes since the influent wastewater contains soluble (0.45 μm) and particulate organic nitrogen that slowly degrade. The settling and decanting phase were characterized by a reactive point-settler model (Kazmi *et al.*, 2001). The simulations were carried out using the WEST simulation package (Vanhooren *et al.*, 2003).

Table 1. ASM2dN based influent wastewater characterization (adapted from Boeije, 1999).

Component	Unit	Concentration	Measurement
Total COD, COD_{tot}	mgCOD/l	411	Lab. analysis
Particulate Inert COD, X_I	mgCOD/l	18	Lab. analysis
Soluble Inert COD, S_I	mgCOD/l	18	Effluent analysis
Biodegradable COD, C_S	mgCOD/l	375	
Fermentable COD, S_F	mgCOD/l	95	Mass balance
Acetate COD, S_A	mgCOD/l	70	GC analysis
Slowly biodegradable COD, X_S	mgCOD/l	210	Mass balance
Ortho-P, S_{PO4}-P	mgP/l	11	Measurement
Total Kjeldahl Nitrogen TKN	mgN/l	63	Lab. analysis
Ammonium nitrogen, NH_4-N	mgN/l	3	Lab. analysis
Soluble biodegradable nitrogen, S_{ND}	mgN/l	10	Mass balance
Particulate biodegradable nitrogen, X_{ND}	mgN/l	50	Mass balance

3. RESULTS AND DISCUSSION

3.1 Measurement campaign results

On-line measurements were performed in the reactor (Figure 2). The nitrification end point, the consumption of nitrate due to denitrification and the phosphate release can be observed from these measurements (Spagni *et al.*, 2001). The corresponding oxygen, O_2, filtered ortho-phosphate, PO_4-P, the nitrate nitrogen, NO_3-N, and ammonia nitrogen, NH_4-N, measurements are presented in Figure 3 and 4. The nitrite nitrogen was found to be negligible. At the beginning of the fill period, a small increase in the oxygen profile occurred because of an inherent oxygen transfer during the feeding and mixing. The gradual pH decrease under anaerobic (filling) conditions can be explained by the net effect of (slow) phosphorus release and denitrification processes. As soon as the consumption of nitrate in the fill phase is completed (Figure 4), a rapid drop in pH can be observed, probably due to fermentation and phosphate release. During the first aerated period, the oxygen concentration is quite low (around 0.3 mg/l) as a result of high oxygen consumption by biomass for readily biodegradable COD degradation with fixed aeration intensity. The effect of CO_2 stripping on the pH profile seems to be higher than that of nitrification up to the mid of the aerated phase

(Figure 2). The oxygen concentration increased up to the controlled band of 2±0.5 mgO_2/L. In the following phases, it decreased to zero just after the termination of aeration (Figure 2 right).

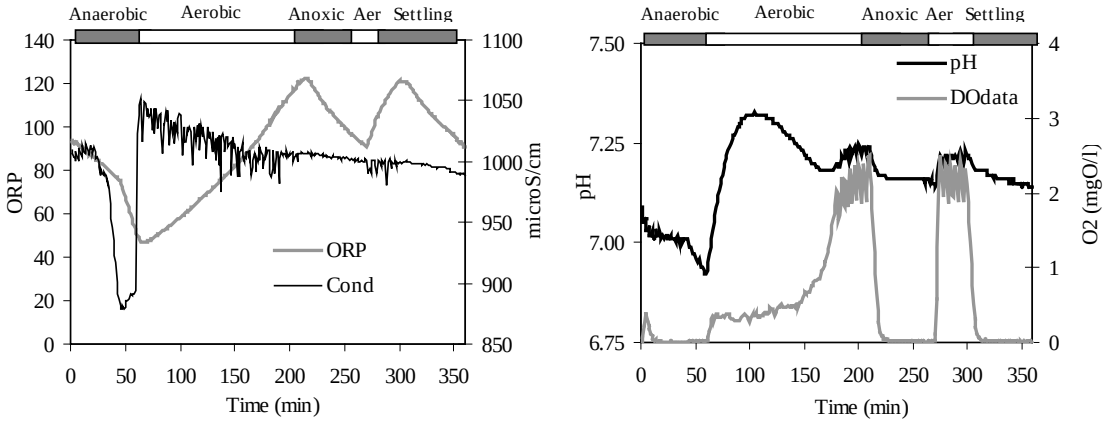

Figure 2. On-line measurements (left) ORP, conductivity and DO, pH (right)

The phosphate concentration increased during the fill phase because of P release (VFA uptake) and filling. Figure 3-right shows that the rate of phosphorus release increased as soon the nitrate was consumed. The remaining VFA was consumed with P-release (Comeau *et al.*, 1990; Kuba *et al.*, 1996). At the end of the first phase, after a steep decline, a gradual increase in the conductivity measurements can be observed after the NO_3 consumption is completed. This can be attributed to phosphorus release which liberates ions into the bulk. In the aerobic phase, the phosphate is taken up again. There is a slight increase in the phosphate concentration during the 2nd anoxic period probably because of endogenous P-release and COD turnover from the endogenous biomass.

The NH_4-N and NO_3-N profiles are quite interesting in terms of their order of magnitude at the end of the aerobic phase (Figure 4-left). The NO_3 generation is much higher than the observed NH_4-N consumption. This observation reveals that organic nitrogen is transformed into NH_4-N and nitrified to NO_3-N directly and that, in fact, only a net NH_4-N conversion rate is measured. Indeed, after the complete oxidation of NH_4-N, the NO_3-N build-up continues until the end of the first aerobic period. So, the degradation of organic nitrogen becomes the rate-limiting step and must be incorporated in the model in such a way that it is controlled by the hydrolysis mechanism. In the 2nd aerobic period, NO_3-N increased from 17 to 20 mgN/L. The organic nitrogen in the effluent water was measured analytically to be around 1.0 mgN/L which is also in agreement with the simulation result (Figure 4-right). It should be stressed that the total phosphate mass balance resulted in a 98% recovery confirming the exact total sludge age of the system. Within the observation period covering the calibration study, consistent long-term data with respect to effluents together with online measurements shows that the system -under constant conditions- is still at steady state and necessitates no more additional validation effort.

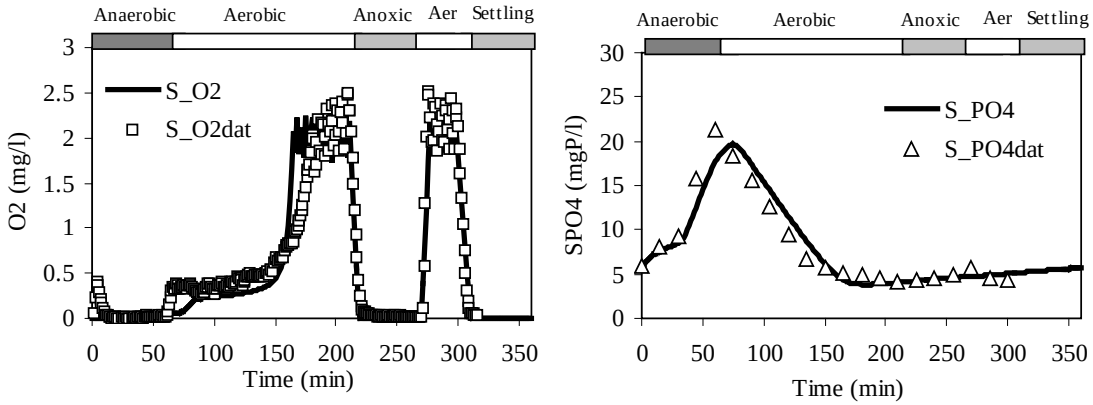

Figure 3. Measurements (symbols) and simulations (lines) of the dissolved oxygen (left) and phosphate (right)

3.2 Model selection

The activated sludge model used was built on the basis of ASM1 and ASM2d (Henze *et al.*, 1987; 1999). According to the influent wastewater characterization, the nitrogen transformations were incorporated as an integral module. An approach similar to ASM1 was used. The particulate nitrogen is first hydrolysed to soluble organic nitrogen, S_{ND}, and then ammonified to NH_4-N by heterotrophic biomass.

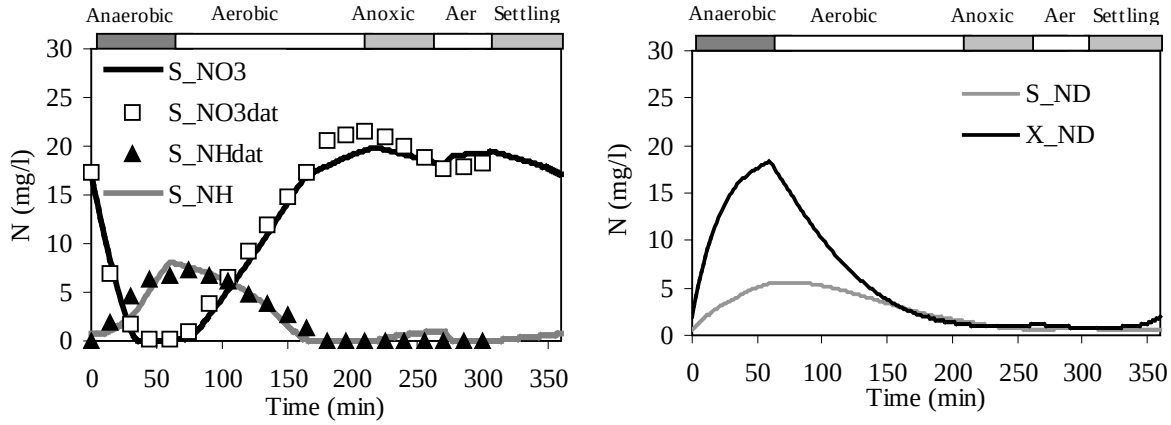

Figure 4. Measurements (symbols) and simulation (lines) of NH_4/NO_3 (left) soluble/particulate nitrogen (right)

The hydrolysis kinetics under anaerobic and anoxic conditions are adapted with correction factors. The kinetics and stoichiometry for autotrophs, the heterotrophs and phosphorus accumulating microorganisms are taken from the ASM2d model except for the anoxic heterotrophic yield, Y_{HNO3}. The default values of the parameters were taken as starting point. The phosphorus components (soluble and particulate) were taken as a fraction of the influent COD

fractions and model components. The conservation of the components was calculated according to Gujer and Larsen (1995).

3.3 Calibration methodology

A step-wise calibration methodology was developed based on long-term simulations in each iteration step (see Figure 5). As illustrated in Figure 5, a calibration methodology based on expert knowledge was constructed by introducing 4 iterative steps in the order of NH_4-N, O_2 , NO_3-N and PO_4-P profiles, respectively. For each iteration, a 30 day-simulation was carried out to ensure that the state variables gave the same trend in each cycle ("steady state"). The starting point is to obtain the proper activity of the autotrophs to generate NO_3-N. In the first long-term simulation with the default parameter values, the autotrophs were washed out from the system. As a result, the nitrogen half saturation coefficient for autotrophs, K_{NHaut}, was decreased because of the low ammonia concentration in the aerobic phase. Next, the maximum growth rate for autotrophs, $\hat{\mu}_A$, had to be increased in order to sustain autotrophic growth. Later on, the oxygen half saturation constants for autotrophs, $K_{NHaut,}$ and heterotrophs, K_{NH}, were changed to promote heterotrophic growth. In addition, the half saturation constant for hydrolysis, K_X, was included in the calibration to get better fitting of the O_2 profile (Figure 3-left). It should be noted here that each iteration step comprises the preceeding steps to maintain good NH_4-N, O_2, NO_3-N and PO_4-P fits.

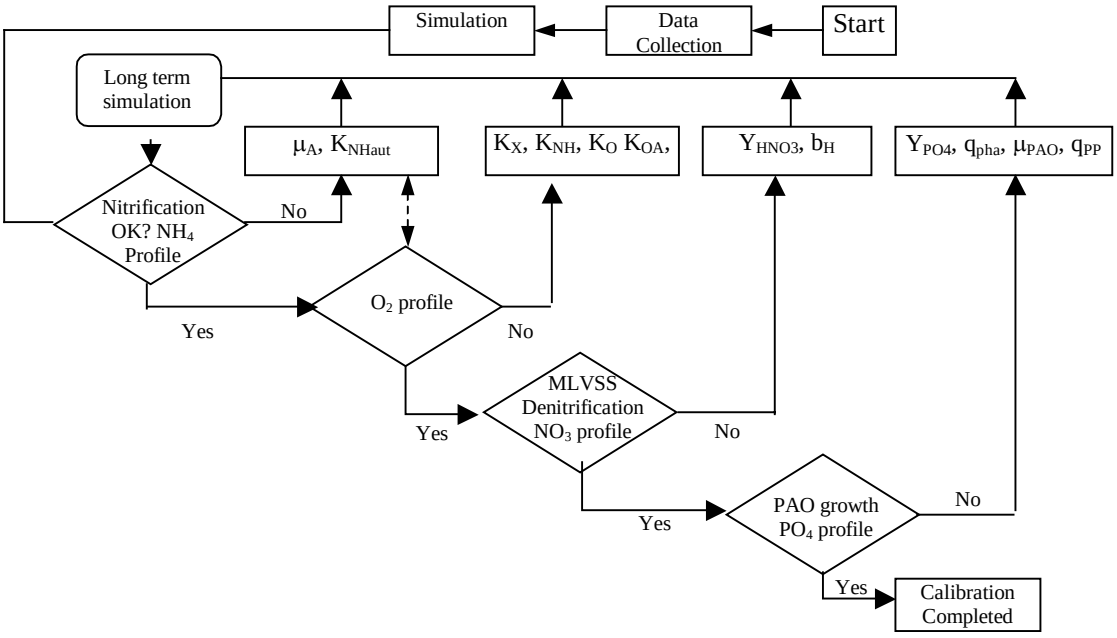

Figure 5. Calibration methodology for the ASM2dN model

In the third step, the anoxic yield was adjusted (0.58 mgCOD/cellCOD) in order to increase the denitrification potential and fit the measured nitrate concentrations. In the literature, the anoxic yield was also reported to be lower than the aerobic yield coefficient (Muller *et al.*, 2003; Orhon *et al.*, 1996). The slope of nitrate during the fill phase was well achieved by the calibration of the

heterotrophic lysis rate, b_H. The MLVSS component could be added to Figure 5, but no additional calibration effort was needed for this case. It was measured and simulated around 2000 mg/l. The simulated soluble, S_{ND}, and particulate nitrogen, X_{ND}, profiles are illustrated in Figure 4-right. Finally, the fourth step deals with the calibration of the kinetic constants for the PAOs. The maximum acetate uptake rate of the PAO's, q_{PHA}, had to be increased in order to have them compete successfully with ordinary heterotrophs during the fill phase in the presence of NO_3-N. The reason is that high NO_3-N concentrations during the first 30 minutes of the fill phase caused a high denitrification rate which consumes VFA before the true anaerobic period begins.

Table 2. Summary of the calibrated ASM2dN parameters

Parameter	Unit	Default	Calibrated
Yield coefficient for phosphate release, Y_{PO4}	MgP/mgCOD	0.4	0.38
Anoxic heterotrophic yield, Y_{HNO3}	MgCOD/mgcellCOD	0.63	0.58
Saturation/Inhibition coefficient for O_2, K_O	mgO/l	0.1	0.06
Saturation coefficient for O_2 (autotrophs), K_{OA}	mgO/l	0.5	0.07
Half saturation constant for hydrolysis, K_X	MgCOD/mgcellCOD	0.1	0.045
Endogenous decay rate for heterotrophs, b_H	day^{-1}	0.4	0.45
Rate constant for storage of PHA, q_{PHA}	gCOD/gPP.d	3.0	6.0
Maximum growth rate for PAOs, μ_{PAO}	day^{-1}	1.0	1.8
Maximum growth rate for autotrophs, $\hat{\mu}_A$	day^{-1}	1.0	1.5
Maximum phosphorus storage rate, q_{PP}	gP/gcellCOD.d	1.5	1.3
Half saturation constant for ammonia (heterotrophs), K_{NH}	mgN/l	0.05	0.01
Half saturation constant for ammonia (autotrophs), K_{NHAUT}	mgN/l	1.0	0.2

The yield for phosphate release, Y_{PO4}, had to be decreased to fit the fill-phase PO_4-P profile. As stated in the ASM2d model, the storage compound, X_{PHA}, is consumed by two simultaneous processes, i.e. the phosphate uptake and the growth of PAOs. During calibration, the concentration of X_{PAOs} was increased by adjusting the maximum growth rate of PAOs, $\hat{\mu}_{PAO}$, to a higher value. Meanwhile, to achieve steeper slope and also to reach the constant PO_4 concentration at the end of the aerobic phase, the maximum phosphate uptake rate, q_{PP}, was increased (Figure 2-left). The calibration task was terminated when the simulated profiles were closest to all measured data (see Figure 2-4). The values of the calibrated parameters together with their default values are listed in Table 2.

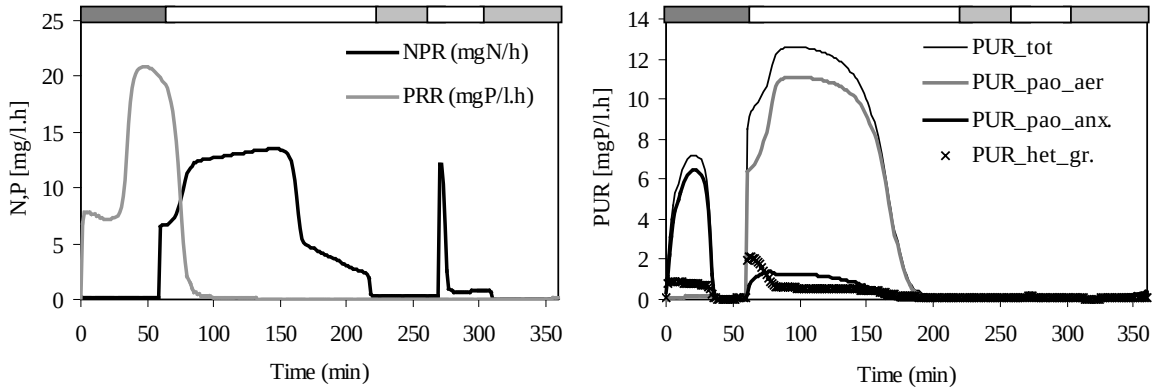

Figure 6. Nitrate production, P-release (left) and segments of phosphate utilization rate (right)

3.4 Systems analysis

Using the calibrated model, the trajectories of the process rates were drawn to visualize the contribution of each process to the overall SBR behaviour. It is obvious from Figure 6-left that the P-release rate after the mid of the fill phase is 2.5 times higher (21 mgP/l.h) than that at the beginning of the phase (7.5 mgP/l.h) because of the removal of NO_3-N. This continues until the external carbon source is consumed completely after around 100 min and the oxygen concentration increases. The nitrate production rate, NPR, immediately increased when aeration is turned on. The rate dropped from 13 mgN/l.h to around 5 mgN/l.h when it became hydrolysis limited. The simulation for the total phosphate utilization rate, PUR, reveals that the maximum contribution pertains to the aerobic phosphate uptake by the PAOs (73% of the overall P uptake) initially exhibiting an uptake rate of 11 mgP/l.h (Figure 6-right). As can be observed from Figure 6-right and Figure 7, P-release, anoxic P-uptake and VFA storage took place simultaneously. It is important to mention here that 19% of the removed P is taken up by the denitrifying PAOs during the fill phase (12%). In the aerobic phase 7% of P is removed (Figure 8). The rate of the anoxic P uptake at the start of the aerobic phase was simulated to be around 1.4 mgP/l.h. The P uptake via heterotrophic growth only covers 8% of the overall P-removal (growth of nitrifiers is neglected).

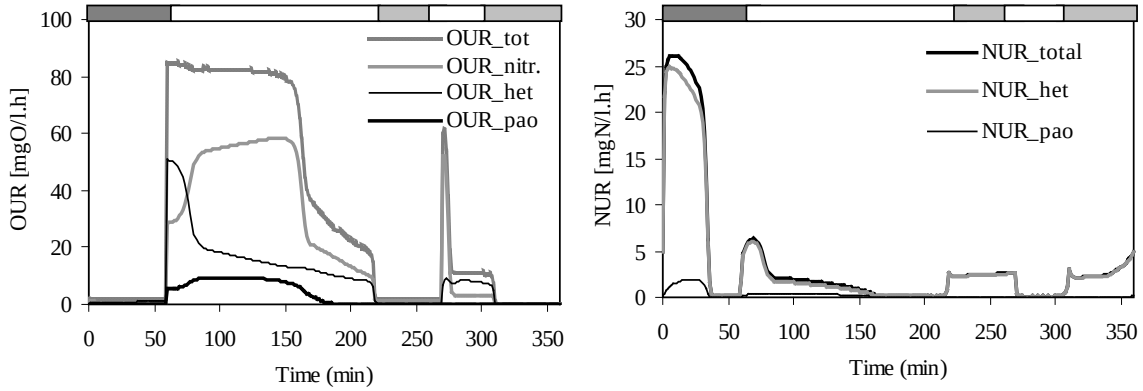

Figure 7. OUR and NUR contributions in a SBR cycle

According to the simulation results, the distribution of denitrified nitrogen over each of the phases can be summarized as follows: (a) 61% of total denitification took place in the first phase (fill phase), (b) 17% was denitrified under aerobic conditions due to simultaneous nitrification-denitrification (Münch *et al.*, 1996), (c) 10% denitrification was achieved in the 2nd anoxic period and (d) 10% denitrification in the settling phase. The simulation based calculations showed that 22 mg/L NO_3-N was denitrified in one cycle which is comparable with the denitrification potential calculation performed according to Artan *et al.* (2001) which led to a value of 18 mgN/l. This difference can be explained as follows. First, it should be acknowledged that the 22 mg/L does not regard the denitrification potential used by the PAOs. Another point is the additional denitrification in the aerobic phase due to low oxygen levels. This is not considered in the stoichiometric calculation. The nitrate utilization rate, NUR, is mainly governed by ordinary heterotrophic activity, i.e. 89% of the total denitrified nitrogen is used up by these microorganisms. Only 11% is consumed in denitrifying PAO activity (Figure 7- right).

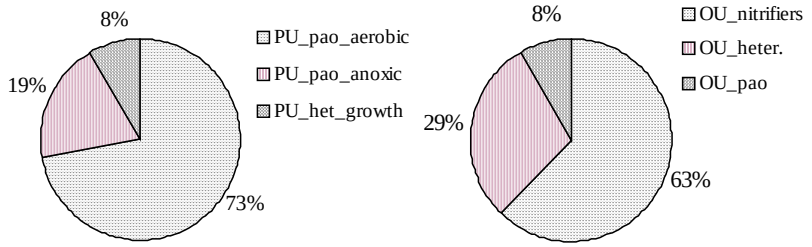

Figure 8. The phosphate and oxygen utilization in one SBR cycle

The maximum total oxygen uptake rate, OUR, is around 82 mgO_2/l.h until 150 min (nitrification end point) and is governed by the oxygen transfer capacity. Within the aerobic phase, the maximum oxygen uptake rates for the autotrophs, heterotrophs and PAOs are around 50, 50 and 10 mgO_2/l.h, respectively. However these maximum rates are reached in different periods of the aerobic phase (see Figure 7). The distribution of cumulative oxygen consumptions over the processes is given in Figure 8-right. The autotrophic biomass accounts for 63% of the total oxygen consumption of the system. The ordinary heterotrophs only consume 29%.

4. CONCLUSIONS

A systematic model calibration methodology was applied successfully to a lab-scale SBR exhibiting simultaneous nitrification-denitrification together with biological phosphorus removal, the so-called 'simultaneous nutrient removal'. The biological processes described in the model were found to occur simultaenously under limited aeration conditions. A low oxygen transfer inherently differentiates the system behaviour from systems under traditional design calculations. As a result, the oxygen transfer should strictly be incorporated in the calibration of biological nutrient removal

to visualize the individual contributions of each process. From this point of view, models may serve as practical tools to evaluate alternatives for the optimization of SBR's. The stepwise calibration methodology applied here is necessary for an effective selection of the relevant parameters to be calibrated.

The systems analysis performed with the calibrated model clearly illustrated that the denitrification at the start of the aerobic phase and during the settling phase has a considerable contribution to the overall denitrification capacity of the system and also affects biological phosphate removal. It therefore warrants further study.

5. ACKNOWLEDGMENTS

This research was financially supported by the Fund for Scientific Research–Flanders (F.W.O.) and the Ghent University Research Fund.

Chapter 5.2

Long-term prediction performance of a calibrated model of an intermittently aerated carrousel plant

ABSTRACT

To gain a better insight and increase confidence in full-scale application of activated sludge models (ASMs), it is very important to have an idea about the life-time of a calibrated model in view of adequately predicting dynamic behaviour of complex wastewater treatment plants (WWTP). In other words, how long and to what extent does a calibrated model remain valid within the frame of adequately representing a WWTP? To address this question, a mathematical model (ASM2d) was calibrated for a municipal wastewater treatment plant (Haaren WWTP, The Netherlands) using a dynamic measurement campaign data (MC1) collected 3 years ago. The calibrated ASM2d model was then used to predict the current dynamic performance using a new measurement campaign (MC2) data. The BIOMATH protocol (Chapter 2) was used in each case to ascertain a standard/systematic calibration procedure.

The calibrated model was observed to remain largely valid over this long-term and was as such able to successfully predict the dynamics of MLSS and NO_3-N in the treatment plant measured 3 years after the calibration period. On the other hand, PO_4-P and NH_4-N trends in the treatment plant could be better predicted by adjusting a few relevant parameters without compromising the good model-fits on the measured MLSS and NO_3-N trends. The results obtained in this study particularly suggest that the life cycle of a calibrated model is compatible with the life cycle of a WWTP (in this case, Haaren WWTP). This is expected to stimulate confidence in mechanistic modelling of WWTPs and the use of calibrated models for further applications e.g. optimisation, upgrade or design of WWTP. However, a detailed characterisation of the influent wastewater (i.e model input) was observed to be the key to a successful model calibration, i.e. it directly determines the quality of the model outputs. Since in both measurement campaigns summer conditions prevailed, the model response (i.e. its prediction performance) should also be checked for different seasons, i.e. winter, spring and autumn.

This chapter is i*n preparation* for publication.

1. INTRODUCTION

Since the promulgation of the EU Directives (91/271/EEC) regarding strict discharge standards for nitrogen and phosphorus, especially in sensitive areas, appropriate design and plant optimisation issues are gaining more importance. Activated sludge plants are the most commonly used technology for removing organic carbon and nutrients (N, P) from domestic and/or industrial wastewaters to meet the discharge criteria. In general, a number of process alternatives have been proposed. Among these alternatives, carrousel systems are associated with plants for small communities, where stability and simplicity of operation are of prime importance in the absence of primary clarification (Grady *et al.*, 1999; Randall *et al.*, 1992). The stability of treatment efficiency, especially with regard to nutrient removal, is often difficult to achieve due to the complex characteristics of biological processes.

The features that distinguish carrousel type systems from other conventional activated sludge plants are (a) it is operated with high sludge age, (b) it has a simplified flow diagram and (c) it possesses channel (plug) flow characteristics. The system provides not only well-stabilized sludge but also flexible operation (i.e. aeration control) alternatives under dynamic conditions. In order to provide phosphorus removal and to prevent excessive growth of filamentous microorganisms, anoxic or anaerobic selectors are introduced prior to the aerobic/anoxic reactors. Another option can be the intermittent feeding or aeration of the mixed liquor (Grady *et al.*, 1999; Randall *et al.*, 1992).

The optimisation of the operation of an activated sludge plant using a model-based approach necessitates successful and reliable calibration of the dynamic mathematical models. In literature, many mathematical models have been used to describe the biological processes. The models concerning carbon and nitrogen removal are described by ASM1 and ASM3 (Gujer *et al.*, 1999). Enhanced Biological Phosphorus Removal (EBPR) together with carbon and nitrogen removal are described by other models (Wentzel *et al.*, 1992; Henze *et al.*, 1995,1999; Barker and Dold, 1997). Metabolic models for EBPR were also proposed which include the maintenance of biomass as a separate process (Smolders *et al.*, 1994; Murnleitner *et al.*, 1997; Filipe and Daigger, 1998).

Several studies have been conducted concerning the calibration of the Enhanced Biological Phosphorus Removal (EBPR) type activated sludge plants, as described by the ASM2 and ASM2d models (Cinar *et al.*, 1997; Carrette *et al.*, 2001; Makinia *et al.*, 2001). From a modelling point of view, the data collection with regard to influent wastewater, environmental influences (i.e. temperature changes) together with biomass characterization play a crucial role to increase the reliability of the model that will be used for retrofitting or process optimisation. On top of that, difficulties in the calibration of the treatment plant are encountered very often because of the limitations in available plant information and the over-

parameterized (too complex) structure of the mathematical models (Ayesa *et al.*, 1995; Weijers and Vanrolleghem, 1997; Brun *et al.*, 2002; Reichert and Vanrolleghem, 2002). Consequently, prior to the calibration, a measuring campaign should be designed in order to collect informative data from the treatment plant (Chapter 2).

In literature, several calibration protocols have been proposed namely STOWA protocol (Hulsbeek *et al.*, 2002), HSG guidelines (Langergraber *et al.*, 2003a) and BIOMATH protocol (Vanrolleghem *et al.*, 2003; Chapter 2). The STOWA protocol is tailored for the SIMBA simulation software and based on extensive experience obtained from dynamic modelling of over 100 activated sludge treatment plants in the Netherlands (Hulsbeek *et al.*, 2002). The HSG guidelines (Langergraber *et al.*, 2003a), on the other hand, summarize the experience of university members from Germany, Austria and Switzerland with the simulation of dynamic activated sludge models. The BIOMATH calibration protocol is based upon the work of Petersen *et al.* (2002b) with dynamic modelling of WWTPs in Belgium and extended in Chapter 2 for general applications. The above-mentioned calibration protocols have a common target: to provide a standardized approach for the calibration of dynamic activated sludge models and thereby to facilitate the application of dynamic models into practice. Subsequently, it is hoped that the standardized approach will improve the calibration accuracy and provide a basis for quality control/reliability check and comparisons between different calibration studies (Hulsbeek *et al*., 2002; Langergraber *et al*., 2003a; Chapter 2).

These protocols differ in their approaches to reach this common target. The STOWA protocol proposes a physical-chemical method combined with BOD measurements for the characterization of influent wastewater (Hulsbeek *et al*., 2002) and it provides a detailed and step-by-step approach for the implementation of a calibration study. The HSG guidelines, on the other hand, focus more on the systematic and detailed documentation of the calibration study rather than providing a detailed procedure on how to calibrate a mathematical model (Langergraber *et al*., 2003a). Finally, in the BIOMATH protocol, a dynamic calibration procedure based on interactive modules is proposed which aims to obtain a minimum effort and cost-effective calibration. To this aim, the calibration procedure was made flexible and interactive where different choices are provided to the user corresponding to different levels of calibration accuracy. Moreover, the optimal experimental design (OED) concept is incorporated at different levels of the calibration procedure in order to provide a cost-effective and information rich experimental designs. In this study, the BIOMATH calibration protocol is applied/followed to ascertain a standard approach for calibrating the activated sludge model in this study it is ASM2d.

An important step in modelling is the validation step, which is a long disputed and controversial issue. In this step, the objective is to check the ability of a calibrated model to

predict the behaviour of a treatment plant under operating conditions (drastically or gradually) different than the calibration period. On the other hand, there is no general agreement on how to validate a model for dynamic activated sludge treatment plants in the above-mentioned calibration protocols (i.e. concerning data collection frequency, period and duration etc.).

From a model-validation point of view, a significant question arises as to what extent/how long a calibrated and/or validated model does indeed represent/predict the behaviour of a treatment plant. In other words, what is the evolution/fate of a calibrated model in time in view of its prediction performance? This aspect of modelling is particularly important in order to ascertain the reliability of a model in view of its long term applicability/performance to simulate the behaviour of the complex WWTP systems before full-scale implementation purposes e.g. process upgrade, optimisation, control or design purposes. To this aim, this study focuses on the evolution of a calibrated model in time. In other words, the validity of a calibrated model is monitored over a long-term with separate and dedicated measurement campaigns to understand and therefore assess the need for re-calibration of the model.

The objective of this study is tested at a municipal wastewater treatment plant located in the Netherlands (Haaren WWTP). A mathematical model (ASM2d), which was calibrated with the measurement campaign (MC1) data performed 3 years ago (Insel *et al*., 2003b), is used. A new measurement campaign (MC2) following the BIOMATH protocol (Chapter 2) is performed for this study to collect information rich dynamic data for validation and/or re-calibration of the Haaren WWTP. It is important to note that the operation strategy of the Haaren WWTP remained the same over the last three years but that influent dynamics were naturally different over past 3 years. The report is structured as follows: First the results of the new measurement campaign (MC2) are given in comparison with the first measurement campaign (MC1). This is followed by the comparison of the predictions/simulations of the model calibrated on the basis of the treatment plant dynamics obtained in the first measurement campaign (MC1) (Insel *et al*., 2003b). Then, the calibrated model is simulated with the new input dynamics obtained from the second measurement campaign (MC2) and the simulation results are compared to the treatment plant performance obtained in the second measurement campaign (MC2). In other words, the validity of the model is evaluated. That means that the long-term prediction ability of the calibrated model (in other words the fit of the calibrated model to the second measurement campaign (MC2) designed 3 years later) is evaluated and the issue of re-calibration of the model is addressed. Finally, the model is re-calibrated and the simulation results are compared to the performance of WWTP in the second measurement campaign (MC2). Last, the recalibrated model is used to understand in depth the dynamic nutrient removal performance in the Haaren WWTP.

2. MATERIALS AND METHODS

2.1 WWTP Definition

The treatment plant under study is located near Haaren, Noord-Brabant, the Netherlands. The activated sludge plant is a carrousel type plant receiving the wastewater of 50000 PE. The average daily influent flow rate of the plant was recorded to be 6500 m^3/day (the average of 4 days during the measurement campaign). An anaerobic selector is present prior to the carrousel tank in order to prevent sludge bulking. The carrousel plant consists of one anaerobic reactor, 2 carrousels and 6 clarifiers. The carrousel reactors are operated in parallel and basically the system has two lanes after the anaerobic selector. In case of high hydraulic loadings, the influent flow bypasses the anaerobic selector and is equally distributed to the carrousels.

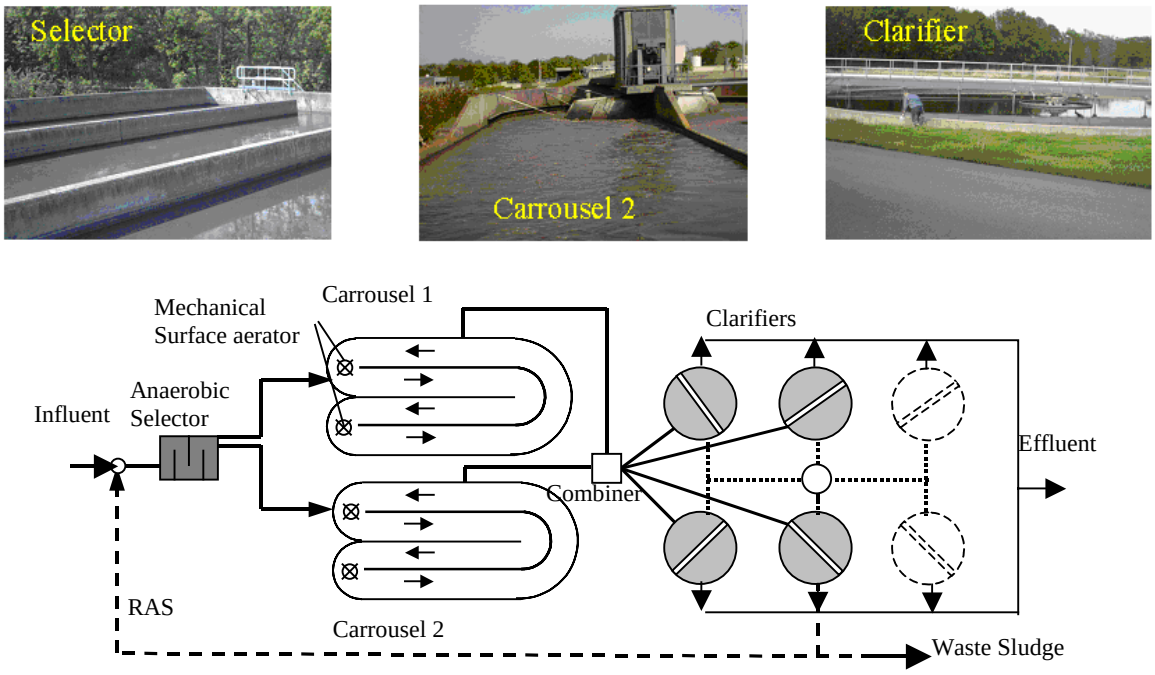

Figure 1. Schematic diagram of the activated sludge plant

Four out of 6 clarifiers are operational under average daily flow loading. The sludge recycle is controlled in order to avoid sludge overflow from the weirs of the clarifiers. During average daily flow loading 4 recycle pumps are activated and the sludge recycle is controlled with these pumps according to manual SVI measurements. The total maximum capacity of the recycle pumps is 600 m^3/h under heavy rain events. The volumes for the anaerobic compartment (1), carrousels (2) and the clarifiers (4), are given in total as 1400 m^3, 10000 m^3 and 2460 m^3 respectively. The operational SRT of the system is around 22 days. The overall hydraulic retention time of the system is 1.8 days.

2.2 Operation/control strategy

The dissolved oxygen concentration is simultaneously controlled in both carrousels. The control strategy is different for day and night operation. During the day period, the 2 aerators in each carrousel are manipulated to keep the dissolved oxygen concentrations in the range between 0.9 mg/l and 1.2 mg/l. In the course of the night period, the carrousels are operated as an alternating plant by turning the aeration on/off in so-called intermittent aeration to stimulate denitrification. In this alternating aeration period, the total cycle time, T_C is set to 110 minutes. The aeration is shut off during 80 minutes and turned on for 30 minutes. In each 30 minutes aeration period, the aerators are operated as during the day period and the dissolved oxygen is controlled in the range of 0.9-1.2 mgO_2/l. It should be noted that during the intermittent aeration one of the aerators was kept at its maximum level (low O_2 transfer) for keeping the MLSS in suspension. The average internal mixed liquor recycle rate in the carrousel is calculated as 635,040 m^3/day which is 108 times the influent flow rate leading to a typical flow velocity of 0.3 m/s. The average sludge recirculation rate (Q_R) through the anaerobic selector is calculated as 8434 m^3/day.

2.3 Measurement campaigns

In the framework of this study, dynamic plant data obtained from 2 different measurement campaigns were used in order to check the success of the prediction of the model as mentioned above. In the first measurement campaign (MC1), an intensive rain event happened just before the first measurement campaign (see Figure 2), which does not reflect the real plant efficiency under daily average loading (Insel *et al*., 2003b). In this respect, the second measurement campaign (MC2) was conducted under dry weather conditions. It is used as a validation data set for the calibrated model (Insel *et al*., 2003b) to give an idea on the real average removal efficiency without any external disturbances. Both measurement campaigns were performed in the summer period.

2.3.1 First measurement campaign (Insel et al., 2003b)

The measurement campaign data comprises the dissolved oxygen (DO), NO_3-N (both on-line); effluent ortho-phosphate and TSS concentrations (lab analyses) in the carrousel for a period starting from 17/07/2000 till 25/07/2000 corresponding to day 7 and 14, respectively. The total/filtered (0.45μm) COD, VFA, BOD_u, total/filtered TKN, NH_4-N, total/filtered phosphate and TSS measurements were performed with a grab sampling interval of 4 hrs during the measurement campaign period. The temperature of the mixed liquor was reported in the range of 17.2-19.2 ^{0}C. The average wastewater and COD characteristics used for the steady state analysis are given in Table 1. The nitrate and the oxygen concentrations were measured in Carrousel 1 with a sampling interval of 15 and 5 minutes, respectively. The ortho-phosphate analyses were performed every day from the effluent of the clarifier. The daily samples for filtered phosphate samples were taken from the effluent.

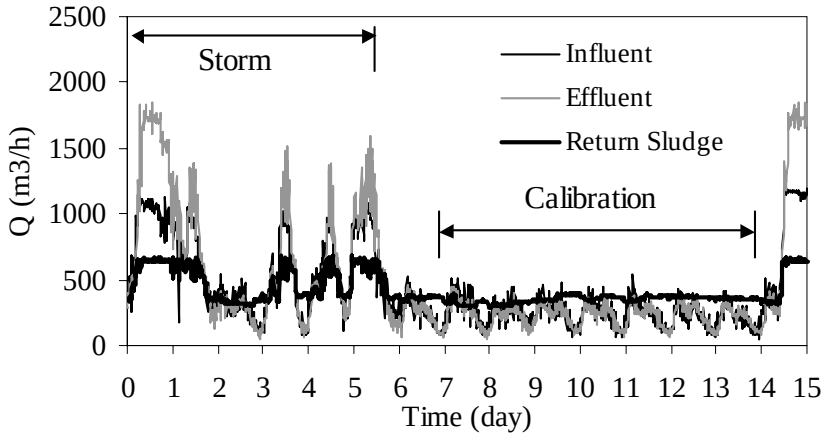

Figure 2. Influent, effluent and RAS flow-rates in the 1st Measurement Campaign (Insel *et al.*, 2003b)

2.3.2 Second measurement campaign (MC2)

The MC2 data comprise on-line DO, NO_3-N and NH_4-N measurements; ortho-phosphate from the selector and the effluent of the plant for 4 days starting from 16th to 19th June 2003. In addition, the total/filtered (0.45μm) COD, VFA, BOD_u, total/filtered TKN, NH_4-N, total/filtered phosphate and TSS measurements for influent wastewater characterisation were also measured from the grab samples taken at different frequencies and locations (see below) during the measurement campaign period. The temperature of the mixed liquor was around 19 ^{0}C. The average influent wastewater characterization, which was used for the steady state analysis is given in Table 1 in the results section below. In addition, flow-rates of the influent, RAS and WAS were also collected from the SCADA system (see Figure 3) and quality of the flow data was checked and improved (see Annex). No sludge blanket was observed during the course of the measurement campaign.

The measurement campaign was designed based on expert knowledge and system analysis (Vanrolleghem *et al.*, 2003; Chapter 2). However, the application of OED as a tool for designing the optimal measurement campaign should be considered for the future studies in order to save cost and time associated with measurement campaigns (Chapter 2). The following sampling frequency and measurements were performed between 16/07/2003 and 19/07/2003:

Influent to the selector: 4-hours flow proportional composite samples were taken automatically every 4 hours (in total 6 samples/day) for the analysis of influent COD, $COD_{filtered}$, TKN, TKN_{filt}, TP, PO_4^{3-}, TSS and VSS. Grab samples were also taken two times a day from the influent for the analysis of BOD, COD (for determination of biodegradable fraction of COD i.e. influent BOD_u/COD_{tot} ratio), VFA (for the determination of VFA/COD

ratio) and NO_3. All the grab samples except for the BOD were filtered in-situ and preserved according to the Standard Methods (APHA, 1995).

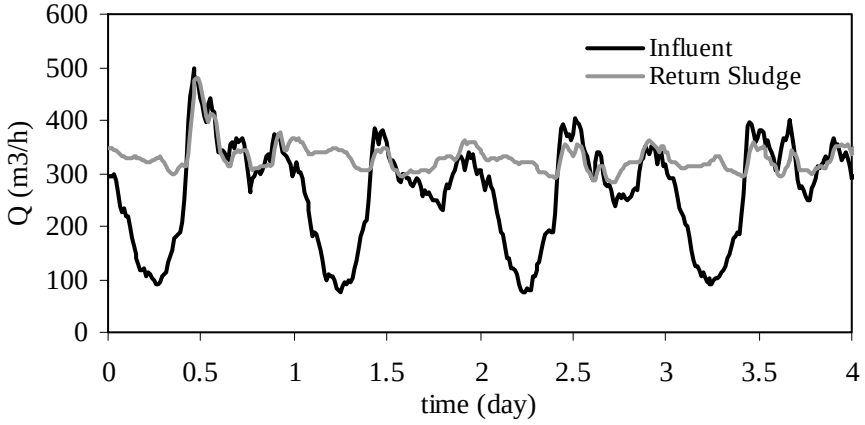

Figure 3. Influent, effluent and sludge recycle flowrate in the 2nd Measurement Campaign

Selector: Two grab samples per day from the first compartment of the selector and two grab samples a day from the output compartment of the selector were taken and manually filtered in situ. These grab samples were used for the analysis of NO_3-N, PO_4^{3-} and VFA in the selector.

Carrousel: 3 grab samples were taken per day and manually filtered for the analysis of PO_4^{3-} and 1 sample per day was taken for the analysis of the COD, TKN, TP (used for determination of the TKN/COD and TP/COD content of the MLSS), MLSS and MLVSS. Moreover, online ammonium and nitrate sensors were positioned next to each other in the 8th compartment of the carrousel (see Figure 5) for the online measurements at 15 minutes interval. One on-line DO sensor, positioned in the middle of the carrousel (6th compartment), provides data every 5 minutes.

Return activated sludge (RAS): One sample was taken manually per day for the analysis of TP and MLSS (used for the mass balance and to check the system SRT). In addition, one sample was also taken every day from the waste activated sludge line for the analysis of TP and to calculate the actual sludge age of the system.

Effluent: 8 hours flow proportional composite samples were automatically taken everyday for the analysis of effluent TSS, COD, TKN, NH_4 and NO_3. One grab sample was also taken every day for the measurement of effluent BOD, COD (for the effluent BOD/COD ratio) and TP (needed to check the system SRT).

In addition, on June 18th 2003 the frequency of the grab samples in the influent, selector and carrousel was doubled (from 2 to 4 samples per day). The reason was simply to monitor the fast dynamics (if any) in the system with grab samples. The sample preservation, transport and analysis were all performed according to Standard Methods and/or Dutch standards unless otherwise mentioned. For the filtering, 0.45μm nylon filters (Millipore) were used. VFA analyses were performed using gas chromatography. BOD measurements were performed with OxiTop (WTW).

2.4 Calibration Methodology

The calibration of the activated sludge plant comprises three main steps (Petersen *et al.*, 2002b; Chapter 2). These are (a) *simple steady state calibration* (b) *steady state calibration* and (c) *dynamic calibration* steps. According to the proposed method, the first step concerns the *simple steady state calibration* after gathering the necessary information about the plant. This step mainly deals with the overall sludge balance over the system. In general, the aim is to obtain and maintain the measured sludge concentration with the simulations. In the simplified layout that is used for this calibration step (Figure 4), S1 and S2 delineate the two sections of the selector (an anoxic and an anaerobic zone) with a total volume of 1400 m^3. Compartments C1 (Aerobic) and C2 (Anoxic) represent the carrousels with a total volume of 10000 m^3. It should be noted here that the DO controllers are not modelled at this stage. Instead, the dissolved oxygen in the aerated reactors was set to 1.2 mg/l. The final clarifier was considered as a point settler in which the solids removal efficiency is almost 100%. In this step, the sludge wastage was estimated under steady state loading (flux based average). During the *steady state calibration* and the *dynamic calibration* steps, the aim is to mimic the real activated sludge plant together with the control strategy under steady state and dynamic loadings.

It should be noted that the parameters that are influential to the biomass compositions e.g. Y_H, b_H and/or X_I were changed only during *the simple steady state* and *steady state calibration* steps. During the dynamic calibration these parameters remained unchanged. For the steady state and dynamic calibration, a more complex layout was devised to reflect the plug flow characteristics of the bioreactor (Figure 5).

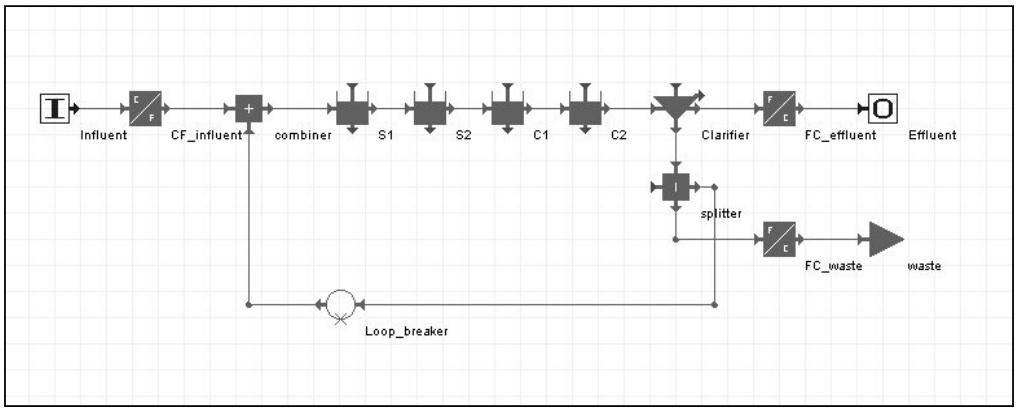

Figure 4. Plant layout for simple steady state calibration (WEST)

According to Abusam and Keesman (1999) the number of CSTRs in series is suggested to be limited to 10 reactors or to the minimum number needed for adequate modelling of the aeration configuration for closed loop reactors. In this respect, the anaerobic and the carrousel reactor were regarded as 4 (S1-S4) and 8 compartments in series (C1-C8), respectively based upon the plant geometry, DO measurements along the reactor and reactor geometry (Figure 5).

The sludge age calculation is of great importance for BNR plants because the TSS balance, active fraction of the biomass and internal storage products are highly influenced by cell residence time (Henze *et al.*, 2002; Rodrigo *et al.*, 1996). Both authors suggest that the most appropriate sludge age for BNR plants is around 20 days. In this study, a mass balance for TP is performed using the TP measurements in the influent, effluent and WAS to verify the SRT of the system, which was found to be around 22 days (see Annex).

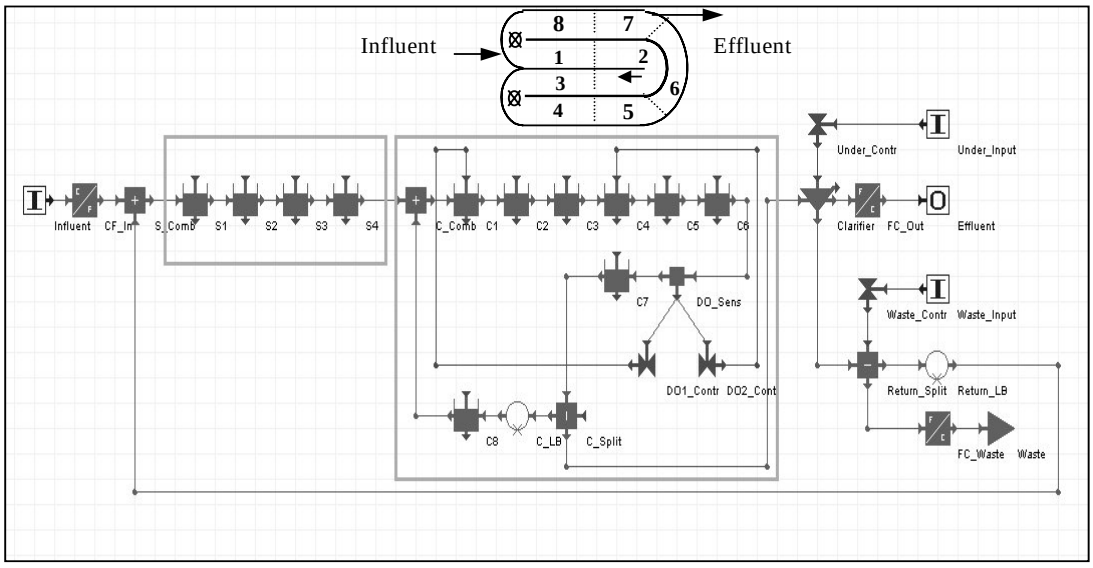

Figure 5. Plant layout implemented in WEST software

In the *steady state calibration*, a flux-based average steady state influent file was applied. The simulations were carried out to find out the initial biomass composition in the reactors under steady state loading that would fit the average measured N, P concentrations. This approach provides the initial values for the state variables that were then used in dynamic simulations. Dynamic simulations were carried out with the dynamic influent file. In order to mimic the smoothing effect of the final clarifier on the effluent N, P concentrations, a non-reactive mixed tank with a 2460 m^3 volume was introduced after the point settler (not shown in Figure 5). The two identical lanes of the activated sludge plant and the clarifiers were combined together in order to decrease the computation time. The model implementation (ASM2d) and simulations were performed using a dedicated simulation package WEST (Vanhooren *et al.*, 2003).

3. RESULTS AND DISCUSSION

3.1 The results of the second measurement campaign (MC2)

3.1.1 Determination of degradable fraction of influent COD

The biodegradable fraction of the influent COD was measured for the first day and second day of the measurement campaign (16-17/06/2003). The BOD was monitored for 28 days respectively and plotted together with the model-fits (see Figure 6). The ultimate BOD, BOD_U was estimated by fitting the following BOD model (Metcalf and Eddy, 1991; Weijers, 1999):

$$BOD_t = BOD_U (1- e^{-kt}) \qquad \text{Eq.1}$$

where t is time, k is the first order degradation constant and BOD_t is the BOD at any time t. The two BOD measurements indicate at least two phases (see Figure 6). In the first phase, the degradation rate of the organic carbon compounds is very fast suggesting that this might be the S_S fraction of the COD (e.g. VFA). This is followed by a slower degradation of the organic which might corresponds to the X_S fraction of the COD. These observations are supported by the study of Weijers (1999) where the BOD curves were analyzed using a simplified ASM1 model for aerobic conditions.

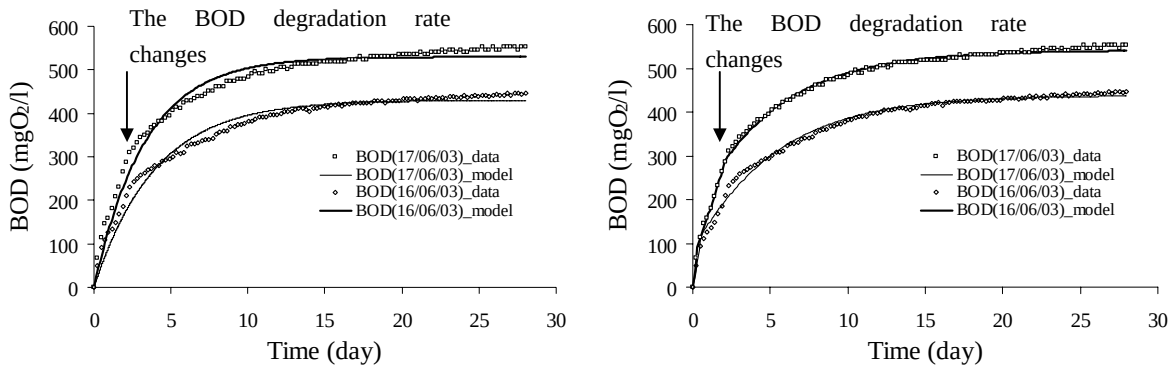

Figure 6. The BOD_U results of the influent grab samples taken at 16/06/2003 and 17/06/2003 respectively and the model fits (left) BOD model (Eq.1) (right) simplified ASM1 model. Note that only every third data points of the BOD measurements is shown in the figure for the sake of clarity.

The model fit to the BOD measurements is observed to be remarkably better using the simplified ASM1 model (see Figure 6-right) than the traditional BOD model given in Eq.1 (see Figure 6-left). The degradable fraction of the influent wastewater predicted by the BOD model was lower (around 6%) than the value predicted by the simplified ASM1 model. This is in contrast to the findings of Weijers (1999) where the BOD_U was clearly higher than the degradable COD, COD_{DB} predicted by the ASM1 model. This discrepancy between the BOD_U and COD_{DB} in this study can be attributed to the fact that the fit of the BOD model to the data (see Figure 6-left) was not as good as the fit of the ASM1 model (see Figure 6-right). It is clearly seen that the BOD_U was underestimated compared to the measurements (see Figure 6-left). This poor fit of the BOD model may have caused the underestimation of the BOD_U.

Table 1. BOD_U estimation results using BOD and simplified ASM1 models and degradable fraction (BOD_U/COD) of influent wastewater. Degradable COD, $COD_{DB} = S_S+X_S$

		BOD model			Simplified ASM1	
Sample	COD	BOD_U	k	BOD_U/COD	COD_{DB}	COD_{DB}/COD
	mgO_2/l	mgO_2/l	d^{-1}		mgCOD/l	
16/06/2003	590	430	0.25	0.73	460	0.78
17/06/2003	710	530	0.3	0.75	561	0.79
Average	650	480	0.275	0.74	510	0.785

In this study, the degradable fraction of the influent COD was determined to be 76% by taking the average of the estimate of both models (BOD model and simplified ASM1, see in Table 1). This value is relatively high which also means that less inert COD is present in the influent compared to other WWTP calibration studies performed in the Netherlands (Roeleveld and Van Loosdrecht, 2002; Weijers, 1999).

3.1.2. Endogenous decay rate of the biomass

To determine the decay rate, the endogenous respiration of the biomass is monitored under continuous aeration for about 15 days in a 2 L batch reactor. As nitrification inhibitor 30 mg/l ATU was added to the batch reactor. The pH and temperature of the reactor were monitored and observed to remain relatively constant around 7.12 and 18.6 ^{0}C respectively.

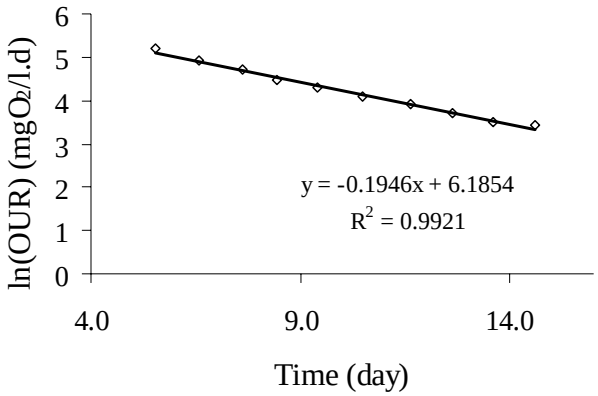

Figure 7. Endogenous respiration rate (OURend - ◊) of biomass over 15 days and the model-fit to the data (—). ATU (30mg/l) is added to inhibit nitrification.

The OUR measurements were started at the 5th day to ensure that the slowly degradable COD, X_S, and internal storage products of the biomass, X_{STO}, present in the mixed liquor were depleted considerably. The experimental results and the model-fit are shown in Figure 7. The aerobic endogenous decay rate of the biomass $b_H^{'}$ was determined to be 0.195 d^{-1} which is well in the range reported in the literature (Henze *et al*., 2000).

The endogenous decay rate corrected for the death-regeneration model of ASM2d (Henze *et al*., 2000) can be calculated straightforwardly to be 0.39 d^{-1} assuming Y_H is 0.63 and f_{XI} is 0.2 (see below). This value is very much close to the default value of the ASM2d (Henze *et al*., 2000) hereby supporting the use of default values of ASM models in case of lack of experimental data.

$$b_H = \frac{b_H^{'}}{1 - Y_H(1 - f_{XI})} = 0.39 \text{ d}^{-1}.$$

3.1.3 Average influent wastewater characterization (flux-based)

The average influent wastewater composition (flux-based) was calculated for the 1st and 2nd measurement campaigns and is given in Table 2. The strength of the influent wastewater in terms of total COD and TP for the 2nd calibration period is higher than that of the 1st calibration period while the TKN concentrations are almost the same (see Table 2). This can

be attributed to the heavy rain event that took place just before the 1st measurement campaign or a change in the wastewater composition in time (see Insel *et al*., 2003b). The prediction of effluent quality of the treatment plants is highly dependent on the COD/TKN and COD/TP ratio as well as the fractionation of the COD components. As stated in Grady *et al.* (1999) and Randall *et al., (*1992), 8-10 mgVFA-COD/l is necessary for the removal of 1 mgP/l from wastewaters. It should be noted here that 6-8 mg VFA-COD is lost when 1 mgNO_3-N is recycled via the internal or sludge recycle streams through the anaerobic reactor.

Table 2. Influent wastewater characterization and COD characterization (flux based average)

Component	**Unit**	**1st Campaign**	**2nd Campaign**	**Remark**
Total COD, COD_{tot}	mgCOD/l	495	590	Measurement
Particulate Inert COD, X_I	mgCOD/l	100	100	Mass balance of solids
Soluble Inert COD, S_I	mgCOD/l	27	30	Effluent soluble COD concentration
Fermentable COD, S_F	mgCOD/l	25	130	Mass balance from soluble COD components
Acetate COD, S_A	mgCOD/l	95	70	GC analysis
Slowly biodegradable COD, X_S	mgCOD/l	248	250	Mass balance from particulate COD fraction
Ortho-phosphate, S_{PO4}-P	mgP/l	5	7.3	Measurement
Total phosphate, TP	mgP/l	8	12	Measurement and mass balance
Ammonium nitrogen, NH_4-N	mgN/l	50	48	Measurement
Total Kjeldahl nitrogen, TKN	mgN/l	63	66	Measurement
Soluble organic nitrogen	mgN/l	NA	6	
COD_{tot} /TKN	-	7.8	8.9	-
COD_{tot} /TP	-	62	50	-

* 28-day biochemical oxygen demand average of two days

Based on the biodegradable fraction of the influent wastewater (see above), the influent COD was fractionated following the BIOMATH protocol (Chapter 2) and is given in Table 2. Using the fraction of the inert particulates in the influent, X_I, calculated above, the average X_I in the influent was determined to be 100 mgCOD/l (see Table 2). It was observed that the steady-state model prediction of the MLSS concentration using the above-determined X_I in the influent was below the measured MLSS concentration in the carrousel, which is 4750 mg/l on average during the measurement campaign. The reason of this discrepancy could be the underestimation of the influent TSS concentration, especially during the flow peaks. Another factor could be the influent slowly biodegradable COD (X_S) can be fractionated further into several sub-classes with different degradation rates *i.e.* settleable, colloidal COD fractions (Orhon *et al*., 2002). These fractions of X_S may act as inert X_I, depending on the SRT of the treatment plant and therefore contribute to the measured MLSS concentration in

the carrousel. However, further research is needed to clarify this discrepancy.

The calculation shows that the average COD/TKN ratio for the 2nd measurement campaign is 8.9, which claims that there is more COD source available for the denitrification compared to the first one. Therefore, it is expected that the effluent NO_3–N concentration should be lower but it was not as it is discussed in detail below.

3.1.4 Diurnal changes in influent wastewater composition

In this section, the diurnal changes in the wastewater composition are addressed on the basis of load changes in COD, TKN and TP concentrations. As shown in Figure 8 (right), the loads of COD, TKN and TP reveal cyclic changes during the measurement campaign. The ratio of COD/TKN and COD/TP calculated based on corresponding fluxes are in the range of 7.5-10.5 and 40-65 respectively which falls in a confident region appropriate for an efficient biological nutrient removal (Orhon and Artan, 1994; Randall, 1992).

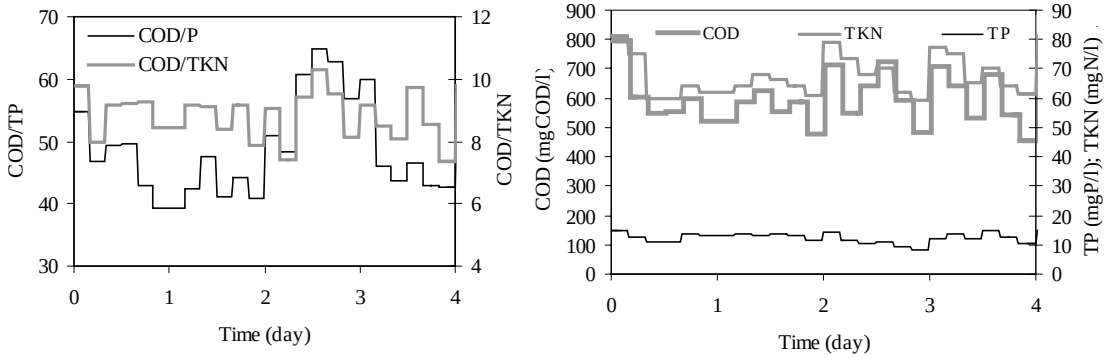

Figure 8. Flux-based influent COD/TKN and COD/TP ratio (left) influent COD, TKN and TP concentrations (right)

Diurnal changes in the influent wastewater composition cause variation in the organic loading rate to the treatment plant (see Figure 8). In this way, the activated sludge is exposed to a dynamic feed pattern, which stimulates storage phenomena (van Loosdrecht and Heijnen, 2002). In this case, it is observed that the COD/TKN and COD/TP ratio were rather low from 3:00 AM until 7:00 AM in the morning (see Figure 8 and Figure 9). On the other hand, between 8:00 to 20:00, the organic loading rate of the plant was sustained at a maximum level but it also reaches a peak load around noontime. These changes in COD load may cause a change in the DO profile along the reactor if there is no aeration control is implemented. For instance, the anoxic fraction, T_{anox}/T_{total} in the biological reactor becomes lower when the aeration is limited during the maximum COD load.

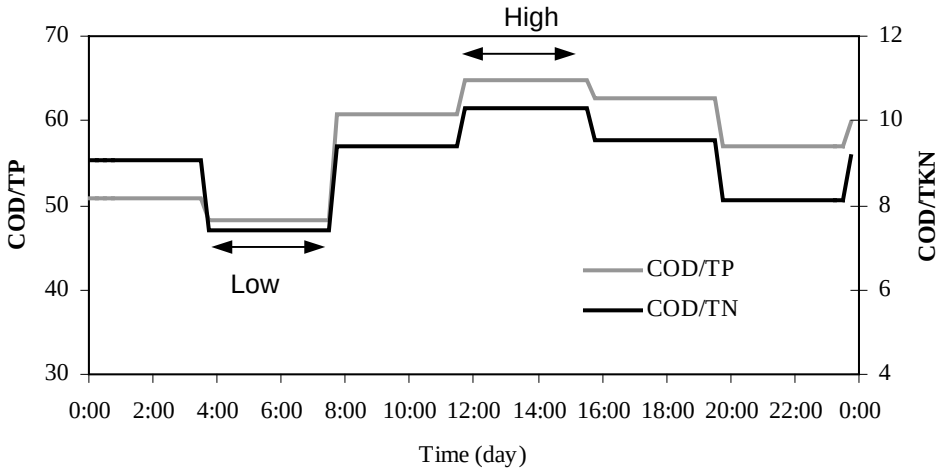

Figure 9. Diurnal changes in COD/TKN and COD/TP load

3.2 The calibrated model: Simulation results (Insel *et al.*, 2003b)

In this section, simulation results using first campaign and obtained with the calibrated model using these first measurement campaign data are presented. The measured and simulated concentrations of nitrate, ammonia nitrogen together with effluent phosphate and dissolved oxygen in the 6th compartment of the carrousel reactor are measured as shown in Figure 10 and Figure 11. According to Figure 10 (left), during day-time, the nitrate can be observed to build up to 15 mgN/l. A reasonably good fit is obtained for the oxygen profile in the middle of the tank (6th reactor). The reason is that aeration is in excess and anoxic conditions cannot be generated for efficient denitrification. It should be noted that only the surface aerators provide mixing in order to keep the mixed liquor in suspension. With this model calibration, nitrification is found to be well described, but effluent phosphorus concentrations are slighlty over-predicted by the model (see Figure 11 right).

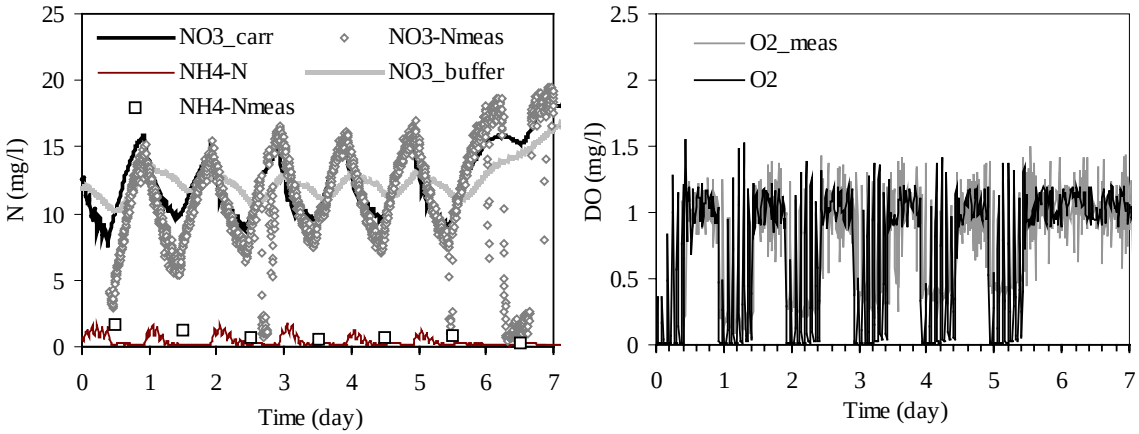

Figure 10. Simulated and measured nitrogen (left) and dissolved oxygen (right) (Insel *et al.*, 2003b)

Another important point is the rain event that happened just before the measurement campaign. This made the system difficult to calibrate in terms of solid balance, process stoichiometry and kinetics (Insel *et al*., 2003b). Figure 11 (left) reflects the simulated and measured MLSS where excessive sludge wastage caused a large drop in the MLSS concentration in the carrousel. The calibrated parameters are given in the 1st calibration column of Table 3. One of the objectives was to keep the number of parameters for calibration to a minimum while getting a good fit on all measured variables.

The calibrated parameters are the anaerobic hydrolysis reduction factor, anoxic hydrolysis correction factor, the oxygen half saturation constant for heterotrophs, the endogenous decay rate for X_{PAOs} X_{PP} X_{PHA}, the half saturation constant for hydrolysis, and the half saturation constant of autotrophs for oxygen. The endogenous decay rate for PAOs was set to 0.14 day^{-1}, which is slightly lower than the default value proposed in ASM2d (0.2 day^{-1}). It was also suggested by Siegrist *et al*. (1999) that comparably reduced decay rates for PAOs could be observed under PHB limiting conditions in which the biomass is subjected to alternating electron acceptor conditions. The half saturation constant for oxygen is lowered to 0.15 mgO_2/l (Carucci *et al.*, 1999) to increase the efficiency of the aerobic processes. Consequently, the value of the half saturation constant for O_2 (X_{AUT}) is also set to 0.2 mgO_2/l, which is in agreement with literature values (Orhon and Artan, 1994; Stenström and Poduska; 1980).

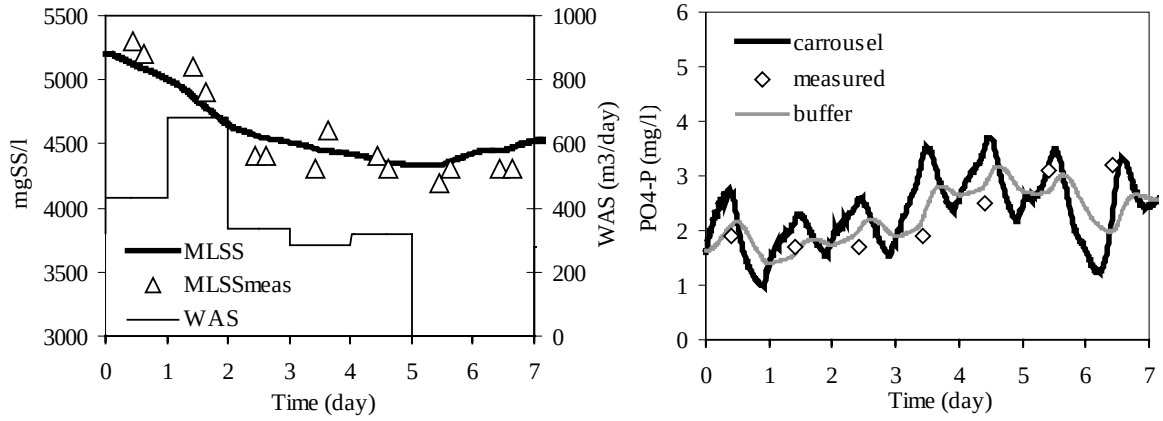

Figure 11. Simulated and measured MLSS (left) and effluent phosphate (right) (Insel *et al*., 2003b)

3.3 The calibrated model: Validation with the second measurement campaign data

The aim of this section is to check the prediction performance of the calibrated model by using the new dynamic influent wastewater characterization (MC2) obtained under different conditions (see Figure 8), i.e. for the 'validation' of the model. Another important point is to determine the reason of a possible discrepancy between the simulations results and the measurements.

For the validation of the model, the following procedure was applied:

1. Use the calibrated model and calibrated parameters
2. Use the new operating conditions prevailing during the new measurement campaign: e.g. sludge wastage, SRT, internal recirculation rates, aeration, return sludge recycle etc.
3. Determine the initial conditions of the model: Simulate the calibrated model for long-time using the new operating parameters of the Haaren WWTP and the average influent wastewater composition obtained from MC2 (see Table 2).
4. Use the new input dynamics obtained during the MC2
5. Perform dynamic simulations: Use the model of step-1, the operating conditions of step-2, the initial conditions determined in step-3 and the dynamic input wastewater composition of step-4.
6. Compare the simulations with the measured dynamic trends in the treatment plant

During the validation as outlined above, the calibrated model and the parameters of the calibrated model (see Table 3) remained the same.

It is important to note that the calibrated model is also used to simulate longer than the duration of the measurement campaign (MC2) that covers only 4-days. The aim of extending these dynamic simulations beyond the measurement campaign duration is solely to monitor for longer period the trends in the dynamics of NH_4-N, NO_3-N and DO measured on-line in the Haaren WWTP. To this aim, the influent wastewater composition/data collected during 4-days of the measurement campaign (MC2) were assumed to be the same and therefore repeated to the following days. For example, the same influent composition of the first and second days of the MC2 were used for simulating plant behavior on the 5^{th} and 6^{th} days respectively. It is clear that measurements should have been preferred instead of this assumption but the associated costs of additional measurements would be too high. It is, however, significant to stress that for these longer simulations the operating conditions such as influent flow, sludge recycle and sludge wastage rates were not assumed, but taken from the SCADA system of the Haaren WWTP.

In the second measurement campaign, additional phosphate and ammonia concentrations were measured at high frequency. It is observed that the simulated phosphate concentration in the selector reached up to around 45 mgP/l on average (see Figure 12-left). The simulated phosphate concentration is higher (around 15 mgP/l on average) than the measured phosphate concentration in the selector. Consequently, this resulted in a much lower simulated phosphate concentration in the effluent than the measured phosphate concentration in the effluent (see Figure 12-left). As shown in Figure 12 (right), a reasonable fit on the dissolved oxygen profile was observed.

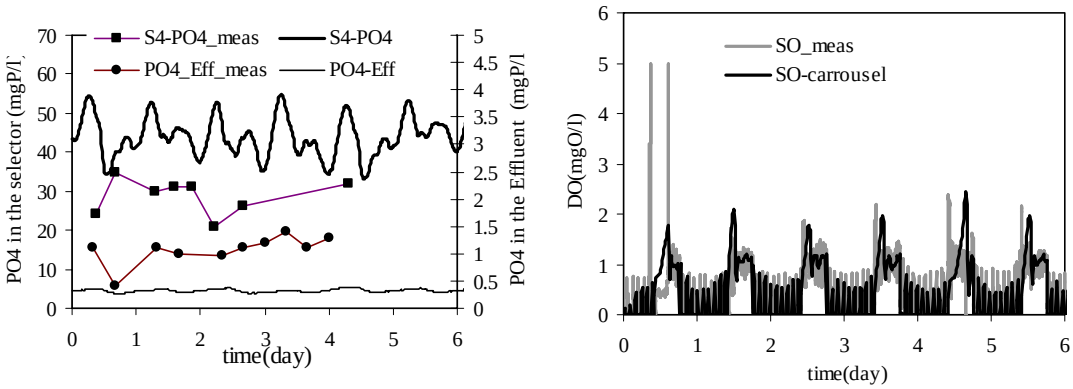

Figure 12. Simulated phosphate (left) and dissolved oxygen (right) concentrations

The simulated nitrate and ammonium trends are compared to the on-line measurements in the carrousel in Figure 13. The simulated trend of nitrate concentrations in the carrousel is observed to agree remarkably well with the nitrate measurements in the carrousel (see Figure 13-left). Although the calibrated model overestimates the peak in the ammonia concentrations, the predicted trend of the ammonium concentration in the carrousel is in acceptable agreement with the on-line measurements (see Figure 13-right).

The simulated nitrate concentrations are observed to deviate slightly from the measurements starting on the 5th and 6th days (a similar observation can also be made for ammonium concentrations on day 5 and 6). It is important to note that the influent wastewater compositions for these two days were assumed (see above). Therefore, it is very much likely that these deviations in the simulated ammonium profiles are caused by the uncertainty in the influent wastewater composition. Despite this uncertainty, however, it is also remarkable that the simulated trends in the nitrate profiles on these two days are fairly acceptable. This observation emphasizes the significance of the quality of the influent characterisation as well as a need for long-term monitoring of the influent to WWTP systems.

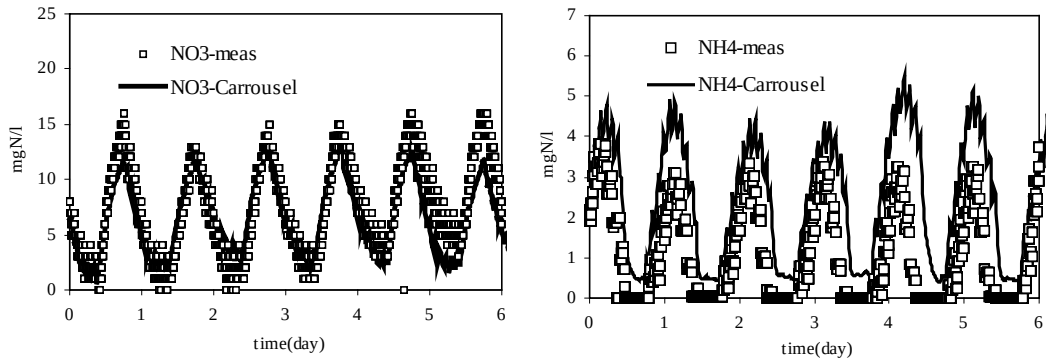

Figure 13. Simulated and measured nitrogen components

Two weeks of simulated MLSS concentrations in the carrousel (on average 4220 mgSS/l) are given in Figure 14 and compared with the daily MLSS measurements (on average 4470 mgSS/l). It is observed that there is a mismatch between the model predictions and the measurements on the first and the third days of the measurement campaign (MC2). However, the general trend observed in the MLSS dynamics in the carrousel is predicted sufficiently well by the calibrated model.

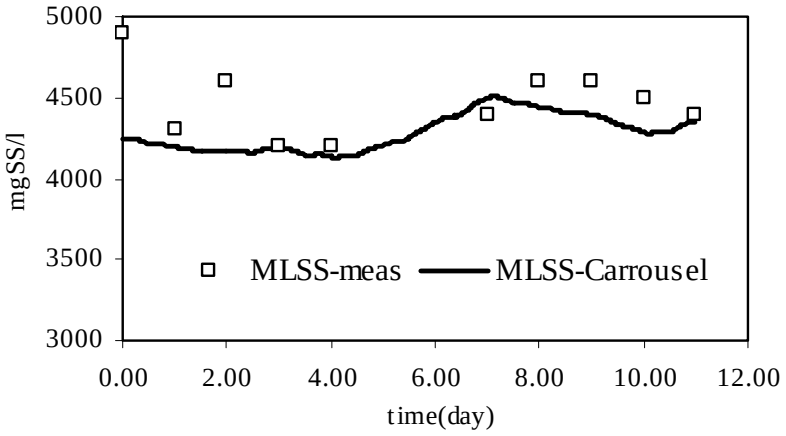

Figure 14. Simulated and measured MLSS concentration in the carrousel

Based on the prediction performance of the calibrated model after 3 years as presented above, it can be said that the model predicted the dynamic behaviour of the Haaren WWTP remarkably well, particularly the measured MLSS, NO_3-N and DO trends in the carrousel. Moreover, the calibrated model was also able to adequately simulate the trend observed in PO_4-P and NH_4-N concentrations but to a lesser accuracy. These outcomes are not surprising since the model was calibrated by only considering on-line NO_3-N, DO and off-line MLSS measurements (see Insel *et al*., 2003b). Overall, the validity of the model is high.

This good model validity indicates the quality of the calibrated model itself. It also indicates the quality of the dynamic measurement campaign data used to simulate the calibrate model. The quality of the measurement campaign data can be attributed particularly to the accurate data collection and detailed influent wastewater characterization (see above). When the dynamic influent wastewater composition is not measured but assumed on day 5 and 6, the model prediction of the nitrate concentrations in the carrousel already deviates from the measurements (see Figure 13-right).

However, as addressed above, the off-line phosphate measurements in the selector (see Figure 12-left) and the ammonium concentrations in the carrousel (see Figure 13-left) were over-predicted by the calibrated model. In the following section, it will be attempted to improve the

prediction performance of the model by fine-tuning some of the parameters. In other words, the calibrated model will be re-calibrated.

3.4 Recalibration of the model

The results obtained in the validation step discussed above show that the calibrated model adequately represents the dynamic behaviour of the Haaren WWTP, even 3-years after the calibration period. However, there are some aspects that can be improved, particularly the ammonium concentrations in the carrousel and the phosphate concentrations in the selector. It was tried to recalibrate the model to improve the model fit to those measurements. It should be noted that the period selected for the MC2 reflects the average behaviour of the plant efficiency under dry weather conditions during summer.

The calibration methodology of Chapter 2 was applied for the recalibration. The model was recalibrated by fine-tuning the anaerobic hydrolysis reduction factor, η_{fe}, the half saturation constant for hydrolysis, K_X, and the affinity constant of autotrophs for ammonium, K_{NH} (see Table 3).

Table 3. Calibrated parameters for the first and re-calibration steps (the re-calibrated parameters are shown in *italics*)

Parameters	Symbol	Unit	Default	1st calibration	Recalibration
Anaerobic hydrolysis reduction factor	η_{fe}	-	0.4	0.8	*0.2*
Anoxic hydrolysis correction factor	η_{NO3hyd}	-	0.6	0.8	0.8
Half saturation constant for oxygen (X_H)	K_O	mgO_2/l	0.2	0.15	0.15
Endogenous lyses rate for X_{PAOs} X_{PP} X_{PHA}	b_{PAO}, b_{PP}, b_{PHA}	day^{-1}	0.2	0.12	0.12
Half saturation constant for hydrolysis	K_X	gCOD /gCOD	0.1	0.03	*0.1*
Half saturation constant for O_2 (X_{AUT})	K_{OAUT}	mgO_2/l	0.5	0.2	0.2
Half saturation constant for NH_4-N (X_{AUT})	K_{NH}	mgN/l	1	1	*0.5*

Compared to the first calibration, it is observed in the recalibration study that the anaerobic hydrolysis correction factor, η_{fe} has a large impact on the PHA pool for EBPR since it liberates readily biodegradable COD in the selector. Moreover, it directly affects the dissolved oxygen concentration in the beginning of the carrousel reactor. The anaerobic hydrolysis correction factor, η_{fe} was therefore used as a recalibration parameter. However, there is little information available about this parameter in the literature (Ekama and Wentzel, 2001; Hu *et al*., 2003). Similarly, the half-saturation constant for the hydrolysis process was also increased compared to the first calibration to decrease the rate of hydrolysis, which is directly affecting the availability of VFA in the selector (see Figure 15-left). Re-calibrating these two parameters was sufficient to improve the model fit to the phosphate measurements in the

selector (see Figure 15-left). That consequently indicates that these two parameters can also be regarded as sensitive parameters for this calibration study. Note that these parameters were also found sensitive in Brun *et al*. (2002). Moreover, the affinity constant of autotrophs for ammonium nitrogen was also re-calibrated to improve the model fit to the ammonium measurements in the carrousel (see below).

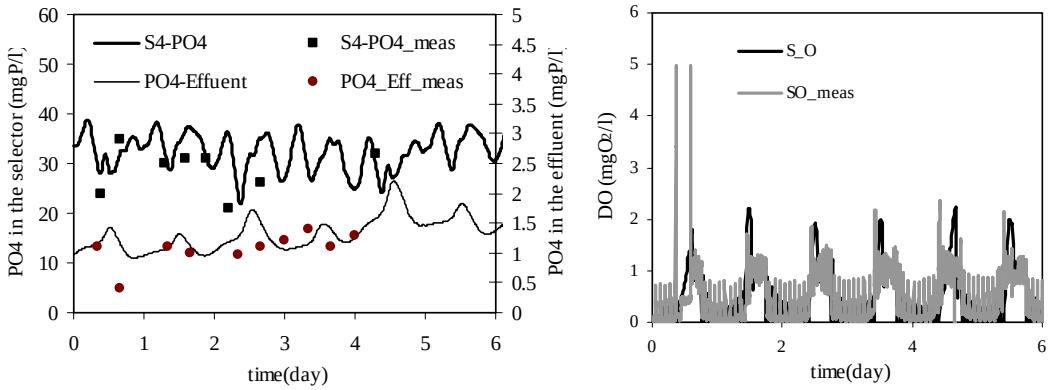

Figure 15. Simulated phosphate and dissolved oxygen concentrations

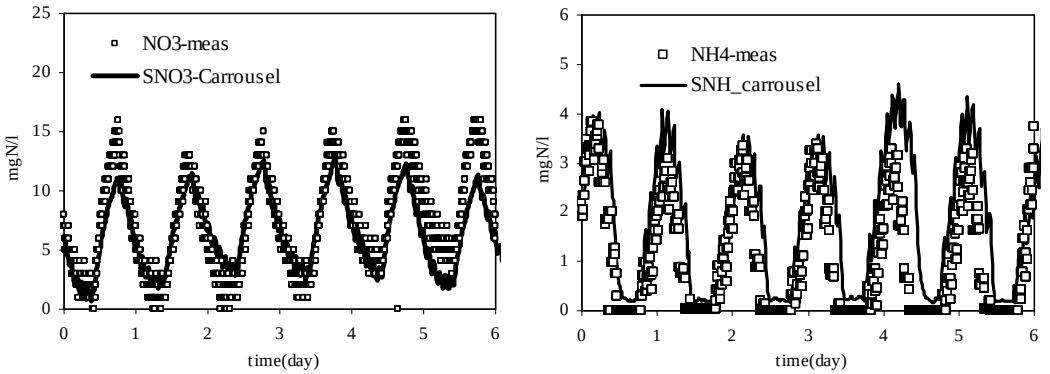

Figure 16. Simulated and measured nitrogen components (a) nitrate (b) ammonium.

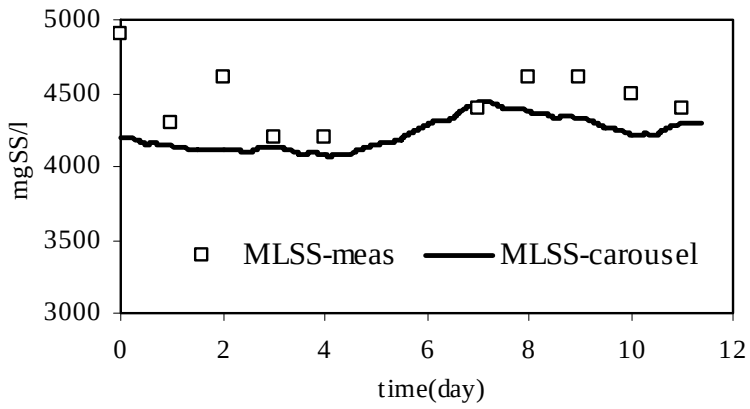

Figure 17. Simulated and measured MLSS concentration in the carrousel

The simulation results with the recalibrated model under dynamic loading (MC2) are compared to the measurements in Figure 15, Figure 16 and Figure 17. The simulated dynamics of ammonium and phosphorous in the Haaren WWTP are improved considerably by the recalibrated model by changing the above-mentioned parameters (see Figure 15, Figure 16 and Figure 17). At the same time, the re-calibrated model was able to simulate the trends of nitrate, oxygen and suspended solids concentrations in the carrousel as good as the first calibrated model.

It is important to also mention that during the process of re-calibration, the parameter i_{NXS}, i.e. the nitrogen fraction of slowly degradable COD, X_S, had to be increased from 0.04 mgN/mgCOD (the average calculated i_{NXS} from the influent wastewater characterisation; see Annex 4) to 0.06 mgN/mgCOD. The value 0.06 mgN/mgCOD was close to the maximum of the measured i_{NXS} fractions in the influent wastewater characterisation (see Annex 4). This increase to 0.06 was required to better fit the measured total nitrogen concentration (NO_3-N and NH_4-N) in the carrousel. Consequently, there is a discrepancy between the measured influent characteristics and the model requirement. In this respect, it is important to point out here that the ASM2d model (Henze *et al*., 2000) assumes a fixed parameter to describe the influent slowly degradable particulate organic nitrogen, X_{ND}, as a function of the influent X_S. However, this may not be the case in reality, as observed in this study too (see the variation of i_{NXS} in Annex 4).

3.5 Model-based analysis of the nutrient removal in the Haaren WWTP

The recalibrated model is used here to study the main biological conversion processes in the treatment plant, which is responsible for the overall nutrient removal performance in the EBPR plants (Wentzel *et al*., 1992).

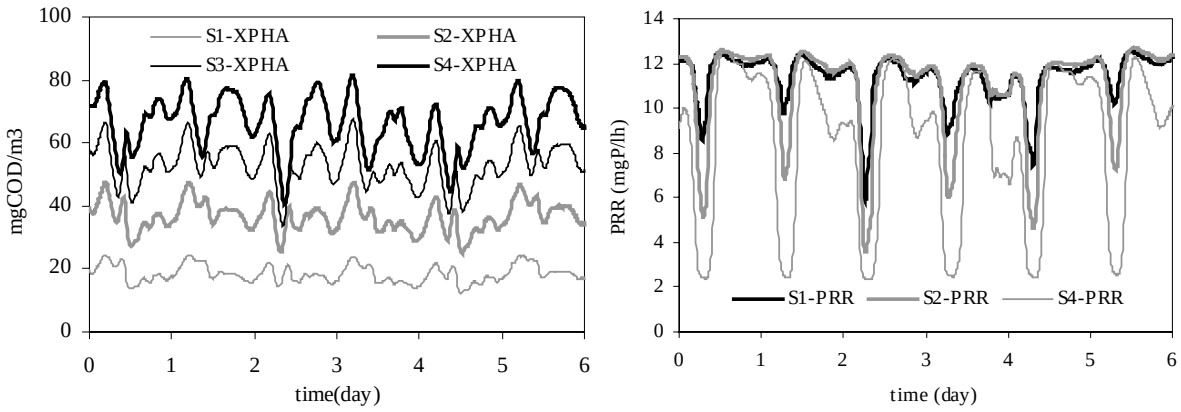

Figure 18. Simulations of the phosphorous release rate, PRR (right) and X_{PHA} (left) in the different sections of the selector

The dynamic influent load, particularly the time when the plant is under high organic-COD loading rate, has a strong effect on the release of phosphorous in the anaerobic selector (see Figure 18-right). Concomitantly, cyclic phosphate fluctuations are simulated in the carrousel reactor, which in turn resulted in a more realistic prediction of phosphate in the effluent (Figure 15-right). It should be noted again that a mixed tank is used just after the carrousel plant in order to simulate the mixing behaviour of the clarifier. During the night period, elevated phosphate concentrations are obtained in the carrousel. However, the phosphate concentration is lowered due to the smoothing effect of the buffer tank that keeps the effluent phosphate concentration below 2 mgP/l during the measurement campaign period.

The X_{PHA} concentrations and the phosphate release rates (PRR) in the selector are also simulated and shown in Figure 18. It was observed that the X_{PHA} concentrations are increasing while moving through the 4 compartments of the selector. Moreover, these internal storage products of PAOs exhibit dynamic fluctuations throughout the selector due to the dynamic variation in the influent wastewater composition (see Figure 8). On the other hand, the PRR is at its maximum during the daytime when the plant is under high COD loads. But this is still not sufficient to increase the X_{PHA} level at the beginning of the selector (see Figure 18-right). During night time, the PRR decreased by more than half which is in agreement with the phosphate concentrations in the carrousel reactor as illustrated in Figure 18-right. The phosphate release rate dropped down to around 8 mgP/l-h in the last compartment in the evening.

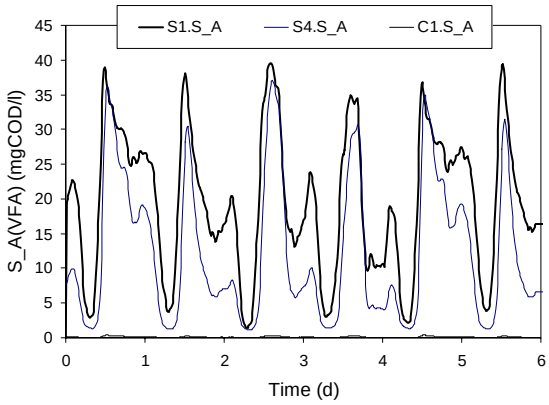

Figure 19. Simulation of S_A (VFA) concentrations in the selector and inlet of the carrousel

The simulations of the VFA concentration in the different compartments of the selector reveal that in the morning, high concentrations of readily biodegradable COD, S_A are still available while denitrification taking place at the head/inlet of the selector (see Figure 19). Meanwhile, as seen in Figure 18-right, the PRR is at its maximum rate of 12 mgP/l.h during daytime, clearly depending on the available VFA. Despite the fact that during night time the nitrate load is reduced under the intermittent aeration mode, the PRR drops drastically by a factor of

2-3 in the selector due to the low influent COD loading (see Figure 19). The same effect of the low influent COD load can be seen on the elevated phosphate concentration profile in the carrousel during night time (results not shown). It is noteworthy that the concentration of S_A in the first compartment of the carrousel is almost zero due to the rapid uptake of the readily degradable COD by the aerobic heterotrophs.

The denitrification rate calculated as the sum of the anoxic activity of heterotrophs and PAOs and expressed as nitrate uptake rate (NUR) of the biomass, reaches up to 250 gN/m^3-d in the first compartment of the selector where the nitrate in the return activated sludge is reduced using the influent readily biodegradable COD (see Figure 20-left). The denitrification rate reduces to almost zero in the following compartments of the selector parallel to the decrease in the nitrate concentration down to zero (see Figure 20-left). On the other hand, the decrease in the denitrification rate favours the phosphorous release activity (PRR) of PAOs (see Figure 18-right). This is particularly true when the influent COD load is too low, because both processes compete for the readily biodegradable COD in the influent, particularly for the volatile fatty acids (Wentzel *et al.*, 1992). The result of this competition also influences the internal storage products content of the PAOs (see Figure 18-right).

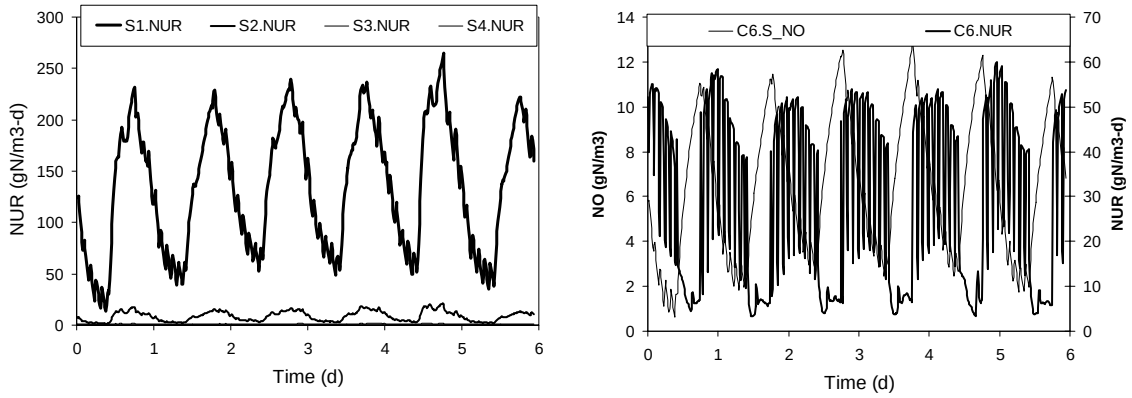

Figure 20. Simulations of the NUR in the selector (left) and the NUR and nitrate in the carrousel (right)

The denitrification activity in the carrousel is observed to reach up to around 60 gN/m^3-d (see Figure 20-right). This is significantly lower than the rate achieved in the selector (see Figure 20-left). The reason for this difference is the limited availability of external carbon source in the carrousel (the only COD sources are the hydrolysis of X_S and endogenous processes) in contrast to the selector where fresh COD is supplied with the influent wastewater.

The nitrification activity was negligible (zero) in the selector (results not shown) as expected since there is no aeration provided in this reactor. However, the nitrification activity in the

carrousel was observed to reach up to 122 gN/m^3-d and 98 gN/m^3-d during nighttime (alternating mode) operating modes and 82 gN/m^3-d and 48 gN/m^3-d during the daytime (full-aeration mode) operation at the inlet and at the end compartments of the carrousel respectively (see Figure 21). In both operation modes, the nitrification activity is higher at the inlet compartment of the carrousel because the oxygen concentrations are higher in this part of the carrousel and then gradually decreasing along the carrousel. These results confirm the plug-flow type behaviour of the carrousel reactor when oxygen is considered (as mentioned above).

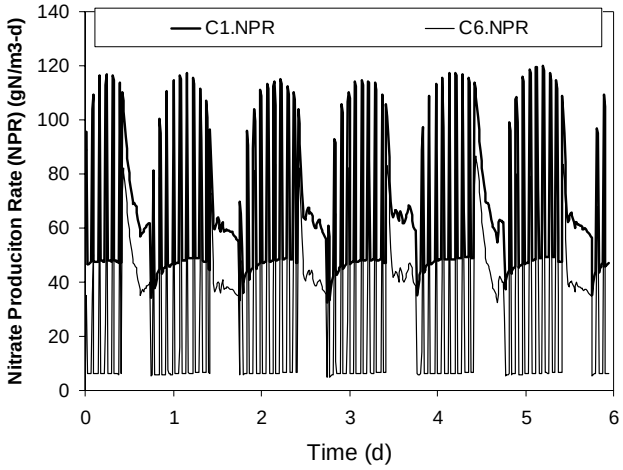

Figure 21. Simulations of the nitrification activity (as nitrate production rate, NPR) in the carrousel.

It is worth mentioning that the re-calibration period (dry-weather conditions) and the design of the measurement campaign itself appear to be sufficiently informative to characterize the plant behaviour and reflect the overall N, P removal efficiency on a yearly basis. This is important since it was shown that a longer period with (approx. 2-3 days) is necessary for the plant to recover full EBPR capability after low organic loadings such as observed during intense rain events (Temmink *et al.* 1996 and Brdjanovic *et al.,* 2000). In this respect, it is crucial to perform a well-designed and dedicated measurement campaign when the plant is under normal loading conditions.

On top of the daily variations, the diurnal variations in the influent also induce remarkable dynamics in the ammonium, nitrate and phosphorous profiles in the Haaren WWTPs. This is because all biological activities are influenced by/depend on the influent wastewater characteristics. For example, influent dynamics are observed to cause a variation in the X_{PHA} content of the PAOs in the selector during the day as presented in Figure 19 (left). These variations, subsequently, cause an oscillation in the phosphorus profile in the carrousel and in the effluent. During night time operation, the nitrate concentrations throughout the carrousel

are significantly decreased (see Figure 16). This is because the plant is operated in alternating mode by turning on/off the aeration as opposed to daytime operation where the aeration is fully on. In this way, the denitrification processes is more enhanced at night time operation (see Figure 19-right). Although the nitrate concentrations are reduced, the influent COD load, particularly the readily biodegradable COD, S_S, was not sufficient to regenerate the storage pools, X_{PHA}, in the PAOs. This is also clear from the PRR simulations in Figure 19 (right). In this respect, it is also important to note that the plant is subjected to higher COD/TKN and COD/TP ratios during night time periods, which further favour denitrification and P-release.

3.6 General discussion: The state and future perspective of model calibration

The mathematical model for Haaren WWTP which was calibrated with a set of dynamic measurement campaign data collected 3 -years ago (Insel *et al*., 2003b) is observed to predict the recent dynamic trends of nutrients in the Haaren WWTP remarkably well. In other words, the calibrated model predictions of the Haaren WWTP were largely valid even after a long time.

Moreover, some aspects of the calibrated model, particularly the predictions of the phosphate concentration in the selector and the ammonium concentration in the carrousel, could be improved further by re-calibrating a few (in total 3) relevant parameters of the model. The re-calibration of the model was performed straightforwardly (required little effort) while these efforts resulted in considerable improvements in the prediction performance of the model.

This long-term prediction capability of the model showed that the model remained largely valid in view of representing the Haaren WWTP. This suggests that the life cycle of a calibrated model can be compatible with the life cycle of a WWTP. This particular result of the long-term model validation encourages the use of the calibrated model for further applications, e.g. optimisation of operation oriented at minimizing aeration costs, optimal control of the WWTP under rain events, upgrade of WWTP and design of new WWTP etc.

The good level of model validity demonstrated in this study indicates the goodness of the calibrated model itself. Moreover, it also indicates the quality of the set of dynamic measurement campaign data used to calibrate the model. The quality of the measurement campaign data can be attributed particularly to the accurate and detailed data collection and influent wastewater characterization.

Having demonstrated the significance of the composition of the influent wastewater in relation to the model outputs, the response of the calibrated model under seasonal changes in the influent wastewater characteristics should also be considered. It is important to emphasize that the model was calibrated and validated with dynamic data collected under summer

conditions. It will certainly be very valuable to evaluate the prediction performance of the calibrated model throughout the year dealing with seasonal changes (autumn, winter and spring) where remarkable differences in the influent wastewater characteristics can be expected (Henze *et al*., 2001).

In this study, the calibration of the model as well as the design of the measurement campaign to collect information rich data about the Haaren WWTP were based on expert knowledge. It is very important to stress that this expert knowledge based calibration approach is tedious and requires considerable amount of time. A cost effective and information rich alternative approach is to use a systematic calibration procedure (Chapter 2):

1. Determine parameter subsets for calibration: assess the identifiable parameter combinations that can be calibrated (Ayesa *et al.*, 1995; Weijers and Vanrolleghem, 1997; Reichert and Vanrolleghem, 2001; Brun *et al*., 2002).
2. Design the measurement campaign using Optimal Experimental Design (OED) principles to obtain information rich data about the system in view of increasing the identifiability of the model/reduce the uncertainty of the calibrated parameters.

The systematic calibration approach is especially useful when the model is over-parameterised with respect to available measurements (Weijers and Vanrolleghem, 1997; Omlin *et al*., 2001; Reichert and Vanrolleghem, 2001; Brun *et al*., 2002). This level of complexity of the models often leads to identifiability problems and uncertainty in the calibrated parameters (Weijers and Vanrolleghem, 1997; Alewel and Manderscheid, 1998; Omlin and Reichert, 1999; Omlin *et al*., 2001; Reichert and Vanrolleghem, 2001;). A systematic calibration approach may offer a promising solution to the above-mentioned obstacles.

4. CONCLUSION AND PERSPECTIVES

In this study, it has been shown that the model which has been calibrated with data collected 3 years before (MC1) predicts the recent dynamic behaviour of the WWTP monitored with a recent measurement campaign data (MC2) remarkably well. In other words, the calibrated model predictions of the Haaren WWTP were largely valid even after a long time.

Some sub-models of the calibrated model, particularly the phosphate concentration in the selector and ammonium concentration in the carrousel, were improved considerably by re-calibrating a few (in total 3) relevant parameters of the model. The re-calibration of the model was performed straightforwardly and required little effort.

This long-term prediction capability of the model suggests that the life cycle of a calibrated model is compatible with the life cycle of a WWTP (in this case, the Haaren WWTP). This in

turn encourages the use of such models for further applications e.g. optimisation, control of operation, upgrade or design of WWTP etc.

The influent wastewater composition is very important in relation to the quality of the model output. Since the two measurement campaigns were both performed in the summer, the model response (i.e. the prediction performance) should also be checked under seasonal changes i.e. winter, spring and autumn, to ascertain the model‘s validity under these conditions too.

The quality and quantity of the influent wastewater characterization is the most expensive yet the impost important aspect of modelling of full-scale wastewater systems. A systematic calibration approaches offers OED based measurement campaign design, which produce information rich design at a cost effective price. This approach is suggested for the future modelling exercises.

ANNEX

Annex 1.

Table A1. Plant performance and average influent wastewater characteristics

Influent wastewater Characteristics	Unit	Measurement
COD_{total}	mgCOD/l	590
COD_{filter}	mgCOD/l	234
TKN	mgN/l	66
TKNsol	mgN/l	6
NH_4-N	mgN/l	48
PO_4-P	mgP/l	7.3
TP	mgP/l	12
TSS	mgSS/l	395
Flowrates		
Average Flowrate, Q_{av} (Dry weather)	m^3/day	6310
Q_{peak}/Q_{av}	-	1.6
Q_{peak}/Q_{min}		5.0
Plant Load		
COD_{total}	kgCOD/day	3723
TKN load	kgN/day	417
TP load	kgP/day	76
COD/TKN	-	8.9
COD/TP	-	49
Effluent wastewater characteristics (yearly average basis)		
COD_{total}	mgCOD/l	33 (30*)
NO_3-N	mgN/l	5.5 (5.4*)
NH_4-N	mgN/l	0.6 (0.6*)
TP	mgP/l	1.3 (1.4*)
TKN	mgN/l	2.6
TSS	mgSS/l	5
Plant operation		
SRT	day	~22
HRT	day	1.8
$Q_{internal}/Q$	-	219
$V_{sel}/V_{total(reac)}$	-	0.12
MLSS(carrousel)	mgSS/l	4700-5000
Sludge Blanket Height (Settler)	m	No blanket

* Flux based steady state simulation

Annex.2

Mass balance to check/verify the SRT of the Haaren WWTP

The mass balance of total-P over the system was calculated in order to determine the exact sludge age of the system. First the average wastage flow-rate, QWAS, is calculated using the TP balance as follows:

$Q_{in.ave} \cdot TP_{in.ave} = Q_{out.ave} \cdot TP_{out.ave} + Q_{was.ave} \cdot TP_{was}$

$Q_{was.ave} = (6310 * 12 - 6030*1.3)/230 = 295\ m^3/d$

The estimated $Q_{was,ave}$ (295 m^3/d) using the TP balance was higher than the reported $Q_{was.ave}$ (280 m^3/d). Therefore, the SRT of the system is calculated using the corrected sludge wastage rate:

$$SRT = \frac{MLSS_{ave} * V_{total}}{Q_{was.ave} * MLSS_{was.ave} + Q_{eff.ave} * TSS_{eff.ave}}$$

$$SRT = \frac{4.6 * 14{,}000}{295 * 8.1 + 6030 * 0.005} = 21.67 days$$

The calculated SRT of the Haaren WWTP based on the corrected wastage flowrate is found to be 21.67 days which is quite close to the reported SRT of the Haaren WWTP which is 22 days. The 1.5% error in the calculated SRT is acceptable for a good quality of calibration studies (Meijer et al., 2001).

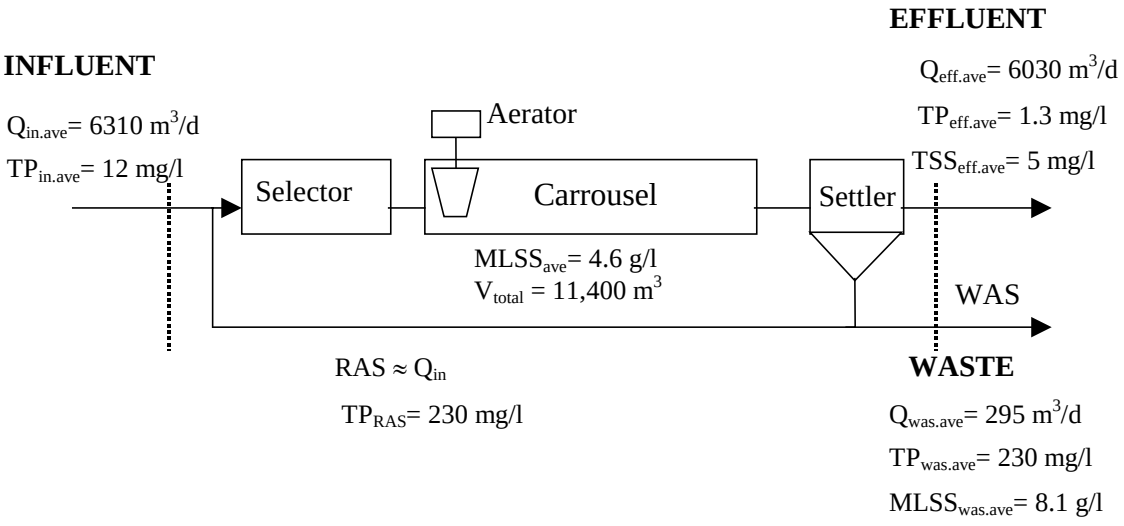

Figure A1. TP mass balance over the system

Evaluation of data quality: Flow balance

The raw flow data obtained from the SCADA system of the Haaren WWTP were analysed prior to use in the dynamic simulations. The raw data from the on-line flow sensors are stored at high frequency, which is 1 data per minute. The flow data set presented in Figure A2 is for the 8 days window that starts on 16/06/2003 as day zero and continues until 23/06/2003. The raw flow data is clearly observed to contain high frequency noise, which is usually the case with on-line sensors in WWTPs (a similar observation is made for the raw effluent flowrate data too, results not shown). This high frequency noise was filtered prior to use in dynamic simulations.

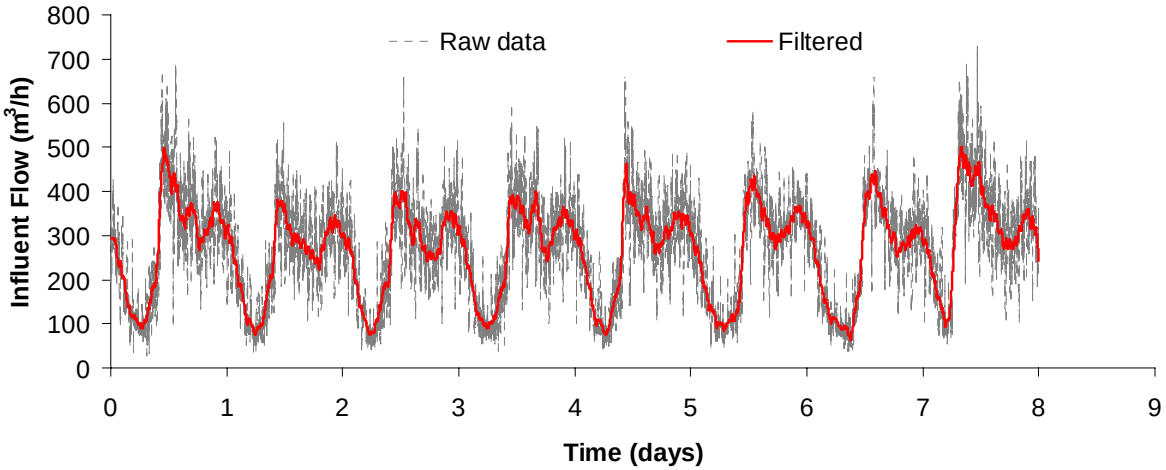

Figure A2. The influent flowrate data; the dashed line represents raw data and the bold line represents the filtered data (Savitzky-Golay with polynomial order 1 and window size 51).

To check the quality of the flow data, a flow balance was performed around the system boundaries shown in Figure A1, both using raw measurements and filtered measurements as follows:

Balance = $Q_{in} - (Q_{eff} + Q_{was})$

Table A1bis. Evaluation of flow data quality

Raw data balance (percentage error)		Filtered data balance (percentage error)	
Average	Standard deviation	Average	Standard deviation
-5.667	38.128	1.4257	8.092

The results of the flow balance are plotted in Figure 2A. The percentage error of the flow balance is calculated as follows:

Flow balance error = (Balance/Q_{in}) *100

The average and standard deviations for the flow balance errors were calculated for raw and filtered flow measurements and given in Table A1bis. The results show that the flow balance had an average error of 5.7% with 38% of standard deviation. Filtering the raw flow data aided to bring the error on the flow balance down to 1.5% with 8% of standard deviation (see Table A1bis). In Figure 3A, the flow balance errors are also plotted for both raw and filtered data which clearly indicates the improvement to the quality of the flow data. Figure 3A indicates that the error on the flow balance was mainly caused by the high frequency noise contained in the raw flow data. This could be considerably decreased after filtering. The filtered and quality-improved flow data are shown in Figure 4A.

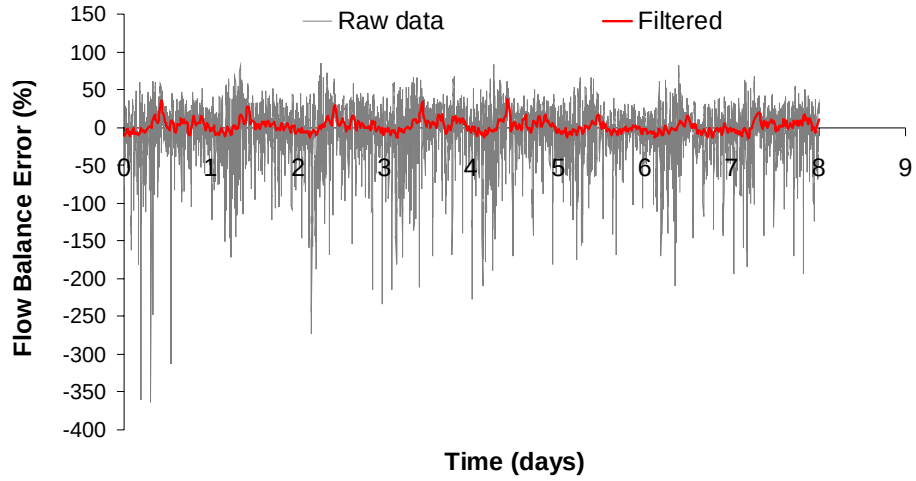

Figure 3A. Flow balance errors calculated for raw flow and filtered data

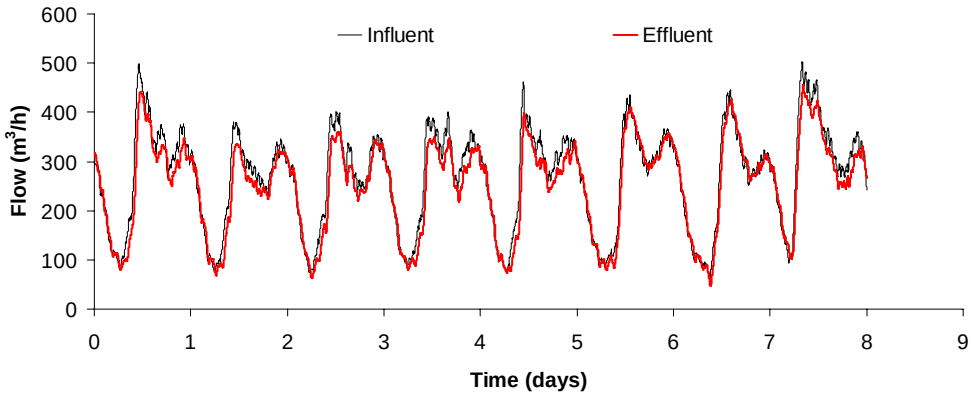

Figure 4A. Filtered (balanced) influent and effluent flow rates. Note that the corrected sludge wastage rate is 12.2 m^3/h (or similarly 295 m^3/day)

Annex 3.

Table A2. The experimental results of the b_H experiment

Date	Time (day)	OUR (mgO_2/l-h)	OUR (mgO_2/l-d)	ln(OUR)
8-May-03	0.0			
13-May-03	5.5	7.5	180	5.19
14-May-03	6.6	5.7	136.8	4.92
15-May-03	7.6	4.6	110.4	4.70
16-May-03	8.4	3.7	88.8	4.49
17-May-03	9.4	3.1	74.4	4.31
18-May-03	10.5	2.5	60	4.09
19-May-03	11.6	2.1	50.4	3.92
20-May-03	12.6	1.7	40.8	3.71
21-May-03	13.6	1.4	33.6	3.51
22-May-03	14.6	1.3	31.2	3.44

Note: pH is 7.1, Temperature is around 19 ^{0}C and ATU is added to the batch reactor at around 30 mg/l.

Annex 4

Table A3. Second measurement campaign (MC2): Influent wastewater characterisation results

Day	Time	COD_T	COD_F	S_I	S_F	S_A	X_S	X_I	NH_4-N	PO_4-P	TKN	TKN_F	TP	TSS	COD_F/COD_T	S_I/CODtot	I_{NSF}	I_{NXS}	COD/TKN	COD/TP
16-Jun	0.00	796.00	226.00	32.00	125.49	68.51	410.96	159.04	56.00	7.60	77.00	61.00	12.00	370.00	0.28	0.04	0.04	0.04	10.34	66.33
16-Jun	0.17	601.00	170.64	24.16	94.75	51.72	310.29	120.08			68.00		9.00	360.00					8.84	66.78
16-Jun	0.33	548.00	256.00	30.00	148.40	77.60	190.48	101.52	43.00	6.70	59.00	49.00	8.90	310.00	0.47	0.05	0.04	0.05	9.29	61.57
16-Jun	0.50	552.00	257.87	30.22	149.48	78.17	191.87	102.26			66.00		10.00	180.00					8.36	55.20
16-Jun	0.67	598.00	264.00	34.00	149.98	80.02	224.48	109.52	46.00	9.10	62.00	52.00	9.80	150.00	0.44	0.06	0.04	0.04	9.65	61.02
16-Jun	0.83	524.00	231.33	29.79	131.42	70.12	196.70	95.97			62.00		10.00	90.00					8.45	52.40
17-Jun	1.00																			
17-Jun	1.17	587.00	259.14	32.00	148.59	78.55	218.98	108.88		9.10	72.00		10.00	180.00		0.05			8.15	58.70
17-Jun	1.33	624.00	266.00	34.02	151.35	80.63	242.26	115.74	49.00	8.00	78.00	67.00	22(!)	190.00	0.43		0.12	0.04	8.00	
17-Jun	1.50	555.00	236.59	29.90	134.97	71.72	215.11	103.30		9.00	66.00		22(!)	350.00		0.05			8.41	
17-Jun	1.67	589.00	255.00	31.73	145.97	77.30	224.37	109.63	46.00	8.50	64.00	60.00	11.00	96.00	0.43		0.09	0.01	9.20	53.55
17-Jun	1.83	480.00	207.81	32.30	112.52	62.99	189.29	82.90		7.90	63.00		9.70	47.00		0.07			7.62	49.48
18-Jun	2.00																			
18-Jun	2.17	716.00	223.00	32.30	123.10	67.60	353.46	139.54	56.00	7.90	76.00	59.00	12.00	200.00	0.31		0.02	0.04	9.42	59.67
18-Jun	2.33	547.00	170.36	31.70	87.02	51.64	277.06	99.58		6.70	61.00		9.70	280.00		0.06			8.97	56.39
18-Jun	2.50	642.00	258.00	37.21	142.59	78.21	267.13	116.87	48.00	5.30	63.00	49.00	7.20	170.00	0.40		0.00	0.05	10.19	89.17
18-Jun	2.67	722.00	290.15	29.40	172.80	87.95	287.97	143.88		5.10	66.00		7.30	310.00		0.04			10.94	98.90
18-Jun	2.83	591.00	245.00	24.07	146.67	74.27	228.23	117.77	44.00	4.50	60.00	52.00	7.50	190.00	0.41		0.05	0.03	9.85	78.80
19-Jun	3.00	483.00	200.23	33.30	106.23	60.69	200.15	82.62		4.60	61.00		8.20	140.00		0.07			7.92	58.90
19-Jun	3.17	710.00	235.00	33.30	130.47	71.23	337.90	137.10	55.00	5.80	76.00	59.00	8.40	200.00	0.33		0.03	0.05	9.34	84.52
19-Jun	3.33	641.00	212.16	30.40	117.45	64.31	305.40	123.44		8.50	61.00		9.80	280.00		0.05			10.51	65.41
19-Jun	3.50	530.00	207.00	25.14	119.12	62.75	220.94	102.06	49.00	7.70	63.00	50.00	9.70	170.00	0.39		0.01	0.05	8.41	54.64
19-Jun	3.67	682.00	266.37	29.00	156.62	80.74	280.95	134.68		8.90	66.00		14.00	310.00		0.04			10.33	48.71
19-Jun	3.83	546.00	200.00	23.22	116.16	60.62	238.18	107.82	47.00	8.10	60.00	52.00	9.80	190.00	0.37		0.04	0.03	9.10	55.71
20-Jun	4.00	455.00	166.67	30.00	86.15	50.52	209.13	79.20		6.90	61.00		9.80	140.00		0.07			7.46	46.43
Average		596.5	230.6	30.4	130.3	69.9	253.1	112.8	49.0	7.3	65.7	55.5	9.7	213.2	0.388	0.054	0.043	0.04	9.1	63.0
STD		85.9	34.2	3.5	23.0	10.4	59.1	20.2	4.7	1.5	6.0	6.0	1.6	90.7	0.058	0.010	0.034	0.01	1.0	13.9

* F stands for filtered; T for total; the rest of the parameters are as defined in ASM2d.

PART 4
-
DEVELOPMENT AND APPLICATION OF A SYSTEMATIC OPTIMISATION PROTOCOL

Chapter 6

Optimal but robust N and P removal in SBRs: A model-based systematic study of operation scenarios

ABSTRACT

In the first part of this study, a systematic approach to determine the optimal operation strategy for nitrogen (N) and phosphorous (P) removal of sequencing batch reactors (SBRs) has been developed and applied successfully to a lab-scale SBR. The methodology developed is based on using a grid of possible scenarios to simulate the effect of the key degrees of freedom in the SBR system. The grid of scenarios is simulated using a calibrated ASM2dN model developed and calibrated in Chapter 5.1. Effluent quality in combination with a robustness index for each of the scenarios is used to select the best scenario. With the best scenario, it is possible to improve/increase the current performance of the SBR system by around 54% and 74% for N and P removal respectively.

In the second part of this chapter, the effect of oxygen set-point and sludge age on the performance and robustness of the SBR system are analysed using a model-based approach. It was found that increasing sludge age has a negative effect on P-removal while it has a positive effect on N-removal. Decreasing the oxygen level in the SBR (i.e. oxygen limited operation) is observed to improve both N and P-removal. Robustness of the system as a function of sludge age and oxygen set-point was observed to have a completely opposite trend with the trend of effluent quality. Improving effluent quality decreases the stability of the SBR performance. This means that under optimal operating conditions, the system is forced to operate close to its limits, thereby making the system fragile against external variations/disturbances.

Main parts of this chapter were presented at the 3rd IWA conference on SBRs:

Sin G., Insel G., Lee D.S. and Vanrolleghem P. A. (2004) Optimal but robust N and P removal in SBRs: A model-based systematic study of operational scenarios. In proceedings: 3rd IWA International conference on SBR, Noosa, Queensland, Australia, February 22 – 26 2004, pp 93-100.

1. INTRODUCTION

Sequencing batch reactor (SBR) technology for nutrient removal has received worldwide attention from the wastewater treatment community in view of the ever-stricter demands on effluent discharge quality (Wilderer *et al*., 2001). Both nitrogen and phosphorous removal from wastewaters have been demonstrated successfully at lab-scale and full-scale installations (Manning and Irvin, 1985; Furumai *et al*., 1999; Keller *et al*., 2001; Wilderer *et al*., 2001; Demoulin *et al*., 2001)

Being flexible to operate, a myriad of operation strategies have been developed to optimise nutrient removal performance in SBRs (Wilderer *et al*., 2001). The operational strategies have been usually tested experimentally at lab-scale (Manning and Irving, 1985; Lin and Jing, 2001; Hvala *et al*., 2001). Increasingly, mathematical models (e.g. ASM1 for N-removal and ASM2d for N and P-removal) have been used for developing and testing optimal operation strategies for biological N and P removal (Demuynck *et al*., 1994; Hvala *et al*., 2001; Artan *et al*., 2002). The main parameters that have been demonstrated in the above-mentioned studies to impose a major effect on the N and P removal capacity of the SBRs until now are the step-feed of the influent (Hvala *et al*., 2001; Lin and Ying, 2001), intermittent aeration (Demuynck *et al*., 1994; Demoulin *et al*., 2001), oxygen set-point in the aerobic react-phase to regulate the extent of simultaneous nitrification and denitrification in the SBR (Munch *et al*., 1996; Artan *et al*., 2002) and length of anaerobic, aerobic and anoxic phases (Wilderer *et al*., 2001; Artan *et al*., 2002).

The objective of this study is to develop a systematic approach to determine the best operation strategy for the optimisation of the N and P removal performance of the SBR technology. The methodology is based on using a grid of scenarios to simulate the effect of different degrees of freedom on the SBR system. The scenarios, i.e. the operation strategies formulated using realistic combinations of the significant degrees of freedom tested so far elsewhere, are simulated using the ASM2dN model developed and calibrated in a previous study (Chapter 5.1). Criteria for the selection of the best scenario are proposed based on not only the effluent quality but also the robustness against deviations of the modelled reality (Vanrolleghem and Gillot, 2002). Finally, the systematic approach has been applied to a lab-scale SBR. Particular attention is given to the oxygen set-point in the aerobic react phase and the sludge age on the overall performance of the SBR system.

2. MATERIAL AND METHODS

A lab-scale sequencing batch reactor (SBR) with a working volume of 80 L was seeded with sludge from the Ossemeersen WWTP (Ghent, Belgium). It is operated in a 6 h cycle mode, each cycle consisting of 60 min fill/anaerobic, 150 min aerobic, 60 min anoxic, 30 min aerobic and 60 settling/draw phases. A synthetic sewage is used as SBR influent, which was

shown to mimic a real pre-settled domestic wastewater. The detailed description of the SBR is given in Chapter 5.1. Simulations were performed using WEST® (Hemmis, Belgium) a dedicated software for the modelling of WWTP that contains a scenario analysis module (Vanhooren *et al.*, 2003).

2.1. A systematic methodology for the optimisation of SBR systems

The model-based optimisation of the lab-scale SBR is performed following the methodology described in Fig.1.

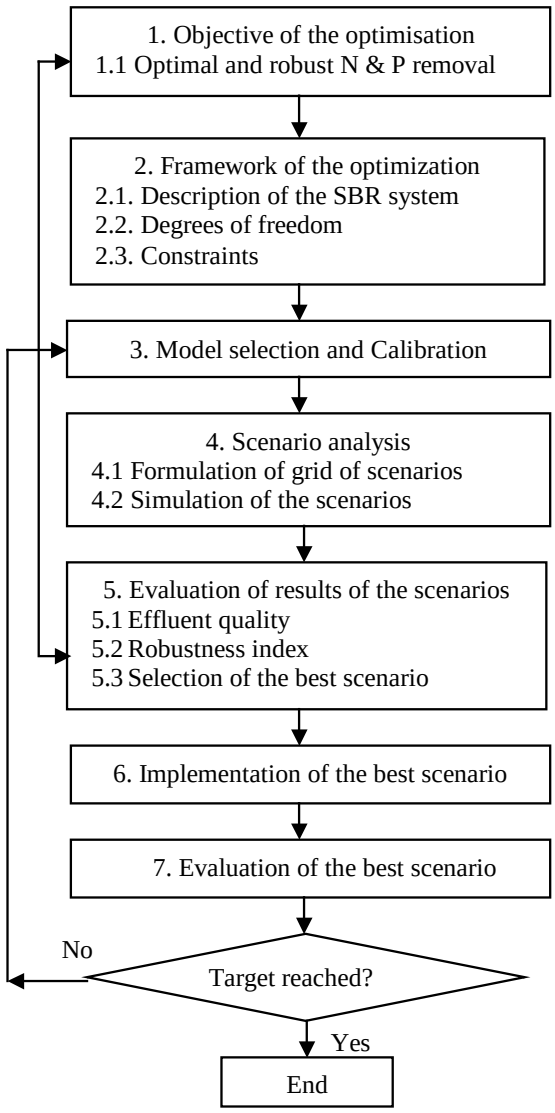

Figure 1. A systematic methodology for the model-based optimisation of SBR systems

The first step is the definition of the objective of the optimisation study. This will determine the required calibration accuracy and serve as the main criterion in selecting the optimal operation strategy for the system. The second step is the description of the system including the definition of the degrees of freedom and constraints of the system, which will determine the framework of the optimisation. This is followed by the model selection and calibration

step to obtain a realistic model-based description of the SBR system. Following this step, i.e. step 4, a grid of scenarios based on the above degrees of freedom and constraints is formulated and simulated using the calibrated model. The results of the scenarios are evaluated in the following step, i.e. step 5. The analysis of the results is expected to provide in-depth insight into the operation scheme of the SBR system. In this step, the optimal scenario is chosen considering the objective of the optimisation. Two criteria are proposed for this purpose: the effluent quality and the robustness of the system to deviations of the modelled system (Vanrolleghem and Gillot, 2002). Afterwards, the best scenario should be implemented to the SBR system. The last step i.e. step 7 is to check if the objective of the optimisation is reached. To this aim, a measurement campaign should be carried out after the SBR system reaches a new steady-state. If the SBR performance under the newly implemented operation conditions is not satisfactory, the procedure should be iterated starting from step 3.

3. RESULTS AND DISCUSSION

3.1 Application of the systematic methodology to a lab-scale SBR

3.1.1 Objective of the optimisation

In this study, the objective of the optimisation is to find an optimal and robust SBR operation scenario that achieves the best possible effluent quality with respect to N and P removal under given physical boundary and influent characteristics.

3.1.2 The framework for the SBR optimisation: Degrees of freedoms and constraints

Being flexible systems to operate, SBR systems offer a large number of operation-variables to be optimised. Ideally, all possible operation variables should be used in the optimisation of the SBR system. However, the number of the degrees of freedom that can be selected must be limited due to the resulting too high computational demand (In this study, simulation of one scenario takes on average 25 min with a 1GHz Pentium III processor). In this study, based on a survey of the relevant literature (see the introduction) and a preliminary model-based analysis of the system (see Chapter 5.1), the following degrees of freedoms were identified and used for the SBR optimisation:

(1) Oxygen set-point (S_O-sp) in the aerobic react phase,
(2) Length of the anaerobic phase (T_{ANB}),
(3) Length of the reaction (aerobic and anoxic) phase (T_R i.e T_{AER}+ T_{ANX}),
(4) Step-feed of the influent organic load ($V_{step\text{-}feed}$) and
(5) Intermittent aeration frequency (IAF), which is explained below.

The constraints of the optimisation study stem from several reasons including the lower and upper boundaries of the degrees of freedoms, the physical boundary of the SBR (e.g. maximum volume of the SBR, influent pump capacity etc.), and the priorities of the objective of the optimisation. In this study, the solids retention time, SRT (10 d), hydraulic retention time, HRT (12 h), the volumetric exchange ratio, i.e. the ratio of the fill volume to the maximum volume of the reactor (0.5), and the total cycle time (360 min) are fixed. Further, the mass transfer coefficient for oxygen (K_La) is fixed to a sufficiently high value (500 d^{-1}) to ensure the oxygen set-point can be maintained effectively with on/off control. The last aerobic react phase is fixed to 30 min to strip the nitrogen gas entrapped in the flocs and to polish the effluent prior to discharge to the receiving water**.** The minimum anaerobic time is set to 60 min based on preliminary simulation results with the SBR model. The length of the settling/draw phase is also fixed to its design value (60 min) as this incorporates a safety margin to provide sufficient settling time in case of a sludge bulking event.

3.1.3 Model selection and calibration

From the dynamic ammonium and nitrate trends in the SBR, it was observed that the degradation of organic nitrogen (i.e. hydrolysis and ammonification) is the rate limiting-step in the over-all nitrogen turnover in the SBR (Chapter 5.1). This was probably due to the high fraction of organic nitrogen present in the influent (ca. 95%), which is not typical for domestic wastewaters for which ASM2d is valid. As a result, the ASM2d model had to be extended with a hydrolysis process for the entrapped organic nitrogen (ASM1) to adequately describe the dynamic N and P trends in the SBR. The calibration of the so-called ASM2dN model is given in Chapter 5.1.

3.1.4 Scenario analysis: Formulation and simulation of grid of scenarios

A grid of scenarios considering the degrees of freedom and the constraints of the system mentioned above was formulated as a full-factorial experimental design (Table 1). The intermittent aeration frequency (IAF) (Table 1) refers to the number of aerobic and anoxic sequences/sub-phases during the reaction phase excluding the last aerobic period. For instance, IAF 2 means that there are 2 aerobic and 2 anoxic (in total 4) sub-phases in the react phase (see Fig.2B). In the implementation of the intermittent aeration for the SBR model (see Fig.2), the length of the total aerobic react phase (T_{AER}) is divided equally by the number of aeration sub-phases, i.e. 1, 2, 4 and 8. For instance, when the aeration frequency is equal to 2, the length of each aerobic sequence is equal to the length of the total aerobic react phase divided by 2, i.e. $T_{AER}/2$. In the same way, the length of the anoxic sequence is equal to the total length of the anoxic-react phase (T_{ANX}) by 2, i.e. $T_{ANX}/2$. Further, the step-feed volume is partitioned equally between the anoxic sequences except for the IAF 8 where some of the sub-phases do not receive any influent COD.

The amount of influent fed to the anaerobic phase is calculated straightforwardly by subtracting the step-feed volume from the total fill volume ($V_{fill} - V_{step\text{-}feed}$). Moreover, the filling time of the SBR cycle depends on the influent feed volume (the influent pump flowrate is fixed to 0.96 m^3/d). Therefore the filling time is 60 min, 52.5 min and 45 min for 40 L, 35 L and 30 L influent volumes respectively. The length of the anaerobic phase (T_{ANB}) is chosen to range between 60 and 80 minutes. The aerobic period of the reaction phase (T_{AER}) (excluding the last aerobic phase) ranges from 130 to 150 minutes. Note that the sum of the lengths of anaerobic (T_{ANB}), aerobic (T_{AER}) and the anoxic (T_{ANX}) phases is constrained to 270 minutes which means that the length of the anoxic phase (T_{ANX}) is also varying for each combination of aerobic and anaerobic durations.

Table 1. The grid of scenarios to simulate the effect of key degrees of freedom on the SBR system

Scenario	Degrees of freedom (d.f.)				Total No.
IAF	S_O-sp (mgO_2/l)	$V_{step\text{-}feed}$ *(L)*	T_{ANB} (min)	T_{AER}(min)	Scenarios
1	[0.2, 0.4, 0.6, 0.8, 1,2]	[0,5,10]	[60,70,80]	[130,140,150]	162
2	[0.2, 0.4, 0.6, 0.8, 1,2]	[0,5,10]	[60,70,80]	[130,140,150]	162
4	[0.2, 0.4, 0.6, 0.8, 1,2]	[0,5,10]	[60,70,80]	[130,140,150]	162
8	[0.2, 0.4, 0.6, 0.8, 1,2]	[0,5,10]	[60,70,80]	[130,140,150]	162

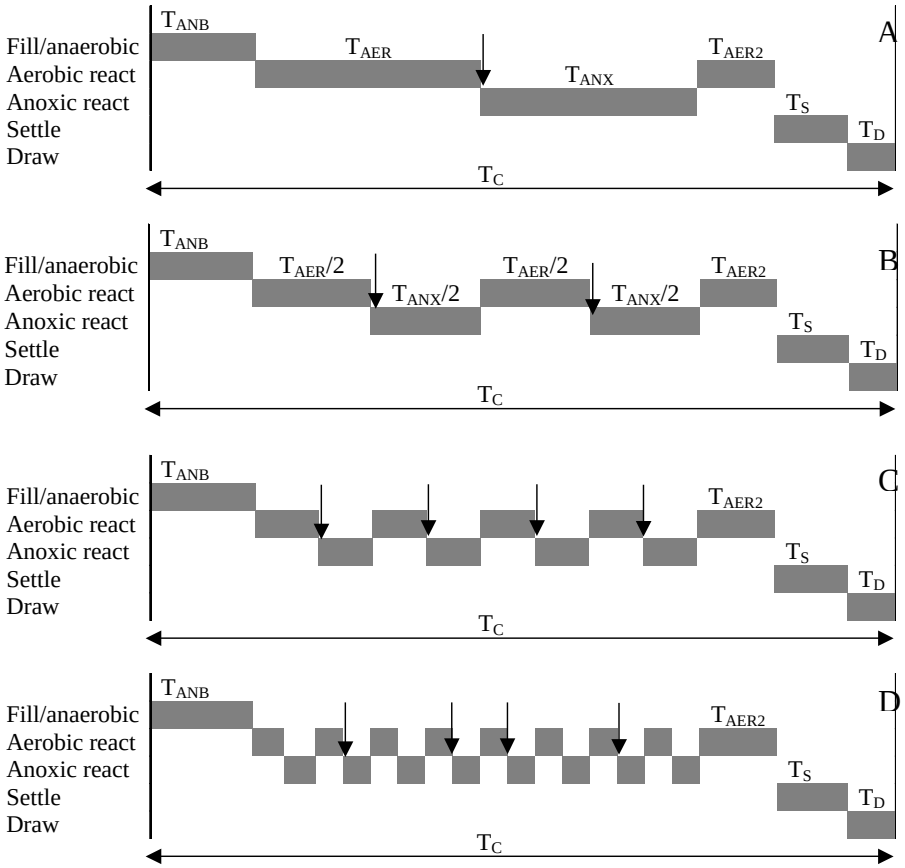

Figure 2. Implementation of IAF with step-feed options to anoxic sub-phases. The arrow indicates the step feed instants. SBR with IAF 1 (A), IAF 2 (B) IAF 4 (C) and IAF 8 (D).

The combination of these degrees of freedom under the above-mentioned constraints results in 648 scenarios, which is expected to be sufficient to provide significant insight into the optimal operational scheme for the SBR system. In this way, the optimal scenario of the SBR operation can be searched using the predefined criteria.

3.1.5 Evaluation of the scenario analysis results

Effluent quality

The grid of scenarios presented in Table 1 is simulated for 30 days, equal to 3 times the system SRT. The steady-state results of the SBR system in each scenario are then recorded, resulting in a huge amount of data. The scenarios are compared in order to find the best scenario according to the predefined criteria, which are the minimum concentrations of NH_4, NO_3 and PO_4 in the effluent (Table 2). Note that total nitrogen (TN) is the sum of NH_4 and NO_3 in the effluent.

The scenario analysis results (SCA) indicate that the best system performance for either N or P-removal are obtained under different operating conditions. The best system performance for N can provide additional 10.62 mg N/l removal (see Table 2 with IAF 8) which means a 57% improvement compared to the existing performance. On the other hand, the best P-removal performance is obtained under IAF1 providing additional 4.73 mgP/l removal, which means an 83% improvement in the existing P-removal performance. Moreover, in all of the best scenarios the effluent total nitrogen contains not only nitrate but also ammonium nitrogen. In this regard, the correct definition of the objective function is crucial. In this study, the objective was set to improve the N removal defined as the sum of NH_4 and NO_3 in the effluent.

Table 2 Summary of the scenario analysis results: the best scenario in each category

Scenarios ID	T_{ANB}	T_{AER}	T_{ANX}	$V_{Step\text{-}feed}$	S_{O_sp}	NH_4	NO_3	PO_4	TN
	min	min	min	L	mgO_2/l	mgN/l	mgN/l	mgP/l	mgN/l
Reference	60	150	60	0	2	0.73	17.10	5.7	17.83
IAF 1	60	130	80	10	0.4	2.50	8.26	0.97	10.76
IAF 2	60	130	80	10	0.4	2.04	7.88	1.04	9.93
IAF 4	60	130	80	10	0.4	1.70	6.67	1.47	8.38
IAF 8	60	130	80	10	0.4	1.88	5.84	1.03	7.72

The scenario analysis results (Table 2) are the result of the sum-up effect of all the evaluated degrees of freedom on the system. Since the number of degrees of freedom is relatively high (i.e. 5), it becomes difficult to distinguish exclusively and quantitatively the effect of each degree of freedom on the overall system performance. The following general remarks are observed from the detailed analysis of the scenario analysis data (unpublished):

- ✓ Increasing the T_{ANB} improves the P-removal efficiency, however, the N-removal performance decreases. Obviously, this favours conditions for phosphorous accumulating organisms (PAOs) to effectively utilise the VFA generated during the anaerobic phase (Wilderer *et al*., 2001).
- ✓ Increasing the T_{AER} slightly improves the performance of the nitrification process. However, this parameter has a negative effect on denitrification process (Artan *et al*., 2002).
- ✓ The S_O-sp appeared to be the most critical parameter in determining the overall behaviour of the system. A detailed discussion is provided below.
- ✓ The step-feed option has a considerable positive effect on the denitrification process. This parameter is essential in improving the denitrification capacity of the system (Hvala *et al*., 2001; Lin and Ying, 2001).
- ✓ Increasing the intermittent aeration frequency in general has a positive effect on the nutrient (N & P) removal capacity of the system (Demuynck *et al*., 1994)

In general, the results of the optimisation study (Table 2) demonstrate that during the filling phase there is a strong competition between PAOs and denitrifiers for the influent COD (particularly VFA), which is in agreement with several studies (Manning and Irvin, 1985; Wilderer *et al*., 2001; Hvala *et al*., 2001; Lin *et al*., 2001; etc.). To improve P removal in SBRs, the fraction of influent COD utilised by PAOs should be increased during the filling phase. This can be achieved by providing sufficient anaerobic time and decreasing the initial NO_3 concentration present at the beginning of the filling phase. Hence, improving N removal in the SBR is not only useful in itself but also enhances P-removal. In this respect the following actions are useful to consider:

(1) step-feed of the influent,
(2) maintain oxygen limited conditions during the aerobic react phase to increase simultaneous nitrification and denitrification (SND) capacity of the system (see below),
(3) high intermittent aeration frequency during react phase and
(4) optimise the length of aerobic and anoxic sub-phases during the react phase.

The systematic methodology presented here significantly facilitates the efforts to find the optimal combination of the above-mentioned parameters to achieve both optimal N and P removal in SBR systems.

Robustness analysis of the best scenarios

The robustness index (RI) introduced by Vanrolleghem and Gillot (2002) is used to assess/measure the robustness of each scenario against a change in the system operation

conditions. The sensitivity of the SBR under different scenarios was determined by applying the following manipulations:

(1) 10 % decrease in the sludge age (SRT),
(2) 10% increase in the hydraulic loading rate,
(3) 10% decrease in the organic (COD) loading rate and
(4) 33% decrease in the temperature (from 15 to 10 ^{0}C). The temperature effect on the system performance was modelled using the Arrhenius equation.

Table 3. Sensitivity analysis and robustness index of the best scenarios (see text for explanation)

	Reference		IAF1		IAF2		IAF4		IAF8	
Parameters (θ)	TN	PO_4	TN	PO_4	TN	PO_4	TN	PO_4	TN	PO_4
1. SRT (-10%)	0.11	0.56	-0.10	0.56	0.00	-0.07	0.05	0.18	0.05	-0.02
2. HRT (+10%)	-0.04	-0.37	-0.07	0.47	-0.08	-0.01	-0.06	0.26	-0.10	0.02
3. COD load (-10%)	0.09	0.79	0.03	0.53	0.22	0.32	0.40	0.81	0.46	0.82
4. Temp. (-33%)	0.13	0.67	2.45	12.10	3.33	7.07	1.22	-0.31	4.17	5.99
Robustness index (RI)*	**9.52**	**1.36**	**0.81**	**0.16**	**0.60**	**0.28**	**1.48**	**1.62**	**0.47**	**0.33**

$^{*}RI = \left(\sqrt{\frac{1}{p}\sum_{i=1}^{p} S_i^2} \right)^{-1}$ where $S_i = \frac{dCost}{d\theta_i} \cdot \frac{\Delta\theta_i}{Cost}$ $i = 1..p$ and $Cost = [TN, PO_4]$

Table 3 provides the relative sensitivities S_i (calculation, see Table footer) of the effluent TN and PO_4 concentration with respect to a change in each operating condition/parameter (defined in the parameter column). The magnitude of the relative sensitivity indicates how strong the resulting effect of a change in a parameter on the SBR system is. The sensitivity analysis of the SBR showed that decreasing the SRT of the system has a negative (although only small) effect, while increasing the hydraulic loading rate has mainly a dilution effect on the effluent N and P concentrations. Further, decreasing the influent COD load resulted in higher concentrations of N and P in the effluent. On the other hand, the temperature induced a sharp decrease in the performance of the SBR, almost leading to system failure.

Based on the comparison of the RI (Table 3), the reference system appeared to be the most robust with respect to N-removal, followed by the best scenario under IAF4. From a P-removal point of view, however, the SBR system is most robust under the best IAF4 scenario followed by the reference system. However, the robustness index does not indicate the goodness of a scenario with respect to effluent quality, it only indicates how stable (good or bad) the performance is under process changes (Vanrolleghem and Gillot, 2002). The robustness of the system is particularly low when the system delivers its best effluent quality, see e.g. IAF1, IAF2 and IAF8 in Table 3. This implies that the optimised SBR is forced to operate close to its limit under the above-mentioned scenarios. Hence, a small deviation in the

input to the system leads to drastic deviations in the performance of the system, even up to system failure where biological N and P removal is no longer achieved. From this perspective, it can be said that the robustness index of a scenario indicates how the SBR system is forced to operate close to its limits/edge and therefore how fragile it becomes against a deviation in the input to the system. This provides significant information, particularly for wastewater treatment plants operated under dynamic input conditions, since the effluent quality should be ensured not for short-term (optimal) but for long-term (variable) operation.

Selection of the best scenario for implementation

The objective of the optimisation study is to optimise the operation of the SBR in such a way that the best effluent quality can be obtained. Obviously, one of the criteria to decide for the best scenario is the effluent quality in each scenario. However, the effluent quality standards (e.g. EC Directives, 91/271/EEC) usually require the treatment plant to deliver the effluent quality over a certain period of the operational time (e.g. 95%). From this perspective, the stability of the system becomes significant and should be considered equally in the final decision. Based on the effluent quality (Table 2) and robustness index of the best scenarios (Table 3), the SBR operation under IAF4 appeared to be the best scenario to provide effluent quality below discharge standards accompanied with good system stability. Under this scenario, the existing SBR performance for the N and P removal is improved by 54% and 74% respectively. The best scenario has been implemented and the SBR performance is expected to reach a new steady-state soon.

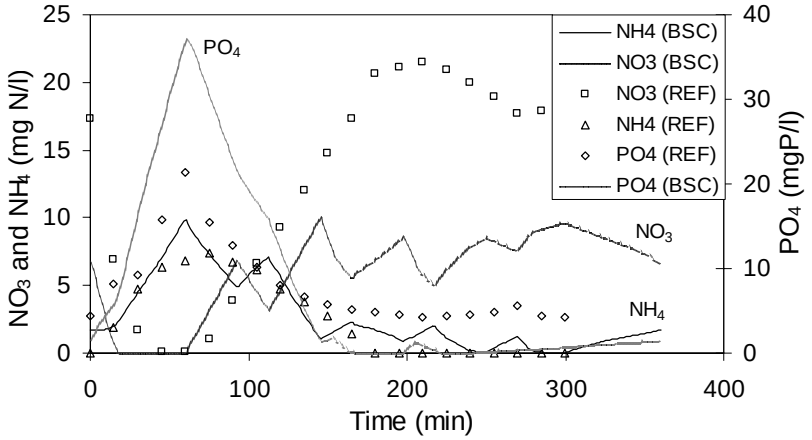

Figure 3. N and P-removal dynamics under the best scenario (BSC) obtained in IAF4 in comparison with the reference (REF) system

In this optimisation study, a fixed length of aerobic and anoxic sequences is assumed to reduce the number of scenarios required for the optimisation. It is clear that the optimisation of the SBR system should also consider the variable length of the aerobic/anoxic sequences, particularly for SBRs subjected to dynamic input conditions. Moreover, the settling properties

of activated sludge are not incorporated in the state-of-the-art activated sludge models such as ASM2dN (Chapter 5.1). Hence, it is not possible to predict the behaviour of activated sludge during the settling phase under different operating conditions. Ideally, this should be a third criterion to consider during the selection of the best scenario.

3.2 Effect of the oxygen set-point and length of the aerobic react phase

An important outcome of the scenario analysis is the fact that the system delivers the best effluent quality (both for N and P criteria) under oxygen-limited conditions (see Table 2). A set-of simulations (224 in total) were carried out to understand the effect of the oxygen set-point on the nitrification and denitrification processes in the SBR system. A grid of scenarios was constructed around a vector of oxygen set-points and a vector of aerobic react phase times. The simulation results obtained under the best IAF4 scenario are shown in Fig.4. Similar trends are observed in the ammonium and nitrate profiles obtained under the best scenarios with IAF1, IAF2 and IAF8 (Mura, 2003).

The simulation results demonstrated that a linear relationship exists between the oxygen set-point or the length of the aerobic react phase (i.e. aerobic SRT) and the effluent nitrogen concentrations (see Fig.4). A certain nitrate concentration (8 mgN/l) can be obtained under different oxygen set- points and aerobic react time (see Fig.4B). This linear relationship can be explained by the changing extent of simultaneous nitrification and denitrification (SND) occurring during the reaction phase of the SBR (Munch *et al*., 1996). Based on the simulation results, it is strongly advised to consider the oxygen set-point in the design of SBRs and probably also for other types of wastewater treatment plants.

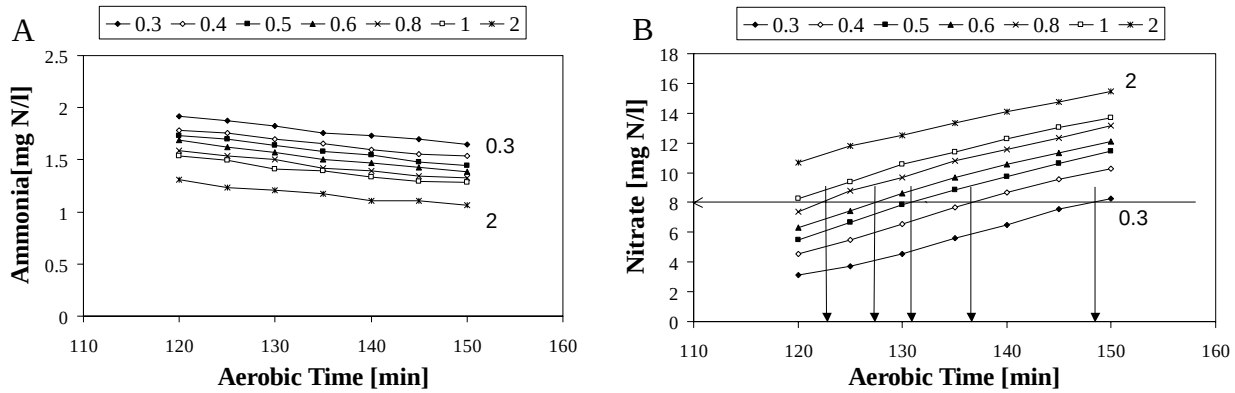

Figure 4. Trend of ammonium (A) and nitrate (B) as function of oxygen set-point under different lengths of aerobic react phase for the SBR operation with IAF4. Arrows indicate combinations of oxygen set-points and aerobic-time corresponding to 8-mgN/l nitrate in the effluent (B).

3.3 Effect of sludge age on the SBR performance and stability

In the previous sections, the scenario analysis is performed under a fixed sludge age equal to the sludge age of the reference system, i.e. 10 days. The question "What is the response of the SBR system under different sludge ages with respect to both effluent quality and robustness criteria?" is addressed in detail in this section to complement the optimisation study carried out at the fixed sludge age of 10 days.

For the simulations presented in this section, the length of the anaerobic phase, the amount of step-feed and the length of the aerobic-react phase were fixed to the values obtained from the best scenarios under the different intermittent aeration frequencies (see Table 2). The effect of sludge age on the SBR performance is investigated under different oxygen set-points, since the oxygen set-point is found to be one of the most critical operating parameters of the SBR. In this way, the response of the SBR system is simulated for each point in the following operation domain: a grid of sludge ages (SRT) – 8, 10, 12, 14, 16, 18, 20, 22, 24, 25 days, versus oxygen set-point – 0.2, 0.3, 0.4, 0.5, 0.6, 0.8, 1, 2 mgO_2/l. This results in 240 simulations in total (i.e. including 3 different categories of intermittent aeration frequency), which is expected to be sufficient to predict the trend in the behaviour of the SBR system as a function of SRT and oxygen concentration.

3.3.1 Effect of sludge age on effluent quality

The effluent quality results as function of SRT and oxygen set-point are shown in 3-D graphs in Figure 5. In these 3-D graphs, the x-axis corresponds to the oxygen set-point, the y-axis corresponds to the sludge age of the SBR system and the z-axis corresponds either to the effluent TN (equal to the sum of NH_4-N and NO_3-N in the effluent) (see Figure 5-left) or to the effluent PO_4-P concentrations respectively (see Figure 5-right).

The effluent quality of the SBR system as function of sludge age has a particular behaviour dictated by the specific conditions/operating variables of the system (see Figure 5). However, the following general conclusions can be deduced from a detailed analysis of the effluent quality results (data not shown explicitly):

1. Below a critical oxygen set-point (in this case 0.2 mg/l), the nitrifiers are washed-out and there is no P-uptake, i.e. a system failure occurs with respect to N and P removal.
2. The P-removal is observed to be optimal for sludge ages around 10-12 days depending on the oxygen set-point in the system (see Figure 5 right-A). This is in accordance with experimental results shown elsewhere (Henze *et al.,* 2000; Smolders *et al.,* 1995). An increase in the SRT of the SBR is observed to have a slight negative effect on the effluent P removal. This might be explained by the amount of storage polymers in the PAOs (X_{PHA}) (Smolders et al., 1995). Since the substrate flux to the system is constant, the concentration of the storage polymers (fixed yield) will be diluted as the

concentration of biomass kept in the system increases (i.e. increasing SRT). Consequently, the P-uptake in the aerobic/anoxic phase will be relatively lower due to decreased level of X_{PHA} in the PAOs.

3. Decreased oxygen set-points have a positive effect on the effluent P concentrations. This is most probably an indirect effect of the reduced effluent TN concentrations.
4. The effluent TN concentrations are observed to decrease parallel to an increase in SRT. Moreover, decreasing oxygen set-points have a remarkable effect on reducing effluent TN concentrations (see Figure5-left). This was discussed in detail in the preceding section. Oxygen limited operation of SBR has shown to considerably improve the N-removal under all different operating SRTs and intermittent aeration frequencies (see Figure 5-left). This confirms/supports the findings that a lower oxygen concentration enhances simultaneous nitrification and denitrification processes.
5. Increasing the intermittent aeration frequency (from 2 to 8 see Figure 5-left) has a positive effect both on N and P removal. This is in accordance with the experimental results shown elsewhere (Hvala *et al*., 2001; Demuynck *et al*., 1994; Lin and Jing, 2001).

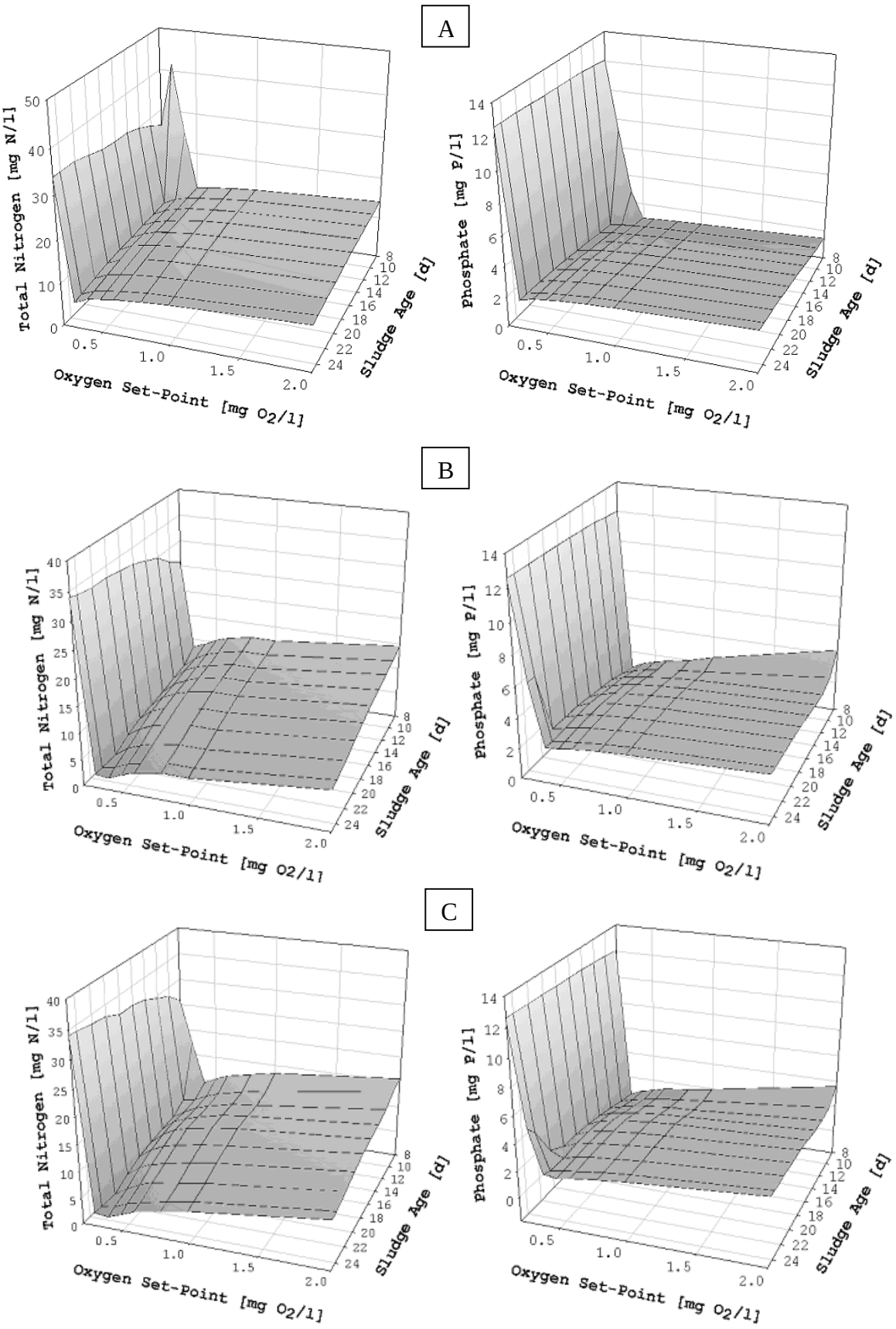

Figure 5. SBR performance with respect to effluent TN (left-hand) and P concentrations (right-hand) as a function of sludge age under different oxygen set points: IAF2 (A) IAF4 (B) and IAF8 (C).

3.3.2 Effect of sludge age on the robustness of the SBR system

The robustness index (RI) or stability of the SBR system under each operating condition are shown in 3-D graphs in Figure 6. The z-axis in Figure 6 corresponds to either the RI of the SBR system towards effluent TN (see Figure 6-left) or to the RI of the SBR system towards effluent PO_4-P concentrations (see Figure 6-right). It is important to note that the magnitude of the RI shown in Figure 6 is meaningful only for comparison purposes.

The trend of the robustness index (RI) of the SBR as a function of sludge age has a particular behaviour, which is dictated by the specific conditions of the system. However, the following general conclusions can be deduced from the robustness analysis:

1. The stability of SBR system has a non-linear trend as function of the system SRT, DO and intermittent aeration frequency. Moreover, the robustness of the system is different for N and P removal (see Figure 6). The trend of RI related to phosphate is clearly increasing (robustness increases parallel to the increase in sludge age) as shown in Figure 6-right. The trend of RI related to TN on the other hand can be said to be decreasing parallel to a decreasing SRT, with a few exceptions (see Figure 6-left).
2. The robustness of the SBR (both for TN and P) is observed to increase parallel to an increase in oxygen concentration (see Figure 6). It is a common characteristic observed in each intermittent aeration category (IAF2, IAF4 and IAF8). An exception should be made for the scenarios with oxygen set-point equal to 0.2 mg/l. In this case, although the robustness of the system is at its maximum (see Figure 6), the effluent quality is worse (see Figure 5). This special case means that for this operation mode, the response of the SBR with respect to effluent quality cannot be altered (either in negative or positive way) resulting in maximum robustness index values.
3. A detailed analysis of the components of the robustness index (results not shown) showed that the temperature has the biggest influence on the nitrification performance of the SBR. The phosphate removal performance, on the other hand, is very sensitive towards a change in the COD load to the SBR. The effect of the hydraulic retention time on the overall system performance is, however, observed to be minimal. The temperature effect on nitrification is well compensated by either increasing the oxygen set-point in the system or equivalently increasing the sludge age of the system (see e.g. left hand side of Figure 5). This is expected since increasing the oxygen set-point (see the section above) indirectly increases the aerobic SRT of the SBR.
4. The stability of nitrogen removal is particularly regulated by the temperature variation in the system. For phosphate removal, on the other hand, it is the change in influent COD that plays an important role. Variation of the hydraulic retention time does not affect the stability of the system considerably.

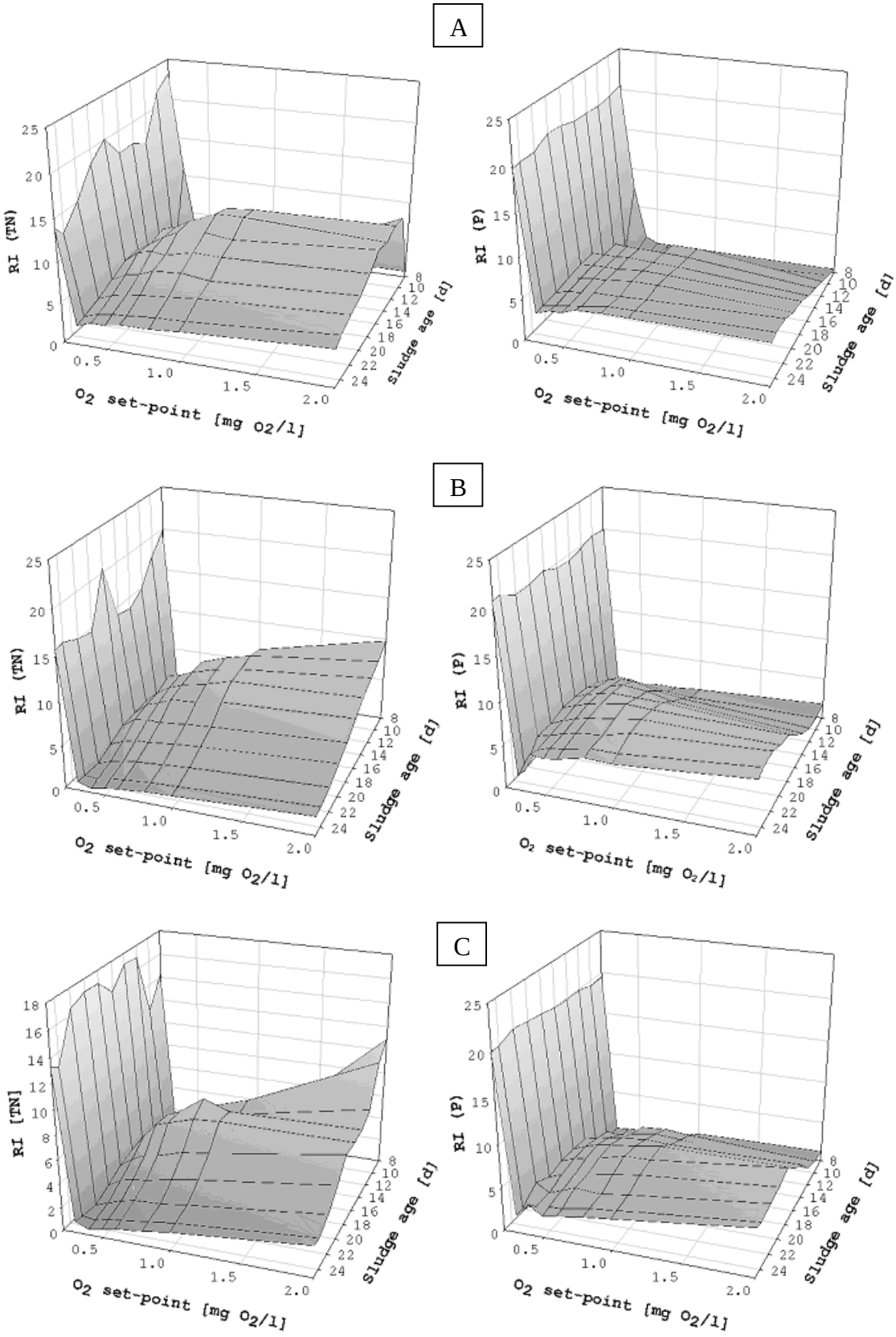

Figure 6. Stability/robustness of the SBR system with respect to TN (left-hand) and P removal (right-hand) as a function of sludge age under different oxygen set points: IAF2 (A) IAF4 (B) and IAF8 (C).

Comparing the effluent quality (Figure 5) and the robustness index (Figure 6) in the SBR system under different operating conditions (particularly as a function of SRT and oxygen) shows that the robustness of the SBR system is decreasing parallel to the improvement in the effluent quality. This was also observed in the preceding section (see 3.1.5 i.e. selection of the best scenario) mentioned above and was observed in Vanrolleghem and Gilliot (2002) too. This supports the above-mentioned argument that optimisation of the SBR system to obtain improved effluent quality asks for operating the SBR system close to its limits. Furthermore, it means that optimised SBR operation asks to sacrifice robustness thereby making the SBR operation fragile against external disturbances. This aspect is particularly significant for the full-scale optimisation of biological systems, which are exposed to dynamic variations and uncertainties in the input to the system. As such robustness analysis of the different operation scenarios should be part of the decision making process.

4. CONCLUSION

In the first part of this research, a systematic approach (methodology) for the optimisation of SBRs using mechanistic models is developed and evaluated at a lab-scale SBR in view of an improvement of effluent N & P discharges. Based on a compromise between the effluent quality and the robustness of the SBR operation, the best scenario for SBR optimisation is found out to be a step-feed with 4 intermittent aeration sub-phases during the react phase. Under this scenario, it is possible to improve the current N and P removal performance of the SBR by 54% and 74% respectively.

In the second part of this study, the model-based study of the effect of SRTs and oxygen set-point on the SBR performance and stability were performed. The results showed that:

- N-removal improves parallel to increasing SRT. Moreover, oxygen-limited operation of SBR remarkably enhances the effluent N.
- P-removal is optimal around 10-12 days depending on the oxygen set-points whereas increasing SRTs have slightly negative effect on P-removal. Similar to N-removal, a decreasing oxygen concentration in the system improves effluent-P quality.
- Under all different SRTs and oxygen set-points, there is an inverse correlation between effluent quality and robustness of the system. In other words, improving N and P removal of the system decreases the stability of the system. This is most probably caused by the fact that the SBR system is pushed to its limits for improving N and P removal, which makes the system less stable against external disturbances.

5. ACKNOWLEDGMENT

This research was financially supported by the Fund for Scientific Research-Flanders (F.W.O.) and the Ghent University Research Fund.

Chapter 7

General discussion, conclusions and perspectives

1. GENERAL DISCUSSION

Modelling biological systems is known to be limited by the non-existence of one "true" model, which is by definition an exact copy of the system (Alewell and Manderscheid, 1998). There are several underlying reasons for the non-existence of the "true" model (Alewell and Manderscheid, 1998) (i) Biological processes are too complex to be known exactly which implies unpredictability, (ii) The availability of experimental data/measurements about the system behaviour is limited. The very first advantage of having a "true" model would be that it doesn't require validation to describe different biological systems since the model parameters would be universal (Alewell and Manderscheid, 1998). In contrast, the Activated Sludge Models (ASMs) of Henze *et al*. (2000), the most widely accepted and successfully used models for the description of complex biological processes ongoing in wastewater treatment plants (WWTPs), do require calibration. Numerous full-scale applications of ASMs (see for a recent review Petersen *et al*., 2003a) have shown that the parameters of the ASMs (Henze *et al*., 2000) are not universal and as such some of those parameters need to be calibrated for each activated sludge system under study (Brun *et al*., 2002). This is not surprising since the ASMs were originally developed as a compromise between the complexity of biological processes and the practical implementation concern (Henze *et al*., 2000). The ASMs are not "true" models, i.e. exact copies of the activated sludge system but they are rather an approximation of reality. This claim is also indirectly supported by the fact that literature contains many studies aiming at contributing to the further development of ASMs.

In short, it becomes clear that ASMs need to be calibrated to successfully model any WWTPs until one "true" model can be developed for activated sludge systems, but this is probably utopian. Further, this also means that model calibration is a key step in obtaining a good

approximation to the system under study. The research carried out in this thesis mainly focused on the continuous development and application of systematic calibration methodologies (see Chapter 2) to improve the quality of the calibration of ASMs for nitrogen removing WWTPs.

THE BIOMATH CALIBRATION PROTOCOL

In Chapter 2, a systematic calibration protocol based on consolidated scientific and engineering experience was developed. The protocol was refined on the basis of the previous protocol developed by Petersen *et al*. (2003a). The BIOMATH protocol was made flexible and consists of a set of interactive and independent modules for the calibration of hydraulic, settling and biological properties of the plant. The main difference between the alternative Dutch approach, i.e. the STOWA protocol (Hulsbeek *et al*., 2002), is that the BIOMATH protocol is based on respirometry for the characterisation of influent wastewater and it incorporates Optimal Experimental Design (OED) methodology for the design of lab experiments and design of full-scale measurement campaigns. As such the BIOMATH protocol is expected to save time and costs without compromising the quality of the calibration exercise.

Further, in the protocol the targets of modelling and the availability of the data for calibration determine the overall procedure/steps to be executed during the calibration. The protocol is therefore clearly objective focused. Also, data collection and quality is recognized to be of crucial importance for a reliable calibration. Hence data quality should be ensured, e.g. by checking mass balances. The significance of the influent wastewater characterization and the solids mass balance of the system (SRT) are also emphasized in the protocol. An iterative procedure is employed in the protocol until a satisfactorily good agreement between simulations and measurements is obtained.

Based on the BIOMATH protocol and a recent thorough review on experimental designs for activated sludge model calibration, two major problems were identified.

(1) There is a lack of robust/simple sensors to quantify the stoichiometric and kinetic parameters of anoxic sludge activity.
(2) Storage phenomena may play a significant role in the respirometric measurements designed for the characterization of influent wastewater (particularly S_S) and for the estimation of stoichiometric and kinetic parameters. The extent of the storage phenomenon should therefore be evaluated for accurate interpretation of respirometric profiles.

Therefore, the main body of the thesis was focused on the development of experimental set-

ups to improve the quality (and the frequency) of the measurements, particularly for those processes occurring under anoxic conditions. As a complementary step of the second part of the thesis, existing model-based methods were improved (see Chapter 4.1) and some other methods (see Chapters 4.2.2 and 4.3) were developed to interpret the experimental data in view of transferring lab-scale data to full-scale model calibration studies. In doing so, ASM1 and ASM3 were also extended to mechanistically improve the model predictions, i.e. to take into account the simultaneous storage and growth phenomena (see Chapters 4.2.2, 4.3) and to describe the fast transient phenomenon observed in batch respirometric measurements (see Chapter 4.4). Parallel to these studies, in the third part of this thesis the BIOMATH systematic calibration protocol developed in Chapter 2 was evaluated both at a pilot-scale SBR (80 L) (see Chapter 5.1) and a full-scale carrousel type WWTP (50,000 PE) (see Chapter 5.2). Finally in the last (fourth) part of this thesis, a systematic protocol for the application of calibrated models was developed and evaluated to optimise the nutrient removing performance of the pilot-scale SBR (80 L).

In what follows, the bottom line of the research results obtained from each abovementioned study is going to be presented and discussed.

PART 1: DEVELOPMENT OF LAB-SCALE EXPERIMENTAL METHODOLOGIES

In Chapter 3.1, an experimental set-up was developed by integrating both the aerobic (Gernaey *et al.*, 2002a) and anoxic (Petersen *et al.*, 2002a) respirometric-titrimetric methodologies in a single set-up. In this way it was made possible to monitor the entire activity of biomass under both aerobic and anoxic conditions of BNR plants, i.e. nitrification, denitrification and carbon source degradation processes. The major advantage of this sensor is that it provides an information rich matrix of data (OUR, Hp, NU or NP) which, moreover, allows to perform internal check for the quality of the measurements. In addition, the anoxic reduction factor for growth, η_g, could be determined straightforwardly by comparing the OUR with the NUR data for the same degradation process. It was already noticed here that the denitrification rate under the famine phase, i.e. in the absence of external substrate, was remarkably lower (at least by 75%) than the denitrification rate under the feast phase. Moreover, the denitrification rate under the famine phase was higher than the endogenous rate of the biomass implying the possible presence of a storage phenomenon, which was studied in detail in the second part of the thesis. The ratio of OUR to NUR was observed to be close to 1 for two different carbon sources (acetate and dextrose). This implies that this ratio reflects the ratio of the substrate uptake rate of biomass under aerobic and anoxic conditions rather than

the anoxic reduction factor for the biomass growth. This issue was also investigated in detail in Chapter 4.3.

The anoxic compartment of the integrated sensor developed in Chapter 3.1 was based on an ion-selective nitrate electrode (ISE). However, long-term experiences with this type of ion-selective electrode showed that the slope of the ISE nitrate sensor drifts usually in a rather random and unpredictable way (Petersen *et al*., 2002a; Malisse, 2002). This makes it rather tedious to work with even during the course of a relatively short (less than 1 hour) batch experiment. Moreover, it was rather sensitive towards the ionic strength of the medium, and also to the nitrite concentration (Malisse, 2002). Further, it was not possible to reliably measure nitrate concentrations below 2 mgNO_3-N/l (Malisse, 2002). In order to circumvent these problems and improve the robustness and quality of the anoxic monitoring of biomass, a novel nitrate biosensor (Larsen *et al*., 2000) was evaluated in Chapter 3.2.

The experimental set-up developed in Chapter 3.2 provides nitrate and also titrimetric measurements for the monitoring of anoxic activated sludge activity similar to the abovementioned set-up. The use of the nitrate biosensor made the anoxic methodology simpler, more robust and more reliable. Indeed the output of the biosensor was linear to the nitrate concentration in the medium and it was rather sensitive to low nitrate concentrations (it can measure down to 0.0028 mgN/l). Moreover, the nitrate biosensor was observed to have a rather fast first order response time constant (0.31 min), which is comparable with the response time constants of Clark-type oxygen electrodes.

This experimental set-up provided high quality and high frequency nitrate measurements, which could be successfully used to calculate the nitrate uptake rate (NUR) of denitrifying biomass every 3 sec. These high frequency and quality NUR measurements for the monitoring of denitrification were possible for the first time unlike high frequency and quality OUR data which were already available for a long time to monitor the aerobic activity of biomass in BNR plants. Further, it was also possible for the first time to study the dynamics of the denitrification process in detail and to compare them with the dynamics observed in the oxygen uptake rate (OUR) measurements of biomass. It was observed that the aerobic and the anoxic activity of biomass display many similarities. This supports the findings of Beun *et al*. (2000a,b) where it was concluded that the metabolism of acetate under aerobic and anoxic conditions (considering simultaneous storage and growth activities) is similar. For instance, the NUR resulting from pulse addition of acetate to endogenously respiring activated sludge sample shows a fast transient (1- 5 minutes) as is also observed in OUR data. This is studied in detail in Chapter 4.4. Moreover, under the famine phase of a batch experiment, the NUR displays a clear storage tail similar to the OUR profile. These two phenomena are studied and modelled in detail in Chapter 4.2.2 and Chapter 4.3 respectively. Finally, it was also noticed

that the NUR data resulting from consecutive additions of acetate to biomass that had been starved for one day demonstrated a slow transient in reaching its maximum nitrate uptake rate (see Figure 6 in Chapter 3.2). Again, this particular "wake-up" behaviour was also observed in the OUR data obtained under aerobic conditions in Vanrolleghem *et al*. (1998).

The titrimetric data resulting from the anoxic batch experiments correlated well with the nitrate uptake profiles. For example, upon addition of acetate to the anoxic reactor, the acid addition accelerated immediately to compensate for the proton consumption during the denitrification process. This acid addition rate decreased sharply to a lower level which was determined only by the pH effect of the CO_2 stripping and endogenous processes under famine conditions, i.e. after all acetate was completely removed from the reactor (see Figure 4 in Chapter 3.2). This indicates a potential for titrimetry to be used for detailed study of the denitrification process, in view of e.g. kinetic parameter estimation. This was already demonstrated to be feasible for the aerobic carbon source degradation process by Gernaey *et al*. (2002a&b). The model-based interpretation of the titrimetric data from the batch denitrification experiments was explored in detail in Chapter 4.3.

The methodology developed in Chapter 3.2 has two main limitations: (1) the nitrate biosensor was also observed to drift albeit that the drift of the slope was stable, i.e. it decreases linearly in time (e.g. -2.65%/day for the pilot-scale SBR experiments). This can easily be corrected for by in-line calibration, i.e. by using the known nitrate additions that are regularly performed in the operation of the sensor. (2) The nitrate biosensor measures NO_X i.e. NO_3^- plus NO_2^-. This necessitates quantifying the NO_2^- during batch denitrification experiments either by using off-line nitrite measurements or a NO_2^- biosensor. In this study, the NO_2^- was measured off-line during the anoxic batch experiments and observed to accumulate negligibly (ca 0.22 mgN/l). Finally, the methodology developed in Chapter 3.2 is expected to be used as an anoxic respirometer to study the anoxic behaviour of activated sludge. It can be used for various purposes similar to aerobic respirometers, e.g. for process control, toxicity monitoring and characterisation of the denitrification process, fractionation of influent wastewater in view of calibration of activated sludge models, etc.

PART 2: DEVELOPMENT OF MODEL-BASED METHODS FOR INTERPRETATION OF LAB-SCALE EXPERIMENTS

Extensions to the titrimetric model of Gernaey *et al*. (2002a)

Gernaey *et al*. (2002a) recently developed a titrimetric model to interpret the titrimetric data resulting from aerobic batch experiments designed for calibration of ASM1. It was also shown to improve the identifiability of the ASM1 model when used together with the OUR measurements. However, the applicability of that titrimetric model was limited to

experimental data collected under strict conditions. To circumvent this problem, the Gernaey model was extended by a dynamic CO_2 model to describe the non-linear effect of gas-liquid CO_2 equilibria on the titrimetric data collected during (aerobic) batch experiments. A simple methodology based on titrimetric data alone was successfully developed to calibrate the dynamic CO_2 model. In this calibration methodology, the mass transfer rate of CO_2, K_La_{CO2}, was determined using the relation with the mass transfer of O_2, K_La_{O2}, and endogenous decay parameters were fixed either to the experimentally found or default values in the ASM1 model. A sensitivity study of the dynamic CO_2 model parameters showed that the reaction rate constant of the bicarbonate equilibrium, k_1, has negligible impact whereas pH, K_La_{CO2} and equilibrium constant, K_1, have a profound effect on the simulated titrimetric data. These results are in accordance with the findings of Noorman *et al*. (1992). The time constant analysis of the titrimetric data showed that the CO_2 transfer rate (CTR) is critically limited by the liquid side equilibrium reaction of CO_2, i.e. the inter-conversion between aqueous CO_2 and HCO_3^- ions. This finding is in fact not surprising and already expected (Ho *et al*., 1987) but it was necessary to be able to understand the mechanism underlying the slow dynamics (with a first order time constant around 100 min) observed in the titrimetric data of a long endogenous experiment (see Figure 5 in Chapter 4.1).

The extended Gernaey model was applied to interpret combined respirometric-titrimetric data resulting from an aerobic carbon source degradation experiment where respirometric data were used to evaluate the performance of the extended model. Similar to Gernaey *et al*. (2002b), the nitrogen content of the biomass, i_{NBM}, becomes identifiable when combined OUR and Hp data are used for parameter estimation. The estimate of i_{NBM} (0.06 mgN/mgCOD) was slightly lower than the default value (0.086 mgN/mgCOD) of ASM1 but in the same range as reported by Gernaey *et al*. (2002b). This discrepancy is believed to be an indirect effect of the storage phenomenon (Gernaey *et al*., 2002b). This becomes clear in Chapter 4.3 when ASM1 and ASM3e models were compared in view of biomass production. It was observed that ASM1 overestimates the biomass production and as such the i_{NBM} parameter was estimated lower than the default value to compensate for this error. Furthermore, the estimated parameters using Hp data and combined OUR and Hp data were compared and a remarkable agreement was found between them (see Table 8 in Chapter 4.1). These results support the validity of the extended titrimetric model developed in this Chapter.

The yield coefficient (0.75), on the other hand, was estimated to be higher than the default value of ASM1 (0.67) indicating the possible existence of storage phenomenon (van Loosdrecht and Heijnen, 2002). In contrast with this, the typical storage tail in the OUR was not observed (see Figure 8 in Chapter 4.1). Even more noteworthy, the OUR profiles could be well described using the non-storage ASM1 model (see Figure 8 in Chapter 4.1). The

comparison of ASM1 and ASM3 models was investigated further in detail in Chapter 4.2.1 in view of the mechanistic description of OUR obtained from full-scale WWTPs.

From the evaluation of the extended titrimetric model, it can be concluded that this titrimetric model can now be reliably applied to model a wide range of titrimetric data collected under different experimental conditions even if a non-linear pH effect of CTR occurs.

It is expected that combined respirometric-titrimetric data contribute to the further improvement of the identifiability of ASMs. One important drawback associated with the presented titrimetric methodology is that the elemental composition of the biomass and carbon source must be known a priori (i.e. the degrees of reduction of biomass and substrate). This is not the case for wastewater, which has a complex composition. However, the extended model is still a valuable and cheap tool for many applications, e.g. to identify two-step nitrification kinetics, or study degradation kinetics of known carbon sources by activated sludge.

Simultaneous storage and growth activities of activated sludge under aerobic conditions

Limitations of ASM1 and ASM3

Parameter estimation using respirometric batch experiments leads to estimated yield coefficients for growth that are often higher than the default values for full-scale application of the models. This is not surprising since it was recently shown by numerous studies that the storage process has a significant role in overall substrate conversion processes occurring in WWTP (van Loosdrecht *et al*., 1997; Beun *et al*., 2000a&b; Dircks *et al*., 2001; Carucci *et al*., 2001; Beccari *et al*., 2002; among many others).

Keeping that in mind, the ASM1 as a growth-based model and ASM3 as a storage-based model were evaluated and compared using the OUR data obtained with sludge collected from full-scale WWTPs to understand the extent of the storage process occurring in full-scale WWTPs (see Chapter 4.2.1). It was found that both models have serious limitations in view of the mechanistic description of aerobic activated sludge activities as measured by OUR in batch experiments. For instance, ASM1 was unable to fit the tail of OUR profiles observed in the famine phase (see Figure 1 in Chapter 4.2.1) unless the endogenous decay coefficient of biomass, b_H, is considerably increased to values much higher than the default reported in ASMs (Henze *et al*., 2000) (results not shown). Consequently, ASM1 would also estimate a growth yield as much as 0.8 (see Table 2 in Chapter 4.2.1). This, however, is too high and not likely from an energetic point of view (Heijnen and van Dijken, 1992). Whereas ASM3 could adequately fit the OUR tail, usually referred to as the storage tail, this occurred at the expense of employing parameter values which no longer have a mechanistic meanings (see Table 2 in

Chapter 4.2.1). For instance, ASM3 would estimate a maximum growth rate for biomass, μ_{MAXH}, as high as 64 d^{-1} which is way higher than the values for slowly growing activated sludge cultures operated under long SRTs (e.g. >5 days) reported in relevant literature up to now (Henze *et al*., 2000; Beun *et al*., 2000a; Beun *et al*., 2002; Vanrolleghem *et al*., 1999; Gernaey *et al*., 2002b; among many others).

These unusual values for the model parameters in both models were required to compensate for the inadequacy of the conceptual basis of the ASM1 and ASM3 models. In other words, ASM1 assumes that the substrate flux is only used for growth whereas ASM3 assumes all substrate flux is first directed to formation of storage products before it is used for growth. Reality is most probably somewhere in between the assumptions of ASM1 and ASM3, i.e. the substrate flux is simultaneously used for growth and storage. This argument is supported by numerous experimental results published in literature (Beun *et al*., 2000a&b; Dircks *et al*., 2001; Beun *et al*., 2002; Carucci *et al*., 2001; Beccari *et al*., 2002; among many others). Finally, it was noticed that the practical identifiability of ASM3 based on batch OUR data was poor. It was particularly observed that μ_H and affinity constant for storage products, K_{STO}, are not identifiable, and that a strong correlation exists between the growth yield on storage products, $Y_{H,STO}$, and μ_H, and $Y_{H,STO}$ and K_{STO}. Results obtained in this Chapter urge to consider an identifiability analysis of the model structure to support future model developments.

Extending ASM3 for simultaneous storage and growth processes

The aforementioned failures of ASM1 and ASM3 in mechanistically describing the aerobic activated sludge activities led to the development of a new mechanistic model. To this aim, several models proposed for the description of simultaneous storage and growth processes under aerobic conditions were evaluated. A new model developed around ASM3 brought two new approaches as a compromise between the complexity of biological processes and practical applicability: (i) Branch-pipe analogy is used to describe the diversion of the substrate flux to simultaneous growth and storage processes. This approach made it possible to explicitly separate the modelling of substrate uptake from the growth of biomass. (ii) Degradation of storage products, X_{STO}, under famine conditions is described using a surface saturation type kinetics for X_{STO}, and a regulation kinetics as a function of the storage content of the biomass, f_{XSTO}. These kinetics expressions result in a second order model.

The new model was evaluated using OUR data from typical batch experiments and was satisfactorily validated using independent PHB measurements (see Figure 6 in Chapter 4.2.2). A practical calibration procedure requiring only OUR data obtained from batch experiments was successfully used for parameter estimation. The parameter estimation results showed that the fraction of substrate used for storage, f_{STO}, ranged from 0.3 to 0.65 mgCOD/mgCOD for

the biomass examined in this study. This means that a considerable fraction of the substrate flux is directed to the formation of storage products. Although the value of 30% is rather low, the 65% storage ratio is in good agreement with the range reported in Beun *et al*. (2002) for slowly growing aerobic heterotrophic biomass.

The biomass growth yield on substrate, $Y_{H,S}$, was estimated to be as low as 0.57 mgCOD-X/mgCOD-S which is a more realistic (thus probably more mechanistic) prediction for the heterotrophic growth yield on soluble substrate (Heijnen and van Dijken, 1992; Henze *et al*., 2000). This is an exciting finding because it indicates that it is possible with this new model to employ mechanistically meaningful/realistic model parameters and still have a good model-fit to the experimental data in this case OUR data. This was not possible both with ASM1 and ASM3 (see Chapter 4.2.1).

The estimate for the maximum growth rate of biomass, μ_{MAXH}, was found to be in the range between 0.7 and 1.3 d^{-1}. This range is significantly lower than the values estimated in the literature for the growth-based ASM models (Henze *et al*., 2000; Vanrolleghem *et al*., 1999; Gernaey *et al*., 2002b; etc.). On the other hand, it is known that biomass in full-scale WWTPs usually function at maintenance level, which is in accordance with the results obtained in this study. As such, it is expected that these lower estimates for μ_{MAXH} are more realistic estimates of the maximum growth rate of biomass in full-scale WWTPs typically operated with long SRTs. In addition, the maximum substrate uptake rate of the biomass, q_{MAX}, is remarkably higher (at least 5 times) than the maximum growth rate of biomass, μ_{MAXH}. This is also in accordance with the conceptual basis of the new model developed here and experimental observations given elsewhere (see e.g. Beun *et al*., 2000a). Moreover, the biomass affinity to storage products, K_{STO}, was observed to be around 0.01 mgCOD/mgCOD which is close to the default value advised in ASM2d for the PAOs (0.01) but higher than the default value suggested by ASM3 which is 1.0 mgCOD/mgCOD (Henze *et al*., 2000). The high default value of ASM3 is believed to be due to parameter correlations (see Chapter 4.2.1). In this respect it is noteworthy that Koch *et al*. (2000) estimated a value for the K_{STO} as low as 0.1 mgCOD/mgCOD.

The practical identifiability analysis results for the ASM3e model are given in Table 1 in comparison with the structurally identifiable parameter combinations of ASM1e determined using the generalisation method of Petersen *et al*. (2003b) assuming no growth and nitrate in excess conditions. Since the ASM3e model was too complex and had a different type of structure than the ASM1 model, it was not possible to apply the generalisation method of Petersen *et al*. (2003b). Instead, the results of the practical identifiability analysis of the ASM3e model were used (see Chapter 4.2.2).

Table 1. Practically identifiable parameters of ASM3e and structurally identifiable parameters combinations of ASM1e (see text for explanation)

NUR	Hp	NUR & Hp
ASM1e model (negligible growth and nitrate in excess)		
$\frac{1-Y_{HNO\,3}}{2.86\cdot Y_{HNO\,3}}\mu_{\max\,H}\eta X_{\,H}(0)$	$\frac{\beta}{Y_{HNO3}}\cdot\mu_{\max H}\eta X_{\,H}(0)$	$\frac{1-Y_{HNO\,3}}{2.86\cdot Y_{HNO\,3}}\mu_{\max\,H}\eta X_{\,H}(0)$
$\frac{1-Y_{HNO\,3}}{2.86}\cdot K_S$	$\beta\cdot K_S$	$\frac{1-Y_{HNO\,3}}{2.86}\cdot K_S$
$\frac{1-Y_{HNO\,3}}{2.86}\cdot S_S(0)$	$\beta\cdot S_S(0)$	$\frac{2.86}{1-Y_{HNO3}}\beta$
		$\frac{1-Y_{HNO\,3}}{2.86}\cdot S_S(0)$
ASM3e model (negligible growth and nitrate in excess)		
q_{MAX}, f_{STO}, δ, K_S, K_1 and K_2	-	q_{MAX}, f_{STO}, δ, K_S, K_1, K_2 and i_{NBM}
ASM3e model (negligible growth and nitrate limiting)		
q_{MAX}, f_{STO}, δ, K_S, K_{NO3}, K_1 and K_2	-	q_{MAX}, f_{STO}, δ, K_S, K_{NO3}, K_1, K_2 and i_{NBM}

Where $\beta=-\frac{m}{8\gamma_S i_{CSS}}+\frac{p}{14}i_{NBM}\cdot Y_{HNO3}-\frac{1}{14}\cdot\frac{1-Y_{HNO3}}{2.86}$

Parameter estimation results with the ASM3e model showed that it is possible to estimate model parameters q_{MAX}, τ, f_{STO}, δ and also K_S using OUR data alone whereas the estimation of parameters related to the degradation of storage products for biomass growth, i.e. K_1 and K_2, are largely correlated, i.e. these two are identifiable but with large confidence intervals. When also considered in the parameters to be estimated from OUR data, the initial concentration of storage products, $X_{STO}(0)$, was observed to cause severe problems (i.e. large confidence intervals). Therefore, it was proposed to fix this parameter either by measuring it or by using a two-step parameter estimation approach (see e.g. Chapter 4.2.2). An iterative Optimal Experimental Design (OED) methodology was implemented to improve parameter estimation accuracy. It was observed that the confidence intervals of parameters K_1 and K_2 could be reduced from 77% and 102% to 12% and 25% respectively. This is a remarkable achievement in view of parameter estimation accuracy and adds credit to the OED methodology.

Simultaneous storage and growth activities of activated sludge under anoxic conditions

The aforementioned new model describing simultaneous storage and growth processes under aerobic conditions was subsequently extended to anoxic conditions. The so-called ASM3e model was evaluated using high frequency and quality NUR data (see Chapter 3.2) and compared to the growth kinetics based ASM1e model (Henze *et al.*, 2000). The ASM3e and

ASM1e models were also extended to describe the pH effect of denitrification processes in view of describing the titrimetric data collected using the set-up developed in Chapter 3.2.

Parameter estimation results showed that around 60% of the substrate (acetate) was used for the synthesis of storage products while the rest was used for the production of new cells. Moreover, the ASM3e model predicted a growth yield for the anoxic heterotrophic growth around 0.49 mgCOD-X/mgCOD-S. This is a more realistic prediction compared to the value estimated by ASM1e which was ca 0.66 mgCOD-X/mgCOD-S. It is important to note here that in ASM1e, the endogenous decay coefficient of biomass, b_H, under anoxic conditions had to be increased by ca 40% to be able to fit the elevated endogenous level after substrate addition. In fact, in this way the storage tail was fitted.

Similar to the results obtained above with aerobic storage phenomena, the maximum growth rate of denitrifiers predicted by ASM3e was remarkably lower (at least 4-5 times) than the maximum growth rate estimated by ASM1e (see e.g. Table 8 in Chapter 4.3). This was expected since the conceptual basis of ASM3e assumes biomass to maximise substrate uptake in lieu of growth rate. This argument was also supported by the estimate of the maximum substrate uptake rate of denitrifiers, q_{MAX}, which was quite higher than the μ_{MAXH} of the denitrifying biomass.

Titrimetric models developed in this study both for ASM1e and ASM3e (see Table 2&4 and Annex 1&2 in Chapter 4.3) adequately described the titrimetric data collected during anoxic batch experiments. However, the parameter estimation results with combined titrimetric and NUR data showed some identifiability problems. In other words, some parameters were estimated with large confidence intervals suggesting that they are not identifiable under the given experimental data (see Table 8 in Chapter 4.3). These identifiability problems are believed to result from an insufficient information content of the titrimetric data under the famine conditions. Application of Optimal Experimental Design (OED) methodology can be expected to solve these problems.

Affinity constants of denitrifiers, K_{NO3} and K_{STO}

The affinity constant of nitrate, K_{NO3}, could be estimated in experiments where nitrate is becoming the limiting nutrient for growth/decay. The K_{NO3}, however, was estimated to be in the order of 0.015 mgN/l (by both ASM1e and ASM3e models), which is low compared to the default values of the ASM1 model, 0.5 mgN/l. The reason of this discrepancy is believed to be the lumped effect of diffusion limitations and imperfect mixing existing in large tanks of full-scale WWTPs. When only looking at the biological phenomenon, such a low value for K_{NO3} was already expected by Betlach and Tiedje (1982).

The denitrifier's affinity constant for storage products, K_{STO}, was found to be ca 0.02 – 0.03 mgCOD/l. This is quite close to the affinity constant found above and the default value of the affinity constant of PAOs for the storage products in ASM2d (Henze *et al*., 2000), which is 0.01 mgCOD/l. These results suggest that K_{STO} of the biomass does not vary significantly as such. Since K_{STO} is the ratio of K_2 over K_1, these two parameters can be fixed to a certain value thereby eliminating the need for simultaneously estimating two parameters. This approach is expected to improve the identifiability of the second order model that describes the degradation of the storage products under famine conditions. However, further research will be necessary to verify this approach.

Effect of initial substrate to biomass, S_0/X_0

In the experimental work reported here, the substrate to biomass ratio, S_0/X_0, was shown to significantly influence the kinetic parameters whereas the yields were not affected. The latter is not unexpected since yields are related to the efficiency of oxidative phosphorylation. Parallel to the increase in S_0/X_0 ratio the maximum growth rate and maximum substrate uptake rate of biomass were observed to increase while the maximum storage rate remained unchanged (see Table 9 in Chapter 4.3). Based on these findings, it is hypothesised that biomass responds in different ways to changing S_0/X_0 ratio in batch reactors. First, at low S_0/X_0, biomass uses a certain fraction of the substrate flux (which van Loosdrecht and Heijnen (2002) assume to be constant for particular WWTPs) to the formation of storage products. Second, as S_0/X_0 increases in the batch reactor, biomass directs the increased substrate influx to the cell for the production of new cells (see Figure 9 in Chapter 4.3). This is possible for the activated sludge by undergoing a physiological adaptation, which results in increased levels of RNA, enzymes and protein synthesis etc. to sustain higher growth rates (Roels, 1983).

If the S_0/X_0 ratio remains high in the batch reactor, the microbial population which grows fast will become dominant in the reactor. In this way, the original microbial population will be significantly changed which results in the microbial selection of the fast growers in the system as explained by Chudoba *et al*. (1992). Based on these findings, it is advised to keep the S_0/X_0 ratio below 0.1 mgCOD/mgCOD during anoxic batch experiments, as they are designed to obtain representative so-called "extant" kinetic parameters (Grady *et al*., 1996) for the full-scale model. However, batch experiments carried out under high S_0/X_0 ratio will certainly be useful and meaningful for the determination of "intrinsic" kinetic parameters of the microbial population which corresponds to unrestricted growth conditions (Grady *et al*., 1996). Further research will be needed to determine an accurate value for this critical S_0/X_0 ratio in batch experiments, which is observed to be different in different studies (Chudoba *et al*., 1992; Grady *et al*., 1996; Vanrolleghem *et al*., 1999; Sperandio and Paul, 2000).

Transient responses of biomass in batch experiments

In this section, the various transient responses of activated sludge observed in batch experiments are summarised. The three different transient responses of biomass are illustrated in Figure 1 for NUR measurements. Note that the same phenomena are also observed in OUR data (Chapter 4.4; Vanrolleghem *et al*., 1998).

The fast transient response is often observed in most of the respirometric measurements, both under aerobic and anoxic conditions, which is studied in detail in Chapter 4.4. This fast response is called "start-up" and defined as the time required for the respiration rate (both NUR and OUR) to reach a maximum level possible under given conditions (see Figure 1). This transient can be characterised by a first order time constant in the order of 2-3 minutes observed in the beginning of a NUR (OUR) profile. The underlying mechanism is hypothesised to be the very nature of the substrate metabolism occurring (refer to Chapter 4.4 for more details). This transient occurs independent of the S_0/X_0 value in the batch reactor.

The second transient phenomenon is slower and observed strictly under low S_0/X_0 values and with biomass subjected to prolonged starvation periods, e.g. 1 day. In this transient phenomenon, the respiration rate of biomass reaches a level following a fast transient. After this point, it still keeps increasing until reaching the maximum respiration rate, which was obtained prior to the starvation period. In the consecutive substrate addition, the biomass does not repeat the slow transient phenomenon (see Figure 1). The time-constant of this phenomenon is in the order of 20-40 minutes. Vanrolleghem *et al*. (1998) hypothesised that it is probably due to enzymatic activation in the activated sludge which tends to be inactivated during starvation periods and as such it is called "wake-up" phenomenon.

The third phenomenon relates to the high S_0/X_0 values in the batch reactors and the time constant of this transient could be from several hours to days (see Figure 1). This phenomenon was studied in detail in Chapter 4.3 (this was also discussed above) and a hypothesis was developed to link the physiological adaptation phenomenon occurring at the hours scale (studied here) to the microbial selection hypothesis occurring at days scale (Chudoba *et al*., 1992). In this phenomenon, the biomass starts to increase its maximum substrate uptake and growth rate by undergoing a physiological adaptation, e.g., increased synthesis rate of RNA, enzymes, proteins, etc. (Roels, 1983; Chudoba *et al*., 1992; Grady *et al*., 1996). If the S_0/X_0 ratio in the batch reactor is maintained sufficiently high and long enough (e.g. by consecutive addition of substrate), then according to the hypothesis of Chudoba *et al*. (1992) it will lead to microbial selection for those microorganisms with the fastest growth kinetics.

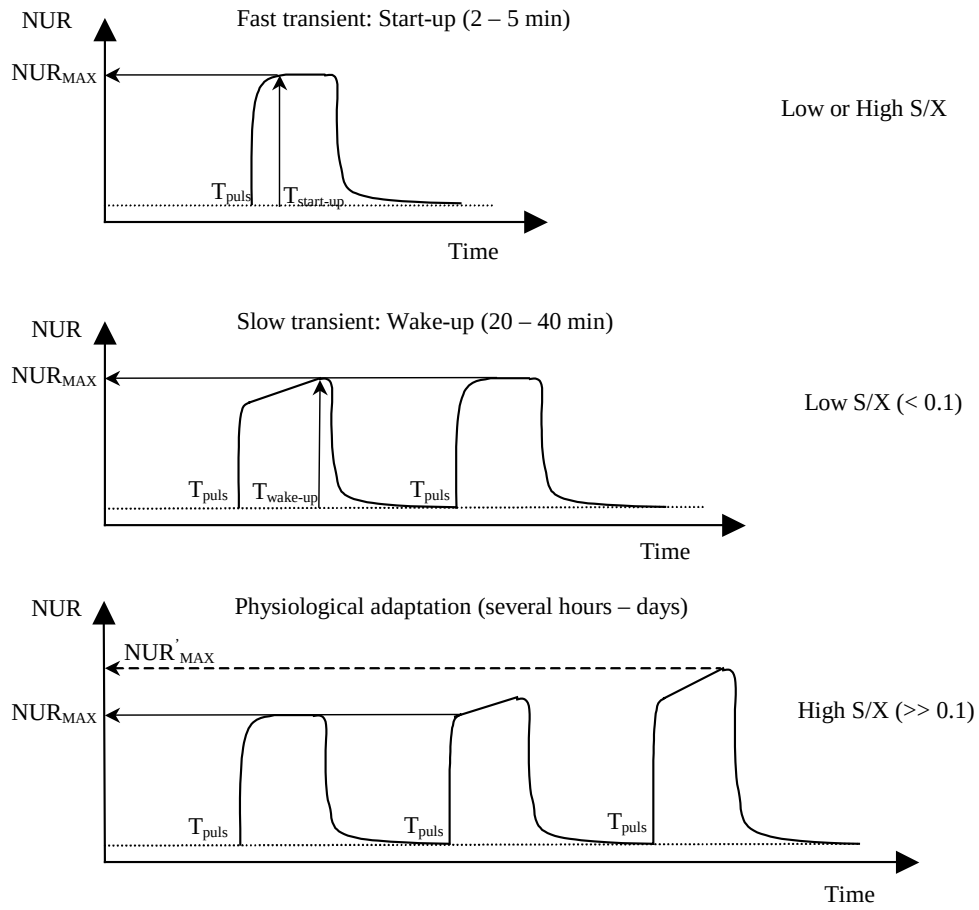

Figure 1. Illustration of three different/distinctive phenomena observed in respirometric measurements of activated sludge activity (here illustrated for NUR but the similar response is also observed in OUR).

The fast and slow transient responses of biomass should be taken into account properly to allow determination of "extant" kinetic parameters. The batch experiments at high S_0/X_0 remain useful for studying "intrinsic" properties of biomass as mentioned above. The modelling of fast transient phenomena is studied in Chapter 4.4.

Modelling the fast transient phenomenon observed in respirometric measurements

Oxygen uptake rate (OUR) measurements resulting from respirometric batch experiments often display a fast transient in minute scale (see e.g. Gernaey *et al.*, 2002), usually taking 2-5 minutes until reaching the maximum OUR level (see Figure 2 in Chapter 4.4). This transient in the OUR profile is not predicted by the current understanding of activated sludge models (e.g. ASM1). Three hypothesis were proposed to explain this discrepancy between the model and the data:

(1) Is the observed discrepancy due to an error or misinterpretation of the experimental data?
(2) Is it due to a physico-chemical phenomenon?
(3) Or is it a modelling error?

The first two hypotheses were evaluated in detail and ruled out because they failed to describe the fast transient in the OUR data. Therefore, the assumption of the ASM1 model that the OUR immediately reaches the maximum level under substrate unlimited conditions is not correct. A hypothesis was developed linking the fast transient phenomenon to the substrate metabolism at the cellular level. It seems very likely that the sequence of intracellular reactions taking place in the substrate degradation pathway is responsible for this transient. Studies with pure cultures (*S. cerevisae* and *E. coli*) performed elsewhere support this hypothesis (Theobald *et al*., 1997; Chassagnole *et al*., 2002). In our hypothesis (see Figure 10 in Chapter 4.4), the substrate uptake process is situated at the beginning of the substrate degradation pathway and does not depend on preceding reactions in the metabolic network of the cell. It has therefore a fast dynamics. Moving down the substrate degradation pathway (consisting of a myriad of reactions) some time passes until electrons of the substrate reach the oxygen reduction sites situated at the end of the metabolic network. This entire process eventually causes a delay in the oxygen uptake measurements in the surrounding environment, which is displayed as a first order transient in the experimental data.

The fast transient can be described by an empirical approach based on a first order model (see Figure 6 in Chapter 4.4). Application of this empirical model to respirometric measurements obtained with various activated sludge activities are summarised in Table 2. These results showed that the titrimetric data (indirectly monitoring the substrate uptake process) has a faster response (0.12 min on average) compared to the dynamics in the OUR data (1.74 min on average), which is particularly reflecting the start-up dynamics of the overall substrate degradation process in the model. Moreover, similar findings were obtained under the anoxic conditions using combined nitrate and titrimetric measurements (see Chapter 4.3 and Table 2). The first order time constant of titrimetric data, τ_{Hp}, was much lower than the first order time constant of the NUR data indicating that again substrate uptake is a faster process than the growth process under anoxic conditions. These results provide additional proof to the above-mentioned hypothesis.

Table 2. Estimates of first order time constants (given as averages see Chapter 4.4 and Chapter 4.3) for various activated sludge activities

Activated sludge activity	τ_{Hp} (min)	τ_{OUR} (min)	τ_{NUR} (min)
Nitrifiers	-	2.27	-
Aerobic heterotrophs	0.12	1.74	-
Denitrifiers	0.1	-	0.75

The implications of this fast transient phenomenon to the modelling of activated sludge systems are twofold. First, from a model calibration point of view, the fast transient occurring in the OUR data is shown to considerably interfere with parameter estimation if not modelled properly. For example, it causes 2.8 %, 11.5% and 16.8% relative errors (average of 3

experiments) on Y_H, μ_{maxH} and K_S respectively in the examined OUR data. Second, proper modelling of this transient phenomenon is expected to contribute fundamentally to a better understanding and modelling of fast alternating plants, e.g. ORBAL, carrousel and SBR. This requires, on the other hand, the extension of the first order model which is applicable only to batch reactors, to continuous systems. To do so, it requires at least three processes namely substrate uptake, substrate metabolism and growth processes. Further research in this direction would be valuable to see the full-scale impact of this fast transient phenomenon.

PART 3: APPLICATION OF THE BIOMATH SYSTEMATIC CALIBRATION PROTOCOL

Systematic calibration of a modified ASM2d to a pilot-scale SBR

The BIOMATH calibration protocol was developed on the basis of experiences gained from calibration studies performed for continuous activated sludge systems (see Chapter 2). Sequencing Batch Reactor (SBR) technology differs considerably in terms of configuration and operation of continuous systems (Wilderer *et al*., 2001). In this study the BIOMATH calibration protocol was evaluated at a pilot-scale SBR system (80L). The aim of the calibration was to obtain a calibrated, reliable model able to adequately describe biological processes occurring in the SBR. This model can then be used for model-based optimisation of nutrient removal (see Chapter 6).

When selecting the most appropriate model, it was observed that hydrolysis and ammonification of organic particulate nitrogen was the bottleneck (rather than the nitrification process) in the turnover of nitrogen species in the first aerobic phase of the SBR operation. This was inferred from the in-cycle nitrogen measurements and the influent wastewater characterization. Therefore, the ASM2d (Henze *et al*., 2000) model was modified by adding the organic nitrogen module of ASM1 (Henze *et al*., 2000) linked to the hydrolysis mechanism.

The BIOMATH calibration protocol was then successfully applied and extended with a methodology that makes it also applicable to SBR systems (see Figure 5 in Chapter 5.1). In this methodology a step-wise calibration procedure for each biological activity namely nitrification, hydrolysis and aerobic ordinary heterotrophs, denitrifiers and PAOs activity was proposed using NH_4-N, O_2, NO_3-N and PO_4-P measurements (every 10-15 minutes) obtained from a cycle of SBR operation. Because SBR operates in a sequence of batches, the in-cycle measurements inherently contain information unique to different biological processes under alternating anaerobic, aerobic and anoxic conditions. In this way, SBR operation already provides the information necessary for the determination of kinetic and stoichiometric parameters of biological processes. This step-wise calibration procedure simplifies the

BIOMATH protocol, as there is no need to perform dedicated lab-scale experiments for the determination of kinetics and stoichiometric parameters.

Following the step-wise calibration procedure described above, the ASM2dN model was successfully calibrated and used for systems analysis. This was performed to determine the contributions of the different biological processes to the overall N and P removal in the SBR. It was found out that 61% of denitrification took place in the anaerobic phase while 17% of total denitrification was performed in the first aerobic phase, indicating that simultaneous nitrification and denitrification is occurring in the system (Munch *et al.*, 1996). This was not surprising since in the first aerobic phase the oxygen was mostly limiting and only around 0.5 mgO_2/l. The activity of autotrophs was observed to consume the major fraction of the oxygen supplied to the system (around 63%). Concerning the P-removal, aerobic P-removal was found dominant over anoxic P-removal, which accounted for 19% of the P-removal in the system.

The nitrogen and phosphorous removal in the SBR was rather poor, around 72% and 53% respectively. In the next step, the calibrated model was used to investigate different scenarios for improving the N and P removal performance of the SBR. The insight obtained into the SBR after the systems analysis was used during the systematic optimisation of the SBR operation as described in detail in Chapter 6.

Long-term evaluation of a calibrated ASM2d model in view of prediction performance

In this study, the validation of activated sludge models is addressed. Validation is important to gain confidence in full-scale applications of activated sludge models (ASMs). Equally important is to know how long a calibrated model remains valid in terms of adequately describing the dynamic behaviour of full-scale WWTPs.

This issue was studied for the ASM2d model which was calibrated for a municipal wastewater treatment plant (Haaren WWTP, The Netherlands) using dynamic measurement campaign data (MC1) collected 3 years ago. Validation of the calibrated ASM2d model was then checked using a new measurement campaign (MC2) that reflected the recent dynamic performance of the Haaren WWTP. The BIOMATH calibration protocol (see Chapter 2) was used to perform a standard/systematic calibration.

The validation study showed that the calibrated model remained largely valid on this long-term period. In other words, it successfully predicted the dynamics of MLSS and NO_3-N in the treatment plant measured 3 years after the calibration period. However, the dynamic PO_4-P and NH_4-N trends in the treatment plant could be better predicted by adjusting a few relevant parameters of the nitrification and PAO processes. This means that part of the model

required a slight re-calibration to correct and therefore improve the predictions of NH_4-N and PO_4-P. It is also important to note that the model was calibrated using only NO_3-N and MLSS data collected 3 years ago. This particular case shows the dependency of the model calibration on the data used for the calibration.

The simulation results with the slightly recalibrated model should still be considered remarkable. This long-term prediction capability of the model suggests that the life cycle of a calibrated model is compatible with the life cycle of WWTP. This is an exciting outcome and is expected to encourage and reinforce confidence in mechanistic modelling of WWTPs. This will be positive for the future use of calibrated models for full-scale applications e.g. optimisation, upgrade and even design of WWTP.

It is also important to mention that accurate characterisation of the influent was observed to be the key to a successful model calibration. In other words, the quality of the model input determines to a large extent the quality of the model outputs. As a result the model response (i.e. prediction performance) should be checked under different seasons i.e. winter, spring and autumn, to check the model validity under these conditions too since the model calibration and re-calibrations were performed only under summer conditions.

PART 4: DEVELOPMENT AND APPLICATION OF A SYSTEMATIC OPTIMISATION PROTOCOL

The calibration of a model is usually *the "means"* whereas the application of the calibrated model is mostly *the aim* of modelling activated sludge systems. As such it is equally significant that the application of calibrated models should also be systematized to ensure objective and optimal outcomes from the modelling exercise. A systematic approach is needed to realise the notion of *optimisation* in its true sense for full-scale applications of calibrated models instead of just comparing few scenarios performed with the calibrated model, which is usually the case. The systematic optimisation approaches are expected to be an intermediate step towards the development of model-based fully automatic optimisation methodologies for activated sludge systems.

Keeping this in mind, a general systematic protocol for model-based optimisation of the operation of activated sludge systems was developed and evaluated at a pilot-scale SBR. The main idea of the protocol is to systematize every step involved in a general optimisation study. The systematic protocol is illustrated in Figure 1 of Chapter 6. The protocol consists of 7 steps and is made iterative. In this way, an optimisation loop is constructed as explained below and iterated until the objective of the modelling is satisfied. This loop includes (1) the definition of the targets of modelling (2) the definition of the system under study, the

selection of the degrees of freedom and constraints of the system, (3) selection and calibration of the model to describe the system (4) construction of grids of scenarios to cover the entire operational diagram of the system under given degrees of freedom and constraints (full-factorial design) (5) evaluation of the scenario analysis considering the objective of modelling and decision for the optimal scenario (6) implementation of the optimal scenario (7) evaluation of the optimal scenario and comparison with the targets. If the results are unsatisfactory, then go to step (3) and iterate the loop again.

Following this protocol, a grid consisting of 648 scenarios resulting from a full-factorial design of the degrees of freedoms under the constraints imposed by the study (see Chapter 6) were simulated. The simulation results were analysed according to effluent quality and robustness criteria. Analysis of effluent quality of the scenarios showed that oxygen set-point, step-feed of the influent and intermittent aeration frequency were the most influential operating parameters. Further, the effluent quality and robustness index criteria were observed to conflict with each other. In other words, scenarios with best effluent quality tended to have the lowest robustness (compare Table 2 and Table 3 in Chapter 6). Therefore a compromise had to be made considering both criteria. The best scenario was chosen to be the one with limiting oxygen (set-point is 0.5 mgO_2/l), 4 intermittent aeration sub-phases during the react phase, step-feed of the influent (ca 24% of the total influent) to the anoxic sub-phases during the react phase and 20 minutes increase in the anoxic length of the react phase. Under this scenario, the model predicted the current N and P removal performance of the SBR to improve by 54% and 74% resulting in N and P effluent concentration complying with the effluent discharge standards.

An important drawback of the protocol is that it is unable to take into account the settling properties of activated sludge and as such it is unable to simulate the settling performance of the SBR under different operating scenarios. This could be significant since it is known that settling properties of activated sludge depend on the operating parameters of the system (Metcalf and Eddy, 1991; Casey *et al*., 1992). To circumvent this problem, one may consult expert knowledge and incorporate this information at the decision-making step in choosing the best scenario. A better approach would be to extend the activated sludge models with settling models but this would complicate the activated sludge modelling even more.

During the optimisation study, the sludge age of the system was fixed at a certain sludge age (10 days). Since SRT is one of the key parameter of the system, its effect on the performance and robustness of the SBR system were also analysed to make sure that the best scenario is not a sub-optimal choice. The response of the system was analysed considering a wide range of SRTs and also as a function of the oxygen set-point in the system. It was found that increasing the sludge age has a negative effect on P-removal while it has a positive effect on

N-removal. Stability of the system as a function of sludge age and oxygen set-point was observed to have a completely opposite trend considering the effluent quality. This means that at different combinations of SRT and oxygen set-point the response of the system remains the same. This is a significant outcome as it implies that the SRT, one of the key design and operation parameter in activated sludge systems, should be considered together with the oxygen set-point in the system.

2 GENERAL CONCLUSIONS

The following main conclusions can be drawn from the research carried out in this thesis:

1. A robust, simple and reliable anoxic respirometer was successfully developed that provides *for the first time* high frequency (every 3 seconds) and high quality nitrate uptake rate (NUR) measurements of denitrifiers. The development of the anoxic respirometer was made possible by the use of a recently developed novel nitrate biosensor (Larsen *et al*., 2000). The use of this high quality and high frequency NUR measurements was shown to be essential both for improving the understanding of denitrifiers activity and for the further extension of the ASM3 model. From this, it is concluded that technical limitations existing in data collection for various activated sludge activities, is one of the main hindrance to the further development of the modelling of activated sludge systems.
2. Simultaneous storage and growth processes were recently shown to be the rule rather than the exception in full-scale WWTPs (SRT > 5days). However, the ASM1 and ASM3 models were shown to be unable to describe this phenomenon. A new mechanistic model was successfully developed to describe the simultaneous storage and growth processes of activated sludge under aerobic and anoxic conditions. In the new model, the substrate uptake kinetics of biomass was *explicitly* separated from the growth kinetics of biomass. Parameter estimation with the new model provided parameter estimates which are *mechanistically more meaningful* than those reported for the ASM models. As such the new model is expected to improve the mechanistic modelling of activated sludge processes in BNR plants.
3. Respirometric measurements of activated sludge from batch experiments both under aerobic (OUR) and anoxic conditions (NUR) showed *three distinctive transient phenomena*. These phenomena were revealed to be closely linked to the initial S_0/X_0 ratio in batch reactors:
    i. A fast-transient so-called “start-up”: phenomenon This phenomenon can be described by a first order response and usually takes 2-5 min until the respiration rate (valid both for OUR or NUR) reaches a maximum level. This phenomenon is hypothesised to result from the very nature of the *substrate metabolism at the cellular level*. Further, it occurs both at low and high S_0/X_0 ratio in batch reactors.

ii. A slow-transient phenomenon at low S_0/X_0, so-called "wake-up effect": This phenomenon usually takes place after biomass undergoes a starvation period, e.g. one-day, and under low S_0/X_0. In this phenomenon, biomass reaches its maximum respiration rate (OUR or NUR) after a relatively longer time than the "start-up" phenomenon and usually takes 20-40 min. Vanrolleghem *et al*. (1998) hypothesised that this might be due to the *enzymatic activation* of biomass.

iii. A slow transient phenomenon at high S_0/X_0: This phenomenon occurs when the initial substrate to biomass ratio, S_0/X_0, is maintained at high levels during batch experiments and continues from several hours to days. In such experiments, biomass *alters its physiological state* (new synthesis of RNA, enzyme, proteins, etc.) to increase its maximum growth rate (Chudoba *et al*., 1992; Grady *et al*., 1996). This subsequently remarkably changes the microbial population and leads to the selection of microorganisms with the fastest growth rate.

4. *Systematic calibration protocols* are needed to ensure an objective and high quality/efficient calibration of activated sludge models. The BIOMATH calibration protocol was further improved and also successfully extended to Sequencing Batch Reactor (SBR) systems. The systematic calibration protocols are expected to lay down preliminary steps to the development of fully automatic calibration methodologies.
5. The ASM2d model calibrated for a municipal WWTP (50,000 pe) was successfully validated over a long-term period (3 years time). This implies that the *lifetime of a calibrated model* is compatible with the lifetime of an activated sludge systems. This is a significant outcome which supports and increases the confidence into mechanistic modelling of full-scale WWTPs for various objectives: optimization, upgrade and design of WWTPs.
6. *A systematic protocol* for the model-based optimization of activated sludge systems was also developed and successfully evaluated at pilot-scale SBR (80 L). This protocol can be used as a guideline to systematize the search for an optimal scenario for various objectives of full-scale model applications.

Finally, the limited availability of data (measurements) and limited understanding (unpredictability) of complex biological processes ongoing in WWTPs are still the major bottlenecks in the continuous development of both the mechanistic models and the systematic calibration of these models for activated sludge systems. With the results obtained in this thesis, it is hoped to have contributed to the further advancement of the mechanistic modelling and the systematic calibration of these systems. Naturally, the research in the aforementioned direction must go on.

References

Abusam A. and Keesman K.J. (1999) Effect of number of CSTRs on the modelling of oxidation ditches: steady state and dynamic analysis. *Med. Fac. Landbouww. Univ.* Gent, **64**/5a.

Alewell C. and Manderscheid B. (1998) Use of objective criteria for the assessment of biogeochemical ecosystem models. *Ecol. Modell.* **107**:213-224.

Almeida J.S., Reis M.A.M. and Carrondo M.J.T. (1995) Competition between nitrate and nitrite reduction in denitrification by *Pseudomonas Fluorescens*. *Biotech. Bioeng.* **46**:476 – 484.

Andrews G.F. (1991) Aerobic wastewater process models. *Biotechnology: Measuring, modeling and control*. Rehm H.-J., Reed G. (eds), 2nd ed., **4**: 408-437.

APHA (1995) Standard methods for the examination of water and wastewater, 19thed. *American Public Health Association*, Washington, DC.

APHA (1998) Standard methods for the examination of water and wastewater, 20th ed. *American Public Health Association*, Washington, DC.

Artan N., Wilderer P., Orhon D., Morgenroth E. and Özgür N. (2001) The mechanism and design of sequencing batch reactor systems for nutrient removal-the state of the art. *Wat. Sci. Tech.* **43**(3): 53-60.

Artan N., Wilderer P., Orhon D., Tasli R. and Morgenroth E. (2002) Model evaluation and optimisation of nutrient removal potential for sequencing batch reactors. *Water SA* **28**(4):423-432.

ASCE (1992) Measurement of oxygen in clean water. 2nd ed, *American Society of Civil Engineers* East 47th Street, New York, NY.

Ayesa E., Oyarbide G., Larrea L. and Garcia-Heras J.L. (1995) Observability of reduced order models –application to a model for control of alpha process. *Wat. Sci. Tech.* **31**(2):161-170.

Baltes M., Scheider R., Sturm C. and Reuss M.(1994) Optimal experimental design for parameter estimation in unstructured growth models. *Biotech. Prog.* **10**:480-488.

Barker P.S. and Dold P.L. (1997) General model for biological nutrient removal activated-sludge systems: model presentation. *Wat. Env. Res.* **69**(5): 969-984.

Batchelor B. (1982) Kinetic-analysis of alternative configurations for single-sludge nitrification denitrification. *J.Water Pollut.Control Fed.* **54**(11): 1493-1504.

Beccari M., Dionisi D., Giuliani A., Majone M. and Ramadori R. (2002) Effect of different carbon sources on aerobic storage by activated sludge. *Wat. Sci. Tech.* **45**(6): 157-168.

Beun J.J., Paletta F., van Loosdrecht M.C.M. and Heijnen J.J. (2000a) Stoichiometry and kinetics of Poly-B-Hydroxybutyrate metabolism in aerobic, slow growing activated sludge cultures. *Biotechnol. Bioeng*. **67**: 379-389

Beun J.J., Verhoef E.V., van Loosdrecht M.C.M. and Heijnen J.J. (2000b) Stoichiometry and kinetics of Poly-β Hydroxybutyrate metabolism under denitrifying conditions in activated sludge culture. *Biotechnol. Bioeng.* **68**: 496-507

Beun J.J., Dircks K., van Loosdrecht M.C.M. and Heijnen J.J. (2002) Poly-B-hydroxybutyrate metabolism in dynamically fed mixed microbial cultures. *Wat. Res.* **36**: 1167-1180.

Betlach M.R. and Tiedje J.M. (1982) Kinetic explanation for accumulation of nitrite, nitric oxide and nitrous oxide during bacterial denitrification. *Appl. Environ. Microbiol.* **42**: 1074 – 1084.

Bishop D.F., Heidman J.A. and Stamberg J.B. (1976) Single stage nitrification/denitrification. *J. Water Pollut. Control Fed.* **48**(3): 520-532.

Boeije G. (1999) Chemical fate prediction for use in geo-referenced environmental exposure assessment. *PhD. Thesis*. Faculty of Agricultural and Applied Biological Sciences. University Gent (http://biomath.ugent/be/theses/).

Bogaert H., Vanderhasselt A., Gernaey K., Yuan Z., Thoeye C. and Verstraete W. (1997) New sensor based on pH effects of denitrification process. *J. Environ. Eng.* **123**: 884 – 891.

Bonarius H.P.J., De Gooijer C.D., Tramper J. and Schmid, G. (1995). Determination of the Respiration Quotient in Mammalian Cell Culture in Bicarbonate Buffered Media. *Biotech. Bioeng*. **45**: 524-535.

Boyle W.C. and Campbell H.J.Jr. (1984) Experiences with oxygen transfer testing of diffused air systems under process conditions. *Wat. Sci. Tech.* **16**: 91-106.

Brun R., Kuhni M., Siegrist H., Gujer W. and Reichert P. (2002). Practical identifiability of ASM2d parameters – systematic selection and tuning of parameter subsets. *Wat. Res.* **36**(16): 4113-4127.

Bundgaard E., Andersen K. and Petersen G. (1989). Bio-Denitro and Bio-Denipho systems - Experiences and advanced model development: The Danish systems for biological N and P removal. *Wat. Sci. Tech*. **21**: 1727-1730.

Capela S., Gillot S. and Héduit A. (1999) Oxygen transfer under process conditions: Comparison of measurement methods. *In: Proceedings 72nd Annual WEF Conference and Exposition*. New Orleans, USA, October 9-13 1999. (on CD-ROM).

Carrette R., Bixio D., Thoeye C., Ockier P. (2001) Full application of the IAWQ ASM No.2d model. *Wat. Sci. Tech.* **44** (2-3): 17-24.

Carucci A., Dionisi D., Majone M., Rolle E. and Smurra P. (2001) Aerobic storage by activated sludge on real wastewater. *Wat. Res.* **35**: 3833-3844.

Carucci A., Rolle E. and Smurra P. (1999a). Management optimisation of a large wastewater treatment plant. *Wat. Sci. Tech.* **39**(4):129-136.

Carucci A., Kühni M., Brun R., Carucci G., Koch G., Majone M. and Siegrist H. (1999b) Microbial competition for the organic substrates and its impact on EBPR systems under conditions of changing carbon feed, *Wat. Sci. Tech.* **39**(1) 75-85.

Casey T.G., Wentzel M.C., Loewenthal R.E., Ekama G.A. and Marais G.v.R. (1992) A hypothesis for the cause of low F/M filament bulking in nutrient removal activated sludge systems. *Wat. Res.* **26**:867-869.

Chambers B. (1992) Design methodology for optimisation of aeration efficiency in activated sludge plants. *In: Proceedings 6th Forum Applied Biotechnology. Med. Fac. Landbouww. Univ. Gent* **57**: 1631-1642.

Chassagnole C., Noisommit-Rizzi N., Schmid J.W., Mauch K. and Reuss M. (2002) Dynamic modelling of the central carbon metabolism of *Escherichia coli*. *Biotechnol. Bioeng.* **79**:53-73.

Cheng C.-Y. and Ribarova I. (1999). Activated sludge system modeling and simulations for improving the effluent water quality. *Wat. Sci.Tech.* **39**(8), 93-98.

Chudoba P., Capdeville B. and Chudoba J. (1992) Explanation of biological meaning of the S0/X0 ratio in batch cultivation *Wat. Sci. Tech.* **26**(3-4): 743-751.

Cinar Ö., Daigger G.T. and Graef S.P. (1998) Evaluation of IAWQ activated sludge model no.2 using steady state data from four full-scale wastewater treatment plants, *Wat. Env. Res*., **70**(6): 1216-1224.

Coen F., Vanderhaegen B., Broonen I., Vanrolleghem P.A. and Van meenen P. (1997). Improved design and control of industrial and municipal nutrient removal plants using dynamic models. *Wat. Sci. Tech.* **35**(10): 53-61.

Comeau Y., Hall, K.J. and Oldham W.K. (1990). Indirect polyphosphate quantification in activated sludge. *Water Pollut. Res. J. Canada* **25**(2): 161-174.

Comeau Y., Hall K.J., Oldham W.K. (1988) Determination of poly-hydroxybutyrate and poly-hydroxyvalerate in activated sludge by gas-liquid chromatography. *Appl. Environ. Microbiol.* **54**: 2325-2327.

Daigger G.T. and Grady C.P.L. (1982) The dynamics of microbial growth on soluble substrates: A unifying theory. *Wat. Res.* **16**: 365-382.

Daigger G.T. and Nolasco D. (1995) Evaluation and design of full scale wastewater treatment plants using biological processes models. *Wat. Sci Tech* **31**(2): 245-255.

Daigger G.T. and Littleton H.X. (2000) Characterization of simultaneous nutrient removal in staged, closed-loop bioreactors. Water Env. Res. **72**:330-339.

De Clercq B., Coen F., Vanderhaegen B. and Vanrolleghem P.A. (1999) Calibrating simple models for mixing and flow propagation in wastewater treatment plants. *Wat. Sci. Tech.* **39**(4): 61-69.

De la Sota A., Larrea L., Novak L., Grau P. and Henze M. (1994) Performance and model calibration of R-N-D processes in pilot plant. *Wat. Sci. Tech.* **30**(6): 355-364

Demoulin G., Rudiger A. and Goronszy M.C. (2001). Cyclic activated sludge technology – recent operating experience with a 90,000 p.e. plant in Germany. *Wat. Sci. Tech.* **43**(3): 331-337.

Demuynck C., Vanrolleghem P.A., Mingneau C., Liessens J. and Verstraete W. (1994) NDBEPR process optimization in SBRs: Reduction of external carbon source and oxygen supply. *Wat. Sci. Tech.* **30**(4):169-179.

Derco J., Králik M. and Kovács A. (2001) Modelling of nutrient removal processes in an intermittently aerated bioreactor. *Chem. Biochem. Eng.* **15**(4): 167-174.

De Pauw D., Sin G., Insel G., Van Hulle S.W.H., Vandenberghe V. and Vanrolleghem P.A. (2003) Discussion of 'Assessing Parameter Identifiability of Activated Sludge Model No. 1' by Pedro Afonso and Maria da Conceicao Cunha, *Journal of Environmental Engineering*. (In press).

De Schryver T. (1992) On-line schatting van de zuurstofoverdrachts- en zuurstofopnamesnelheidskarakteristieken met de RODTOX-biosensor. *Engineers Thesis*. Faculty of Agricultural Sciences. Ghent University, Belgium. pp. 99 (in Dutch).

Dionisi D., Majone M., Ramadori R. and Beccari M. (2001) The storage of acetate under anoxic conditions. *Wat. Res*. **35**: 2661 –2668.

Dircks K., Henze M., van Loosdrecht M.C.M., Mosbaek H. and Aspegren H. (2001). Storage and degradation of poly-B-hydroxybutyrate in activated sludge under aerobic conditions. *Wat. Res*. **35**:2277-2285.

Dochain D., and Vanrolleghem, P.A. (2001). Dynamical modelling and estimation in wastewater treatment processes. *IWA Publishing*, London, UK.

Dudlry J., Buck, G., Ashley R., and Jack A. (2001) Experience and extensions to the ASM2 family of models. *In Proceedings: 5th Kollekolle Seminar on Activated Sludge Modelling, Processes in Theory and Practice*, Kopenhagen, Denmark, September 10-12, 2001.

Dupont R. and Sinkjaer O. (1994) Kinetic constants of nitrification. *Wat. Sci. Tech.* **30**(4): 181-190.

Ekama G.A., Dold P.L. and Marais G.V. (1986) Procedures for determining influent cod fractions and the maximum specific growth-rate of heterotrophs in activated-sludge systems. *Wat. Sci. Tech.* **18**(6): 91-114.

Ekama G.A., Barnard J.L., Gunthert F.W., Krebs P., McCorquodale J.A., Parker D.S. and Wahlberg E.J. (1997) Secondary Settling Tanks: Theory, Modelling, Design and Operation. *IWA Scientific and Technical Report No.6* . IWA publishing, London.

Ficara E., Musumeci A. and Rozzi A. (2000) Comparison and combination of titrimetric and respirometric techniques to estimate the nitrification kinetics parameters. *Water SA* **26**:217-224.

Filipe C.D.M. and Daigger G.T. (1998) Development of a revised metabolic model for the growth of phosphorus-accumulating organisms, *Wat. Env. Res.* **70**(1): 67-79.

Foxon K.M., Brouckaert C.J., Buckley C.A. and Rozzi A. (2002) Denitrifying activity measurements using an anoxic titration (pHstat) bioassay. *Wat. Sci.Tech.* **46**(9): 211–218.

Furumai H., Kazmi A.A., Fujita M., Furuya Y. and Sasaki K. (2001) Modelling long-term nutrient removal in a sequencing batch reactor. *Wat.Res.* **33**: 2708-2714.

Gernaey K., Bogaert H., Massone A., Vanrolleghem P. and Verstraete W. (1997) On-line nitrification monitoring in activated sludge with a titrimetric sensor. *Environ. Sci. Tech*. **31**: 2350 - 2355.

Gernaey K., Vanrolleghem P. and Verstraete W. (1998) On-line estimation of kinetic parameters of NH4+ oxidizing bacteria in activated sludge samples using titration in-sensor-experiments. *Wat. Res.* **32**: 71-80.

Gernaey K., Petersen B., Ottoy J.P. and Vanrolleghem P. (2001a) Activated sludge monitoring with combined respirometric - titrimetric measurements. *Wat. Res*. **35**: 1280 -1294.

Gernaey K., Vanrolleghem P. and Lessard P. (2001b). Modelling of a reactive primary clarifier, *Wat. Sci. Tech.* **43** (7): 73-81.

Gernaey K., Petersen B., Nopens I., Comeau Y. and Vanrolleghem P.A. (2002a) Modelling aerobic carbon source degradation processes using titrimetric data and combined respirometric-titrimetric data: Experimental data and model structure. *Biotech. Bioeng*., **79**: 741-753.

Gernaey K., Petersen B., Dochain D. and Vanrolleghem P.A. (2002b) Modelling aerobic carbon source degradation processes using titrimetric data and combined respirometric-titrimetric data: Structural and practical identifiability. *Biotech. Bioeng*. **79**: 754-769.

Gijzen HJ and Mulder A (2001). The nitrogen cycle out of balance. *Water 21* **8**: 38 - 40.

Gillot S., Deronzier G. and Héduit A. (1997) Oxygen transfer under process conditions in an oxidation ditch equipped with fine bubble diffusers and slow speed mixers. *In: Proceedings 70th Annual WEF Conference and Exposition*. Chicago, USA, October 18-22 1997. **1**: 385-392.

Gillot S. (2002) Personal Communication.

Govoreanu R., Seghers D., Nopens I., De Clercq B., Saveyn H., Capalozza C., Van der Meeren P., Verstraete W., Top E. and Vanrolleghem P.A. (2003) Linking floc structure and settling properties to activated sludge population dynamics in an SBR. *Wat. Sci. Tech.* **47**(12): 9-18.

Grady C.P.L. Jr., Smets B.F. and Barbeau D.S. (1996) Variability in kinetic parameter estimates: a review of possible causes and a proposed terminology. *Wat. Res.* **30**: 742-748

Grady C.P.L.Jr., Daigger G.T. and Lim H.C. (1999) Biological wastewater treatment, *Marcel Dekker Inc.*, New York.

Gujer W. and Larsen T.A. (1995) The implementation of biokinetics and conservation principles in ASIM. *Wat. Sci. Tech.* **31**(2): 257-266.

Gujer W., Henze M., Mino T. and van Loosdrecht M.C.M. (2000) Activated Sludge Model No.3. In: *Activated Sludge Models ASM1, ASM2, ASM2D and ASM3*, Henze M., Gujer W., Mino T., van Loosdrecht M.C.M. (eds.) *IWA Scientific and Technical Report* **9**. IWA London.

Guisasola A., Baeza J.A., Carrera J., Casas C. and Lafuente J. (2004) An off-line respirometric procedure to determine inhibition and toxicity of biodegradable compounds in biomass from an industrial WWTP. *Wat. Sci. Tec.* **48**(11-12): 267-275.

Guisasola A., Pijuan M., Baeza J.A., Casas C. and Lafuente F.J. (In press) Aerobic phosphorus release linked to acetate uptake in bio-P-sludge. Process modelling using oxygen uptake rate measurements. *Biotech. Bioeng*.

Guisasola A., Sin G., Baeza J.A., Carrera J. and Vanrolleghem P. (Submitted) Limitations of ASM1 and ASM3: a comparison based on batch OUR profiles from different full-scale WWTPs. *IWA 4th World Water Congress,* 19-24 September 2004, Marrakech, Morocco.

Hanhan O., Artan N. and Orhon D. (2003) Retrofitting activated sludge systems to intermittent aeration for nitrogen removal, *Wat. Sci. Tech*. **46**(8): 75-82.

Hatziconstantinou G.J., Kalergis C.M. and Grivas A.P. (1995). Upgrading of a small wastewater treatment plant: design and operation aspects. *Wat. Sci. Tech.* **32**(7): 111-117.

Heijnen J.J. (1999) Bioenergetics of microbial growth. *In: Encyclopedia of Bioprocess Technology: Fermentation, Biocatalysis and Bioseparation*. Ed. Flickinger M.C. and Drew S.W. John Wiley & Sons Inc.: 267-291.

Heijnen J.J. and van Dijken J.P. (1992) In search of a thermodynamic description of biomass yields for the chemotrophic growth of microorganisms. *Biotech. Bioeng.* **39**: 833 - 858.

Henze M., Grady C.P.L.Jr., Gujer W., Marais G.v.R. and Matsuo T. (1987). Activated sludge model No.1. *IAWPRC Sci. and Tech. Report* **1**, IAWPRC, London

Henze M., Gujer W., Mino T., Matsuo T., Wentzel M.C. and Marais G.v.R. (1995a). Activated Sludge Model No.2. *IAWPRC Task Group on Mathematical Modelling for Design and Operation of Biological Treatment*, IAWQ, London.

Henze M, Harremoës P, Jansen JC and Arvin E (1995b) Biological and Chemical Processes :In Wastewater Treatment, *Springer-Verlag*, Berlin.

Henze M., Gujer W., Mino T., Matsuo T., Wentzel M.C., Marais G.v.R. (1995c) Wastewater and biomass characterization for the activated sludge model no-2 - biological phosphorus removal. *Wat. Sci. Tech.* **31**(2): 13-23.

Henze M., Gujer W., Mino T., Matsuo T., Wentzel M.C., Marais G.v.R., van Loosdrecht M.C.M. (1999) Activated Sludge Model No.2d, ASM2d. *Wat. Sci. Tech.* **39**(1): 165-182.

Henze M., Gujer W., Mino T. and van Loosdrecht M.C.M. (2000) Activated Sludge Models ASM1, ASM2, ASM2d and ASM3. *IWA Scientific and Technical Report* **9** IWA. London.

Henze M., Aspegren H., Jansen J.L., Nielsen P.H. and Lee N. (2002) Effect of solids retention time and wastewater characteristics on biological phosphorus removal. *Wat. Sci. Tech.* **45**(6): 137-144 2002

Ho C.S., Smith M.D. and Shanahan J.F. (1987) Carbon dioxide tranfer in biochemical reactors. *Adv. Biochem. Eng.Biotechnol*. **35**:83-125.

Hulsbeek J.J.W., Kruit J., Roeleveld P.J. and van Loosdrecht M.C.M. (2002) A practical protocol for dynamic modelling of activated sludge systems. *Wat. Sci. Tech.* **45** (6): 127-136.

Hvala N., Zec M., Ros M. and Strmcnik S. (2001) Design of a sequencing batch reactor sequence with an input load partition in a simulation-based experimental environment. *Water Environ. Res.* **73**:146 –153.

Insel G., Orhon D. and Vanrolleghem P.A. (2003a) Identification and modeling of aerobic hydrolysis mechanism-application of optimal experimental design, *J. Chem. Tech. Biotech.* **78**(4): 437-445.

Insel G., De Pauw D, Lee DS and Vanrolleghem PA (2003b) Dynamic calibration of an intermittently aerated carrousel plant-Report No.1, *BIOMATH Technical Report*.

Irvine R.L., Wilderer P.A. and Flemming H.C. (1997) Controlled unsteady state processes and technologies-an overview. *Wat. Sci. Tech.* **35**(1): 11-18.

Ip S.Y., Bridger J.S. and Mills N.F. (1987) Effect of alternating aerobic and anaerobic conditions on the economics of the activated-sludge system. *Wat. Sci. Tech.* **19**(5-6): 911-918.

Isaacs S., Hansen J.A., Schimdt K. and Henze M. (1995) Examination of the activated sludge model No:2 with an alternating process, *Wat. Sci. Tech*. **31**(2): 55-66.

Iversen J.J.L., Thomsen J.K. and Cox R.P. (1994) On-line growth measurement in bioreactors by titrating metabolic proton exchange. *Appl. Microbiol. Biotechnol*. **42**: 256 – 262.

Kappeler J. and Gujer W. (1992). Estimation of kinetic parameters of heterotrophic biomass under aerobic conditions and characterization of wastewater for activated sludge modelling. *Wat. Sci.Tech.* **25**(6): 125-139.

Karahan-Gül Ö., van Loosdrecht M.C.M. and Orhon D. (2003). Modification of Activated Sludge nº3 considering direct growth on primary substrate. *Wat. Sci. Technol.* **47**(11): 219-225.

Kazmi A.A., Fujita M. and Furumai H. (2001) Modeling effect of remaining nitrate on phosphorus removal in SBR. *Wat. Sci. Tech.* **43**(3): 175-182.

Keesman K.J., Spanjers H. and van Straten G. (1997) Analysis of endogenous process behaviour in activated sludge. *Biotech. Bioeng.* **57**: 155-163.

Keller J., Watts S., Battye-Smith W. and Chong R. (2001) Full-scale demonstration of biological nutrient removal in a single tank process. *Wat. Sci. Tech.* **43**(3): 355-362.

Ketchum L.H.Jr. (1997) Design and physical features of sequencing batch reactors. *Wat. Sci. Tech.* **35**(1): 1-10.

Kim B.H., Hao O.J. and Mc Avoy T.J. (2001a) SBR system for phosphorus removal: ASM2 and simplified linear model. *Journal Env. Eng.* **127**(2): 98-104.

Kim B.H., Hao O.J. and Mc Avoy T.J. (2001b) SBR system for phosphorus removal: linear model based optimization. *Journal Env. Eng.* **127**(2): 105-111.

Koch G., Kühni M., Gujer W. and Siegrist H. (2000) Calibration and validation of activated sludge model nº3 for Swiss municipal wastewater. *Wat. Res*. **34**: 3580-3590.

Kong Z., Vanrolleghem P., Willems P. and Verstraete W. (1996). Simultaneous determination of inhibition kinetics of carbon oxidation and nitrification with a respirometer. *Wat. Res.* **30**: 825-836.

Kotte K. (2002) Reducing uncertainty of activated sludge model (ASM1) parameters. *M.Sc. Thesis*. Faculty of Agricultural and Applied Biological Sciences. Ghent University. pp. 114.

Kramer R. and Sprenger G. (1991) Metabolism. *In Biotechnology*: *Biotechnological fundamentals*. Rehm H.-J., Reed G. (eds.), 2nd ed., **2**: (50-90).

Kristensen H.G., Elberg Jørgensen P. and Henze M. (1992) Characterisation of functional microorganism groups and substrate in activated sludge and wastewater by AUR, NUR and OUR. *Wat. Sci. Tech.* **25**(6): 43 - 57.

Kristensen H.G., la Cour Janssen J. and Elberg Jorgensen, P. (1998) Batch test procedures as tools for calibration of the activated sludge model- A pilot scale demonstration. *Wat. Sci Tech.* **37**(4-5): 235-242.

Krishna C. and van Loosdrecht M.C.M. (1999) Substrate flux into storage and growth in relation to activated sludge modelling. *Wat. Res.* **33**(14): 3149-3161.

Kuba T., Wachtmeiser A., van Loosdrecht M.C.M. and Heijnen J.J. (1994) Effect of nitrate on phosphorus release in biological phosphorus removal systems. *Wat. Sci. Tech.* **30**(6): 263-269.

Kuba T., van Loosdrecht M.C.M. and Heijnen J.J. (1996) Effect of cyclic oxygen exposure on the activity of denitrifying phosphorus removing bacteria, *Wat. Sci. Tech.* **34**(1-2): 33-40.

Langergraber G., Rieger L., Winkler S., Alex J., Wiese J., Owerdieck C., Ahnert M., Simon J. and Maurer M. (2003a). A guideline for simulation studies of wastewater treatment plants. *In proceedings*: *9th IWA conference on Design Operation and Economics of LWWTP*. 1-4 September 2003, Praha, Czech Republic: 201-208.

Langergraber G., Fleischmann N. and Hofstädter F. (2003b) A multivariate calibration procedure for UV/VIS spectrometric quantification of organic matter and nitrate in wastewater. *Water Sci. Tech.* **47**(2): 63-71.

Larrea L., Irizar I. and Hidalgo M.E. (2001) Improving the predictions of ASM2d through modelling in practice. *In Proceedings: 5th Kollekolle Seminar on Activated Sludge Modelling, Processes in Theory and Practice,* Kopenhagen, Denmark, September 10-12.

Larsen L.H., Damgaard L.R., Kjaer T., Stenstrom T., Lynggaard-Jensen A. and Revsbech N.P. (2000) Fast responding biosensor for on-line determination of nitrate/nitrite in activated sludge. *Wat. Res.* **34**: 2463-2468.

Lee Y.H. and G.T. Tsao (1979) Dissolved oxygen electrodes. *Adv. Biochem. Eng*. **13**: 35-86.

Lesouef A., Payraudeau M., Rogalla F. and Kleiber B. (1992) Optimising nitrogen removal reactor configuration by on-site calibration of the IAWPRC activated sludge model. *Wat. Sci. Tech.* **25**(6): 105-123.

Li D. and Ganczarczyk J. (1992) Advective transport in activated sludge flocs. *Water Environ. Res.* **64**: 236-240.

Lin K.C. and Tsang K.W.R. (1989) Nitrogen removal in an intermittently aerated completely mixed reactor. *Env. Tech. Lett.* **10**(1): 1-8.

Lin Y.-F. and Jing S.-R. (2001) Characterization of denitrification and nitrification in a step-feed alternating anoxic-oxic sequencing batch reactors. *Water Environ. Res.* **73**: 526-533.

Lynggaard-Jensen A. (1999) Trends in monitoring of wastewater systems. *Talanta*. **50**: 707-716.

Makinia J. and Wells S.A. (2000) A general model of the activated sludge reactor with dispersive flow-I. Model development and parameter estimation. *Wat. Res.* **34**: 3987-3996.

Makinia J, Swinarski M and Dobiegala E (2002) Experiences with computer simulation at two large wastewater treatment plants in northern Poland. *Wat. Sci. Tech.*, **45**(6) 209-218.

Malisse K. (2002) Monitoring van de denitrificatie in actief slib aan de hand van nitraat- en titrimetrische gegevens. *Engineers Thesis.* Faculty of Agricultural and Applied Biological Sciences. Ghent University. pp 130. (In Dutch).

Mamais D., Jenkins D. and Pitt P. (1993) A rapid physical chemical method for the determination of readily biodegradable soluble COD in municipal wastewaters. *Wat. Res.* **27**: 195-197.

Manning J.F. and Irvin R.L. (1985) The biological removal of phosphorous in a sequencing batch reactor. *J. Water Pollut. Control. Fed.* **57**: 87-94.

Massone A., Antonelli M. and Rozzi A. (1996) The Denicon: A novel biosensor to control denitrification in biological wastewater treatment plants. *Med. Fac. Landbouww. Univ. Gent*, **61**: 1709 – 1714.

McClintock S.A., Sherrard J.H., Novak J.T. and Randall C.W. (1988) Nitrate versus oxygen respiration in the activated sludge process. *J. Water Pollut. Control Fed.* **60**: 342 – 350.

McMurray S.H., Meyer R.L., Zeng R.J., Yaun Z. and Keller J. (2004) Integration of titrimetric measurement, off-gas analysis and NO_x^- biosensors to investigate the complexity of denitrification processes. In proceedings: *2nd IWA* conference on Automation in Water Quality Monitoring (AutMoNet2004), April 19-20, Vienna, Austria, pp 53-59.

Meijer S.C.F., van der Spoel H., Susanti S., Heijnen J.J. and van Loosdrecht M.C.M. (2002) Error diagnostics and data reconciliation for activated sludge modelling using mass balances. *Wat. Sci. Tech.* **45**(6):145-156.

Meirlaen (2002) Immision based real-time control of the integrated urban wastewater system. *PhD Thesis*. Faculty of Applied Biological Sciences, Ghent University, pp 243.

Metcalf and Eddy (1991) Wastewater engineering: Treatment, disposal and reuse. Revised by Tchobanoglous Y. and Burton L., 3rd ed. McGraw Hill, Inc.

Mino T., San Pedro C.D. and Matsuo T. (1994). Estimation of the rate of slowly biodegradable COD (SBCOD) hydrolysis under anaerobic anoxic and aerobic conditions by experiments using starch as model substrate. *Wat. Sci. Tech.* **31** (2): 95-103

Mueller J. and Boyle W. (1988) Oxygen transfer under process conditions. *J. Water Pollut. Control Fed.* **60**: 332-341.

Muller A., Wentzel M.C., Loewenthal R.E. and Ekama G.A. (2003) Heterotrophic anoxic yield in anoxic aerobic activated sludge systems treating municipal wastewater. *Wat. Res.* **37**(10): 2435-2441.

Münch E.V., Lant P. and Keller J. (1996) Simultaneous nitrification and denitrification in bench-scale sequencing batch reactors. *Wat. Res.* **30**(2): 277-284.

Mura G. (2003) Model-based optimisation of SBRs: Effect of oxygen set-point and SRT. *Master thesis*. Faculty of Applied Biological Sciences, Ghent University, 120 pp.

Murnleitner E., Kuba T., van Loosdrecht M.C.M. and Heijnen J.J. (1997) An integrated metabolic model for the aerobic and denitrifying biological phosphorus removal. *Biotechnol Bioeng*. **54**(5): 434-450.

Naidoo V., Urbain V. and Buckley C.A. (1998) Characterisation of wastewater and activated sludge from European municipal wastewater treatment plants using the NUR test. *Wat. Sci. Tech.* **38**(1): 303 – 310.

Nakanaishi H., Fukagawa M., Takeuchi M., Ishikawa M., Ukita M. and Murakami S. (1990) Biological nitrogen removal in a complete mixing type aerator with ORP control. *Wat. Sci. Tech.* **22**(7/8): 269-270.

Nelder J.A. and Mead R. (1964) A simplex method for function minimization. *Computer Journal* **7** : 308-313.

Nielsen J., Villadsen J. and Lidén G. (2003) Bioreaction engineering principles. *Kluwer Academic/Plenum Publishers 2nd ed.,* Dordrecht, The Netherlands.

Ning Z., Patry G.G. and Spanjers H. (2000) Identification and quantification of nitrogen nutrient deficiency in the activated sludge process using respirometry. *Wat. Res*. **34**: 3345-3354.

Noorman H.J., Luijkx G.C.A., Luyben K.Ch.A.M. and Heijnen J.J. (1992) Modeling and experimental validation of carbon dioxide evolution in alkalophilic culture. *Biotech. Bioeng.* **39**: 1069-1079.

Novák L., Larrea L. and Wanner J. (1994) Estimation of maximum specific growth rate of heterotrophic and autotrophic biomass: A combined technique of mathematical modelling and batch cultivations. *Wat. Sci. Tech*. **30**(11):171-180.

Oh J. and Silverstein J. (1999) Acetate limitation and nitrite accumulation during denitrification. *J. Environ. Eng.* **125** (3): 234-242.

Omlin M. and Reichert P. (1999) A comparison of techniques for the estimation of model prediction uncertainty. *Ecol. model.* **115**:45-59.

Omlin M., Brun R. and Reichert P. (2001) Biogeochemical model of lake Zurich: sensitivity, identifiability and uncertainty analysis. *Ecol. Modell.* **141**:105-123.

Orhon D. and Artan N. (1994) Modelling of activated sludge systems. *Technomic Publishing Inc*., London.

Orhon D., Yildiz G., Cokgor E.U. and Sozen S. (1995) Respirometric evaluation of the biodegradation of confectionary wastewaters. *Wat.Sci.Tech*. **32**(12):11-19.

Orhon D., Sözen S. and Artan N. (1996) The effect of heterotrophic yield on the assessment of the correction factor for anoxic growth. *Wat. Sci. Tech.* **34**(5-6): 67-74.

Orhon D., Ubay Çokgör E. and Sözen S. (1998) Dual hydrolysis model of the slowly biodegradable substrate in activated sludge systems. *Biotechnol. Tech.* **12**(10): 737-741.

Orhon D., Ubay Çokgör E. and Sözen S. (1999) Experimental basis for the hydrolysis of slowly biodegradable substrate in different wastewaters. *Wat. Sci.Tech.* **39**(1): 87-95.

Orhon D., Okutman D. and Insel G. (2002) Characterization and biodegradation of settleable organic matter for domestic wastewater. *Water SA,* **28**(3): 299-305.

Pedersen K.M., Kümmel M. and Soeberg H. (1990) A real time measurement system for an activated sludge wastewater treatment plant. *In: Advances in Water Pollution Control. Ed. Briggs R.*, Pergamon Press, London: 171-178.

Pedersen J. and Sinkjaer O. (1992) Test of activated sludge models capabilities as a prognostic tool on a pilot scale wastewater treatment plant. *Wat. Sci. Tech.* **25**(6): 185-194.

Petersen B. (2000) Calibration, identifiability and optimal experimental design of activated sludge models. *Ph.D. Thesis*, Ghent University, Faculty of Agricultural and Applied Biological Science, Belgium. (http://biomath.rug.ac.be/ publications /download /petersenbritta_phd.pdf)

Petersen B., Gernaey K. and Vanrolleghem P.A. (2002a) Anoxic activated sludge monitoring with combined nitrate and titrimetric measurements. *Water Sci. Tech.* **45**(4-5): 181–190.

Petersen B., Gernaey K., Henze M. and Vanrolleghem P.A. (2002b) Evaluation of an ASM1 model calibration procedure on a municipal–industrial wastewater treatment plant. *J. Hydroinformatics* **4**:15-38.

Petersen B., Gernaey K., Henze M. and Vanrolleghem P.A. (2003a) Calibration of activated sludge models: A critical review of experimental designs. In: *Biotechnology for the Environment: Wastewater Treatment and Modeling, Waste Gas Handling*. Eds. Agathos S.N. and Reineke W., Kluwer Academic Publishers, Dordrecht, The Netherlands. 101-186.

Petersen B., Gernaey K., Devisscher M., Dochain D. and Vanrolleghem P.A. (2003b) A simplified method to assess structurally identifiable parameters in Monod-based activated sludge models. *Wat. Res.* **38**: 2893-2904.

Philichi T. and Stenstrom M. (1989) Effects of dissolved oxygen probe lag on oxygen transfer parameter estimation. *J. Wat. Pollut. Control Fed*. **61**:83-86.

Pratt, S., Yuan, Z., Gapes, D., Dorigo, M., Zeng, R and Keller, J. (2003) Development of a novel titration and off-gas analysis (TOGA) sensor for study of biological processes in wastewater treatment systems. *Biotech. Bioeng.* **81**: 482-495.

Press W.H., Teukolsky S.A., Vetterling W.T. and Flannery B.P. (1992) *Numerical Recipes in C: The art of scientific computing*. 2nd edition, Cambridge University Press.

Randall CW, Barnard LB and Stensel HD (1992) Design and retrofit of wastewater treatment plants for biological nutrient removal. *Technomic Publishing Inc*., Lancaster, PA.

Ramadori R., Rozzi A. and Tandoi V. (1980) An automated system for monitoring the kinetics of biological oxidation of ammonia. *Wat. Res*. **14**: 1555 – 1557.

Rieger L., Siegrist H., Winkler S., Saracevic E., Votava R. and Nadler J. (2002) In-situ measurement of ammonium and nitrate in the activated sludge process. *Wat. Sci. Tech.* **45**(4-5): 93-100.

Roeleveld P.J. and Van Loosdrecht M.C.M. (2002) Experiences with guidelines for wastewater characterization in The Netherlands. *Wat. Sci. Tech.* **45**(6): 77-87.

Rodrigo MA, Seco A, PenyaRoja JM, Ferrer J (1996) Influence of sludge age on enhanced phosphorus removal in biological systems, *Wat. Sci. Tech.* **34**(1-2): 41-48.

Roels, J.A. (1983). Energetics and kinetics in biotechnology : chapter 8. *Elsevier Biomedical Press*, Amsterdam.

Roig B., Pouet M.-F. and Thomas O. (2002) Trends in UV monitoring. In: *Proceedings International IWA conference on Automation in Water Quality and Monitoring.* Vienna, Austria, May 21-22, 2002.17-24.

Royce, P.N. (1992). Effect of changes in the pH and carbon dioxide evolution rate on the measured respirometry quotient of fermentation. *Biotech. Bioeng*. **40**: 1129-1138.

Satoh H., Okuda E., Mino T. and Matsuo T. (2000) Calibration of kinetic parameters in the IAWQ activated sludge model: a pilot scale experience. *Wat. Sci. Tech.* **42** (3-4): 29-34.

Siegrist H. and Tschui, M. (1992) Interpretation of experimental data with regard to the activated sludge model no. 1 and calibration of the model for municipal wastewater treatment plants. *Wat. Sci. Tech.* **25**(6): 167-183.

Siegrist H., Brunner I., Koch G, Linh C. P. and Van Chieu L. (1999) Reduction of biomass decay rate under anoxic and anaerobic conditions, *Wat. Sci. Tech.* **39**(1): 129-137.

Sin G., Van Hulle S.W.H., Volcke E.I.P. and Vanrolleghem, P.A. (2001). Activated Sludge Model No. 1 Extended with Anammox and Sharon Processes. *Biomath Technical Report.* Ghent University, Belgium.

Sin G., Malisse K. and Vanrolleghem P. (2003) An integrated sensor for the monitoring of aerobic and anoxic activated sludge activities in biological nitrogen removal plants. *Wat. Sci. Tech*. **47**(2): 141-148.

Sin G. and Vanrolleghem P.A. (2004) A nitrate biosensor based methodology for monitoring anoxic activated sludge activity. *In proceedings: 2nd international IWA conference* on Automation in Water Quality Monitoring AutMoNet2004, Vienna, Austria, 19 – 20 April 2004, pp 61-68.

Smolders G.J.F., van der Meij J., van Loosdrecht M.C.M. and Heijnen J.J. (1994) Model of the anaerobic metabolism of the biological phosphorus removal process, *Biotechnol. Bioeng*. **43**: 461-470.

Smolders G. J. F., Klop J.M., van Loosdrecht M. and Heijnen J. J. (1995) A metabolic model of the biological Phosphorus removal process: I. Effect of the sludge retention time. *Biotechnol. Bioeng.* **48** (3): 222-233

Sollfrank U. and Gujer W. (1991) Characterization of domestic wastewater for mathematical modelling of the activated sludge process. *Wat. Sci. Tech.* **23** (4-6): 1057-1066.

Sözen S., Cokgör E.U., Orhon D. and Henze M. (1998) Respirometric analysis of activated sludge behaviour - II. Heterotrophic growth under aerobic and anoxic conditions. *Wat. Res.* **32**(2): 476-488.

Spagni A., Buday J., Ratini P. and Bortone G. (2001) Experimental considerations on monitoring ORP, pH, conductivity and dissolved oxygen in nitrogen and phosphorus biological removal processes. *Wat. Sci. Tech.* **43**(11): 197-204.

Spanjers H. and Vanrolleghem P. (1995). Respirometry as a tool for rapid characterization wastewater and activated sludge. *Wat. Sci. Tech.* **31**(2): 105-114.

Spanjers H., Vanrolleghem P.A., Olsson G. and Dold P.L. (1998) Respirometry in Control of the Activated Sludge Process: Principles. *IAWQ Scientific and Technical Report No. 7*. London, UK.

Spérandio M. and Paul E. (1997) Determination of carbon dioxide evolution rate using on-line gas analysis during dynamic biodegradation experiments. *Biotech. Bioeng*. **53**: 243-252.

Sperandio M. and Paul E. (2000). Estimation of wastewater biodegradable COD farctions by combining respirometric experiments in various So/Xo ratios, *Water Res*. **34**(4): 1233-1244.

Stamou A.I. (1997) Modelling of oxidation ditches using an open channel flow 1-D advection dispersion equation and ASM1 process description. *Wat. Sci. Tech.* **36**(5): 269-276.

Stasinakis A.A., Mamais D., Paraskevas P.A. and Lekkas T.D. (2003) Evaluation of different methods for the determination of maximum heterotrophic growth rates. *Water Environ. Res.* **75**: 549-552.

Stenström M.K. and Poduska R.A. (1980) The effect of dissolved oxygen concentration on nitrification. *Wat. Res.* **14**(6): 643-649.

Stephanopoulos G. and Stafford D.E. (2002) Metabolic engineering: a new frontier of chemical reaction engineering. *Chem. Eng. Sci.* **57**: 2595-2602.

Stokes L., Takacs I., Watson B. and Watts J.B. (1993) Dynamic modelling of an A.S.P. sewage works- A Case study. *Wat. Sci. Tech.* **28**(11-12): 151-161.

Strotmann U.J., Geldern A., Kuhn A., Gendig C. and Klein S. (1999) Evaluation of a respirometric test method to determine the heterotrophic yield coefficient of activated sludge bacteria. *Chemosphere* **38** :3555-3570.

Stumm W. and Morgan J. J. (1996) Aquatic Chemistry: chemical equilibria and rates in natural waters. 3rd ed., John Wiley & Sons, Inc.

Takacs I., Patry G. and Nolasco D. (1991) A dynamic model of the clarification – thickening process. *Wat. Res*. **25**(10): 1263-1275.

Teichgräber B., Schreff D., Ekkerlein C. and Wilderer P.A. (2001) SBR technology in Germany - An overview. *Wat. Sci. Tech.* **43**(3): 323-330.

Temmink H., Petersen B., Isaccs S. and Henze M. (1996) Recovery of Biological phosphorus removal after periods of low organic loading. *Wat. Sci. Tech.* **34**(1-2): 1-8.

Theobald U., Mailinger W., Baltes M., Rizzi M. and Reuss M. (1997) In vivo analysis of metabolic dynamics in *Saccharomyces Cerevisiae*: I. Experimental observations. *Biotechnol. Bioeng*. **55**: 305-316.

Thomsen J.K., Geest T. and Cox R.P. (1994) Mass Spectrometric studies of the effect of pH on the accumulation of intermediates in denitrification by *Paracoccus denitrificans*, *Appl. Environ. Microbiol.* **60**: 536 – 541.

Tusseau-Vuillemin M.-H., Lagarde F., Chauviere C. and Heduit A. (2002) Hydrogen peroxide (H_2O_2) as a source of dissolved oxygen in COD-degradation respirometric experiments. *Wat. Res.* **36**:793-798

UNESCO (2003) http://www.unesco.org/water/wwap/facts_figures/basic_needs.shtml

van Aalst-van Leeuwen M.A., Pot M.A, van Loosdrecht M.C.M. and Heijnen J.J (1997) Kinetic modelling of polyβ-hydroxybutyrate) production and consumption by *Paracoccus pantotrophus* under dynamic substrate supply. *Biotechnol. Bioeng*. **55**(5): 773-782

van Loosdrecht M.C.M., Pot M.A. and Heijnen J.J. (1997) Importance of bacterial storage polymers in bioprocesses. *Wat Sci. Tech.* **35**(1): 41-47

van Loosdrecht M.C.M. and Heijnen J.J. (2002) Modelling of activated sludge processes with structured biomass. *Wat. Sci Tech.* **45**(6): 12-23

van Veldhuizen H.M., van Loosdrecht M.C.M. and Brandse F.A. (1999). Model based evaluation of plant improvement strategies for biological nutrient removal. *Wat. Sci. Tech.* **39**(4): 45-53.

van Vooren L. (2000) Buffer capacity based multipurpose hard- and software sensor for environmental applications. *PhD Thesis*. Faculty of Agricultural and Applied Biological Sciences. Ghent University, Belgium. (http://biomath.ugent.be/publications/download /vanvoorenlieven_phd.pdf)

Vanhooren H., Meirlaen J., Amerlinck Y., Claeys F., Vangheluwe H. and Vanrolleghem P.A. (2003) WEST: Modelling biological wastewater treatment. *J. Hydroinformatics* **5**: 27-50.

Vanrolleghem P.A., Kong Z., Rombouts G. and Verstraete W. (1994) An on-line respirographic biosensor for the characterization of load and toxicity of wastewaters. *J. Chem. Technol. Biotechnol.* **59**: 321-333.

Vanrolleghem P.A., Van Daele M. and Dochain D. (1995) Practical identifiability of a biokinetic model of activated sludge respiration. *Wat. Res*. **29**:2561-2570

Vanrolleghem P.A., Gernaey K., Coen F., Petersen B., De Clercq B. and Ottoy J.P. (1998) Limitations of short-term experiments designed for identification of activated sludge biodegradation models by fast dynamic phenomena. In: *Proceedings 7th IFAC conference on Computer Applications in Biotechnology CAB7,* Osaka, Japan, May 31-June 4 1998: 567 – 572.

Vanrolleghem P.A. and Spanjers H. (1998) A hybrid respirometric method for more reliable assessment of activated sludge model parameters. *Wat. Sci. Tech.* **37**(12): 237 – 246.

Vanrolleghem P.A., Spanjers H., Petersen B., Ginestet P. and Takacs I. (1999) Estimating (combinations of) Activated Sludge Model No.1 parameters and components by respirometry. *Wat. Sci. Tech*. **39**(1): 195-214.

Vanrolleghem P.A. and Gillot S. (2002) Robustness and economic measures as control benchmark performance criteria. *Wat. Sci. Tech.* **45**(4-5): 117-126.

Vanrolleghem P.A., Insel G., Petersen B., Sin G., De Pauw D., Nopens I., Weijers S. and Gernaey K. (2003) A comprehensive model calibration procedure for activated sludge models. *In Proceedings*: *WEFTEC 2003: 76th Annual Technical Exhibition & Conference*. October 11 - 15, 2003, Los Angeles, California U.S.A. (on CD-ROM)

Vanrolleghem P.A., Sin G. and Gernaey K. (2004) Transient response of aerobic and anoxic activated sludge activities to sudden concentration changes. *Biotechnol. Bioeng.* 86: 277-290.

Wanner O., Kappeler J. and Gujer W. (1992) Calibration of an activated sludge model based on human expertise and on a mathematical optimization technique- A comparison. *Wat. Sci. Tech.* **25**(6): 141-148.

Water 21 (2003) Water's peace paradigm. *IWA magazine*. February 2003, 13-16.

Weijers S. R. and Vanrolleghem P.A. (1997) A procedure for selecting best identifiable parameters in calibrating activated sludge model no. 1 to full scale plant data. *Wat. Sci. Tech.* **36**(5): 69-79.

Weijers S. R. (1999) On BOD tests for the determination of biodegradable COD for calibrating activated sludge model no.1. *Wat. Sci. Tech.* **39**(4): 177-184.

Wilderer P., Irvine RL. and Goronszy M.C. (2001) Sequencing Batch Reactor Technology, *IWA Scientific and Technical Report No:10,* London.

Wentzel M.C., Dold P.L., Ekama G.A. and Marais G.v.R (1985) Kinetics of biological phosphorus release. *Wat. Sci. Tech.* **17**(11-1): 57-71.

Wentzel M.C., Ekama G., Loewenthal R., Dold P. and Marais G.v.R. (1989) Enhanced polyphosphate organism cultures in activated sludge systems, Part II: Experimental behavior, *Water SA*, **15**(2): 71-88.

Wentzel M.C., Ekama G.A. and Marais G.v.R. (1992) Processes and modelling of nitrification denitrification biological phosphorus removal systems – a review. *Wat. Sci. Tech.* **25**(6): 59-82.

WERF (2003) Using of activated sludge models. *WEFTEC 2003 workshop number 122,* Los Angeles, California U.S.A., October 12, 2003.

Wouters-Wasiak K., Héduit A., Audic J.M. and Lefèvre F. (1994) Real-time control of nitrogen removal at full-scale using oxidation reduction potential. *Wat. Sci. Tech.* **30**(4): 207-210.

Xu S. and Hultman B. (1996). Experiences in wastewater characterization and model calibration for the activated sludge processes. *Wat. Sci. Tech.* **33**(12): 89-98.

Yegneswaren P.K., Gray M.R. and Thompson B.G. (1990) Kinetics of CO_2 hydration in fermentor: pH and pressure effects. *Biotechnol. Bioeng.* **36**: 92-96.

Yuan Z. and Bogaert H. (2001) A titrimetric respirometer measuring the nitrifiable nitrogen in wastewater using insensor-experiment. *Wat. Res.* **35**:180-188.

List of abbreviations

a	Mole of hydrogen in 1 mol-C of biomass
ASM	Activated sludge model
ASM1	Activated sludge model number 1
ASM2	Activated sludge model number 2
ASM2d	Activated sludge model number 2d
ASM2dN	Activated sludge model number 2d extended with the hydrolysis of organic nitrogen module of the ASM1 model
ASM3	Activated sludge model number 3
ASM1e	Extended activated sludge model number 1(this thesis)
ASM3e	Extended activated sludge model number 3 (this thesis)
ATU	Alyyl-thio-urea
AUR	Ammonium uptake rate (mg NH_4-N/l-min)
b	Mole of oxygen in 1 mol-C of biomass
b_H	Endogenous decay coefficient of biomass (d^{-1})
b_{STO}	Endogenous decay of storage products (d^{-1})
BNR	Biological nitrogen removal
BOD	Biological oxygen demand (mgO_2/l)
BOD_∞	Ultimate biological oxygen demand (mgO_2/l)
BOD_{st}	Short-term biological oxygen demand (mgO_2/l)
BOD_t	Biological oxygen demand at time *t* (mgO_2/l)
BOD_U	Ultimate biological oxygen demand (mgO_2/l)
c	mol of nitrogen in 1 mol-C of biomass
$CH_aO_bN_c$	Molecular composition of biomass (1 mol-C)
CH_pO_q	Molecular composition of a storage polymer/product (1 mol-C)
CH_yO_z	Molecular composition of a substrate (carbon) (1 mol-C)
C/N	Initial COD to nitrogen ratio (g COD/g N)
COD	Chemical oxygen demand ((mgCOD/l)
$COD^{Degraded}$	Amount of COD degraded (mgCOD/l)
CODsol	Soluble COD (mgCOD/l)
$CODsol_{influent}$	Influent soluble COD (mgCOD/l)
$CODsol_{effluent}$	Effluent soluble COD (mgCOD/l)
COD_{st}	Short-term chemical oxygen demand (mgCOD/l)

COD_{tot}	Total COD (mgCOD/l)
COV	Covariance matrix (inverse of FIM)
CO_2	Dissolved carbon dioxide (mmol/l)
CPR_{end}	Endogenous carbon dioxide production (mmol/l-min)
C_{Tinit}	Initial concentration of total inorganic carbon (mmol/l)
CTR	Carbon dioxide transfer rate
Det	Determinant
DO	Dissolved oxygen concentration (mgO_2/l)
E	Output of the DO electrode (mg O_2/l)
FIM	Fisher Information Matrix
f_{XI}	Inert fraction of biomass (mgCOD/mgCOD)
f_{XSTO}^{REG}	Regulation constant of biomass controlling degradation rate of X_{STO} as function of f_{XSTO}, mgCOD
$f_{XSTO}(0)$	Initial fraction of X_{STO} in biomass i.e. $X_{STO}(0)/X_H(0)$, mgCOD
f_{XSTO}	Fraction of X_{STO} in biomass i.e. $X_{STO}(0)/X_H(0)$, mgCOD
f_{STO}	Fraction of substrate used for storage, mgCOD-X_{STO}/mgCOD-S_S
H^+	Hydrogen (mole)
Hp	Cumulative proton production (meq H^+/l)
HpR	Proton production rate (meq H^+/l-min)
i_{CSS}	Carbon content of substrate (C-mol/mole)
i_{NBM}	Nitrogen content of biomass (mgN/mgCOD)
i_{NXI}	Nitrogen content of the inert fraction of biomass (mgN/mgCOD)
i_{XB}	Nitrogen content of biomass (mgN/mgCOD)
IAF1	Intermittent aeration with 1 sequence of aerobic and anoxic sub
IAF2	Intermittent aeration with 2 sequences of aerobic and anoxic sub
IAF4	Intermittent aeration with 2 sequences of aerobic and anoxic sub
IAF8	Intermittent aeration with 2 sequences of aerobic and anoxic sub
J	Weighted sum of squared errors
K_H	Henry coefficient for CO_2 (mole/(atm.l))
$K_La_{wastewater}$	Volumetric mass transfer coefficient O_2 in wastewater (h^{-1})
K_La_{water}	Volumetric mass transfer coefficient O_2 in clean water, (h^{-1})
K_La_{CO2}	Surface-mass transfer coefficient for CO_2 (d^{-1})
K_La_{O2}	Surface-mass transfer coefficient for O_2 (d^{-1})
K_{NH}	Affinity constant for ammonium (mgN/l)
K_{NO3}	Affinity constant for nitrate (mgN/l)
K_O	Affinity constant for oxygen (mgO_2/l)
K_S	Substrate affinity constant (mgCOD/l)
K_{S_HP}	K_S estimate based on Hp data (mg COD/l)
K_{S_OUR}	K_S estimate based on OUR data (mg COD/l)

K_{STO}	Biomass affinity constant for X_{STO} (mgCOD/l)
k_{STO}	Maximum storage rate of biomass (d^{-1})
k_1	Forward reaction rate for aqueous CO_2 equilibrium (min^{-1})
K_1	Regulation constant of biomass controlling degradation rate of X_{STO} as function of f_{XSTO}, (mgCOD-X_{STO}/mgCOD-X_H)
K_2	A lumped parameter related to the affinity of biomass to storage fraction of biomass i.e. f_{STO}, (mgCOD-X_{STO}/mgCOD-X_H)
LFS	Flowing gas-static liquid respirometer
m	Degree of mixing
MLSS	Mixed liquor suspended solids (mgSS/l)
MLVSS	Mixed liquor volatile suspended solids (mgSS/l)
Mod-E	Modified E criterion
N_2	Dinitrogen gas (mgN/l)
NH_4–N	Ammonium (concentration) (mg N/l)
NH_3	Ammonia nitrogen (mgNH_3-N/l)
NO_2–N	Nitrite nitrogen (mgNO_2-N/l)
NO_3–N	Nitrate nitrogen (mgNO_3-N/l)
NP	Nitrate production (mg NO_3-N/l)
NUR	Nitrate uptake rate (mg NO_3-N/l-min)
NU	Nitrate uptake (mg NO_3-N/l)
ORP	Oxidation reduction potential
OED	Optimal Experimental Design
OUR	Oxygen uptake rate (mg O_2/l-min)
OUR_{end}	Endogenous oxygen uptake rate (mg O_2/l-min)
OUR_{ex}	Exogenous oxygen uptake rate (mg O_2/l-min)
PHB	Poly-β-hydroxybutyrate (mgCOD/l)
p	Mole of hydrogen in 1 mol-C of storage product
PAO	Phosphorous accumulating organisms
P_{CO2}	Partial pressure of CO_2 in air (atm)
pH	Negative logarithm of proton concentration
PHA	Poly-hydroxyalkanoates
pK_A	Negative logarithm of dissociation constant for acetate
pK_{NH}	Negative logarithm of dissociation constant for ammonium
pK_1	Negative logarithm of the first acidity constant in the CO_2 equilibrium
PO_4 –P	Concentration of phosphate (mgP/l)
Q_i	Weights
q	Mole of oxygen in 1 mol-C of storage product
q_{MAX}	Maximum substrate uptake rate (d^{-1})
$r_{H,S}$	Specific growth rate on substrate (mgCOD/l)

$r_{H,STO}$	Specific growth rate on storage products (mgCOD/l)
r_{O2}	Oxygen uptake rate (mg O_2/l-min)
r_S	Specific substrate uptake rate (mgCOD/l)
r_{STO}	Specific storage rate (mgCOD/l)
RQ	Respiratory quotient
SBR	Sequencing batch reactor
S_{CO2}^*	Equilibrium concentration of CO_2 with air 1 (mmol/l)
S_I	Inert suspended solids (mgCOD/l)
$S_{I,effluent}$	Effluent inert suspended solids (mgCOD/l)
$S_{I,influent}$	Influent inert suspended solids (mgCOD/l)
SND	Simultaneous nitrification and denitrification
S_{ND}	Soluble degradable organic nitrogen (mgN/l)
$S_{NH}(0)$	Initial ammonium concentration (mg N/l)
S_{NH}	Ammonium concentration (mg N/l)
$S_{NO3}(0)$	Initial nitrate concentration (mg N/l)
S_{NO3}	Nitrate concentration (mgN/l)
S_{N2}	Nitrogen gas (mgN/l)
S_0/X_0	Initial substrate to biomass ratio (mgCOD/mgCOD)
S/X	Substrate to biomass ratio (mgCOD/mgCOD)
S_{O2}^*	Oxygen saturation concentration (mgO_2/l)
S_O	Oxygen concentration (mgO_2/l)
S_O_sp	Oxygen set-point (mgO_2/l)
SRT	Solids retention time or sludge age (days)
S_S	Soluble readily degradable COD (mgCOD/l)
$S_{S,effluent}$	Effluent soluble readily degradable COD (mgCOD/l)
$S_{S,influent}$	Influent soluble readily degradable COD (mgCOD/l)
s(t)	Concentration of tracer at time *t*
s_0	Initial concentration of tracer
s_∞	Concentration of tracer as $t \rightarrow \infty$
T_{AER}	length of aerobic time (min)
T_{ANB}	length of anaerobic time (min)
T_{ANX}	length of anoxic time (min)
TKN	total kjeldhal nitrogen (mgN/l)
t_m	Mixing time (min)
TN	Total nitrogen (mgN/l)
t_{pulse}	Time of pulse addition of substrate (min)
Trans	First order dynamic transient term (-)
WWTP	Wastewater treatment plant
y	Mole of hydrogen in 1 mol-C of substrate

Y_A	Autotrophic yield coefficient (mg COD/ mg NH_4-N)
Y_H	Heterotrophic yield coefficient (mg COD/ mg COD)
$Y_{H,S}$	Yield coefficient for growth on substrate (mgCOD-X_H/mgCOD-S_S)
$Y_{H,STO}$	Yield coefficient for growth on storage products (mgCOD-X_H/mgCOD-X_{STO})
Y_{STO}	Yield coefficient for storage on substrate (mgCOD-X_{STO}/mgCOD-S_S)
Y_{SX}	Yield coefficient for growth on substrate (mol-X_H/mol-S_S)
X_A	Autotrophic biomass concentration (mg COD/l)
X_I	Inert particulate COD (mgCOD/l)
X_H	Heterotrophic biomass (mgCOD/l)
$X_H(0)$	Initial concentration of heterotrophic biomass (mgCOD/l)
X_{ND}	Particulate degradable organic nitrogen (mgN/l)
X_S	Slowly degradable particulate COD (mgCOD/l)
$X_{STO}(0)$	Initial concentration of storage polymers/products in biomass (mgCOD/l)
X_{STO}	Concentration of storage polymers/products in biomass (mgCOD/l)
z	Mole of oxygen in 1 mol-C of substrate

Griek Symbols

α	Correction factor for the oxygen transfer in wastewater
δ	Efficiency of oxidative phosphorylation (mol/mol)
δ_n	Efficiency of oxidative phosphorylation under anoxic conditions (mol/mol)
ε_R	Relative error (%)
η_g	Anoxic growth reduction factor
γ_{NO3}	Degree of reduction of nitrate (mole)
γ_S	Degree of reduction of substrate (mole)
γ_{STO}	Degree of reduction of storage products (mole)
γ_X	Degree of reduction of biomass (mole)
μ	growth rate for heterotrophic biomass (1/min)
μ_{maxA}	Maximum growth rate for autotrophic biomass (1/min)
μ_{maxH}	Maximum growth rate for heterotrophic biomass (1/min)
μ_{obs}	Observed growth rate for heterotrophic biomass (1/min)
$\mu_{MAX,S}$	Maximum growth rate of biomass on substrate (d)
$\mu_{MAX,STO}$	Maximum growth rate on storage products (d)
τ	First order time constant (min)
τ_A	First order time constant observed in autotrophic activity (min)
τ_H	First order time constant observed in heterotrophic activity (min)
τ_{HP}	First order time constant observed in titrimetric data (min)
τ_{NO}	First order time constant observed in NUR (min)

τ_{OUR}	First order time constant observed in OUR (min)

Summary

There is a good deal of experiences/reasons accumulated over the past decade concerning the full-scale application of mechanistic models (e.g. Activated Sludge Models (ASM) of Henze *et al*. (2000)) that stimulate and encourage further investment/research in this field. First of all, these ASMs are objective and represent the state-of-the-art in understanding of the complex activated sludge processes ongoing in wastewater treatment plants (WWTPs). Second, they have been successfully applied worldwide on many cases for the optimisation of full-scale operation of WWTPs, e.g. for cost reduction, control, improving effluent quality etc. Third, modelling of WWTPs further increases the in-depth understanding of complex activated sludge processes, which in turn is used to further develop the existing models (an interactive/constructive cycle). Last but not least, they enable dynamic simulation of WWTPs, which is valuable to cross check existing designs of WWTPs based on steady-state approaches and/or rules of thumb.

Because the parameters of the ASMs are not universal, model calibration is strictly required prior to full-scale application. This step critically determines the overall quality of the model application. The research carried out in this thesis is, therefore, situated in the quest to further develop the systematic calibration of Activated Sludge Models (ASMs) and particularly to improve and standardize the quality of the calibration of ASMs for nitrogen removing WWTPs.

In Chapter 2 therefore, a previously proposed calibration methodology (Petersen *et al*., 2003a) is further improved on the basis of rigorous scientific and engineering experiences with the systematic calibration of activated sludge models. The main motivation of the so-called BIOMATH protocol was to systematize the calibration exercise such that different model calibration studies can be compared and the quality of the calibration study itself can be checked. The two distinctive properties of the BIOMATH protocol are the respirometry based influent characterisation procedure and the incorporation of the Optimal Experimental Design (OED) methodology. From the systematic calibration protocol it becomes clear that lab-scale

batch experiments are very much important and are mostly used in full-scale model calibrations (i) to improve the identifiability of the complex ASMs, e.g. by providing estimates to the kinetic and stoichiometric parameters of the model and (ii) for the influent wastewater characterisation. However, the use of batch experiments has so far been limited to aerobic conditions because an appropriate sensor to collect data under anoxic conditions was lacking.

Keeping that in mind, in Chapter 3.1, an integrated sensor was developed by combining the aerobic set-up of Gernaey *et al*. (2002a) and the anoxic set-up of Petersen *et al*. (2002a) in one single unit. The integrated sensor provides an information rich matrix of data consisting of oxygen uptake rate (OUR), nitrate production (NP), nitrate uptake (NU) and proton production (Hp), and was successfully used to sequentially monitor aerobic and anoxic activated sludge activities in BNR plants. In Chapter 3.2, the ion selective electrode (ISE) used for nitrate measurements in the integrated sensor was replaced with a novel nitrate biosensor (Larsen *et al*., 2000). The anoxic set-up developed in Chapter 3.2 successfully provided for the first time high quality and high frequency nitrate uptake rate (NUR) measurements of activated sludge, i.e. every 3 secs. This high quality NUR data allowed to compare the anoxic activity of biomass with the aerobic activity in detail. This was also shown to be essential for model development purposes (see Chapter 4.3).

A complementary step to the use of batch experiments is the *accurate* interpretation of the resulting data in view of parameter estimation for full-scale models of WWTPs. Therefore, the in-depth/mechanistic understanding and the model-based interpretation of the results obtained from the short-term batch experiments were the prime focus of the second part of the thesis. In Chapter 4.1, the titrimetric model of Gernaey *et al*. (2002a) was successfully extended to model the time-varying CO_2 transfer rate (CTR) observed in the titrimetric data resulting from aerobic carbon source degradation. This extension made it possible to apply the Gernaey model to adequately interpret titrimetric data collected under a wider range of experimental conditions.

In Chapter 4.2 the oxygen uptake rate (OUR) data collected under aerobic carbon source degradation process were analysed in depth in view of mechanistic interpretation/modelling. In Chapter 4.2.1, it was shown that neither ASM1 nor ASM3 were able to mechanistically describe OUR data collected with biomass from different full-scale WWTPs. This failure was

hypothesised to be due to the conceptual basis of both models: ASM1 assumes that in feast phase substrate is only used for growth while in the endogenous phase biomass only decay. ASM3 assumes that substrate is used only for storage in the feast phase while it grows on the stored substrate in the endogenous/famine phase. This hypothesis was supported by the numerous results obtained elsewhere with the research on storage phenomena by activated sludge. To improve the mechanistic description of activated sludge activity, a simultaneous storage and growth model was successfully developed using a new approach. In this new approach, (i) the substrate uptake kinetics was explicitly separated from the growth kinetics of biomass and (ii) degradation of storage products was modelled using a second order model. This new model was successfully evaluated using OUR data and validated using independent PHB measurements. The model was shown to provide realistic and mechanistically more meaningful parameter estimates. For example, the yield of heterotrophic growth was estimated to be around 0.59, which is much lower than the estimate of ASM1, e.g. 0.75 mgCOD/mgCOD.

In Chapter 4.3 the simultaneous storage and growth model developed in Chapter 4.2.2 was adapted to anoxic conditions and called ASM3e. The ASM3e includes the pH effect of denitrification process since titrimetry was shown to be positive on improving the identifiability of complex models. It was shown here that the ASM3e model could better describe the NUR data collected in Chapter 3.2 and provides more realistic parameter estimates compared to the ASM1e model (the ASM1 model extended with the pH effect of denitrification). Moreover, it was observed that it was possible to estimate the nitrate affinity constant of denitrifiers, K_{NO3}, in experiments with nitrate as limiting substrate, thanks to the high frequency and high quality NUR data. The K_{NO3} was estimated to be in the order of 0.015 mgN/l which is low compared to the default values in ASMs (Henze *et al*., 2003). Both models were shown to adequately describe the anoxic titrimetric data but the identifiability of both models when using the titrimetric data should be further studied to eliminate parameter correlation problems. The initial substrate to biomass ratio, S_0/X_0, was studied in detail here and observed to be a key factor influencing the response of heterotrophic biomass in anoxic batch experiments. It is advised to keep this ratio low (below 0.1 mgCOD/mgCOD) to obtain representative “extant” parameter estimates for full-scale models. Increasing this ratio in batch experiments was shown to change the estimates of the kinetic parameters of denitrifiers due to physiological adaptation of biomass. A hypothesis complementary to the hypothesis of

Chudoba *et al*. (1992) was developed to explain the physiological adaptation of biomass occurring in response to increasing the S_0/X_0 level in anoxic batch experiment.

In Chapter 4.4 the fast transient phenomena often observed in high frequency respirometric measurements obtained under both aerobic (OUR) and anoxic (NUR) conditions were addressed in detail. Referring to dynamic metabolic network modelling of pure cultures (e.g. Chassagnole *et al*., 2002), it appears that this fast transient phenomenon (which takes 2-5 minutes) results from the substrate metabolism at the cellular level, i.e. it takes some time until the electrons of the substrate reach the electron acceptor (e.g., oxygen, nitrate, etc.) reduction sites in the cell. This is reflected as a first order response in the (oxygen or nitrate) measurements obtained in the external environment. This phenomenon could therefore be modelled using a first order model. The first order time constants observed in both OUR and NUR profiles were higher than those of the titrimetric data which appear to reflect the substrate uptake dynamics. These results further support the abovementioned hypothesis. Moreover, it was shown that it is necessary to account for this transient in model-based parameter estimation using respirometric data, otherwise it will induce error into the separate (unique) parameter estimates (e.g. in μ_{maxH} and K_S parameters). It is also expected that this fast transient occurs regularly in particular WWTPs (e.g., carrousel, SBRs with short cycles of intermittent aeration, anaerobic selectors in WWTPs etc.) and should be studied in detail.

In the third part of the thesis the focus was turned to the evaluation of the BIOMATH systematic calibration protocol. In Chapter 5.1, the BIOMATH protocol was evaluated using the ASM2dN model of a lab-scale nutrient removing SBR (80 L). The BIOMATH protocol was extended with a step-wise calibration procedure for different biological processes in the ASM2dN model. This was possible because the SBR operates batch-wisely thereby providing information relevant for each process under anaerobic, aerobic and anoxic conditions. The calibrated ASM2dN model was also used for the systems analysis to understand in-depth the contributions of each process to the overall N and P removal in the SBR. This type of analysis is important to find out the key degrees of freedom of the system to be used in the process optimisation which is studied in detail in Chapter 6.

A very important aspect of mechanistic modelling of WWTPs is the model validation. In other words, once a model is calibrated to a WWTP, how long does this calibrated model remain valid in terms of adequately representing the WWTP? To answer this question, in

Chapter 5.2 the ASM2d model calibrated 3 years ago to the Haaren WWTP (50,000 PE, The Netherlands) was validated using a new measurement campaign reflecting the recent behaviour of the Haaren WWTP. The BIOMATH calibration protocol was followed for both designing the measurement campaign and performing the validation exercise. The validation results were in general quite positive, i.e. it was still possible to adequately predict the dynamic trends observed in the MLSS and NO_3-N measurements but a few parameters needed to be calibrated slightly to better fit the dynamic trends in PO_4-P and NH_4-N data. This positive outcome of the validation study implies that the lifetime of a calibrated model may be compatible with the lifetime of the WWTP. This certainly reinforces confidence into full-scale mechanistic modelling of WWTPs. However, since the model calibration and validation were performed in the summer period, it will be quite relevant and useful to validate the model under different periods, e.g. spring or winter.

In the final part of the thesis, the attention was focused on the application of calibrated models. Within this frame, in Chapter 6 an iterative systematic protocol was developed and evaluated on a lab-sale SBR (80 L). The particular aim of this protocol was to systematize the model-based search for an optimal operation scenario for activated sludge systems. The application of this protocol to the lab-scale SBR in view of improving both effluent quality and robustness of the SBR operation revealed that it was possible to improve the existing N and P removal by 54% and 74% respectively. However, this protocol can be and should be further improved by incorporating the change in settling properties of activated sludge when different operation scenarios are considered in the systematic search.

Samenvatting

De ervaring die de laatste 10 jaar is opgebouwd rond de toepassing van mechanistische modellen voor actief slib-processen (vb. Activated Sludge Models (ASM) (Henze et al., 2000)), stimuleert verdere investeringen en onderzoek in dit vakgebied. Ten eerste bevatten de ASM-modellen de 'state-of-the-art'-kennis voor het begrijpen en interpreteren van de complexe actief slib-processen in waterzuiveringsinstallaties (WZI's). Ten tweede zijn deze modellen wereldwijd reeds succesvol toegepast bij verschillende studies voor de optimalisatie van WZI's, meer bepaald voor kostenbesparing, controle en het verbeteren van de effluentkwaliteit. Ten derde verhoogt de modellering van WZI's de kennis over deze complexe actief slib-processen. Deze kennis kan op zich weer gebruikt worden voor de verdere ontwikkeling van bestaande modellen (i.e. een interactieve/constructieve cyclus). Tenslotte kunnen dynamische simulaties gebruikt worden om het ontwerp van WZI's te controleren, aangezien dit ontwerp gebaseerd is op 'steady-state'-aannames en vuistregels.

Aangezien de modelparameters niet universeel toepasbaar zijn, is modelcalibratie strikt noodzakelijk vooraleer de ASM-modellen te gebruiken voor volleschaaltoepassingen. Deze stap bepaalt dan ook de uiteindelijke kwaliteit van de modeltoepassing. Het onderzoek uitgevoerd in dit proefschrift concentreert zich daarom op de verdere ontwikkeling van de systematische calibratie van actief slib-modellen en meer in het bijzonder het verbeteren en standaardiseren van de kwaliteit van de calibratie van modellen voor stikstofverwijderende waterzuiveringsinstallaties.

In Hoofdstuk 2 wordt daarom een eerder beschreven calibratiemethodologie (Petersen et al., 2003a) verder verbeterd op basis van wetenschappelijke en technische ervaring met systematische calibratie van actief slib-modellen. De belangrijkste motivatie voor het opstellen van dit zogenaamde 'BIOMATH-protocol' was de systematisering van de calibratie-oefening zodat verschillende modelcalibratiestudies met elkaar kunnen vergeleken worden en de kwaliteit van de calibratiestudie op zich kan gecontroleerd worden. Kenmerkende eigenschappen van het BIOMATH-protocol zijn ten eerste de influentkarakterisering die

gebaseerd is op respirometrie en ten tweede het gebruik van Optimaal Experimenteel Ontwerp (Optimal Experimental Design, OED). Vanuit dit systematische calibratieprotocol werd duidelijk dat het uitvoeren van batch-experimenten op laboschaal bij calibratiecalibratiestudies van volle schaal-modellen heel belangrijk is om (i) de identificeerbaarheid van de complexe ASM-modellen te verbeteren, bijvoorbeeld door schatting van de kinetische en stoichiometrische parameters van het model en (ii) het influent te karakteriseren. Nochtans is het gebruik van batch-experimenten tot nu toe beperkt gebleven tot aërobe omstandigheden omdat een geschikte sensor voor datacollectie onder anoxische omstandigheden nog niet voorhanden was.

In Hoofdstuk 3.1 wordt een geïntegreerde sensor ontwikkeld door het combineren van de aërobe opstelling van Gernaey et al. (2002a) en de anoxische opstelling van Petersen et al. (2002a) in één opstelling. Deze geïntegreerde sensor genereert een informatierijke matrix van data bestaande uit de zuurstofopnamesnelheid (oxygen uptake rate, OUR), de nitraatproductiesnelheid (NP), de nitraatopname (nitrate uptake, NU) en de protonproductie (Hp). Deze sensor werd succesvol toegepast voor de sequentiële monitoring van aërobe en anoxische activiteit van actief slib in installaties met biologische stikstofverwijdering. In Hoofdstuk 3.2 wordt de ionselectieve elektrode (ISE) voor nitraatmetingen in de geïntegreerde sensor vervangen door een nieuw ontwikkelde nitraat-biosensor (Larsen et al., 2000). Met de resulterende anoxische opstelling, beschreven in Hoofdstuk 3.2, werd voor het eerst een hoogfrequente (i.e. elke 3 seconden), kwaliteitsvolle meting van de de nitraatopnamesnelheid (nitrate uptake rate, NUR) bekomen. Dankzij deze NUR-data van hoge kwaliteit kon de anoxische activiteit in detail vergeleken worden met de aërobe activiteit. Deze vergelijking was essentieel voor de modelontwikkeling beschreven in Hoofdstuk 4.3.

Bij het gebruik van batch-experimenten is het belangrijk dat de verkregen data nauwkeurig geïnterpreteerd worden met het oog op parameterschatting voor volle schaal-modellen van WZI's. In het tweede deel van de thesis ligt de nadruk daarom op het mechanistisch begrijpen en de modelgebaseerde interpretatie van de resultaten van de kortetermijn batch-experimenten. Hoofdstuk 4.1 beschrijft de succesvolle uitbreiding van het titrimetrisch model van Gernaey et al. (2002a) voor het modelleren van de tijdsvariante CO_2-uitwisselingssnelheid (CO_2 transfer rate, CTR), waargenomen in de titrimetrische data van aërobe koolstofverwijdering. Deze uitbreiding maakte het mogelijk om het model van

Gernaey toe te passen voor de interpretatie van titrimetrische data in een breder bereik van experimentele condities.

In Hoofdstuk 4.2 worden de data m.b.t. de zuurstofopnamesnelheid (oxygen uptake rate, OUR), verzameld tijdens aërobe koolstofverwijderingsexperimenten, grondig geanalyseerd met het oog op mechanistische interpretatie/modellering. In Hoofdstuk 4.2.1 wordt aangetoond dat noch ASM1, noch ASM3, in staat zijn om de OUR-data, verzameld in experimenten met biomassa van verschillende volleschaalinstallaties, mechanistisch te beschrijven. Dit falen werd toegeschreven aan de conceptuele basis van beide modellen: ASM1 neemt aan dat in de 'feast'-fase substraat alleen gebruikt wordt voor groei, terwijl er in de endogene fase alleen afsterving is. ASM3 neemt aan dat substraat alleen opgeslagen wordt in de 'feast'-fase, terwijl er groei is op dit opslagproduct tijdens de endogene of 'famine'-fase. Deze hypothese werd gesteund door talrijke studies over de opslag van substraat in actief slib. Om de mechanistische beschrijving van de activiteit van actief slib te verbeteren, werd een model met simultane opslag en groei succesvol ontwikkeld. Dit gebeurde aan de hand van een nieuwe aanpak, namelijk (i) de kinetiek van substraatopname werd expliciet gescheiden van de kinetiek van biomassagroei en (ii) de afbraak van opslagproducten werd gemodelleerd m.b.v. een tweede orde model. Dit nieuwe model werd succesvol geëvalueerd op basis van OUR-data. Vervolgens werd dit model gevalideerd met onafhankelijke PHB-metingen. Het model gaf realistische en mechanistisch betekenisvolle parameterschattingen. De opbrengstcoëfficiënt voor heterotrofe groei werd bijvoorbeeld geschat op 0.58 mgCOD/mgCOD, wat veel lager is dan de schatting met ASM1, die 0.75 mgCOD/mgCOD bedraagt.

In Hoofdstuk 4.3 wordt het in Hoofdstuk 4.2.2 ontwikkelde model met simultane opslag en groei aangepast om ook anoxische condities te beschrijven. Dit model werd ASM3e genoemd. Het omvat ook het pH-effect van het denitrificatieproces. Er is immers aangetoond dat titrimetrie de identificeerbaarheid van complexe modellen kan verbeteren. Het ASM3e model kon de NUR-data, verzameld in Hoofdstuk 3.2, beter beschrijven en voorzag in meer realistische parameterschattingen in vergelijking met ASM1e (het ASM1 model uitgebreid met het pH effect van denitrificatie). Het is zelfs mogelijk gebleken om dankzij de hoge frequentie en kwaliteit van de NUR-data, de nitraataffiniteitsconstante van de denitrificeerders, K_{NO3}, te schatten in experimenten met nitraat als limiterend substraat. Voor deze K_{NO3} werd een waarde gevonden in de orde van 0.015 mgN/l wat laag is in vergelijking

met de standaardwaarden in de ASM-modellen (Henze et al., 2003). Beide modellen konden de anoxische titrimetrische data adequaat beschrijven. De identificeerbaarheid van beide modellen bij het gebruik van titrimetrische data moet echter verder onderzocht worden om parametercorrelatieproblemen te voorkomen. De initiële verhouding van substraat tot biomassa, S_0/X_0, werd hier in detail bestudeerd en bleek een bepalende factor te zijn in de respons van heterotrofe biomassa in anoxische batch-experimenten. Deze verhouding moet laag gehouden worden (beneden 0.1 mgCOD/mgCOD) om representatieve 'extant' parameterschattingen te verkrijgen voor volle schaal-modellen. Studies hebben immers aangetoond dat het verhogen van deze verhouding kan leiden tot andere schattingen voor de kinetische parameters van denitrificeerders. Dit is te wijten aan fysiologische adaptatie van de biomassa. Een hypothese, complementair aan de hypothese van Chudoba et al. (1992), werd ontwikkeld om de fysiologische adaptatie van biomassa te verklaren tengevolge van verhoogde S_0/X_0 verhoudingen in anoxische batch experimenten.

In Hoofdstuk 4.4 werd aandacht besteed aan de snelle overgangsverschijnsels ('fast transient phenomena') die vaak worden waargenomen tijdens respirometrische metingen met hoge frequentie, zowel onder aërobe (OUR) als anoxische (NUR) omstandigheden. Op basis van de dynamische metabolische netwerk-modellering van pure culturen (e.g. Chassagnole et al., 2002), kan gesteld worden dat zo'n snel overgangsverschijnsel (dat ongeveer 2-5 minutes duurt) een gevolg is van het substraatmetabolisme op celniveau. Dit betekent dat het enkele minuten duurt vooraleer de elektronen van het substraat de reductieplaatsen in de cel van de elektronacceptor (zuurstof, nitraat, etc.) bereiken. Dit uit zich als een eerste orde antwoord in de gemeten (zuurstof- of nitraat-)waarden buiten de cel. Dit fenomeen kan dan ook beschreven worden met een eerste orde model. De waargenomen eerste orde-tijdsconstanten in zowel de OUR- als de NUR-profielen waren hoger dan deze van de titrimetrische data die blijkbaar de dynamica van de substraatopname weerspiegelen. Deze resultaten ondersteunen de bovenvermelde hypothese verder. Meer nog, er werd aangetoond dat het nodig was om dit overgangsverschijnsel in rekening te brengen tijdens modelgebaseerde parameterschattingen met respirometrische data. Anders zal dit leiden tot fouten in de individuele (unieke) parameterschattingen (e.g. μ_{maxH} en K_S). Het kan ook verwacht worden dat dit verschijnsel regelmatig optreedt in specifieke WZI's (e.g. carrousel, SBR's met korte periodes van intermitterende beluchting, anaërobe selectoren in WZIs). Het is dan ook aangeraden om in deze installaties dit verschijnsel in detail te bestuderen.

In het derde deel van deze thesis ligt de nadruk op de evaluatie van het BIOMATH-protocol voor systematische calibratie. In Hoofdstuk 5.1 wordt het BIOMATH-protocol geëvalueerd, gebruik makend van het ASM2dN-model van een SBR met nutriëntverwijdering op laboschaal (80 L). Het BIOMATH-protocol werd uitgebreid met een stapsgewijze calibratieprocedure voor de verschillende biologische processen in het ASM2dN-model. Dit was mogelijk omdat de SBR batchgewijs werkt, waardoor er relevante informatie beschikbaar is over elk proces onder anaërobe, aërobe en anoxische condities. Het gekalibreerde ASM2dN-model werd ook gebruikt voor een grondige analyse van de bijdrage van elk proces tot de totale N- en P- verwijdering in de SBR. Deze analyse is cruciaal om de belangrijkste vrijheidsgraden van het systeem te identificeren. Deze vrijheidsgraden zullen immers in Hoofdstuk 6 gebruikt worden om het proces te optimaliseren.

Een belangrijk aspect van mechanistische modellering van WZI's is de modelvalidatie, meer bepaald de geldigheidsduur van een gekalibreerd model. Hoe lang het model een juiste weergave is van de werkelijkheid, wordt beantwoord in Hoofdstuk 5.2. Een ASM2d-model, dat 3 jaar geleden gekalibreerd werd voor de WZI van Haaren (50,000 IE, Nederland), werd in dit hoofdstuk gevalideerd op basis van een nieuwe meetcampagne die het gewijzigde gedrag van de WZI weerspiegelt. Het BIOMATH-calibratieprotocol werd gevolgd voor zowel het ontwerp van de meetcampagne als de modelvalidatie. De validatieresultaten waren in het algemeen positief. Het was namelijk steeds mogelijk om de dynamische trends van MLSS en NO_3-N metingen adequaat te voorspellen. Enkele parameters moesten echter lichtjes aangepast worden om de dynamische trends in PO_4-P en NH_4-N data te voorspellen. Dit resultaat wijst erop dat de levensduur van een gekalibreerd model vergelijkbaar wordt met de levensduur van een WZI. Dit versterkt het vertrouwen in volle schaal mechanistische modellering van WZI. Het model werd echter gekalibreerd en gevalideerd tijdens de zomerperiode. Het lijkt daarom interessant en nuttig om het model verder te valideren met data van een ander seizoen.

In het laatste deel van dit proefschrift werd de nadruk gelegd op de toepassing van gekalibreerde modellen. Hoofdstuk 6 beschrijft de ontwikkeling van een iteratief systematisch protocol en de evaluatie ervan m.b.v. een SBR op laboschaal (80 L). Het eigenlijke doel van dit protocol was de systematisering van de modelgebaseerde zoektocht naar de optimale bedrijfsvoering van actief slib-systemen. De toepassing van dit protocol voor de optimalisatie van de SBR op laboschaal in termen van effluentkwaliteit en robuustheid, toonde aan dat de

bestaande N- en P-verwijdering kon verbeterd worden met respectievelijk 54% and 74%. Dit protocol moet echter verder uitgebreid worden om rekening te houden met veranderingen, bijvoorbeeld, in slibbezinkingseigenschappen ten gevolge van het toepassen van de verschillende scenario's voor bedrijfsvoering die beschouwd werden in de systematische zoektocht.

Gürkan Sin

Environmental Engineer, M.Sc.

PERSONAL DATA

Nationality: Turkish
Date of Birth: 29.07.1976
Place of Birth: Samandag, Hatay, Turkey.
Marital Status: Single.
Address: Raas van Gaverestraat, 3/1, 9000 Gent, Belgium.
E-mail: gurkan@biomath.ugent.be **or** Gurkan.Sin@ugent.be **or** Gurkan.Sin@lycos.com
Telephone: +32 9 264 5937, GSM: +32 474 309 238

EDUCATION

2000 – present	Doctoral study (PhD) in the Faculty of Applied Biological Sciences: Environmental Technology, Ghent University, Ghent, Belgium. **Supervisor:** Prof. Dr. ir. Peter A. Vanrolleghem **Title:** Systematic calibration of activated sludge models
1998 – 2000	M.Sc. Environmental Engineering Middle East Technical University, Ankara, Turkey.
1994 – 1998	B.Sc. Environmental Engineering Middle East Technical University, Ankara, Turkey
1993 – 1994	English Language School Middle East Technical University, Ankara, Turkey

RESEARCH EXPERIENCE

2000 – present	Research Assistant in the Department of Applied Mathematics, Biometrics and Process Control (BIOMATH) Ghent University, Ghent, Belgium
1998 – 2000	Teaching/research Assistant in Environmental Engineering Department Middle East Technical University (METU), Ankara, Turkey

WORK EXPERIENCE

2003 – 2004	Dynamic calibration and optimisation of an intermittently aerated carrousel type wastewater treatment plant –Haaren WWTP, the Netherlands: Representability of the calibrated model in time **Summary:** The aim of this project is to check the validity i.e. the representability of the calibrated model (ASM2d) for Haaren WWTP (50,000 pe) in time. The long-term representability of the model is of profound importance before the model can be concluded reliable to be used for not only full-scale optimisation but also for optimal design of new WWTPs. The BIOMATH calibration protocol –a minimum effort/cost-effective calibration protocol developed for full-scale continuous WWTPs, was used as a guideline to re-calibrate the model (ASM2d).

2002 –2004	Development of calibration and optimisation protocols for optimal but robust N and P removal in sequential batch reactors (SBRs): **Summary:** A calibration and optimisation protocol is applied to model nutrient removal performance in an 80 L lab-scale SBR. The optimisation study aimed not only at improving the nutrient removal performance but also the stability of the SBR operation. Finally, the optimised operation strategy is shown to provide a 54% and an 82% improvement in N and P removal capacity respectively with an increased stability of the SBR system.
2001 –2004	Improved control and application of nitrogen cycle bacteria for Nitrogen removal from wastewater: IcoN project **Summary:** IcoN is a RTD (Research Technology and Development) project under the fifth Framework Research Program of the European Commission, which is awarded to a consortium of academic and individual partners. As part of this project, BIOMATH (Ghent University) is responsible for modelling and control of the Anammox process. As part of the BIOMATH responsibility, an integrated sensor was developed for the monitoring of aerobic and anoxic activated sludge activities. The integrated sensor was shown to deliver information-rich data for in-depth study of carbon oxidation, nitrification and denitrification processes. Further, model-based methodologies were developed for identification/quantification of aerobic carbon source degradation and denitrification processes using the sensor data.
1999-2000	Modelling a large-scale (3.5 million pe) wastewater treatment plant for upgrade to nitrogen removal: Ankara WWTP, Turkey. **Summary:** The Ankara WWTP was commissioned for operation late in 1997 for only carbon-pollutants removal. As part of the second stage of the project, the WWTP was to be upgraded to nitrogen removal. For this purpose, the ASM1 model was calibrated successfully using field and lab-sale experimental data. The model-based analysis of the WWTP showed that the WWTP was highly over-designed with respect to the existing organic loading rate. The calibrated model was presented for management of the Ankara WWTP and for testing several operation/upgrade strategies.

LANGUAGE SKILLS

English	Fluent
Turkish	Fluent
Dutch	Proficient
Arabic	Native Speaker

COMPUTER SKILLS

Operating Systems

Microsoft Win 95, 98 and 2000	Proficient user & system administrator level
Linux Red Hat 7.2 & 8.0 distribution	Proficient user & system administrator level

Software (some examples)

WEST, Hemmis	A general purpose WWTP simulation platform
Matlab	Advanced mathematical tools and simulation platform
MS Office products	MS Excel, Word and Powerpoint 1997 and 2000
Sigma Plot	Advanced data analysis tool
Labview	A graphical programming language oriented at data acquisition and control
MYSQL	A database management program (Linux version)
Apache	A web server (Linux version)

System Administration

Webmaster (2001 – present)	Webmaster of the official website of BIOMATH, Ghent University (http://biomath.ugent.be/)

Computer Languages

C++	Good
MSL	Very good
Labview-G	Very good
HTML	Very good
PHP	Very good

AWARDS

Graduated top *first* in 1997/1998 academic year from the Environmental Engineering department. Middle East Technical University, Ankara, Turkey. 1998.

MEMBERSHIPS IN PROFESSIONAL SOCIETIES

International Water Association (IWA)
Türk Eğitim Derneği (TED)- Association of Turkish Education.
Turkish Union of Chambers of Engineers and Architects. Chamber of Environmental Engineers.

PUBLICATIONS

Refereed International Journals

Vanrolleghem P.A., **Sin G.** and Gernaey K. (2004) Transient response of aerobic and

anoxic activated sludge activities to sudden substrate concentration changes. Biotechnol and Bioeng. 86:277-290.

De Pauw D.J.W., **Sin G.,** Insel G., van Hulle S., Vandenberghe V. and Vanrolleghem P.A. (2004) Discussion of 'Assessing Parameter Identifiability of Activated Sludge Model No. 1' by Pedro Afonso and Maria da Conceicao Cunha. Journal of Environmental Engineering. 130(1): 110-112.

Sin G., Malisse K. and Vanrolleghem P.A. (2003) An integrated sensor for the monitoring of aerobic and anoxic activated sludge activities in biological nitrogen removal plants. *Wat. Sci. Tech.*. 47(2):141 –148.

Conference Proceedings

Vanrolleghem P.A., Van Hulle S.W.H., Volcke E.I.P. and **Sin G.** (2004) Modelling, control and optimization of autotrophic nitrogen removal. EU 5th framework IcoN symposium on Anammox. Ghent, Belgium, 21-23 January 2004.

Guisasola A., **Sin G.,** Baeza J.A., Carrera J. And Vanrolleghem P. Limitations of ASM1 and ASM3: a comparison based on batch OUR profiles from different full-scale WWTPs. *IWA 4th World Water Congress*,19-24 September 2004, Marrakech, Morocco. *Accepted.*

Sin G. and Vanrolleghem (2004) A nitrate biosensor-based methodology for monitoring anoxic activated sludge activity. *In proceedings: 2nd International IWA Conference on Automation in Water Quality Monitoring: AutMoNet2004.19-20 April 2004, Vienna, Austria, pp 61-68.*

Sin G., Insel G., Lee D.S. and Vanrolleghem P.A. (2004) Optimal but robust N and P removal in SBRs: A systematic study of operating scenarios. *In proceedings: 3rd IWA international Conference on SBRs, 22-26 February 2004, Noosa, Queensland, Australia, pp 93-100. (Accepted for Water Science & Technology).*

Insel G., **Sin G.,** Lee D.S. and Vanrolleghem P. A. (2004) A calibration methodology and model-based systems analysis for SBR's removing nutrients under limited aeration conditions. *In proceedings: 3rd IWA international Conference on SBRs*, 22-26 February 2004, Noosa, Queensland, Australia (on CD-ROM).

Gökçay C.F. and **Sin G.** (2003) Modeling of a large-scale wastewater treatment plant for efficient operation. *In proceedings:* 9th IWA conference on LWWTPs, 1-4 September 2003, Praha, Czech Republic, pp 193-200.

Sin G., Petersen B., Gernaey K. and Vanrolleghem P.A. (2001). Combined nitrate and titrimetric measurements for identification of the denitrification process: In calibration of ASMs for BNR systems. Med. Fac. Landbouw. Univ. Gent, 66/4, pp 245-252.

Workshops

Sin G. and Vanrolleghem P.A. (2003). Anoxic monitoring of activated sludge activity: A

nitrate biosensor based methodology.3rd Nitrification day, 24 November 2003, IHE – TUDELFT, Delft, Holland.

Sin G., Malisse K. and Vanrolleghem P.A. (2002). Quantifying aerobic and anoxic activated sludge activities in BNR plants using simultaneous titrimetric, respirometric and nitrate measurements. 2nd Nitrification day, 25 March 2002, IHE – TUDELFT, Delft, Holland.

Technical Reports

Sin G., Van Hulle, S.W.H., Volcke E.I.P., & Vanrolleghem P.A. (2001). Activated Sludge Model No. 1 Extended with Anammox and Sharon Processes. Biomath Technical report. Ghent University, Belgium.

CONFERENCES & WORKSHOPS

2004

2nd International IWA Conference on Automation in Water Quality Monitoring: AutMoNet2004.19-20 April 2004, Vienna, Austria,
3rd IWA international Conference on SBRs, 22-26 February 2004, Noosa, Queensland, Australia,

2003

Biological nutrient removal in industrial wastewater treatment plants and the prevention and remediation of related operational disorders (MicroSurvey)" October 28 - 29, 2003. Brasschaat, Belgium.
TNAV Workshop on "New developments in measurement and automation techniques in the watersector" (Nieuwe ontwikkelingen op het gebied van meet- en regeltechniek in de watersector) October 22, 2003. Edegem, Belgium.
17th FORUM FOR APPLIED BIOTECHNOLOGY, 24th and 25th September 2003.Gent, Belgium,

2002

International IWA conference "From Nutrient Removal to recovery" October 2-4, 2002.Amsterdam, Netherlands.
International IWA conference on Automation in Water Quality Monitoring: AutMoNet 2002 May 21-22, 2002.Vienna, Austria.
8th FLTBW PhD Symposium 22 October 2002, Gent University.

2001

De Reele Kosten van Water an Afwalwater in de Publieke en Industriele Sector. Workshop by Technologisch Instituut. 27 November 2001, Antwerp, BELGIUM.
7th FLTBW PhD Symposium, 10 October 2001, Gent University.
15th FORUM FOR APPLIED BIOTECHNOLOGY, 24th and 25th September 2001, Gent, Belgium.
Advance Course on Environmental Biotechnology at The institute for Biotechnology Studies

– Delft University of Technology and Leiden University.20-29 June 2001, Kluyver Laboratory of TU-DELFT, The Netherlands.

2000

WATERMATEX 2000 - 5th International Symposium on Systems Analysis and Computing in Water Quality Management. Gent, Belgium, 18-20 September 2000.
New Trends in Mathematical Modeling and Numerical Methods. November 16-17, 2000. Leuven, Belgium.

1999

Tacis-Tempus 2nd International Conference on Industry, Technology, Environment (ITE) - Education in Technical Universities for the Twenty-first Century. Moscow State University of Technology "STANKIN". Moscow, Russia. 1999.
Third National Congress of Environmental Engineering. İzmir, Turkey. 1999.

1997

Second National Congress of Environmental Engineering. Istanbul, Turkey. 1997.

HOBBIES

Cinema	I closely follow the 7th art. Two things I value most in a movie: the uniqueness of the script, the consistency and coherence of the story throughout the movie and the audio-visual effects of the movie. I enjoy particularly the short films and also the animations.
Sport	I enjoy playing mini-football and squash.
Literature	My current favourite kind in literature is the science fiction. I find it as a brilliant and awesome reflection of human imagination. Few names whom I adore: Arthur C. Clark, Frank Herbert, Isaac Asimov….
Webmaster	I enjoy working with internet. I am part of a team that maintains and upgrades regularly the BIOMATH website (http://biomath.ugent.be/).

ISBN 90-5989-024-8